

Synthesis, Characterisation and Biological Evaluation of Novel *N*-  
Ferrocenyl Amino Acid and Dipeptide Derivatives as Potential  
Anticancer Agents.

By

**Rachel Tiedt B. Sc (Hons.)**

A thesis presented for the degree of Doctor of Philosophy

At

Dublin City University

Under the supervision of Dr. Peter T. M. Kenny



*OllScoil Chathair Bhaile Átha Cliath*

*School of Chemical Sciences*

*July 2014*

*I hereby certify that this material, which I now submit for assessment on the programme of study leading to the award of Ph.D. is entirely my own work, that I have exercised reasonable care to ensure that the work is original, and does not to the best of my knowledge breach any law of copyright, and has not been taken from the work of others save and to the extent that such work has been cited and acknowledged within the text of my work.*

Signed: \_\_\_\_\_

ID No. \_\_\_\_\_

Rachel Tiedt

Date: \_\_\_\_\_



Synthesis and structural characterisation of ferrocenyl amino acid and dipeptide derivatives.....	49
2.1. Introduction .....	49
2.2. The synthesis of <i>N</i> -(6-ferrocenyl-2-naphthoyl), <i>N</i> -{ <i>para</i> -(ferrocenyl)cinnamoyl} and <i>N</i> -{ <i>para</i> -(ferrocenyl)benzoyl} amino acid and dipeptide derivatives.....	55
2.2.1.1. Preparation of ferrocenyl carboxylates.....	58
2.2.1.2. Preparation of ferrocenyl naphthalene-2-carboxylic acid.....	59
2.2.1.3. Preparation of dipeptides.....	59
2.2.1.4. Amide bond formation.....	60
2.2.1.4.1. Acyl chlorides.....	61
2.2.1.4.2. Anhydrides.....	61
2.2.1.4.3. Carbodiimides.....	63
2.2.1.4.3.1. Racemisation.....	63
2.2.1.4.3.2. Intramolecular acyl transfer.....	64
2.2.1.4.3.3. Auxiliary nucleophiles.....	65
2.2.2. Purification and yields of <i>N</i> -(6-ferrocenyl-2-naphthoyl), <i>N</i> -{ <i>para</i> -(ferrocenyl)cinnamoyl} and <i>N</i> -{ <i>para</i> -(ferrocenyl)benzoyl} amino acid and dipeptide derivatives.....	66
2.2.3. <sup>1</sup> H NMR studies of <i>N</i> -(6-ferrocenyl-2-naphthoyl), <i>N</i> -{ <i>para</i> -(ferrocenyl)cinnamoyl} and <i>N</i> -{ <i>para</i> -(ferrocenyl)benzoyl} amino acid and dipeptide derivatives.....	68
2.2.4. <sup>1</sup> H NMR study of <i>N</i> -(6-ferrocenyl-2-naphthoyl)-glycine-L-alanine methyl ester (106).....	70
2.2.5. <sup>1</sup> H NMR study of <i>N</i> -{ <i>para</i> -(ferrocenyl)cinnamoyl}-γ-aminobutyric acid ethyl ester (115).....	71
2.2.6. <sup>1</sup> H NMR study of <i>N</i> -{ <i>para</i> -(ferrocenyl)benzoyl}-glycine-glycine benzyl ester (123).....	73
2.2.7. Variable temperature study of <i>N</i> -(6-ferrocenyl-2-naphthoyl)-sarcosine-glycine methyl ester.....	75
2.2.8. <sup>13</sup> C NMR and DEPT 135 NMR studies of <i>N</i> -(6-ferrocenyl-2-naphthoyl), <i>N</i> -{ <i>para</i> -(ferrocenyl)cinnamoyl} and <i>N</i> -{ <i>para</i> -(ferrocenyl)benzoyl} amino acid and dipeptide derivatives.....	79
2.2.9. <sup>13</sup> C NMR and DEPT 135 NMR study of <i>N</i> -{ <i>para</i> -(ferrocenyl)cinnamoyl}glycine-L-alanine ethyl ester (116).....	80

2.2.10. HSQC study of <i>N</i> -{ <i>para</i> -(ferrocenyl)cinnamoyl}-glycine-L-alanine ethyl ester (116).....	83
2.2.11. Infra red studies of <i>N</i> -(6-ferrocenyl-2-naphthoyl), <i>N</i> -{ <i>para</i> -(ferrocenyl)cinnamoyl} and <i>N</i> -{ <i>para</i> -(ferrocenyl)benzoyl} amino acid and dipeptide derivatives.....	85
2.2.12. UV-Vis studies of <i>N</i> -(6-ferrocenyl-2-naphthoyl), <i>N</i> -{ <i>para</i> -(ferrocenyl)cinnamoyl} and <i>N</i> -{ <i>para</i> -(ferrocenyl)benzoyl} amino acid and dipeptide derivatives.....	87
2.2.13. Mass spectrometric studies of <i>N</i> -(6-ferrocenyl-2-naphthoyl) amino acid and dipeptide derivatives.....	89
2.3. Approaches to the synthesis and structural characterisation of <i>N</i> -(1-ferrocenyl-5-naphthoyl) amino acid and dipeptide derivatives.....	90
2.3.1. Introduction.....	90
2.3.2. Synthesis of <i>N</i> -(5-ferrocenyl-1-naphthoyl) dipeptides.....	92
2.3.2.1. Preparation of Boc protected dipeptides with a free hydroxyl group.....	93
2.3.2.2. Preparation of <i>N</i> -5-acetyl-1-aminonaphthalene.....	94
2.3.2.2.1. <i>t</i> -Butoxycarbonyl (Boc) protecting groups.....	94
2.3.2.2.2. Acetyl protecting groups.....	96
2.3.3. Discussion.....	97
2.4. Conclusions.....	98
Experimental Procedures.....	100
References.....	143
Chapter 3.....	145
Biological evaluation of <i>N</i> -(6-ferrocenyl-2-naphthoyl), <i>N</i> -{ <i>para</i> -(ferrocenyl)cinnamoyl} and <i>N</i> -{ <i>para</i> -(ferrocenyl)benzoyl} amino acid and dipeptide derivatives.....	145
3.1. Introduction .....	145
3.1.1. Cell culture.....	145
3.2. Biological evaluation of <i>N</i> -(6-ferrocenyl-2-naphthoyl)-glycine-glycine esters.....	147
3.2.1. <i>In vitro</i> evaluation on A549 and H1299 lung cancer cell lines.....	149
3.2.2. <i>In vitro</i> evaluation in Lox-IMVI, Malme-3M and HT-144 metastatic melanoma cell lines.....	150
3.2.3. <i>In vitro</i> evaluation in normal human dermal fibroblast (NDHF) cells.....	152

3.2.4. In <i>vitro</i> evaluation in resistant cell lines.....	152
3.2.5. Apoptosis assays.....	153
3.2.5.1. Cell cycle analysis.....	154
3.2.5.2. TUNEL assay.....	156
3.3. Biological evaluation of <i>N</i> -{ <i>para</i> -(ferrocenyl)cinnamoyl} and <i>N</i> -{ <i>para</i> - (ferrocenyl)benzoyl} amino acid and dipeptide derivatives.....	158
3.4. Solubility studies.....	158
3.5 Conclusions.....	159
Experimental procedures.....	161
References.....	164
Chapter 4.....	165
Mode of action studies and drug targeting.....	165
4.1. Introduction .....	165
4.1.1. Cancer cells.....	166
4.1.2. The cell cycle.....	166
4.1.3. Abnormal signalling pathways.....	167
4.1.4. Apoptosis.....	168
4.1.5. Cell immortality.....	168
4.1.6. Angiogenesis.....	169
4.1.7. Metastasis.....	169
4.2. DNA binding assays.....	169
4.2.1. Targeting DNA.....	169
4.2.2. DNA binding.....	170
4.2.2.1. Classical DNA intercalators.....	171
4.2.2.2. Threading intercalators.....	173
4.2.2.3. Groove binders.....	173
4.2.2.4. Electrostatic backbone binders.....	175
4.2.2.5. Metallointercalators.....	176
4.2.3. <i>N</i> -(6-ferrocenyl-2-naphthoyl) amino acid and dipeptide esters as potential intercalating agents.....	177
4.3. Redox modulation in cancer therapy.....	178
4.3.1. Reactive oxygen species (ROS).....	178
4.3.2. Oxidative stress and cancer.....	179
4.3.3. Antioxidant therapy.....	179

4.3.4. Prooxidant therapy.....	179
4.3.4.1. Agents that generate ROS.....	180
4.3.4.2. Agents that inhibit antioxidants.....	182
4.3.5. Oxidative DNA damage.....	183
4.3.6. Guanine oxidation studies.....	187
4.3.6.1. <i>N</i> -(ferrocenylmethylamino acid) fluorinated benzene carboxamide derivatives.....	188
4.3.7. <i>N</i> -(6-ferrocenyl-2-naphthoyl)-glycine-glycine ethyl ester (70) and <i>N</i> -(ferrocenylmethyl-L-alanine)-3,4,5-trifluorobenzene carboxamide (75g) mediated DNA damage.....	190
4.4. Drug targeting.....	194
4.4.1. Introduction.....	194
4.4.2. Drug targeting for <i>N</i> -(6-ferrocenyl-2-naphthoyl) dipeptide derivatives.....	197
4.5. Conclusions.....	202
Experimental Procedures.....	188
References.....	189
5.1. Discussion.....	200
5.2. Conclusion.....	201
Experimental procedures.....	204
References.....	205
Appendix A – Abbreviations.....	210
Appendix B – Publications .....	219

## Abstract

The aim of this research thesis was to extend the structure activity relationship (SAR) of ferrocenyl peptide bioconjugates, a novel class of potential anticancer agents, and to investigate their mode of action in preparation for *in vivo* testing. A series of *N*-(6-ferrocenyl-2-naphthoyl), *N*-{*para*-(ferrocenyl)cinnamoyl} and *N*-{*para*-(ferrocenyl)benzoyl} amino acid and dipeptide derivatives was prepared. Both the conjugated linker and the ester portions of the molecule were varied. The compounds were fully characterised by spectroscopic techniques including <sup>1</sup>H NMR, <sup>13</sup>C NMR, IR, UV-Vis and MS.

A further SAR study was undertaken varying both the substitution pattern of the conjugated linker and replacement of the ester portion of the molecule with the free amine *N*-terminus on the amino acid or dipeptide. The synthesis of *N*-(5-ferrocenyl-1-naphthoyl) amino acid and dipeptide esters was attempted by coupling of 1-amino-5-ferrocenyl-naphthalene with the *C*-terminus of the amino acid or dipeptide.

Biological evaluation was performed *in vitro* in A549 and H1299 non small cell lung cancer and HT-144, Lox-IMVI and Malme-3M metastatic melanoma. The most active derivative, *N*-(6-ferrocenyl-2-naphthoyl)-glycine-glycine methyl ester had an IC<sub>50</sub> of 0.2 μM on A549, Lox-IMVI and HT-144 and 0.3 μM on H1299 and Malme-3M cells. Toxicity studies demonstrated a similar level of toxicity to cisplatin while evaluation in resistant cell lines showed that *N*-(6-ferrocenyl-2-naphthoyl)-glycine-glycine methyl ester does not share cross resistance with temozolomide on the Malme-3M cell line. Cell cycle analysis showed a significant increase in the sub G<sub>0</sub> phase while the TUNEL assay confirmed that the compounds undergo apoptosis leading to cell death.

Guanine oxidation studies were carried out via HPLC-EC for *N*-(6-ferrocenyl-2-naphthoyl)-glycine-glycine ethyl ester and *N*-(ferrocenylmethyl-L-alanine)-3,4,5-trifluorobenzene carboxamide). This confirmed that both classes of compounds are capable of generating reactive oxygen species (ROS) via Fenton chemistry. DNA binding as a possible mode of action was explored and a B<sub>12</sub> conjugate was prepared as a potential drug delivery vehicle to overcome drug solubility issues *in vivo*.



## Acknowledgements

Firstly I would like to thank Dr. Peter Kenny for allowing me to carry out this research under his supervision and for all his patience and support over the years.

I would like to thank;

The Health Research Board (HRB) for providing the funding for my research project with grant number HRA/09/86.

Dr Norma O' Donovan in the National Institute for Cellular Biotechnology (NICB) for her assistance with the biological testing aspects of the project.

Dr. Blánaid White and Dr. Michele Kelly of the school of chemical sciences for their supervision and assistance with high performance liquid chromatography electrochemical detection (HPLC-EC) guanine oxidation studies.

Dr. Fabio Zobi of the University of Switzerland for his assistance with B<sub>12</sub> conjugation studies.

The technical staff of the school of chemical sciences; Veronica, Ambrose, Damien, John, Brendan, Vinny and Catherine, for being some of the most genuinely pleasant people to work with and on many occasions going out of their way to offer assistance.

The Peter Kenny Research Group (PKRG) that I had the pleasure to work with; Lingli Lu, James Murphy, Dr William Butler, Dr. Andy Harry and Dr. Áine Mooney and our summer students Aoife Kinahan, Camille Remeur and Laura Stella and masters student Sue Ryeo Kim.

I would like to thank the 'Tea Gang'; Aoife, Brian, Nicky (even though she doesn't drink tea), Sean, Leeanne, Laura, Orla, Hannah, Andy, Alan, Sarah, Hazel, Declan, Gill and Keana for ensuring there is always someone around for a cup of tea and a chat. You guys have kept me going.

I would like to thank my best friends Gaëlle, Chaz and Zowie for being there for me even though I haven't had much free time to see them recently.

Finally I would like to thank my family. Thank you Mum and Dad for supporting me through the last five years. Thank you for pushing me to continue when I felt I should have given up. I would like to thank my auntie Helen for her support and our chats. I would especially like to thank my little brother Aaron for keeping me distracted with streamed TV shows and

helping me by eating half of the chocolate. I dedicate this thesis to my little brother Aaron.  
You've been comparing report cards for years. I challenge you – beat this!

*For my little brother Aaron.*



## Chapter 1

### Cancer, chemotherapy and bioorganometallic anticancer agents.

#### 1.1 Cancer

##### 1.1.1 Introduction

Cancer is the term used to describe a set of diseases characterised by abnormal and uncontrolled cell growth which evolves into a population of cells that can invade tissues and metastasise to other parts of the body. It is a major cause of death worldwide. There were 12.7 million cases of cancer in 2008 and it is expected to rise to 21 million by 2030<sup>1</sup>.

It is estimated that approximately 70 % of cancers are preventable through diet and lifestyle. Few cancers are hereditary with environmental factors such as smoking, infectious agents, radiation, industrial chemicals, pollution, medication, nutrition, physical activity and body composition having a large impact. The world cancer research fund makes several recommendations for the reduction of lifestyle related cancers; to be as lean as possible within a healthy body weight, daily physical activity, the reduction of calorie dense foods, a high consumption of plant based foods, the reduction of red meats, alcohol and salt, and an adequate intake of nutrients through diet as opposed to supplementation<sup>2</sup>.

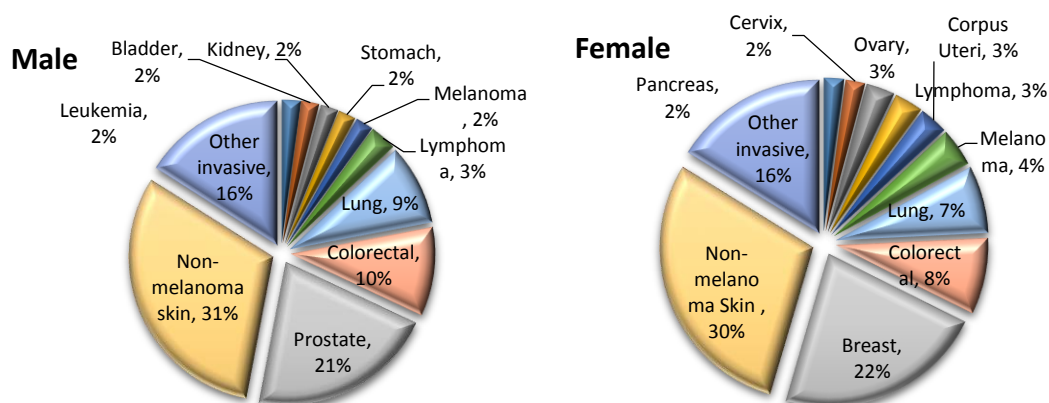


**Figure 1.1:** Relative frequency of the main invasive cancers diagnosed 2008-2010 reproduced from the annual report of the national cancer registry 2013<sup>3</sup>.

According to the annual report of the national cancer registry, cancer was the second most common cause of death in Ireland after circulatory diseases in 2010<sup>3</sup>. In the period 2008-2010 an average of 32,500 cases of cancer were reported per year. The cumulative risk of developing cancer is 1 in 3 for Irish men and 1 in 4 for Irish women with the most commonly

diagnosed cancers being breast, prostate, colorectal and lung cancers. These also represent almost 50 % of all cancer deaths in Ireland as can be seen in figure 1.1

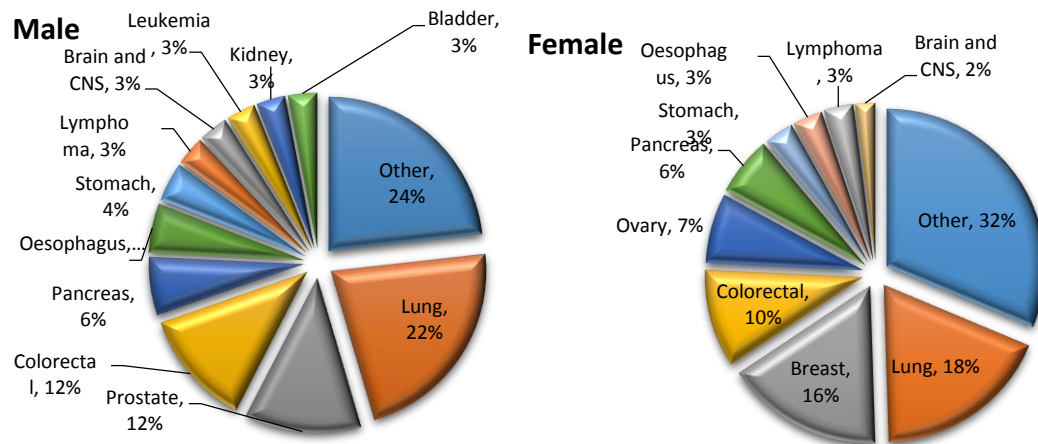


**Figure 1.2:** Relative frequency of the main cancer deaths 2010 reproduced from the annual report of the national cancer registry 2013<sup>3</sup>.

### 1.1.2 Lung cancer

Lung cancer is the most common cancer in the world. In 2008 it accounted for 12.7 % of all new cancers and 1.61 million new cases. It was also the most common cause of death from cancer with 1.38 million deaths (18.2 % of total cancer deaths)<sup>4</sup>. In Ireland it was the third most commonly diagnosed type of cancer in men and women between 2005 and 2009<sup>3</sup>. It accounted for 20 % of all cancer deaths in Ireland in 2010. It has a relatively poor survival rate compared to its incidence rate as can be seen from figures 1.1 and 1.2. It has a poor 5 year relative survival rate of just over 10 % based on figures between 2005 and 2009. Smoking is well known to be the greatest cause of lung cancer as it is responsible for 85 % of lung cancers. There are two main types of lung cancer, small cell lung cancer (SCLC) and non-small cell lung cancer (NSCLC). NSCLC represents approximately 84 % of all lung cancers<sup>5</sup>.

### 1.1.3 Melanoma

Melanoma accounted for 4.4 % of all cancer deaths in Ireland in the period 2008-2010. While melanoma comprises of only 5 % of skin cancers it accounts for 77 % of skin cancer deaths worldwide<sup>5</sup>. Early stage melanoma is very treatable and easy to detect however advanced melanoma is aggressive with a tendency to form metastases and is resistant to chemotherapy. It is one of the most aggressive forms of skin cancer and is one of the most rapidly increasing cancers in the world. While the five year survival rate for localised

melanoma is 98 %, advanced metastatic melanoma has a poor prognosis with a five year survival rate of just 15 %.

#### **1.1.4 Cancer chemotherapy**

Cancer is characterised by abnormal, unregulated cell growth. This growth may be benign or malignant. Malignant growths are characterised by their ability to form metastases; secondary growths which may often be distant from the location of the original tumour<sup>6</sup>. Cancer may be treated by surgery, radiotherapy, chemotherapy or a combination of these.

Many classical cancer chemotherapy drugs target cell replication as cancer cells are reproducing at a faster rate than most normal cells. However, they will also kill cells which divide rapidly under normal conditions such as those in the bone marrow, the lining of the digestive tract and in the hair follicles. This can lead to some of the more common side effects associated with cancer such as myelosuppression, inflammation of the digestive tract and loss of hair.

Resistance to chemotherapeutic drugs may be intrinsic; a property already possessed by the tumour before exposure to chemotherapeutic drugs, or acquired; resistance that occurs when a tumour is initially responsive to chemotherapy and later becomes resistant.

Tumours may become resistant to cancer drugs through loss of cell surface receptors or transporters for a drug or alteration of the target molecule of a drug; however these result in resistance only to a small number of related drugs<sup>7</sup>. Multiple drug resistance (MDR) may occur when protein efflux pumps remove toxic chemotherapeutic chemicals from the cell or when there is decreased cellular uptake of these compounds by transporter proteins<sup>8</sup>. Phosphoglycoprotein (Pgp), the multidrug transporter, normally expels toxins from cells. Pgp is widely expressed in many human cancers and can detect and bind to a wide variety of hydrophobic drug molecules as they enter the plasma membrane thus leading to multidrug resistance.

Much work has been undertaken to counter these effects by finding a drug that will actively compete with or inhibit Pgp and counter drug resistance<sup>9</sup>. As MDR occurs when a tumour becomes resistant to more than one compound used to treat it, many chemotherapeutics are given in combination therapy. Combination therapy offers several advantages to treatment with a single agent in that the drugs used differ in their mechanism of action. This

allows the agents to be used at lower dosages reducing toxicity as well as the chance of resistance to a particular agent.

#### 1.1.4.1 Alkylating agents

Alkylating agents are highly electrophilic and react with the nucleophilic regions of DNA in one or both strands to form strong covalent bonds. They act by causing crosslinking, creating DNA strand breaks and abnormal base pairing<sup>10</sup> which leads to the inhibition of cell division. Undesirable effects include acute toxicity, acquired resistance and the formation of secondary cancers. They are effective during all phases of the cell cycle but proliferating cells are more sensitive to them. These compounds are often prescribed in combination therapy. The nitrogen mustards were the first class of modern chemotherapeutic agents to be used *in vivo*. It was noticed during World War II that soldiers exposed to sulphur mustard gas were myelosuppressed. It was thought that they may also be used on cancer cells. They were first implemented in the 1940's when the nitrogen mustard, chlormethine **1**, which is closely related to the sulphur mustard gas that was used in World War II, was used to treat a patient with non-Hodgkins' lymphoma<sup>11</sup>.

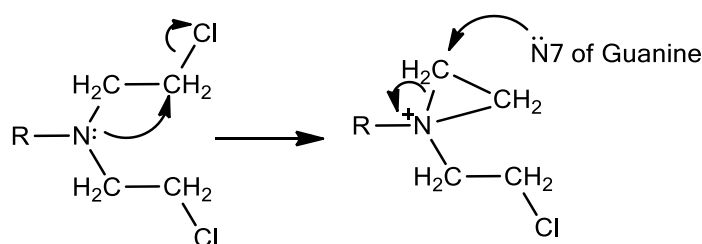
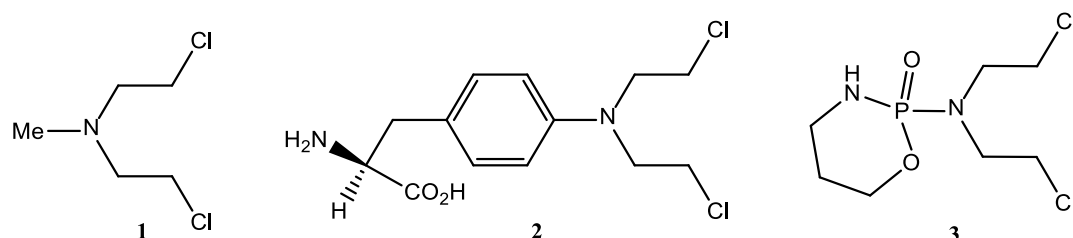


**Figure 1.3:** Mechanism for the formation of DNA crosslinks by the aliphatic nitrogen mustards<sup>12</sup>.

The weakly electrophilic  $\beta$ -carbon of aliphatic nitrogen mustards such as **1** is converted to the highly electrophilic aziridinium ion by internal nucleophilic substitution. This is followed by nucleophilic attack by the N7 of guanine. As the molecule contains two chloride ligands, both chains can react with guanine residues to form a cross link. As these molecules are highly electrophilic they can react with other nucleophilic molecules within the cell causing unwanted toxicity. Chlormethine is too reactive to be administered orally and has to be injected intravenously.

In order to reduce unwanted side effects attempts have been made to stop formation of the aziridinium ion. Drugs such as melphalan **2** contain an electron withdrawing benzene ring which

reduces the nucleophilic nature of the nitrogen atom. These agents react by direct substitution of the  $\beta$ -chlorine atoms by guanine. This allowed for the oral administration of nitrogen mustards.



Cyclophosphamide **3** is the most widely used alkylating agent in chemotherapy. It acts as a prodrug and is oxidised to the active form *in vivo*. It was believed the high concentration of phosphoramidases contained in tumours would hydrolyse the phosphorous group however it has been shown that its activity is due to the formation of a phosphoramidate mustard upon oxidation by microsomal enzymes in the liver (figure 1.4).

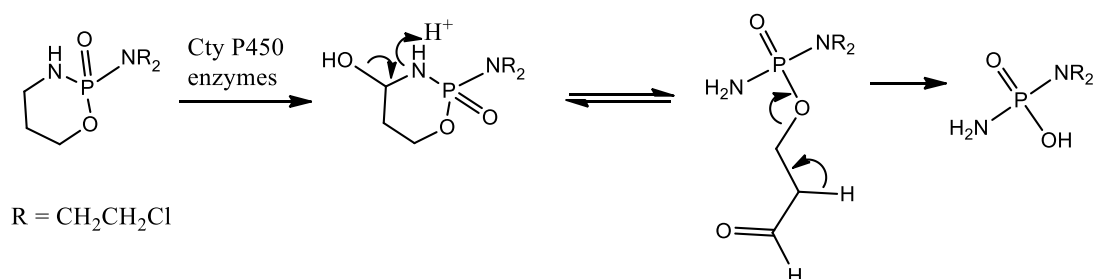


**Figure 1.4:** Formation of cytotoxic phosphoramidate mustard.

Nitrosoureas such as carmustine **4** and lomustine **5** act by attaching a chloroethyl group to a nucleic acid base to cause crosslinking. They are lipophilic and thus can cross the blood brain barrier and are used in the treatment of brain tumours.



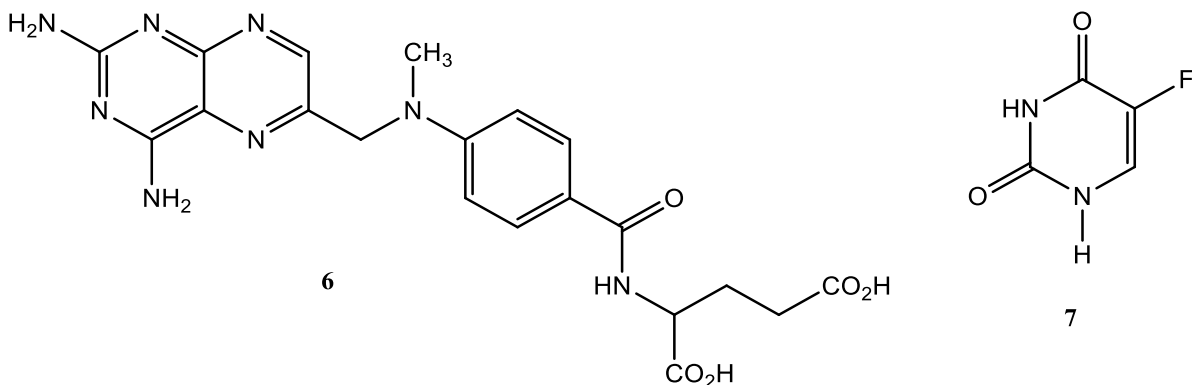


#### 1.1.4.2 Antimetabolites

Antimetabolites were discovered shortly after the introduction of the alkylating agents. Unlike the alkylating agents they act by inhibiting the enzymes involved in DNA and nucleotide synthesis. The first antimetabolites, the antifolates, came to light when it was realised that supplementation of folic acid caused proliferation of acute lymphoblastic leukaemia cells in affected children<sup>13</sup>.

Methotrexate **6** is one of the most commonly used antimetabolites used in cancer chemotherapy. It acts on dihydrofolate reductase (DHFR). This enzyme is required for the maintenance of the cofactor tetrahydrofolate, which in turn is essential for the generation of DNA synthesis precursors. Methotrexate mimics the structure of the natural folates and has a stronger binding affinity for DHFR than the cofactor tetrahydrofolate and thus depletes levels in the cell causing a reduction in DNA synthesis and cell division.

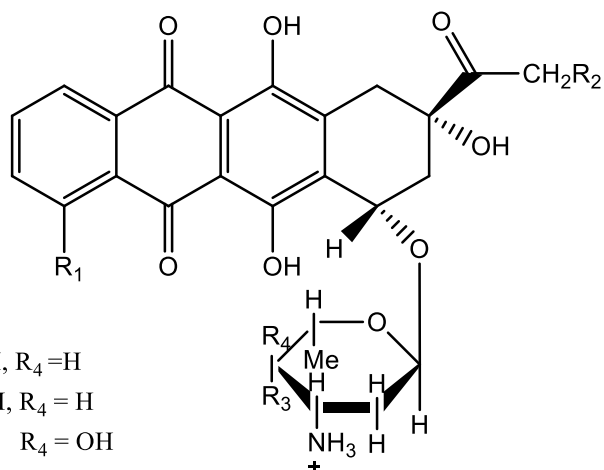
5-Fluorouracil **7** inhibits thymidylate synthase. It forms a suicide substrate by binding irreversibly with the enzyme and disrupting the synthesis of thymidine from uridine. This halts DNA synthesis and cell replication. It is often used in combination therapy with methotrexate.



#### 1.1.4.3 Agents acting on DNA topoisomerase.

Topoisomerases are nuclear enzymes which act on DNA topology by breaking and re-joining the DNA strand. There are two types, topoisomerase I and topoisomerase II. Topoisomerase I acts by inducing a single strand break while topoisomerase II acts by inducing a double strand break. Agents which interfere with topoisomerase activity may act as topoisomerase poisons or inhibitors<sup>14</sup>. Topoisomerase poisons do not prevent the enzyme from functioning rather just slow it by stabilising the DNA enzyme complex.

Intercalators contain a planar aromatic ring system which can fit into the DNA sequence and distorts the structure. Anthracyclins such as doxorubicin **8**, epirubicin **9**, danorubicin **10** and idarubicin **11** intercalate and stabilise the DNA enzyme complex at the point where the strand is cut.



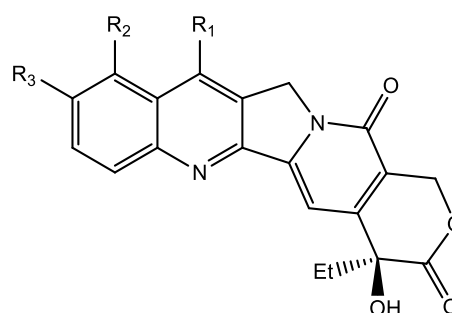
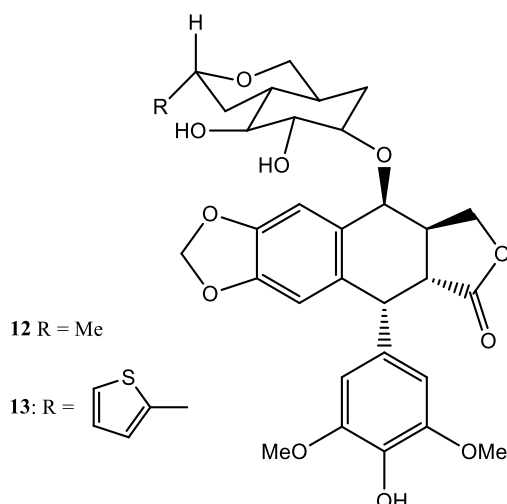
**8**  $R_1 = \text{OMe}, R_2 = \text{OH}, R_3 = \text{OH}, R_4 = \text{H}$

**9**  $R_1 = \text{OMe}, R_2 = \text{OH}, R_3 = \text{OH}, R_4 = \text{H}$

**10**  $R_1 = \text{OMe}, R_2 = \text{H}, R_3 = \text{H}, R_4 = \text{OH}$

**11**  $R_1 = \text{H}, R_2 = \text{H}, R_3 = \text{H}, R_4 = \text{OH}$

Etoposide **12** and teniposide **13** are semi synthetic derivatives of the natural product podophyllotoxin extracted from the dried rhizome and roots of *Podophyllum hexandrum*. These compounds act by stabilising the intermediate formed at the 5' break of the DNA strand, preventing the rejoining of the strand by topoisomerase II, thus causing double strand breaks and cell death. Etoposide is used for treatment of small cell lung cancer, testicular cancer, and lymphomas while teniposide is used in paediatric neuroblastoma.



**15**  $R_1 = \text{Et}, R_2 = \text{H}, R_3 =$

**16**  $R_1 = \text{H}, R_2 = \text{CH}_2\text{NMe}_2, R_3 = \text{OH}$

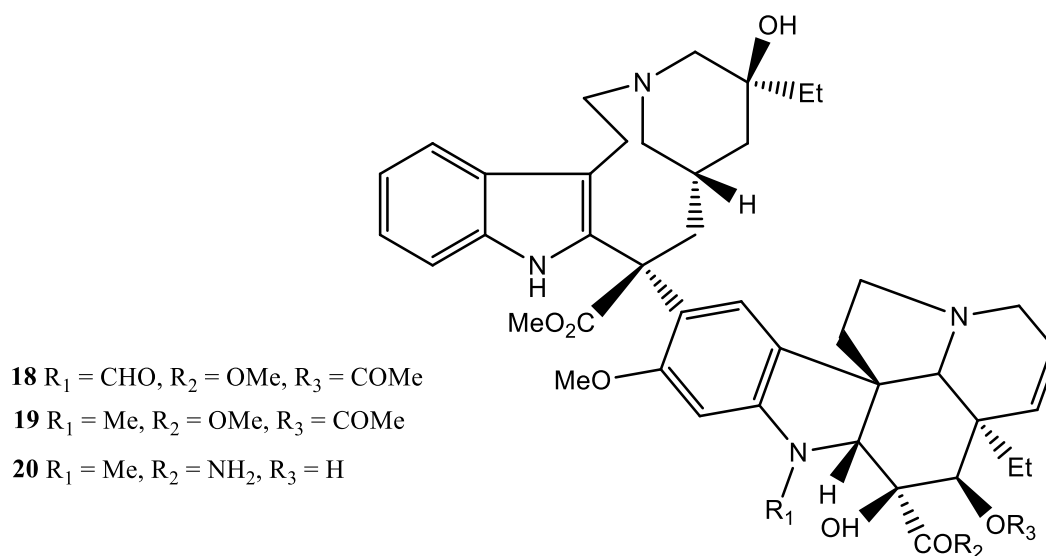
Camptothecin **14** acts on topoisomerase I. It is a natural product which was extracted from the ornamental Chinese tree *Camptotheca acuminata* (Nyssaceae) in 1966<sup>15</sup>. It was found to have activity against leukaemia and lung cancer in 1971<sup>16</sup>. It has shown poor activity *in vivo*

due to poor water solubility and has unacceptable renal toxicity. It wasn't until 1996 that a camptothecin derivative; irinotecan **15** was approved for use by the food and drug administration (FDA)<sup>17</sup>. Topotecan **16** was also developed, however these drugs are prone to resistance.

#### 1.1.4.4 Anti-microtubule agents

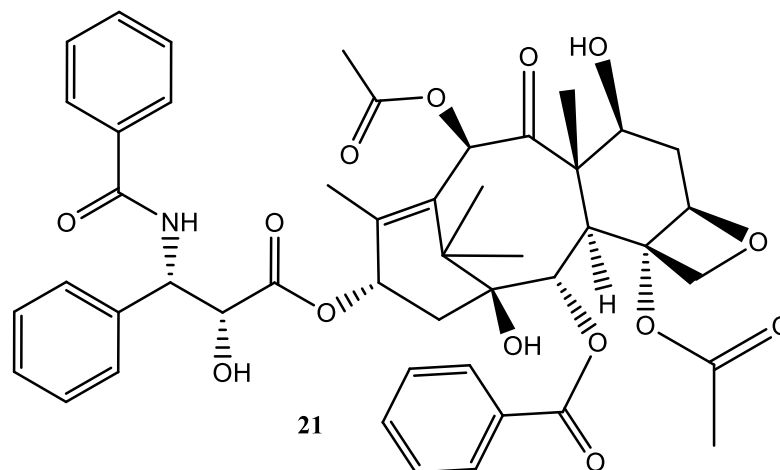
Tubulin is essential to cell division. Tubulin binding proteins help to polymerise or depolymerise of microtubules during cell division. Agents acting on microtubules may either bind to tubulin and stop polymerisation or bind to the microtubules themselves and prevent depolymerisation. This results in the inability of the cell to divide and induces cell death.

The vinca alkaloids vincristine **18** and vinblastine **19** are natural products derived from the Madagascar periwinkle plant *Cartharanthus roseus* and have been used in chemotherapy for over 35 years<sup>18</sup>. Their antiproliferative effect was first noticed by the Eli Lilly natural products group in 1963<sup>19</sup>. Vincristine is used in the treatment of childhood leukaemia as well as lymphomas, small cell lung cancer, cervical cancers and breast cancers. Vinblastine is used mainly in the treatment of Hodgkin's disease. Semisynthetic derivatives including vindesine **20** have also shown anticancer activity. They inhibit polymerisation of microtubules, particularly spindle microtubules and block the cell cycle at M phase, halting mitosis and inducing apoptosis.



First extracted from the bark of the pacific yew, *Taxus brevifolia*, and identified as antitumour agents in 1971<sup>20,21</sup> taxanes such as paclitaxel **21** inhibit depolymerisation by binding to the  $\beta$ -subunit of tubulin and promoting the production of unusually stable microtubules.

Depolymerisation is then unable to occur during cell division. Paclitaxel is used in the treatment of ovarian and breast cancer, small cell lung cancer and cancers of the head and neck.



## 1.2 Bioorganometallic chemistry

Bioorganometallic chemistry is the study of biologically active molecules which contain a direct carbon metal bond. In the late 1970's the field of organometallic chemistry was mainly concerned with the well-established area of catalysis, when an interest in its biological applications began to unfold. Up until then it was believed that metal complexes rarely played a role in biological processes. The discovery of the structure of vitamin B<sub>12</sub> and its coenzyme methylcobalamin in 1954 showed one of the first naturally occurring metal carbon bonds<sup>22</sup>. The term bioorganometallic chemistry was first used in 1985 to describe the study of organometallic species with biological applications<sup>23, 24</sup>. As a topic it has expanded significantly over the last 20 years as can be seen in figure 1.5.

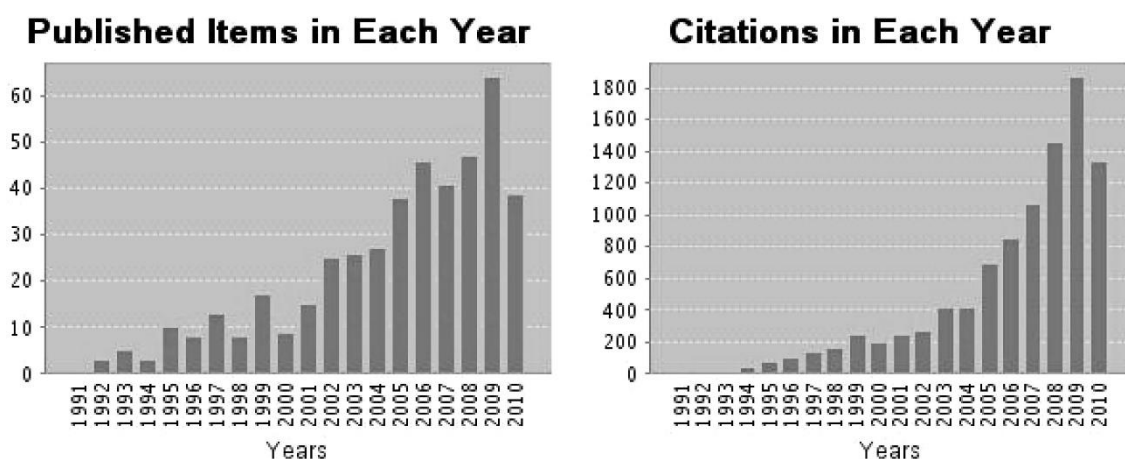
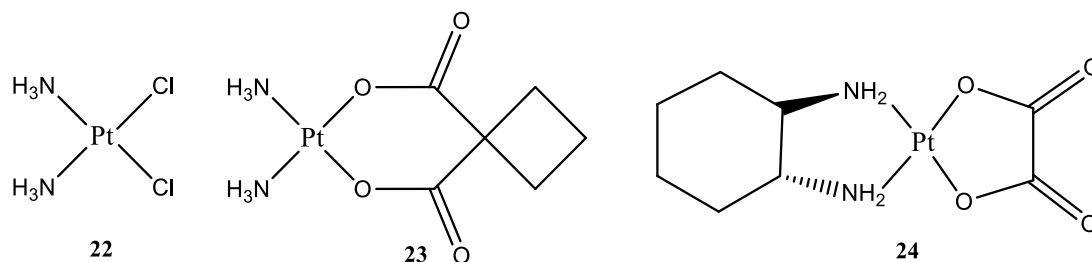


**Figure 1.5:** Number of articles published and their citations for the last 20 years using the query “bioorganometallic” for a search of the Web of Science database (September 2010)<sup>25</sup>.

## 1.2.1 Organometallic anticancer agents

### 1.2.1.1 Platinum metal complexes

The most widely used and well known anticancer metal complex (cis-diaminedichloroplatinum) cisplatin **22**, was first synthesised in 1844 by Michele Peyrone and was known as Peyrone’s chloride<sup>26</sup>. It is a platinum II square planar complex. It was not until 1965 that its anticancer properties were discovered by Rosenberg, who was investigating the effect of electric field on the growth of *E. coli*<sup>27</sup>. He noticed that the platinum conducting plates inhibited cell division and postulated that this may also be used to stop tumour growth. Clinical trials began in 1971 led by Bristol Myers Squib (BMS) and the National Cancer Institute (NCI) and in 1978 the drug was licensed by the Food and Drug Administration for the treatment of ovarian and testicular cancer<sup>28</sup>. Before its introduction survivors of testicular cancer were rare. Today the survival rate is over 85 % when used in combination therapy. It has also been used with some success in ovarian cancer and for palliative treatment of small cell lung cancer, bladder cancer, head and neck cancer and cervical cancer.



Following its huge success much research was carried out on platinum complexes as anticancer agents and soon after many other derivatives entered clinical trials. Its narrow spectrum of activity, toxicity and the development of resistance led to the development and licensing of several other platinum based compound. Among the most well known of these are carboplatin **23** and oxaliplatin **24**. Carboplatin was introduced to the clinic in 1981. It had a similar activity to cisplatin with less harsh side effects, specifically reduced nephrotoxicity, however it shares cross resistance with cisplatin. Oxaliplatin received approval in 1999 and shows activity on tumours which are cisplatin resistant e.g. colorectal cancer. It shows a better safety profile than cisplatin or carboplatin and does not share cross resistance with cisplatin or carboplatin. Other platinum agents were developed but to date no others have received as widespread clinical approval.

Cisplatin is an alkylating agent and owes its antitumour activity to its DNA binding abilities. Cisplatin is administered intravenously. Cisplatin itself is unreactive; high chloride concentrations in the extracellular fluid suppress aquation reactions of the ligands and allow the uncharged species to penetrate the cell membrane. The chloride concentration in the blood is approximately 100 mM, whereas the concentration in the cytoplasm is about 20 mM. The low concentration of chloride ions in the cytoplasm causes the replacement of the chloride ligands with neutral water ligands to give the reactive positively charged species (figure 1.6). This occurs to a greater extent once the compound reaches the nucleus where chloride concentrations are approximately 4 mM<sup>29</sup>. Aquated cisplatin is reactive towards nucleophilic centres on DNA, RNA and proteins as H<sub>2</sub>O is a better leaving group than Cl. Carboplatin owes its stability to its bidentate dicarboxylate ligand, which is more than 100 times more resistant to these aquation reactions, giving it extra stability and a longer half life than cisplatin<sup>30</sup>.

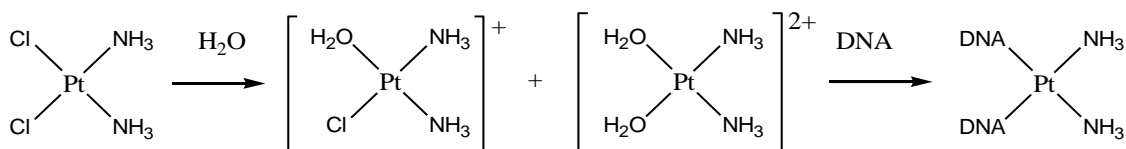


**Figure 1.6:** Loss of chlorine ligands in water and binding to DNA<sup>31</sup>.

DNA binding occurs to the N7 atom of the imidazole rings of guanine and adenine, as these are the most accessible and reactive sites of the double helix, to produce intra strand 1,2 and 1,3 crosslinks which block replication and/or prevent transcription<sup>32</sup>. It is most likely that 1,2 intra strand crosslinks are responsible for activity as the inactive compound transplatin is unable to form these and they are the least effectively removed from DNA by repair enzymes. These adducts then inhibit translation and replication triggering cellular apoptosis.

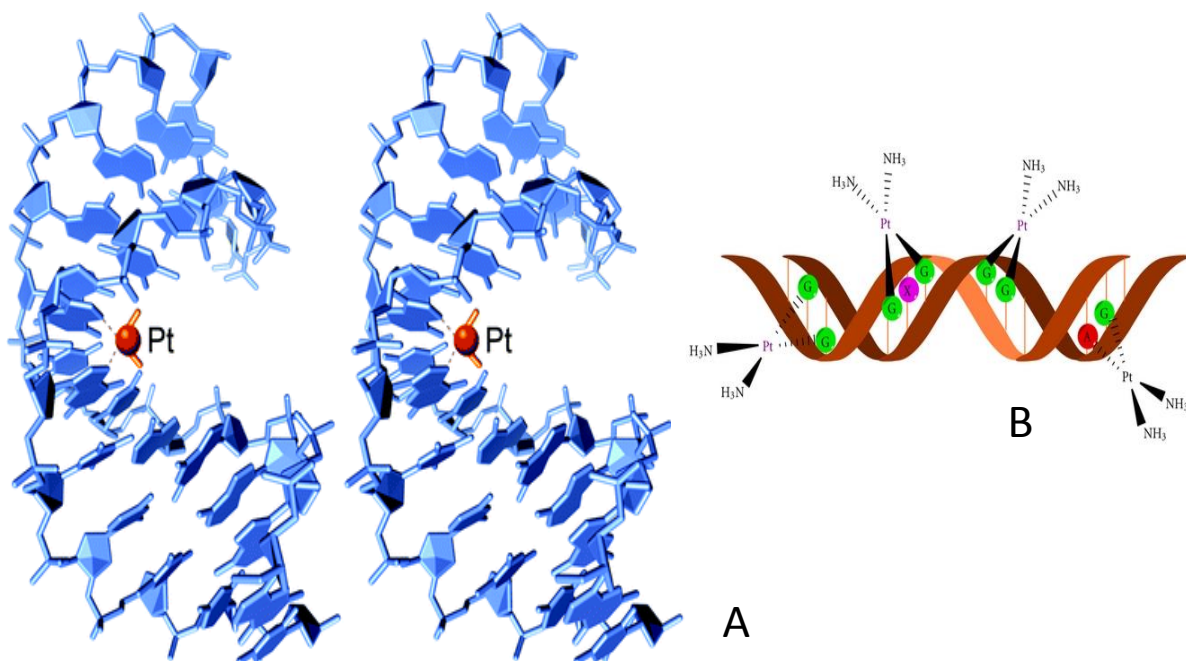
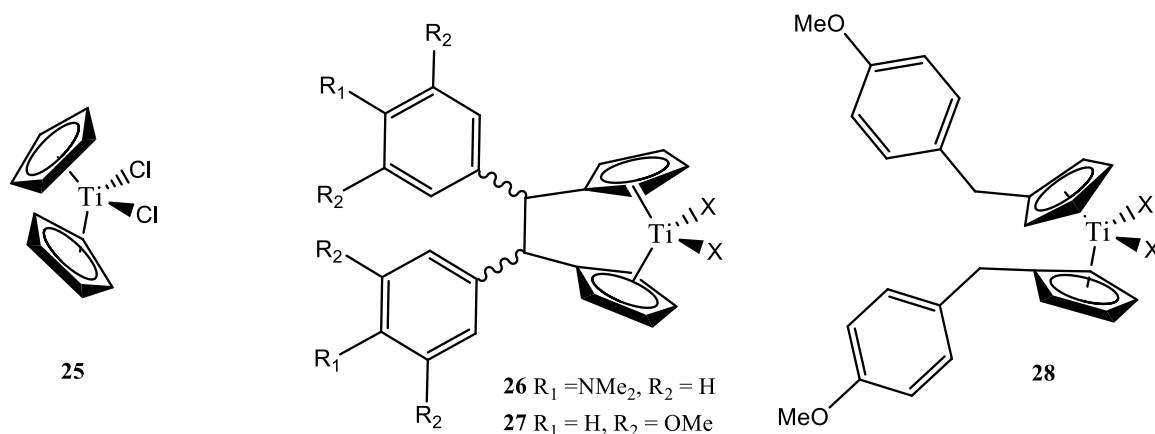


**Figure 1.7:** Two representations of cisplatin DNA binding. (A) Stereo view of X-ray structure of DNA crosslinked with cisplatin<sup>33</sup> and (B) schematic view of cisplatin with guanine units of DNA<sup>34</sup>.

### 1.2.1.2 Non platinum metal complexes

Transition metal complexes are often used in the development of complexes for treating cancer. Interesting physical properties including electronic structure, bonding, chemical and spectroscopic properties have led to their increasing use in medicinal chemistry. Among the metal complexes shown recently to have potential in cancer treatment are titanocene, vanadacene, molybdenocene, ferrocene and zirconocene<sup>35</sup>.



Titanocene **25** was the first metallocene reported with antitumour activity. It was shown to have strong cytotoxic activity against implanted Ehrlich ascites tumours (EATs) in mice in 1979 by Köpf and Köpf-Maier<sup>36</sup>.

It was studied in phase I clinical trials in 1993<sup>37,38, 39</sup> however dose limiting effects were noted including nephrotoxicity, hypoglycaemia, nausea and a reversible metallic taste. It reached some phase II clinical trials in metastatic breast carcinoma and advanced renal cell carcinomas. It was dropped after phase II as it had no significant advantages over cisplatin and was experiencing formulation problems due to low water solubility.

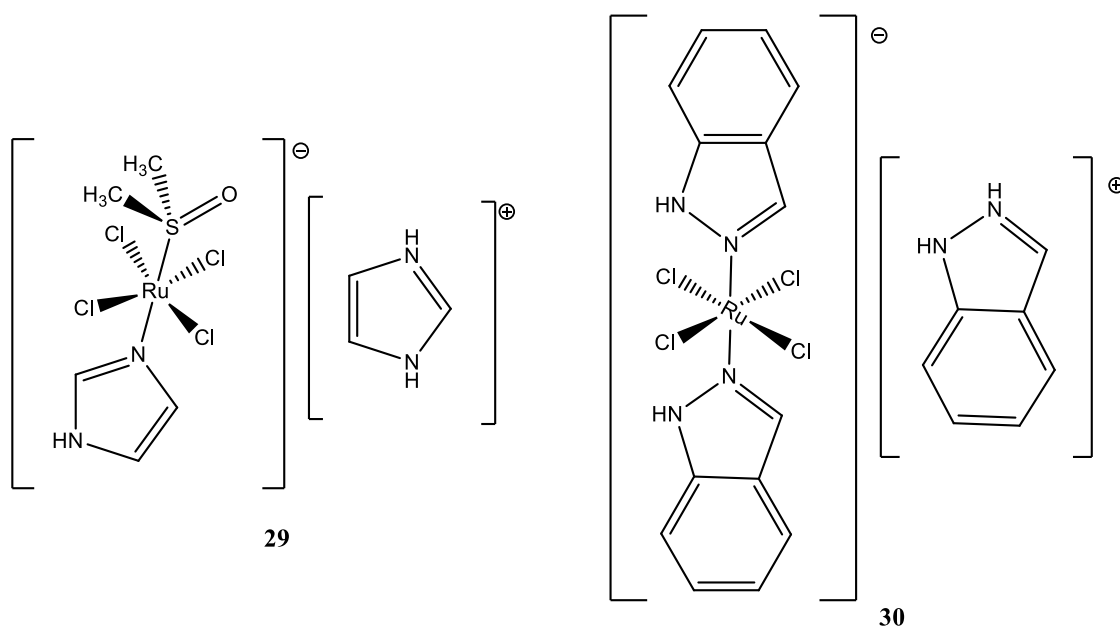
Recent work has focused on the preparation of different derivatives of titanocene with interesting anticancer properties. *Ansa* derivatives **26, 27** were prepared to increase water solubility and stability. *Ansa* metallocenes are linked by a bridging group between the two cyclopentadienyl rings. The cyclopentadienyl rings were linked for additional stability via a chelate effect and the water solubility was increased through the amino moieties<sup>40</sup>. Titanocene **Y 28**, the *para* methoxybenzyl derivative, was found to be active against a panel of 36 human tumour cell lines and has displayed promising activity *in vivo*<sup>41</sup>. In an attempt to improve the hydrolytic stability of the compounds the chlorine atoms were replaced with carboxylate ligands to give equally active compounds with more favourable pharmacokinetics.

As alternatives to platinum have been sought among the transition metals, ruthenium has also shown some promise as an antitumour and antimetastatic agent. It is considered a good replacement for platinum as the compounds are less toxic and have shown some specificity for cancer cells.



Ruthenium has three properties which make it suitable for medicinal use. Slow ligand exchange kinetics, multiple accessible oxidation states; ruthenium can access (II) (III) and (IV) oxidation states under physiological conditions, and the ability to mimic iron binding through albumin and transferrin<sup>42</sup>.

To date two ruthenium compounds have made it to human clinical trials NAMI-A **29** and KP1019 **30**<sup>43</sup>. NAMI-A shows no direct inhibition but has anti metastatic properties<sup>44</sup> whereas KP1019 has shown antitumour activity on human tumour explants by inducing apoptosis.



Both NAMI-A and KP1019 are Ru(III) complexes. Originally it was thought that these operated through the same mechanism as cisplatin, however ruthenium appears to accumulate preferentially in neoplastic masses. It is believed that it uses iron transport proteins albumin and transferrin to enter tumours. The lower oxygen content and higher acidity of the tumour environment then reduces the inactive Ru(III) compound to the active Ru(II) form.

NAMI-A was the first of these to reach human clinical trials. Phase I ran from 1999 and was reported in 2004. The majority of patients showed disease progression in this dose escalation study<sup>45</sup>. It has not yet undergone phase II trials. KP1019 has also been tested in a phase I dose escalation study. The majority of patients showed disease stabilisation however there was difficulty administering the maximum dosage as the compound has limited water solubility.

### 1.2.2 Ferrocene

Ferrocene was first discovered accidentally in 1951 by Pauson and Kealy while trying to synthesise fulvalene<sup>46, 47</sup>. They reported a yellow compound that contained two cyclopentadienyl rings and an iron atom, that was stable in water, in the presence of both strong acid and alkali and on heating to high temperatures. The structures shown in Figure 1.8 were initially reported. However the correct structure was not proposed until 1952 independently by both Fischer and Wilkinson<sup>48</sup>. X-ray crystallographic data was published shortly afterwards confirming the sandwich nature of ferrocene<sup>49</sup>. Until then it was believed that bonds between transition metals and hydrocarbons were unstable. After the structure of ferrocene was published, synthesis was attempted using most of the other transition metals giving rise to the generation of complexes known as sandwich complexes or metallocene chemistry.

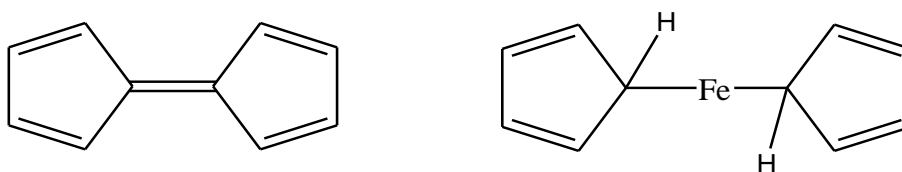


**Figure 1.8:** Initially proposed structures for ferrocene.

Ferrocene's sandwich structure is due to orbital overlap between the  $\pi$  electrons in the p orbitals of the cyclopentadienyl rings with the d orbitals of the iron atom<sup>50</sup>. The complex follows the 18 electron rule; it forms a stable complex, with a relative energy minimum and the electron configuration of the next noble gas, when the sum of the metal d electrons, electrons from the ligands and the overall charge of the complex equals 18. The iron centre is usually assigned the +2 oxidation state. Each ring is given a single negative charge, corresponding to 6  $\pi$  electrons. These are then shared with the 6 d electrons of the metal via covalent bonding.

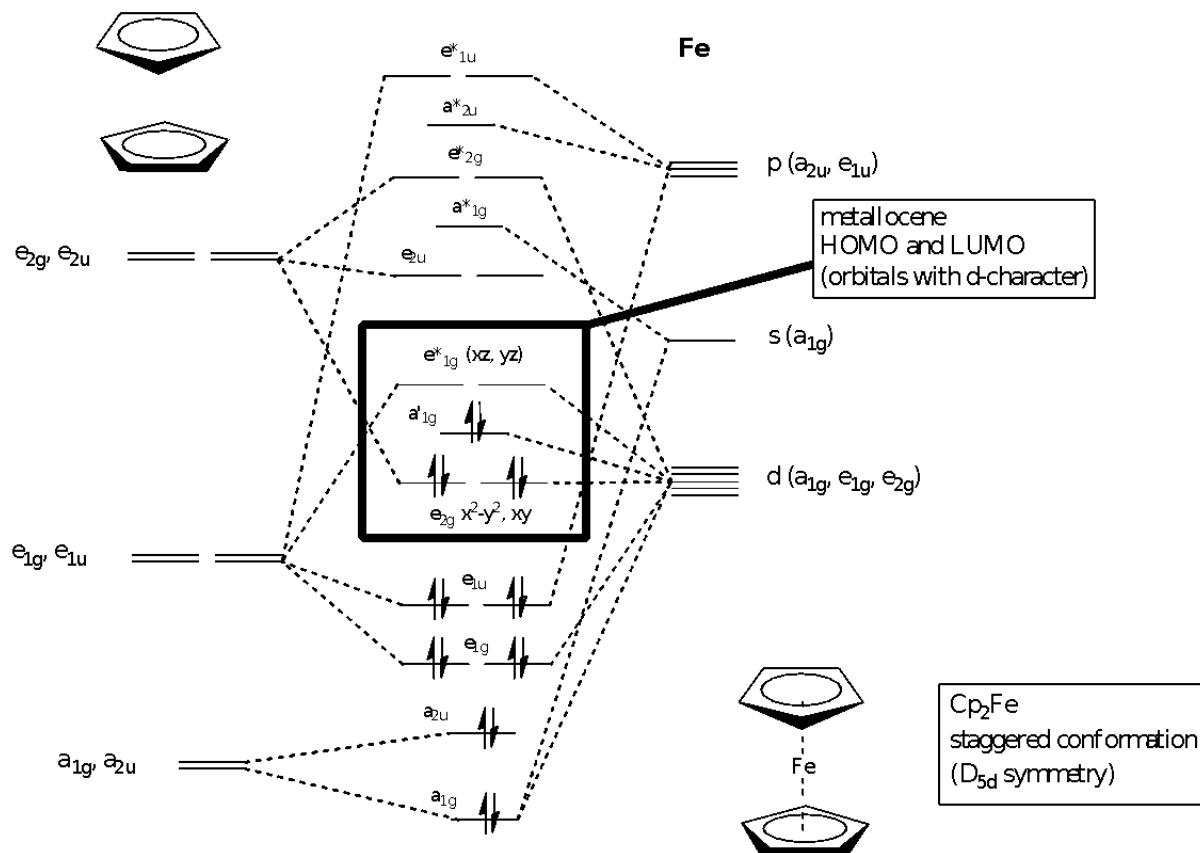


**Figure 1.9:** Molecular orbital diagram of ferrocene.

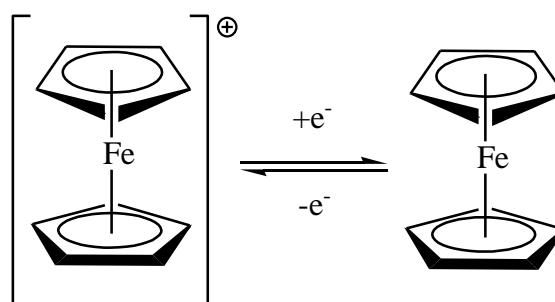
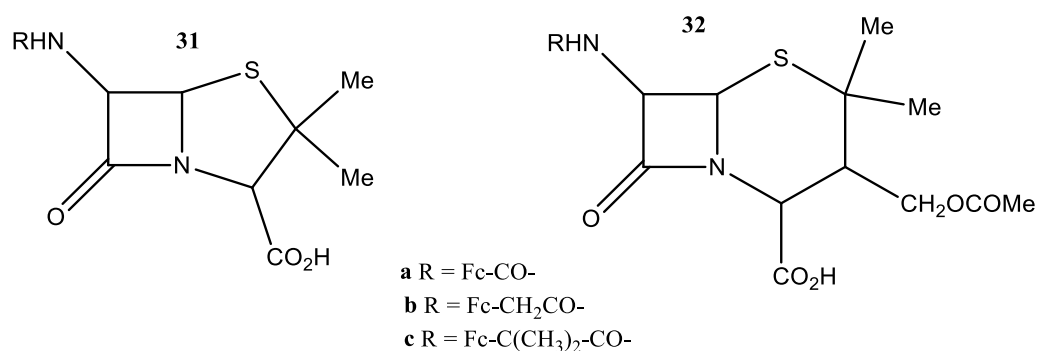


**Figure 1.10:** Ferrocene and ferricenium ion.

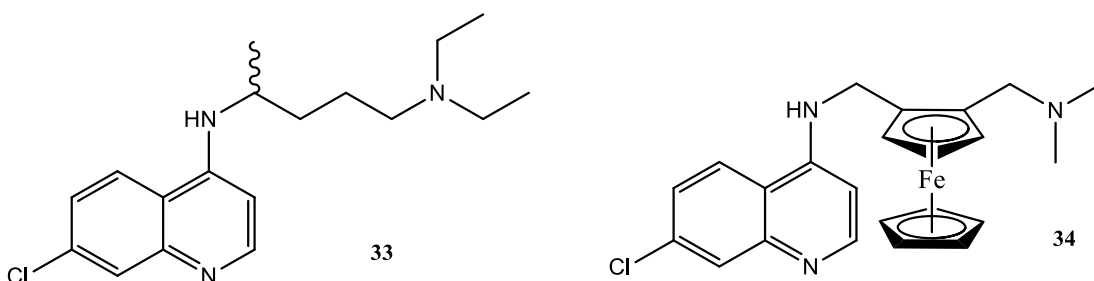
The cyclopentadienyl rings adopt a staggered conformation around the central iron atom. Due to its aromaticity it is often used as a bioisosteric replacement for benzene. Thus the name ferrocene was coined. Sometimes bioisosteric replacement with ferrocene has very little effect as in the case of ferrocenyl penicillins and sometimes it gives rise to an activity not possessed by the purely organic derivative. Ferrocene readily undergoes one electron oxidation from the Fe(II) to the Fe(III) oxidation state to give the ferricenium species which is blue green in dilute solution.

### 1.2.2.1 Medicinal chemistry of ferrocene

Ferrocene has shown many potential medicinal applications as antitumour, antiinfective antiviral, antibacterial and antifungal<sup>51</sup> agents. Some of the first ferrocenyl antibiotic derivatives were prepared in the late 70's by Edwards *et al.* in an attempt to address the issue of acquired resistance to antibiotics<sup>52, 53, 24</sup>. They developed ferrocenyl penicillins **31** and ferrocenyl cephalosporins **32** as  $\beta$ -lactamase inhibitors.



Edwards replaced the organic moieties with ferrocene. When the ferrocene was placed too close to the lactam ring **31a** and **32a**, antibiotic activity was decreased. When it was attached with a methylene spacer **31b** and **32b**, activity was similar to the organic derivative. When attached with a C(CH<sub>3</sub>)<sub>2</sub> spacer **31c** and **32c**, the desired increase in  $\beta$ -lactamase inhibition was achieved but the antibiotic activity decreased.



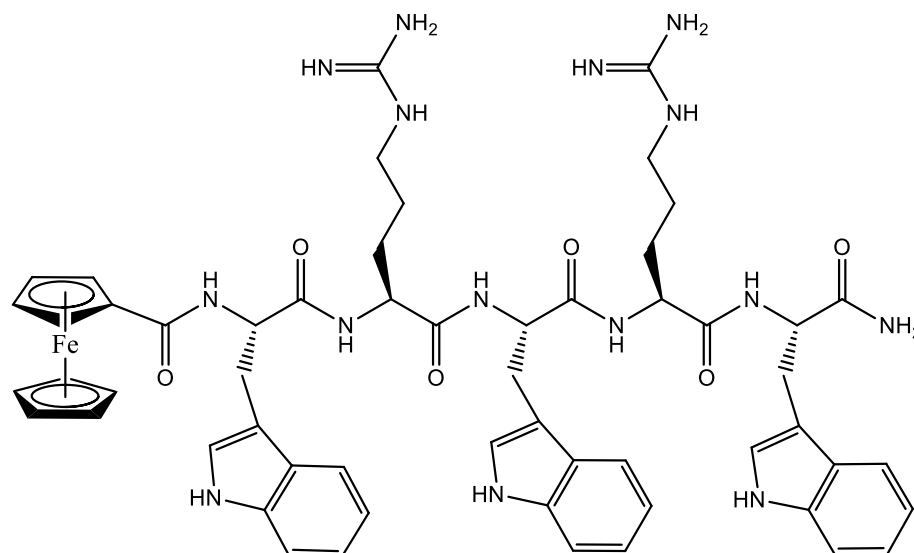
In the mid 90's using a similar strategy to the group of Jaouen, Biot modified the main antimalarial drugs in use at the time by attaching a ferrocene moiety<sup>54</sup>. Analogues of chloroquine **33**, quinine, mefloquine, artemisinin and atovoquine were synthesised. The chloroquine analogue, ferroquine **34** was the most promising compound against both chloroquine susceptible and resistant strains of *Plasmodium falciparum*, the most dangerous of the five plasmodium strains responsible for malaria.

The mode of action of ferroquine is thought to differ from that of the parent compound. More than one potential mode of action has been proposed.

The parasite ingests haemoglobin as its primary source of amino acids. Ferroquine is believed to act in part by forming a complex with haematin and inhibit conversion to hemozoin similarly to chloroquine, however it does not accumulate resistance in the same way<sup>55</sup>. Resistance to ferroquine could not be induced in either *in vivo* or *in vitro*<sup>56</sup>. More recently it has been shown that the generation of oxidative damage by the ferrocene moiety also plays a role in its antimalarial activity<sup>57</sup>. Increased levels of the HO• radical were detected in the digestive vacuole of the parasite after treatment with ferroquine. It is believed that alteration of the redox status of the cell causes the breakdown of the membrane and death of the parasite.

Ferroquine finished phase II clinical trials in 2011, at which point clinical testing was discontinued for the drug after a decision to further modify the development strategy of the drug. No safety issues or unexpected activity was noted during these studies<sup>58</sup>.

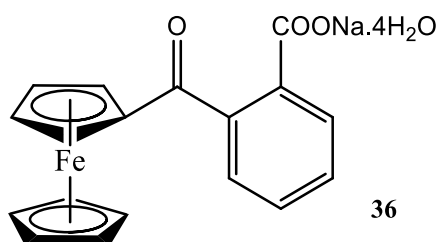
The group of Metzler-Nolte has worked on the synthesis of antimicrobial peptides (AMPs) as antibacterial drugs. In 2005 Chantson *et al.* prepared peptide sequences incorporating a ferrocenyl unit. These sequences varied in length from 3 to 5 amino acids composed of arginine, tryptophan and phenylalanine with glycine as a linker<sup>59</sup>. The chains were prepared by solid phase peptide synthesis (SPPS) and the ferrocenyl moiety was attached at the *N*-terminus. The compounds were tested against *Escherichia coli* (gram negative), *Pseudomonas aeruginosa* (gram negative) and *Staphylococcus aureus* (gram positive) using the minimum inhibitory concentration (MIC) test. However these were not found to be very active with the most active having a value of 57 µg mL<sup>-1</sup> in the *E. coli* and *S. aureus*. In 2006<sup>60</sup> the amino acid sequence was modified to a hexapeptide sequence containing just arginine and tryptophan. While the compounds showed better activity most did not show any particular benefit of the organometallic moiety compared to the organic sequence. Compound **35** however was found to be more active than the organic moiety against *S. aureus*. It had an activity of 7.1 µg mL<sup>-1</sup> and showed greater activity than the pilosulin control.



35

Interestingly El Arbi *et al.* tested ferrocenyl tamoxifen derivatives for their bactericidal and fungicidal activity compared with purely organic analogues<sup>61</sup>. They were tested against the bacteria *P. aeruginosa*, *S. aureus* and the fungus *Candida albicans*. 27 compounds were tested; 20 ferrocenyl derivatives and 7 organic compounds. Doxycyclin was used as a positive control and the compounds were evaluated using the MIC test. The bactericidal and fungicidal activity showed no apparent correlation with the cytotoxicity of the compounds. The organic and ferrocenyl derivatives were found to have similar activities with the most active derivatives bearing two alkylamino side chains.

One of the few ferrocene based compounds to make it to clinical approval is ferrocerone **36**. It was licensed in the USSR for the treatment of iron deficient anaemia<sup>62</sup>.

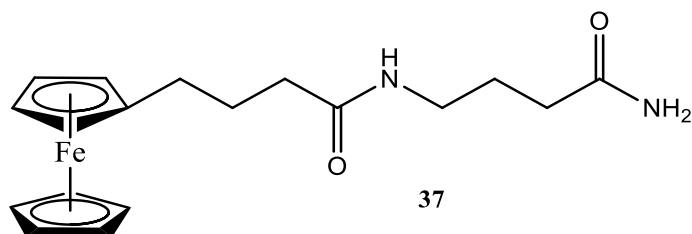


36

### 1.2.2.2 Ferrocene and cancer

The antitumour potential of ferrocene was first noted in 1978 by Fiorina *et al*<sup>63</sup>. A series of ferrocenylpolyamides including *N*-(4-ferrocenylbutyryl)- $\gamma$ -aminobutyramide **37** were tested

for their antitumour activity *in vivo* on murine P-388 lymphocytic leukaemia. Their activity was low but showed that the incorporation of a ferrocene moiety could enhance the antitumour activity of a compound.



#### 1.2.2.2.1 Ferricenium salts

The antitumour activity of ferricenium salts was first reported by Köpf-Maier *et al.* in 1984<sup>64</sup>. They examined the activity of several ferricenium complexes against Erhlich ascites tumours in rats. Ferricenium picrate **38** and ferricenium trichloroacetate **39** obtained the best anti neoplastic activity. These complexes differed from others at the time in that they were water soluble and deviated from the trend for cisplatin analogues.

It was known that ferrocene can convert from the (+2) oxidation state to the ferricenium ion (+3) oxidation state at biological potentials. Osella *et al.* tested several ferrocene species and their corresponding ferricenium salts for their cytotoxicity. He showed that only the ferricenium salts had activity against Erhlich ascites tumour cells. It was shown that this was independent of water solubility or redox potential<sup>65</sup>.

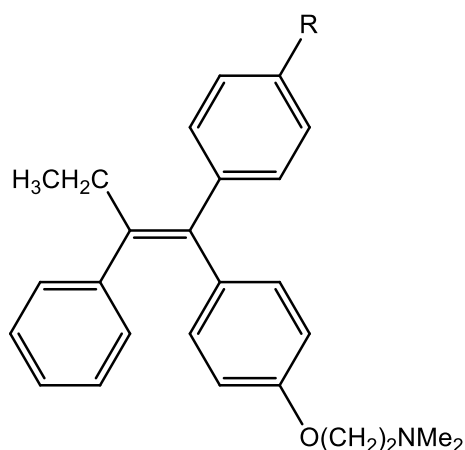
More recently they investigated the activity of five ferricenium complexes in MCF-7 cell lines. Ferricenium tetrafluoroborate, decamethylferricenium tetrafluoroborate **40**, ferricenium carboxylic acid tetrafluoroborate, ferricenium boronic acid tetrafluoroborate and 1,1-dimethyl tetrafluoroborate complexes were prepared and tested. All compounds showed a general cytotoxic effect with the decamethylferricenium salt having the highest IC<sub>50</sub> value of 37  $\mu$ M and the others around 300  $\mu$ M. It was also shown that these compounds caused DNA damage through oxidative stress<sup>66</sup>.

#### 1.2.2.2.2 Organometallic selective estrogen receptor modulators

Breast cancer can be divided into two groups; hormone dependant breast cancers, those which express the estrogen receptor [ER $\alpha$ (+)] and hormone independant cancers, those which do not express [ER $\alpha$ (-)]. About two thirds are [ER $\alpha$ (+)] and are treatable using selective estrogen receptor modulators (SERMs). SERMs bind to the estrogen receptor and may act as

estrogen agonists or antagonists. Tamoxifen **41** and its active metabolite, hydroxytamoxifen **42**, are the most common drugs in this class which are used for the treatment of [ER $\alpha$ (+)] tumours. A second estrogen receptor ER $\beta$  has also been discovered. Malignant breast tissue may express ER $\alpha$ , ER $\alpha$  and ER $\beta$ , no ER and in rare cases ER $\beta$  alone. The ligand binding domain of both receptors shows some similarity and SERMS may bind equally well to both, however patients diagnosed with ER $\alpha$ (+) breast cancer have a better prognosis than those that have ER $\alpha$ (-) suggesting that the receptors do not share the same mechanism of action.

Tamoxifen acts as an antagonist of the estrogen receptor in breast cancer tissue. It was originally designed as a contraceptive agent by Imperial Chemical Industries. Ironically, claims in the original patent that it may be useful as a breast cancer treatment, had to be removed as they were considered to be 'fantastical and lacking evidence'<sup>67</sup>. The compound failed in clinical trials as a contraceptive, however, during the 1970's research began investigating its use in breast cancer treatment.

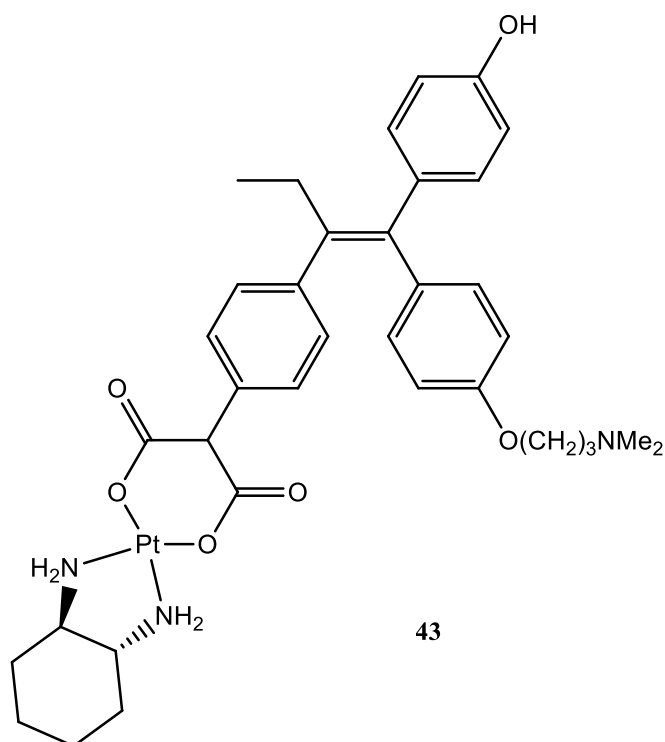


**41** R=H  
**42** R=OH

To solve problems associated with tamoxifen's resistance, side effects and narrow spectrum of activity, the group of Gerard Jaouen modified the structure of tamoxifen by attaching an organometallic moiety. It was hoped that these organometallic derivatives could combine the estrogenic activity with the cytotoxic activity of several known compounds. They wished to develop a targeted therapy using tamoxifen as a vector to deliver a cytotoxic agent directly to the area of interest. The group tried several different approaches using multiple organometallic compounds.

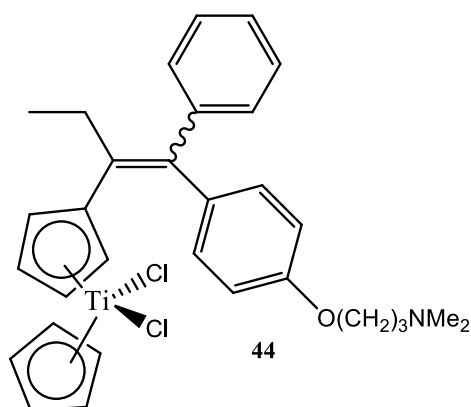


Given the success of cisplatin, it was initially proposed that a tamoxifen derivative of a platinum agent may be useful in targeting breast cancer. They achieved this by attaching a malonate derivative of oxaliplatin to tamoxifen in the hope of transporting a cisplatin analogue directly to the estrogen receptor<sup>68</sup>. Compound **43** was shown to have an IC<sub>50</sub> value of 4.0 μM in MCF-7 cells compared with the literature value of 7.4 μM for oxaliplatin and a value of 6.3 μM for the unvectorised malonate compound<sup>69</sup>. The antiproliferative effect was however attributed to the cytotoxicity of the platinum and at the concentrations tested it was not felt that they brought any benefit to the SERMS. It was proposed that the Pt-N coordination bond was too weak, the metal was unable to react with its target as hydrolysis occurred too quickly and the compound was too bulky. Results in mammary tumours were poor and thus they turned to looking at other potential cytotoxic organometallics to attach to SERMS. The group prepared derivatives incorporating Ti, Ru, Re, CO, as well as osmium clusters and manganese<sup>70, 71, 72, 73</sup>.



A series of ruthenocene analogues of tamoxifen was prepared. These displayed a very high relative binding affinity (RBA) for the estrogen receptor and had an antiproliferative effect similar to tamoxifen in MCF-7 cells, however they had no effect on MDA-MB-231. Therefore it was determined that they act in an antiestrogenic fashion with the organometallic moiety imparting no particular advantage.

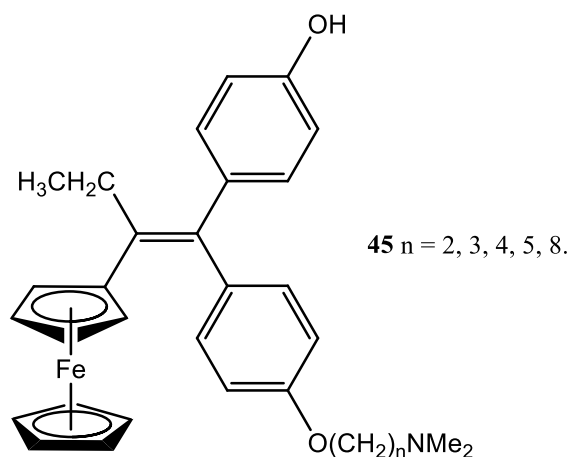
The work of Köpf-Maier on dichlorotitanocene ((Cp)<sub>2</sub>TiCl<sub>2</sub>) showed that the molecule had cytotoxic properties against various tumour types *in vivo* and *in vitro*. As titanocene was shown to have activity against Ehrlich's ascite tumour Anne Vessières *et al.* prepared a tamoxifen derivative incorporating the dichlorotitanocene moiety **44**<sup>74</sup>. The cytotoxicity of the compound was studied in MCF-7 cells. Results showed that **44** acts as an estrogen instead of an antiestrogen as expected due to the presence of the dimethylamino chain thought to be responsible for the activity of tamoxifen.



Perhaps the most successful and well known works of Jaouen are the ferrocifens **45**. The group of Jaouen first prepared ferrocenyl hydroxytamoxifen derivatives in 1996<sup>75</sup>. They decided to attach an antitumour agent and hydroxytamoxifen was the active metabolite of tamoxifen. These compounds are typically prepared by McMurry coupling of the ferrocenyl ketone<sup>76</sup>, which results in a mixture of 50 % (*E*) and (*Z*) isomers. These isomers were shown to rapidly interconvert in protic solutions, which is also true for Tamoxifen and other stilbene based compounds. As this is typical of biological conditions most studies were conducted using a mixture of (*E*) and (*Z*) isomers.

Studies showed a good relative binding affinity (RBA) for the estradiol receptor and IC<sub>50</sub> values of 4.9 μM and 3.4 μM in MCF-7 cells for (*E*) and (*Z*) isomers of hydroxyferrocifen (n=2) compared with a value of 6.4 μM for tamoxifen under the same conditions. However it was found that *in vivo* hydroxytamoxifen caused a large increase in tumour volume of over 50 % in atymic nude mice xenografted with T47D breast cancer cells.

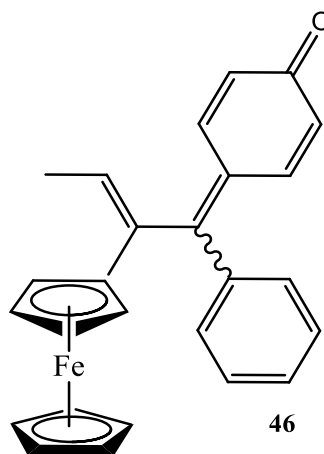
The structure of the ligand binding domain (LBD) of the estrogen receptor requires a basic or polar side chain to deform the receptor to an open conformation and inhibit activation. It was believed that the more bulky ferrocene moiety stopped the compound from deforming the ER to its open conformation. It was proposed that increasing the side chain by 1 or 2 carbons could reverse this<sup>77</sup>.



A series of hydroxyferrocifens was prepared<sup>78</sup> keeping the hydroxyl group and the dimethyl amino side chain that are necessary for binding to the LBD of the ER and thus antiestrogenic activity, while varying carbon chain length with  $n = 2, 3, 4, 5$  and  $8$ <sup>79</sup>. All of the compounds were shown to have antiestrogenic effects but that activity was dependant on chain length. Where  $n = 2$  and  $8$ , RBA values lower than hydroxytamoxifen were observed. For  $n = 3-5$  values were similar or slightly better in ER(+) MCF-7 cells. Cytotoxicity of the compounds was established using a DNA damage detection (3D) test, showing that they have a dual activity, as acting as an antiestrogen and a cytotoxic agent<sup>80</sup> When these derivatives were also tested on ER(-) MDA-MB-231 cells they were found to have a hormone independant mechanism of action<sup>81</sup>. They were also most effective when  $n = 3-5$ . Tamoxifen has no effect on ER(-) cell lines. This showed ferrocifens to be both useful against ER(+) and ER(-) cell lines.

It was initially thought that the ferrocifens induced DNA damage through oxidative stress however fluorescence activated cell sorting (FACS) analysis showed that hydroxyferrocifen produces negligible DNA damage compared to the parent compound hydroxytamoxifen<sup>82</sup>. Further work on the mode of action was carried out using cyclic voltammetry with the addition of pyridine as a base<sup>83</sup>. A reaction mechanism which proceeded via a quinone methide was proposed. The ferrocene is initially electrochemically oxidised. This imparts partial positive to the hydroxyl group which acidifies the proton and allows it to be abstracted

by the pyridine resulting in a phenoxy species with the radical on the alpha carbon to the ferrocene. It is then oxidised a second time to give the quinone methide **46**. The drug will only be activated in the presence of basic species such as DNA nucleobases or peptides, where it can cause cellular damage leading to cell death.



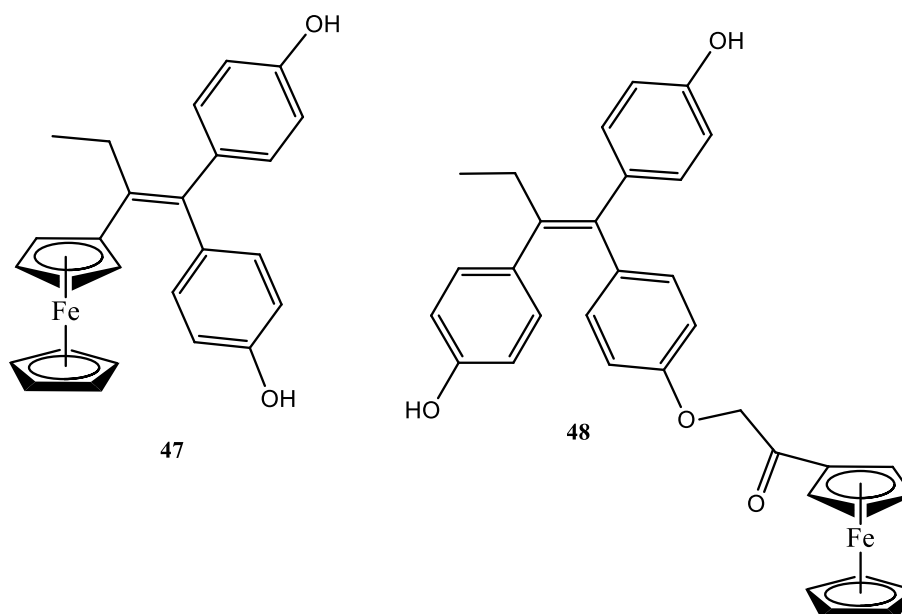
Oxidation to a reactive quinone methide has been shown to be the mechanistic basis of many phenolic anticancer drugs including tamoxifen. Cell damaging pathways for tamoxifen include metabolism to o-quinones, quinone methides and carbocations<sup>84</sup>. These quinone methides may form adducts with DNA, glutathione (GSH) or proteins<sup>85</sup>.

The group moved to further establish this mechanism showing that the proposed quinone methides are indeed formed upon oxidative metabolism in rat liver microsomes<sup>86</sup>. Four ferrocifens were tested and quinone methides were isolated and characterised by high performance liquid chromatography-mass spectrometry (HPLC-MS) as the major products of metabolism.

In further structure activity relationship (SAR) studies the group prepared a series of derivatives, the most active of which was **47** with an  $IC_{50}$  value of 0.44  $\mu$ M in MDA-MB-231 cells. From this study it was determined that the ferrocene moiety is necessary for activity but not sufficient to elicit a response alone. The phenyl group must be oriented *trans* to the ferrocene and the two phenyl groups must be attached to the same carbon atom. The position of the hydroxyl group was important with the *para* group preferred over the *meta*. No proton coupled intramolecular electron transfer occurred in the case of the *meta*. It was also noted that one ferrocene moiety was more effective than two<sup>87</sup>. Replacement of the phenol group with an alanine or acetanilide further increased the cytotoxic activity<sup>88</sup>.

These compounds have increased lipophilicity compared to the purely organic drug tamoxifen due to the presence of the ferrocene moiety. This makes it easier for them to penetrate the cell membrane, however, they have poor bioavailability due to the high hydrophobicity caused by the phenyl rings. Thus it was necessary to investigate methods of formulation to aid drug delivery. The group looked at several formulation strategies. Swollen micelles were found to be ineffective as they had poor uptake by the cytoplasm and no biological activity. Among the strategies developed to improve solubility was the formulation of ferrocenyl tamoxifen adducts with cyclodextrins<sup>89, 90</sup>. It was found that compounds with hydroxyl groups on the phenyl ring formed ferrocifen-cyclodextrin complexes that are soluble in polar solvents. On addition of base dissociation of the ferrocene from the cyclodextrin occurs allowing conversion to the ferricenium cation. It was found that cytotoxicity to MDA-MB-231 cells was unaffected by the cyclodextrin complex making it a viable method for increasing water solubility for use *in vivo*.

Two promising potential drug candidates, Fc-diOH **47** and DFO **48** showed good activity in both MCF-7 and MDA-MB-231 breast cancer cells *in vitro* but were poorly soluble in biological fluids. The group prepared two types of stealth nanoparticles; PEG/PLA nanospheres and nanocapsules to address the problem of formulation<sup>91</sup>. Stealth nanocapsules are designed to evade the immune response, increasing the circulation time. This gave the slow release of both compounds. They were found to arrest the cell cycle in S-phase and induce apoptosis. Given their small size they have the ability to undergo endocytosis and protect the drug from hydrolysis and oxidation.



Fc-di-OH loaded lipid nanocapsules between 20-100 nm were found to be effective on 9L-glioma cells, with an IC<sub>50</sub> value of 0.6 μM. They also showed low toxicity when tested on normal cells. Using this strategy the group were able to carry out their first *in vivo* studies in rats showing a significant reduction in both tumour mass and volume evolution<sup>92</sup>.

The group also prepared a series of pro-drugs of Fc-diOH using either acetyl group or palmitate<sup>93</sup>. These LNC prodrugs have to be activated *in situ* by enzymatic hydrolysis. The acetyl pro-drug had similar effects to that of the parent, whereas the palmitate showed a loss of activity.

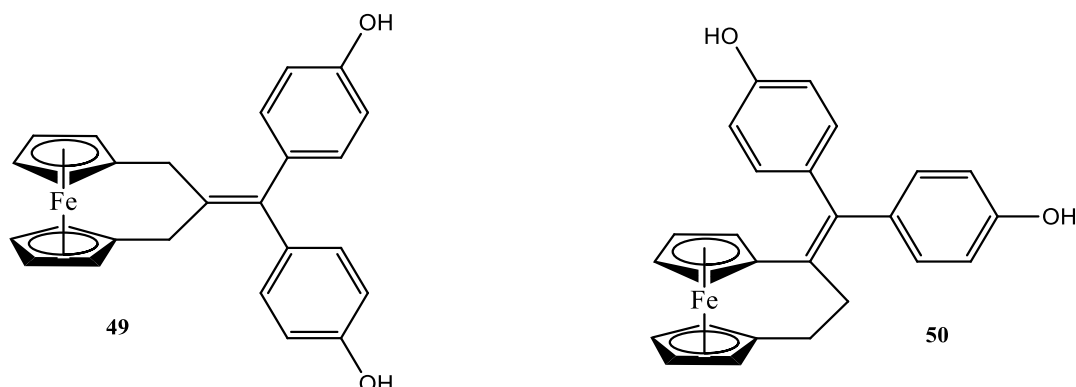
Fc-diOH LNC were tested in intracerebral 9L glioma *in vitro* and *in vivo* in conjunction with external radiotherapy. It was shown that chemotherapy followed by radiotherapy had better results than the reverse which was attributed to a radiosensitising effect. It was shown that they acted in synergy and not only additive effects were observed<sup>94</sup>.

In another study LNCs were incorporated into MIAMI mesenchymal cells. It was found that they did not cause cell death and maintained both their stem cell properties and migration capacity. These were shown to have a cytotoxic effect both *in vitro* and *in vivo* after intertumoural injection in a heterotopic U87MG glioma model in nude mice<sup>95</sup>.

More recently they used ferrocenyl hydroxytamoxifen LNCs *in vivo* in mice bearing xenografted triple negative breast cancer tumours. Both stealth and conventional nanocapsules were prepared and tested *in vitro* with IC<sub>50</sub> values for both types approximately 2 μM. *In vivo* a significant reduction in tumour growth was observed with a 36 % reduction after 38 days<sup>96</sup>.

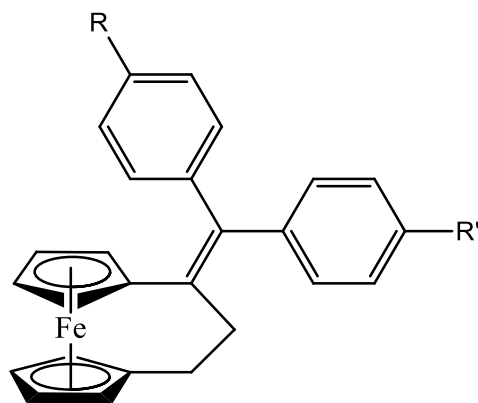
The most active derivatives to date produced by the Jaouen group are the ferrocenophanes. These contain a 3 carbon bridge joining the cyclopentadiene rings. Based on the previous work which had shown a great effect with modification of the phenol rings, derivatives were prepared maintaining the bis substituted phenol rings and incorporating a 3 ferrocenophane structure<sup>97</sup>. These derivatives were estimated to have IC<sub>50</sub> values of approximately 1 and 4 μM in MCF-7 cells and 0.09 and 0.96 μM in the MDA-MB-231 cells. When the olefin was moved from the 2 position **50** to the 1 position **49** on the bridge, activity decreased by an order of magnitude. However, they showed mixed estrogenic and antiestrogenic activity and

were thus determined to be more suitable for hormone independent cancers. These results were significantly lower than those of the ferrociphenol lead compound.



A second series of analogues was prepared using aniline and acetylene ferrocenophane and ferrocifen derivatives. In each case, the ferrocenophane was shown to be more active than the ferrocene derivative<sup>98</sup>.

Given that the bis-substituted phenol compound showed twice the activity of the mono substituted derivative in both the ferrocene and ferrocenophane series, with a value of 0.09  $\mu\text{M}$  compared to 0.47  $\mu\text{M}$  for ferrocenophane and 0.65  $\mu\text{M}$  to 1.1  $\mu\text{M}$  for ferrocene, a series of compounds with either mixed or identical bis substitution with protic groups on both phenyl rings was prepared **51**<sup>99</sup>. As was expected the bis-substituted compounds were found to be more active with  $\text{IC}_{50}$ s in the nanomolar range in the MDA-MB-231 cells (0.05-0.92  $\mu\text{M}$ ) and similar when tested in PC-3 prostate cells (0.02-2.43  $\mu\text{M}$ ). The exception to this was the case of the derivative with two amide groups, which has  $\text{IC}_{50}$  values of 5.64  $\mu\text{M}$  and 12.45  $\mu\text{M}$  in the MDA-MB-231 and PC-3 cells respectively. This showed that *para* substitution of both rings with protic groups and the 3-ferrocenophane moiety give rise to the most active derivatives produced by the group.



- a. R=OH R'=H
- b. R=NH<sub>2</sub> R'=H
- c. R=NHAc R'=H
- d. R=R'=OH
- e. R=NH<sub>2</sub> R'=OH
- f. R=R'=NHAc
- g. R=NHAc R'=OH
- h. R=R'=NH<sub>2</sub>

51

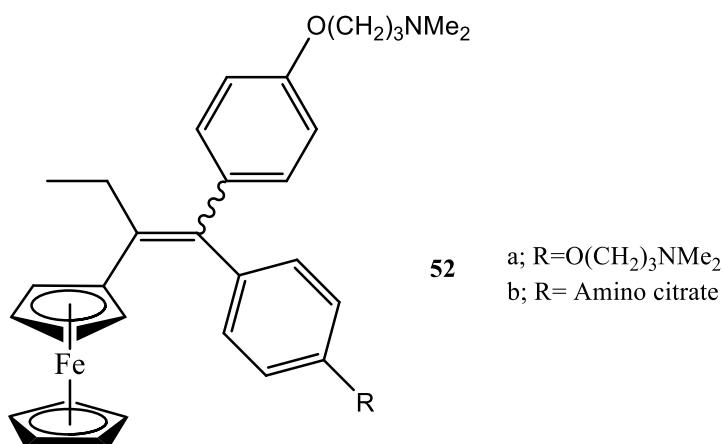
Given that the dianiline species (**51h**) had been their most active derivative to date a further series of dianilines was prepared varying the length of the carbon chain attached<sup>100</sup>. It was found that for increasing number of hydrocarbons the activity of the compound on MDA-MB-21 cells decreased. It was also shown that the purely organic moiety was less active than the ferrocenophane derivative but more active than the ferrocenyl derivative. For tetra methylated aniline derivatives the activity was lost, showing that the protic groups are required for activity. It is proposed that these groups can be oxidised to an imine methide in a similar fashion to the phenol groups.

Pigeon *et al.* prepared derivatives of tamoxifen possessing two amino alkyl side chains of the form O(CH<sub>2</sub>)<sub>3</sub>NMe<sub>2</sub> based on both the ferrocenophane motif and the open conformation<sup>101</sup>. Despite having no protic groups these analogues had both a strong affinity for the estrogen receptor and excellent antiproliferative activity on both hormone dependant and independent cell lines. These are believed to operate via a different mechanism to the previous derivatives as they cannot form either quinone methides or quinone imines. The organic analogues have a similar activity to the ferrocenyl derivatives in these compounds.

The activity of 27 of the organometallics SERMS derivatives were investigated on a panel of other human cancer cell lines. Ferrocenyl substituted tamoxifens and stilbene analogues were tested on SF-295 (human glioblastoma), HCT-8 (human colon cancer) MDA-MB-435 (human melanoma) HL-60 (human promylocytic leukaemia) cells and evaluated for antiproliferative activity, ROS generation and haemolytic activity<sup>102</sup>. These compounds were found to be least active in the melanoma cell line with low micromolar activities. They were most active in the HL-60 cell line with an average IC<sub>50</sub> of 2 μM.



Previously studied compound **52a** and its citrate salt **52b** were found to be most active in all cell lines. The di substituted diaminoalkyl compound had been previously shown to have good activity on MDB-MA231 cells with an IC<sub>50</sub> value of 0.45 μM as well as showing good antibacterial and antifungal activity<sup>61</sup>.



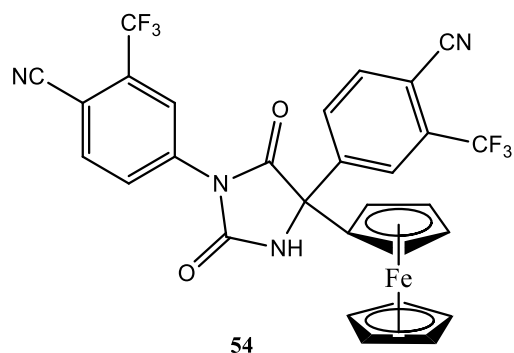
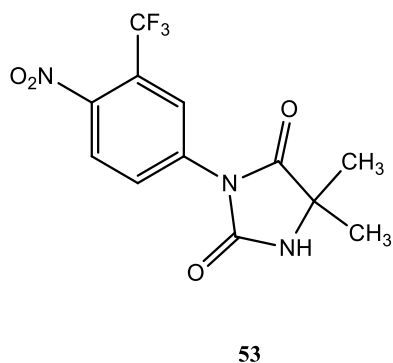
The compounds, bearing no protic groups cannot form a quinone methide species. The ROS studies showed no correlation of ROS generation with antiproliferative activity. Most compounds showed no ROS generation in the HL-60 cell line indicating that they operate via a mechanism unrelated to oxidative stress. To this effect the haemolytic activity of the compounds was investigated. Six of the compounds, including **52** and tamoxifen showed some haemolytic activity suggesting that these compounds may generate cell membrane damage. Compounds with high antiproliferative activity and low haemolytic activity were considered to present interesting opportunities for further development.

Besides their activity against breast cancer the ferrocifens have also shown some activity against melanoma<sup>103</sup>. Ferrocifen and ferrociphenol were tested for activity against primary WM35, WM793 and metastatic WM9 melanoma cells as well as melanocytes. They were found to be selective for the melanoma cells over melanocytes when tested *in vitro* on hair follicles they showed ejection of the hair shaft from the follicle suggesting hair loss may be a possible side effect if used as a chemotherapeutic. These were also tested on BR95 and MM98 mesothelioma cells where both compounds were found to be more effective at stopping cell proliferation than cisplatin.

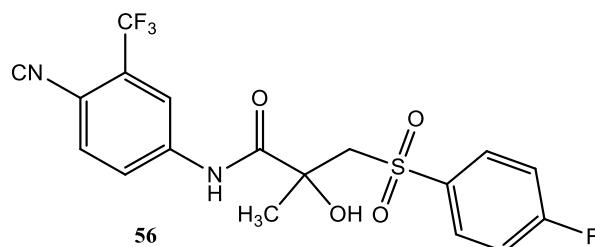
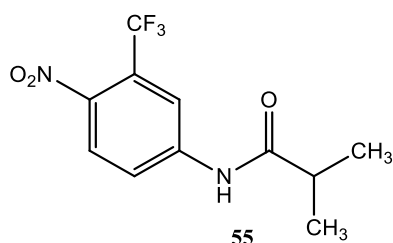
### 1.2.2.2.3 Other ferrocenyl compounds with anticancer activity

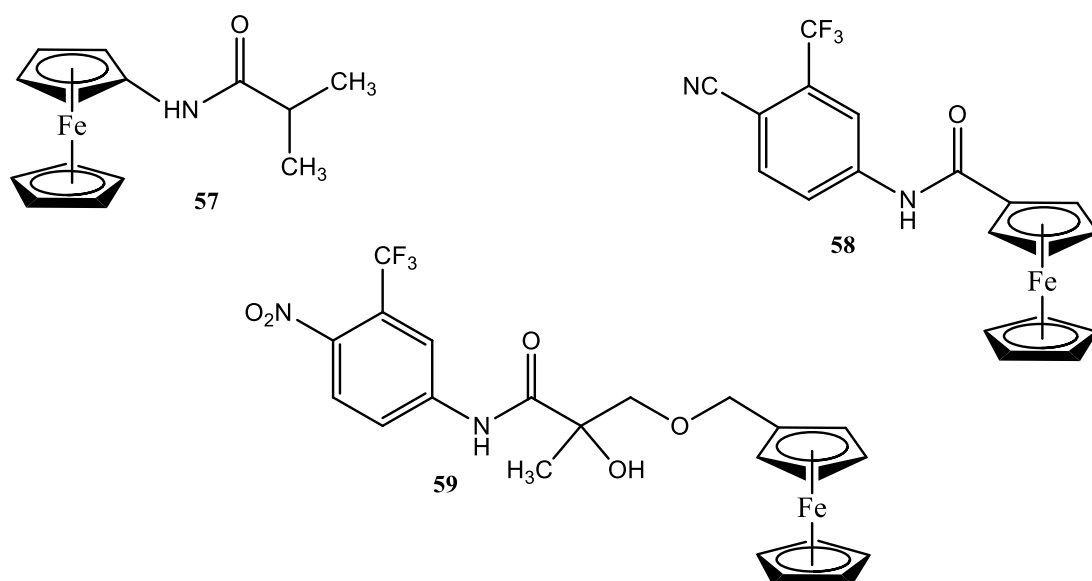
Apart from the work carried out on SERMS the group of Jaouen has also investigated derivatising several other types of bioactive compounds with ferrocene. In 2008 they

prepared derivatives of the nonsteroidal antiandrogen nilutamide **53**<sup>104</sup>. These were tested against prostate cancer cells. Those substituted at the N1 position of the hydantoin ring showed only weak antiproliferative effects while those substituted at the C5 position showed good cytotoxic activity however this could not be attributed to the organometallic moiety as the organic analogue had similar activity on replacement of the ferrocene moiety.



Derivatives of flutamide **55** and bicalcutamide **56** were synthesised<sup>105</sup>. Compounds had a low binding affinity for the androgen receptor and activity was attributed to cytotoxicity rather than hormonal effects. The most active bicalcutamide derivative **59** had an  $IC_{50}$  of 17  $\mu$ M in the PC-3 cells but the flutamide derivatives **57** and **58** showed almost no activity against hormone dependant LNCaP or hormone independant PC-3 prostate cancer cells.





A series of derivatives based on flavonoid structures was synthesised<sup>106,107</sup>. These biological compounds are credited with numerous health benefits which have been attributed to their antioxidant properties. The B ring of the flavonoid was replaced with the ferrocenyl moiety. Aurones, chalcones, flavones and flavonols were prepared and tested *in vitro* against B16 murine melanoma cells and endothelial cells. The compounds displayed only modest cytotoxic activity; the aurone derivatives having the best activity with IC<sub>50</sub> values of 12-18  $\mu$ M. They showed some antivasular activity though these did not seem to correlate.

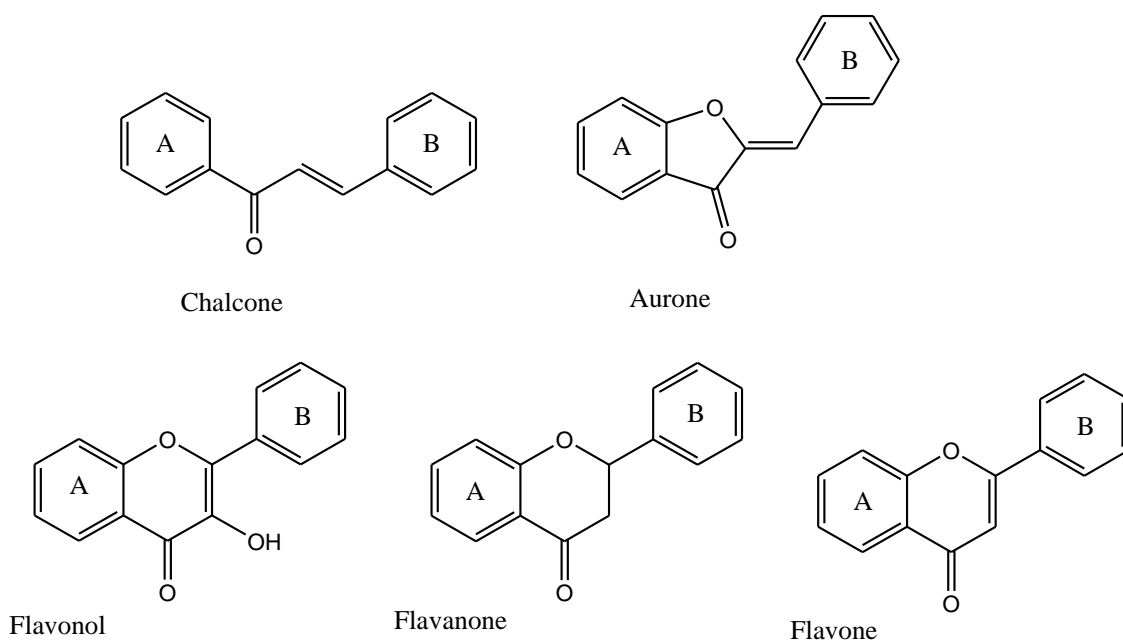
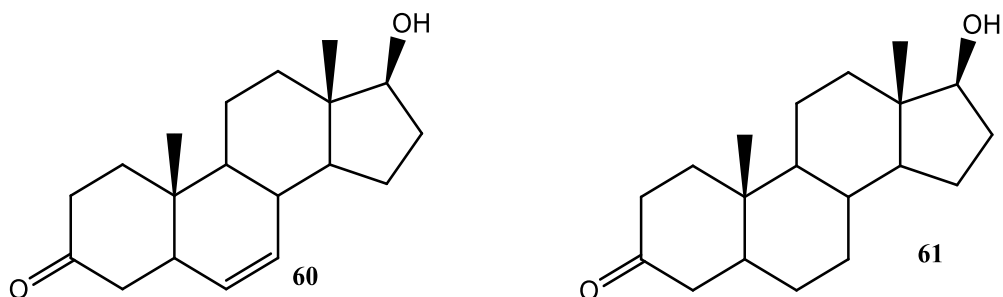
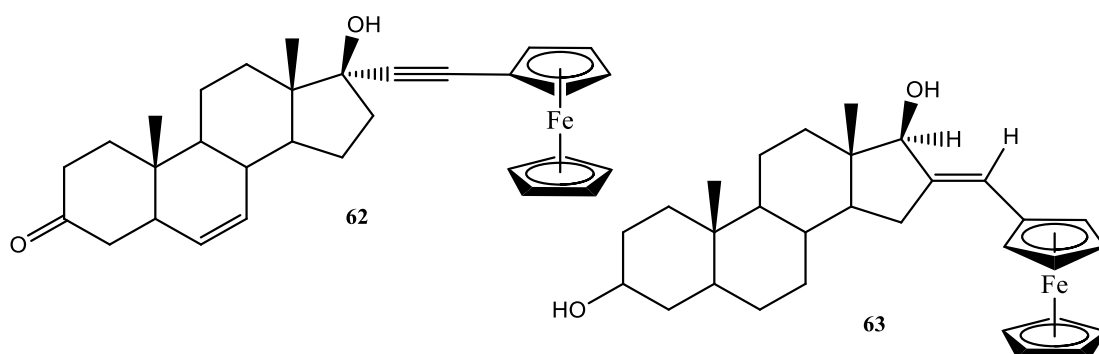


**Figure 1.11:** Structures of flavonoids.



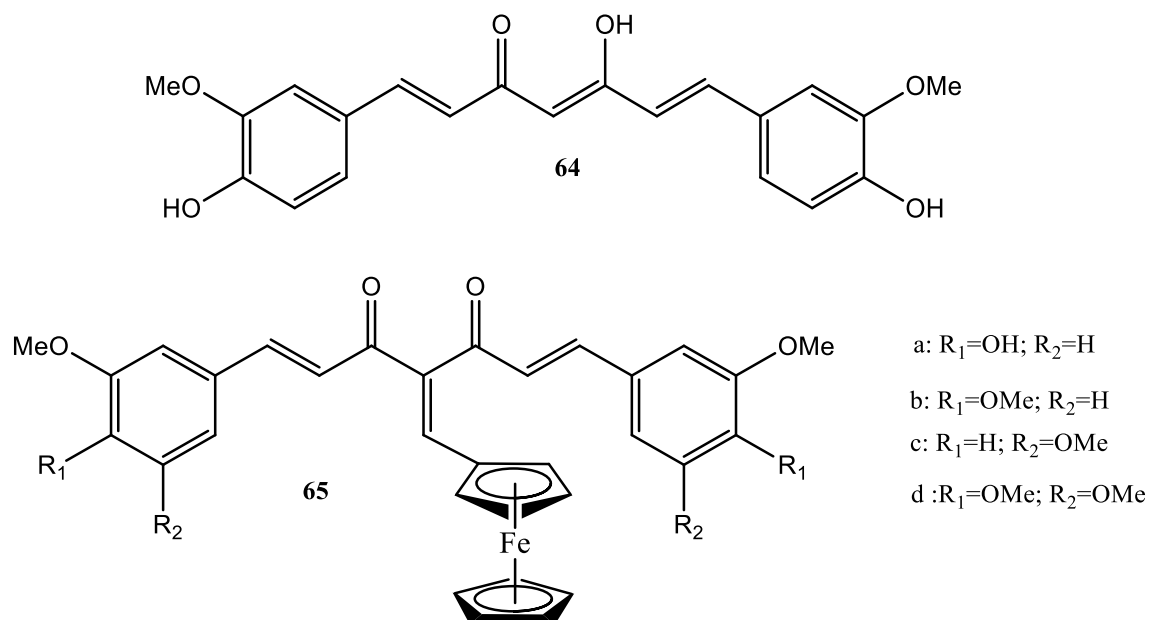
Given the success the group achieved targeting the estrogen receptor with the ferrocifens and ferrocophanes against breast cancer, the group undertook a similar approach with derivatives of the steroidal androgens testosterone **60** and dihydrotestosterone **61** in prostate cancer cells<sup>108</sup>. Several ferrocenyl ethynyl testosterone well as ethynyl ferrocenyl and vinyl ferrocenyl androstanes were prepared. Sandwich and semi-sandwich complexes of chromium, manganese and rhenium were also prepared, however the ferrocenyl derivatives showed the best activity.



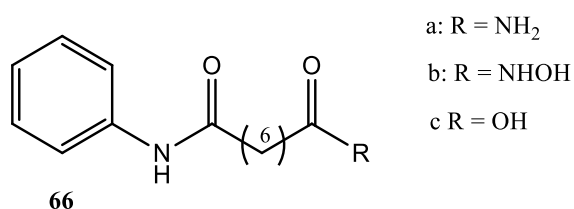
A C17 ethynyl ferrocenyl derivative of testosterone **62** and the corresponding dihydrotestosterone showed  $IC_{50}$  values of 4.7 and 8.3  $\mu M$  respectively in PC-3 prostate cancer cells. While a C17  $\beta$  androstane diol showed an  $IC_{50}$  value of 5.5  $\mu M$  and the C16 derivative with a ferrocenyl vinyl unit **63** showed and  $IC_{50}$  of 12.2  $\mu M$ .

Curcumin **64** is a naturally occurring antioxidant responsible for the yellow colour of turmeric. Several ferrocenyl curcuminoid **65a-d** derivatives were prepared using either a propanone, methylene or ethanone spacer to attach ferrocene via the central carbon atom of curcumin<sup>109</sup>. The substitution pattern of the ring was also varied. The compounds were tested in B16 murine melanoma cells. Curcumin has an  $IC_{50}$  value of 8.5  $\mu M$  in this cell line. The ferrocenyl derivatives with a methylene side chain were found to be most cytotoxic with  $IC_{50}$  values of 2.2 to 7.1  $\mu M$ . The compounds also showed some selectivity for cancer cells

with higher IC<sub>50</sub> values in normal cells lines. These compounds were also tested for their tubulin binding ability and antivasular activity. Ferrocenyl compounds with a propanone spacer group were found to have the best tubulin polymerisation inhibition and antivasular properties. It was noted that the derivatives with 3, 4-dimethoxy substitution pattern were most active.



Some of the most recent work undertaken by the group was the addition of suberamides **66** such as suberoylanilide hydroxamic acid (SAHA) **a** and *N*<sup>1</sup>-phenylsuberamide (PSA) **b** and 8-oxo-8-(phenylamino)octanoic acid (OPOA) **c** to the ferrocifen<sup>110</sup> and ferrocenophane<sup>111</sup> structures, replacing the dimethylaminoalkoxy side chain. SAHA is a histone deacetylase inhibitor (HDACi) and is used in the treatment of cutaneous T cell lymphoma. It inhibits transcription by adopting a closed conformation with DNA which transcription factors cannot access.

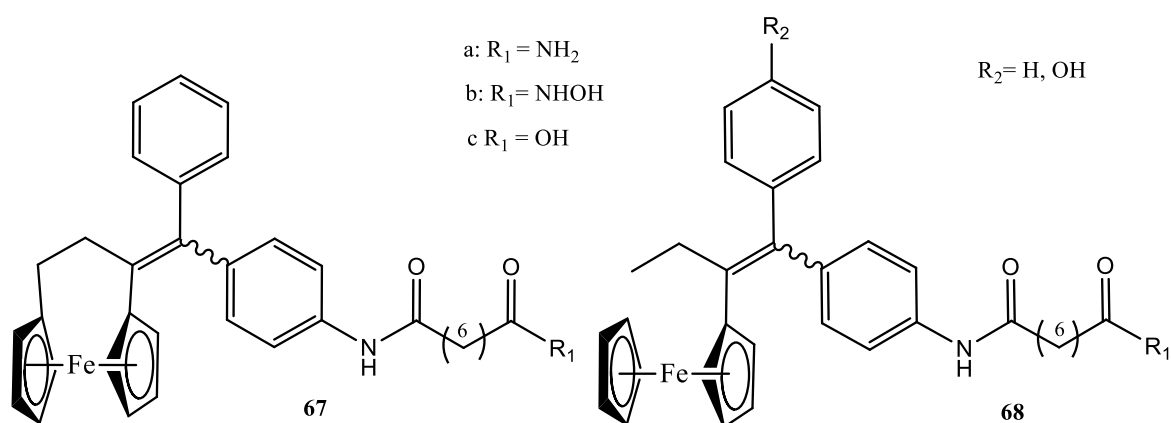


These new compounds were tested in MDA-MB-21 cells and MCF-7 cell lines. It was found that the antiproliferative activity of the compounds was not due to an affinity for the estrogen receptor or their ability to inhibit histone deacetylase activity.

In the MDA-MB-21 cells the  $IC_{50}$  values ranged from 0.5 to 0.9  $\mu\text{M}$  compared with 3.6  $\mu\text{M}$  for SAHA alone. The most active derivative was the ferrocenyl PSA derivative. The ferrocenyl derivatives were shown to have a greater activity than the purely organic tamoxifen derivatives or the suberamides alone.

In the MCF-7 cell line values ranged from 0.87  $\mu\text{M}$  for the ferrocenophanic SAHA **67a** to 2.0  $\mu\text{M}$ , however SAHA alone was quite active with a value of 1  $\mu\text{M}$ . Still these represent the most active derivatives synthesised by the group to date. OPOA derivatives were prepared but had low activity.

Phenolic derivatives analogous to hydroxytamoxifen were also synthesised **68**<sup>112</sup>. These were found to have  $IC_{50}$  values ranging from 1.3 to 4.5  $\mu\text{M}$  in MDA-MB-231 cells and 1.5 to 6.6  $\mu\text{M}$  in MCF-7 cells. Compared to organic derivatives with a phenol ring the ferrocenyl derivatives were again shown to be more active illustrating that the organometallic derivative contributed to the activity. The OPOA derivatives in this instance were found to be more active with the phenolic group.

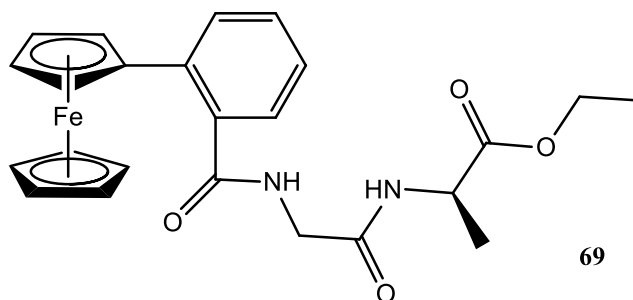


#### 1.2.2.2.4 Ferrocenyl peptide conjugates

*N*-ferrocenyl derivatives were prepared by Sheehy *et al*<sup>113</sup>. The ferrocenyl moiety was coupled directly to amino acid esters with an initial goal of exploring the potential of ferrocenyl peptide conjugates as novel sensor compounds, peptide mimetics or unnatural

drugs<sup>114</sup>. A benzene ring was added as a conjugated linker and *N-para*<sup>115</sup>, *ortho*<sup>116</sup> and *meta*<sup>117</sup>-ferrocenyl benzoyl amino acid esters were synthesised, also initially as potential anion sensing agents, however an *in vitro* screen showed some cytotoxicity. The *N-ortho* ferrocenyl benzoyl glycine ethyl ester was found to have an IC<sub>50</sub> of 48 μM against H1299 lung cancer cells<sup>118</sup>. *N-ortho*<sup>119</sup>, *meta*<sup>120</sup> and *para*<sup>121</sup>-ferrocenyl benzoyl dipeptide esters were synthesised and evaluated.

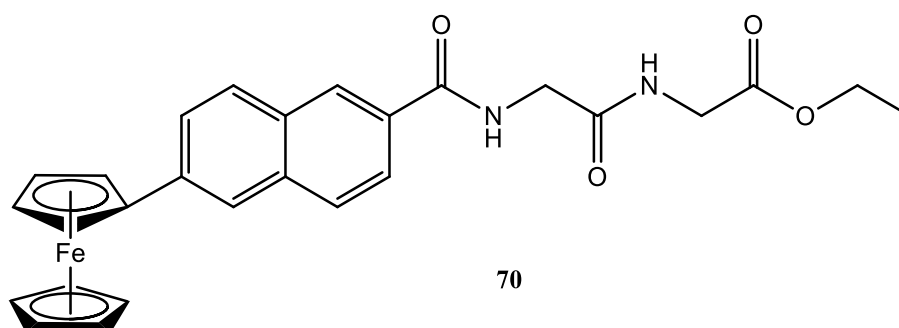
The *N*-(*ortho*-(ferrocenyl)benzoyl)-glycine-L-alanine ethyl ester derivative **69** was found to have a strong antiproliferative effect in the H1299 cell line with an IC<sub>50</sub> value of 5.3 μM. The *meta* and *para* had similar IC<sub>50</sub> values of 4.0 and 6.6 μM respectively<sup>122</sup>. The dipeptide chain was subsequently extended to tripeptide and tetrapeptide chains, however, this led to a significant decrease in antiproliferative activity, showing that the dipeptide chain is required for activity<sup>123</sup>.



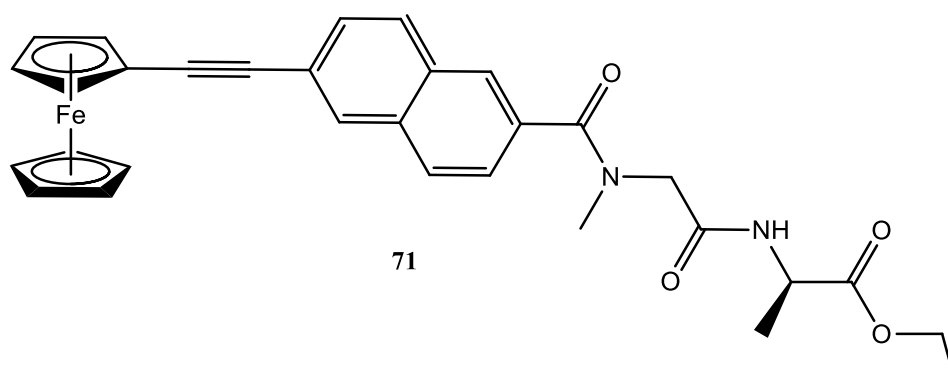
Mooney *et al.* subsequently replaced the benzoyl linker with a naphthoyl linker, generating a series of *N*-(3-ferrocenyl-2-naphthoyl) dipeptide ethyl and *N*-(6-ferrocenyl-2-naphthoyl) dipeptide ethyl esters<sup>124</sup>. The *N*-ferrocenyl-naphthoyl derivatives were found to have IC<sub>50</sub> values in the H1299 cell line ranging from 7.8 μM to 1.3 μM all of which were more active than their benzoyl analogues. The most active of these was *N*-(6-ferrocenyl-2-naphthoyl)-glycine-L-alanine ethyl ester with an IC<sub>50</sub> value of 1.3 ± 0.1 μM which is lower than that of the clinically employed anticancer drug cisplatin (IC<sub>50</sub> 1.5 ± 0.1 μM in H1299 cells).

Further work utilising the naphthoyl spacer involved the synthesis of *N*-(ferrocenyl)naphthoyl amino acid esters. These were evaluated in both H1299 lung cancer cells and in Sk-Mel-28 malignant melanoma cell lines<sup>125</sup>. These compounds showed strong antiproliferative effects in the H1299 cells, while the Sk-Mel-28 cells were slightly more resistant. The most active of these compounds was found to be the *N*-(6-ferrocenyl-2-naphthoyl)-γ-aminobutyric acid ethyl ester with an IC<sub>50</sub> value of 0.62 ± 0.07 μM in the H1299 cell line and 1.41 ± 0.04 μM in the Sk-Mel-28 cell line.

Further structure activity relationship studies on the *N*-(6-ferrocenyl-2-naphthoyl) dipeptide ethyl esters investigated the effect on antiproliferative effect of incorporating either  $\alpha$ -amino acids with branched allyl or aromatic side chains into the dipeptide chain<sup>126</sup>. Thus a series of dipeptide analogues were prepared using either glycine or L-alanine as the first amino acid residue and glycine, L-alanine, L-leucine or L-phenylalanine as the second amino acid residue. The D-alanine analogue was also synthesised and found to be four times more active in the H1299 cell line than the L-alanine with an  $IC_{50}$  value of  $0.33 \pm 0.02 \mu\text{M}$ . The most active derivative however, was determined to be *N*-(6-ferrocenyl-2-naphthoyl)-glycine-glycine ethyl ester **70** with an  $IC_{50}$  value of  $1.10 \pm 0.13 \mu\text{M}$  in the Sk-Mel-28 cell line and  $0.13 \pm 0.02 \mu\text{M}$  in the H1299 cell line, more than 10 times that of cisplatin.

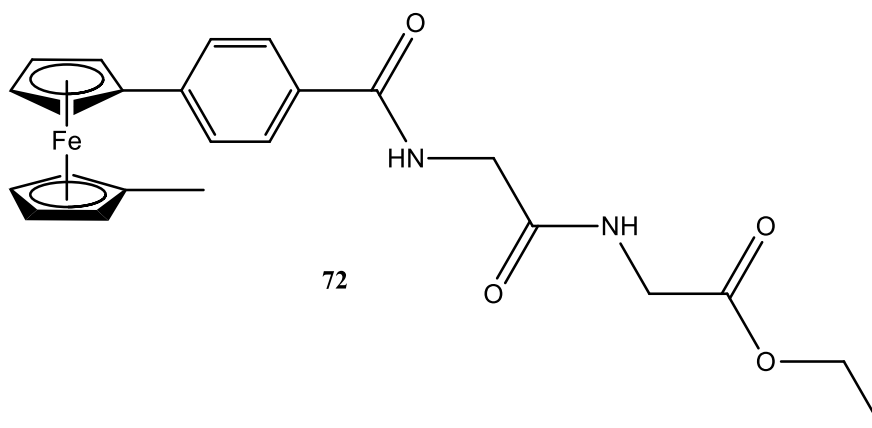


Given that the redox activity of ferrocene has been implicated in its mode of action, modification of the structure to generate compounds which could potentially lower the oxidation potential of the ferrocenyl moiety has been investigated. One potential route to compounds with a lower oxidation potential is the incorporation of an ethynyl spacer. It was shown that increasing conjugation by the introduction of a naphthalene moiety in place of a benzene increased activity. Thus a series of derivatives was prepared further extending the conjugation of the molecule with an ethynyl spacer placed between the redox active core and the naphthalene ring<sup>127</sup>.





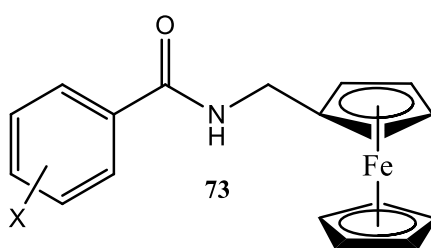
*N*-{6-(ferrocenyl) ethynyl-2-naphthoyl} amino acid and dipeptide ethyl esters were synthesised using GABA(OEt), Gly-Gly(OEt), Gly-Ala(OEt), Sar-Gly(OEt), Pro-Gly(OEt), Sar-Ala(OEt) and Pro-Ala(OEt). Compounds were evaluated in H1299 NSCLC cells. They had IC<sub>50</sub>'s ranging from 3.2 μM - 7.2 μM. The oxidation potential was found to be higher than the *N*-(6-ferrocenyl-2-naphthoyl) dipeptide derivatives but lower than the ferrocenyl dipeptide derivatives. The most active compound was *N*-{6-(ferrocenyl) ethynyl-2-naphthoyl}-sarcosine alanine ethyl ester **71**, which also had the lowest oxidation potential of the series, however the incorporation of an ethynyl spacer did not result in compounds with lower oxidation potentials or an increase in cytotoxicity.



A series of 1-alkyl-1'-*N-para*-(ferrocenyl) benzoyl dipeptide esters were prepared by Harry *et al*<sup>128</sup>. It was believed that introduction of an alkyl group could further lower the oxidation potential of the ferrocene moiety and thus improve cytotoxicity. The cyclopentadienyl ring was substituted with methyl, ethyl and propyl chains while dipeptides Gly-L-Ala(OEt), Gly-L-Leu(OEt) and Gly-L-Phe(OEt) were used. It was found that as expected the oxidation potential for the compounds was significantly lower than the unsubstituted compounds and compounds bearing no aromatic moiety. Compounds were tested in H1299 NSCLC cell lines. IC<sub>50</sub> values of 4.5 μM to 6.6 μM were obtained. It was also noted that Gly-L-Ala derivatives were more active than the Gly-L-Leu derivatives which in turn were more active than the Gly-L-Phe derivatives; showing that chiral side chains with bulky groups decrease the activity of the compounds. It was found that activity decreased with increasing alkyl chain length, however both methyl and ethyl side chains were more active than the unsubstituted compounds. The 1-methyl-1'-*N-para*-(ferrocenyl) benzoyl glycine-L-alanine ethyl ester was found to be most active.

1-Alkyl-1'-*N-meta*-(ferrocenyl) benzoyl dipeptide esters and 1-alkyl-1'-*N-ortho*-(ferrocenyl) benzoyl dipeptide esters were also prepared using Gly-Gly(OEt) as well as the Gly-L-Ala(OEt), Gly-L-Leu(OEt) and Gly-L-Phe(OEt) used previously coupled to methyl, ethyl and propyl ferrocenyl benzoic acids<sup>129</sup>. All compounds were screened at 10  $\mu\text{M}$  in H1299 cells. The 1-alkyl-1'-*N-ortho*-(ferrocenyl) benzoyl dipeptide esters displayed poor growth inhibition ranging from 14-48 % and were not further evaluated. The previously synthesised *N*-{*ortho*-(ferrocenyl) benzoyl}-glycine-L-alanine ethyl ester **69** bearing an unsubstituted cyclopentadienyl ring had an  $\text{IC}_{50}$  of 5.3  $\mu\text{M}$ . This shows a significant decrease in cytotoxicity for the *ortho* derivatives on alkylation of the cyclopentadienyl ring. The most active compounds were the *N*-{*meta*-(ferrocenyl) benzoyl}-glycine-glycine ethyl ester and *N*-{*meta*-(ferrocenyl) benzoyl}-glycine-L-alanine ethyl ester derivatives with 70 % or higher growth inhibition. Similarly to the 1-alkyl-1'-*N*-{*para*-(ferrocenyl) benzoyl} dipeptides it was found that cytotoxicity decreases with increasing alkyl chain length and increasing peptide side chain size. The 1-methyl-1'-*N*-{*meta*-(ferrocenyl) benzoyl}-glycine-L-alanine ethyl ester had an  $\text{IC}_{50}$  of 6.7  $\mu\text{M}$  compared with 4.0  $\mu\text{M}$  for the unsubstituted cyclopentadienyl ring derivative. Thus cytotoxicity is decreased for *ortho* and *meta* derivatives bearing an alkyl group on the ferrocene. The most active derivative was 1-methyl-1'-*N*-{*meta*-(ferrocenyl) benzoyl}-glycine-glycine ethyl ester **72** with an  $\text{IC}_{50}$  of 2.6  $\mu\text{M}$ .

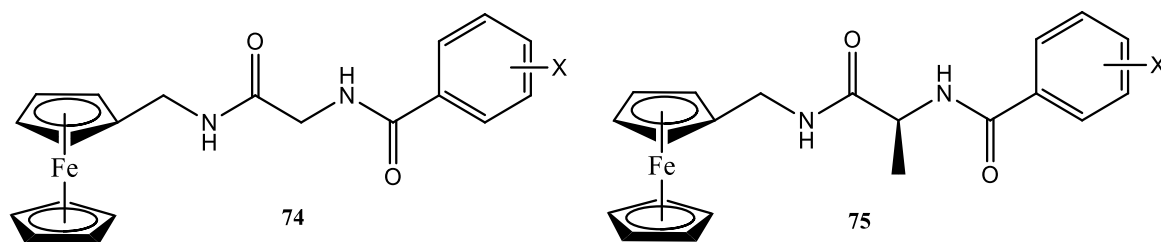
A series of *N*-(ferrocenylmethyl)fluorobenzene carboxamide derivatives **73** were prepared by Kelly *et al*<sup>130</sup>. These were shown to have an antiproliferative effect on MDA-MB-435-S-F breast cancer cells with the most active 4-fluoro derivative having an  $\text{IC}_{50}$  value of 11-14  $\mu\text{M}$ .



X = H, 2F, 3F, 4F, 2 and 6F, 2,3,4,5 and 6F.

Continuing this work Butler *et al.* prepared a series of *N*-(ferrocenylmethyl amino acid) fluorinated benzene-carboxamide derivatives using glycine **74** and L-alanine **75** linkers<sup>131</sup>. The compounds were evaluated in MCF-7 cells. The most active compound *N*-(ferrocenylmethyl-L-alanine)-3,4,5-trifluorobenzene-carboxamide had an  $\text{IC}_{50}$  value of 2.84  $\mu\text{M}$  compared to a value of 16.3 for cisplatin in this cell line. Guanine oxidation studies carried

out on this derivative showed that this class of compounds is capable of generating oxidative DNA damage via a reactive oxygenated species mediated mechanism.



a X: 2F  
 b X: 3F  
 c X: 4F  
 d X: 2F and 6F

e X: 2F and 4F  
 f X: 3F and 5F  
 g X: 3F, 4F and 5F  
 h X: 2F, 3F, 4F, 5F and 6F

### 1.3 Conclusion

Cancer is a disease which may affect any of the organs of the body. It is a major cause of death worldwide. Cancer and chemotherapy represent an extensively studied area in the fields of both chemistry and biology with the treatment of cancer costing millions each year.

The field of organometallic chemistry offers a diverse range of potential compounds which can be incorporated into unnatural drugs for the treatment of cancer. Transition metal compounds in particular offer a number of different potential bonding modes and oxidation states which lend unusual properties to potential drug candidates. To this effect ruthenium, titanium, iron, platinum, zinc, vanadium and molybdenum complexes among others have been studied extensively.

Ferrocene complexes in particular have been extensively studied. Ferrocene is nontoxic and stable and its ease of derivatisation and redox activity made it an ideal candidate for incorporation as a potential chemotherapeutic drug candidate. Ferrocene has been shown to undergo oxidation to the ferricenium ion and to generate ROS at biological potentials, while ferricenium salts have been shown to have antitumour activity. ROS can potentially generate DNA damage and cell death through increased oxidative stress within the cell.

The incorporation of ferrocene into drug molecules has been used as a strategy in antiviral, antibacterial and antifungal compounds among others. It has been seen to increase the activity of many potential drug compounds, particularly in the case of the organometallic tamoxifen analogues, the ferrocifens, against breast cancer. Ferrocene based compounds

which have been used in a clinical setting include the antimalarial ferroquine which made it to phase II clinical trials and ferrocenone which was used in the former USSR for the treatment of iron deficient anaemia.

A strong body of evidence has accumulated from recent work within this group to indicate that ferrocenyl peptide conjugates may be strong candidates as potential anticancer agents.

## References

---

- <sup>1</sup>World Cancer Research Fund (Globcon **2008** database V1.2 <http://globcon.iarc.fr>)
- <sup>2</sup>World Cancer Research Fund/American Institute for Cancer Research, Food and nutrition for the Prevention of Cancer; A Global Perspective, Washington DC, AICR, **2007**.
- <sup>3</sup>Annual report of the National Cancer registry **2013**.
- <sup>4</sup>World Cancer Research Fund International (<http://www.wcrf.org>)
- <sup>5</sup>The Cancer Research Institute (CRI) [www.cancerresearch.org](http://www.cancerresearch.org)
- <sup>6</sup>J. R. Hanson, *Chemistry and Medicines*, first edition, RSC Publishing, **2006**.
- <sup>7</sup>M. M. Gotteman, *Annual Review of Medicine*, **2002**, 53, 615-627.
- <sup>8</sup>F. S. Liu, *Taiwan Journal of Obstetrics and Gynecology*, **2009**, 48 (3), 239-244.
- <sup>9</sup>C. Atalay, *Expert Opinion in Therapeutic Patents*, **2007**, 17 (5), 511-520.
- <sup>10</sup>R. Ralhan, J. Kaur, *Expert Opinion in Therapeutic Patents*, **2007**, 17 (9), 1061-1075.
- <sup>11</sup>L. S. Goodman, M. M. Wintrobe, W. Dameshek, M. J. Goodman, A. Gilman, *Journal of the American Medical Association*, **1946**, 132(3), 126-132.
- <sup>12</sup>G. Thomas, *Medicinal Chemistry: An Introduction*, first edition, Wiley, **2000**.
- <sup>13</sup>S. Faber as cited by B. A. Chabner, T. G. Roberts Jr, *Nature Reviews/Cancer*, **2005**, 5, 65-72.
- <sup>14</sup>Z. Topcu, *Journal of Clinical Pharmacy and Therapeutics*, **2001**, 26, 405-416.
- <sup>15</sup>M. E. Wall, M. C. Wani, C. E. Cook, K. H. Palmer, A. T. McPhail, G. A. Sim, *Journal of the American Chemical Society*, **1966**, 88 (16), 3888-3890.
- <sup>16</sup>F. M. Mugga as cited by Z. Topcu, *Journal of Clinical Pharmacy and Therapeutics*, **2001**, 26, 405-416.
- <sup>17</sup>L. B. Saltz, J. V. Cox, C. Blanke, L. S. Rosen, L. Fehrenbacher, M. J. Moore, J. A. Maroun, S. P. Ackland, P. K. Locker, N. Pirotta, G. L. Elfring, L. L. Miller, *New England Journal of Medicine*, **2000**, 343 (13), 905-914.
- <sup>18</sup>F. Mollinedo, C. Gajate, *Apoptosis*, **2003**, 8, 413-450.
- <sup>19</sup>L. S. Johnson, J. G. Armstrong, M. Gorman, J. P. Burnett Jr., *Cancer Research*, **1963**, 23 (8) 1390-1427.
- <sup>20</sup>M. C. Wani, H. L. Taylor, M. E. Wall, P. Coggon, A. T. McPhail, *Journal of the American Chemical Society*, **1971**, 93 (9), 2325-2327.
- <sup>21</sup>B. A. Chabner and T. G. Roberts Jr., *Nature Reviews: Cancer*, **2005**, 5, 65-72.
- <sup>22</sup>D. Hodgkin, *Acta Crystallographica*, **1954**, 7 (10), 616-617.

- 
- <sup>23</sup>S. Top, G. Jaouen, A. Vessières, J. P. Abjean, D. Davoust, C. A. Rodger, G. B. Sayer and M. J. McGlinchey, *Organometallics*, **1985**, 4, 2143-2150.
- <sup>24</sup>G. Jaouen, *Bioorganometallics: Biomolecules, Labelling, Medicine*, **2006**.
- <sup>25</sup>E. A. Hillard and G. Jaouen, *Organometallics*, **2011**, 30, 20-27.
- <sup>26</sup>G. B. Kauffman, *Platinum Metals Review*, **2010**, 54 (4), 250-256.
- <sup>27</sup>B. Rosenberg, L. Van Camp and T. Krigas, *Nature*, **1965**, 205, 698-699.
- <sup>28</sup>D. Lebwhol, R. Canetta, *European Journal of Cancer*, **1998**, 34 (10), 1522-1534.
- <sup>29</sup>I. Romero-Canelón, P. J. Sadler, *Inorganic Chemistry*, **2013**, 52, 12276-12291.
- <sup>30</sup>L. R. Kelland, *Uses of Inorganic Chemistry in Medicine*, Royal Society of Chemistry, **1999**.
- <sup>31</sup>G. L. Patrick, *An Introduction to Medicinal Chemistry*, fifth edition, Oxford University Press, **2013**.
- <sup>32</sup>M. A. Fuertes, C. Alonso and J. M. Perez, *Chemical reviews*, **2003**, 103, 646-662.
- <sup>33</sup>D. Roeland Boer, A. Canals, M. Coll, *Dalton Transactions* **2009**, 399-414.
- <sup>34</sup>S. Gómez-Ruiz, D. Maksimović-ivanić, S. Mijatović, G. Kaluđerović, *Bioinorganic Chemistry and Applications*, **2012**, 2012.
- <sup>35</sup>P. Köpf-Maier, H. Köpf, *Chemical Reviews*, **1987**, 87 (5), 1137-1152.
- <sup>36</sup>H. Köpf, P. Köpf-Maier, *Angewentie Chemisty International Edition-England*, **1979**, 18, 477-478.
- <sup>37</sup>A. Korfel, M. E. Scheulen, H. J. Schmoll, O. Grundel, A. Harstrick, M. Knoche, L. M. Fels, M. Skorsec, F. Bach, J. Baumgart, G. Sass, S. Seeber, E. Thiel, W. E. Berdel, *Clinical Cancer Research*, **1998**, 4 (11) 2701-2708.
- <sup>38</sup>C. V. Christodoulou, D. R. Ferry, D. W. Fyfe, *Journal of Clinical Oncology*, **1998**, 16 (8) 2761-2769.
- <sup>39</sup>K. Mross, P. Robben-Bathe, L. Edler *Onkologie*, **2000**, 23 (6), 576-579.
- <sup>40</sup>M. Tacke, M. T. Allen, L. Cuffe, W. M. Gallagher, Y. Lou, O. Mendoza, H. Muller-Bunz, F. J. K. Rhemann, N. Sweeney, *Journal of Organometallic Chemistry*, **2004**, 689, 2242-2249.
- <sup>41</sup>N. J. Sweeny, O. Mendoza, H. Muller-Bunz, C. Pampillion, F. J. K. Rehmann, K. Strohfeldt, M. Tacke, *Journal of Organometallic chemistry*, **2005**, 690, 4537-4544.
- <sup>42</sup>W. H. Ang, P. J. Dyson, *European Journal of Inorganic Chemistry*, **2006**, 4003-4018.
- <sup>43</sup>E. S. Antonarakis, A. Emadi, *Cancer Chemotherapy Pharmacology*, **2010**, 66, 1-9.
- <sup>44</sup>G. Sava, I. Capozzi, K. Clerici, G. Gagliardi, E. Alessio, G. Mestroni, *Clinical Experiments in Metastases*, **1998**, 16, 371-379.

- 
- <sup>45</sup>J. M. Rademaker-Lakhai, D. Van de Bongard, D. Pluim, J. H. Beijnin, J. H. M. Schellens, *Clinical Cancer Research*, **2004**, 10, 2717-2727.
- <sup>46</sup>T. J. Kealy, P. L. Pauson, *Nature*, **1951**, 168, 1039.
- <sup>47</sup>P. L. Pauson, *Journal of Organic Chemistry*, **2001**, 367-369, 3-6.
- <sup>48</sup>G. Wilkinson, M. Rosenblum, M. C. Whiting, R. B. Woodward; *Journal of the American Chemical Society* **1952**, 74(8), 2125-2126.
- <sup>49</sup>J. D. Dunitz, L. E. Orgel, A. Rich, *Acta Crystallographica*, **1956**, 9, 373.
- <sup>50</sup>N. J. Long, *Metallocenes*, first edition, Blackwell Science Ltd., **1998**.
- <sup>51</sup>C. Chochan, *Applied Organometallic Chemistry*, **2006**, 20, 112-116.
- <sup>52</sup>E. I. Edwards, R. Epton, G. Marr, *Journal of Organometallic Chemistry*, **1976**, 122, C49-C51.
- <sup>53</sup>E. I. Edwards, R. Epton, G. Marr, *Journal of Organometallic Chemistry*, **1976**, 107, 351-357.
- <sup>54</sup>C. Biot, I. Fraisse, D. Ter-Minassian, J. Khalife, D. Dive, *Parasite*, **2011**, 18, 207-214.
- <sup>55</sup>C. Biot, N. Chavain, F. Dubar, B. Pradines, X. Trivelli, J. Brocard, I. Forfar, D. Dive, *Journal of Organometallic Chemistry*, **2009**, 845-854.
- <sup>56</sup>W. Daher, C. Biot, T. Fandeur, H. Jouin, L. Pelinski, E. Viscogliosi, L. Fraisse, B. Pradines, J. Brocard, J. Khalife, D. Dive, *Malaria Journal*, **2006**, 5(1), 11.
- <sup>57</sup>F. Dubar, C. Slomianny, J. Khalife, D. Dive, H. Kalamou, Y. Guérardel, P. Grellier, C. Biot, *Angewandte chimie International Edition*, **2013**, 52, 7690-7693.
- <sup>58</sup>Clinical Sciences and Operations Sanofi; In *ClinicalTrials.gov*, Bethesda (MD), National Library of Medicine (US), **2011**, NLM Identifier; NCT00988507. Available from: <http://clinicaltrials.gov/ct2/show/study/NCT00988507>.
- <sup>59</sup>J. T. Chantson, M. V. V. Falzacappa, S. Crovella, N. Metzler-Nolte, *Journal of Organometallic Chemistry*, **2005**, 690, 4564-4572.
- <sup>60</sup>J. T. Chantson, M. V. V. Falzacappa, S. Crovella, N. Metzler-Nolte, *ChemMedChem*, **2006**, 1, 1268-1274.
- <sup>61</sup>M. El Arbi, P. Pigeon, S. Top, A. Rhouma, S. Aifa, A. Rebai, A. Vessières, M-A. Plamont, G. Jaouen, *Journal of Organometallic Chemistry*, **2011**, 696, 1038-1048.
- <sup>62</sup>A. N. Nesmayan, N. G. Bogomolo, I. G. Andriano, V. D. Vilchevs, N. S. Kochetko, *Khimiko-Farmatsevticheskii Zhurnal*, **1972**, 6(4), 61-67.
- <sup>63</sup>V. J. Fiorina, R. J. Dubois, S. Byrnes, *Journal of Medicinal Chemistry*, **1978**, 21(4) 393-395.
- <sup>64</sup>P. Köpf-Maier, H. Köpf, E. W. Neuse, *Journal of cancer Research and Clinical Oncology*, **1984**, 108, 3, 336-340.
- <sup>65</sup>D. Osella, M. Ferrali, P. Zanello, F. Laschi, M. Fontani, C. Nervi, G. Cavigliolio, *Inorganica Chimica Acta*, **2000**, 42-48.

- 
- <sup>66</sup>G. Tabbì, C. Cassino, G. Cavigiolio, D. Colangelo, A. Ghiglia, I. Viano, D. Osella, *Journal of Medicinal Chemistry*, **2002**, 45, 5786-5796.
- <sup>67</sup>V. C. Jordan, *European Journal of Cancer*, **2008**, 44, 30-38.
- <sup>68</sup>S. Top, E. B. Kaloun, A. Vessières, G. Lerclercq, I. Laois, M. Ourevitch, C. Deuschel, M. J. McGlinchey, G. Jaouen, *Chembiochem*, **2003**, 4(8) 754-761.
- <sup>69</sup>A. Vessières, S. Top, W. Beck, E. Hillard, G. Jaouen., *Dalton Transactions*, **2006**, 529-541.
- <sup>70</sup>P. Pigeon, S. Top, A. Vessières, M. Huché, E. A. Hillard, E. Salomon, G. Jaouen, *Journal of Medicinal Chemistry*, **2005**, 48, 2814-2821.
- <sup>71</sup>K. Nikitin, Y. Ortin, H. Müller-Bunz, M-A. Plamont, G. Jaouen, A. Vessières, M. J. McGlinchey, *Journal of Organometallic Chemistry*, **2010**, 695,595-608.
- <sup>72</sup>K. H. Chan, W. K. Leong, G. Jaouen, L. Leclercq, S. Top, A. Vessières, *Journal of Organometallic Chemistry*, **2006**, 691, 9-19.
- <sup>73</sup>T. Dallagi, M. Saidi, G. Jaouen, S. Top, *Applied Organometallic Chemistry*, **2012**, 27(1), 28-35.
- <sup>74</sup>A. Vessières, S. Top, W. Beck, E. Hillard, G. Jaouen, *Dalton Transactions*, **2006**, 4, 529-541.
- <sup>75</sup>S. Top, J. Tang, A. Vessières, D. Carrez, C. Provot, G. Jaouen, *Chemical Communications*, **1996**, 8, 955-966.
- <sup>76</sup>S. Top, B. Dauer, J. Vaissermann, G. Jaouen, *Journal of Organometallic Chemistry*, **1997**, 541 (1-2), 355-361.
- <sup>77</sup>G. Jaouen, S. Top, A. Vessières, G. Leclercq, J. Quivy, L. Jin, A. Croisy, *Comptes rendus de l'Académie des sciences. Series IIC, Chemistry*, **2000**, 3(2), 89-93.
- <sup>78</sup>G. Jaouen, S. Top., A. Vessières, G. Leclercq, M. McGlinchey, *Current Medicinal Chemistry*, **2004**, 11, 2505-2517.
- <sup>79</sup>S. Top, A. Vessières, G. Leclercq, J. Quivy, J. Tang, J. Vaissermann, M. Huche, G. Jaouen, *Chemistry- A European Journal*, **2003**, 9, 5223-5236.
- <sup>80</sup>S. Top, A. Verrières, C. Cabestaing, I. Laois, G. Leclercq, C. Provot, G. Jaouen, *Journal of Organometallic Chemistry*, **2001**, 637-639, 500-506.
- <sup>81</sup>A. Vessières, C. Corbet, J. M. Heldt, N. Lories, N. Juoy, I. Laois, G. Laclercq, G. Jaouen, R. A. Toillon, *Journal of Inorganic Biochemistry*, **2010**, 104 (5), 503-511.
- <sup>82</sup>D. Osella, H. Mahboobi, D. Colangelo, G. Cavigiolio, A. Vessières, G. Jaouen, *Inorganica Chimica Acta*, **2005**, 358, 1993-1998.
- <sup>83</sup>E. Hillard, A. Vessières, L. Thouin, G. Jaouen, C. Amatore, *Angewandte chemie*, **2006**, 45, 285-290.



- 
- <sup>84</sup>P. W. Fan, F. Zhang, J. L. Bolton, *Chemical Results in Toxicology*, **2000**, 13, 45-52.
- <sup>85</sup>M. M. Marques, F.A. Beland, *Carcinogenesis*, **1997**, 18(10), 1949-1954.
- <sup>86</sup>D. Hamels, P. M. Dansette, E. A. Hillard, S. Top, A. Vessières, P. Herson, G. Jaouen, D. Mansuy, *Angewante Chemie International Edition*, **2009**, 48, 9124-9126.
- <sup>87</sup>E. A. Hillard, P. Pigeon, A. Vessières, C. Amatore, G. Jaouen, *Dalton Transactions*, **2007**, 5073-5081.
- <sup>88</sup>P. Pigeon, S. Top, O. Zekri, E. A. Hillard, A. Vessières, M. A. Plamont, O. Buriez, E. Labbé, M. Huché, S. Boutamine, C. Amatore, G. Jaouen, *Journal of Organometallic Chemistry*, **2009**, 694, 895-901.
- <sup>89</sup>O. Buriez, J. M. Heldt, E. Labbé, A. Vessières, G. Jaouen, C. Amatore, *Chemistry - A European Journal*, **2008**, 14, 8195-8203.
- <sup>90</sup>O. Mertins, O. Buriez, E. Labbé, P-P. Fang, E. Hillard, A. Vessières, G. Jaouen, Z-Q. Tian, C. Amatore, *Journal of Electroanalytical Chemistry*, **2009**, 635, 13-19.
- <sup>91</sup>A. Nguyen, V. Marsaud, C. Bouclier, S. Top, A. Vessières, P. Pigeon, R. Gref, P. Legrand, G. Jaouen, J. M. Renoir, *International Journal of Pharmaceutics*, **2008**, 347, 128-135.
- <sup>92</sup>E. Allard, C. Passirani, E. Gaarcion, P. Pigeon, A. Vessières, G. Jaouen, J. P. Benoit, *Journal of Controlled Release*, **2008**, 130, 146-153.
- <sup>93</sup>E. Allard, N. T. Huynh, A. Vessières, P. Pigeon, G. Jaouen, J-P. Benoit, C. Passirani, *International journal of Pharmaceutics*, **2009**, 379, 317-323.
- <sup>94</sup>E. Allard, D. Jarnet, A. Vessières, S. Vinchon-Petit, G. Jaouen, J. P. Benoit, C. Passirani, *Pharmaceutical Research*, **2009**, 27, 56-64.
- <sup>95</sup>M. Roger, A. Clavreul, N. T. Huynh, C. Passirani, P. Schiller, A. Vessières, C. Montero-Menei, P. Menei., *International Journal of Pharmaceutics*, **2012**, 423, 63-68.
- <sup>96</sup>A-L. Lainé, E. Adriaenssens, A. Vessières, G. Jaouen, C. Corbet, E. Desruelles, P. Pigeon, R-A. Toillon, c. Passirani, *Biomaterials*, **2013**, 34, 6949-6956.
- <sup>97</sup>D. Plažuk, A. Vessières, E.A.Hillard, O. Buriez, E. Labbé, P. Pigeon, M. A. Plamont, C. Amatore, A. Zakrewski, G. Jaouen., *Journal of Medicinal Chemistry*, **2009**, 52, 4964-4967.
- <sup>98</sup>M. Görmen., D. Palžuk, P. Pigeon, E.A. Hillard, M-A, Plamont, S. Top, A. Vessières, G.Jaouen, *Tetrahedron Letters*, **2010**, 51, 118-120.
- <sup>99</sup>M. Görmen, P. Pigeon, S. Top, A. Vessières, M-A. Plamont, E. A. Hillard, G. Jaouen, *Medicinal Chemistry Communications*, **2010**, 1, 149-151.
- <sup>100</sup>J. D. Cázares-Marinero, E. Labbé, S. Top, O. Buriez, C. Amatore, G. Jaouen, *Journal of Organometallic chemistry*, **2013**, 744, 92-100.

- 
- <sup>101</sup>P. Pigeon, S. Top, A. Vessières, M. Huché, M. Görmen, M. El Arbi, M-A. Plamont, M. J. McGlinchey, G. Jaouen, *New Journal of Chemistry*, **2011**, 35, 2212-2218.
- <sup>102</sup>A. C. DeOliveira, E. A. Hillard, P. Pigeon, D. D. Rocha, F. A. R. Rodrigues, R. C. Montenegro, L. V. Costa-Lotuf, M. O. F. Goulart, G. Jaouen, *European Journal of Medicinal Chemistry*, **2011**, 46, 3778-3787.
- <sup>103</sup>Q. Michard, G. Jaouen, A. Vessières, B. A. Bernard, *Journal of Inorganic Biochemistry*, **2008**, 102, 1980-1985.
- <sup>104</sup>O. Payen, S. Top, A. Vessières, E. Brulé, M-A. Plamont, M. J. McGlinchey, H. Müller-Bunz, G. Jaouen, *Journal of Medicinal Chemistry*, **2008**, 51, 1791-1799.
- <sup>105</sup>O. Payne, S. Top, A. Vessières, E. Brulé, A. Lauzier, M-A. Plamont, M. J. McGlinchey, H. Müller-Bunz, G. Jaouen, *Journal of Organometallic Chemistry*, **2011**, 696, 1049-1056.
- <sup>106</sup>K. N. Tiwari, J. P. Monserrat, F. D. Montigny, G. Jaouen, M. N. Rager, E. A. Hillard, *Organometallics*, **2011**, 30, 5424-5432.
- <sup>107</sup>J. P. Monserrat, K. N. Tiwari, L. Quentin, P. Pigeon, G. Jaouen, A. Vessières, G. G. Chabot, E. A. Hillard, *Journal of Organometallic Chemistry*, **2013**, 734, 78-85.
- <sup>108</sup>S. Top, C. Thibaudeau, A. Vessières, E. Brulé, F. Le Bideau, J-M. Joerger, M-A. Plamont, S. Samreth, A. Edgar, J. Marrot, P. Herson, G. Jaouen, *Organometallics*, **2009**, 28, 1414-1424.
- <sup>109</sup>A. Arezki, G. G. Chabot, L. Quentin, D. Scherman, G. Jaouen, E. Brulé, *MedChemComm*, **2011**, 2, 190-195.
- <sup>110</sup>J. D. Cázares-Marinero, M. Lapierre, V. Cavallès, R. Saint-Fort, A. Vessières, S. Top, G. Jaouen, *Dalton Transactions*, **2013**, 42, 15489-15501.
- <sup>111</sup>J. D. Cázares-Marinero, O. Buriez, E. Labbè, S. Top, C. Amatore, G. Jaouen, *Organometallics*, **2013**, 32, 5926-5934.
- <sup>112</sup>J. D. Cázares-Marinero, S. Top, A. Vessières, G. Jaouen, *Dalton Transactions*, **2014**, 43, 817-830.
- <sup>113</sup>M. J. Sheehy, J. F. Gallagher, M. Yamashita, Y. Ida, J. White-Colangelo, J. Johnson, R. Orlando, P. T. M. Kenny, *Journal of Organometallic Chemistry*, **2004**, 689 (9), 1511-1520.
- <sup>114</sup>D. Savage, J. F. Gallagher, Y. Ida, P. T. M. Kenny, *Inorganic Chemistry Communications*, **2002**, 5 (12), 1034-1040.
- <sup>115</sup>D. Savage, G. Malone, J. F. Gallagher, Y. Ida, P. T. M. Kenny, *Journal of Organometallic Chemistry*, **2005**, 690 (2), 383-393.
- <sup>116</sup>D. Savage, G. Malone, S. R. Alley, J. F. Gallagher, A. Goel, P. N. Kelly, H. Mueller-Bunz, P. T. M. Kenny, *Journal of Organometallic Chemistry*, **2006**, 691 (3), 463-469.

- 
- <sup>117</sup>D. Savage, N. Neary, G. Malone, S. R. Alley, J. F. Gallagher, P. T. M. Kenny, *Inorganic Chemistry Communications*, **2005**, 8 (5), 429-432.
- <sup>118</sup>A. J. Corry, Ph.D Thesis, **2009**.
- <sup>119</sup>A. J. Corry, A. Goel, S. R. Alley, P. N. Kelly, D. O'Sullivan, D. Savage, P. T. M. Kenny, *Journal of Organometallic Chemistry*, **2007**, 692, 1405-1410.
- <sup>120</sup>D. Savage, S. R. Alley, J. F. Gallagher, A. Goel, P. N. Kelly, P. T. M. Kenny, *Inorganic Chemistry Communications*, **2006**, 9 (2), 152-155.
- <sup>121</sup>D. Savage, S. R. Alley, A. Goel, T. Hogan, Y. Ida, P. N. Kelly, L. Lehmann, P. T. M. Kenny, *Inorganic Chemistry Communications*, **2006**, 9 (12), 1267-1270.
- <sup>122</sup>A. J. Corry, N. O'Donovan, Á. Mooney, D. O'Sullivan, D. K. Rai, P. T. M. Kenny, *Journal of Organometallic Chemistry*, **2009**, 694, 880-885.
- <sup>123</sup>A. J. Corry, Á. Mooney, D. O'Sullivan, P. T. M. Kenny, *Inorganica Chimica Acta*, **2009**, 362, 2957-2961.
- <sup>124</sup>Á. Mooney, A. J. Corry, D. O'Sullivan, D. K. Rai, P. T. M. Kenny, *Journal of Organometallic Chemistry*, **2009**, 694, 886-894.
- <sup>125</sup>Á. Mooney, A. J. Corry, C. N. Ruairc, T. Mahgoub, D. O'Sullivan, N. O'Donovan, J. Crown, S. Varughese, S. M. Draper, D. K. Rai, P. T. M. Kenny, *Dalton Transactions*, **2010**, 39, 8228-8239.
- <sup>126</sup>Á. Mooney, R. Tiedt, T. Maghoub, N. O'Donovan, J. Crown, B. White, P. T. M. Kenny, *Journal of Medicinal Chemistry*, **2012**, 55 (11), 5455-5466.
- <sup>127</sup>A. G. Harry, J. Murphy, W. E. Butler, R. Tiedt, Á. Mooney, J. C. Manton, M. T. Pryce, N. O'Donovan, N. Walsh, J. Crown, D. K. Rai, P. T. M. Kenny, *Journal of Organometallic Chemistry*, **2013**, 734, 86-92.
- <sup>128</sup>A. G. Harry, W. E. Butler, J. C. Manton, M. T. Pryce, N. O'Donovan, J. Crown, D. K. Rai, P. T. M. Kenny, *Journal of Organometallic Chemistry*, **2014**, 757, 28-35.
- <sup>129</sup>A. G. Harry, W. E. Butler, J. C. Manton, M. T. Pryce, N. O'Donovan, J. Crown, D. K. Rai, P. T. M. Kenny, *Journal of Organometallic Chemistry*, **2014**, 766, 1-12.
- <sup>130</sup>P. N. Kelly, A. Prêtre, S. Devoy, I. O'Reilly, R. Devery, A. Goel, J. Gallagher, A. J. Lough, P. T. M. Kenny, *Journal of Organometallic Chemistry*, **2007**, 692, 1327-1331.
- <sup>131</sup>W. E. Butler, P. N. Kelly, A. G. Harry, R. Tiedt, B. White, R. Devery, P. T. M. Kenny, *Applied Organometallic Chemistry*, **2013**, 27, 361-365.

## Chapter 2

### **Synthesis and structural characterisation of *N*-(6-ferrocenyl-2-naphthoyl), *N*-{*para*-(ferrocenyl)cinnamoyl} and *N*-{*para*-(ferrocenyl)benzoyl} amino acid and dipeptide derivatives.**

#### **2.1 Introduction**

Although any compound containing both an amino group and a carboxylic acid may be termed an amino acid, the term is most often used to refer to an  $\alpha$ -amino acid in which the amine and the carboxylic acid groups are attached to the same carbon atom. There are 20 standard amino acids which are found in proteins, nine of which are essential meaning that they cannot be synthesised in the body and must be taken in through the diet. In addition to the standard amino acids there are other amino acids which have biologically important roles such as  $\gamma$ -aminobutyric acid (GABA) which acts a neurotransmitter. Amino acids are often used in medicinal chemistry as they offer a wide range of shapes, different charges and have side chains which may form hydrogen bond interactions.

L-amino acids are the predominant stereoisomer found in nature however D-amino acids are also found<sup>1</sup>. D-amino acids such as D-alanine and D-glutamic acid are found principally in the peptidoglycan cell wall of bacteria. In humans they have specific roles. D-aspartate plays a regulatory role in adult neurogenesis while D-serine acts as a co-agonist of *N*-methyl-D-aspartate type glutamate receptors in the brain, which are involved in learning, memory and behaviour in mammals. Some peptides contain D-amino acids. D-configured amino acid residues in peptides provide resistance to proteases, which generally exhibit specificity for the L-isomers.

The incorporation of amino acids in drug design is a common strategy in medicinal chemistry. Amino acid prodrugs may be made for drug delivery to take advantage of amino acid transporters within the body<sup>2</sup>.

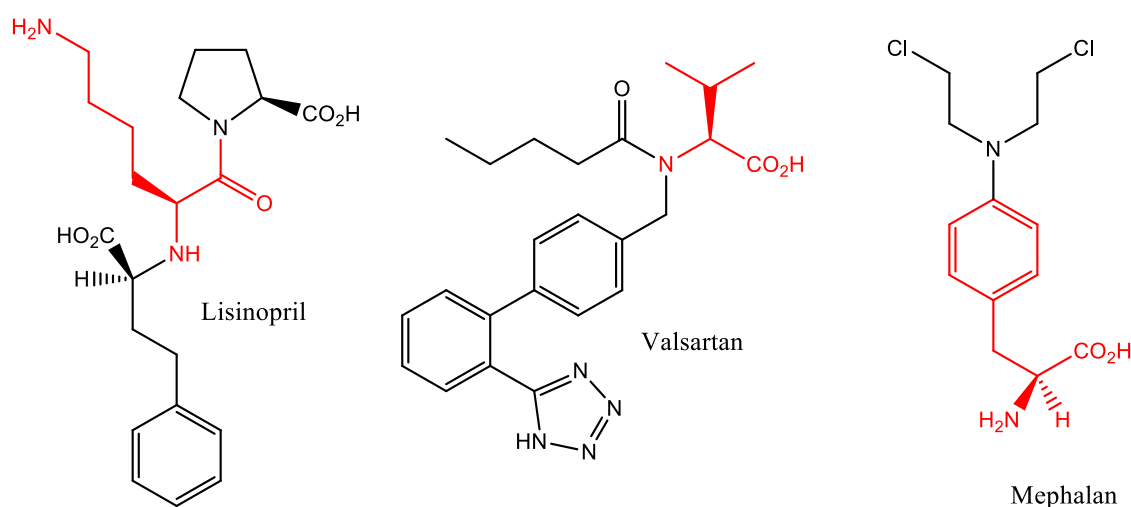
Such transporters largely consist of the solute carrier (SLC) family of transporters of which there are over 370 members<sup>3</sup>. These transporters have a huge variety of functions within the cell and are responsible for the transport of neurotransmitters, nutrients, lipid derivatives, nucleotides and nucleosides, cations and anions as well

as amino acids and short peptides. 59 functional amino acid transporters have been identified in 12 different SLC subfamilies<sup>4</sup>. The SLC36 family have been shown to transport small, unbranched, zwitterionic  $\alpha$ ,  $\beta$  and  $\gamma$  amino acids.

L-type amino acid transporters 1 (LAT1) and 2 (LAT2) are a subfamily of SCL7 and SCL3 heterodimeric amino acid transporters<sup>5</sup>. They transport large neutral amino acids from the extracellular fluid into the cell and are expressed in various tissues including the intestinal wall, the blood brain barrier and the kidneys. Only a few drugs are substrates of these transporters, including levodopa and melphalan.

Two peptide transporters 1 (PEPT1) SLC15A1 and 2 (PEPT2) SLC15A2 have been identified in mammals<sup>6</sup>. The physiological substrates of these transporters are dipeptides and tripeptides composed of the 20 proteinogenic L- $\alpha$ -amino acids. They have been shown to be responsible for the transport of angiotensin converting enzyme (ACE) inhibitors such as Lisinopril.

This is a strategy often used to increase a drug's bioavailability. Compounds currently on the market which contain amino acids in order to increase uptake by use of transport proteins include the antihypertensive agents Lisinopril and Valsartan and the DNA alkylating agent Mephalan. Lisinopril is a lysine derivative of enalapril and is transported by transport proteins for dipeptides. Valsartan is an angiotensin II receptor agonist. Mephalan is a nitrogen mustard alkylating agent. It is a phenylalanine derivative of chlormethine **1**.



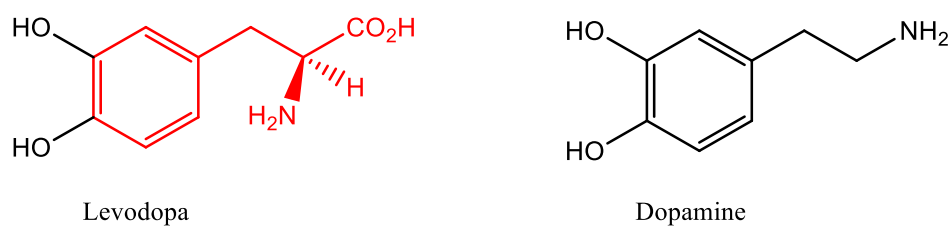


**Figure 2.1:** Structures of currently used drugs containing amino acids.

Similarly the Levodopa is a prodrug for the neurotransmitter dopamine. It is used in the treatment of Parkinson's disease, a condition caused by a deficiency of the neurotransmitter in the brain. Dopamine is too polar to cross the blood brain barrier. Levodopa is even more polar, however it is an amino acid and thus is recognised by the amino acid transporters and carried across the cell membrane<sup>7</sup>. It is transported by the phenylalanine transporter.

Organometallic compounds offer a wide range of potential structures and bonding modes, making them an ideal starting point for the synthesis of potential drug compounds. The use of metals in medicine can be traced back over 5000 years<sup>7</sup>. The first important organometallic drug was salvarsan which was an arsenic based compound discovered in 1908 and used to treat syphilis<sup>8</sup>. The discovery of cisplatin's anticancer activity in 1965 was a major breakthrough for metal based drugs<sup>9</sup>. Today it is estimated that platinum based coordination complexes are used in 50-70 % of chemotherapeutic schedules used to treat cancer patients<sup>8</sup>.

Ferrocene is an attractive motif for use in medicinal chemistry because it is stable and non-toxic, it is aromatic and easily undergoes derivitisation. Ferrocene has been shown to have anti-tumour, antiinfective, antiviral<sup>10</sup> and antifungal<sup>11</sup> activity as well as anticancer activity. The first organometallic bioconjugates of ferrocene were reported in 1957<sup>12</sup>. Schlögl *et al.* reported the synthesis and characterisation of ferrocenylalanine and *para*-ferrocenyl phenylalanine as well as the first *N*-ferrocenyl methyl amino acid. Ferrocene itself is not cytotoxic, however many of its derivatives including ferrocenium species have been shown to be. Their ability to produce reactive oxygen species (ROS) which are capable of damaging DNA and other biomolecules is thought to be important to their mode of action. Jaouen *et al.* have prepared the most successful series of ferrocene based anticancer drug candidates, which selectively target hormone dependant tumours such as breast cancer<sup>13</sup>.

Thus the preparation of ferrocenyl peptide conjugates offers an attractive method to target cancer cells. Recent research within this group has proved this to be an effective strategy for the generation of cytotoxic agents. Mooney *et al.* identified 5 lead compounds that had an

excellent anti-proliferative activity against the H1299 NSCLC and Sk-Mel-28 metastatic melanoma cell line<sup>14</sup>. Compounds **70** and **76-79** all showed activity greater than that of cisplatin, with four of the compounds having an activity in the nanomolar (nm) range in the H1299 cell line (table 2.1).

**Table 2.1:** IC<sub>50</sub> values for the most active compounds in the *N*-(6-ferrocenyl-2-naphthoyl) series.

Compound	H1299 (μM)	Sk-Mel-28 (μM)
<b>22</b> Cisplatin	1.50 ± 0.10	-
<b>70</b> <i>N</i> -(6-ferrocenyl-2-naphthoyl)-glycine-glycine-OEt	0.13 ± 0.02	1.10 ± 0.13
<b>76</b> <i>N</i> -(6-ferrocenyl-2-naphthoyl)-sarcosine-glycine-OEt	0.14 ± 0.02	1.06 ± 0.05
<b>77</b> <i>N</i> -(6-ferrocenyl-2-naphthoyl)-γ-aminobutyric acid-OEt	0.62 ± 0.07	1.41 ± 0.04
<b>78</b> <i>N</i> -(6-ferrocenyl-2-naphthoyl)-glycine-L-alanine-OEt	1.30 ± 0.10	3.74 ± 0.37
<b>79</b> <i>N</i> -(6-ferrocenyl-2-naphthoyl)-glycine-D-alanine-OEt	0.33 ± 0.02	1.83 ± 0.04

The objective of this research was to further extend the SAR study of these molecules. Four key areas have been identified for modification of these compounds (figure 2.2). These are 1; the electroactive ferrocene core, 2; the conjugated linker, 3; the dipeptide chain and 4; the ester protecting group.

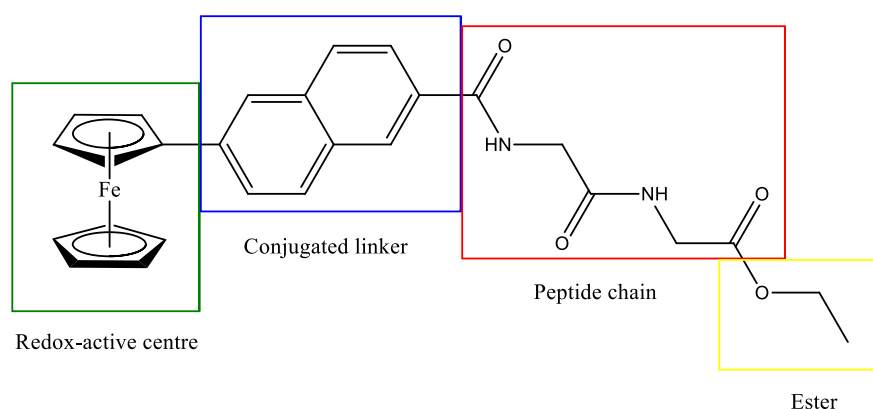
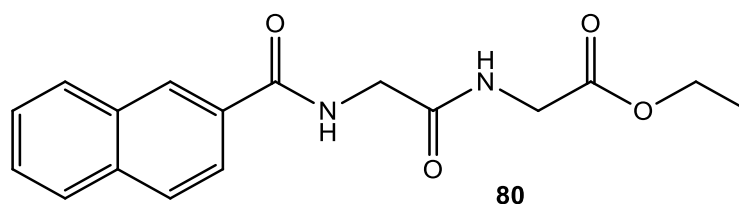


**Figure 2.2:** SAR regions of *N*-(6-ferrocenyl-2-naphthoyl)-glycine-glycine ethyl ester.

The first region for consideration is the ferrocene core of the molecule. The redox active ferrocene core has been shown to be required for activity. Mooney *et al.* prepared a 2-naphthoyl-glycine-glycine ethyl ester **80** analogue of the *N*-(6-ferrocenyl-2-naphthoyl)-glycine-glycine ethyl ester **70**. The non-organometallic analogue was tested alongside the other dipeptide esters. It did not show any inhibitory effect against either H1299 lung cancer

or Sk-Mel-28 melanoma cell lines when tested at 1  $\mu$ M. Percentage cell growth was  $87.6 \pm 18.4$  and  $95.6 \pm 10.9$  for H1299 cells and Sk-Mel-28 cells respectively.



Replacement of the electroactive core by an alternative metallocene is another plausible strategy. The most common approach is the substitution of ferrocene by ruthenocene. Ruthenium undergoes electrochemical oxidation more readily than ferrocene and a low oxidation potential is believed to be necessary for antiproliferative activity. However the oxidation of ruthenocene has been reported as both a one electron and a two electron irreversible oxidation process<sup>15</sup>. Pigeon *et al.* prepared ruthenocene analogues of the organometallic tamoxifen derivatives. However a loss of activity in the ER (-) breast cancer cell line was reported on replacement of the ferrocene with ruthenocene<sup>16</sup>. As the reversible redox properties displayed by the *N*-(6-ferrocenyl-2-naphthoyl) and *N*-{*para*-(ferrocenyl)benzoyl} amino acid and dipeptide derivatives are thought to have an important role in the mode of action of these compounds it is unlikely that ruthenocenyl analogues would have the same biological activity.

The second region for modification is the conjugated linker. Corry *et al.* prepared *N-ortho*, *meta* and *para* ferrocenyl benzoyl amino acid and dipeptide derivatives, the most active of which, *N*-{*ortho*-(ferrocenyl)benzoyl} glycine-L-alanine ethyl ester **69** had an  $IC_{50}$  of 4.0  $\mu$ M in H1299 cells<sup>17</sup>. Mooney *et al.* replaced benzoyl linker with a naphthoyl linker. The conjugating ability of the linker is thought to be important in decreasing the redox potential of these compounds. Thus increasing the conjugation of the ring system seemed a logical approach. Both *N*-(3-ferrocenyl-2-naphthoyl) and *N*-(6-ferrocenyl-2-naphthoyl) derivatives were prepared. The *N*-(6-ferrocenyl-2-naphthoyl) derivatives were significantly more active with the *N*-(6-ferrocenyl-2-naphthoyl)-glycine-L-alanine ethyl ester **78** having an  $IC_{50}$  of 1.3  $\mu$ M<sup>14</sup>. This is three times more active than the *N*-{*ortho*-(ferrocenyl)benzoyl}-glycine-L-alanine ethyl ester **69**.

There are many possible further modifications to the conjugated linker available, and many conjugated aromatic systems available which could be used to replace the benzoyl linker. The use of a cinnamoyl linker is an interesting strategy as it also offers a more conjugated



system than the benzoyl linker but without having a fully fused ring system as in the case of the naphthoyl linker (figure 2.3). This modification may increase the flexibility of the molecule. It is an interesting modification for the SAR study as it may help to determine whether the fully fused ring is essential for activity.

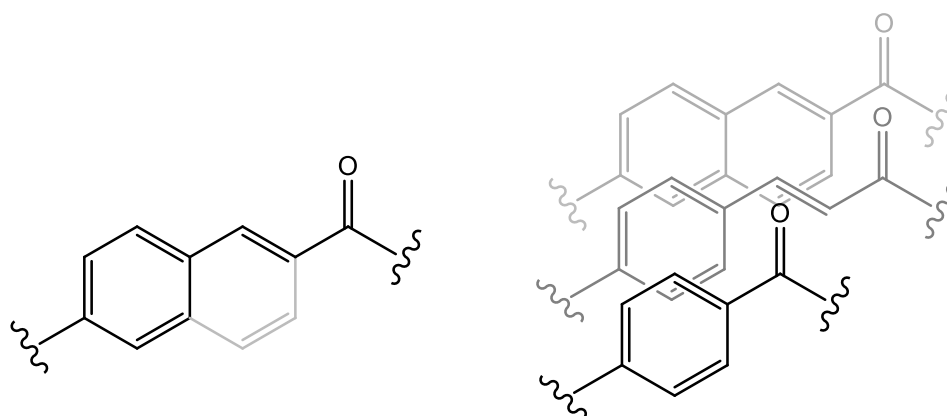


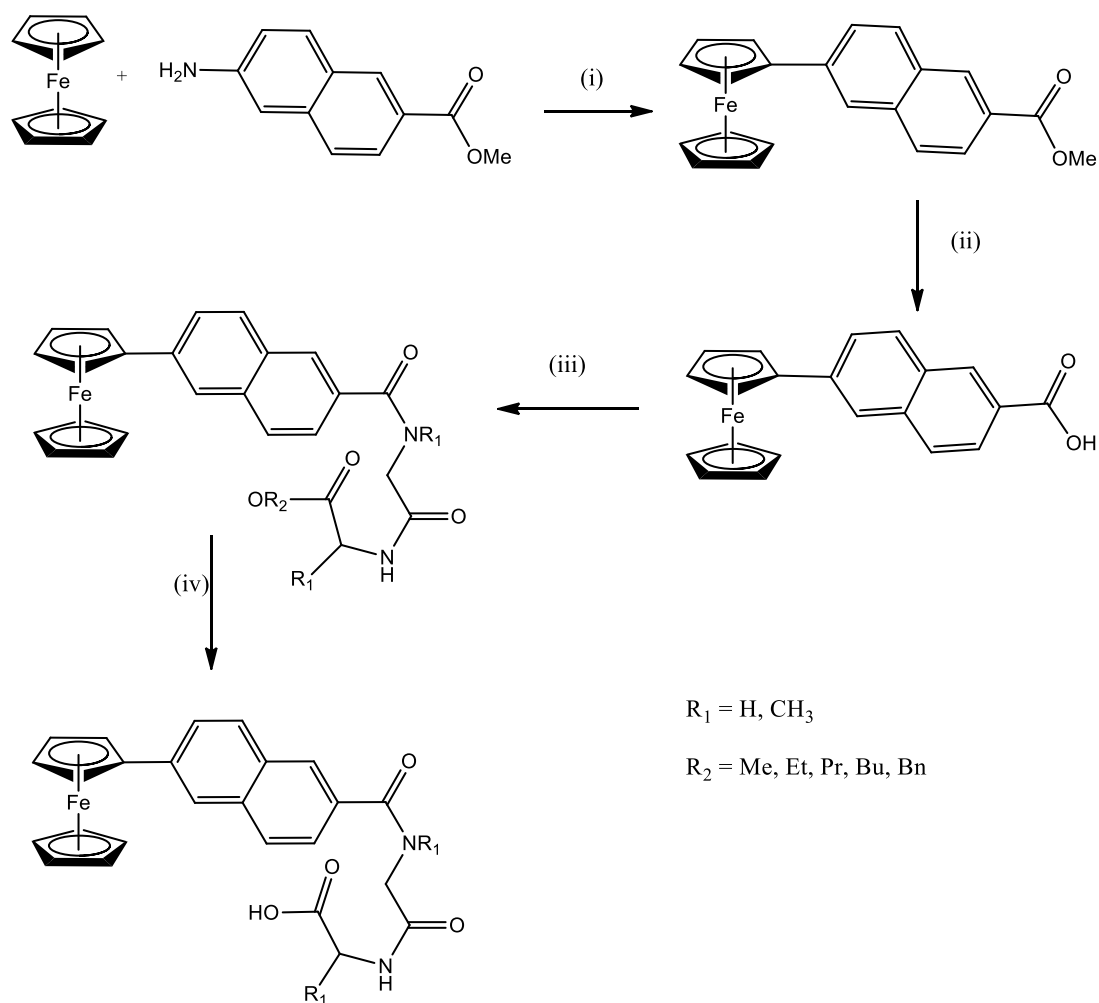
**Figure 2.3:** Variations of the conjugated linker.

The peptide region of the compounds has been extensively studied<sup>18</sup>. It has been shown that an amino acid or dipeptide is essential for the cytotoxic activity of the molecule. Methyl-6-ferrocenylnaphthalene-2-carboxylate **82** was tested against H1299 and Sk-Mel-28 cell lines and displayed no activity<sup>19</sup>. Tripeptide and tetrapeptide chains have been synthesised, however this led to a decrease in activity. Dipeptide derivatives have proved most successful when small neutral  $\alpha$ -amino acids have been incorporated into the chain. The most active of the *N*-(6-ferrocenyl-2-naphthoyl) amino acid and dipeptide esters are given in table 2.1. The amino acid and dipeptide chain configurations from table 2.1 have been maintained in the current study.

The final moiety of the compounds which can be modified is the ester protecting group. To date this area of the compound has not been modified. The simplest alteration to this region of the molecule is to prepare a series of esters of differing sizes to investigate if ester chain length exerts an influence on the cytotoxicity of the molecule.

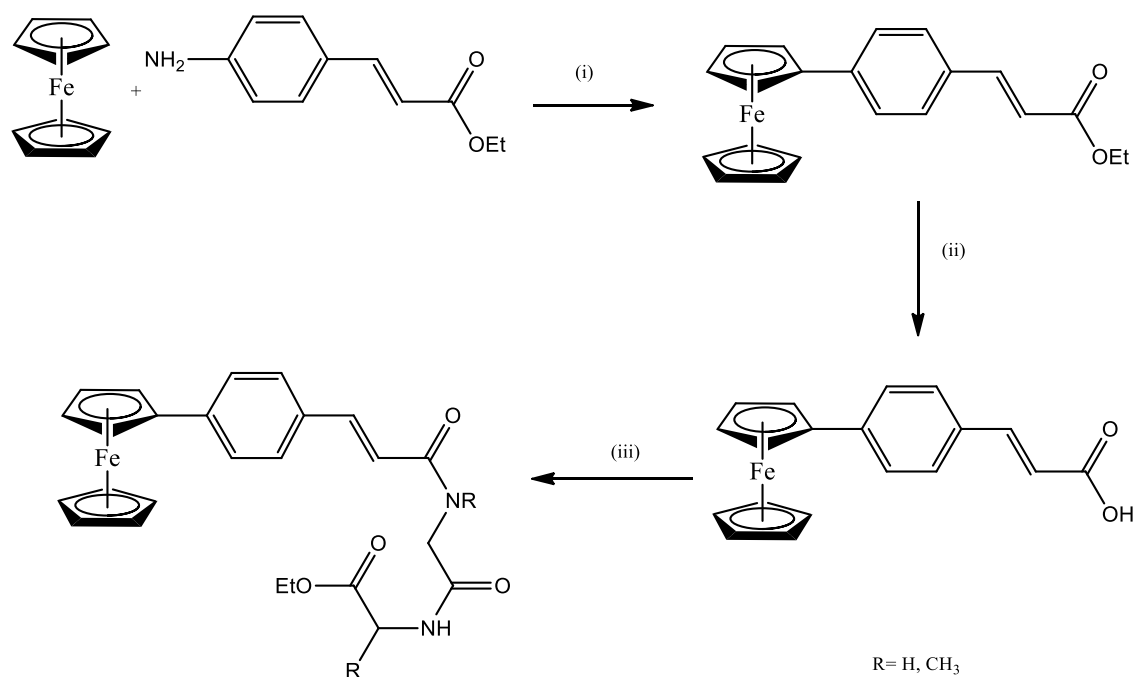
## 2.2 The synthesis of *N*-(6-ferrocenyl-2-naphthoyl), *N*-{*para*(ferrocenyl)cinnamoyl} and *N*-{*para*-(ferrocenyl)benzoyl} amino acid and dipeptide derivatives.

The *N*-(6-ferrocenyl-2-naphthoyl), *N*-{*para*-(ferrocenyl)cinnamoyl} and *N*-{*para*-(ferrocenyl)benzoyl} amino acid and dipeptide derivatives were prepared via standard peptide coupling methods using *N*-(3-dimethylaminopropyl)-*N'*-ethylcarbodiimide hydrochloride (EDC) and *N*-hydroxysuccinamide (NHS). A solution of the appropriate ferrocenyl carboxylic acid ester in dichloromethane at 0 °C, was treated with EDC, NHS and triethylamine (Et<sub>3</sub>N) and allowed to stir for an hour. An equimolar amount of the corresponding amino acid or dipeptide was then added to the solution with stirring. Scheme 2.1 outlines the synthetic route for the *N*-(6-ferrocenyl-2-naphthoyl) amino acid and dipeptide derivatives. *N*-*para*-(ferrocenyl)cinnamoyl (scheme 2.2) and *N*-{*para*-(ferrocenyl)benzoyl} derivatives (scheme 2.3) and were prepared following the same strategy.



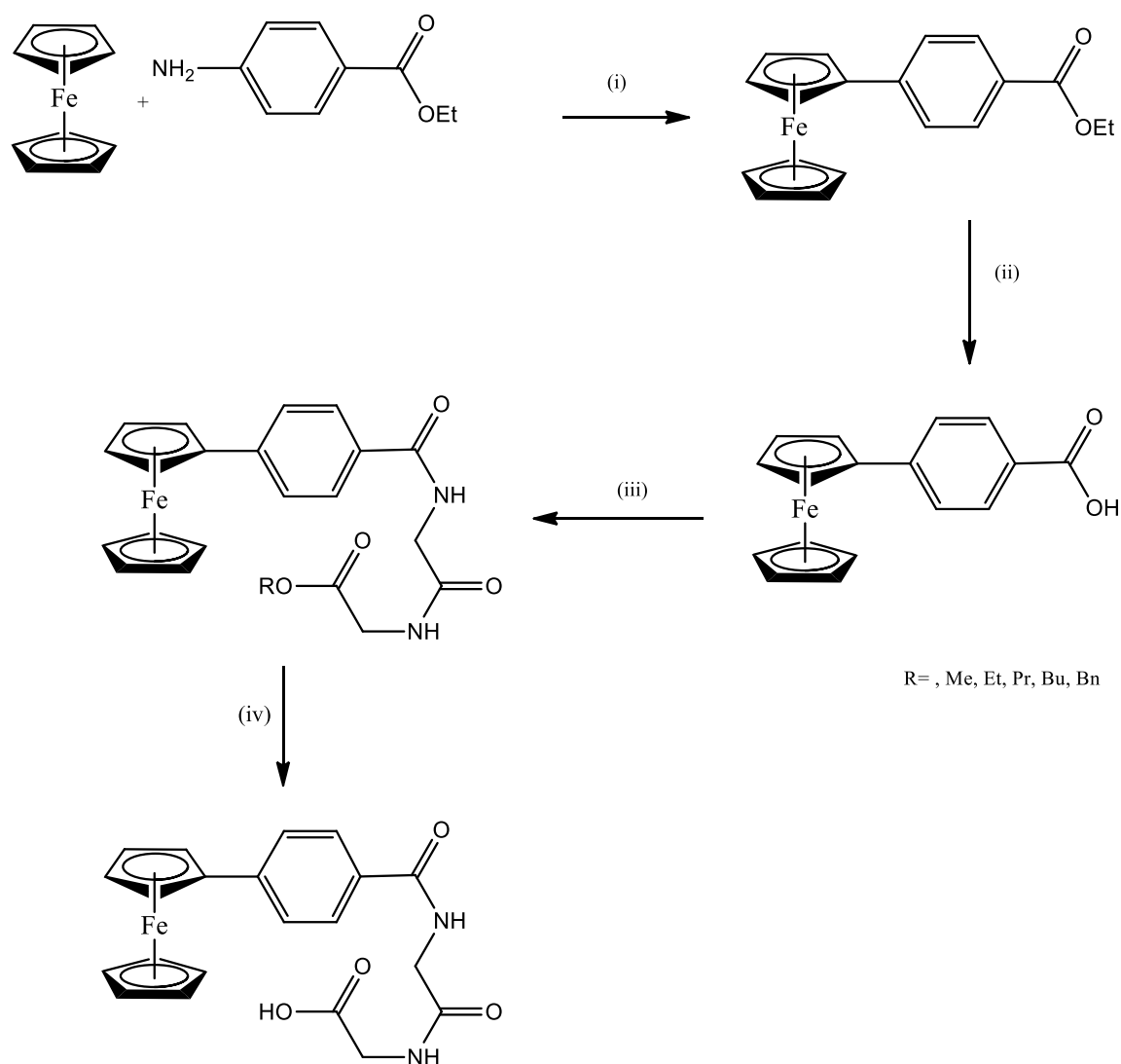
(i)  $\text{NaNO}_2$ ,  $\text{HCl}$ ,  $5^\circ \text{C}$ ; (ii)  $\text{NaOH/MeOH}$ ,  $\text{H}_2\text{O}$ ; (iii)  $\text{EDC}$ ,  $\text{NHS}$ ,  $\text{Et}_3\text{N}$ , amino acid/dipeptide (iv)  $\text{NaOH/MeOH}$ ,  $\text{H}_2\text{O}$ .

**Scheme 2.1:** General reaction scheme for the synthesis of *N*-(6-ferrocenyl-2-naphthoyl) amino acid and dipeptide derivatives.



(i) NaNO<sub>2</sub>, HCl, 5° C; (ii) NaOH/MeOH, H<sub>2</sub>O; (iii) EDC, NHS, Et<sub>3</sub>N, amino acid/dipeptide.

**Scheme 2.2:** General reaction scheme for the synthesis of *N*-{*para*-(ferrocenyl)cinnamoyl} amino acid and dipeptide ethyl esters.

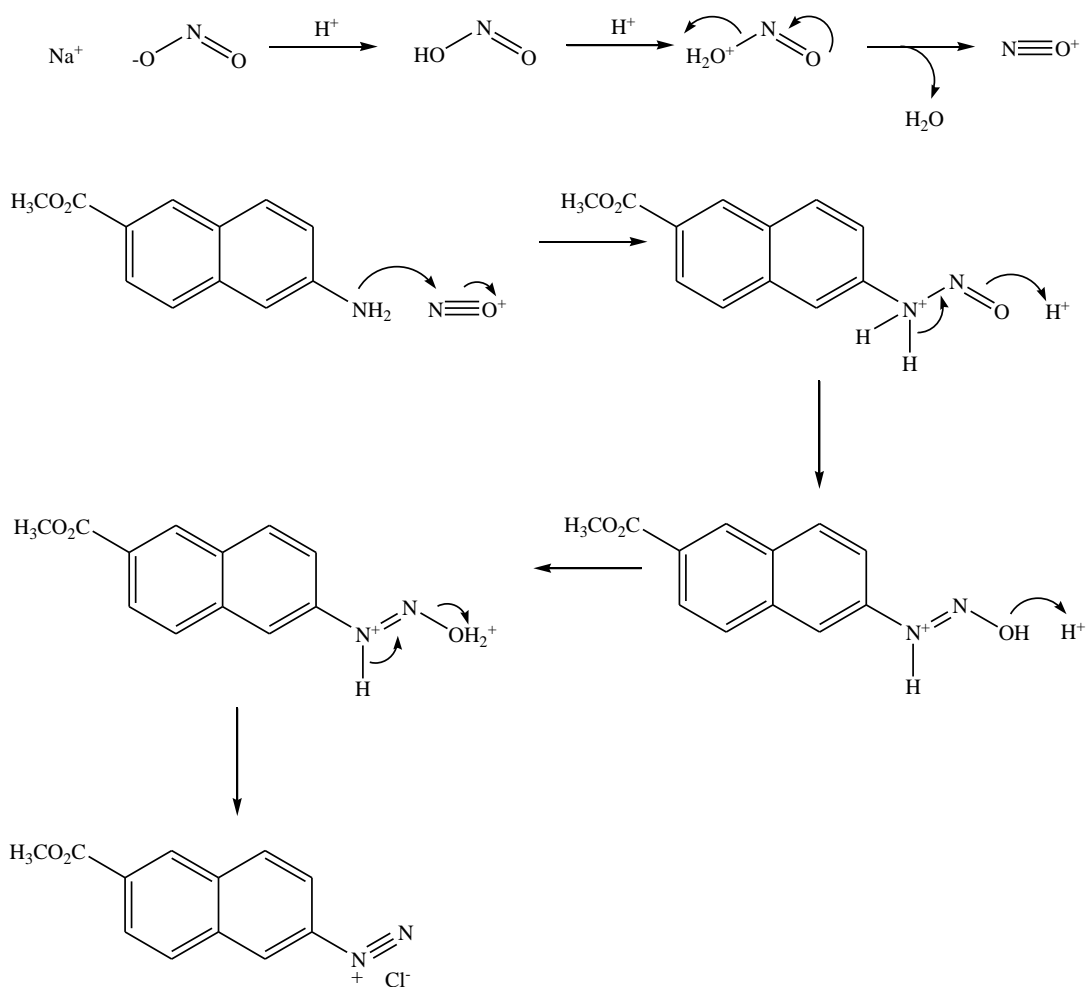


(i)  $\text{NaNO}_2$ ,  $\text{HCl}$ ,  $5\text{ }^\circ\text{C}$ ; (ii)  $\text{NaOH}/\text{MeOH}$ ,  $\text{H}_2\text{O}$ ; (iii)  $\text{EDC}$ ,  $\text{NHS}$ ,  $\text{Et}_3\text{N}$ , amino acid/dipeptide (iv)  $\text{NaOH}/\text{MeOH}$ ,  $\text{H}_2\text{O}$ .

**Scheme 2.3:** General reaction scheme for the synthesis of *N*-{*para*-(ferrocenyl)benzoyl} dipeptide derivatives.

### 2.2.1.1 Preparation of ferrocenyl carboxylates

The appropriate naphthoyl, cinnamoyl or benzoyl carboxylate ester was treated with sodium nitrite in the presence of hydrochloric acid at a temperature below  $5\text{ }^\circ\text{C}$  to yield the diazonium salt (scheme 2.4). Above  $5\text{ }^\circ\text{C}$  the diazonium salt decomposes resulting in the formation of an aryl carbocation and the evolution of  $\text{N}_2$  gas. Ferrocene present *in situ* reacts with the aryl carbocation via electrophilic aromatic substitution to give the ferrocenyl carboxylate ester as an orange solid.



**Scheme 2.4:** Diazonium salt formation.

### 2.2.1.2 Preparation of ferrocenylnaphthalene-2-carboxylic acid.

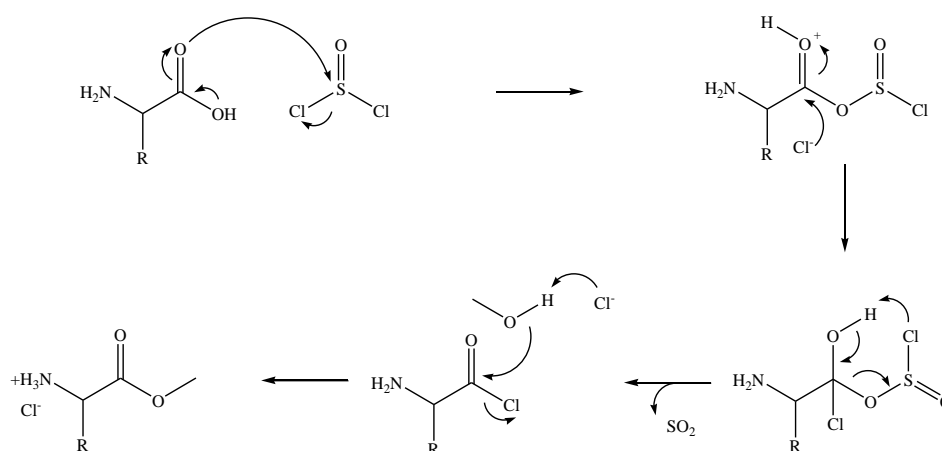
Hydrolysis of the ferrocenyl carboxylate ester in 10 % sodium hydroxide removes the ester group to produce ferrocenyl carboxylate.

### 2.2.1.3 Preparation of dipeptides

Dipeptides were prepared by EDC coupling of the *N*-terminus of one amino acid with the *C*-terminus of the other. In order to achieve regiospecific coupling it was necessary to protect the *C*-terminus of the amino acids or dipeptides prior to condensation with the ferrocenyl carboxylic acid. The most common method of protection is esterification. This increases the compounds solubility in organic solvent, ensures that an amide bond rather than an anhydride is formed and that only mono addition products are formed.

The conversion of the carboxylic acid to the ester was achieved by treatment of the amino acid or dipeptide with thionyl chloride in the presence of the appropriate alcohol to give the

ester hydrochloride salt (scheme 2.5). The hydrochloride salt may be neutralised to give the corresponding free base, however, these decompose rapidly at room temperature. They are therefore generated as required *in situ* by neutralisation with triethylamine (Et<sub>3</sub>N).



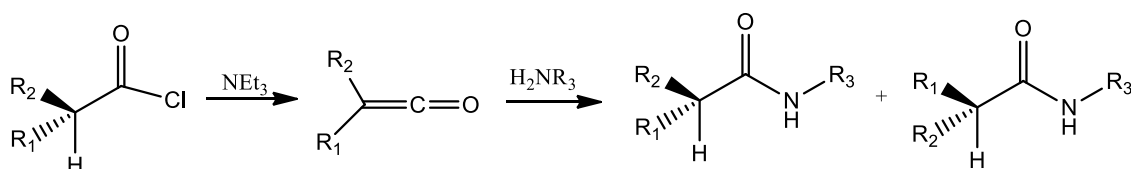
**Scheme 2.5:** Ester formation using thionyl chloride and methanol.

#### 2.2.1.4 Amide bond formation

Carboxylic acids are capable of reacting with amines to form an amide bond, however elevated temperatures are required in the range of 160-180 °C. These temperatures are detrimental to complex peptides. As a result peptide synthesis is usually performed at or below room temperature and either the amino group or the carboxylic acid is activated. A practical method of activating the amino group has not been found. Electron donating groups should increase the nucleophilicity of the nitrogen, however it has been found that this also decreases the rate of acylation. Therefore activation of the carboxyl group remains the method used in peptide bond formation. It is required that the carboxylic acid is activated since carboxylic acids form salts with amines at room temperature under normal conditions. The sensitivity of the carbonyl towards nucleophilic attack is reduced by the hydroxyl group particularly if the nucleophile is sufficiently basic to form a carboxylate anion. Therefore the -OH group of the acid must be converted into a good leaving group before treatment with the amine. This is typically achieved using peptide coupling reagents.

#### 2.2.1.4.1 Acyl chlorides

The simplest way of creating an amide bond is by converting the carboxylic acid to an acyl chloride before coupling. The acyl chloride is reacted with the desired amine. Acyl chlorides are formed using reagents such as thionyl chloride ( $\text{SOCl}_2$ ), oxalyl chloride ( $\text{COCl}_2$ ), phosphorus trichloride ( $\text{PCl}_3$ ), phosphorus oxychloride ( $\text{POCl}_3$ ) and phosphorus pentachloride ( $\text{PCl}_5$ ). Additional base is usually required to trap the HCl generated and avoid conversion of the amine to the unreactive HCl salt. Couplings are normally performed in dry solvents in the presence of a non-nucleophilic tertiary amine such as  $\text{Et}_3\text{N}$ . Acyl chlorides have limited value in peptide coupling because of the danger of hydrolysis, racemisation and cleavage of protecting groups. The tendency of acyl chlorides to racemise under basic conditions can be illustrated by the standard synthesis of ketenes (scheme 2.6). Ketenes are formed by reacting the  $\alpha$ -proton of an acyl chloride with  $\text{Et}_3\text{N}$ . The ketene can then react with an amine to yield the corresponding addition product with a loss of chirality.

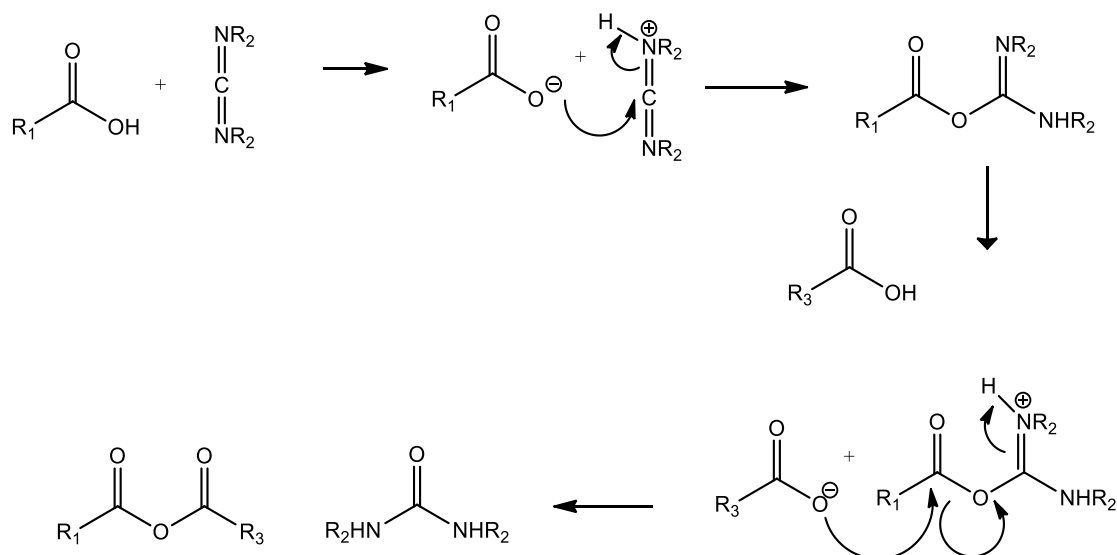


**Scheme 2.6:** Potential racemisation via ketene formation.

#### 2.2.1.4.2 Anhydrides

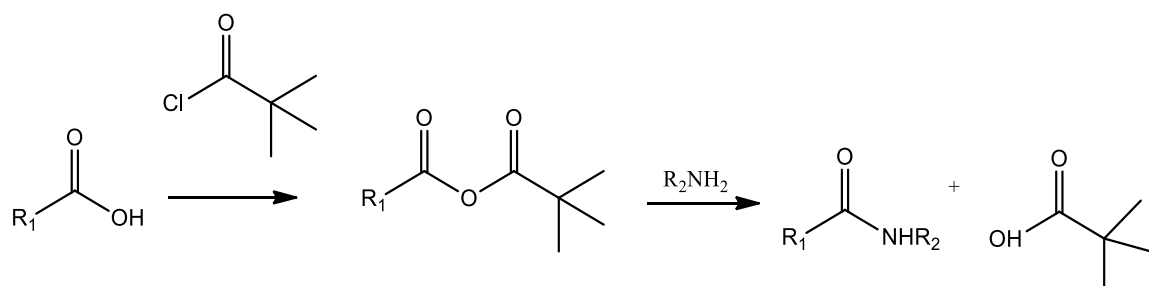
Symmetrical and mixed anhydrides have been used in amide bond formation. The desired anhydride is usually prepared beforehand. This is usually achieved by heating the acid or reacting two equivalents of the acid with one equivalent of a reagent such as 1,3-dicyclohexylcarbodiimide (DCC) to prepare a symmetrical anhydride (scheme 2.7). The driving force of the reaction is the formation of a urea by product. The anhydride is then reacted with the selected amine. In theory no base is required as a carboxylate anion is generated *in situ*. The main limitation is that only half of the acid is effectively coupled with the second half wasted.





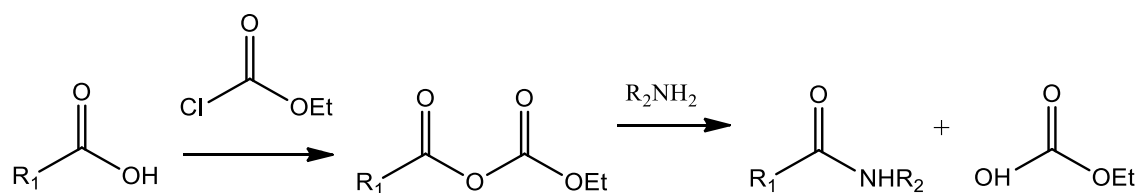
**Scheme 2.7:** Formation of a symmetrical anhydride.

To overcome the problem of waste, mixed anhydride methods have been developed where the second molecule of acid is cheap and easy to couple to the carboxyl moiety. However difficulty can occur in mixed carboxylic anhydrides getting regioselectivity of nucleophilic addition. Mixed pivalic anhydrides will give the desired aminolytic selectivity due to the presence of the bulky tert-butyl group (scheme 2.8)<sup>20</sup>.



**Scheme 2.8:** Coupling via mixed pivalic anhydride.

Mixed carbonic anhydrides give excellent selectivity (scheme 2.9). The carbonate electrophilic centre is more reactive than the carboxylic site as it is less stabilised by resonance.



**Scheme 2.9:** Coupling via mixed carbonic anhydrides.

#### 2.2.1.4.3 Carbodiimides

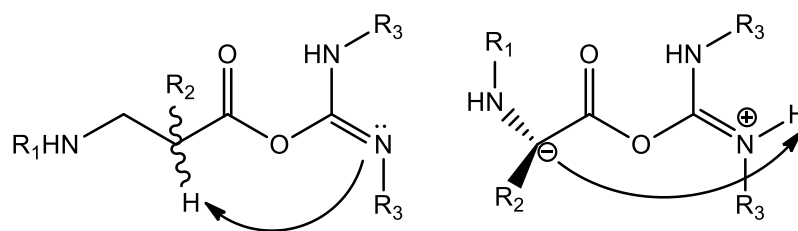
Carbodiimides are used to activate carboxylic acids towards nucleophilic attack. In 1955 Sheehan and Hess proposed DCC as a peptide bond forming reagent<sup>21</sup>. Activation occurs through addition to an N=C double bond in the diimide. Commonly used carbodiimides include 1,3-dicyclohexylcarbodiimide (DCC), *N,N*-diisopropylcarbodiimide (DIC), *N*-(3-dimethylaminopropyl)-*N'*-ethylcarbodiimide hydrochloride (EDC). The first step of peptide coupling involves addition of the carboxylic acid to the carbodiimide to give an *O*-acylisourea intermediate.

There are several disadvantages to the use of carbodiimides as coupling reagents for amide bond formation. The *N,N'*-dicyclohexylurea by-product is insoluble in most organic solvents, however it is not entirely insoluble especially in the presence of other dissolved materials. It therefore frequently contaminates the product of coupling. This can be avoided by the use of water soluble carbodiimides. The salts of the urea derivatives may be removed by extraction with water.

Of the 20 amino acids constituent of proteins only alanine and leucine are immune to side chain reactions, though not racemisation. A common cause of these side reactions is the presence of tertiary bases present in the reaction mixture during activation and coupling. These can be somewhat reduced by the avoidance of tertiary bases and the use of unprotected amines, as well as amine salts.

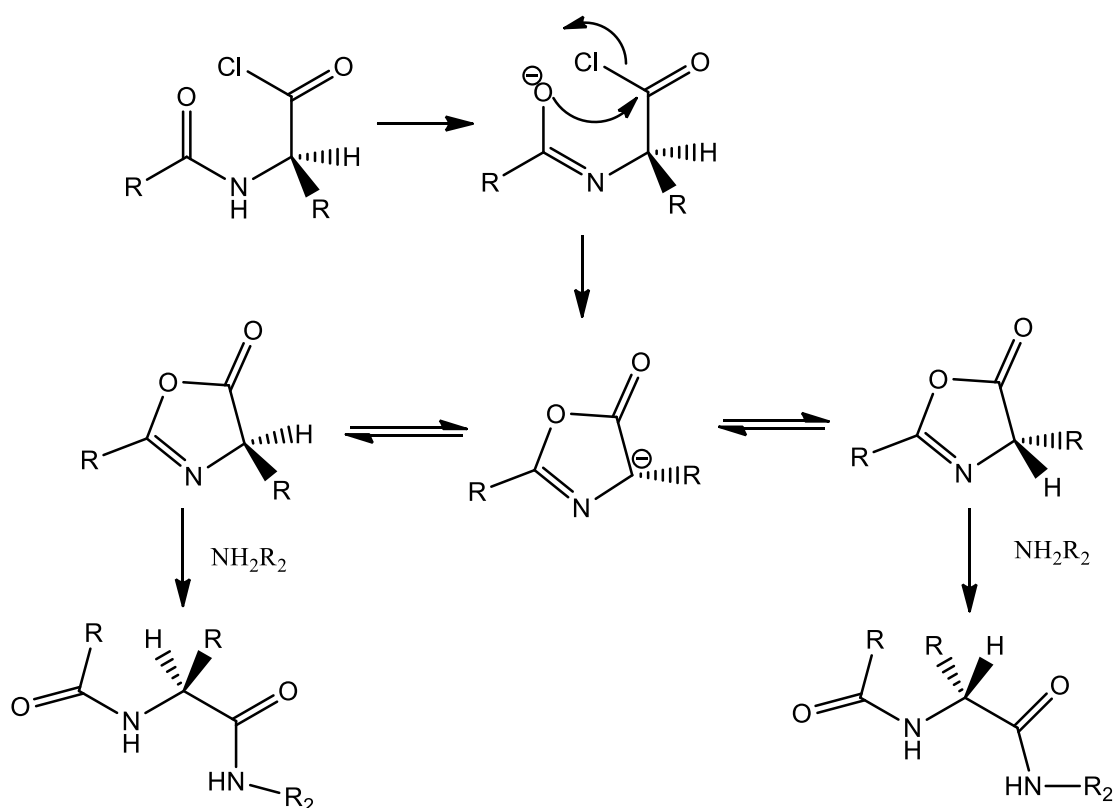
##### 2.2.1.4.3.1 Racemisation.

Racemisation is an almost exclusively base induced side reaction and is usually only a problem at activation and coupling. Deprotonation can occur at the  $\alpha$ -carbon of an  $\alpha$ -amino acid. This results in a carbanion intermediate which may reprotonate on either side (scheme 2.10).



**Scheme 2.10:** Racemisation by proton abstraction

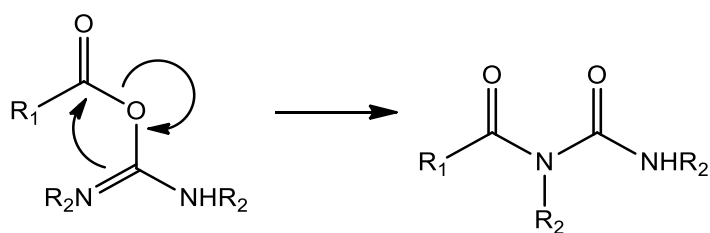
Racemisation may also occur through oxazolone formation. Activated acyl amino acids and peptides will cyclise under the influence of base to give oxazolones (scheme 2.11). The oxazolones are themselves activated towards aminolysis and will lead to peptide formation, however, racemisation can occur via the stabilised carbanion.



**Scheme 2.11:** Racemisation via acyl chlorides.

#### 2.2.1.4.3.2 Intramolecular acyl transfer.

Carbodiimides may also be subject to several side reactions which can limit product yield and interfere with product purification. Intramolecular rearrangement of the *O*-acylisourea derivative is a possible side reaction with the use of carbodiimides (scheme 2.12). Attack of the nearby nucleophile on the activated carbon can result in an *O* to *N* shift giving an *N*-acylurea as a by-product<sup>22</sup>.

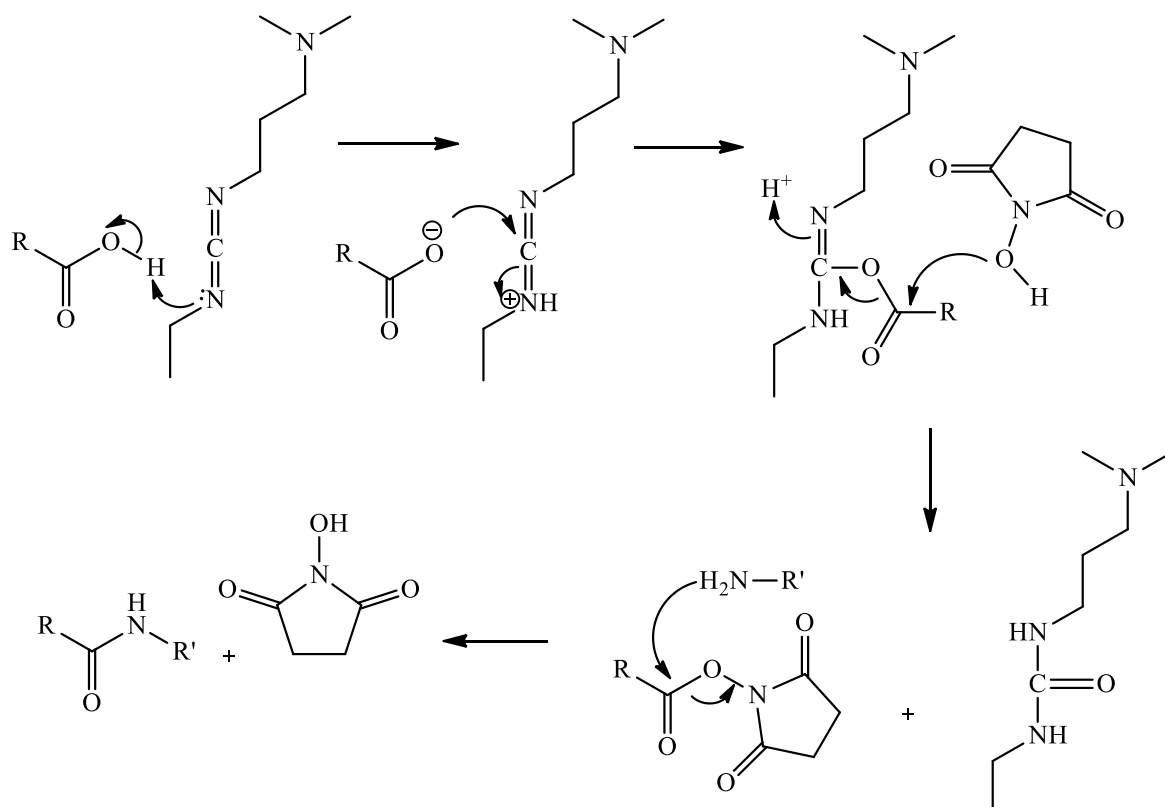


**Scheme 2.12:** Acyl transfer from *O*-acylisourea to *N*-acylurea.

This is undesirable not only because it results in a loss of the desired product but separation of these from the desired product may be difficult. Use of DCC may also be accompanied by racemisation at the carboxyl terminal residue.

#### 2.2.1.4.3.3 Auxiliary Nucleophiles

Some of the shortcomings of DCC can be overcome by the use of additives. 1-hydroxybenzotriazole (HOBt), *N*-hydroxysuccinimide (NHS) and 3-hydroxy-3,4-dihydro-1,2,3-benzotriazin-4-one (HOObt) are some of the most frequently used. These were initially introduced to reduce the racemisation of the peptides. These act as a secondary nucleophile and accelerate the reaction and convert overactive intermediates of the reaction to less reactive esters of HOBt or NHS (scheme 2.13).



**Scheme 2.13:** Peptide coupling using EDC and NHS.

### 2.2.2 Purification and yields of *N*-(6-ferrocenyl-2-naphthoyl), *N*-{*para*-(ferrocenyl)cinnamoyl} and *N*-{*para*-(ferrocenyl)benzoyl} amino acid and dipeptide derivatives.

The *N*-(6-ferrocenyl-2-naphthoyl), *N*-{*para*-(ferrocenyl)cinnamoyl} and *N*-{*para*-(ferrocenyl)benzoyl} amino acid and dipeptide derivatives were prepared by standard peptide coupling conditions. The corresponding carboxylic acid was coupled with the *N*-terminal of the Boc protected dipeptide. The crude product was purified by column chromatography using ethyl acetate and hexane as an eluent. The purified compounds were obtained as orange or red solids with yields ranging from 15 % to 96 %. All compounds gave spectroscopic and analytical data in accordance with their proposed structures.

Yields obtained for the *N*-(6-ferrocenyl-2-naphthoyl)-glycine-glycine esters were generally better than those obtained for the *N*-{*para*-(ferrocenyl)benzoyl}-glycine-glycine esters. The *N*-{*para*-(ferrocenyl)cinnamoyl} dipeptide esters showed the lowest yields overall. Given that none of the substituents are closely positioned around the conjugated linker and that the amino acid chains do not possess any bulky side groups this is unlikely to be due to steric effects as has been noted in the case of *N*-*ortho* and *meta* (ferrocenyl)benzoyl dipeptide

esters<sup>23</sup> and *N*-(3-ferrocenyl-2-naphthoyl) dipeptide esters<sup>24</sup>. Yields are typically low for secondary amino acids such as sarcosine which has been attributed to the spontaneous formation of diketopiperazine on removal of the Boc group.

Yields for the free carboxylic acid compounds were generally higher than the esters as a simple hydrolysis of the ester followed by filtration resulted in the final compound without need for further purification.

**Table 2.2:** Percentage yields for *N*-(6-ferrocenyl-2-naphthoyl) amino acid and dipeptide derivatives.

Compound	Number	%Yield
<i>N</i> -(6-ferrocenyl-2-naphthoyl)-Gly-Gly-OMe	100	51 %
<i>N</i> -(6-ferrocenyl-2-naphthoyl)-Gly-Gly-OPr	101	55 %
<i>N</i> -(6-ferrocenyl-2-naphthoyl)-Gly-Gly-OBu	102	78 %
<i>N</i> -(6-ferrocenyl-2-naphthoyl)-Gly-Gly-OBn	103	66 %
<i>N</i> -(6-ferrocenyl-2-naphthoyl)-Sar-Gly-OMe	104	20 %
<i>N</i> -(6-ferrocenyl-2-naphthoyl)-GABA-OMe	105	50 %
<i>N</i> -(6-ferrocenyl-2-naphthoyl)-Gly-L-Ala-OMe	106	26 %
<i>N</i> -(6-ferrocenyl-2-naphthoyl)-Gly-D-Ala-OMe	107	47 %
<i>N</i> -(6-ferrocenyl-2-naphthoyl)-Gly-Gly-OH	108	59 %
<i>N</i> -(6-ferrocenyl-2-naphthoyl)-Sar-Gly-OH	109	72 %
<i>N</i> -(6-ferrocenyl-2-naphthoyl)-GABA-OH	110	90 %
<i>N</i> -(6-ferrocenyl-2-naphthoyl)-Gly-L-Ala-OH	111	95 %
<i>N</i> -(6-ferrocenyl-2-naphthoyl)-Gly-D-Ala-OH	112	96 %

**Table 2.3:** Percentage yields for *N*-{*para*-(ferrocenyl)cinnamoyl} and *N*-{*para*-(ferrocenyl)benzoyl} amino acid and dipeptide derivatives.

Compound	Number	% Yield
<i>N</i> -{ <i>para</i> -(ferrocenyl)cinnamoyl}-Gly-Gly-OEt	113	46 %
<i>N</i> -{ <i>para</i> -(ferrocenyl)cinnamoyl}-Sar-Gly-OEt	114	16 %
<i>N</i> -{ <i>para</i> -(ferrocenyl)cinnamoyl}-GABA-OEt	115	46 %
<i>N</i> -{ <i>para</i> -(ferrocenyl)cinnamoyl}-Gly-L-Ala-OEt	116	36 %
<i>N</i> -{ <i>para</i> -(ferrocenyl)cinnamoyl}-Gly-D-Ala-OEt	117	18 %
<i>N</i> -{ <i>para</i> -(ferrocenyl)benzoyl}-Gly-Gly-OH	118	92 %
<i>N</i> -{ <i>para</i> -(ferrocenyl)benzoyl}-Gly-Gly-OMe	119	15 %
<i>N</i> -{ <i>para</i> -(ferrocenyl)benzoyl}-Gly-Gly-OEt	120	82 %
<i>N</i> -{ <i>para</i> -(ferrocenyl)benzoyl}-Gly-Gly-OPr	121	60 %
<i>N</i> -{ <i>para</i> -(ferrocenyl)benzoyl}-Gly-Gly-OBu	122	46 %
<i>N</i> -{ <i>para</i> -(ferrocenyl)benzoyl}-Gly-Gly-OBn	123	24 %

### 2.2.3 <sup>1</sup>H NMR studies of *N*-(6-ferrocenyl-2-naphthoyl), *N*-{*para*-(ferrocenyl)cinnamoyl} and *N*-{*para*-(ferrocenyl)benzoyl} amino acid and dipeptide derivatives.

All of the <sup>1</sup>H NMR experiments were carried out in DMSO-*d*<sub>6</sub> as the compounds showed limited solubility in other deuterated solvents. The amide protons appear downfield in the range  $\delta$  8.06-8.96. The appearance of these signals in the lowfield region is due to hydrogen bonding between the S=O group of the DMSO and the proton of the amide. In CDCl<sub>3</sub> amide protons typically appear further upfield.

In the *N*-(6-ferrocenyl-2-naphthoyl) amino acid and dipeptide derivatives the aromatic region shows a singlet, singlet, multiplet doublet doublet splitting pattern, integrating for one, one, three and one protons respectively. In the *N*-{*para*-(ferrocenyl)cinnamoyl} amino acid and dipeptide derivatives the aromatic region shows the characteristic *para* disubstituted splitting pattern of two apparent doublets integrating for two protons each. The *trans* olefinic protons appear as two doublets each integrating for 2 protons in the range  $\delta$  6.5-7.5 with coupling constants of 16 Hz. Similarly in the *N*-{*para*-(ferrocenyl)benzoyl} amino acid and dipeptide derivatives the aromatic region shows the characteristic *para* disubstituted splitting pattern of two apparent doublets.

The aromatic peaks of the ferrocene appear upfield of the aromatic region. The protons of ferrocene experience more shielding than the protons of benzene as ferrocene is more electron dense. The ferrocenyl region of *N*-(6-ferrocenyl-2-naphthoyl), *N*-{*para*-(ferrocenyl)cinnamoyl} and *N*-{*para*-(ferrocenyl)benzoyl} amino acid and dipeptide derivatives are relatively similar and confirm the presence of a monosubstituted ferrocene ring. In the *N*-(6-ferrocenyl-2-naphthoyl) derivatives the *ortho* protons appear as a fine triplet or singlet in the range  $\delta$  4.96-5.03. The *meta* protons typically appear as a fine triplet or singlet from  $\delta$  4.45-4.46 and the unsubstituted ( $\eta^5$ -C<sub>5</sub>H<sub>5</sub>) protons appear as a singlet at  $\delta$  4.04 - 4.05. In the *N*-{*para*-(ferrocenyl)cinnamoyl} derivatives the signals are slightly further upfield. The *ortho* protons appear at  $\delta$  4.90, the *meta* at  $\delta$  4.39-4.45 and the ( $\eta^5$ -C<sub>5</sub>H<sub>5</sub>) protons appear at  $\delta$  4.02-4.09. For the *N*-{*para*-(ferrocenyl)benzoyl} derivatives the *ortho* protons typically appear as a fine triplet or singlet from  $\delta$  4.45-4.46, the *meta* from  $\delta$  4.41-4.42 and the ( $\eta^5$ -C<sub>5</sub>H<sub>5</sub>) protons from  $\delta$  4.02-4.09.

**Table 2.4:** Selected  $^1\text{H}$  NMR spectral data ( $\delta$ ,  $\text{DMSO-}d_6$ ) for *N*-(6-ferrocenyl-2-naphthoyl), *N*-{*para*-(ferrocenyl)cinnamoyl} and *N*-{*para*-(ferrocenyl)benzoyl} amino acid and dipeptide derivatives.

Compound	NH's	N(CH <sub>3</sub> )	$\alpha\text{H}$	<i>ortho</i> $\eta^5(\text{C}_5\text{H}_4)$	<i>meta</i> $\eta^5(\text{C}_5\text{H}_4)$	$\eta^5(\text{C}_5\text{H}_5)$
100	8.42, 8.95	-	-	4.97	4.46	4.05
101	8.40, 8.95	-	-	4.96	4.45	4.05
102	8.39, 8.95	-	-	4.97	4.46	4.05
103	8.06, 8.96	-	-	4.96	4.45	4.05
104	8.59 & 8.51	3.02	-	5.03	4.95	4.04
105	8.66	-	-	4.96	4.45	4.05
106	8.85, 8.45	-	4.34	4.97	4.46	4.05
107	8.85, 8.46	-	4.34	4.97	4.46	4.05
108	8.96, 8.46	-	-	4.96	4.45	4.05
109	8.66 & 8.57	3.01	-	4.97	4.46	4.05
110	8.66	-	-	4.96	4.45	4.04
111	8.30, 8.85	-	4.26	4.97	4.45	4.04
112	8.27, 8.90	-	4.23	4.98	4.45	4.05
113	8.36 - 8.42	-	-	4.85	4.40	4.03
114	8.58 & 8.37	3.20 & 2.93	-	4.87	4.40	4.08
115	8.12	-	-	4.84	4.39	4.03-4.09
116	8.40, 8.31	-	4.27	4.85	4.40	4.02
117	8.42, 8.31	-	4.27	4.85	4.40	4.03
118	7.98, 8.81	-	-	4.87	4.41	4.03
119	8.78, 8.37	-	-	4.90	4.42	4.02
120	8.79, 8.35	-	-	4.90	4.41	4.07
121	8.78, 8.36	-	-	4.90	4.42	3.96-4.02
122	8.78, 8.35	-	-	4.90	4.42	4.02-4.11
123	8.80, 8.40	-	-	4.90	4.42	4.02



#### 2.2.4. $^1\text{H}$ NMR study of *N*-(6-ferrocenyl-2-naphthoyl)-glycine-L-alanine methyl ester (**106**).

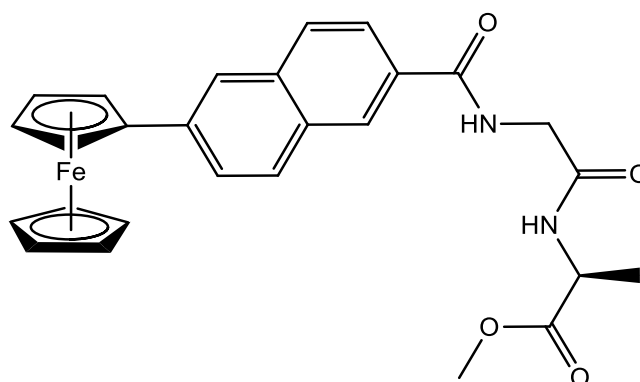


**Figure 2.4:** *N*-(6-ferrocenyl-2-naphthoyl)-glycine-L-alanine methyl ester **106**.

In the  $^1\text{H}$  NMR spectrum of *N*-(6-ferrocenyl-2-naphthoyl)-glycine-L-alanine methyl ester **106** the naphthoyl amide proton peak appears downfield at  $\delta$  8.85 as a triplet due to coupling with the methylene protons of glycine. The second amide proton signal overlaps with a singlet due to an aromatic proton in the range  $\delta$  8.44-8.45. The remainder of the aromatic region appears in the range  $\delta$  7.83-8.06 and has the characteristic singlet, multiplet, doublet doublet splitting pattern integrating for one, three and one protons respectively which has been seen for the 2,6-disubstituted naphthalene ring<sup>24</sup>. In the ferrocenyl region the *ortho* ( $\eta^5\text{-C}_5\text{H}_4$ ) protons appear furthest downfield as a fine triplet at  $\delta$  4.97 with a coupling constant of 1.6 Hz, while the *meta* ( $\eta^5\text{-C}_5\text{H}_4$ ) protons appear also as a triplet at  $\delta$  4.46. Each integrates for 2 protons. The  $\alpha$ -proton of the L-alanine residue appears at  $\delta$  4.34 as a quintet. The signal for the unsubstituted ( $\eta^5\text{-C}_5\text{H}_5$ ) ring appears at  $\delta$  4.05. The methylene protons of the glycine residue are observed as two doublets of doublets at  $\delta$  3.93 and 4.02. The splitting pattern is due to the chiral centre in the molecule. The methylene protons of the glycine residue are diastereotopic due to the presence of the L-alanine and geminal coupling is observed with a coupling constant of 10.8 Hz together with coupling to the amide proton with a coupling constant of 6 Hz. The methyl ester appears as a singlet integrating for 3 protons at  $\delta$  3.64 and the L-alanine methyl group appears as a doublet at  $\delta$  1.32.

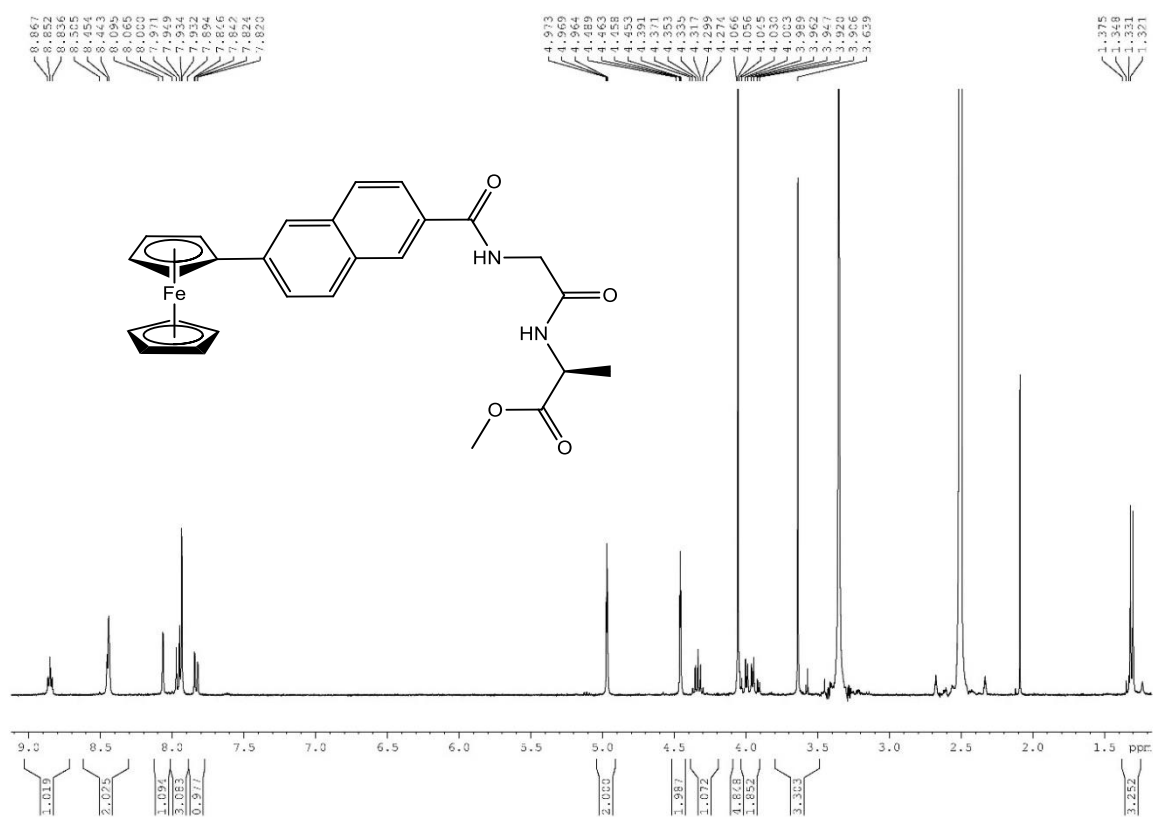


**Figure 2.5:** <sup>1</sup>H NMR spectrum of *N*-(6-ferrocenyl-2-naphthoyl)-glycine-L-alanine methyl ester **106**.

### 2.2.5 <sup>1</sup>H NMR study of *N*-{*para*-(ferrocenyl)cinnamoyl}- $\gamma$ -amino butyric acid ethyl ester (**115**).

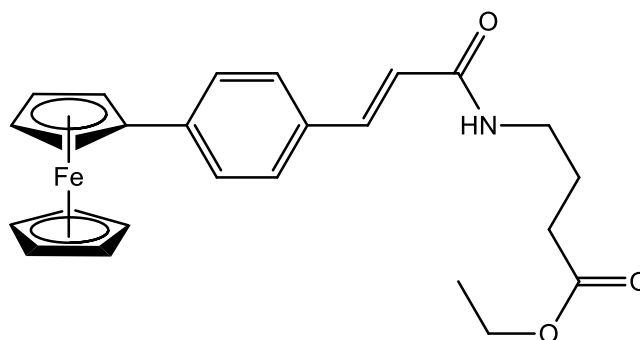


**Figure 2.6:** *N*-{*para*-(ferrocenyl)cinnamoyl}- $\gamma$ -amino butyric acid ethyl ester **115**.

In the <sup>1</sup>H NMR spectrum of *N*-{*para*-(ferrocenyl)cinnamoyl}- $\gamma$ -amino butyric acid ethyl ester **115** the amide proton peak appears downfield at  $\delta$  8.12. The signal appears as a triplet due to coupling with the adjacent methylene protons of the  $\gamma$ -aminobutyric acid. The aromatic protons appear downfield at  $\delta$  7.57 and 7.48. They display the characteristic *para* splitting pattern of a disubstituted benzene ring with two apparent doublets. The olefinic protons



### 2.2.6 $^1\text{H}$ NMR study of *N*-{*para*-(ferrocenyl)benzoyl}-glycine-glycine benzyl ester (123).

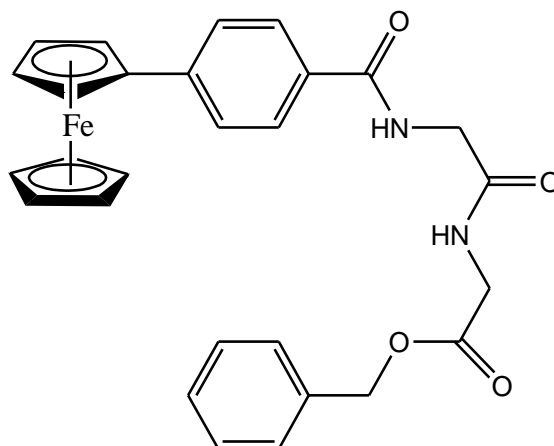


**Figure 2.8:** *N*-{*para*-(ferrocenyl)benzoyl}-glycine-glycine benzyl ester **123**.

In the  $^1\text{H}$  NMR spectrum of *N*-{*para*-(ferrocenyl)benzoyl}-glycine-glycine benzyl ester **123** the amide proton peaks appear downfield at  $\delta$  8.80 and 8.40. Each appears as a triplet due to coupling with the methylene protons of the glycine residue. The aromatic protons appear as two apparent doublets at  $\delta$  7.84 and 7.64 as is characteristic of *para* disubstituted aromatic compounds. The aromatic protons of the benzyl ester appear as a multiplet integrating from  $\delta$  7.40-7.30. The methylene protons of the ester appear as a singlet at  $\delta$  5.14. In the ferrocenyl region the *ortho* protons on ( $\eta^5\text{C}_5\text{H}_4$ ) appear as a fine triplet with a coupling constant of 1.6 Hz at  $\delta$  4.90. The *meta* protons on ( $\eta^5\text{C}_5\text{H}_4$ ) also appear as a fine triplet at  $\delta$  4. The singlet due to the unsubstituted ( $\eta^5\text{C}_5\text{H}_5$ ) appears at 4.02 and integrates for 5 protons. The methylene protons of the glycine residues appear as a doublet at  $\delta$  3.94.

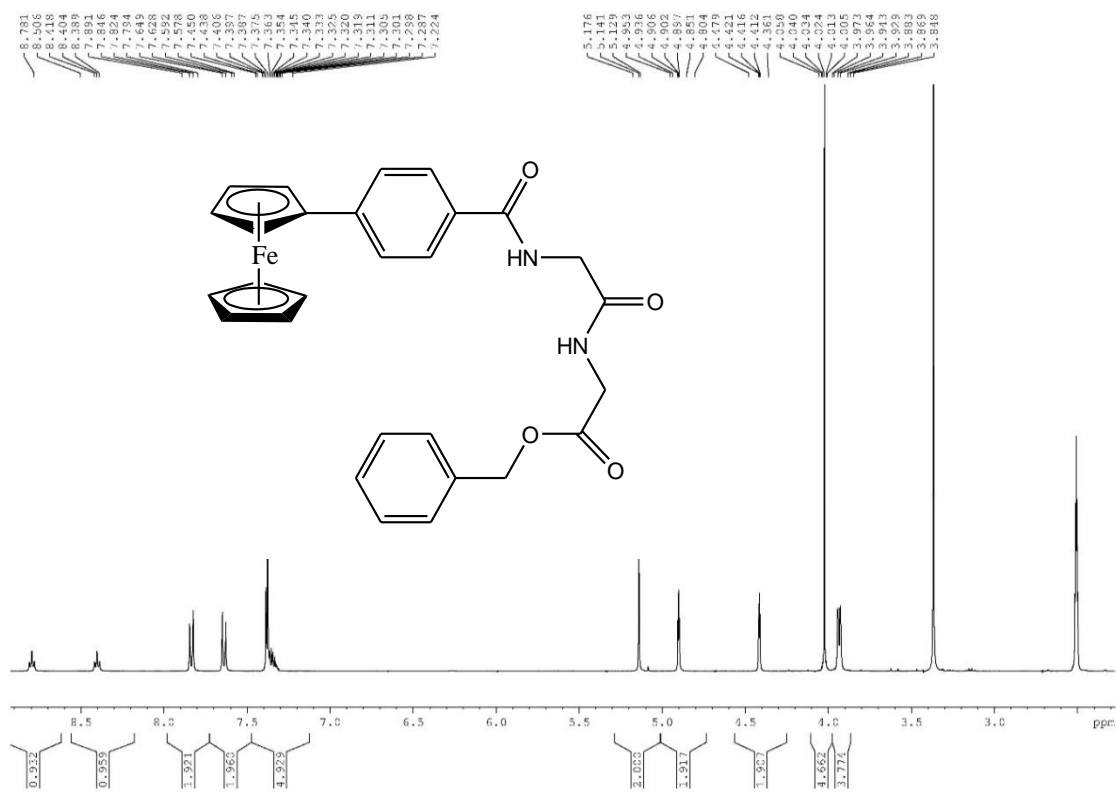


**Figure 2.9:** <sup>1</sup>H NMR spectrum of *N*-{*para*-(ferrocenyl)benzoyl}-glycine-glycine benzyl ester **123**.

### 2.2.7 Variable temperature study of *N*-(6-ferrocenyl-2-naphthoyl)-sarcosine-glycine methyl ester (**104**).

Rotamers are conformational isomers in which rotations around formally single bonds are restricted. The presence of rotamers in solution complicates the  $^1\text{H}$  NMR spectrum. The *N*-methyl group gives rise to multiple signals in the  $^1\text{H}$  NMR spectrum. The amide bond is characterised by short bond lengths, co-planarity and restricted rotation around the C-N bond. Rotation about the C-N bond is intrinsically hindered due to its significant double bond nature.

Usually the *trans* conformers of peptide amide bonds are thermodynamically favoured as there is less steric hindrance from the groups at either end of the C-N bond than with the *cis* isomer. This is the case for secondary amides where the *cis* isomer concentration is less than 1 %, however in tertiary amides the steric hindrance is similar for both *cis* and *trans* isomers.

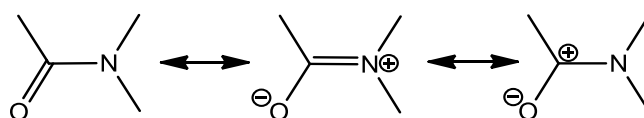


**Figure 2.10:** Resonance structures of the amide bond<sup>25</sup>.

Rotations around single bonds are restricted by a rotational energy barrier which must be overcome to interconvert one form to another. When the solution is heated to the coalescence temperature the barrier is overcome and the two forms may interconvert and a single broad signal is seen. As the temperature is raised the two forms interconvert more rapidly and a sharp signal is seen.

The  $^1\text{H}$  NMR spectrum of *N*-(6-ferrocenyl-2-naphthoyl)-sarcosine-glycine methyl ester gives rise to multiple signals in the NMR due to the presence of rotamers in solution caused by the presence of the *N*-methyl group. The rate of interconversion of the rotamers is slow on the NMR timescale, therefore NMR experiments must be performed at a higher temperature to increase the rate of interconversion.

A variable temperature study of the  $^1\text{H}$  NMR spectrum of *N*-(6-ferrocenyl-2-naphthoyl)-sarcosine-glycine methyl ester (**104**) was performed at 20, 30, 40, 50, 60, 70 and 80 °C in DMSO- $d_6$  (figure 2.12).

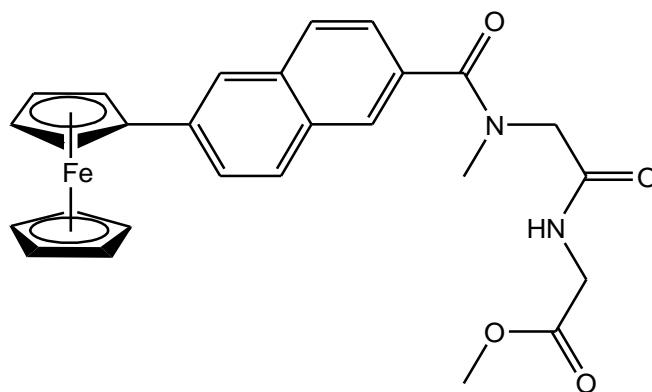


**Figure 2.11:** *N*-(6-ferrocenyl-2-naphthoyl)-sarcosine-glycine methyl ester **104**.

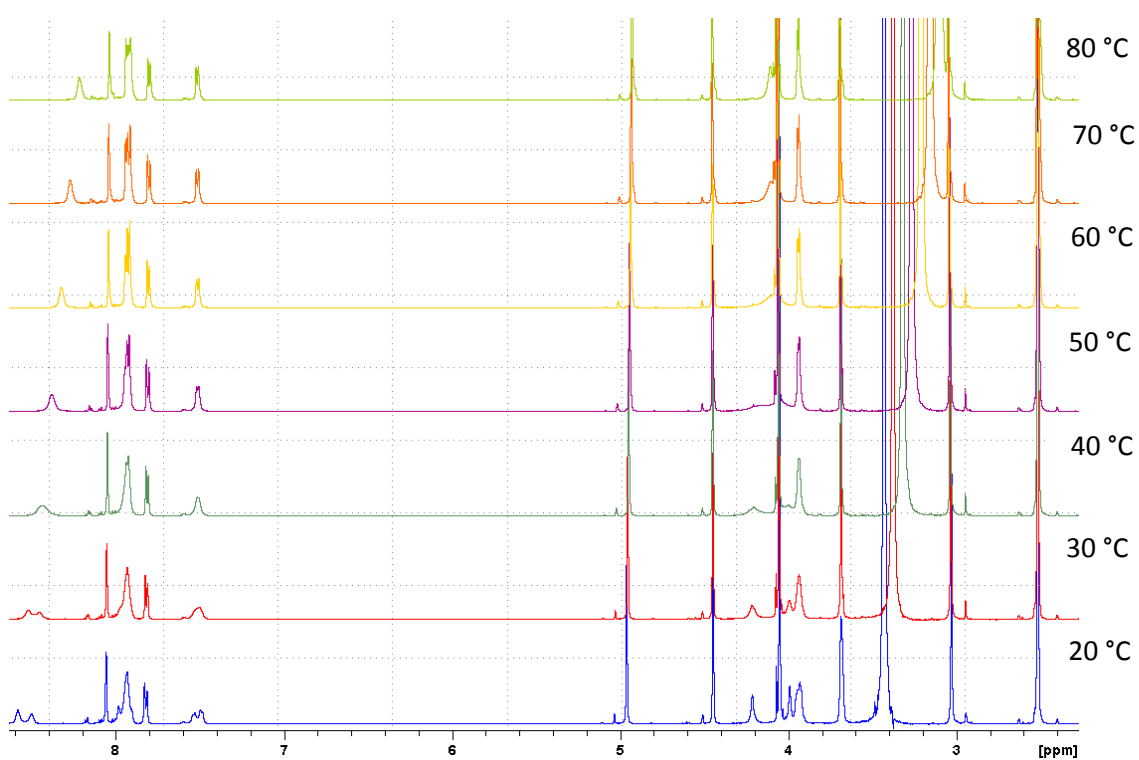


**Figure 2.12:** The  $^1\text{H}$  NMR spectrum of *N*-(6-ferrocenyl-2-naphthoyl)-sarcosine-glycine methyl ester **104** at 20, 30, 40, 50, 60, 70, and 80 °C.

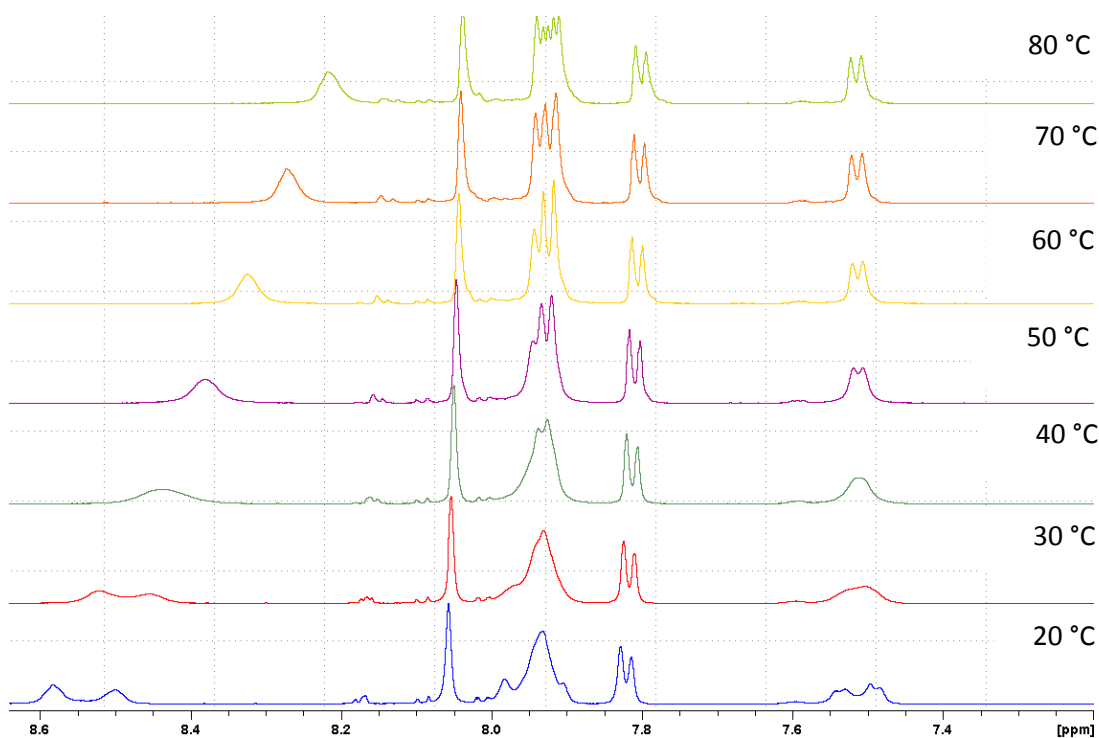


**Figure 2.13:** Variable temperature  $^1\text{H}$  NMR study of *N*-(6-ferrocenyl-2-naphthoyl)-sarcosine-glycine methyl ester **104**: the aromatic region (7.4-8.6 ppm).

At the coalescence temperature the signals due to separate rotamers coalesce to give a single broad signal. Above this the signal will become a sharp peak as the exchange between rotamers is rapid. In the aromatic region the amide proton of the glycine residue gives rise to two broad singlets at  $\delta$  8.59 and 8.51 at 20 °C (figure 2.13). As the temperature is raised these singlets broaden further, shifting slightly upfield and coalesce at 40 °C. Above 40 °C the signal sharpens.



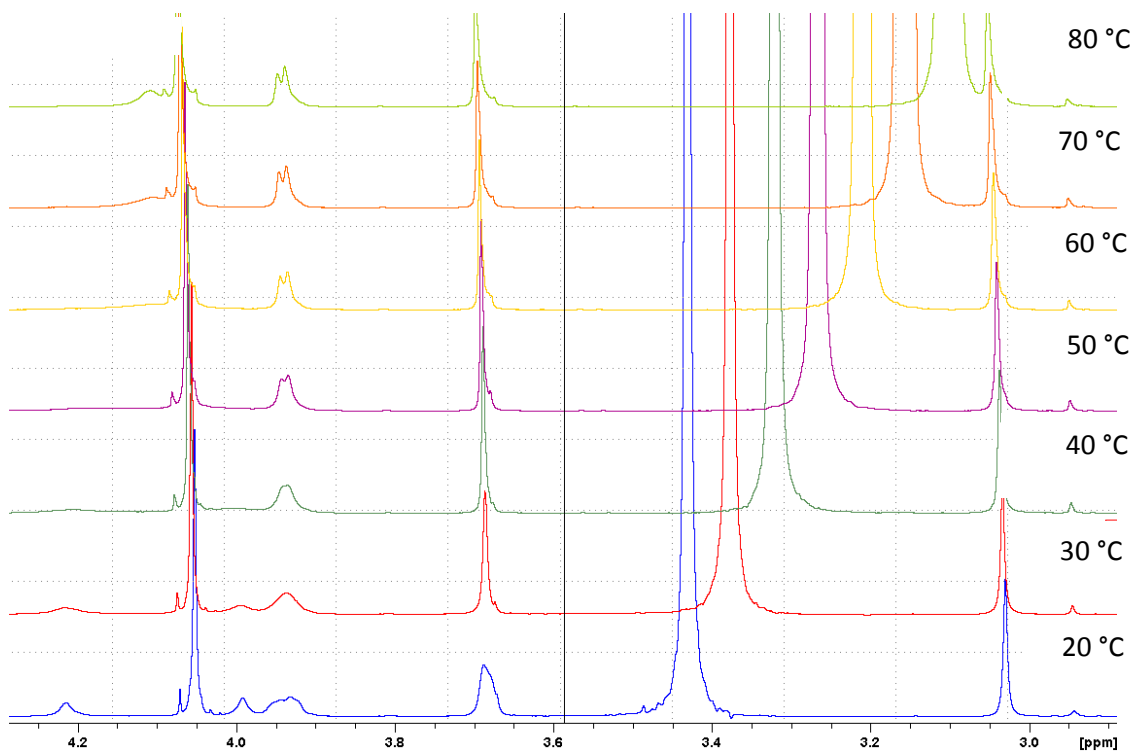


**Figure 2.14:** Variable temperature  $^1\text{H}$  NMR study of *N*-(6-ferrocenyl-2-naphthoyl)-sarcosine-glycine methyl ester **104**; the *N*-methyl region (3.0-4.3 ppm).

In the ferrocenyl region of the spectrum the methylene protons of the sarcosine residue appear at  $\delta$  4.2 and 4.0 as 2 broad singlets (figure 2.14). These broaden further as the temperature is raised. At 80 °C a broad singlet can be seen at  $\delta$  4.11. The methyl ester group appears as a broad singlet at  $\delta$  3.66 at 20 °C, however from 30 °C this becomes a sharp signal.

### 2.2.8 $^{13}\text{C}$ NMR and DEPT 135 NMR studies of *N*-(6-ferrocenyl-2-naphthoyl), *N*-{*para*-(ferrocenyl)cinnamoyl} and *N*-{*para*-(ferrocenyl)benzoyl} amino acid and dipeptide derivatives.

In the DEPT 135 spectrum methylene carbons typically appear negative, while methyl and methine carbons appear positive. Non proton bearing carbons do not appear in the DEPT spectrum.

In the  $^{13}\text{C}$  NMR the carbonyl groups due to the amide and ester groups are found in the range  $\delta$  165.1-175.2. In the *N*-(6-ferrocenyl-2-naphthoyl) derivatives the aromatic carbons appear as 10 signals in the range  $\delta$  122.7 - 138.9. The four quaternary carbons were identified using DEPT 135. In the  $^{13}\text{C}$  NMR of the *N*-{*para*-(ferrocenyl)cinnamoyl} derivatives the aromatic carbons appear as 4 signals in the range  $\delta$  120.6 – 140.9. The olefinic carbons of the *N*-{*para*-(ferrocenyl)cinnamoyl} derivatives appear in the range  $\delta$  120.7 - 140.9. In the  $^{13}\text{C}$  NMR of the *N*-{*para*-(ferrocenyl)benzoyl} derivatives the aromatic carbons appear as 4 signals in the range  $\delta$  125.3-148.3.

In the ferrocenyl region carbon signals appear in the range  $\delta$  66.4 - 88.4. In the  $^{13}\text{C}$  NMR of the *N*-(6-ferrocenyl-2-naphthoyl) derivatives the *ipso* carbon on the substituted cyclopentadienyl ring appears from  $\delta$  84.0 - 84.1. The unsubstituted ( $\eta^5\text{-C}_5\text{H}_5$ ) ring appears at  $\delta$  69.4-69.5. The signal due to the *meta* ( $\eta^5\text{-C}_5\text{H}_4$ ) carbons is in close proximity to ( $\eta^5\text{-C}_5\text{H}_5$ ) or overlapping at  $\delta$  69.4, while the *ortho* carbons appear at  $\delta$  66.6.

In the  $^{13}\text{C}$  NMR of the *N*-{*para*-(ferrocenyl)cinnamoyl} derivatives the location of the ferrocenyl signals is similar, with the *ipso* ( $\eta^5\text{-C}_5\text{H}_4$ ) carbon appearing at  $\delta$  83.7, the ( $\eta^5\text{-C}_5\text{H}_5$ ) carbon appearing at  $\delta$  69.4 and the *meta* and *ortho* carbons appearing at  $\delta$  69.3 and  $\delta$  66.4-66.5. In the  $^{13}\text{C}$  NMR of the *N*-{*para*-(ferrocenyl)benzoyl} derivatives the signals appear over a slightly wider range, with the *ipso* ( $\eta^5\text{-C}_5\text{H}_4$ ) carbon at  $\delta$  83.2-88.4, the ( $\eta^5\text{-C}_5\text{H}_5$ ) carbon at  $\delta$  69.5-74.8 and the *meta* and *ortho* carbons at  $\delta$  69.5-75.8 and  $\delta$  66.6-71.8 respectively.

The methylene carbons of the dipeptides appear negative in the DEPT 135 spectrum in the range  $\delta$  31.2-47.6

**Table 2.5:** Selected  $^{13}\text{C}$  NMR spectral data ( $\delta$ ,  $\text{DMSO-}d_6$ ) for *N*-(6-ferrocenyl-2-naphthoyl), *N*-{*para*-(ferrocenyl)cinnamoyl} and *N*-{*para*-(ferrocenyl)benzoyl} amino acid and dipeptide derivatives.

Compound	C=O	<i>ipso</i> ( $\eta^5\text{-C}_5\text{H}_4$ )	<i>ortho</i> ( $\eta^5\text{-C}_5\text{H}_4$ )	<i>meta</i> ( $\eta^5\text{-C}_5\text{H}_4$ )	( $\eta^5\text{-C}_5\text{H}_5$ )
100	170.3-166.5	84.0	66.6	69.4	69.5
101	169.9-166.6	84.0	66.6	69.4	69.5
102	169.8-166.5	84.0	66.6	69.4	69.5
103	169.9	84.0	66.6	69.4	69.5
104	171.1-168.9	84.1	66.6	69.5	69.5
105	173.2-166.3	84.1	66.6	69.4	69.4
106	173.0-166.4	84.1	66.6	69.4	69.4
107	173.0-166.4	84.0	66.6	69.4	69.4
108	171.2-166.5	84.0	66.6	69.4	69.5
109	171.6-168.2	84.1	66.6	69.4	69.5
110	174.3-166.3	84.1	66.6	69.4	69.4
111	174.0-166.4	84.1	66.6	69.4	69.4
112	174.0-166.5	84.0	66.6	69.4	69.5
113	169.7-165.4	83.7	66.4	69.3	69.4
114	169.7-166.1	83.7	66.4	69.4	69.3
115	172.6-165.1	83.7	66.4	69.3	69.4
116	172.5-165.4	83.7	66.5	69.3	69.4
117	172.5-165.4	83.7	66.4	69.3	69.4
118	172.2-166.3	83.2	66.6	69.5	69.5
119	170.3-166.3	83.2	66.6	69.5	69.5
110	169.8-166.3	83.2	66.6	69.5	69.5
111	175.2	88.2	71.8	75.8	74.8
112	175.1-171.5	88.4	71.8	74.7	74.7
113	169.7-166.3	83.2	66.6	69.5	69.5

**2.2.8  $^{13}\text{C}$  and DEPT 135 NMR study of *N*-{*para*-(ferrocenyl)cinnamoyl}-glycine-L-alanine ethyl ester 116.**

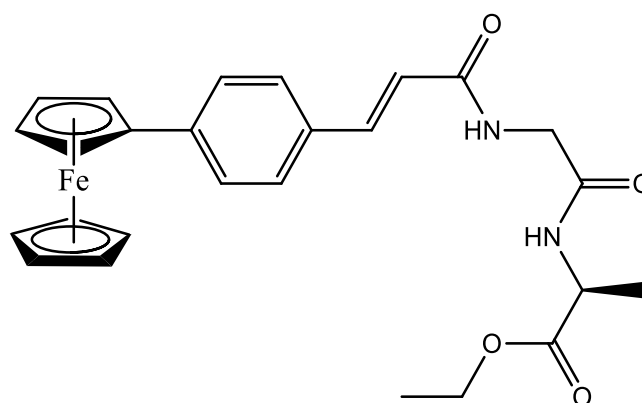


**Figure 2.15:** Structure of *N*-{*para*-(ferrocenyl)cinnamoyl}-glycine-L-alanine ethyl ester 116.

The  $^{13}\text{C}$  NMR of *N*-{*para*-(ferrocenyl)cinnamoyl}-glycine-L-alanine ethyl ester **116** shows three carbonyl carbons at  $\delta$  172.5, 168.8 and 165.4 which are absent in the DEPT 135. The aromatic region shows six signals. The signals at  $\delta$  140.9 and 132.2 are not present in the DEPT 135 spectrum, indicating that they are the quaternary carbons of the benzene ring. The signals at  $\delta$  138.9 and 120.7 correspond to the olefinic carbons and the remaining signals at  $\delta$  127.7 and 126.2 correspond to the remaining carbons on the benzene ring. The signal at  $\delta$  83.7 is not present in the DEPT spectrum and can be attributed to the *ipso* carbon. At  $\delta$  69.4 the signal of the unsubstituted ( $\eta^5\text{-C}_5\text{H}_5$ ) ring is present. The *meta* ( $\eta^5\text{-C}_5\text{H}_4$ ) carbon is in close proximity at  $\delta$  69.3 and the *ortho* ( $\eta^5\text{-C}_5\text{H}_4$ ) carbon appears at  $\delta$  66.5. The signal at  $\delta$  60.5 is negative in the DEPT 135 spectrum and can be assigned to the methylene carbon of the ethyl ester. The signal at  $\delta$  40.0 is also negative in the DEPT 135 and may be assigned to the methylene carbon of the glycine residue. The signals at  $\delta$  47.6 and 17.0 correspond to the methine and methyl carbons atoms of the L-alanine residue respectively, while the signal at  $\delta$  14.0 corresponds to the methyl carbon of the ethyl ester.

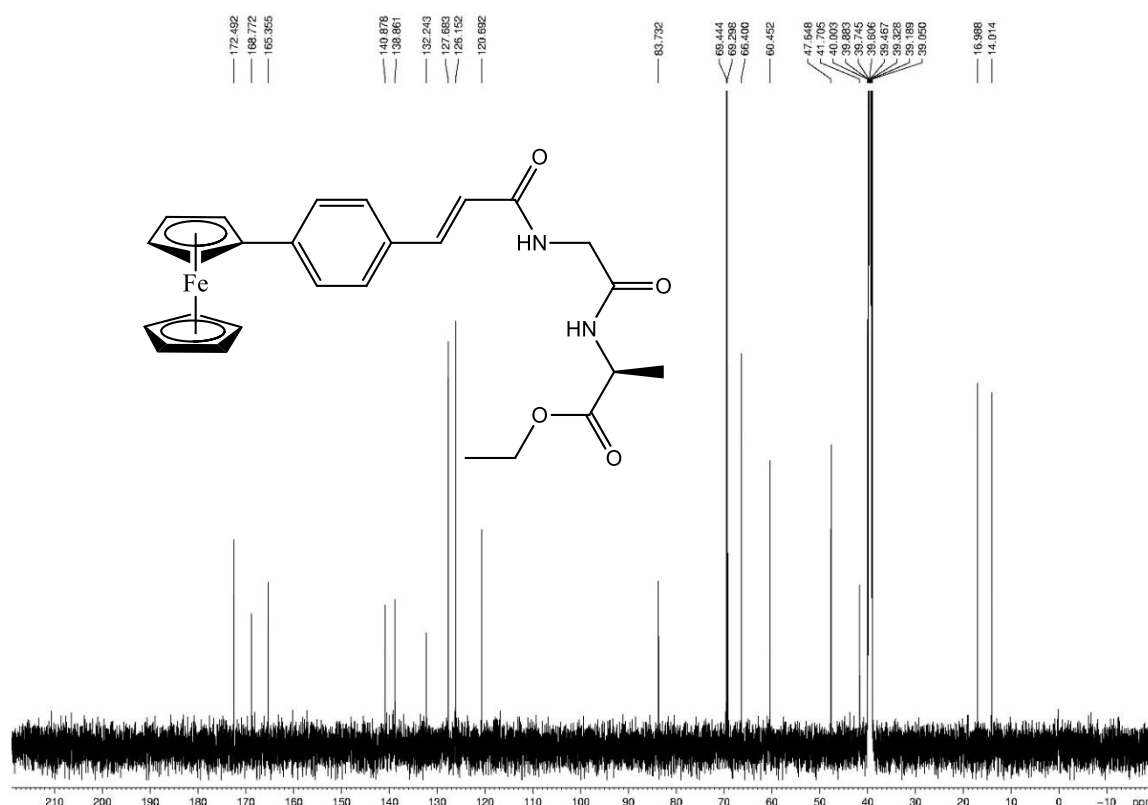


**Figure 2.16:**  $^{13}\text{C}$  NMR spectrum of *N*-{*para*-(ferrocenyl)cinnamoyl}-glycine-L-alanine ethyl ester **116**.

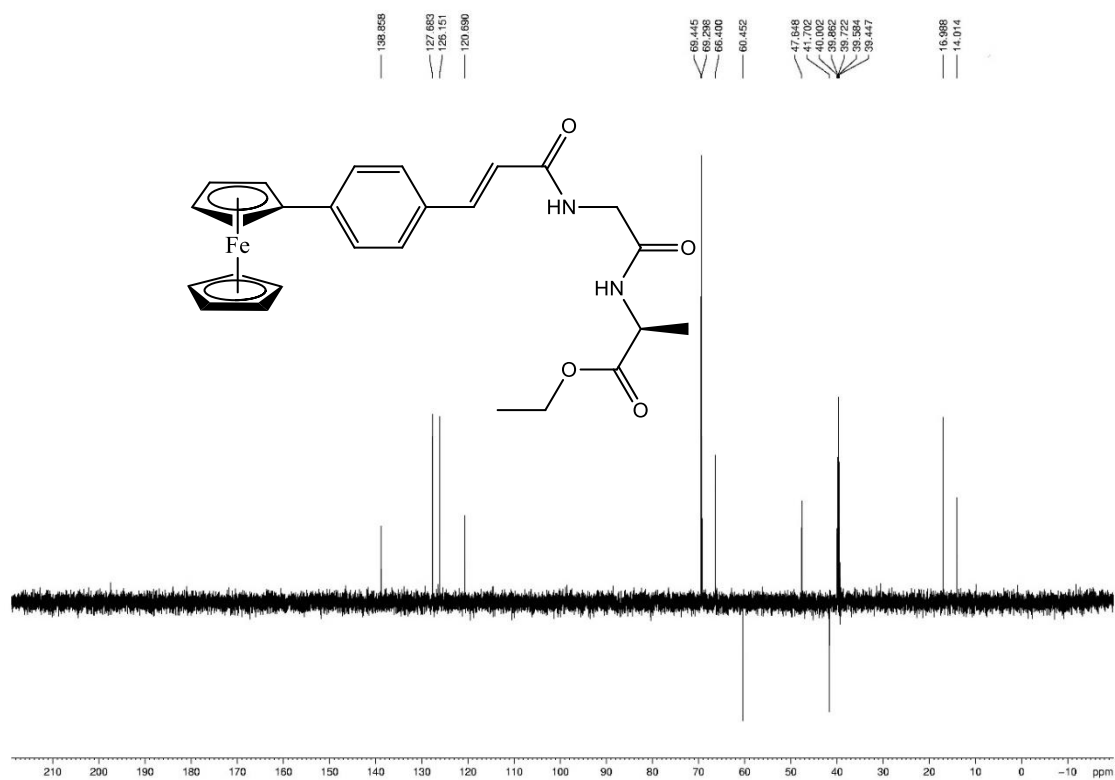


**Figure 2.17:** DEPT 135 NMR spectrum of *N*-{*para*-(ferrocenyl)cinnamoyl}glycine-L-alanine ethyl ester **116**.

### 2.2.9 HSQC study of *N*-{*para*-(ferrocenyl)cinnamoyl}-glycine-L-alanine ethyl ester (116).

HSQC (Heteronuclear Single Quantum Coherence) is a 2D NMR technique that correlates each  $^{13}\text{C}$  atom to the proton to which it is directly attached, thus allowing for complete assignment of proton and carbon spectra.

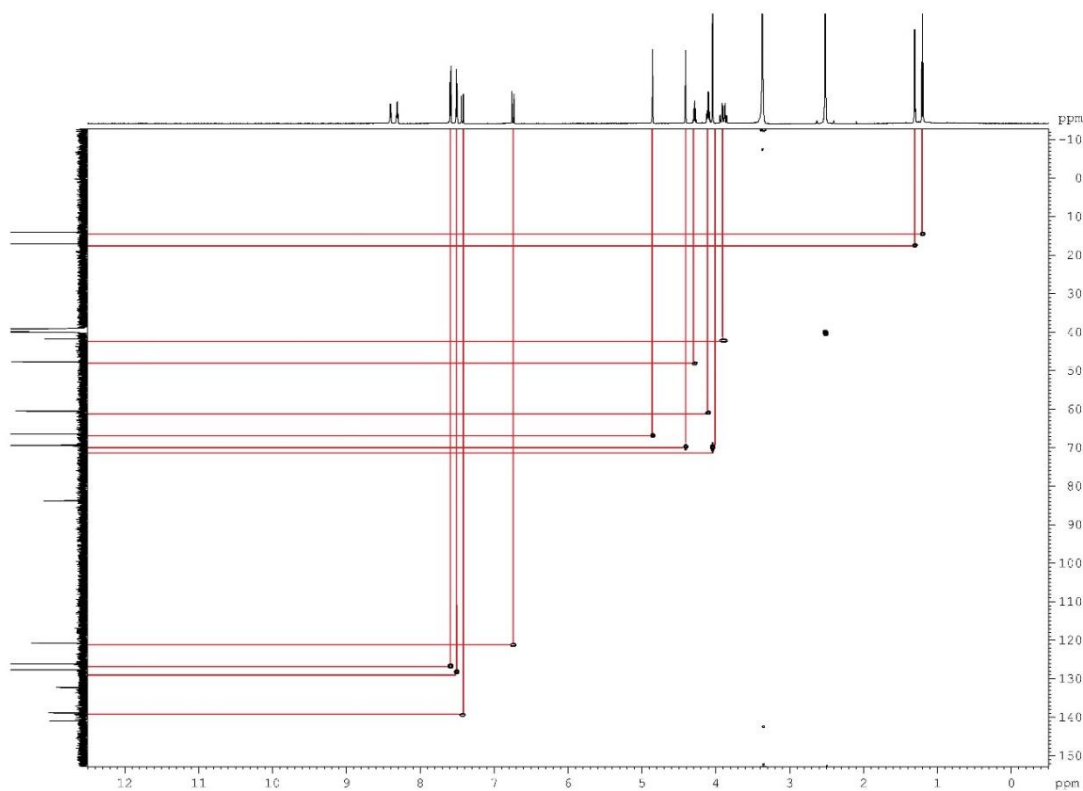


**Figure 2.18:** HSQC of *N*-{*para*-(ferrocenyl)cinnamoyl}-glycine-L-alanine ethyl ester **116**.

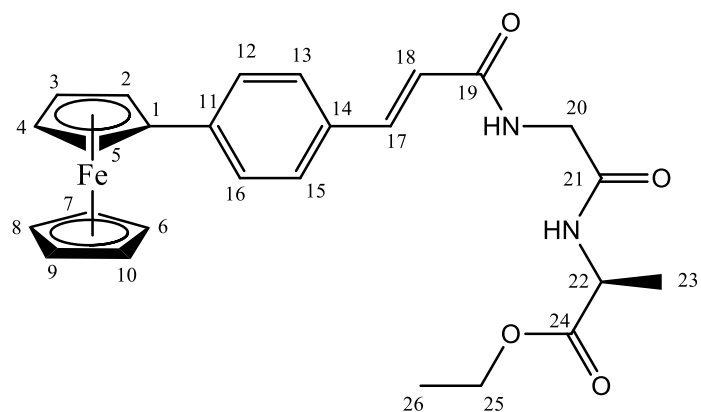


**Figure 2.19:** *N*-{*para*-(ferrocenyl)cinnamoyl}-glycine-L-alanine ethyl ester **116**.

**Table 2.6:** HSQC data for *N*-{*para*-(ferrocenyl)cinnamoyl}-glycine-L-alanine ethyl ester **116**.

Site	<sup>1</sup> H NMR	<sup>13</sup> C NMR	HSQC
1		83.7	
2,5	4.85		66.4
3,4	4.40		69.3
6 to 10	4.04		69.4
11		132.2	
12, 16	7.58		126.2
13, 15	7.49		127.7
14		140.9	
17	6.73		120.7
18	7.46		138.9
19		165.4	
20	3.86 & 3.92		40.0
21		168.8	
22	4.27		47.6
23	1.29		17.0
24		173.5	
25	4.09		60.5
26	1.19		14.0

**2.2.10 Infra red studies of *N*-(6-ferrocenyl-2-naphthoyl), *N*-{*para*-(ferrocenyl)cinnamoyl} and *N*-{*para*-(ferrocenyl)benzoyl} amino acid and dipeptide derivatives.**

Any compound which has covalent bonds absorbs frequencies of electromagnetic radiation in the infrared region of the electromagnetic spectrum. The region lies at wavelengths that are longer than visible light. Molecules are excited to a higher state when they absorb infrared radiation. Radiation in this energy range corresponds to stretching and bending vibrational frequencies of the covalent bonds in molecules. Only bonds which have a dipole moment that changes as a function of time at the same frequency as the incoming infrared radiation are capable of absorbing it.

**Table 2.7:** Selected IR data for *N*-(6-ferrocenyl-2-naphthoyl), *N*-{*para*-(ferrocenyl)cinnamoyl} and *N*-{*para*-(ferrocenyl)benzoyl} amino acid and dipeptide derivatives. Values are given in  $\text{cm}^{-1}$

Compound No.	N-H	amide I	amide II	C=O ester/acid
100	3418, 3313	1638, 1622	1512	1741
101	3281	1653	1523	1753
102	3298	1645	1544	1749
103	3263	1645	1544	1749
104	3291	1624	1543	1742
105	3305	1624	1547	1729
106	3305	1627	1516	1734
107	3292	1624, 1645	1513	1747
108	-	1628, 1600	1544	1690
109	-	1624	1548	1720
110	-	1615	1543	1712
111	2932, 3092	1626	1534	1727
112	2930, 3094	1628	1535	1723
113	3287	1626	1549	1732
114	3293	1642	1592	1745
115	3277	1616	1563	1739
116	3310	1621	1529	1732
117	3307	1622	1527	1729
118	-	1640	1522	1737
119	3274	1655	1514, 1550	1727
120	3389	1644	1515, 1543	1727
121	3367, 3274	1643	1542, 1515	1727
122	3298	1633	1549, 1518	1738
123	3310	1628, 1609	1548, 1519	1734



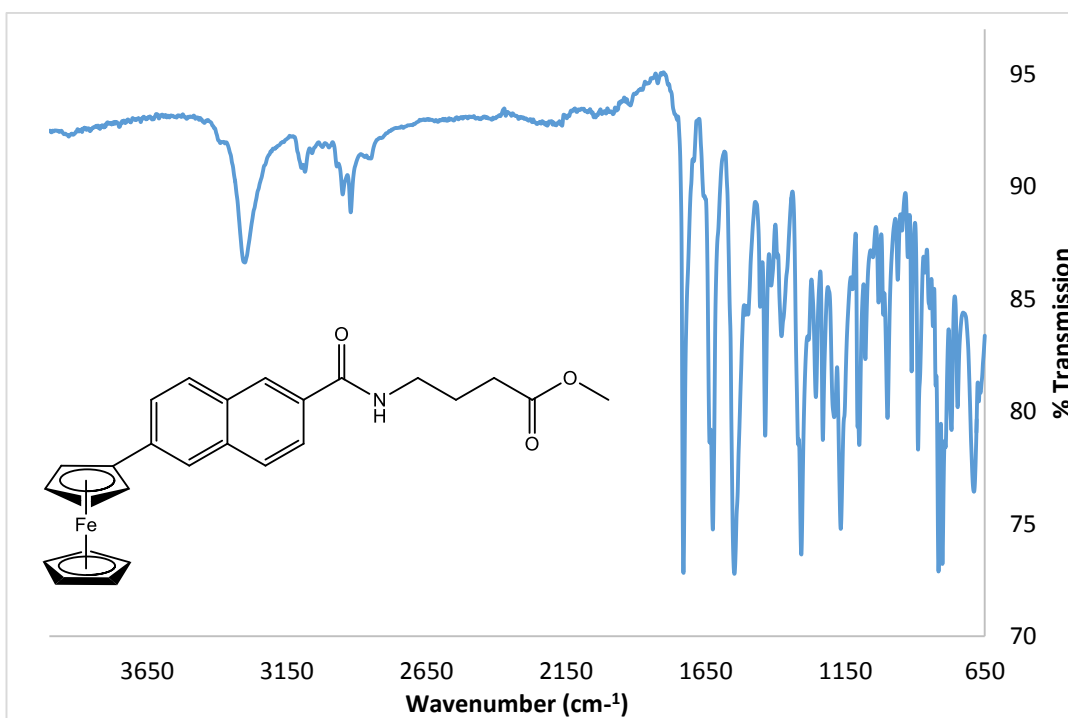


**Figure 2.20** IR spectrum of *N*-(6-ferrocenyl-2-naphthoyl)- $\gamma$ -aminobutyric acid methyl ester **105**.

The fundamental absorptions arise from excitation from the ground state to the lowest energy excited state. However the spectrum is complicated by the presence of weak overtone, combination and difference bands. Overtones result from excitation from the ground state to higher energy levels, combination bands arise when two vibrational frequencies combine to give a vibration of a new frequency and difference bands result a new frequency arises from the difference of two frequencies<sup>26</sup>.

The IR spectra of *N*-(6-ferrocenyl-2-naphthoyl), *N*-{*para*-(ferrocenyl)cinnamoyl} and *N*-{*para*-(ferrocenyl)benzoyl} amino acid and dipeptide derivatives were obtained as pure solids. The spectra usually show two bands above 3000  $\text{cm}^{-1}$  which correspond to the secondary amide groups. In the carbonyl region there are usually at least two bands which correspond to primary and secondary amides. The higher frequency band is known as the amide I band and the lower frequency band is known as the amide II band. The amide I band appears between 1673 and 1600  $\text{cm}^{-1}$  and corresponds to the stretching vibration of the C=O band, while the amide II band appears between 1563 and 1512  $\text{cm}^{-1}$  and corresponds to the bending vibration of the N-H bond. The C=O of the ester appears at a higher frequency between 1753 and 1712  $\text{cm}^{-1}$ .

**2.2.11 UV-Vis studies of *N*-(6-ferrocenyl-2-naphthoyl), *N*-{*para*-(ferrocenyl)cinnamoyl} and *N*-{*para*-(ferrocenyl)benzoyl} amino acid and dipeptide derivatives.**

**Table 2.8:** Selected UV-Vis data for *N*-(6-ferrocenyl-2-naphthoyl), *N*-{*para*-(ferrocenyl)cinnamoyl} and *N*-{*para*-(ferrocenyl)benzoyl} amino acid and dipeptide derivatives.

Compound No.	$\lambda_{\max 1}$ (nm)	$\epsilon_1$	$\lambda_{\max 2}$ (nm)	$\epsilon_2$
100	369	3093	451	1344
101	373	2600	448	1086
102	375	2717	452	1174
103	379	2908	452	1281
104	359	2744	452	1027
105	371	3127	452	1213
106	376	3210	452	1302
107	363	3682	452	1403
108	373	1545	452	673
109	365	2513	452	1038
110	371	1562	451	641
111	374	2843	450	1158
112	369	1875	451	862
113	378	3436	457	1378
114	387	3487	455	1522
115	370	3001	452	1059
116	387	3487	455	1522
117	313	4118	436	550
118	351	1987	450	356
119	354	2858	452	865
120	354	1584	451	570
121	355	1737	450	552
122	356	1532	425	487
123	313	4835	449	587

The UV-Vis spectrum ranges from 190-800 nm. The transitions that result in the absorption of electromagnetic radiation in this region of the spectrum correspond to transitions between the electronic energy levels. As the molecule absorbs energy an electron is promoted from an occupied orbital to an unoccupied orbital of higher potential energy. The most probable transition is from the highest unoccupied energy level (HOMO) to the lowest unoccupied energy level (LUMO). For most molecules the lowest energy occupied levels correspond to  $\sigma$  bonds. The  $\pi$  orbitals lie at higher energy levels while non-bonding ( $n$ )

orbitals lie at higher levels still. The highest energy levels correspond to antibonding ( $\sigma^*$  and  $\pi^*$ ) orbitals<sup>26</sup>.

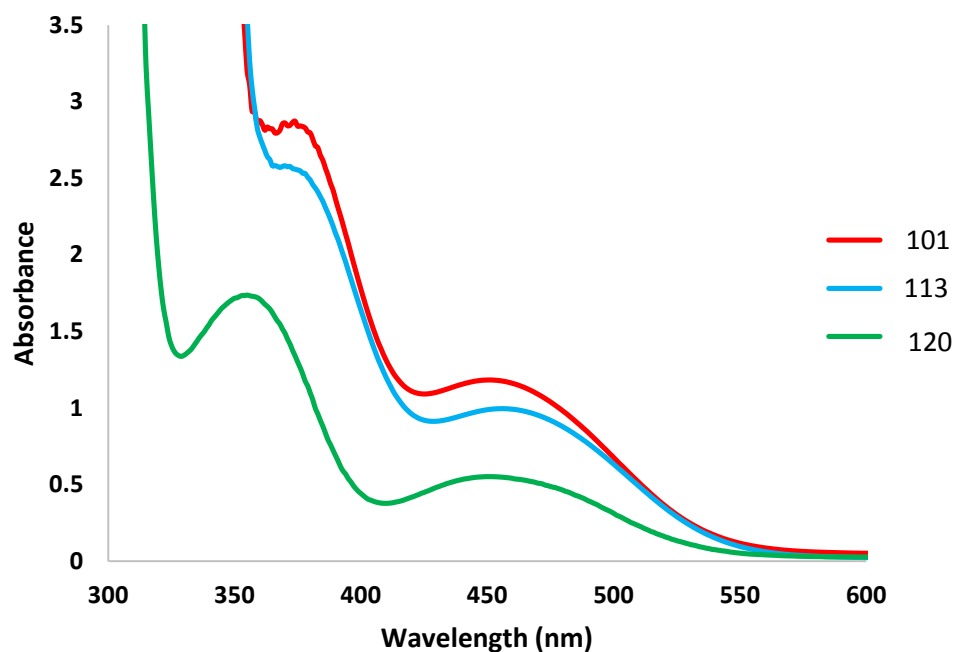


**Figure 2.21:** UV-Vis spectra of *N*-(6-ferrocenyl-2-naphthoyl)-glycine-glycine propyl ester **101**, *N*-*para*-(ferrocenyl)-cinnamoyl-glycine-glycine ethyl ester **113** and *N*-*para*-(ferrocenyl)-benzoyl-glycine-glycine ethyl ester **120**.

The *N*-(6-ferrocenyl-2-naphthoyl)-glycine-glycine amino acid and dipeptide esters have the strongest absorptions in the UV spectrum with local maxima at 375 nm and 450 nm respectively. The *N*-*para*-(ferrocenyl)-benzoyl dipeptide esters have local maxima at 355 nm and 450 nm respectively. The absorptions are less intense and occur at slightly shorter wavelengths. The UV-Vis spectra of the *N*-(6-ferrocenyl-2-naphthoyl)-glycine-glycine amino acid and dipeptide esters are similar to those of the *N*-*para*-(ferrocenyl)-cinnamoyl amino acid and dipeptide esters. The absorbances for the *N*-(6-ferrocenyl-2-naphthoyl) and *N*-*para*-(ferrocenyl)cinnamoyl derivatives are stronger than those of the *N*-*para*-(ferrocenyl)benzoyl derivatives as they have a higher degree of conjugation.

The absorbance at 375 nm can be attributed to a  $\pi$  to  $\pi^*$  transition of the aromatic moiety while the absorbance at 450 nm is attributed to a metal to ligand charge transfer band (MLCT). The extinction coefficient  $\epsilon$  is calculated from the Beer-Lambert Law  $A=\epsilon Cl$ , where  $A$  is the absorbance,  $C$  is the concentration and  $l$  is the path length of the cell. All spectra were

obtained at a concentration of  $1 \times 10^{-4}$  M. The extinction coefficients are a function of how efficiently a chromophore absorbs UV or visible radiation.

### 2.2.12 Mass Spectrometric studies of *N*-(6-ferrocenyl-2-naphthoyl)-glycine-glycine esters (**100-103**).

Mass spectrometric studies were carried out for *N*-(6-ferrocenyl-2-naphthoyl)-glycine-glycine esters **100-103**. The *N*-(6-ferrocenyl-2-naphthoyl)-glycine-glycine esters are non volatile and a soft ionisation technique is employed in their analysis. The *N*-(6-ferrocenyl-2-naphthoyl)-glycine-glycine esters were analysed by electrospray ionisation (ESI) mass spectrometry, which confirmed the correct relative molecular mass for each compound. Examination of the mass spectra revealed the presence of radical cation species,  $[M]^+$ , as well as  $[M+H]^+$  species at one mass unit higher. Sequence specific fragment ions were of low intensity in the mass spectra. The mass spectrum for *N*-(6-ferrocenyl-2-naphthoyl)-glycine-glycine methyl ester **100** is shown (figure 2.22). The signal at  $m/z$  339 is due to cleavage at the naphthoyl carbonyl while the signal seen at  $m/z$  396 is cleavage after the first glycine residue (figure 2.23).

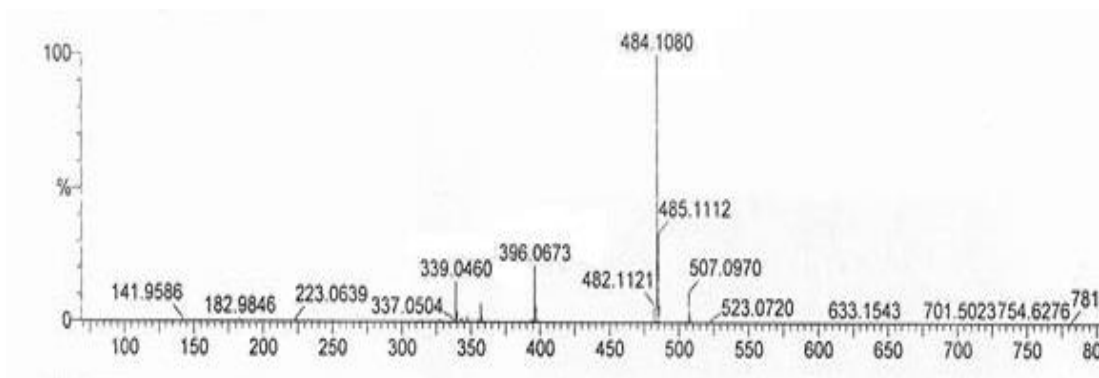


**Figure 2.22:** Mass spectrum of *N*-(6-ferrocenyl-2-naphthoyl)-glycine-glycine methyl ester (**100**).

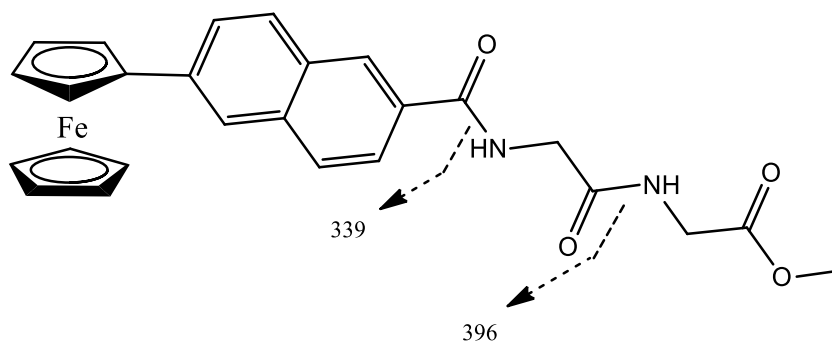


**Figure 2.23:** Product ions observed in the mass spectrum of *N*-(6-ferrocenyl)-glycine-glycine methyl ester (**100**).

## 2.3 Approaches to the synthesis and structural characterisation of *N*-(5-ferrocenyl-1-naphthoyl) amino acid and dipeptide derivatives.

### 2.3.1 Introduction

The preliminary structure activity relationship (SAR) carried out by the group on ferrocenyl bioconjugates has shown the importance of a conjugated linker which is believed to lower the oxidation potential of the ferrocene moiety. Previously modification of the conjugated linker has been shown to have a significant impact on the biological activity of this class of compounds. Replacement of the benzoyl moiety by the naphthalene unit has been shown to have a dramatic effect on activity. The most active of the ferrocenyl benzoyl derivatives, *N*-{*para*-(ferrocenyl)benzoyl} glycine-L-alanine ethyl ester, had an  $IC_{50}$  of 4.0  $\mu$ M. The introduction of the naphthalene linker resulted in an increase in the activity of all of the analogues. The *N*-(6-ferrocenyl-2-naphthoyl) glycine-L-alanine ethyl ester **78** had an  $IC_{50}$  of 1.3  $\mu$ M by comparison.

Also the position of the substituents on the aromatic linker has been shown to be of importance. *N*-{*para*-(ferrocenyl)benzoyl} derivatives were more active than the *ortho* and *meta* counterparts, while *N*-(6-ferrocenyl-2-naphthoyl) amino acid and dipeptide ester derivatives were found to be more active than the *N*-(3-ferrocenyl-2-naphthoyl) derivatives. Therefore as part of the ongoing SAR study of these compounds the preparation of a series of *N*-(5-ferrocenyl-1-naphthoyl) derivatives looks to be a logical strategy.

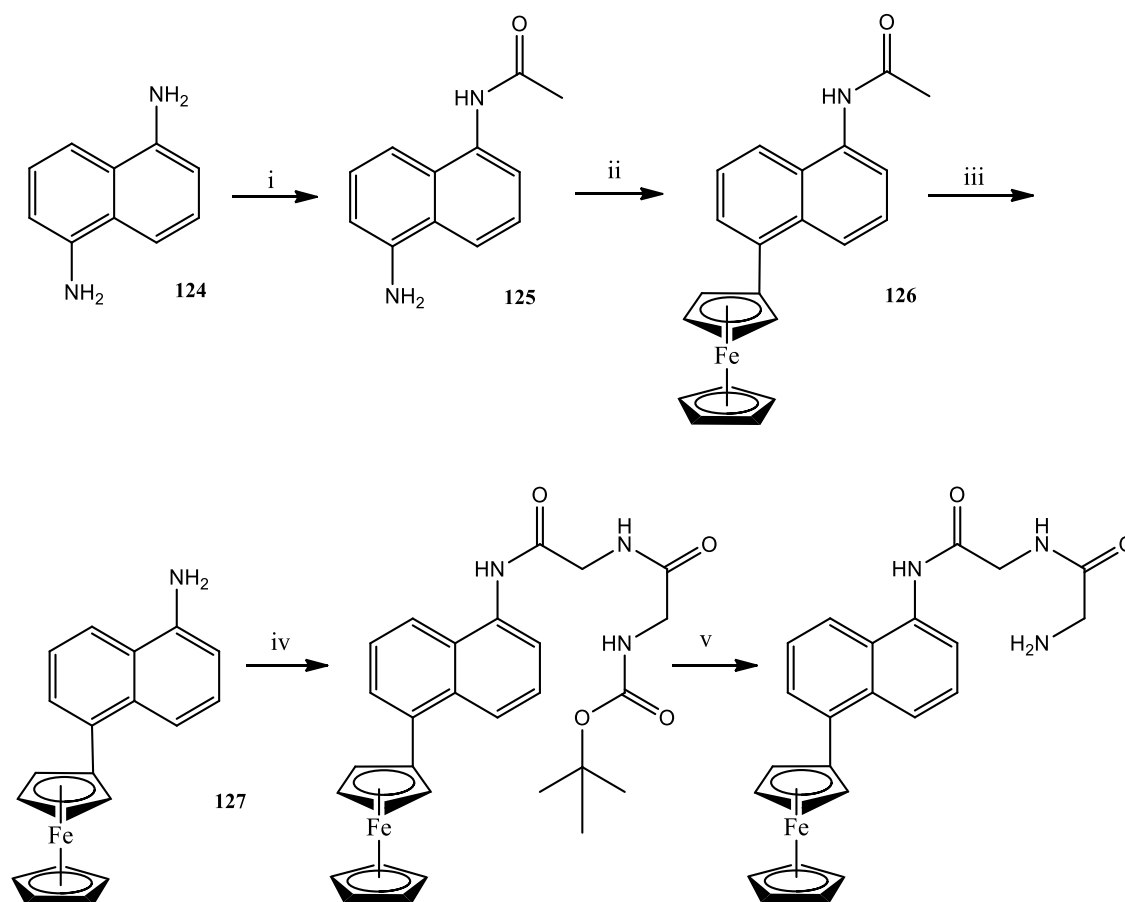
The proposed synthesis of these *N*-(5-ferrocenyl-1-naphthoyl) amino acid and dipeptide esters follows a different synthetic route than the previously made compounds. As no 5-amino-1-naphthoic acid was available commercially, 1,5-diaminonaphthalene **124** was sourced as a suitable alternative. This starting material would allow an alternative synthesis

to structurally similar targets, while utilising mostly synthetic methods well established within the group.

As 1,5-diaminonaphthalene **124** is a symmetrical molecule, either amino group could be protected to give the desired product. Ferrocene could then be introduced via standard diazonium coupling. Deprotection would leave a free amino group compared with the usual carboxylic acid. This would require a dipeptide moiety with a free hydroxyl group to couple with the amine. The dipeptide would thus terminate in an amine as opposed to the usual ester group. This can be achieved through standard dipeptide coupling by preparing a dipeptide with an ester protecting group on the C-terminus and a Boc protecting group on the N-terminus. The ester is removed prior to coupling with the naphthalene linker and the Boc group is removed after to give the terminal amino group.

A series of peptides will be prepared using the most active amino acid and dipeptide conformations noted previously from among the *N*-(6-ferrocenyl-2-naphthoyl) amino acid and dipeptide esters; Gly Gly-NH<sub>2</sub>, GABA-NH<sub>2</sub>, Gly-L-Ala-NH<sub>2</sub>, Gly-D-Ala-NH<sub>2</sub> and Sar-Gly-NH<sub>2</sub>. Given that peptide chain order has shown a significant impact on activity and that the dipeptides will be attached via the C-terminus rather than the N-terminus, the L-Ala-Gly-NH<sub>2</sub>, D-Ala-Gly-NH<sub>2</sub> and the Gly-Sar-NH<sub>2</sub> derivatives will also be synthesised.

### 2.3.2 Synthesis of *N*-(5-ferrocenyl-1-naphthoyl) dipeptides.



(i) Pyridine, acetic anhydride, RT, overnight. (ii) Ferrocene,  $\text{NaNO}_2$ , HCl. (iii) MeOH, NaOH, reflux. (iv) Boc-dipeptide, EDC, NHS, TEA. (v) TFA, DCM.

**Scheme 2.14:** General reaction scheme for the synthesis of *N*-(5-ferrocenyl-1-naphthoyl) dipeptides.

The 1-amino-5-acetyl-naphthalene **125** is prepared by acetylation of the 1, 5-diaminonaphthalene with acetic anhydride in pyridine. The ferrocene moiety is introduced via diazonium coupling to give the 1-acetyl-5-ferrocenyl naphthalene **126**. The acetyl group is then cleaved by base hydrolysis to give the 1-amino-5-ferrocenyl naphthalene **127**. The Boc protected dipeptide can then be coupled to the free amino group by standard peptide coupling to give the 5-ferrocenyl-1-naphthoyl Boc dipeptide. The Boc protecting group is then cleaved by trifluoroacetic acid to give the desired 5-ferrocenyl-1-naphthoyl dipeptide.

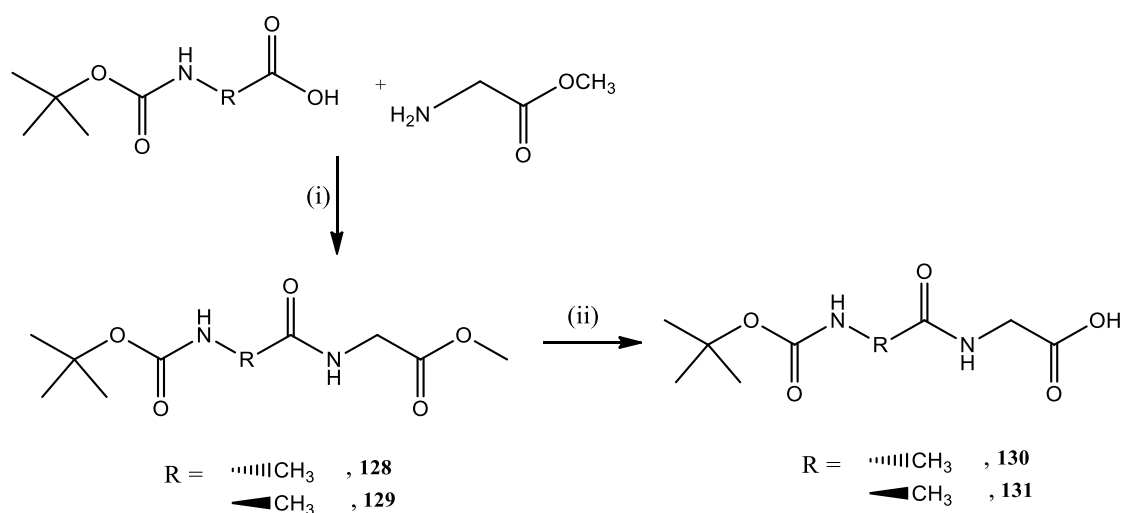
Protection of the of the amino groups of **124** was attempted using Boc anhydride, however the reaction gave either low conversion of starting material to products or multiple by-

products which made purification difficult. As the molecule possesses two amino groups, protection of one or both amino groups may occur. To reduce the potential for protection of the second amino group only one equivalent of Boc anhydride was used. Both the di protected moiety and the starting material must be removed by column chromatography.

An alternative route using acetic anhydride was then employed to protect the amino groups via acetylation. Conversion to approximately 50 % of the protected amino group was achieved with little or no evidence of the protection of the second amine. Removal of unreacted starting material was achieved by column chromatography.

The *N*-acetyl ferrocenyl naphthalene **126** was prepared using the standard diazonium coupling procedures as outlined previously with only a 9 % yield. The acetyl group was removed by base hydrolysis using 30 % sodium hydroxide.

### 2.3.2.1 Preparation of Boc protected dipeptides with a free hydroxyl group.



(i) EDC, NHS, TEA, (ii) 10 % NaOH, MeOH, reflux, 12 h.

#### Scheme 2.15: General procedure for the synthesis of Boc protected dipeptides.

Boc protected dipeptides with a free carboxylic acid were prepared by standard peptide coupling methods using EDC, NHS and TEA in DCM. First the C-terminus of the desired peptide was protected with a methyl group followed by peptide coupling with the Boc protected moiety using standard peptide coupling procedures. The methyl group was then removed by base hydrolysis in 10 % NaOH. This gave the free C-terminus for coupling with

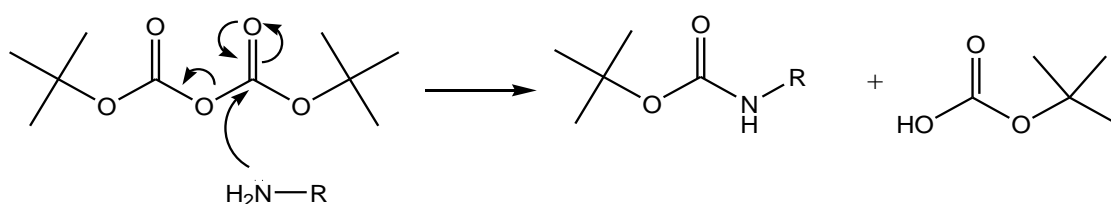


the amino ferrocenyl naphthoic acid. The Boc protecting group could then be removed with TFA to give the final product with the free amine group.

### 2.3.2.2 Preparation of *N*-5-acetyl-1-aminonaphthalene

#### 2.3.2.2.1 *t*-Butoxycarbonyl (Boc) protecting groups

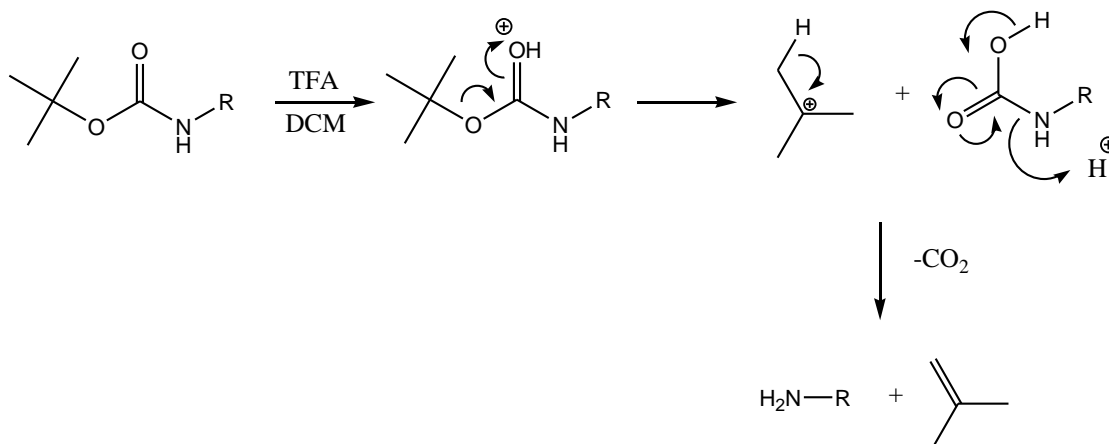
One of the most commonly employed amine protection strategies is protection using the *t*-Boc group. It is regularly used in peptide synthesis and has already been employed during the preparation of dipeptide esters. The *t*-Boc protecting group is introduced using di-*tert*-butyl dicarbonate ( $\text{Boc}_2\text{O}$ ).



**Scheme 2.16:** Introduction of the *t*-Boc protecting group with di-*tert*-butyl dicarbonate.

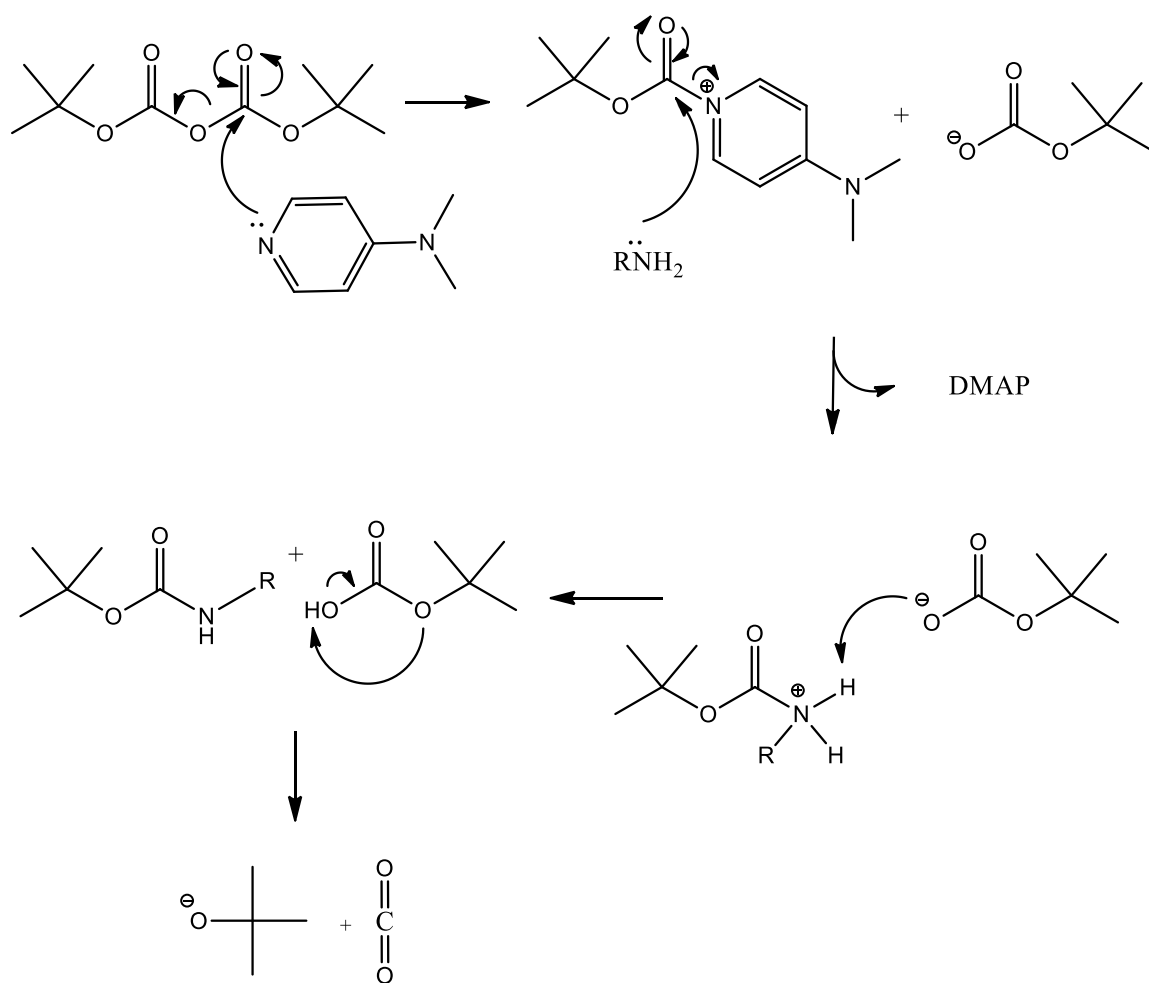
It is resistant to basic and nucleophilic attack as well as catalytic hydrogenation due to the steric bulk of the *t*-butyl group which protects the carbonyl group from attack. It can be readily cleaved by hydrolysis in acid such as TFA which causes a loss of the *t*-butyl cation

followed by decarboxylation. This allows the removal of the BOC group without the cleavage of peptide or ester bonds.



**Scheme 2.17:** Removal of the *t*-Boc group with trifluoroacetic acid.

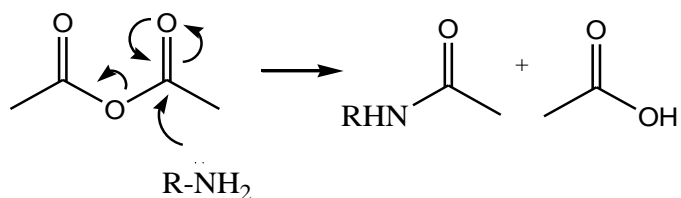
While alkyl amines react readily without a catalyst, secondary, tertiary and aryl amines react poorly and can require a catalyst<sup>27</sup>. Often a tertiary amine such as 4-dimethylaminopyridine (DMAP) or pyridine is added as a catalyst. DMAP increases the rate of reaction, however it also increases the number of possible side reactions.



**Scheme 2.18:** Boc protection using DMAP as a catalyst.

### 2.3.2.2.2 Acetyl protecting groups.

The acetyl group may be used to protect both hydroxyl groups and amines. It is introduced via acetic anhydride with stirring in pyridine.



**Scheme 2.19:** Acetylation of an amine using acetic anhydride.

The acetyl group which is stable during the diazonium coupling procedure is then cleaved by base hydrolysis using methanol and 30 % NaOH solution to furnish the 1-amino-5-ferrocenyl naphthalene **127**.

### 2.3.3 Discussion

The preparation of Boc protected dipeptides was achieved using the usual synthetic route followed by hydrolysis to give the free acids required for coupling. The acetylation of 1,5-diaminonaphthalene **124** gave good yields of up to 80 % and was used without further purification after filtering. The diazonium coupling of 1-amino-5-acetyl-naphthalene **125**, however, gave very low yields of only 9 % after purification. Despite scaling up the quantity of starting material used, after hydrolysis of the *N*-1-acetyl-5-ferrocenyl naphthalene **126**, which had a yield of 56 %, the quantity remaining of 1-amino-5-ferrocenyl-naphthalene **127** was impractical to continue synthesis of the target compounds. Coupling of the 1-amino-5-ferrocenyl-naphthalene **127** to Boc- $\gamma$ -aminobutyric acid was attempted, however no evidence of the desired product was detected by NMR after purification was attempted. Given that a further two reactions were required reach the desired target, the method was deemed impractical for the synthesis of a series of these target compounds.

A potential reason for the poor yield of the 1-acetyl-5-ferrocenyl naphthalene **126** compared with the same reaction of methyl-6-ferrocenylnaphthalene-2-carboxylate **82** may be that the NHCOR group is electron donating while the RCOOR group is electron withdrawing.

Sterically, the 1,5 orientation of the substitution is no more hindered than the 2,6 substitution. Indeed the effect of steric hindrance does not greatly affect the yield at the diazonium coupling stage as the synthesis of methyl-6-ferrocenylnaphthalene-2-carboxylate **82** gave a yield of 21 % while methyl-3-ferrocenylnaphthalene-2-carboxylate gave a yield of 30 %<sup>24</sup>, however it is possible that the effect of the substituent groups may have a role in the poor yield of this reaction.

An electron withdrawing group *para* to the azo group increases the electrophilicity of the diazonium ion. This can be seen in the case of the benzenediazonium cation and the *p*-nitrobenzenediazonium cation in figure 5.1. However, in the synthesis of 1-acetyl-5-ferrocenyl naphthalene **126** the electron withdrawing methyl ester group is replaced by an electron donating amide group opposite to the azo group. It is possible that the electrophilicity of the diazonium cation is reduced by this substituent effect and undergoes electrophilic aromatic substitution less readily than its methyl-6-ferrocenylnaphthalene-2-carboxylate **82** counterpart.

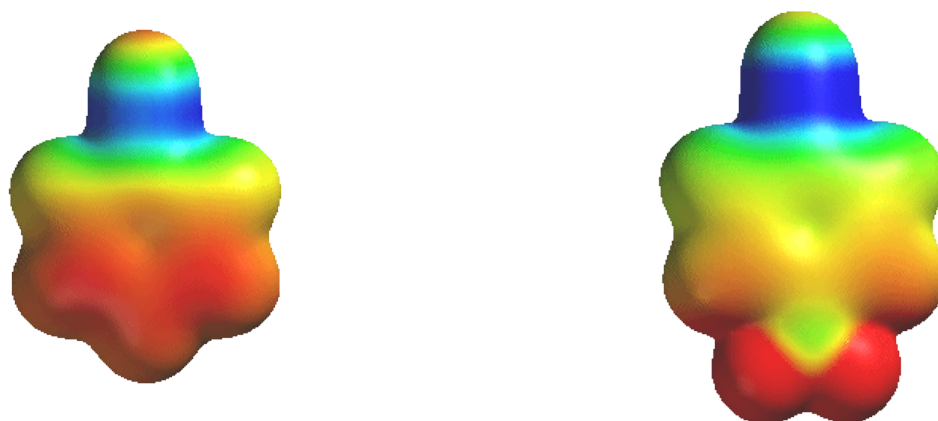


**Figure 2.24:** Electrostatic potential diagrams of the benzenediazonium cation compared with the *p*-nitrosobenzenediazonium cation. Positive potential areas are shown in blue whilst areas of negative potential are shown in red<sup>28</sup>.

## 2.4 Conclusions.

The *N*-(6-ferrocenyl-2-naphthoyl) dipeptide ethyl esters were previously identified as potential anticancer agents with excellent cytotoxicity against H1299 NSCLC cells and Sk-Mel-28 melanoma cells. This project sought to further explore the SAR of these compounds to optimise their cytotoxicity. This was carried out by modification of the previously uninvestigated ester region of the compounds in both *N*-(6-ferrocenyl-2-naphthoyl) and *N*-{*para*(ferrocenyl)benzoyl} derivatives as well as the introduction of a cinnamoyl linker. Thus *N*-(6-ferrocenyl-2-naphthoyl), *N*-{*para*(ferrocenyl)benzoyl} and *N*-{*para*(ferrocenyl)cinnamoyl} amino acid and dipeptide derivatives have been prepared. These novel compounds have been characterised by <sup>1</sup>H NMR, <sup>13</sup>C NMR, DEPT 135, HSQC, IR, UV-Vis and MS. Each compound gave spectra in accordance with their proposed structures.

The synthesis of *N*-(5-ferrocenyl-1-naphthoyl) amino acid and dipeptide derivatives was proposed as an interesting strategy for the exploration of the structure activity relationship of *N*-ferrocenylnaphthoyl amino acid and dipeptide derivatives. It was hoped that this series of derivatives could be prepared utilising similar chemistry to the previously prepared compounds. As described previously the 1-amino-5-acetyl-naphthalene **125** was prepared in sufficient yield, however upon diazonium coupling a poor yield was obtained of approximately 9 %. This was attributed to a potential electron donating substituent effect of

the NHCOH group and this route to the preparation of *N*-(5-ferrocenyl-1-naphthoyl) amino acid and dipeptide derivatives was abandoned.

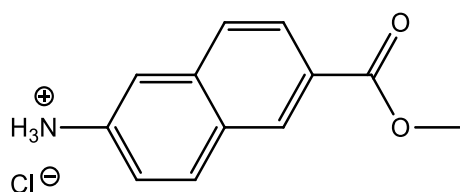
An alternative route, however, has been employed where the Boc protected amino acid or dipeptide is first attached to the protected naphthalene ring. The acetyl group is then cleaved and the ferrocene is coupled secondly. This would eliminate the problematic coupling of the acetylated naphthalene ring and circumvent the need for an electron donating protecting group at the time of coupling. Preliminary results have shown this method to be more successful with diazonium coupling yields in the range of 20 - 30 % in line with those reported previously<sup>24</sup>[Error! Bookmark not defined.](#).

## Experimental Procedures

All chemicals were purchased from Sigma-Aldrich, Fluorochem Limited or Tokyo Chemical Industry UK Limited; and used as received. Commercial grade reagents were used without further purification. Riedel-Haën silica gel was used for thin layer and column chromatography. Melting points were determined using a Stuart melting point (SMP3) apparatus and are uncorrected. Infrared spectra were recorded on a Perkin Elmer Spectrum 100 FT-IR with ATR. UV-Vis spectra were recorded on a Hewlett Packard 8452 A diode array UV-Vis spectrophotometer.  $^1\text{H}$  and  $^{13}\text{C}$  NMR spectra were recorded in deuterated solvents on either a Bruker Avance 400 or 600 NMR. The  $^1\text{H}$  and  $^{13}\text{C}$  NMR chemical shifts are reported in ppm (parts per million). Tetramethylsilane (TMS) or the residual solvent peaks were used as an internal reference. All coupling constants ( $J$ ) are in Hertz. The abbreviations for the peak multiplicities are as follows: s (singlet), d (doublet), dd (doublet of doublets), t (triplet), q (quartet), qt (quintet), m (multiplet) and br (broad). Electrospray ionisation mass spectra were performed on a Micromass LCT mass spectrometer or a Brüker Daltonics Esquire-LC ion trap mass spectrometer. Elemental analysis was carried out by the microanalytical laboratory at University College Dublin.

***General procedure for the preparation of starting materials for N-(6-ferrocenyl-2-naphthoyl), N-{para-(ferrocenyl)cinnamoyl} and N-{para-(ferrocenyl)benzoyl} amino acid and dipeptide derivatives.***

**Methyl-6-aminonaphthalene-2-carboxylate hydrochloride 81.**

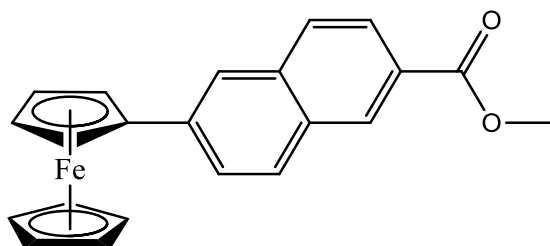


6-Amino-2-naphthoic acid (5.05 g, 27.0 mmol) was dissolved in methanol (30 mL). The solution was cooled on ice and thionyl chloride (5 mL) was added. This was heated at reflux for 24 h. The solution was cooled and the precipitate was isolated via vacuum filtration to yield the title compound as a brown solid (5.48 g, 85 %), mp 250-251 °C (lit<sup>24</sup> 156-158 °C);

$^1\text{H}$  NMR (600 MHz)  $\delta$  (DMSO- $d_6$ ): 8.56 (1H, s, ArH), 8.09 (1H, d,  $J$  8.4 Hz, ArH), 7.94 (1H, d,  $J$  9 Hz, ArH), 7.90 (1H, d,  $J$  8.4 Hz, ArH), 7.53 (1H, s, ArH), 7.37 (1H, d,  $J$  8.4 Hz), 3.90 (3H, s, -OCH<sub>3</sub>);

$^{13}\text{C}$  NMR (150 MHz)  $\delta$  (DMSO- $d_6$ ): 166.3 (C=O), 135.9 (C<sub>q</sub>), 135.4 (C<sub>q</sub>), 131.1, 130.5, 128.5 (C<sub>q</sub>), 127.1, 125.6, 125.1 (C<sub>q</sub>), 121.1, 117.6, 52.1 (-OCH<sub>3</sub>).

### Methyl-6-ferrocenylnaphthalene-2-carboxylate **82**.



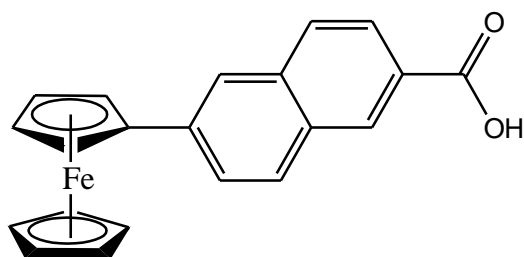
To a solution of methyl-6-aminonaphthalene-2-carboxylate hydrochloride (6.80 g, 28.6 mmol) in water (20 mL) was added conc. HCl (5 mL). A solution of sodium nitrite (2.30 g, 34.3 mmol) in water (20 mL) was then added slowly with stirring while the temperature was kept below 5 °C to yield the diazonium salt. This was then added to a solution of ferrocene (6.38 g, 34.3 mmol) in diethyl ether (40 mL) and allowed to stir for 24 hours. The reaction mixture was washed with water, the organic layer was dried over magnesium sulphate and the solvent was removed *in vacuo* to yield the crude product. It was purified by column chromatography (eluent 5 % diethyl ether: 95 % hexane) to yield the title compound as an orange solid (2.63 g, 25 %), mp 130 °C (lit<sup>24</sup> 158-159 °C);

$^1\text{H}$  NMR (400 MHz)  $\delta$  (DMSO- $d_6$ ): 8.58 (1H, s, ArH), 8.10 (1H, s, ArH), 8.08 (1H, d,  $J$  12 Hz, ArH), 7.93-7.99 (2H, m, ArH), 7.86 (1H, dd,  $J$  12 Hz and 2 Hz, ArH), 4.99 {2H, t,  $J$  2 Hz, *ortho* on ( $\eta^5$ -C<sub>5</sub>H<sub>4</sub>)}, 4.47 {2H, t,  $J$  2 Hz, *meta* on ( $\eta^5$ -C<sub>5</sub>H<sub>4</sub>)}, 4.06 (5H, s,  $\eta^5$ -C<sub>5</sub>H<sub>5</sub>), 3.92 (3H, s, -OCH<sub>3</sub>);

$^{13}\text{C}$  NMR (100 MHz)  $\delta$  (DMSO- $d_6$ ): 166.4 (C=O), 140.0 (C<sub>q</sub>), 135.4 (C<sub>q</sub>), 130.6 (C<sub>q</sub>), 130.4, 129.2, 127.8, 126.1, 125.8 (C<sub>q</sub>), 125.1, 122.7, 83.7 (C<sub>ipso</sub>  $\eta^5$ -C<sub>5</sub>H<sub>4</sub>), 69.6 ( $\eta^5$ -C<sub>5</sub>H<sub>5</sub>), 69.5 (C<sub>meta</sub>  $\eta^5$ -C<sub>5</sub>H<sub>4</sub>), 66.8 (C<sub>ortho</sub>  $\eta^5$ -C<sub>5</sub>H<sub>4</sub>), 52.2 (-OCH<sub>3</sub>).



### 6-Ferrocenylnaphthalene-2-carboxylic acid **83**

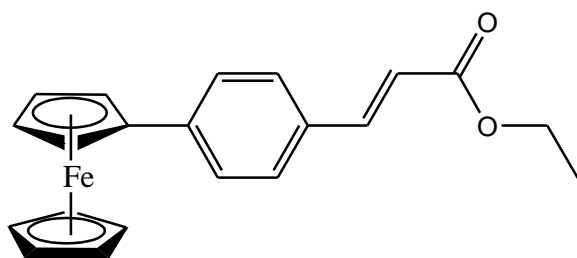


Sodium hydroxide (15 mL, 10 %) was added to a solution of methyl-6-ferrocenylnaphthalene-2-carboxylate (0.30 g, 8.1 mmol) in methanol (15 mL) and allowed to reflux for 24 hours. The solution was cooled on ice and acidified to pH 2 with conc. HCl. The product was isolated by vacuum filtration as an orange solid (0.27 g, 94 %), mp {lit<sup>24</sup> 205 °C (decomp)};

<sup>1</sup>H NMR (600 MHz)  $\delta$  (DMSO-*d*<sub>6</sub>): 12.6 (1H, br.s, -COOH), 8.41 (1H, s, ArH), 7.96 (1H, s, ArH), 7.92-7.88 (2H, m, ArH), 7.80 (1H, d, *J* 8.4 Hz, ArH), 7.72 (1H, d, *J* 8.4 Hz, ArH), 4.87 {2H, s, *ortho* on ( $\eta^5$ -C<sub>5</sub>H<sub>4</sub>)}, 4.36 {2H, s, *meta* on ( $\eta^5$ -C<sub>5</sub>H<sub>4</sub>)}, 3.96 (5H, s,  $\eta^5$ -C<sub>5</sub>H<sub>5</sub>);

<sup>13</sup>C NMR (100 MHz)  $\delta$  (DMSO-*d*<sub>6</sub>): 168.2 (C=O), 138.7 (C<sub>q</sub>), 134.8 (C<sub>q</sub>), 130.8 (C<sub>q</sub>), 129.7, 128.9, 127.5 (C<sub>q</sub>), 127.1, 126.2, 125.6, 122.7, 84.2 (C<sub>ipso</sub>  $\eta^5$ -C<sub>5</sub>H<sub>4</sub>), 69.4 ( $\eta^5$ -C<sub>5</sub>H<sub>5</sub>, C<sub>meta</sub>  $\eta^5$ -C<sub>5</sub>H<sub>4</sub>), 66.6 (C<sub>ortho</sub>  $\eta^5$ -C<sub>5</sub>H<sub>4</sub>).

### *para*-Ferrocenyl-ethyl cinnamate **84**



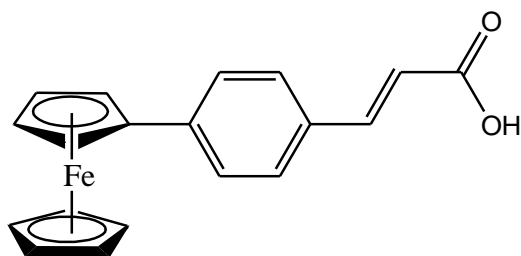
To a solution of ethyl-4-amino cinnamate (1.00 g, 5.2 mmol) in water (20 mL) was added conc. HCl (5 mL). A solution of sodium nitrite (0.43 g, 6.3 mmol) in water (20 mL) was then added slowly with stirring while the temperature was kept below 5 °C to furnish the diazonium salt. This was then added to a solution of ferrocene (1.17 g, 6.3 mmol) in diethyl ether (40 mL) and allowed to stir for 24 hours. The reaction mixture was washed with water, the organic layer was dried over magnesium sulphate and the solvent was removed *in vacuo*

to yield the crude product. It was purified by column chromatography (eluent 5 % diethyl ether: 95 % hexane) to yield the title compound as an orange solid (0.30 g, 16 %), mp 94 °C;

$^1\text{H}$  NMR (400 MHz)  $\delta$  (DMSO- $d_6$ ): 7.65 (5H, m, ArH, =CH-), 6.61 (1H, d,  $J$  10 Hz, -CH=), 4.87 {2H, t,  $J$  2 Hz, *ortho* on ( $\eta^5$ -C<sub>5</sub>H<sub>4</sub>)}, 4.41 {2H, t,  $J$  1.6 Hz, *meta* on ( $\eta^5$ -C<sub>5</sub>H<sub>4</sub>)}, 4.19 (2H, q,  $J$  7.2 Hz, 6.8 Hz, -OCH<sub>2</sub>CH<sub>3</sub>), 4.02 (5H, s,  $\eta^5$ -C<sub>5</sub>H<sub>5</sub>), 1.27 (3H, t,  $J$  7.2 Hz, -OCH<sub>2</sub>CH<sub>3</sub>);

$^{13}\text{C}$  NMR (100 MHz)  $\delta$  (DMSO- $d_6$ ): 166.4 (C=O), 144.3 (-CH=), 142.1 (C<sub>q</sub>), 131.4 (C<sub>q</sub>), 128.5, 126.0, 116.7 (-CH=), 83.4 (C<sub>ipso</sub>  $\eta^5$ -C<sub>5</sub>H<sub>4</sub>), 69.5 ( $\eta^5$ -C<sub>5</sub>H<sub>5</sub>), (C<sub>meta</sub>  $\eta^5$ -C<sub>5</sub>H<sub>4</sub>), 66.5 (C<sub>ortho</sub>  $\eta^5$ -C<sub>5</sub>H<sub>4</sub>), 59.9 (-OCH<sub>2</sub>CH<sub>3</sub>), 14.2 (-OCH<sub>2</sub>CH<sub>3</sub>).

### ***para*-Ferrocenyl-cinnamic acid 85**

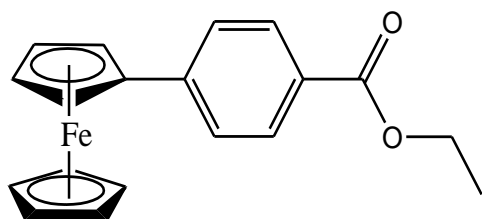


Sodium hydroxide (15 mL, 10 %) was added to a solution of *para*-ferrocenyl-ethyl cinnamate (0.30 g, 8.3 mmol) in methanol (15 mL). This was heated and allowed to reflux for 24 hours. The solution was cooled on ice and acidified to pH 2 with conc. HCl. The product was isolated by vacuum filtration as an orange solid (0.26 g, 94 %), mp 253-254 °C;

$^1\text{H}$  NMR (400 MHz)  $\delta$  (DMSO- $d_6$ ): 12.37 (1H, br.s, -OH), 7.61-7.51 (5H, m, ArH, =CH-), 6.52 (1H, d,  $J$  16 Hz, -CH=), 4.86 {2H, s, *ortho* on ( $\eta^5$ -C<sub>5</sub>H<sub>4</sub>)}, 4.40 {2H, s, *meta* on ( $\eta^5$ -C<sub>5</sub>H<sub>4</sub>)}, 4.02 {5H, s, ( $\eta^5$ -C<sub>5</sub>H<sub>5</sub>)};

$^{13}\text{C}$  NMR (100 MHz)  $\delta$  (DMSO- $d_6$ ): 167.8 (C=O), 143.9 (-CH=), 141.8 (C<sub>q</sub>), 131.6 (C<sub>q</sub>), 128.4, 126.0, 117.8 (-CH=), 83.5 (C<sub>ipso</sub>  $\eta^5$ -C<sub>5</sub>H<sub>4</sub>), 69.5 ( $\eta^5$ -C<sub>5</sub>H<sub>5</sub>), 69.4 (C<sub>meta</sub>  $\eta^5$ -C<sub>5</sub>H<sub>4</sub>), 66.5 (C<sub>ortho</sub>  $\eta^5$ -C<sub>5</sub>H<sub>4</sub>).

### ***para*-Ferrocenyl ethyl benzoate 86**

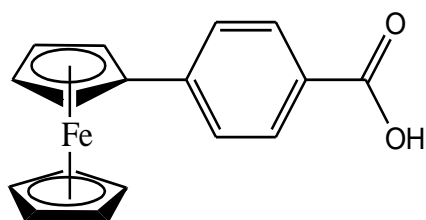


To a solution of ethyl-4-amino benzoate (1.90 g, 11.5 mmol) in water (20 mL) was added conc. HCl (5 mL). A solution of sodium nitrite (1.00 g, 13.8 mmol) in water (20 mL) was then added slowly with stirring while the temperature was kept below 5 °C to furnish the diazonium salt. This was then added to a solution of ferrocene (2.57 g, 13.8 mmol) in diethyl ether (40 mL) and allowed to stir for 24 hours. The reaction mixture was washed with water, the organic layer was dried over magnesium sulphate and the solvent was removed *in vacuo* to yield the crude product. It was purified by column chromatography (eluent 5 % diethyl ether: 95 % hexane) to yield the title compound as an orange solid (0.81 g, 21 %), mp 92°C (lit<sup>23</sup> 92-94 °C);

<sup>1</sup>H NMR (600 MHz)  $\delta$  (DMSO-*d*<sub>6</sub>): 8.09 (2H, d, *J* 8.4 Hz, ArH), 7.88 (2H, d, *J* 8.4 Hz, ArH), 4.91 {2H, t, *J* 1.8 Hz, *ortho* on ( $\eta^5$ -C<sub>5</sub>H<sub>4</sub>)}, 4.46 {2H, t, *J* 1.8 Hz, *meta* on ( $\eta^5$ -C<sub>5</sub>H<sub>4</sub>)}, 4.32 (2H, q, *J* 7.2 Hz, 6.6 Hz, -OCH<sub>2</sub>CH<sub>3</sub>-), 4.04 (5H, s,  $\eta^5$ -C<sub>5</sub>H<sub>4</sub>), 1.34 (3H, t, *J* 6.6 Hz, -OCH<sub>2</sub>CH<sub>3</sub>);

<sup>13</sup>C NMR (100 MHz)  $\delta$  (DMSO-*d*<sub>6</sub>): 165.7 (C=O), 145.1 (C<sub>q</sub>), 129.2, 126.8 (C<sub>q</sub>), 125.7, 82.6 (C<sub>ipso</sub>  $\eta^5$ -C<sub>5</sub>H<sub>4</sub>), 69.8 ( $\eta^5$ -C<sub>5</sub>H<sub>5</sub>), 69.6 (C<sub>meta</sub>  $\eta^5$ -C<sub>5</sub>H<sub>4</sub>), 66.8 (C<sub>ortho</sub>  $\eta^5$ -C<sub>5</sub>H<sub>4</sub>), 60.5 (-OCH<sub>2</sub>CH<sub>3</sub>), 14.2 (-OCH<sub>2</sub>CH<sub>3</sub>).

### ***para*-Ferrocenyl benzoic acid 87**

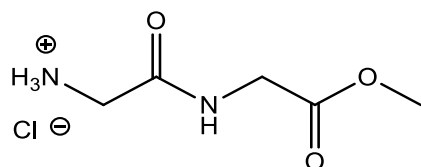


Sodium hydroxide (15 mL, 10 %) was added to a solution of *para*-ferrocenyl-ethyl benzoate (0.74 g, 2.2 mmol) in methanol (15 mL) and allowed to reflux for 24 hours. The solution was cooled on ice and acidified to pH 2 with conc. HCl. The product was isolated by vacuum filtration as an orange solid (0.67 g, 99 %), mp. {lit<sup>23</sup> 203°C (decomp.)};

$^1\text{H}$  NMR (600 MHz)  $\delta$  (DMSO- $d_6$ ): 12.7 (1H, br.s, -COOH), 7.78 (2H, d,  $J$  8.4 Hz, ArH), 7.58 (2H, d,  $J$  7.8 Hz, ArH), 4.82 {2H, s, *ortho* on ( $\eta^5$ -C<sub>5</sub>H<sub>4</sub>)}, 4.36 {2H, s, *meta* on ( $\eta^5$ -C<sub>5</sub>H<sub>4</sub>)}, 3.96 {5H, s, ( $\eta^5$ -C<sub>5</sub>H<sub>5</sub>)};

$^{13}\text{C}$  NMR (150 MHz)  $\delta$  (DMSO- $d_6$ ): 167.3 (C=O), 144.6 (C<sub>q</sub>), 129.4, 127.7 (C<sub>q</sub>), 125.6, 82.9 (C<sub>ipso</sub>  $\eta^5$ -C<sub>5</sub>H<sub>4</sub>), 69.7 ( $\eta^5$ -C<sub>5</sub>H<sub>5</sub>), 69.5 (C<sub>meta</sub>  $\eta^5$ -C<sub>5</sub>H<sub>4</sub>), 66.8 (C<sub>ortho</sub>  $\eta^5$ -C<sub>5</sub>H<sub>4</sub>).

### Glycine-glycine methyl ester hydrochloride **88**

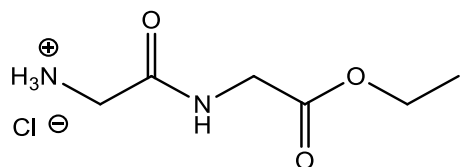


Glycine-glycine (4.00 g, 30.3 mmol) was dissolved in methanol (40 mL). Thionyl chloride (5 mL) was added slowly with cooling. The solution was allowed to stir at room temperature for two days. The solvent was removed *in vacuo* to yield the title compound as a white solid (4.12 g, 74 %), mp 107-109 °C;

$^1\text{H}$  NMR (400 MHz)  $\delta$  (DMSO- $d_6$ ): 9.07 (1H, t,  $J$  5.6 Hz, -CONH-), 8.39 (3H, br.s, NH<sub>3</sub>CH<sub>2</sub>-), 3.93 (2H, d,  $J$  6 Hz, -NHCH<sub>2</sub>-), 3.64 (3H, s, -OCH<sub>3</sub>), 3.60 (2H, s, -NH<sub>3</sub>CH<sub>2</sub>-);

$^{13}\text{C}$  NMR (100 MHz)  $\delta$  (DMSO- $d_6$ ): 170.6 (C=O), 166.5 (C=O), 52.5 (-NHCH<sub>2</sub>-), 51.8 (NH<sub>3</sub>CH<sub>2</sub>-), 40.6 (-OCH<sub>3</sub>).

### Glycine-glycine ethyl ester hydrochloride **89**

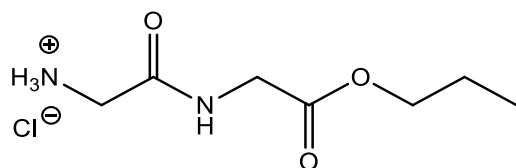


The synthesis followed that of **88** using the following reagents; glycine-glycine (0.51 g, 3.8 mmol), ethanol (40 mL), thionyl chloride (5 mL). The solvent was removed *in vacuo* to yield the title compound as a white solid. (0.52 g, 70 %), mp 178-179 °C;

$^1\text{H}$  NMR (400 MHz)  $\delta$  (DMSO- $d_6$ ): 8.95 (1H, t,  $J$  6 Hz, -CONH-), 8.26 (3H, br.s, -NH $_3$ ), 4.11 (2H, q,  $J$  6.8 Hz, -OCH $_2$ CH $_3$ ), 3.93 (2H, d,  $J$  5.6 Hz, -NHCH $_2$ -), 3.60 (2H, s, NH $_3$ CH $_2$ -), 1.20 (3H, t,  $J$  6.8 Hz, -OCH $_2$ CH $_3$ );

$^{13}\text{C}$  NMR (100 MHz)  $\delta$  (DMSO- $d_6$ ): 169.4 (C=O), 166.5 (C=O), 60.6 (-OCH $_2$ CH $_3$ ), 40.7 (NH $_3$ CH $_2$ -), 40.6 (-NHCH $_2$ -), 14.0 (-OCH $_2$ CH $_3$ ).

### Glycine-glycine propyl ester hydrochloride 90

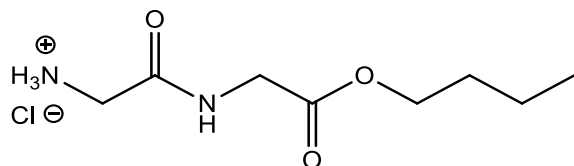


The synthesis followed that of **88** using the following reagents; glycine-glycine (0.51 g, 3.8 mmol), propanol (40 mL), thionyl chloride (5 mL). The solvent was removed *in vacuo* to yield the title compound as a white solid. (0.61 g, 76 %), mp 161 °C;

$^1\text{H}$  NMR (400 MHz)  $\delta$  (DMSO- $d_6$ ): 8.95 (1H, t,  $J$  6 Hz, -CONH-), 8.25 (3H, br.s, -NH $_3$ ), 4.03 (2H, t,  $J$  6.8 Hz, -OCH $_2$ CH $_2$ -), 3.95 (2H, d,  $J$  6 Hz, -NHCH $_2$ -), 3.60 (2H, s, NH $_3$ CH $_2$ -), 1.60 (2H, m, -CH $_2$ CH $_3$ ), 0.89 (3H, t,  $J$  7.6 Hz, -CH $_2$ CH $_3$ );

$^{13}\text{C}$  NMR (100 MHz)  $\delta$  (DMSO- $d_6$ ): 169.5 (C=O), 166.5 (C=O), 66.0 (-OCH $_2$ -), 40.6 (-NHCH $_2$ -), 39.9 (NH $_3$ CH $_2$ -), 21.5 (-CH $_2$ CH $_3$ ), 10.2 (-CH $_2$ CH $_3$ ).

### Glycine-glycine butyl ester hydrochloride 91

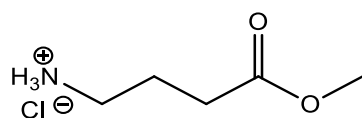


The synthesis followed that of **88** using the following reagents; glycine-glycine (0.50 g, 3.8 mmol), butanol (20 mL), thionyl chloride (5 mL). The solvent was removed *in vacuo* to yield the title compound as a white solid. (0.59 g, 69 %), mp 155-156°C;

$^1\text{H}$  NMR (400 MHz)  $\delta$  (DMSO- $d_6$ ): 8.98 (1H, t,  $J$  5.6 Hz, -CONH-), 8.28 (3H, br.s, -NH $_3$ ), 4.06 (2H, t,  $J$  6.8 Hz, -OCH $_2$ CH $_2$ -), 3.93 (2H, d,  $J$  5.6 Hz, -NHCH $_2$ -), 3.60 (2H, s, NH $_3$ CH $_2$ -), 1.56 (2H, qt,  $J$  6.8 Hz, -CH $_2$ CH $_2$ CH $_2$ -), (2H, m, -CH $_2$ CH $_3$ ), 0.89 (3H, t,  $J$  7.2 Hz, -CH $_2$ CH $_3$ );

$^{13}\text{C}$  NMR (100 MHz)  $\delta$  (DMSO- $d_6$ ): 169.4 (C=O), 166.5 (C=O), 64.2 (-OCH $_2$ -), 40.6 (-NHCH $_2$ -), 39.8 (NH $_3$ CH $_2$ -), 30.1 (-OCH $_2$ CH $_2$ -), 18.5 (-CH $_2$ CH $_3$ ), 13.5 (-CH $_3$ ).

### $\gamma$ -Aminobutyric acid methyl ester hydrochloride **92**

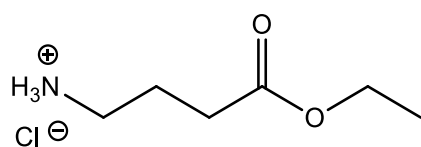


The synthesis followed that of **88** using the following reagents;  $\gamma$ -aminobutyric acid (5.00 g, 48.5 mmol), methanol (40 mL), thionyl chloride (5 mL). The solvent was removed *in vacuo* to yield the title compound as a white solid. (4.33 g, 58 %), mp 115 °C;

$^1\text{H}$  NMR (400 MHz)  $\delta$  (DMSO- $d_6$ ): 8.14 (3H, br.s, -NH $_3$ ), 3.60 (3H, s, -OCH $_3$ ), 2.78 (2H, t,  $J$  7.6 Hz, -COCH $_2$ -), 2.44 (2H, t,  $J$  7.6 Hz, NH $_3$ CH $_2$ -), 1.81 (2H, qt,  $J$  7.6 Hz, -CH $_2$ CH $_2$ CH $_2$ -);

$^{13}\text{C}$  NMR (100 MHz)  $\delta$  (DMSO- $d_6$ ): 172.6 (C=O), 51.4 (-OCH $_3$ ), 38.1 (-COCH $_2$ -), 30.2 (NH $_3$ CH $_2$ -), 22.4 (-CH $_2$ CH $_2$ CH $_2$ -).

### $\gamma$ -Aminobutyric acid ethyl ester hydrochloride **93**



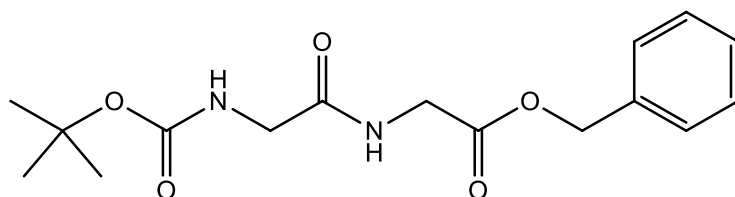
The synthesis followed that of **88** using the following reagents;  $\gamma$ -aminobutyric acid (2.05 g, 19.9 mmol), ethanol (30 mL), thionyl chloride (5 mL). The solvent was removed *in vacuo* to yield the title compound as a white solid. (2.19 g, 66 %), mp 47-48 °C;

$^1\text{H}$  NMR (600 MHz)  $\delta$  (DMSO- $d_6$ ): 8.24 (3H, br. s, -NH $_3$ CH $_2$ -), 4.06 (2H, q,  $J$  7.2 Hz, -OCH $_2$ CH $_3$ ), 2.79 (2H, t,  $J$  7.2 Hz, -COCH $_2$ -), 2.43 (2H, t,  $J$  7.8 Hz, NH $_3$ CH $_2$ -), (2H, qt,  $J$  7.2 Hz, -CH $_2$ CH $_2$ CH $_2$ -), 1.19 (3H, t,  $J$  7.2 Hz, -OCH $_2$ CH $_3$ );

$^{13}\text{C}$  NMR (100 MHz)  $\delta$  (DMSO- $d_6$ ): 172.1 (C=O), 59.9 (-OCH<sub>2</sub>CH<sub>3</sub>), 38.0 (-COCH<sub>2</sub>-), 30.4 (NH<sub>3</sub>CH<sub>2</sub>-), 22.3,(-CH<sub>2</sub>CH<sub>2</sub>CH<sub>2</sub>-) 14.1 (-OCH<sub>2</sub>CH<sub>3</sub>).

## General procedure for the preparation of Boc protected dipeptide esters

### Boc glycine-glycine benzyl ester **94**

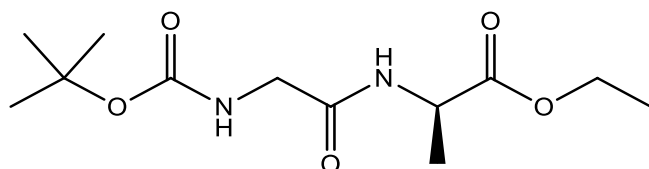


To a solution of Boc-Glycine-OH (0.62 g, 3.5 mmol) in DCM (50 mL) was added ethyl dimethylaminopropyl carbodiimide (EDC) (1.13 g, 5.9 mmol), *N*-hydroxy succinimide (NHS) (0.17 g, 1.5 mmol) and triethylamine (5 mL). The solution was allowed to stir at 0 °C for one hour. Glycine benzyl ester *p*-toluenesulfonate (1.00 g, 3.0 mmol) was then added. The solution was allowed to stir for a further 20 minutes at 0 °C before the temperature was raised and the solution was allowed to stir at room temperature for 48 hours. The solvent was removed in vacuo and the crude product was purified by column chromatography (eluent 50 % ethyl acetate: 50 % hexane) to afford the product as a white solid (0.46 g, 41 %), mp 76-77 °C;

<sup>1</sup>H NMR (400 MHz)  $\delta$  (DMSO-*d*<sub>6</sub>): 8.31 (1H, t, *J* 5.6 Hz, -CONH-), 7.47-7.37 (5H, m, ArH), 7.10 (1H, t, *J* 6 Hz, -CONH-), 5.20 (2H, s, -OCH<sub>2</sub>Ph), 3.97 (2H, d, *J* 6 Hz, -NHCH<sub>2</sub>-), 3.65 (2H, d, *J* 6.4 Hz, -NHCH<sub>2</sub>-), 1.44 {9H, s, -(CH<sub>3</sub>)<sub>3</sub>};

<sup>13</sup>C NMR (100 MHz)  $\delta$  (DMSO-*d*<sub>6</sub>): 170.0 (C=O), 169.7 (C=O), 167.3 (C=O), 155.8 (C<sub>q</sub>), 128.4, 128.3, 128.2, 86.3 (C<sub>q</sub>), 65.8 (OCH<sub>2</sub>), 43.0 (NHCH<sub>2</sub>), 40.6 (NHCH<sub>2</sub>), 28.2 {(CH<sub>3</sub>)<sub>3</sub>}.

### Boc-glycine-L-alanine-ethyl ester **95**



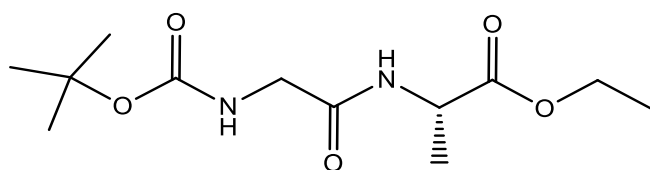
The synthesis followed that of **94** using the following reagents; Boc-glycine-OH (0.86 g, 5.0 mmol), L-alanine ethyl ester hydrochloride (1.17 g, 7.6 mmol), NHS (0.32 g, 2.8 mmol), EDC (2.15 g, 11.2 mmol). The product was purified by column chromatography (eluent 50 % ethyl acetate: 50 % hexane) to yield the title compound as a transparent oil (0.73 g, 53 %);



$^1\text{H}$  NMR (400 MHz)  $\delta$  (DMSO- $d_6$ ): 8.19 (1H, d,  $J$  7.2 Hz, -CONH-), 6.93 (1H, t,  $J$  6 Hz, -CONH-), 4.25 (1H, qt,  $J$  7.2 Hz, -NHCH-), 4.08 (2H, q,  $J$  7.2 Hz, -OCH<sub>2</sub>CH<sub>3</sub>), 3.57 (1H, dd,  $J$  10.4 Hz and 6.4 Hz, -NHCH<sub>2</sub>-), 3.52 (1H, dd,  $J$  10.4 Hz and 6.4 Hz, -NHCH<sub>2</sub>-), 1.38 {9H, s, -C(CH<sub>3</sub>)<sub>3</sub>}, 1.27 (3H, d,  $J$  7.2 Hz, -CHCH<sub>3</sub>), 1.18 (3H, t,  $J$  8 Hz, -OCH<sub>2</sub>CH<sub>3</sub>);

$^{13}\text{C}$  NMR (100 MHz)  $\delta$  (DMSO- $d_6$ ): 172.5 (C=O), 169.2 (C=O), 155.7 (C=O), 77.9 (C<sub>q</sub>), 60.4 (-OCH<sub>2</sub>CH<sub>3</sub>-), 47.5 (-NHCH<sub>2</sub>-), 42.7 (-NHCH<sub>2</sub>-), 28.1 {-C(CH<sub>3</sub>)<sub>3</sub>}, 17.0 (-OCH<sub>2</sub>CH<sub>3</sub>), 14.0 {-C(CH<sub>3</sub>)<sub>3</sub>}.

#### Boc-glycine-D-alanine-ethyl ester **96**

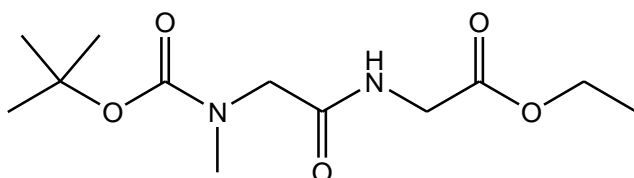


The synthesis followed that of **94** using the following reagents; Boc-glycine-OH (6.03 g, 34.4 mmol), D-alanine ethyl ester hydrochloride (5.00 g, 32.5 mmol), NHS (1.94 g, 16.8 mmol), EDC (11.0 g, 57.4 mmol). The product was purified by column chromatography (eluent 50 % ethyl acetate: 50 % hexane) to yield the title compound as a transparent oil (2.54 g, 32 %)

$^1\text{H}$  NMR (400 MHz)  $\delta$  (DMSO- $d_6$ ): 8.19 (1H, d,  $J$  7.2 Hz, -CONH-), 6.92 (1H, t,  $J$  6 Hz), 4.26 (1H, qt,  $J$  7.6 Hz, -NHCH-), 4.07 (2H, q,  $J$  7.2 Hz, -OCH<sub>2</sub>CH<sub>3</sub>-), 3.60 (1H, dd,  $J$  10.4 Hz and 6.4 Hz, -NHCH<sub>2</sub>-), 3.52 (1H, dd,  $J$  10.8 Hz and 6 Hz, -NHCH<sub>2</sub>-), 1.38 {9H, s, -C(CH<sub>3</sub>)<sub>3</sub>}, 1.27 (3H, d,  $J$  7.2 Hz, -CHCH<sub>3</sub>), 1.18 (3H, t,  $J$  6.8 Hz, -OCH<sub>2</sub>CH<sub>3</sub>)

$^{13}\text{C}$  NMR (100 MHz)  $\delta$  (DMSO- $d_6$ ): 172.5 (C=O), 169.2 (C=O), 155.7 (C=O), 77.9 (C<sub>q</sub>), 60.4 (-OCH<sub>2</sub>), 47.5 (-CHCH<sub>3</sub>), 42.7 (-NHCH<sub>2</sub>-), 28.1 {-C(CH<sub>3</sub>)<sub>3</sub>}, 17.0 (-OCH<sub>2</sub>CH<sub>3</sub>), 14.0 (-CHCH<sub>3</sub>).

#### Boc-sarcosine-glycine-ethyl ester **97**



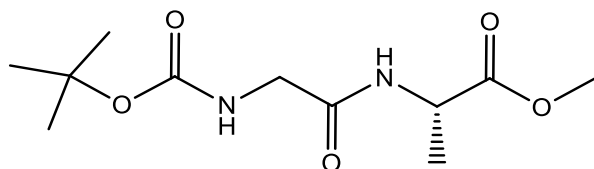
The synthesis followed that of **94** using the following reagents; Boc-sarcosine-OH (9.04 g, 51.6 mmol), glycine ethyl ester hydrochloride (6.00 g, 43.0 mmol), NHS (2.47 g, 21.5 mmol),

EDC (16.48 g, 85.9 mmol). The product was purified by column chromatography (eluent 50 % ethyl acetate: 50 % hexane) to yield the title compound as a transparent oil (3.2 g, 27 %);

$^1\text{H}$  NMR (400 MHz)  $\delta$  (DMSO- $d_6$ ): 8.29 (1H, br.s, -CONH-), 4.10 (2H, q,  $J$  7.2 Hz, -OCH<sub>2</sub>CH<sub>3</sub>), 3.74-3.84 {4H, m, -NHCH<sub>2</sub>-, -N(CH<sub>3</sub>)CH-}, 2.77 {3H, s, -N(CH<sub>3</sub>)}, 1.40 {9H, s, -C(CH<sub>3</sub>)<sub>3</sub>}, 1.19 (3H, t,  $J$  8 Hz, -OCH<sub>2</sub>CH<sub>3</sub>);

$^{13}\text{C}$  NMR (100 MHz)  $\delta$  (DMSO- $d_6$ ): 169.6 (C=O), 168.9 (C=O), 156.1 (C=O), 79.3 (C<sub>q</sub>), 62.0 (-OCH<sub>2</sub>CH<sub>3</sub>-), 59.5 {-N(CH<sub>3</sub>)CH}, 41.4 (-NHCH<sub>2</sub>-), 36.1 {-N(CH<sub>3</sub>)}, 28.7 {-C(CH<sub>3</sub>)<sub>3</sub>}, 14.2 (-OCH<sub>2</sub>CH<sub>3</sub>).

### Boc-glycine-D-alanine-methyl ester **97**

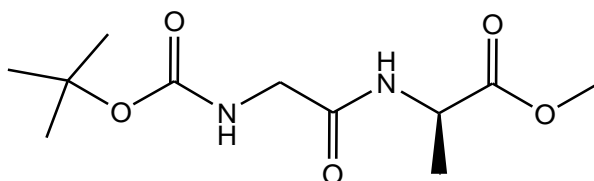


The synthesis followed that of **94** using the following reagents: Boc-glycine-OH (1.63 g, 9.3 mmol), EDC (3.00 g, 15.6 mmol), NHS (0.45 g, 3.9 mmol) and D-alanine methyl ester hydrochloride (1.09 g, 7.8 mmol). The product was purified by column chromatography (eluent 50 % ethyl acetate: 50 % hexane) to yield the title compound as a transparent oil (0.63 g, 31 %);

$^1\text{H}$  NMR (400 MHz)  $\delta$  (DMSO- $d_6$ ): 8.22 (1H, d,  $J$  7.2 Hz, -CONH-), 6.93 (1H, t,  $J$  6 Hz, -CONH-), 4.28 (1H, qt,  $J$  7.2 Hz, -NHCH-), 3.62 (3H, s, -OCH<sub>3</sub>), 3.60-3.49 (2H, m, -NHCH<sub>2</sub>-), 1.38 {9H, s, -C(CH<sub>3</sub>)<sub>3</sub>}, 1.27 (3H, d,  $J$  7.2 Hz, -CHCH<sub>3</sub>);

$^{13}\text{C}$  NMR (100 MHz)  $\delta$  (DMSO- $d_6$ ): 178.3 (C=O), 174.4 (C=O), 161.0 (C=O), 83.2 (C<sub>q</sub>), 57.1 (-OCH<sub>3</sub>), 52.6 (-NHCH-), 48.0 (-NHCH<sub>2</sub>-), 33.4 {-C(CH<sub>3</sub>)<sub>3</sub>}, 22.32 (-CHCH<sub>3</sub>).

### Boc-glycine-L-alanine-methyl ester **98**

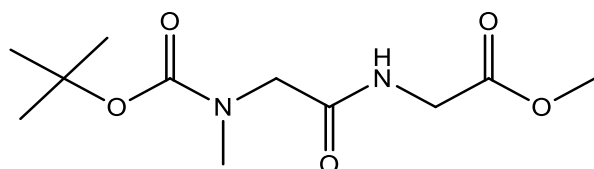


The synthesis followed that of **94** using the following reagents: Boc-glycine-OH (6.02 g, 34.4 mmol), EDC (11.0 g, 57.4 mmol), NHS (1.65 g, 14.4 mmol) and L-alanine methyl ester hydrochloride (4.00 g, 28.7 mmol). The product was purified by column chromatography (eluent 50 % ethyl acetate: 50 % hexane) to yield the title compound as a transparent oil (2.63 g, 35 %);

$^1\text{H}$  NMR (400 MHz)  $\delta$  (DMSO- $d_6$ ): 8.22 (1H, d,  $J$  7.2 Hz, -CONH-), 6.93 (1H, t,  $J$  6 Hz, -CONH-), 4.28 (1H, qt,  $J$  7.2 Hz, -NHCH-), 3.62 (3H, s, -OCH<sub>3</sub>), 3.60-3.42 (2H, m, -NHCH<sub>2</sub>-), 1.38 {9H, s, -C(CH<sub>3</sub>)<sub>3</sub>}, 1.27 {3H, d,  $J$  7.2 Hz, -C(CH<sub>3</sub>)<sub>3</sub>};

$^{13}\text{C}$  NMR (100 MHz)  $\delta$  (DMSO- $d_6$ ): 173.0 (C=O), 169.2 (C=O), 155.7 (C=O), 77.9 (C<sub>q</sub>), 51.9 (-OCH<sub>3</sub>-) 47.4 (-NHCH-), 42.7 (-NHCH<sub>2</sub>-), 28.2 {-C(CH<sub>3</sub>)<sub>3</sub>}, 17.1 (-CHCH<sub>3</sub>).

### Boc-sarcosine-glycine-methyl ester **99**



The synthesis followed that of **94** using the following reagents: Boc-sarcosine-OH (6.00 g, 31.7 mmol), EDC (12.16 g, 63.4 mmol), NHS (1.82 g, 15.9 mmol) and glycine methyl ester hydrochloride (4.70 g, 37.4 mmol). The product was purified by column chromatography (eluent 50 % ethyl acetate: 50 % hexane) to yield the title compound as a transparent oil (1.23 g, 15 %);

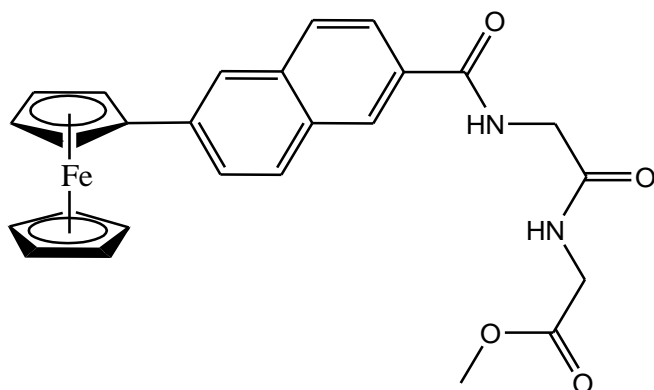
$^1\text{H}$  NMR (400 MHz)  $\delta$  (DMSO- $d_6$ ): 8.31 (1H, br.s, -NHCH<sub>2</sub>-), 3.79-3.87 (4H, m, -NHCH<sub>2</sub>-, -N(CH<sub>3</sub>)CH<sub>2</sub>-), 3.63 (3H, s, -OCH<sub>3</sub>), 2.79 (3H, s, -NCH<sub>3</sub>), 1.40 and 1.35 {9H, s, s, -(CH<sub>3</sub>)<sub>3</sub>}.

$^{13}\text{C}$  NMR (100 MHz)  $\delta$  (DMSO- $d_6$ ): 170.3 (C=O), 170.2 (C=O), 169.3 (C=O), 78.7 (C<sub>q</sub>), 51.7 (-OCH<sub>3</sub>), 51.4 (-NCH<sub>3</sub>CH<sub>2</sub>-), 40.4 (-NHCH<sub>2</sub>-), 35.3 & 35.1(-NCH<sub>3</sub>), 28.0 & 27.8 {C(CH<sub>3</sub>)<sub>3</sub>}.



**General procedure for the synthesis of N-(6-ferrocenyl-2-naphthoyl)-glycine-glycine esters.**

**N-(6-ferrocenyl-2-naphthoyl)-glycine-glycine methyl ester 100.**



Glycine-glycine methyl ester hydrochloride (0.35 g, 1.9 mmol) was added to a solution of 6-ferrocenylnaphthalene-2-carboxylic acid (0.40 g, 1.1 mmol), 1-hydroxybenzotriazole (0.27 g, 2.0 mmol), *N*-(3-dimethylaminopropyl)-*N'*-ethylcarbodiimide hydrochloride (0.37 g, 2.4 mmol) and triethylamine (5 mL) in dichloromethane (50 mL) at 0 °C. The temperature was raised to room temperature after 30 minutes and the reaction was allowed to stir for 48 h. The reaction mixture was washed with water and the organic layer was dried over MgSO<sub>4</sub> and the solvent was removed *in vacuo*. The product was purified by column chromatography (eluent 20 % ethyl acetate: 80 % hexane -100 % ethyl acetate) to yield the title compound as an orange solid (0.27 g, 51 %), mp 197-198 °C;

Anal. calc. for C<sub>26</sub>H<sub>24</sub>N<sub>2</sub>O<sub>4</sub>Fe: C, 64.48; H, 4.99; N, 5.78 %. Found: C, 64.47; H, 5.05; N, 5.65;

*m/z* (ESI) 484.1080 [M]<sup>+</sup>. C<sub>26</sub>H<sub>24</sub>N<sub>2</sub>O<sub>4</sub>Fe requires 484.1085;

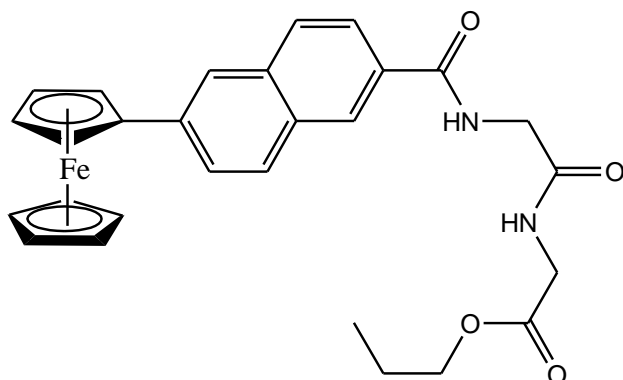
UV-Vis λ<sub>max</sub> (CH<sub>3</sub>CN)/nm 369 (ε/dm<sup>3</sup>mol<sup>-1</sup>cm<sup>-1</sup> 3093), 451 (1344);

I.R. ν<sub>max</sub> (neat)/ cm<sup>-1</sup> 3418, 3313, 1741, 1638, 1622, 1512, 1211;

<sup>1</sup>H NMR (400 MHz) δ (DMSO-*d*<sub>6</sub>): 8.95 (1H, t, *J* 5.6 Hz, -CONH-), 8.46 (1H, s, ArH), 8.42 (1H, t, *J* 5.6 Hz, -CONH-), 8.07 (1H, s, ArH), 7.94-7.97 (3H, m, ArH), 7.83 (1H, dd, *J* 7.2 Hz and 1.6 Hz, ArH), 4.97 {2H, t, *J* 1.6 Hz, *ortho* on (η<sup>5</sup>-C<sub>5</sub>H<sub>4</sub>)}, 4.46 {2H, t, *J* 1.6 Hz, *meta* on (η<sup>5</sup>-C<sub>5</sub>H<sub>4</sub>)}, 4.05 (5H, s, η<sup>5</sup>-C<sub>5</sub>H<sub>5</sub>), 3.98 (2H, d, *J* 5.6 Hz, -NHCH<sub>2</sub>-), 3.89 (2H, d, *J* 6 Hz, -NHCH<sub>2</sub>-), 3.64 (3H, s, -OCH<sub>3</sub>);

<sup>13</sup>C NMR (100 MHz) δ (DMSO-*d*<sub>6</sub>): 170.3 (C=O), 169.6 (C=O), 166.5 (C=O), 138.8 (C<sub>q</sub>), 134.5 (C<sub>q</sub>), 130.6 (C<sub>q</sub>), 130.4 (C<sub>q</sub>), 128.7, 127.6, 127.3, 125.9, 124.6, 122.7, 84.0 (C<sub>ipso</sub> η<sup>5</sup>-C<sub>5</sub>H<sub>4</sub>), 69.5 (η<sup>5</sup>-C<sub>5</sub>H<sub>5</sub>), 69.4 (C<sub>meta</sub> η<sup>5</sup>-C<sub>5</sub>H<sub>4</sub>), 66.6 (C<sub>ortho</sub> η<sup>5</sup>-C<sub>5</sub>H<sub>4</sub>), 51.7 (-OCH<sub>3</sub>), 42.4 (-NHCH<sub>2</sub>), 40.6 (-NHCH<sub>2</sub>).

***N*-(6-ferrocenyl-2-naphthoyl)-glycine-glycine propyl ester 101.**



The synthesis followed that of **100** using the following reagents; glycine-glycine propyl ester hydrochloride (0.24 g, 1.1 mmol) and ferrocenylnaphthalene-2-carboxylic acid (0.40 g, 1.1 mmol). The product was purified by column chromatography (eluent 20 % ethyl acetate: 100 % hexane -100 % ethyl acetate) to yield the title compound as an orange solid (0.31 g, 55 %), mp 115-117 °C;

$m/z$  (ESI) 512.1380 [M]<sup>+</sup>. C<sub>28</sub>H<sub>28</sub>N<sub>2</sub>O<sub>4</sub>Fe requires 512.1398;

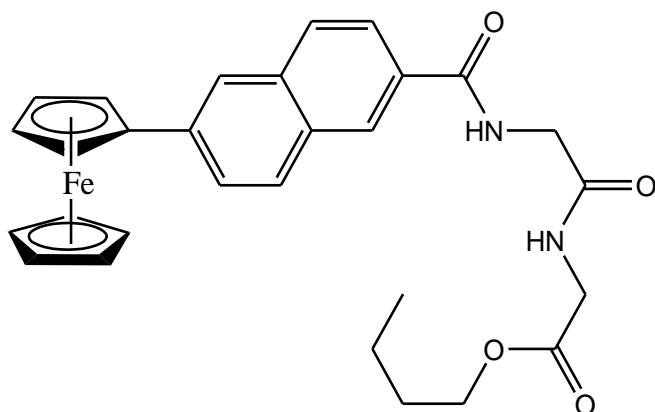
I.R.  $\nu_{\max}$  (neat)/cm<sup>-1</sup> 3281, 1753, 1653, 1523, 1203;

UV-Vis  $\lambda_{\max}$  (CH<sub>3</sub>CN)/nm 373 ( $\epsilon$ /dm<sup>3</sup>mol<sup>-1</sup>cm<sup>-1</sup> 2600), 448 (1086);

<sup>1</sup>H NMR (400 MHz)  $\delta$  (DMSO-*d*<sub>6</sub>): 8.95 (1H, t, *J* 6 Hz, -CONH-), 8.46 (1H, s, ArH), 8.40 (1H, t, *J* 6 Hz, -CONH-), 8.06 (1H, s, ArH), 7.94-7.97 (3 H, m, ArH), 7.83 (1H, dd, *J* 7.2 Hz and 1.6 Hz, -ArH), 4.96 {2H, t, *J* 1.6 Hz, *ortho* on ( $\eta^5$ -C<sub>5</sub>H<sub>4</sub>)}, 4.45 {2H, t, *J* 2 Hz, *meta* on ( $\eta^5$ -C<sub>5</sub>H<sub>4</sub>)}, 4.05-3.98 {9H, m, ( $\eta^5$ -C<sub>5</sub>H<sub>5</sub>), -NHCH<sub>2</sub>CO, -OCH<sub>2</sub>CH<sub>2</sub>-}, 3.89 (2H, d, *J* 6, -NHCH<sub>2</sub>-), 1.59 (2H, m, -CH<sub>2</sub>CH<sub>3</sub>), 0.88 (3H, t, *J* 7.2 Hz, -CH<sub>2</sub>CH<sub>3</sub>);

<sup>13</sup>C NMR (100 MHz)  $\delta$  (DMSO-*d*<sub>6</sub>): 169.9 (C=O), 169.6 (C=O), 166.6 (C=O), 138.8 (C<sub>q</sub>), 134.5 (C<sub>q</sub>), 130.6 (C<sub>q</sub>), 130.4 (C<sub>q</sub>), 128.7, 127.6, 127.3, 125.9, 124.6, 122.7, 84.0 (C<sub>ipso</sub>  $\eta^5$ -C<sub>5</sub>H<sub>4</sub>), 69.5 ( $\eta^5$ -C<sub>5</sub>H<sub>5</sub>), 69.4 (C<sub>meta</sub>  $\eta^5$ -C<sub>5</sub>H<sub>4</sub>), 66.6 (C<sub>ortho</sub>  $\eta^5$ -C<sub>5</sub>H<sub>4</sub>), 65.8(-OCH<sub>2</sub>CH<sub>2</sub>-), 42.5(-NHCH<sub>2</sub>), 40.6(-NHCH<sub>2</sub>), 21.5(-OCH<sub>2</sub>CH<sub>2</sub>-), 10.2(-CH<sub>3</sub>).

### **N-(6-ferrocenyl-2-naphthoyl)-glycine-glycine butyl ester 102**



The synthesis followed that of **100** using-glycine-glycine butyl ester hydrochloride (0.26 g, 1.2 mmol) and ferrocenylnaphthalene-2-carboxylic acid (0.50 g, 1.4 mmol). The product was purified by column chromatography (eluent 20 % ethyl acetate: 80 % hexane -100 % ethyl acetate) to yield the title compound as an orange solid (0.49 g, 78 %), mp 134-135 °C;

$m/z$  (ESI) 526.1541 [M]<sup>+</sup>. C<sub>29</sub>H<sub>30</sub>N<sub>2</sub>O<sub>4</sub>Fe requires 526.1555 ;

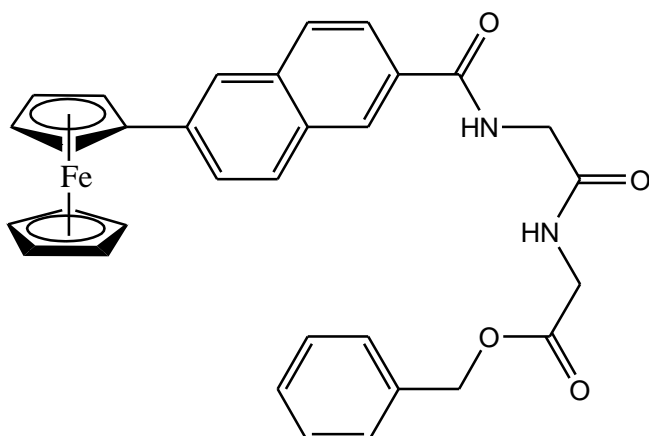
I.R.  $\nu_{\max}$  (neat)/cm<sup>-1</sup> 3298, 1749, 1645, 1544, 1175;

UV-Vis  $\lambda_{\max}$  (CH<sub>3</sub>CN)/nm 375 ( $\epsilon$ /dm<sup>3</sup>mol<sup>-1</sup>cm<sup>-1</sup> 2717), 452 (1174);

<sup>1</sup>H NMR (400 MHz)  $\delta$  (DMSO-*d*<sub>6</sub>): 8.95 (1H, t, *J* 6 Hz, -CONH-), 8.46 (1H, s, ArH), 8.39 (1H, t, *J* 6 Hz, -CONH-), 8.06 (1H, s, ArH), 7.92-7.97 (3H, m, ArH), 7.83 (1H, dd, *J* 6.8 Hz and 1.6 Hz, ArH), 4.96 {2H, t, *J* 2 Hz, *ortho* on ( $\eta^5$ -C<sub>5</sub>H<sub>4</sub>)}, 4.45 {2H, t, *J* 1.6 Hz, *meta* on ( $\eta^5$ -C<sub>5</sub>H<sub>4</sub>)}, 3.99-4.07 (7H, m, ( $\eta^5$ -C<sub>5</sub>H<sub>5</sub>) -OCH<sub>2</sub>CH<sub>2</sub>-), 3.98 (2H, d, *J* 6 Hz, -NHCH<sub>2</sub>-) 3.88 (2H, d, *J* 5.6 Hz, -NHCH<sub>2</sub>-), 1.56 (2H, qt, *J* 4.4 Hz, -OCH<sub>2</sub>CH<sub>2</sub>-), 1.32 (2H, sex, *J* 7.6 Hz, -CH<sub>2</sub>CH<sub>3</sub>), 0.88 (3H, t, *J* 7.6 Hz, -CH<sub>2</sub>CH<sub>3</sub>);

<sup>13</sup>C NMR (100 MHz)  $\delta$  (DMSO-*d*<sub>6</sub>): 169.8 (C=O), 169.6 (C=O), 166.5 (C=O), 138.8 (C<sub>q</sub>), 134.5 (C<sub>q</sub>), 130.6 (C<sub>q</sub>), 130.4 (C<sub>q</sub>), 128.7, 127.6, 127.3, 125.9, 124.6, 122.7, 84.0 (*C*<sub>ipso</sub>  $\eta^5$ -C<sub>5</sub>H<sub>4</sub>), 69.5 ( $\eta^5$ -C<sub>5</sub>H<sub>5</sub>), 69.4 (*C*<sub>meta</sub>  $\eta^5$ -C<sub>5</sub>H<sub>5</sub>), 66.6 (*C*<sub>ortho</sub>  $\eta^5$ -C<sub>5</sub>H<sub>4</sub>), 64.0 (-OCH<sub>2</sub>CH<sub>2</sub>-), 42.5 (-NHCH<sub>2</sub>-), 40.7 (-NHCH<sub>2</sub>-), 30.1 (-OCH<sub>2</sub>CH<sub>2</sub>-), 18.5 (-CH<sub>2</sub>CH<sub>3</sub>), 13.5 (-CH<sub>3</sub>).

### ***N*-(6-ferrocenyl-2-naphthoyl)-glycine-glycine benzyl ester 103**



The synthesis followed that of **100** using the following reagents; boc-glycine-glycine benzyl ester (0.34 g, 1.1 mmol) and ferrocenylnaphthalene-2-carboxylic acid (0.30 g, 0.8 mmol). The product was purified by column chromatography (eluent 20 % ethyl acetate: 80 % hexane - 100 % ethyl acetate) to yield the title compound as an orange solid (0.31 g, 66 %), mp 137-139 °C;

$m/z$  (ESI) 560.1392 [M]<sup>++</sup>. C<sub>32</sub>H<sub>28</sub>N<sub>2</sub>O<sub>4</sub>Fe requires 560.1398;

I.R.  $\nu_{\max}$  (neat)/cm<sup>-1</sup> 3263, 1749, 1645, 1544, 1175;

UV-Vis  $\lambda_{\max}$  (CH<sub>3</sub>CN)/nm 379 ( $\epsilon$ /dm<sup>3</sup>mol<sup>-1</sup>cm<sup>-1</sup> 2908), 452 (1281);

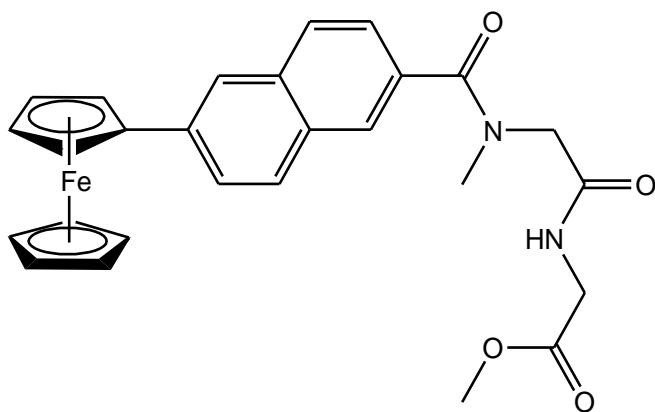
<sup>1</sup>H NMR (400 MHz)  $\delta$  (DMSO-*d*<sub>6</sub>): 8.96 (1H, t, *J* 6 Hz, -CONH-), 8.45 (2H, m, ArH, -CONH-), 8.07 (1H, s, ArH), 8.06 (1H, s, ArH), 7.94-8.04 (3H, m, ArH), 7.83 (1H, dd, *J* 7.2 Hz and 1.6 Hz, ArH), 7.31-7.38 (5H, m, ArH), 5.14 (2H, s, -OCH<sub>2</sub>Ph), 4.96 {2H, t, *J* 2 Hz, *ortho* on ( $\eta^5$ -C<sub>5</sub>H<sub>4</sub>)}, 4.45 {2H, t, *J* 1.6 Hz, *meta* on ( $\eta^5$ -C<sub>5</sub>H<sub>4</sub>)}, 4.05 (5H, s,  $\eta^5$ -C<sub>5</sub>H<sub>5</sub>), 3.99 (2H, d, *J* 5.6 Hz, -NHCH<sub>2</sub>-), 3.95 (2H, d, *J* 6 Hz, -NHCH<sub>2</sub>-);

<sup>13</sup>C NMR (100 MHz)  $\delta$  (DMSO-*d*<sub>6</sub>): 169.9 (C=O), 169.7 (C=O), 166.6 (C=O), 138.9 (C<sub>q</sub>), 135.9 (C<sub>q</sub>), 134.5 (C<sub>q</sub>), 130.6 (C<sub>q</sub>), 130.4 (C<sub>q</sub>), 128.7, 128.4, 128.1, 127.9, 127.6, 127.3, 125.9, 124.6, 122.7, 84.0 (C<sub>ipso</sub>  $\eta^5$ -C<sub>5</sub>H<sub>4</sub>), 69.5 ( $\eta^5$ -C<sub>5</sub>H<sub>5</sub>), 69.4 (C<sub>meta</sub>  $\eta^5$ -C<sub>5</sub>H<sub>4</sub>), 66.6 (C<sub>ortho</sub>  $\eta^5$ -C<sub>5</sub>H<sub>4</sub>), 65.8{-CH<sub>2</sub>(C<sub>6</sub>H<sub>5</sub>)-}, 42.5 (-NHCH<sub>2</sub>-), 40.7 (-NHCH<sub>2</sub>-).



**General procedures for the synthesis of N-(6-ferrocenyl-2-naphthoyl)-dipeptides and amino acids esters.**

**N-(6-ferrocenyl-2-naphthoyl)-sarcosine-glycine methyl ester 104.**



Sarcosine-glycine methyl ester trifluoroacetate salt (1.00 g, 3.5 mmol) was added to a solution of 6-ferrocenylnaphthalene-2-carboxylic acid (1.47 g, 4.1 mmol), EDC (1.32 g, 6.9 mmol), NHS (0.20 g, 1.7 mmol) and triethylamine (5 mL) in dichloromethane (50 mL) at 0 °C. The temperature was raised to room temperature after 30 minutes and the reaction was allowed to stir for 48 h. The reaction mixture was washed with water and the organic layer was dried over MgSO<sub>4</sub> and the solvent was removed *in vacuo*. The product was purified by column chromatography (eluent 20 % ethyl acetate: 80 % hexane -100 % ethyl acetate) to yield the title compound as an orange solid (0.33 g, 20 %), mp 86-87 °C;

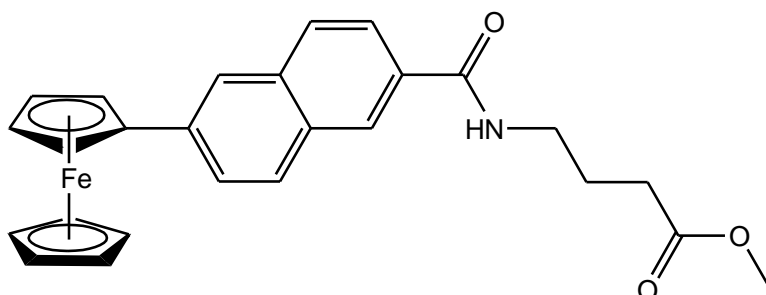
I.R.  $\nu_{\max}$  (neat)/cm<sup>-1</sup> 3291, 1742, 1624, 1543, 1205;

UV-Vis  $\lambda_{\max}$  (CH<sub>3</sub>CN)/nm 359 ( $\epsilon$ /dm<sup>3</sup>mol<sup>-1</sup>cm<sup>-1</sup> 2744), 452 (1027);

<sup>1</sup>H NMR (400 MHz)  $\delta$  (DMSO-*d*<sub>6</sub>): 8.59 & 8.51 (1H, br.s, br.s, -CONH-), 8.08 (1H, s, ArH), 8.05-7.89 (3H, m, ArH), 7.81 (1H, d, *J* 8.4 Hz, ArH), 7.65-7.58 (1H, m, ArH), 5.0 {2H, t, *J* 1.6 Hz, *ortho* on ( $\eta^5$ -C<sub>5</sub>H<sub>4</sub>)}, 4.48 {2H, t, *J* 1.6 Hz, *meta* on ( $\eta^5$ -C<sub>5</sub>H<sub>4</sub>)}, 4.20 {1H, s, -N(CH<sub>3</sub>)CH<sub>2</sub>-}, 3.92-4.04 {9H, m, ( $\eta^5$ -C<sub>5</sub>H<sub>5</sub>), -N(CH<sub>3</sub>)CH<sub>2</sub>-, -NHCH<sub>2</sub>-}, 3.66 (3H, d, *J* 6.4 Hz, -OCH<sub>3</sub>), 3.02 {3H, s, -N(CH<sub>3</sub>)};

<sup>13</sup>C NMR (100 MHz)  $\delta$  (DMSO-*d*<sub>6</sub>): 171.1 (C=O), 170.2 (C=O), 168.9 (C=O), 138.2 (C<sub>q</sub>), 133.5 (C<sub>q</sub>), 132.4 (C<sub>q</sub>), 130.7 (C<sub>q</sub>), 128.6, 127.5, 126.5, 125.9, 124.8, 122.8, 84.1 (*C*<sub>ipso</sub>  $\eta^5$ -C<sub>5</sub>H<sub>4</sub>), 69.5 ( $\eta^5$ -C<sub>5</sub>H<sub>5</sub>), 69.4 (*C*<sub>meta</sub>  $\eta^5$ -C<sub>5</sub>H<sub>4</sub>), 66.6 (*C*<sub>ortho</sub>  $\eta^5$ -C<sub>5</sub>H<sub>4</sub>), 53.8 (-NHCH<sub>2</sub>-), 49.7 {-N(CH<sub>3</sub>)CH<sub>2</sub>-}, 51.8 (-OCH<sub>3</sub>), 38.4 & 34.1 {-N(CH<sub>3</sub>)}.

***N*-(6-ferrocenyl-2-naphthoyl)- $\gamma$ -aminobutyric acid-methyl ester **105**.**



The synthesis followed that of **104** using the following reagents;  $\gamma$ -aminobutyric acid methyl ester (0.20 g, 1.3 mmol) and 6-ferrocenyl-naphthalene-2-carboxylic acid (0.39 g, 1.1 mmol), EDC (0.42 g, 2.2 mmol), NHS (0.06g, 0.6 mmol). The product was purified by column chromatography (eluent 20 % ethyl acetate: 80 % hexane -100 % ethyl acetate) to yield the title compound as an orange solid (0.25 g, 50 %), mp 128-129 °C;

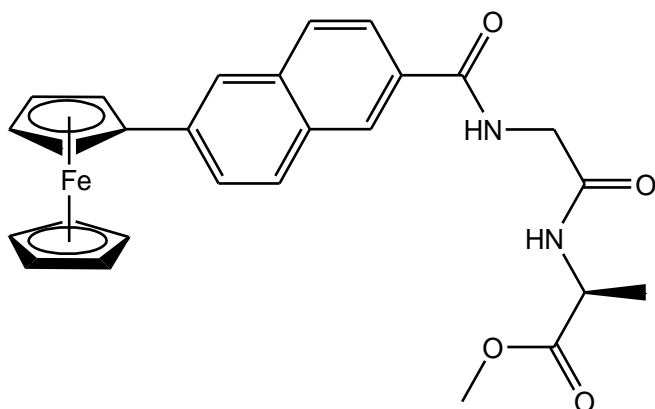
I.R.  $\nu_{\max}$  (neat)/ $\text{cm}^{-1}$  3305, 1729, 1624, 1547, 1166;

UV-Vis  $\lambda_{\max}$  ( $\text{CH}_3\text{CN}$ )/nm 371 ( $\epsilon/\text{dm}^3\text{mol}^{-1}\text{cm}^{-1}$  3127), 452 (1213);

$^1\text{H}$  NMR (400 MHz)  $\delta$  ( $\text{DMSO}-d_6$ ): 8.66 (1H, t,  $J$  5.6 Hz, -CONH-), 8.37 (1H, s, ArH), 7.96-7.89 (3H, m, ArH), 7.82 (1H, dd,  $J$  7.2 Hz and 1.6 Hz, ArH), 4.96 {2H, t,  $J$  1.6 Hz, *ortho* on ( $\eta^5$ - $\text{C}_5\text{H}_4$ )}, 4.45 {2H, t,  $J$  1.6 Hz, *meta* on ( $\eta^5$ - $\text{C}_5\text{H}_4$ )}, 4.05 {5H, s, ( $\eta^5$ - $\text{C}_5\text{H}_5$ )}, 3.62 (3H, s, - $\text{OCH}_3$ ), 2.43 (2H, t,  $J$  6.4 Hz, - $\text{COCH}_2$ -), 1.83 (2H, quin,  $J$  7.2 Hz, - $\text{CH}_2\text{CH}_2\text{CH}_2$ -), 1.17 (2H, t,  $J$  7.2 Hz, - $\text{NHCH}_2$ -);

$^{13}\text{C}$  NMR (100 MHz)  $\delta$  ( $\text{DMSO}-d_6$ ): 173.2 (C=O), 166.3 (C=O), 138.6 ( $\text{C}_q$ ), 134.4 ( $\text{C}_q$ ), 131.0 ( $\text{C}_q$ ), 130.7 ( $\text{C}_q$ ), 128.7, 127.3, 127.2, 125.9, 124.5, 122.7, 84.1 ( $\text{C}_{\text{ipso}}$   $\eta^5$ - $\text{C}_5\text{H}_4$ ), 69.4 ( $\eta^5$ - $\text{C}_5\text{H}_5$ ), ( $\text{C}_{\text{meta}}$   $\eta^5$ - $\text{C}_5\text{H}_4$ ), 66.6 ( $\text{C}_{\text{ortho}}$   $\eta^5$ - $\text{C}_5\text{H}_4$ ), 51.3 (- $\text{OCH}_3$ ), 38.6 (- $\text{NHCH}_2$ -), 30.8 (- $\text{COCH}_2$ -), 24.5 (- $\text{CH}_2\text{CH}_2\text{CH}_2$ -).

**N-(6-ferrocenyl-2-naphthoyl)-glycine-L-alanine-methyl ester 106.**



The synthesis followed that of **104** using the following reagents; glycine-L-alanine methyl ester trifluoroacetate salt (1.46 g, 5.1 mmol), 6-ferrocenylnaphthalene-2-carboxylic acid (1.50 g, 4.2 mmol), EDC (1.61 g, 8.42 mmol), NHS (0.24 g, 2.1 mmol) and triethylamine (5 mL). The product was purified by column chromatography (eluent 20 % ethyl acetate: 80 % hexane -100 % ethyl acetate) to yield the title compound as an orange solid (0.53 g, 26 %), mp 137-139°C;

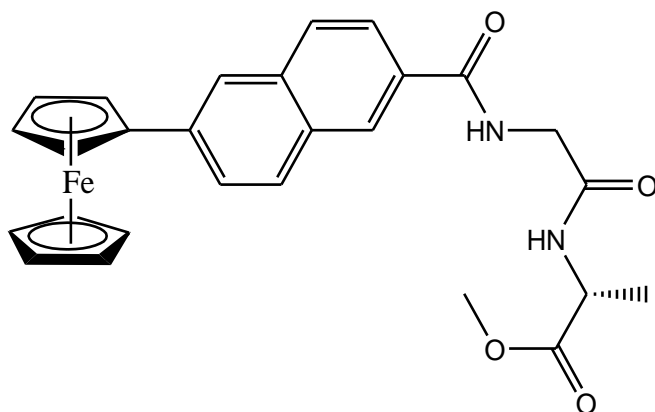
I.R.  $\nu_{\max}$  (neat)/ $\text{cm}^{-1}$  3305, 1734, 1627, 1516, 1200;

UV-Vis  $\lambda_{\max}$  (CH<sub>3</sub>CN)/nm 376 ( $\epsilon/\text{dm}^3\text{mol}^{-1}\text{cm}^{-1}$  3210), 452 (1302);

<sup>1</sup>H NMR (400 MHz)  $\delta$  (DMSO-*d*<sub>6</sub>): 8.85 (1H, t, *J* 5.6 Hz, -CONH-), 8.45 (2H, s, ArH), 8.06 (1H, s, ArH), 7.97-7.93 (2H, m, ArH), 7.83 (1H, dd, *J* 6.8 Hz and 1.6 Hz, -CONH-), 4.97 {2H, t, *J* 1.6 Hz, *ortho* on ( $\eta^5$ -C<sub>5</sub>H<sub>4</sub>)}, 4.46 {2H, t, *J* 2 Hz, *meta* on ( $\eta^5$ -C<sub>5</sub>H<sub>4</sub>)}, 4.34 (1H, qt, *J* 7.2, -NHCH-), 4.05 (5H, s,  $\eta^5$ -C<sub>5</sub>H<sub>4</sub>), 3.98 (2H, qd, *J* 10.8 Hz, 6 Hz, -NHCH<sub>2</sub>-), 3.64 (3H, s, -OCH<sub>3</sub>), 1.31 (3H, d, *J* 7.2 Hz, -CHCH<sub>3</sub>);

<sup>13</sup>C NMR (100 MHz)  $\delta$  (DMSO-*d*<sub>6</sub>): 173.0 (C=O), 168.9 (C=O), 166.4 (C=O), 138.8 (C<sub>q</sub>), 134.5 (C<sub>q</sub>), 130.6 (C<sub>q</sub>), 130.4 (C<sub>q</sub>), 128.7, 127.6, 127.3, 125.9, 124.5, 122.7, 84.1 (C<sub>ipso</sub>  $\eta^5$ -C<sub>5</sub>H<sub>4</sub>), 69.4 ( $\eta^5$ -C<sub>5</sub>H<sub>5</sub>), (C<sub>meta</sub>  $\eta^5$ -C<sub>5</sub>H<sub>4</sub>), 66.6 C<sub>ortho</sub>  $\eta^5$ -C<sub>5</sub>H<sub>4</sub>), 51.8 (-OCH<sub>3</sub>), 47.5 (-NHCH<sub>2</sub>-), 40.1 (NHCH-), 17.1 (-CHCH<sub>3</sub>).

***N*-(6-ferrocenyl-2-naphthoyl)-glycine-D-alanine-methyl ester **107**.**



The synthesis followed that of **104** using the following reagents; glycine-D-alanine methyl ester trifluoroacetate salt (0.29 g, 1.0 mmol) and 6-ferrocenylnaphthalene-2-carboxylic acid (0.30 g, 0.8 mmol), EDC (0.33 g, 1.7 mmol), NHS (0.05 g, 0.4 mmol). The product was purified by column chromatography (eluent 20 % ethyl acetate: 80 % hexane -100 % ethyl acetate) to yield the title compound as an orange solid (0.19 g, 47 %), mp 142-144 °C;

I.R.  $\nu_{\max}$  (neat)/ $\text{cm}^{-1}$  3292, 1747, 1624, 1645, 1513, 1206;

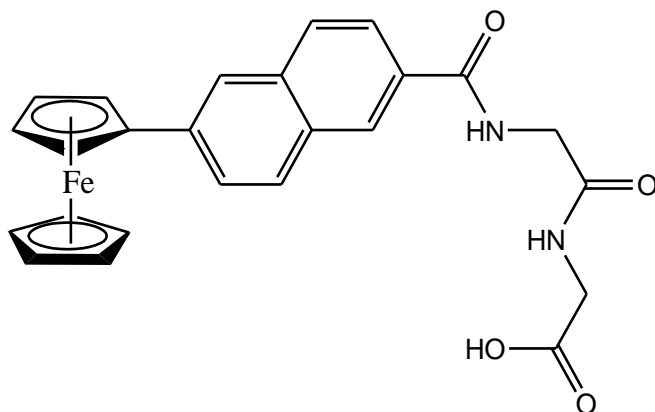
UV-Vis  $\lambda_{\max}$  ( $\text{CH}_3\text{CN}$ )/nm 363 ( $\epsilon/\text{dm}^3\text{mol}^{-1}\text{cm}^{-1}$  3682), 452 (1403);

$^1\text{H}$  NMR (400 MHz)  $\delta$  ( $\text{DMSO}-d_6$ ): 8.85 (1H, t,  $J$  5.6 Hz, -CONH-), 8.46 (2H, m, -CONH-, ArH), 8.06 (1H, s, ArH), 7.97-7.93 (3H, m, ArH), 7.83 (2H, dd,  $J$  6.8 Hz and 1.6 Hz, ArH), 4.97 {2H, t,  $J$  1.6 Hz, ortho on ( $\eta^5\text{-C}_5\text{H}_4$ )}, 4.46 {2H, t,  $J$  2 Hz, meta on ( $\eta^5\text{-C}_5\text{H}_4$ )}, 4.34 (1H, qt,  $J$  7.2 Hz, -NHCH-), 4.05 {5H, s, ( $\eta^5\text{-C}_5\text{H}_5$ )}, 3.98 (2H, dd,  $J$  10.8 Hz and 6 Hz, -NHCH<sub>2</sub>-), 3.64 (3H, s, -OCH<sub>3</sub>);

$^{13}\text{C}$  NMR (100 MHz)  $\delta$  ( $\text{DMSO}-d_6$ ): 173.0 (C=O), 168.9 (C=O), 166.4 (C=O), 138.8 (C<sub>q</sub>), 134.5 (C<sub>q</sub>), 130.6 (C<sub>q</sub>), 130.4 (C<sub>q</sub>), 128.7, 127.5, 127.3, 125.9, 124.5, 122.7, 84.0 (C<sub>ipso</sub>  $\eta^5\text{-C}_5\text{H}_4$ ), 69.4 ( $\eta^5\text{-C}_5\text{H}_5$ ), (C<sub>ortho</sub>  $\eta^5\text{-C}_5\text{H}_4$ ), 66.6 (C<sub>meta</sub>  $\eta^5\text{-C}_5\text{H}_4$ ), 51.9 (-OCH<sub>3</sub>), 47.5 (-NHCH<sub>2</sub>-), 42.2 (NHCH-), 17.1 (-NHCH<sub>3</sub>).

**General procedures for the synthesis of N-(6-ferrocenyl-2-naphthoyl)-dipeptides and amino acids.**

**N-(6-ferrocenyl-2-naphthoyl)-glycine-glycine-OH 108.**



N-(6-ferrocenyl-2-naphthoyl)-glycine-glycine ethyl ester (0.09 g, 0.2 mmol) was dissolved in methanol (15 mL) and sodium hydroxide (15 mL, 0.5 M) and allowed to reflux 24 hours. The solution was cooled on ice and acidified to pH 2. The product was isolated by vacuum filtration as an orange solid (0.05 g, 59 %), mp 155-157 °C;

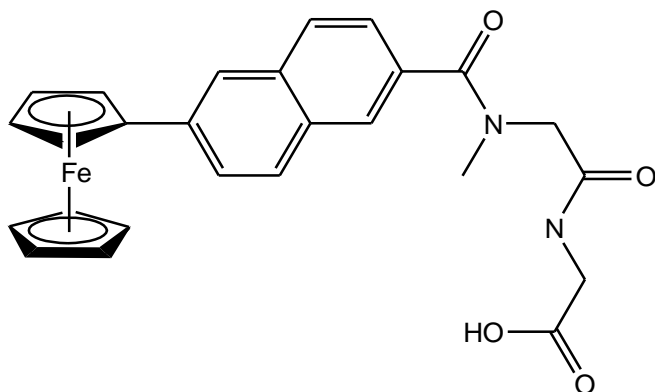
I.R.  $\nu_{\max}$  (neat)/ $\text{cm}^{-1}$  3277, 1690, 1628, 1600, 1544, 1392, 1243;

UV-Vis  $\lambda_{\max}$  (CH<sub>3</sub>CN)/nm 373 ( $\epsilon/\text{dm}^3\text{mol}^{-1}\text{cm}^{-1}$  1545), 452 (673);

<sup>1</sup>H NMR (400 MHz)  $\delta$  (DMSO-*d*<sub>6</sub>): 12.79 (1H, br.s, -OH), 8.96 (1H, t, *J* 5.6 Hz, -CONH-), 8.46-8.44 (1H, m, ArH), 8.29 (1H, t, *J* 6 Hz, -CONH-), 8.06 (1H, s, ArH), 7.98-7.91 (3H, m, ArH), 7.83 (1H, d, *J* 8.4 Hz, ArH), 4.96 {2H, s, *ortho* on ( $\eta^5$ -C<sub>5</sub>H<sub>4</sub>)}, 4.45 {2H, t, *J* 1.6 Hz, *meta* on ( $\eta^5$ -C<sub>5</sub>H<sub>4</sub>)}, 4.05 {5H, s, ( $\eta^5$ -C<sub>5</sub>H<sub>5</sub>)}, 3.98 (2H, d, *J* 5.6 Hz, -NHCH<sub>2</sub>-), 3.80 (2H, d, *J* 6 Hz, -NHCH<sub>2</sub>-);

<sup>13</sup>C NMR (100 MHz)  $\delta$  (DMSO-*d*<sub>6</sub>): 171.2 (C=O), 169.4 (C=O), 166.5 (C=O), 138.8 (C<sub>q</sub>), 136.9 (C<sub>q</sub>), 134.6 (C<sub>q</sub>), 130.4 (C<sub>q</sub>), 128.8, 127.6, 127.3, 125.9, 124.6, 122.7, 84.0 (C<sub>ipso</sub>  $\eta^5$ -C<sub>5</sub>H<sub>4</sub>), 69.5 ( $\eta^5$ -C<sub>5</sub>H<sub>5</sub>), 69.4 (C<sub>ortho</sub>  $\eta^5$ -C<sub>5</sub>H<sub>4</sub>), 66.6 (C<sub>meta</sub>  $\eta^5$ -C<sub>5</sub>H<sub>4</sub>), 42.5 (-NHCH<sub>2</sub>-), 40.6 (-NHCH<sub>2</sub>-).

***N*-(6-ferrocenyl-2-naphthoyl)-sarcosine-glycine-OH 109.**



The synthesis followed that of **108** using *N*-(6-ferrocenyl-2-naphthoyl)-sarcosine-glycine methyl ester (0.30 g, 0.6 mmol) as the starting material. This yielded the title compound as an orange solid (0.21 g, 72 %), mp 132 °C;

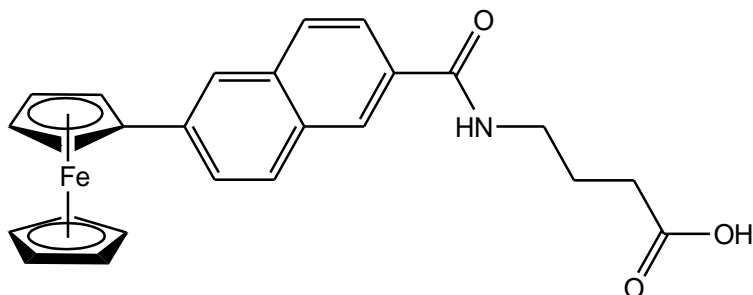
I.R.  $\nu_{\max}$  (neat)/ $\text{cm}^{-1}$  3301, 1720, 1624, 1548, 1310, 1235;

UV-Vis  $\lambda_{\max}$  ( $\text{CH}_3\text{CN}$ )/nm 365 ( $\epsilon/\text{dm}^3\text{mol}^{-1}\text{cm}^{-1}$  2513), 452 (1038);

$^1\text{H}$  NMR (400 MHz)  $\delta$  ( $\text{DMSO}-d_6$ ): 13.1 (1H, br.s, -OH), 8.66 & 8.57 (1H, br.s, br.s, -NHCH<sub>2</sub>-), 8.24 (1H, s, ArH), 7.85-8.21 (3H, m, ArH), 7.84 (1H, s, ArH), 7.39 (1H, d, *J* 8.4 Hz, ArH) 4.97 {2H, s, *ortho* on ( $\eta^5$ -C<sub>5</sub>H<sub>4</sub>)}, 4.46 {2H, s, *meta* on ( $\eta^5$ -C<sub>5</sub>H<sub>4</sub>)}, 4.20-3.74 {9H, m, ( $\eta^5$ -C<sub>5</sub>H<sub>5</sub>), N(CH<sub>3</sub>)CH<sub>2</sub>-, -NHCH<sub>2</sub>-}, 3.01 {3H, s, -N(CH<sub>3</sub>)}.

$^{13}\text{C}$  NMR (100 MHz)  $\delta$  ( $\text{DMSO}-d_6$ ): 171.6 (C=O), 170.0 (C=O), 168.2 (C=O), 138.2 (C<sub>q</sub>), 133.5 (C<sub>q</sub>), 132.4 (C<sub>q</sub>), 130.7 (C<sub>q</sub>), 128.6, 127.5, 126.5, 125.9, 124.8, 122.8, 84.1 (C<sub>ipso</sub>  $\eta^5$ -C<sub>5</sub>H<sub>4</sub>), 69.5 ( $\eta^5$ -C<sub>5</sub>H<sub>5</sub>), 69.4 (C<sub>meta</sub>  $\eta^5$ -C<sub>5</sub>H<sub>4</sub>), 66.6 (C<sub>ortho</sub>  $\eta^5$ -C<sub>5</sub>H<sub>4</sub>), 53.8 (-NHCH<sub>2</sub>-), 49.7 {-N(CH<sub>3</sub>)CH<sub>2</sub>-}, 38.4 & 34.1 {-N(CH<sub>3</sub>)}.

***N*-(6-ferrocenyl-2-naphthoyl)- $\gamma$ -aminobutyric acid **110**.**



The synthesis followed that of **108** using *N*-(6-ferrocenyl-2-naphthoyl)- $\gamma$ -aminobutyric acid methyl ester (0.20 g, 0.4 mmol) as the starting material. This yielded the title compound as an orange solid (0.17 g, 90 %), mp 213 °C (decomp.);

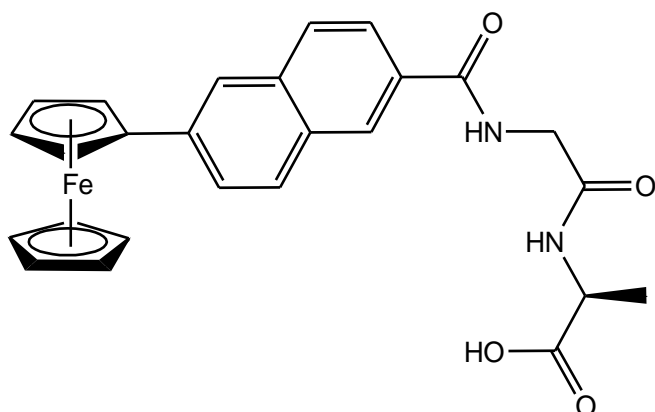
I.R.  $\nu_{\max}$  (neat)/ $\text{cm}^{-1}$  3276, 1712, 1615, 1543, 116, 1220;

UV-Vis  $\lambda_{\max}$  ( $\text{CH}_3\text{CN}$ )/nm 371 ( $\epsilon/\text{dm}^3\text{mol}^{-1}\text{cm}^{-1}$  1562), 451 (641);

$^1\text{H}$  NMR (400 MHz)  $\delta$  ( $\text{DMSO}-d_6$ ): 8.66 (1H, t,  $J$  5.6 Hz, -CONH-), 8.39 (1H, s, ArH), 8.05 (1H, s, ArH), 7.96-7.88 (3H, m, ArH), 7.82 (1H, dd,  $J$  6.8 Hz and 1.6 Hz, ArH), 4.96 {2H, t,  $J$  2 Hz, *ortho* on ( $\eta^5\text{-C}_5\text{H}_4$ )}, 4.45 {2H, t,  $J$  1.6 Hz, *meta* on ( $\eta^5\text{-C}_5\text{H}_4$ )}, 4.04 {5H, s, ( $\eta^5\text{-C}_5\text{H}_5$ )}, 3.36-3.31 (2H, m, -COCH<sub>2</sub>), 2.32 (2H, t,  $J$  7.2 Hz, -NHCH<sub>2</sub>-), 1.80 (2H, qt,  $J$  7.2, -CH<sub>2</sub>CH<sub>2</sub>CH<sub>2</sub>-);

$^{13}\text{C}$  NMR (100 MHz)  $\delta$  ( $\text{DMSO}-d_6$ ): 174.3 (C=O), 166.3 (C=O), 138.6 (C<sub>q</sub>), 134.4 (C<sub>q</sub>), 131.0 (C<sub>q</sub>), 130.7 (C<sub>q</sub>), 128.7, 127.3, 127.2, 125.9, 124.5, 122.7, 84.1 (C<sub>ipso</sub>  $\eta^5\text{-C}_5\text{H}_4$ ), 69.4 ( $\eta^5\text{-C}_5\text{H}_5$ , C<sub>meta</sub>  $\eta^5\text{-C}_5\text{H}_4$ ), 66.6 (C<sub>ortho</sub>  $\eta^5\text{-C}_5\text{H}_4$ ), 38.7 (-COCH<sub>2</sub>), 31.2 (-NHCH<sub>2</sub>-), 24.5 (-CH<sub>2</sub>CH<sub>2</sub>CH<sub>2</sub>-).

***N*-(6-ferrocenyl-2-naphthoyl)-glycine-L-alanine-OH 111.**



The synthesis followed that of **108** using *N*-(6-ferrocenyl-2-naphthoyl)-glycine-L-alanine methyl ester (0.14 g, 0.3 mmol) as the starting material. This yielded the title compound as an orange solid (0.13 g, 95 %), mp 125 °C;

I.R.  $\nu_{\max}$  (neat)/ $\text{cm}^{-1}$  3308, 3092, 2932, 1727, 1626, 1534, 1401, 1227;

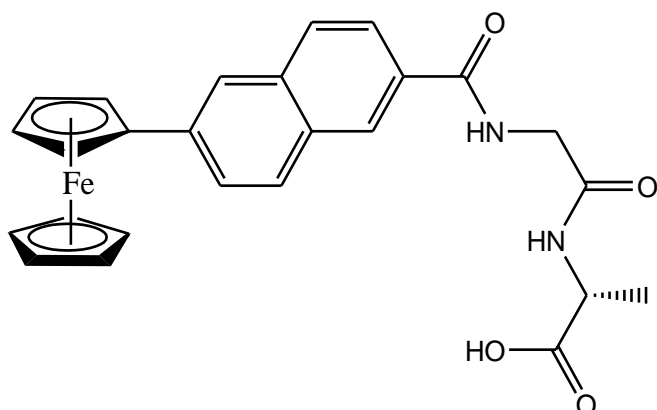
UV-Vis  $\lambda_{\max}$  ( $\text{CH}_3\text{CN}$ )/nm 374 ( $\epsilon/\text{dm}^3\text{mol}^{-1}\text{cm}^{-1}$  2843 ), 450 (1158);

$^1\text{H}$  NMR (400 MHz)  $\delta$  ( $\text{DMSO-}d_6$ ): 8.85 (1H, t,  $J$  8 Hz, -CONH-), 8.44 (1H, s, ArH), 8.30 (1H, d,  $J$  7.2 Hz -CONH-), 8.06 (1H, s, ArH), 7.93-7.96 (3H, m, ArH), 7.83 (1H, dd,  $J$  6.4 Hz and 1.2 Hz, ArH), 4.97 {2H, t,  $J$  1.6 Hz, *ortho* on ( $\eta^5\text{-C}_5\text{H}_4$ )}, 4.45 {2H t,  $J$  2 Hz, *meta* on ( $\eta^5\text{-C}_5\text{H}_4$ )}, 4.26 (1H, qt,  $J$  6.8 Hz, -CHCH<sub>3</sub>), 4.04 {5H, s, ( $\eta^5\text{-C}_5\text{H}_5$ )}, 4.01 (1H, dd,  $J$  10.8 Hz and 4.8 Hz, -NHCH<sub>2</sub>-), 3.93 (1H, dd,  $J$  10.8 Hz and 6.4Hz, -NHCH<sub>2</sub>-), 1.30 (3H, d,  $J$  7.2 Hz, -CCH<sub>3</sub>);

$^{13}\text{C}$  NMR (100 MHz)  $\delta$  ( $\text{DMSO-}d_6$ ): 174.0 (C=O), 168.7 (C=O), 166.4 (C=O), 138.8 (C<sub>q</sub>), 134.5 (C<sub>q</sub>), 130.7 (C<sub>q</sub>), 130.5 (C<sub>q</sub>), 128.7, 127.6, 127.3, 125.9, 124.5, 122.7, 84.1 (C<sub>ipso</sub>  $\eta^5\text{-C}_5\text{H}_4$ ), 69.4 ( $\eta^5\text{-C}_5\text{H}_5$ ), (C<sub>meta</sub>  $\eta^5\text{-C}_5\text{H}_4$ ), 66.6 (C<sub>ortho</sub>  $\eta^5\text{-C}_5\text{H}_4$ ), 47.5 (-NHCH-), 42.3 (-NHCH<sub>2</sub>-), 17.3 (-NHCH<sub>3</sub>).



***N*-(6-ferrocenyl-2-naphthoyl)-glycine-D-alanine-OH 112.**



The synthesis followed that of **108** using *N*-(6-ferrocenyl-2-naphthoyl)-glycine-D-alanine methyl ester (0.50 g, 10.0 mmol) as the starting material. This yielded the title compound as an orange solid (0.47 g, 96 %), mp 185°C;

I.R.  $\nu_{\max}$  (neat)/ $\text{cm}^{-1}$  3311, 3094, 2930, 1723, 1628, 1535, 1410, 1228;

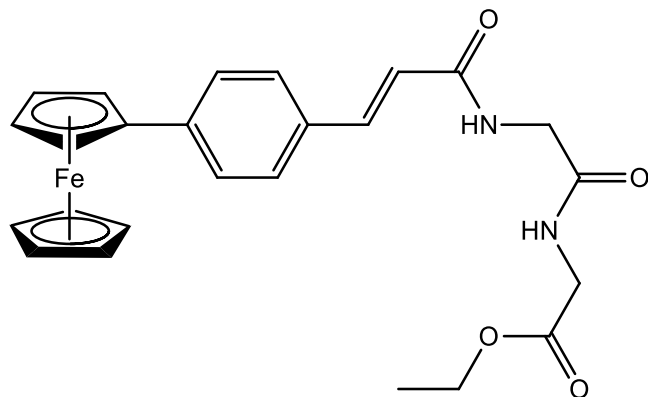
UV-Vis  $\lambda_{\max}$  (CH<sub>3</sub>CN)/nm 369 ( $\epsilon/\text{dm}^3\text{mol}^{-1}\text{cm}^{-1}$  1875), 451 (862);

<sup>1</sup>H NMR (400 MHz)  $\delta$  (DMSO-*d*<sub>6</sub>): 8.90 (1H, t, *J* 6 Hz, -CONH-), 8.44 (1H, s, ArH), 8.27 (1H, d, *J* 4 Hz, -CONH-), 8.06 (1H, s, ArH), 7.93-7.96 (3H, m, ArH), 7.80 (1H, dd, *J* 8 Hz and 1.2 Hz, ArH), 4.98 {1H, s, *ortho* on ( $\eta^5$ -C<sub>5</sub>H<sub>4</sub>)}, 4.45 {1H, s, *meta* on ( $\eta^5$ -C<sub>5</sub>H<sub>4</sub>)}, 4.23 (1H, m, -CHCH<sub>3</sub>), 3.90-4.05 {7H, m, ( $\eta^5$ -C<sub>5</sub>H<sub>4</sub>), -NHCH<sub>2</sub>-}, 1.30 (3H, d, *J* 4.8 Hz, -CHCH<sub>3</sub>).

<sup>13</sup>C NMR (100 MHz)  $\delta$  (DMSO-*d*<sub>6</sub>): 174.0 (C=O), 168.7 (C=O), 166.5 (C=O), 138.8 (C<sub>q</sub>), 134.5 (C<sub>q</sub>), 130.7 (C<sub>q</sub>), 130.4 (C<sub>q</sub>), 128.8, 127.6, 127.4, 125.9, 124.5, 122.7, 84.0 (*C*<sub>ipso</sub>  $\eta^5$ -C<sub>5</sub>H<sub>4</sub>), 69.5 ( $\eta^5$ -C<sub>5</sub>H<sub>5</sub>), 69.4 (*C*<sub>ortho</sub>  $\eta^5$ -C<sub>5</sub>H<sub>4</sub>), 66.6 (*C*<sub>meta</sub>  $\eta^5$ -C<sub>5</sub>H<sub>4</sub>), 47.6 (-NHCH-), 42.3 (-NHCH<sub>2</sub>-), 17.3 (-NHCH<sub>3</sub>).

**General procedure for the synthesis of *N*-{*para*-(ferrocenyl)cinnamoyl} dipeptide esters.**

***N*-{*para*-(ferrocenyl)cinnamoyl}-glycine-glycine ethyl ester 113.**



To a solution of *N*-*para*-(ferrocenyl)cinnamic acid (0.30 g, 0.9 mmol) in DCM (50 mL) was added ethyl dimethylaminopropyl carbodiimide (EDC) (0.34 g, 1.8 mmol), *N*-hydroxysuccinimide (NHS) (0.05 g, 4.5 mmol) and triethylamine (5 mL). The solution was allowed to stir at 0 °C for one hour. Glycine-glycine ethyl ester hydrochloride (0.17 g, 0.9 mmol) was then added. The solution was allowed to stir at 0 °C for a further 20 minutes the temperature was raised and the solution was allowed to stir at room temperature for 48 hours. The product was washed with water and dried over MgSO<sub>4</sub>. The solvent was removed in vacuo and the crude product was purified by column chromatography (eluent 20 ethyl acetate: 80 % hexane – 100 % hexane) to afford the product as an orange solid (0.20 g, 46 %), mp 203-204 °C;

*m/z* (ESI) 474.1220 [M]<sup>+</sup>. C<sub>26</sub>H<sub>24</sub>N<sub>2</sub>O<sub>4</sub>Fe requires 474.1242;

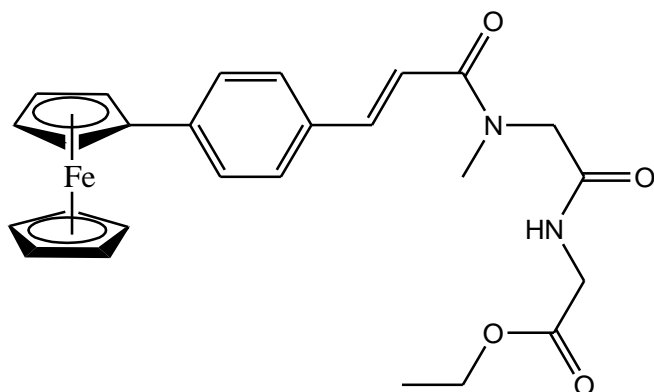
I.R.  $\nu_{\max}$  (neat)/ cm<sup>-1</sup>: 3287, 3089, 1732, 1651, 1626, 1549, 1211;

UV-Vis  $\lambda_{\max}$  (CH<sub>3</sub>CN)/nm 378 ( $\epsilon$ /dm<sup>3</sup>mol<sup>-1</sup>cm<sup>-1</sup> 3436), 457 (1378);

<sup>1</sup>H NMR (400 MHz)  $\delta$  (DMSO-*d*<sub>6</sub>): 8.36-8.42 (2H, m, -NHCH<sub>2</sub>-, -NHCH<sub>2</sub>-), 7.58 (2H, d, *J* 8 Hz, ArH), 7.50 (2H, d, *J* 8.4 Hz, ArH), 7.43 (1H, d, *J* 16 Hz, -CH=), 6.73 (1H, d, *J* 16 Hz, -CH=), 4.85 {2H, t, *J* 1.6 Hz, *ortho* on ( $\eta^5$ -C<sub>5</sub>H<sub>4</sub>)}, 4.40 {2H, t, *J* 1.6 Hz, *meta* on ( $\eta^5$ -C<sub>5</sub>H<sub>4</sub>)}, 4.10 (2H, q, *J* 7.2 Hz, -CH<sub>2</sub>CH<sub>3</sub>), 4.03 (5H, s,  $\eta^5$ -C<sub>5</sub>H<sub>5</sub>), 3.89 (2H, d, *J* 6 Hz, -NHCH<sub>2</sub>-), 3.86 (2H, d, *J* 5.6 Hz, -NHCH<sub>2</sub>-), 1.20 (3H, t, *J* 7.2 Hz, -CH<sub>2</sub>CH<sub>3</sub>);

$^{13}\text{C}$  NMR (100 MHz)  $\delta$  (DMSO- $d_6$ ): 169.7 (C=O), 169.5 (C=O), 165.4 (C=O), 140.9 (=CH-), 138.9 ( $C_q$ ), 132.2 ( $C_q$ ), 127.7, 126.2, 120.6 (=CH-), 83.7 ( $C_{ipso}$   $\eta^5$ - $\text{C}_5\text{H}_4$ ), 69.4 ( $\eta^5$ - $\text{C}_5\text{H}_5$ ), 69.3 ( $C_{meta}$   $\eta^5$ - $\text{C}_5\text{H}_4$ ), 66.4 ( $C_{ortho}$   $\eta^5$ - $\text{C}_5\text{H}_4$ ), 60.4 (-OCH<sub>2</sub>CH<sub>3</sub>), 41.9 (-NHCH<sub>2</sub>-), 40.6 (-NHCH<sub>2</sub>-), 14.0 (-OCH<sub>2</sub>CH<sub>3</sub>).

***N*-{*para*-(ferrocenyl)-cinnamoyl}-sarcosine-glycine ethyl ester **114**.**



The synthesis followed that of **113** using the following reagents; sarcosine-glycine ethyl ester trifluoroacetate salt (0.31 g, 1.1 mmol) and *N*-{*para*-(ferrocenyl)cinnamic acid (0.30 g, 0.9 mmol), EDC (0.35 g, 1.8 mmol), NHS (0.05 g, 0.5 mmol). The product was purified by column chromatography (eluent 20 % ethyl acetate: 80 % hexane - 100 % ethyl acetate) to yield the title compound as an orange solid (0.07 g, 16 %), mp 145°C;

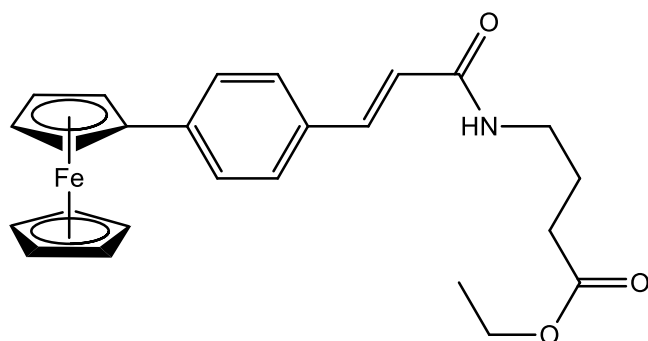
I.R.  $\nu_{\text{max}}$  (neat)/ $\text{cm}^{-1}$  3293, 3095, 1745, 1674, 1673, 1642, 1592, 1526, 1200;

UV-Vis  $\lambda_{\text{max}}$  (CH<sub>3</sub>CN)/nm 387 ( $\epsilon/\text{dm}^3\text{mol}^{-1}\text{cm}^{-1}$  3487), 455 (1522);

$^1\text{H}$  NMR (400 MHz)  $\delta$  (DMSO- $d_6$ ): 8.58 & 8.37 (1H, t, t,  $J$  5.6 Hz, 6 Hz, -CONH-), 7.44-7.72 (5H, m, ArH, =CH-), 7.21 & 7.03 (1H, d, d,  $J$  15.2 Hz, =CH-), 4.87 {2H, s, *ortho* on ( $\eta^5$ - $\text{C}_5\text{H}_4$ )}, 4.40 {2H, s, *meta* on ( $\eta^5$ - $\text{C}_5\text{H}_4$ )}, 4.27 {1H, s, -N(CH<sub>3</sub>)CH<sub>2</sub>-}, 4.09-4.13 {3H, m, -OCH<sub>2</sub>, -N(CH<sub>3</sub>)CH<sub>2</sub>-}, 4.08 {5H, s, ( $\eta^5$ - $\text{C}_5\text{H}_4$ )}, 3.87 (2H, dd,  $J$  10 Hz and 6 Hz, -NHCH<sub>2</sub>-), 3.20 & 2.93 (3H, s, s, -N(CH<sub>3</sub>)CH<sub>2</sub>-), 1.15-1.24 (3H, m, -OCH<sub>2</sub>CH<sub>3</sub>);

$^{13}\text{C}$  NMR (100 MHz)  $\delta$  (DMSO- $d_6$ ): 169.7- (C=O), 168.9 (C=O), 166.1 (C=O), 141.5 ( $C_q$ ), 141.1 ( $C_q$ ), 128.2, 128.1, 126.0, 125.9, 117.1 (-CH=), 116.9 (-CH=) 83.7 ( $C_{ipso}$   $\eta^5$ - $\text{C}_5\text{H}_4$ ), 69.4 ( $\eta^5$ - $\text{C}_5\text{H}_5$ ), 69.3 ( $C_{meta}$   $\eta^5$ - $\text{C}_5\text{H}_4$ ), 66.4 ( $C_{ortho}$   $\eta^5$ - $\text{C}_5\text{H}_4$ ), 60.5 (-OCH<sub>2</sub>-), 52.0 & 50.0 (-N(CH<sub>3</sub>)CH<sub>2</sub>-), 40.6 (-NHCH-), 39.0 & 36.2 {-N(CH<sub>3</sub>)}, 14.0 (-OCH<sub>2</sub>CH<sub>3</sub>).

***N*-{*para*-(ferrocenyl)-cinnamoyl}- $\gamma$ -aminobutyric acid ethyl ester **115**.**



The synthesis followed that of **113** using the following reagents;  $\gamma$ -aminobutyric acid ethyl ester hydrochloride (0.09 g, 0.6 mmol) and *N*-*para*-(ferrocenyl)cinnamic acid (0.23 g, 0.7 mmol), EDC (0.22 g, 1.2 mmol) and NHS (0.03 g, 0.3 mmol). The product was purified by column chromatography (eluent 20 % ethyl acetate: 80 % hexane -100 % ethyl acetate) to yield the title compound as an orange solid (0.12 g, 46 %), mp 152-153 °C;

$m/z$  (ESI) 445.1344 [M]<sup>++</sup>. C<sub>26</sub>H<sub>24</sub>N<sub>2</sub>O<sub>4</sub>Fe requires 445.1340;

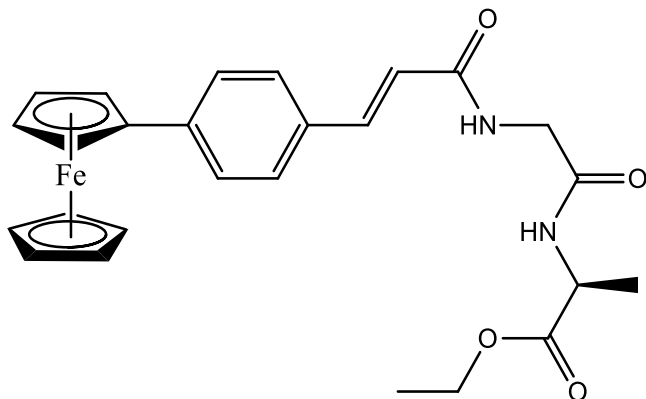
I.R.  $\nu_{\max}$  (neat)/ cm<sup>-1</sup>: 3277, 3093, 1739, 1652, 1616, 1563, 1176;

UV-Vis  $\lambda_{\max}$  (CH<sub>3</sub>CN)/nm 370 ( $\epsilon$ /dm<sup>3</sup>mol<sup>-1</sup>cm<sup>-1</sup> 3001), 452 (1059);

<sup>1</sup>H NMR (400 MHz)  $\delta$  (DMSO-*d*<sub>6</sub>): 8.12 (1H, t, *J* 5.6 Hz, -CONH-), 7.57 (2H, d, *J* 8.4 Hz, ArH), 4.48 (2H, d, *J* 8.4 Hz, ArH), 7.40 (1H, d, *J* 15.6 Hz, =CH-), 6.59 (1H, d, *J* 15.6 Hz, =CH-), 4.84 {2H, t, *J* 1.6 Hz, *ortho* on ( $\eta^5$ -C<sub>5</sub>H<sub>4</sub>)}, 4.39 {2H, t, *J* 2 Hz, *meta* on ( $\eta^5$ -C<sub>5</sub>H<sub>4</sub>)}, 4.03-4.09 {7H, m, -OCH<sub>2</sub>CH<sub>3</sub>, ( $\eta^5$ -C<sub>5</sub>H<sub>4</sub>)}, 3.20 (2H, q, *J* 6.8 Hz, -NHCH<sub>2</sub>-), 2.34 (2H, t, *J* 7.2 Hz, -CH<sub>2</sub>C=O-), 1.72 (2H, qt, *J* 7.2 Hz, -CH<sub>2</sub>CH<sub>2</sub>CH<sub>2</sub>-), 1.19 (3H, t, *J* 6.8 Hz, -OCH<sub>2</sub>CH<sub>3</sub>);

<sup>13</sup>C NMR (100 MHz)  $\delta$  (DMSO-*d*<sub>6</sub>): 172.6 (C=O), 165.1 (C=O), 140.8 (=CH-), 138.5(C<sub>q</sub>), 132.3(C<sub>q</sub>), 127.6, 126.1, 120.9 (=CH-), 83.7(C<sub>*ipso*</sub>  $\eta^5$ -C<sub>5</sub>H<sub>4</sub>), 69.4 ( $\eta^5$ -C<sub>5</sub>H<sub>5</sub>), 69.3 (C<sub>*meta*</sub>  $\eta^5$ -C<sub>5</sub>H<sub>4</sub>), 66.4 (C<sub>*ortho*</sub>  $\eta^5$ -C<sub>5</sub>H<sub>4</sub>), 59.8 (-OCH<sub>2</sub>CH<sub>3</sub>), 38.0 (-NHCH<sub>2</sub>-), 31.0 (-CH<sub>2</sub>C=O-), 24.6 (-CH<sub>2</sub>CH<sub>2</sub>CH<sub>2</sub>-), 14.1 (-OCH<sub>2</sub>CH<sub>3</sub>).

***N*-{*para*-(ferrocenyl)-cinnamoyl}-glycine-L-alanine ethyl ester **116**.**



The synthesis followed that of **113** using the following reagents; glycine-L-alanine ethyl ester trifluoroacetate salt (0.31 g, 1.1 mmol) and *N*-*para*-(ferrocenyl)cinnamic acid (0.30 g, 0.9 mmol), EDC (0.35 g, 1.8 mmol) and NHS (0.5 g, 0.5 mmol). The product was purified by column chromatography (eluent 20 % ethyl acetate: 80 % hexane -100 % ethyl acetate) to yield the title compound as an orange solid (0.16 g, 36 %), mp 201-202 °C;

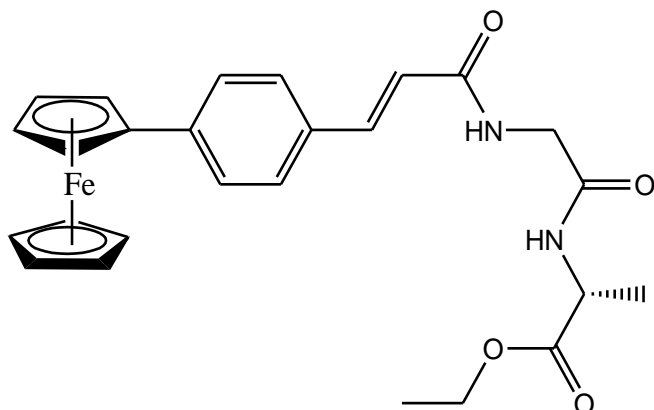
I.R.  $\nu_{\max}$  (neat)/  $\text{cm}^{-1}$ : 3310, 3083, 1732, 1684, 1621, 1529, 1200;

UV-Vis  $\lambda_{\max}$  (CH<sub>3</sub>CN)/nm 387 ( $\epsilon/\text{dm}^3\text{mol}^{-1}\text{cm}^{-1}$  3487), 455 (1522);

<sup>1</sup>H NMR (600 MHz)  $\delta$  (DMSO-*d*<sub>6</sub>): 8.40 (1H, d, *J* 7.2 Hz, -CONH-), 8.31 (1H, t, *J* 5.6 Hz, -CONH-), 7.58 (2H, d, *J* 8.4 Hz, ArH), 7.49 (2H, d, *J* 8.4 Hz, ArH), 7.46 (1H, d, *J* 16 Hz, =CH-), 6.73 (1H, d, *J* 16 Hz, =CH-), 4.85 {2H, t, *J* 2 Hz, *ortho* on ( $\eta^5$ -C<sub>5</sub>H<sub>4</sub>)}, 4.40 {2H, t, *J* 1.6 Hz, *meta* on ( $\eta^5$ -C<sub>5</sub>H<sub>4</sub>)}, 4.27 (1H, qt, *J* 7.2 Hz, -NHCH-), 4.09 (2H, q, *J* 6.8 Hz, -OCH<sub>2</sub>CH<sub>3</sub>), 4.02 (5H, s,  $\eta^5$ -C<sub>5</sub>H<sub>5</sub>), 3.92 (1H, dd, *J* 11.4 Hz and 5.4 Hz, -NHCH<sub>2</sub>-), 3.86 (1H, dd, *J* 10.8 Hz and 6 Hz, -NHCH<sub>2</sub>-), 1.29 (3H, d, *J* 7.2 Hz, -CH<sub>3</sub>), 1.19 (3H, t, *J* 7.2 Hz, -OCH<sub>2</sub>CH<sub>3</sub>);

<sup>13</sup>C NMR (150 MHz)  $\delta$  (DMSO-*d*<sub>6</sub>): 172.5 (C=O), 168.8 (C=O), 165.4 (C=O), 140.9 (=CH-), 138.9 (C<sub>q</sub>), 132.2 (C<sub>q</sub>), 127.7, 126.2, 120.7 (=CH-), 83.7 (C<sub>ipso</sub>  $\eta^5$ -C<sub>5</sub>H<sub>4</sub>), 69.4 ( $\eta^5$ -C<sub>5</sub>H<sub>5</sub>), 69.3 (C<sub>meta</sub>  $\eta^5$ -C<sub>5</sub>H<sub>4</sub>), 66.5 (C<sub>ortho</sub>  $\eta^5$ -C<sub>5</sub>H<sub>4</sub>), 60.5 (-OCH<sub>2</sub>-), 47.6 (-CHCH<sub>3</sub>), 41.7 (-NHCH<sub>2</sub>-), 17.0 (-CHCH<sub>3</sub>), 14.0 (-OCH<sub>2</sub>CH<sub>3</sub>).

***N*-{*para*-(ferrocenyl)-cinnamoyl}-glycine-D-alanine ethyl ester **117**.**



The synthesis followed that of **113** using the following reagents; glycine-D-alanine ethyl ester trifluoroacetate salt (0.31 g, 1.1 mmol) and *N*-*para*-(ferrocenyl)cinnamic acid (0.3 g, 0.9 mmol), EDC (0.35 g, 1.8 mmol), NHS (0.05 g, 0.5 mmol). The product was purified by column chromatography (eluent 20 % ethyl acetate: 80 % hexane -100 % ethyl acetate) to yield the title compound as an orange solid (0.08 g, 18 %), mp 202-203 °C;

I.R.  $\nu_{\max}$  (neat)/  $\text{cm}^{-1}$ : 3307, 2925, 1729, 1646, 1622, 1527, 1216;

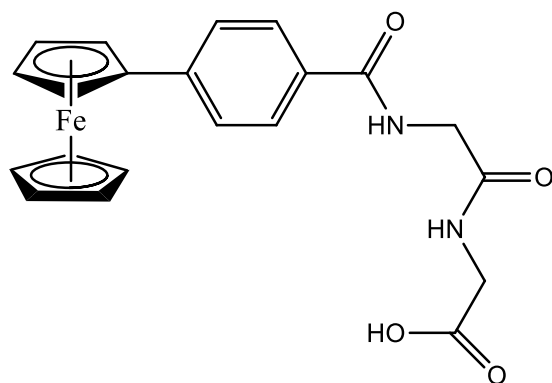
UV-Vis  $\lambda_{\max}$  ( $\text{CH}_3\text{CN}$ )/nm 313 ( $\epsilon/\text{dm}^3\text{mol}^{-1}\text{cm}^{-1}$  4118), 436 (550);

$^1\text{H}$  NMR (400 MHz)  $\delta$  ( $\text{DMSO}-d_6$ ): 8.42 (1H, d,  $J$  7.2 Hz, -CONH-), 8.31 (1H, t,  $J$  5.6 Hz, -CONH-), 7.58 (2H, d,  $J$  8.4 Hz, ArH), 7.49 (2H, d,  $J$  8.4 Hz, ArH), 7.46 (1H, d,  $J$  16 Hz, =CH-), 6.73 (1H, d,  $J$  16 Hz, =CH-), 4.85 {2H, t,  $J$  2 Hz, *ortho* on ( $\eta^5$ - $\text{C}_5\text{H}_4$ )}, 4.40 {2H, t,  $J$  1.6 Hz, *meta* on ( $\eta^5$ - $\text{C}_5\text{H}_4$ )}, 4.27 (1H, qt,  $J$  7.2 Hz, -NHCH-), 4.09 (2H, q,  $J$  6.8 Hz, - $\text{OCH}_2\text{CH}_3$ ), 4.03 (5H, s,  $\eta^5$ - $\text{C}_5\text{H}_5$ ), 3.82-3.95 (2H, m, - $\text{NHCH}_2$ -), 1.29 (3H, d,  $J$  7.2 Hz, - $\text{CH}_3$ ), 1.19 (3H, t,  $J$  7.2 Hz, - $\text{OCH}_2\text{CH}_3$ );

$^{13}\text{C}$  NMR (100 MHz)  $\delta$  ( $\text{DMSO}-d_6$ ): 172.5 (C=O), 168.8 (C=O), 165.4 (C=O), 140.9 (=CH-), 138.9 ( $\text{C}_q$ ), 132.2 ( $\text{C}_q$ ), 127.7, 126.2, 120.7 (=CH-), 83.7 ( $\text{C}_{\text{ipso}} \eta^5$ - $\text{C}_5\text{H}_4$ ), 69.4 ( $\eta^5$ - $\text{C}_5\text{H}_5$ ), 69.3 ( $\text{C}_{\text{meta}} \eta^5$ - $\text{C}_5\text{H}_4$ ), 66.4 ( $\text{C}_{\text{ortho}} \eta^5$ - $\text{C}_5\text{H}_4$ ), 60.5 (- $\text{OCH}_2\text{CH}_3$ ), 47.6 (-CH $\text{CH}_3$ ), 41.7(-NHCH $_2$ -), 17.0 (-CH $\text{CH}_3$ ), 14.0 (- $\text{OCH}_2\text{CH}_3$ ).

**General procedures for the synthesis of *N*-{*para*-(ferrocenyl)-benzoyl}-glycine-glycine esters.**

***N*-{*para*-(ferrocenyl)-benzoyl}-glycine-glycine 118.**



*N*-{*para*-(ferrocenyl)benzoyl}-glycine-glycine ethyl ester (0.30 g, 0.7 mmol) was dissolved in methanol (15 mL) and sodium hydroxide (15 mL, 0.5 M) and allowed to reflux 24 hours. The solution was cooled on ice and acidified to pH 2. The product was isolated by vacuum filtration as an orange solid (0.26 g, 92 %), mp 162-164 °C;

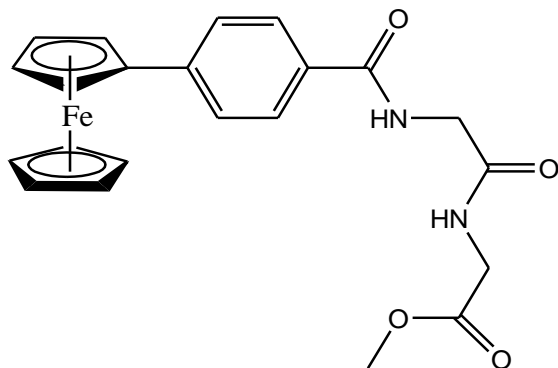
I.R.  $\nu_{\max}$  (neat)/ $\text{cm}^{-1}$  3334, 1737, 1640, 1522, 1345, 1230;

UV-Vis  $\lambda_{\max}$  ( $\text{CH}_3\text{CN}$ )/nm 351 ( $\epsilon/\text{dm}^3\text{mol}^{-1}\text{cm}^{-1}$  1987), 450 (556);

$^1\text{H}$  NMR (400 MHz)  $\delta$  ( $\text{DMSO}-d_6$ ): 8.81 (1H, t,  $J$  5.2 Hz, -CONH-), 7.98 (1H, t,  $J$  8 Hz, -CONH-), 7.83 (2H, d,  $J$  8 Hz, ArH), 7.63 (2H, d,  $J$  8 Hz, ArH), 4.87 {2H, s, *ortho* on ( $\eta^5\text{-C}_5\text{H}_4$ )}, 4.41 {2H, s, *meta* on ( $\eta^5\text{-C}_5\text{H}_4$ )}, 4.03 {5H, s, ( $\eta^5\text{-C}_5\text{H}_5$ )}, 3.90 (2H, d,  $J$  5.6 Hz, -NHCH<sub>2</sub>-), 3.65 (2H, d,  $J$  4.8 Hz, -NHCH<sub>2</sub>-).

$^{13}\text{C}$  NMR (100 MHz)  $\delta$  ( $\text{DMSO}-d_6$ ): 171.2 (C=O), 169.0 (C=O), 166.3 (C=O), 142.8 (C<sub>q</sub>), 131.0 (C<sub>q</sub>), 127.5, 125.3, 83.2 (C<sub>ipso</sub>  $\eta^5\text{-C}_5\text{H}_4$ ), 69.5 ( $\eta^5\text{-C}_5\text{H}_5$ , C<sub>meta</sub>  $\eta^5\text{-C}_5\text{H}_4$ ), 66.6 (C<sub>ortho</sub>  $\eta^5\text{-C}_5\text{H}_4$ ), 42.5 (-NHCH<sub>2</sub>-), 41.5 (-NHCH<sub>2</sub>-).

***N*-{*para*-(ferrocenyl)-benzoyl}-glycine-glycine methyl ester 119.**



To a solution of *para*-ferrocenyl benzoic acid (0.37 g, 1.2 mmol) in DCM (50 mL) was added ethyl dimethylaminopropyl carbodiimide (EDC) (0.38 g, 2.0 mmol), *N*-hydroxy succinimide (NHS) (0.23 g, 0.5 mmol) and triethylamine (5 mL). The solution was allowed to stir at 0 °C for one hour. Glycine-glycine methyl ester hydrochloride (0.19 g, 1.0 mmol) was then added. The solution was allowed to stir at 0 °C for a further 20 minutes before the temperature was raised and the solution was allowed to stir at room temperature for 48 hours. The product was washed with water and dried over MgSO<sub>4</sub>. The solvent was removed in vacuo and the crude product was purified by column chromatography (eluent 20 % ethyl acetate: 80 % hexane -100 % ethyl acetate) to afford the product as an orange solid (0.67 g, 15 %), mp 170-171 °C;

I.R.  $\nu_{\max}$  (neat)/cm<sup>-1</sup> 3274, 1727, 1655, 1550, 1514, 1221;

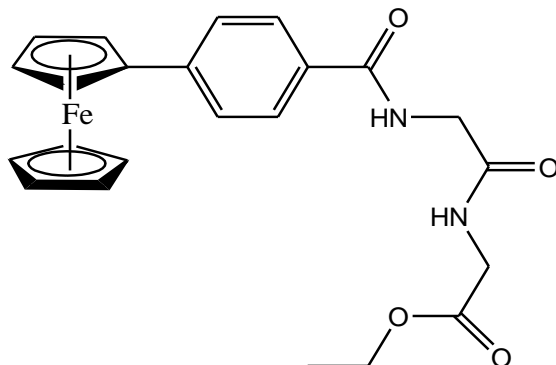
UV-Vis  $\lambda_{\max}$  (CH<sub>3</sub>CN)/nm 354 ( $\epsilon$ /dm<sup>3</sup>mol<sup>-1</sup>cm<sup>-1</sup> 2858), 452 (865);

<sup>1</sup>H NMR (400 MHz)  $\delta$  (DMSO-*d*<sub>6</sub>): 8.78 (1H, t, *J* 5.6 Hz, -CONH-), 8.37 (1H, t, *J* 5.6 Hz, -CONH-), 7.83 (2H, d, *J* 8.4 Hz, ArH), 7.64 (2H, d, *J* 8.4 Hz, ArH), 4.90 (2H, t, *J* 2 Hz, *ortho* on ( $\eta^5$ -C<sub>5</sub>H<sub>4</sub>)), 4.42 (2H, t, *J* 1.6 Hz, *meta* on ( $\eta^5$ -C<sub>5</sub>H<sub>4</sub>)), 4.02 (5H, s, ( $\eta^5$ -C<sub>5</sub>H<sub>4</sub>)), 3.92 (2H, d, *J* 6 Hz, -NHCH<sub>2</sub>-), 3.87 (2H, d, *J* 5.6 Hz, -NHCH<sub>2</sub>-), 3.64 (3H, s, -OCH<sub>3</sub>);

<sup>13</sup>C NMR (100 MHz)  $\delta$  (DMSO-*d*<sub>6</sub>): 170.3 (C=O), 169.7 (C=O), 166.3 (C=O), 142.8 (C<sub>q</sub>), 131 (C<sub>q</sub>), 127.5, 125.3, 83.2 (C<sub>ipso</sub>  $\eta^5$ -C<sub>5</sub>H<sub>4</sub>), 69.5 ( $\eta^5$ -C<sub>5</sub>H<sub>5</sub>, C<sub>meta</sub>  $\eta^5$ -C<sub>5</sub>H<sub>4</sub>), 66.6 (C<sub>ortho</sub>  $\eta^5$ -C<sub>5</sub>H<sub>4</sub>), 51.7 (-OCH<sub>3</sub>), 42.4 (-NHCH<sub>2</sub>-), 40.5 (-NHCH<sub>2</sub>-).



***N*-{*para*-(ferrocenyl)-benzoyl}-glycine-glycine ethyl ester **120**.**



The synthesis followed that of **119** using the following reagents; glycine-glycine ethyl ester hydrochloride (0.19 g, 1.0 mmol) and *N*-*para*-(ferrocenyl)benzoic acid (0.37 g, 1.2 mmol), EDC (0.36 g, 1.9 mmol), NHS (0.06g, 0.5 mmol). The product was purified by column chromatography (eluent 20 % ethyl acetate: 80 % hexane -100 % ethyl acetate) to yield the title compound as an orange solid. (0.32 g, 82 %), mp 134-135 °C;

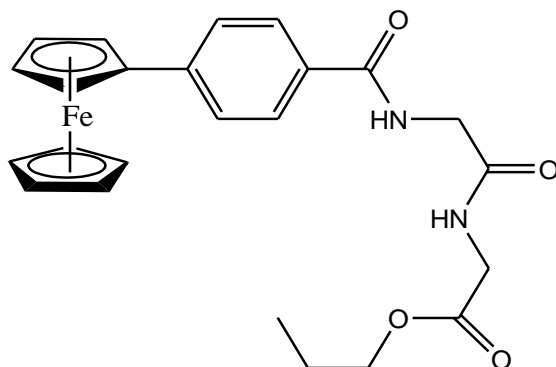
I.R.  $\nu_{\max}$  (neat)/  $\text{cm}^{-1}$ : 3389, 3274, 1727, 1644, 1543, 1515, 1214;

UV-Vis  $\lambda_{\max}$  ( $\text{CH}_3\text{CN}$ )/nm 354 ( $\epsilon/\text{dm}^3\text{mol}^{-1}\text{cm}^{-1}$  1584), 451 (570);

$^1\text{H}$  NMR (400 MHz)  $\delta$  ( $\text{DMSO}-d_6$ ): 8.79 (1H, t,  $J$  6 Hz, -CONH-), 8.35 (1H, t,  $J$  6 Hz, -CONH-), 7.84 (2H, d,  $J$  8.4 Hz, ArH), 7.63 (2H, d,  $J$  8.4 Hz, ArH), 4.90 {2H, t,  $J$  1.6 Hz, *ortho* on ( $\eta^5\text{-C}_5\text{H}_4$ )}, 4.41 {2H, t,  $J$  1.6 Hz, *meta* on ( $\eta^5\text{-C}_5\text{H}_4$ )}, 4.11 (2H, q,  $J$  13.2 Hz, (-OCH<sub>2</sub>CH<sub>3</sub>)), 4.07 {5H, s, ( $\eta^5\text{-C}_5\text{H}_5$ )}, 3.92 (2H, d,  $J$  6, -NHCH<sub>2</sub>-), 3.85 (2H, d,  $J$  6 Hz, -NHCH<sub>2</sub>-), 1.19 (3H, t,  $J$  7.2 Hz, -OCH<sub>2</sub>CH<sub>3</sub>);

$^{13}\text{C}$  NMR (100 MHz)  $\delta$  ( $\text{DMSO}-d_6$ ): 169.8 (C=O), 169.7 (C=O), 166.3 (C=O), 142.8 (C<sub>q</sub>), 131.0 (C<sub>q</sub>), 127.5, 125.3, 83.2 (C<sub>ipso</sub>  $\eta^5\text{-C}_5\text{H}_4$ ), 69.5 ( $\eta^5\text{-C}_5\text{H}_5$ ), (C<sub>meta</sub>  $\eta^5\text{-C}_5\text{H}_4$ ), 66.6 (C<sub>ortho</sub>  $\eta^5\text{-C}_5\text{H}_4$ ), 60.4 (-OCH<sub>2</sub>-), 42.4 (-NHCH<sub>2</sub>-), 40.7 (-NHCH<sub>2</sub>-), 14.1 (-OCH<sub>2</sub>CH<sub>3</sub>).

***N*-{*para*-(ferrocenyl)-benzoyl}-glycine-glycine propyl ester **121**.**



The synthesis followed that of **119** using the following reagents; glycine-glycine propyl ester hydrochloride (0.17 g, 0.8 mmol) and *para*-(ferrocenyl)benzoic acid (0.30 g, 1.0 mmol), EDC (0.31, 1.6 mmol) and NHS (0.05g, 0.4 mmol). The product was purified by column chromatography (eluent 20 % ethyl acetate: 80 % hexane -100 % ethyl acetate) to yield the title compound as an orange solid (0.23 g, 60 %), mp 115-117 °C;

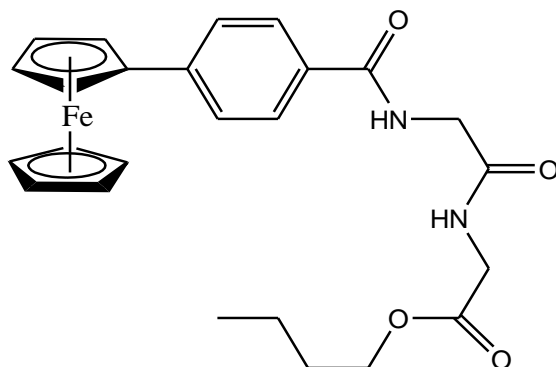
I.R.  $\nu_{\max}$  (neat)/  $\text{cm}^{-1}$ : 3367, 3274, 1727, 1644, 1543, 1515, 1215;

UV-Vis  $\lambda_{\max}$  ( $\text{CH}_3\text{CN}$ )/nm 355 ( $\epsilon/\text{dm}^3\text{mol}^{-1}\text{cm}^{-1}$  1737), 450 (552);

$^1\text{H}$  NMR (400 MHz)  $\delta$  ( $\text{DMSO}-d_6$ ): 8.78 (1H, t,  $J$  6 Hz, -CONH-), 8.36 (1H, t,  $J$  6 Hz, -CONH-), 7.83 (2H, d,  $J$  8.4 Hz, ArH), 7.64 (2H, d,  $J$  8.4 Hz, ArH), 4.90 {2H, t,  $J$  1.6 Hz, *ortho* on ( $\eta^5\text{-C}_5\text{H}_4$ )}, 4.42 {2H, t,  $J$  1.6 Hz, *meta* on ( $\eta^5\text{-C}_5\text{H}_4$ )}, 3.96-4.02 (7H, m,  $\eta^5\text{-C}_5\text{H}_5$ , - $\text{OCH}_2\text{CH}_2$ -), 3.92 (2H, d,  $J$  5.6 Hz, - $\text{NHCH}_2$ -), 3.86 (2H, d,  $J$  6 Hz, - $\text{NHCH}_2$ -), 1.59 (2H, m, - $\text{OCH}_2\text{CH}_2$ -), 0.90 (3H, t,  $J$  13.2 Hz, - $\text{CH}_2\text{CH}_3$ );

$^{13}\text{C}$  NMR (100 MHz)  $\delta$  ( $\text{DMSO}-d_6$ ): 175.2 (C=O), 175.2 (C=O), 172.0 (C=O), 148.3 ( $\text{C}_q$ ), 135.9 ( $\text{C}_q$ ), 132.8, 130.6, 88.2 ( $\text{C}_{\text{ipso}} \eta^5\text{-C}_5\text{H}_4$ ), 74.8 ( $\eta^5\text{-C}_5\text{H}_5$ ), 74.8 ( $\text{C}_{\text{meta}} \eta^5\text{-C}_5\text{H}_4$ ), 71.8 ( $\text{C}_{\text{ortho}} \eta^5\text{-C}_5\text{H}_4$ ), 71.3 (- $\text{OCH}_2\text{CH}_2$ -), 47.6 (- $\text{NHCH}_2$ -), 45.9 (- $\text{NHCH}_2$ -), 26.6 (- $\text{OCH}_2\text{CH}_2$ -), 15.4 (- $\text{CH}_2\text{CH}_3$ ).

***N*-{*para*-(ferrocenyl)-benzoyl}-glycine-glycine butyl ester **122**.**



The synthesis followed that of **119** using the following reagents; glycine-glycine butyl ester hydrochloride (0.20 g, 0.9 mmol) and *para*-(ferrocenyl)benzoic acid (0.33 g, 1.1 mmol), EDC (0.34 g, 1.8 mmol) and NHS (0.05 g, 0.4 mmol). The product was purified by column chromatography (eluent 20 % ethyl acetate: 80 % hexane -100 % ethyl acetate) to yield the title compound as an orange solid. (0.20 g, 46 %), mp 134-135 °C;

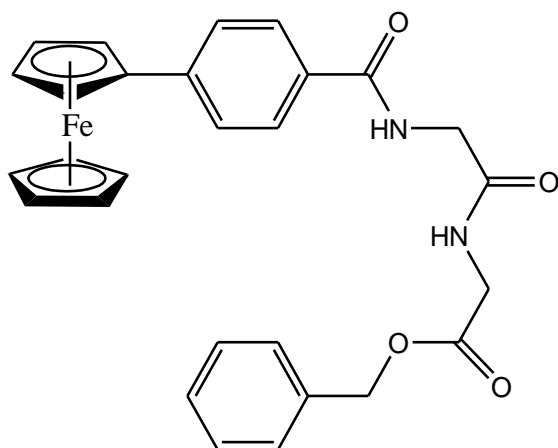
I.R.  $\nu_{\max}$  (neat)/  $\text{cm}^{-1}$ : 3298, 1738, 1633, 1549, 1518, 1235;

UV-Vis  $\lambda_{\max}$  ( $\text{CH}_3\text{CN}$ )/nm 356 ( $\epsilon/\text{dm}^3\text{mol}^{-1}\text{cm}^{-1}$  1532), 425 (487);

$^1\text{H}$  NMR (400 MHz)  $\delta$  ( $\text{DMSO}-d_6$ ): 8.78 (1H, t,  $J$  6 Hz, -CONH-), 8.35 (1H, t,  $J$  6 Hz, -CONH-), 7.83 (2H, d,  $J$  8.4 Hz, ArH), 7.64 (2H, d,  $J$  8.4 Hz, ArH), 4.90 {2H, t,  $J$  2 Hz, *ortho* on ( $\eta^5\text{-C}_5\text{H}_4$ )}, 4.42 {2H, t,  $J$  1.6 Hz, *meta* on ( $\eta^5\text{-C}_5\text{H}_4$ )}, 4.02-4.11 {7H, m, ( $\eta^5\text{-C}_5\text{H}_5$ ), - $\text{OCH}_2\text{CH}_2$ -}, 3.92 (2H, d,  $J$  5.6 Hz, - $\text{NHCH}_2$ -), 3.86 (2H, d,  $J$  6 Hz, - $\text{NHCH}_2$ -), 1.55 (2H, qt,  $J$  6.8 Hz, - $\text{OCH}_2\text{CH}_2$ -), 1.32 (2H, m, - $\text{CH}_2\text{CH}_3$ ), 0.88 (3H, t,  $J$  13.2 Hz, - $\text{CH}_2\text{CH}_3$ );

$^{13}\text{C}$  NMR (100 MHz)  $\delta$  ( $\text{DMSO}-d_6$ ): 175.1 (C=O), 174.9 (C=O), 171.5 (C=O), 148.0 ( $\text{C}_q$ ), 136.2 ( $\text{C}_q$ ), 132.8, 130.5, 88.4 ( $\text{C}_{ipso}$   $\eta^5\text{-C}_5\text{H}_4$ ), 74.7 ( $\eta^5\text{-C}_5\text{H}_5$ ,  $\text{C}_{meta}$   $\eta^5\text{-C}_5\text{H}_4$ ), 71.8 ( $\text{C}_{ortho}$   $\eta^5\text{-C}_5\text{H}_4$ ), 69.3 (- $\text{OCH}_2\text{CH}_2\text{CH}_2$ -), 47.6 (- $\text{NHCH}_2$ -), 45.9 (- $\text{NHCH}_2$ -), 35.4 (- $\text{OCH}_2\text{CH}_2\text{CH}_2$ -), 23.8 (- $\text{CH}_2\text{CH}_3$ ), 18.8 (- $\text{CH}_2\text{CH}_3$ ).

***N*-{*para*-(ferrocenyl)-benzoyl}-glycine-glycine benzyl ester 123.**



The synthesis followed that of **119** using the following reagents; glycine-glycine benzyl ester (0.48 g, 1.5 mmol) and *para*-(ferrocenyl)benzoic acid (0.38 g, 1.2 mmol), EDC (0.48 g, 2.5 mmol) and NHS (0.07 g, 0.6 mmol). The product was purified by column chromatography (eluent 20 % ethyl acetate: 80 % hexane-100 % ethyl acetate) to yield the title compound as an orange solid. (0.15 g, 24 %), mp 137-139 °C;

I.R.  $\nu_{\max}$  (neat)/  $\text{cm}^{-1}$  3310, 1734, 1628, 1609, 1548, 1519, 1235;

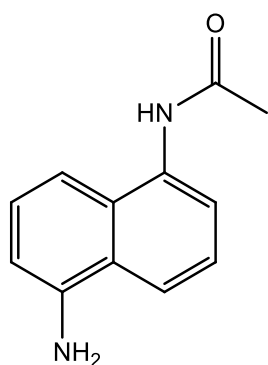
UV-Vis  $\lambda_{\max}$  ( $\text{CH}_3\text{CN}$ )/nm 313 ( $\epsilon/\text{dm}^3\text{mol}^{-1}\text{cm}^{-1}$  4835), 449 (587);

$^1\text{H}$  NMR (400 MHz)  $\delta$  ( $\text{DMSO-}d_6$ ): 8.80 (1H, t,  $J$  6 Hz, -CONH-), 8.40 (1H, t,  $J$  5.6 Hz, -CONH-), 7.84 (2H, d,  $J$  8.8 Hz, ArH), 7.64 (2H, d,  $J$  8.4 Hz, ArH), 7.40-7.30 (5H, m, ArH), 5.14 {2H, s, -OCH<sub>2</sub>(C<sub>6</sub>H<sub>5</sub>)}, 4.90 {2H, t,  $J$  1.6 Hz, *ortho* on ( $\eta^5$ -C<sub>5</sub>H<sub>4</sub>)}, 4.42 {2H, t,  $J$  2 Hz, *meta* on ( $\eta^5$ -C<sub>5</sub>H<sub>4</sub>)}, 4.02 {5H, s, ( $\eta^5$ -C<sub>5</sub>H<sub>5</sub>)}, 3.94 (4H, d,  $J$  5.6 Hz, -NHCH<sub>2</sub>-);

$^{13}\text{C}$  NMR (100 MHz)  $\delta$  ( $\text{DMSO-}d_6$ ): 169.7 (C=O), 169.7 (C=O), 166.3 (C=O), 142.8 (C<sub>q</sub>), 135.9 (C<sub>q</sub>), 131.0 (C<sub>q</sub>), 128.4, 128.0, 127.9, 127.5, 125.3, 83.2 (C<sub>ipso</sub>  $\eta^5$ -C<sub>5</sub>H<sub>4</sub>), 69.5 ( $\eta^5$ -C<sub>5</sub>H<sub>5</sub>, C<sub>meta</sub>  $\eta^5$ -C<sub>5</sub>H<sub>4</sub>), 66.6 (C<sub>ortho</sub>  $\eta^5$ -C<sub>5</sub>H<sub>4</sub>), 65.8 {-OCH<sub>2</sub>(C<sub>6</sub>H<sub>5</sub>)}, 42.4 (-NHCH<sub>2</sub>-), 40.7 (-NHCH<sub>2</sub>-).

**General procedures for the preparation of the starting materials of N-(5-ferrocenyl-1-naphthoyl) amino acid and dipeptide derivatives.**

**N-1-amino-5-acetyl-naphthalene 125.**

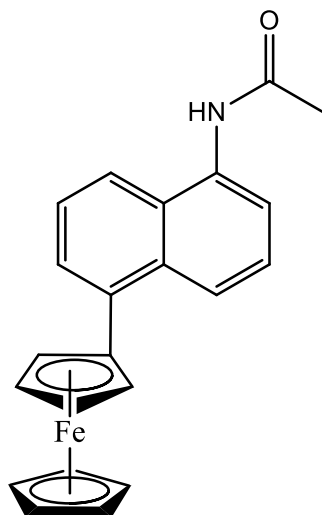


Acetic anhydride (3 mL, 27.2 mmol) was added to 1, 5-diaminonaphthalene acid (3.0 g, 19.0 mmol) in a solution of water (70 mL) and pyridine (5 mL). The reaction was allowed to stir overnight at room temperature. The reaction mixture was poured onto 10% HCl on ice and the product was collected by vacuum filtration to yield a grey-purple solid (3.13 g, 82 %), mp (decomp.) 214 °C (lit<sup>29</sup> 166 °C).

<sup>1</sup>H NMR (400 MHz)  $\delta$  (DMSO-*d*<sub>6</sub>): 9.96 (1H, s, -CONH-), 7.92 (1H, d, *J* 8.4 Hz, ArH), 7.69 (1H, d, *J* 7.2 Hz, ArH), 7.52 (1H, t, *J* 8 Hz, ArH), 7.23 (1H, d, *J* 7.2 Hz, ArH), 7.06 (1H, t, *J* 7.6 Hz, ArH), 6.60 (1H, d, *J* 7.2 Hz, ArH), 5.43 (2H, s, -NH<sub>2</sub>-), 2.19 (3H, s, -COCH<sub>3</sub>).

<sup>13</sup>C NMR (100 MHz)  $\delta$  (DMSO-*d*<sub>6</sub>): 168.9 (C=O), 144.5 (C<sub>q</sub>), 133.9 (C<sub>q</sub>), 128.5 (C<sub>q</sub>), 125.4, 124.3, 123.7 (C<sub>q</sub>), 121.9, 119.9, 110.0, 107.4, 23.4 (-COCH<sub>3</sub>).

**N-1-acetyl-5-ferrocenyl naphthalene 126.**

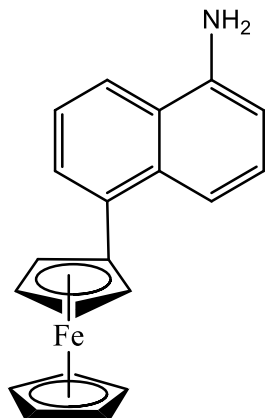


To a solution of 1-amino-5-acetyl naphthalene (3.00 g, 15.0 mmol) in water (50 mL) was added conc. HCl (5 mL). A solution of sodium nitrite (1.24 g, 18.0 mmol) in water (20 mL) was then added slowly with stirring while the temperature was kept below 5 °C to give the diazonium salt. This was then added to a solution of ferrocene (3.35 g, 18.0 mmol) in diethyl ether (40 mL) and allowed to stir overnight. The reaction mixture was washed with water, the organic layer was dried over magnesium sulphate and the solvent was removed *in vacuo* to yield the crude product. It was purified by column chromatography (eluent 20-40 % diethyl ether: 80-60 % hexane) to obtain an orange-brown solid (0.35 g, 9 %), mp 178 °C.

$^1\text{H}$  NMR (400 MHz)  $\delta$  (DMSO- $d_6$ ): 10.02 (1H, s, -NH-), 8.33 (1H, d,  $J$  8.4 Hz, ArH), 7.99 (1H, d,  $J$  8.4 Hz, ArH), 7.91 (1H, d,  $J$  6.8 Hz, ArH), 7.61 (1H, d,  $J$  7.2 Hz, ArH), 7.52 (2H, q,  $J$  8,  $J$  6.8, ArH), 4.68 {2H, t,  $J$  2 Hz, *ortho* on ( $\eta^5$ -C<sub>5</sub>H<sub>4</sub>)}, 4.46 {2H, t,  $J$  2 Hz, *meta* on ( $\eta^5$ -C<sub>5</sub>H<sub>4</sub>)}, 4.21 {5H, s, ( $\eta^5$ -C<sub>5</sub>H<sub>5</sub>)}, 2.19 (3H, s, -COCH<sub>3</sub>).

$^{13}\text{C}$  NMR (100 MHz)  $\delta$  (DMSO- $d_6$ ): 169.0 (C=O), 135.8 (C<sub>q</sub>), 134.0 (C<sub>q</sub>), 133.5, 131.9 (C<sub>q</sub>), 128.5 (C<sub>q</sub>), 128.1, 125.1, 123.0, 121.8, 121.6, 86.4 (C<sub>ipso</sub>  $\eta^5$ -C<sub>5</sub>H<sub>4</sub>), 70.2 ( $\eta^5$ -C<sub>5</sub>H<sub>5</sub>), 69.5 (C<sub>meta</sub>  $\eta^5$ -C<sub>5</sub>H<sub>4</sub>), 68.2 (C<sub>ortho</sub>  $\eta^5$ -C<sub>5</sub>H<sub>4</sub>), 23.4 (-COCH<sub>3</sub>).

### ***N*-1-amino-5-ferrocenyl-naphthalene 127.**



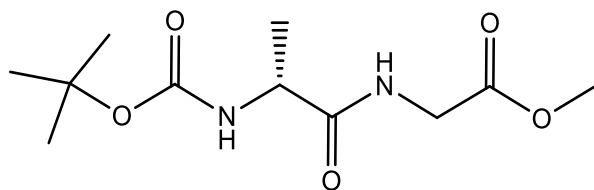
1-acetyl-5-ferrocenyl naphthalene (0.71 g, 19.2 mmol) was dissolved in methanol (10 mL) . To this was added sodium hydroxide (10 %, 10 mL). The mixture was heated to reflux for 24 hours. The solution was cooled on ice and acidified to pH 2. Vacuum filtration yielded a brown solid (0.35 g, 56 %), mp 157-158 °C.

$^1\text{H}$  NMR (400 MHz)  $\delta$  (DMSO- $d_6$ ): 7.99 (1H, d,  $J$  8.4 Hz, ArH), 7.8 (1H, d,  $J$  6 Hz, ArH), 7.61 (1H, d,  $J$  8.8 Hz, ArH), 7.35 (1H, t,  $J$  7.2 Hz, ArH), 7.19 (1H, t,  $J$  8.4 Hz, ArH), 6.66 (1H, d,  $J$  7.2 Hz, ArH), 5.68 (2H, s, -NH<sub>2</sub>), 4.62 {2H, t,  $J$  1.6 Hz, *ortho* on ( $\eta^5$ -C<sub>5</sub>H<sub>4</sub>)}, 4.41 {2H, t,  $J$  1.6 Hz, *meta* on ( $\eta^5$ -C<sub>5</sub>H<sub>4</sub>)}, 4.20 {5H, s, ( $\eta^5$ -C<sub>5</sub>H<sub>5</sub>)}.

$^{13}\text{C}$  NMR (100 MHz)  $\delta$  (DMSO- $d_6$ ): 144.9 (C<sub>q</sub>), 135.1 (C<sub>q</sub>), 132.4 (C<sub>q</sub>), 127.8, 126.3, 123.0 (C<sub>q</sub>), 122.9, 121.0, 113.4, 107.3, 87.3 (C<sub>ipso</sub>  $\eta^5$ -C<sub>5</sub>H<sub>4</sub>), 70.1 ( $\eta^5$ -C<sub>5</sub>H<sub>5</sub>), 69.5 (C<sub>meta</sub>  $\eta^5$ -C<sub>5</sub>H<sub>4</sub>), 69.4 (C<sub>ortho</sub>  $\eta^5$ -C<sub>5</sub>H<sub>4</sub>).

### ***General procedures for the preparation of Boc protected dipeptide esters.***

#### **Boc-D-alanine-glycine-methyl ester 128**

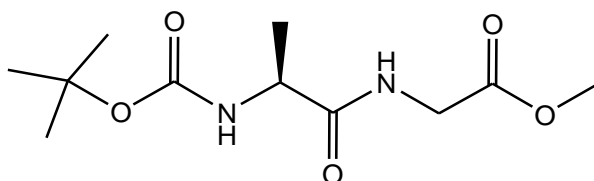


The synthesis followed that of **Boc glycine glycine benzyl ester** using the following reagents; Boc-D-alanine-OH (9.04 g, 47.8 mmol), glycine methyl ester hydrochloride (5.0 g, 39.8 mmol), NHS (2.29 g, 19.9 mmol), EDC (15.3 g, 79.6 mmol). The product was purified by column chromatography (eluent 50 % ethyl acetate: 50 % hexane) to give the title compound as a transparent oil (3.08 g, 30 %)

$^1\text{H}$  NMR (400 MHz)  $\delta$  (DMSO- $d_6$ ): 8.25 (1H, t,  $J$  5.6 Hz, -CONH-), 6.98 (1H, d,  $J$  7.6 Hz, -CONH-), 4.01 (1H, qt,  $J$  7.2 Hz, -NHCH-), 3.93 (1H, dd,  $J$  6 Hz,  $J$  11.2 Hz, -NHCH $_2$ -), 3.84 (1H, dd,  $J$  6 Hz,  $J$  11.6 Hz, -NHCH $_2$ -), 3.67 (3H, s, -OCH $_3$ ), 1.43 (9H, s, -C(CH $_3$ ) $_3$ ), 1.23 (3H, d,  $J$  7.2 Hz, -CHCH $_3$ ).

$^{13}\text{C}$  NMR (100 MHz)  $\delta$  (DMSO- $d_6$ ): 178.5 (C=O), 175.5 (C=O), 160.2 (C=O), 83.2 (C $_q$ ), 56.9 (-OCH $_3$ ), 54.7 (-NHCH $_2$ -), 45.7 (-NHCH-), 33.4 {C(CH $_3$ ) $_3$ }, 23.4 (-CHCH $_3$ ).

#### **Boc-L-alanine-glycine-methyl ester 129**



The synthesis followed that of **Boc glycine glycine benzyl ester** using the following reagents: Boc-L-alanine-OH (9.04 g, 47.8 mmol), EDC (15.26 g, 79.6 mmol), NHS (2.29 g, 19.9 mmol) and glycine methyl ester hydrochloride (5.00 g, 39.8 mmol). The product was purified by column chromatography (eluent 50 % ethyl acetate: 50 % hexane) to give the title compound as a transparent oil (3.75 g, 36 %).

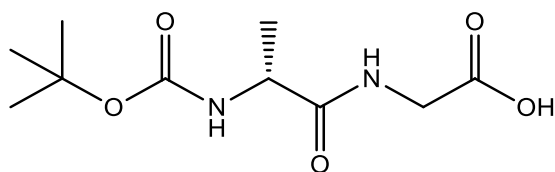
$^1\text{H}$  NMR (400 MHz)  $\delta$  (DMSO- $d_6$ ): 8.19 (1H, t,  $J$  5.6 Hz, -CONH-), 6.94 (1H, d,  $J$  7.6 Hz, -CONH-), 4.04 (1H, qt,  $J$  6.8 Hz, -COCH-), 3.89 (1H, dd,  $J$  11.2 Hz, 6.4 Hz, -NHCH $_2$ -), 3.80 (1H, dd,  $J$  12 Hz, 5.6 Hz, -NHCH $_2$ -), 3.62 (3H, s, -OCH $_3$ ), 1.38 (1H, s, -CH(CH $_3$ ) $_3$ ), 1.19 (3H, d,  $J$  7.2 Hz, -CHCH $_3$ ).

$^{13}\text{C}$  NMR (100 MHz)  $\delta$  (DMSO- $d_6$ ): 173.3 (C=O), 170.3 (C=O), 155.0 (C=O), 77.9 (C $_q$ ), 59.7 (-OCH $_3$ ), 51.6 (-NHCH $_2$ -), 49.4 (-NHCH-), 28.1 {-C(CH $_3$ ) $_3$ }, 18.1 (-CHCH $_3$ ).

#### **General procedures for the preparation of Boc protected dipeptides.**

##### **Boc-D-alanine-glycine-OH 130**



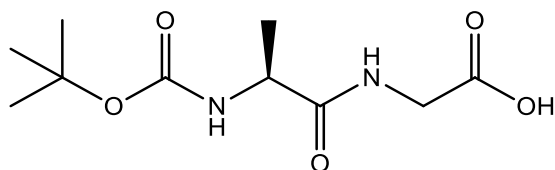


Boc-D-alanine-glycine methyl ester (1.24 g, 4.8 mmol) was dissolved in methanol (10 mL). To this was added sodium hydroxide (0.5 M, 10 mL). The solution was heated to reflux for 24 h. The solution was acidified with citric acid and the solvent was removed *in vacuo* to yield the product as a transparent oil (1.11 g, 93 %).

$^1\text{H}$  NMR (600 MHz)  $\delta$  (DMSO- $d_6$ ): 7.24 (1H, br.s, -CONH-), 7.19 (1H, d,  $J$  7.8 Hz, -CONH-), 3.93 (1H, qt,  $J$  7.8 Hz, -CHCH $_3$ ), 3.26 (2H, d,  $J$  4.2 Hz, -NHCH $_2$ -), 1.36 (3H, s, -CHCH $_3$ ), 1.49 {9H, s, -C(CH $_3$ ) $_3$ }.

$^{13}\text{C}$  NMR (100 MHz)  $\delta$  (DMSO- $d_6$ ): 174.6 (C=O), 171.4 (C=O), 170.3 (C=O), 78.0 (C $_q$ ), 49.9 (-CHCH $_3$ ), 44.0 (-NHCH $_2$ -), 28.2 {-CHCH $_3$ } $_3$ , 25.3 (-CHCH $_3$ ).

#### Boc-L-alanine-glycine-OH **131**.



The synthesis followed that of **135** using the following reagents; Boc-L-alanine-glycine methyl ester (3.50 g, 13.4 mmol), to yield the product as a transparent oil (2.91 g, 88 %).

$^1\text{H}$  NMR (400 MHz)  $\delta$  (DMSO- $d_6$ ): 7.32 (1H, t,  $J$  4.4 Hz, -CONH-), 7.17 (1H, d,  $J$  9.6 Hz, -CONH-), 3.94 (1H, qt,  $J$  7.2 Hz, -COCH-), 3.35 (2H, d,  $J$  4 Hz, -COCH $_2$ -), 1.38 (9H, s, -C(CH $_3$ ) $_3$ ), 1.16 (3H, d,  $J$  6.4 Hz, -CHCH $_3$ ).

$^{13}\text{C}$  NMR (100 MHz)  $\delta$  (DMSO- $d_6$ ): 171.7 (C=O), 171.5 (C=O), 155.1 (C=O), 78.1 (C $_q$ ), 49.8 (-CHCH $_3$ ), 43.7(-NHCH $_2$ -), 28.1 {-CHCH $_3$ } $_3$ , 25.1 (-CHCH $_3$ ).

## References

---

- <sup>1</sup> F. Cava, H. Lam, M. A. dePedro, M. K. Waldor, *Cell and Molecular Life Sciences*, **2011**, 68 (5), 817-831.
- <sup>2</sup> T. Hatanaka, M. Haramura, Y. J. Fei, S. Miyauchi, C. C. Brigdges, P. S. Ganapathy, S. B. Smyth, V. Ganapathy, M. E. Ganapathy, *The Journal of Pharmacology and Experimental Therapeutics*, **2003**, 308 (3), 1138-1147.
- <sup>3</sup> S. Alexander, *British Journal of Pharmacology*, **2011**, 164 (7), 1751-1752.
- <sup>4</sup> D. T. Thwaites, C. M. H. Anderson, *British Journal of Pharmacology*, **2011**, 164, 1802-1816.
- <sup>5</sup> E. M. El Amo, A. Urtti, M. Yliperttula, *European Journal of Pharmaceutical Sciences*, **2008**, 35, 161-174.
- <sup>6</sup> I. Rubio-Aliaga, H. Daniel, *TRENDS in Pharmacological Sciences*, **2002**, 23 (9), 434-440.
- <sup>7</sup> G. L. Patrick, *An Introduction to Medicinal Chemistry*, fifth edition, Oxford University Press, **2013**.
- <sup>8</sup> C. G. Hartinger, P. J. Dyson, *Chemical Society Reviews*, **2008**, 38 (2), 391-401.
- <sup>9</sup> B. Rosenberg, L. Van Camp and T. Krigas, *Nature*, **1965**, 205, 698-699.
- <sup>10</sup> C. Biot, I. Fraisse, D. Ter-Minassian, J. Khalife, D. Dive, *Parasite*, **2011**, 18, 207-214.
- <sup>11</sup> C. Chochan, *Applied Organometallic Chemistry*, **2006**, 20, 112-116.
- <sup>12</sup> K. Schlögl, *Monatshefte für Chemie*, **1957**, 88, 601-607.
- <sup>13</sup> G. Jaouen, *Bioorganometallics: Biomolecules, Labelling, Medicine*, **2006**.
- <sup>14</sup> A. Mooney, R. Tiedt, T. Maghoub, N. O'Donovan, J. Crown, B. White, P. T. M. Kenny, *Journal of Medicinal Chemistry*, **2012**, 55 (11), 5455-5466.
- <sup>15</sup> N. J. Long, *Metallocenes*, first edition, Blackwell Science Ltd., **1998**.
- <sup>16</sup> P. Pigeon, S. Top, A. Vessieres, M. Huché, E. A. Hillard, E. Salomon, G. Jaouen, *Journal of Medicinal Chemistry*, **2005**, 48, 2814-2821.
- <sup>17</sup> A. J. Corry, N. O'Donovan, A. Mooney, D. O'Sullivan, D. K. Rai, P. T. M. Kenny, *Journal of Organometallic Chemistry*, **2009**, 694, 880-885.
- <sup>18</sup> A. J. Corry, A. Mooney, D. O'Sullivan, P. T. M. Kenny, *Inorganica Chimica Acta*, **2009**, 362, 2957-2961.

- 
- <sup>19</sup> A. Mooney, A. J. Corry, C. N. Ruairc, T. Mahgoub, D. O'Sullivan, N. O'Donovan, J. Crown, S. Varughese, S. M. Draper, D. K. Rai, P. T. M. Kenny, *Dalton Transactions*, **2010**, 39, 8228-8239.
- <sup>20</sup> C. A. G. N. Montalbetti, V. Flaque, *Tetrahedron*, **2005**, 61, 10827-10852.
- <sup>21</sup> M. Bodanszky, *Principles of Peptide synthesis*, second edition, Springer, **1993**.
- <sup>22</sup> J. Jones, *Amino Acid and Peptide Synthesis*, first edition, Oxford University Press, **1992**.
- <sup>23</sup> A. J. Corry, Ph.D Thesis, Dublin City University, **2009**.
- <sup>24</sup> A. Mooney, Ph.D Thesis, Dublin City University, **2010**.
- <sup>25</sup> J. C. Micheau, J. Zhao, *Journal of Physical Organic Chemistry*, **2007**, 20, 810-820.
- <sup>26</sup> D. L. Pavia, G. M. Lampman, G. S. Kris, *Introduction to Spectroscopy*, third edition, Brooks/Cole Thomson Learning, **2001**.
- <sup>27</sup> R. Dalpozzo, G. Bartoli, M. Bosco, P. Melchiorre, L. Sambri, *Current Organic Synthesis*, **2009**, 6, 79-101.
- <sup>28</sup> Chemgaroo, Chemgapedia, Wiley-VHC, available from:  
[http://www.chemgapedia.de/vsengine/vlu/vsc/en/ch/12/oc/vlu\\_organik/aromaten/reaktionen/ar\\_se\\_beispiele.vlu/Page/vsc/en/ch/12/oc/aromaten/reaktionen/ar\\_se/azokupplung/azokupplung.vscml.html](http://www.chemgapedia.de/vsengine/vlu/vsc/en/ch/12/oc/vlu_organik/aromaten/reaktionen/ar_se_beispiele.vlu/Page/vsc/en/ch/12/oc/aromaten/reaktionen/ar_se/azokupplung/azokupplung.vscml.html)
- <sup>29</sup> J. C. Bradley, A. Williams, A. Lang, Jean-Claude Bradley Open Melting Point Dataset, 2014, <http://dx.doi.org/10.6084/m9.figshare.1031637>

## Chapter 3

### Biological evaluation of *N*-(6-ferrocenyl-2-naphthoyl), *N*-{*para*-(ferrocenyl)cinnamoyl} and *N*-{*para*-(ferrocenyl)benzoyl} amino acid and dipeptide derivatives.

#### 3.1 Introduction

As previously discussed *N*-(6-ferrocenyl-2-naphthoyl)-glycine-glycine ethyl ester **70** has been shown to be the most active of the *N*-ferrocenyl amino acid and dipeptide esters to date with an IC<sub>50</sub> value of 0.13 ± 0.02 μM in H1299 NSCLC cells and 1.10 ± 0.13 μM in Sk-Mel-28 metastatic melanoma cells. The aims of this research project were to extend the SAR study of the ferrocenyl peptide conjugates, to investigate the mode of action of this class of compounds and to begin *in vivo* studies. In order to extend the SAR study of the project *N*-(6-ferrocenyl-2-naphthoyl), *N*-{*para*-(ferrocenyl)cinnamoyl} and *N*-{*para*-(ferrocenyl)benzoyl} amino acid and dipeptide derivatives have been prepared maintaining the most active dipeptide configurations previously used whilst altering both the conjugated linker and the ester functionality. *N*-(6-ferrocenyl-2-naphthoyl)-glycine-glycine ethyl ester **70** as prepared by Dr. Aine Mooney was evaluated in conjunction with the newly synthesised compounds for comparison. The compounds were evaluated on a panel of lung cancer and melanoma cell lines; H1299 and A549 lung cancer and HT-144, Lox-IMVI and Malme-3M melanoma cells. It was necessary to carry out preliminary evaluation of all the compounds prepared in *in vitro* studies, both for initial assessment and to identify the most promising compounds for the commencement of *in vivo* studies. Biological evaluation was carried out by James Murphy<sup>1</sup>.

##### 3.1.1 Cell culture

The historical development of cell culture began in 1907 when Ross Harrison grew embryonic nerve cells on microscope slides<sup>2</sup>. He developed the hanging drop technique by suspending nerve tissue from frog embryos in lymph fluid as a drop on the underside of a microscope slide and was able to study cell growth for several weeks. Burrows and Carrel developed techniques for the culture of a range of mammalian cells achieving sub culture of the cells for several years without infection. Before 1940 the widespread use of culture techniques was limited by the sterility controls necessary. It was not until the late 1940's with the development of antibiotics that further developments in cell culture took place. Large scale cultures were first considered when it was discovered that viruses could be propagated in cell cultures and used as vaccines. In the early 1950's Earle and Eagle analysed the nutritional

requirements of cultured cells and in 1955 Eagle's minimum essential medium (EMEM) was developed for HeLa cancer cells. Since the 1950's the range of cell lines available has increased considerably.

Cell culture was devised as a means of studying animal cells free of systematic changes which might occur *in vivo* during normal homeostasis or due to the stress of an experiment<sup>3</sup>. Cell culture offers several advantages over animal testing. It allows the ability to control physiochemical parameters such as pH, temperature, pressure, and O<sub>2</sub> and CO<sub>2</sub>. Cell culture is homogenous as it is randomly mixed with each sub culture. It allows for greater economy as cultures may be exposed to a reagent at a lower and defined concentration with direct access to the cell. Thus less reagent is required for injection than *in vivo* where up to 90 % may be lost by excretion and distribution to tissues other than those desired. Screening tests with many replicates and variables are cheaper and the legal and ethical evaluations associated with animal testing are avoided. The use of multi well plates or robotics have allowed an increase in scale and reduction in time.

*In vitro* miniaturised colorimetric assays are used extensively in the determination of a substance's ability to enhance cell growth or promote cell death<sup>4</sup>. The most commonly used measure of toxicity is inhibition of cell growth determined by reduced cell numbers compared with untreated controls. Colorimetric endpoint assays will not distinguish between cytotoxic and cytostatic effects when used after 6 or 7 days of exposure to the test chemical. Cytotoxic agents cause irreversible cell death through apoptosis, necrosis or autophagy, while cytostatic agents have only a temporary effect on growth and growth rates return to normal once the cytostatic agent is removed. Several *in vitro* miniaturised colorimetric assays have been developed for the quantification of cell growth. These include the 3-(4,5-dimethylthiazol-2-yl)-2,5-diphenyltetrazolium bromide (MTT) assay, neutral red assay and staining with crystal violet or sulforhodamine B and the acid phosphatase assay<sup>5</sup>.

Cell viability assays often rely on a breakdown in membrane integrity measured by the uptake of a dye to which the cell is normally impermeable or the release of a dye which is normally retained. The MTT colourimetric endpoint assay was introduced in 1983<sup>6</sup>. This technique relies on the metabolic reduction of tetrazolium dye in viable cells to a coloured formazan product before reading the optical density. The formazan product is insoluble in aqueous media and an extra solubilisation step must be taken before reading the optical density. The neutral red assay is based on the release of the neutral red dye which is normally taken up and retained by viable cells. The absorbance of the eluted dye is measured at 570

nm. The crystal violet assay and the sulforhodamine B assays are protein staining assays. Sulphordamine B has been shown to differentiate between cytotoxicity and cytostatic behaviour.

The acid phosphatase assay is based on the ability of the acid phosphatase enzyme in the lysosome of cells to hydrolyze *p*-nitrophenyl phosphate yielding the *p*-nitrophenyl chromophore. This can be measured in strong alkali at 405 nm. It has fewer steps and fewer reagents than the MTT assay and is more convenient as the product does not require an extra solubilisation step. The reproducibility between replicate wells is excellent and in many cases has been found to be better than the neutral red or MTT assays<sup>7</sup>. The acid phosphatase end point assay was the chosen endpoint assay for the biological evaluation of the *N*-(6-ferrocenyl-2-naphthoyl) amino acid and dipeptide esters.

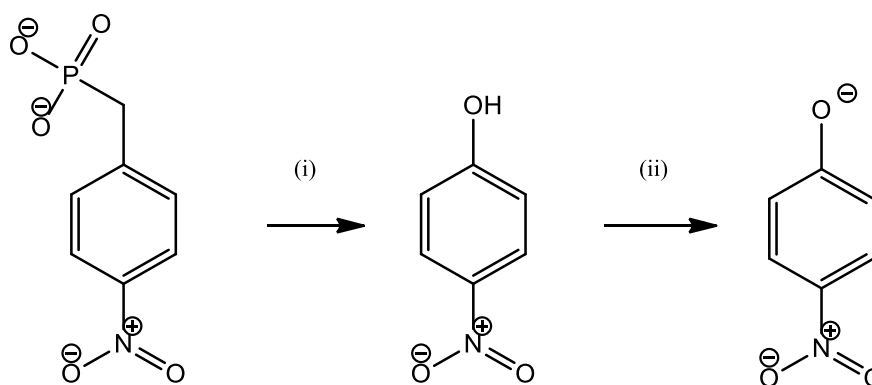


**Figure 3.1:** Acid phosphatase end-point assay: (i) Phosphatase catalysed reaction in water; (ii) colour reaction in base (NaOH).

### 3.2 Biological evaluation of *N*-(6-ferrocenyl-2-naphthoyl)-glycine-glycine esters.

The most active derivative to date of the *N*-(6-ferrocenyl-2-naphthoyl) amino acid and dipeptide ester series was determined to be the *N*-(6-ferrocenyl-2-naphthoyl)-glycine-glycine ethyl ester **70** with an IC<sub>50</sub> value of 0.13 ± 0.02 μM in H1299 non-small cell lung cancer cells and 1.10 ± 0.13 μM in Sk-Mel-28 melanoma cells<sup>8</sup>. Therefore the series of *N*-(6-ferrocenyl-2-naphthoyl)-glycine-glycine esters were prepared and evaluated for their biological activity. *N*-(6-ferrocenyl-2-naphthoyl)-glycine-glycine methyl ester **100**, *N*-(6-ferrocenyl-2-naphthoyl)-glycine-glycine ethyl ester **70**, *N*-(6-ferrocenyl-2-naphthoyl) propyl ester **101**, *N*-(6-ferrocenyl-2-naphthoyl)-glycine-glycine butyl ester **102** and *N*-(6-ferrocenyl-2-naphthoyl)-glycine-glycine benzyl ester **103** were evaluated against a panel of A549 lung cancer, Malme-3M, Lox-IMVI and HT144 melanoma cell lines. All compounds were screened

at 10  $\mu\text{M}$  and 1  $\mu\text{M}$ . The results of the preliminary screen are presented in figures 3.1 and 3.2.

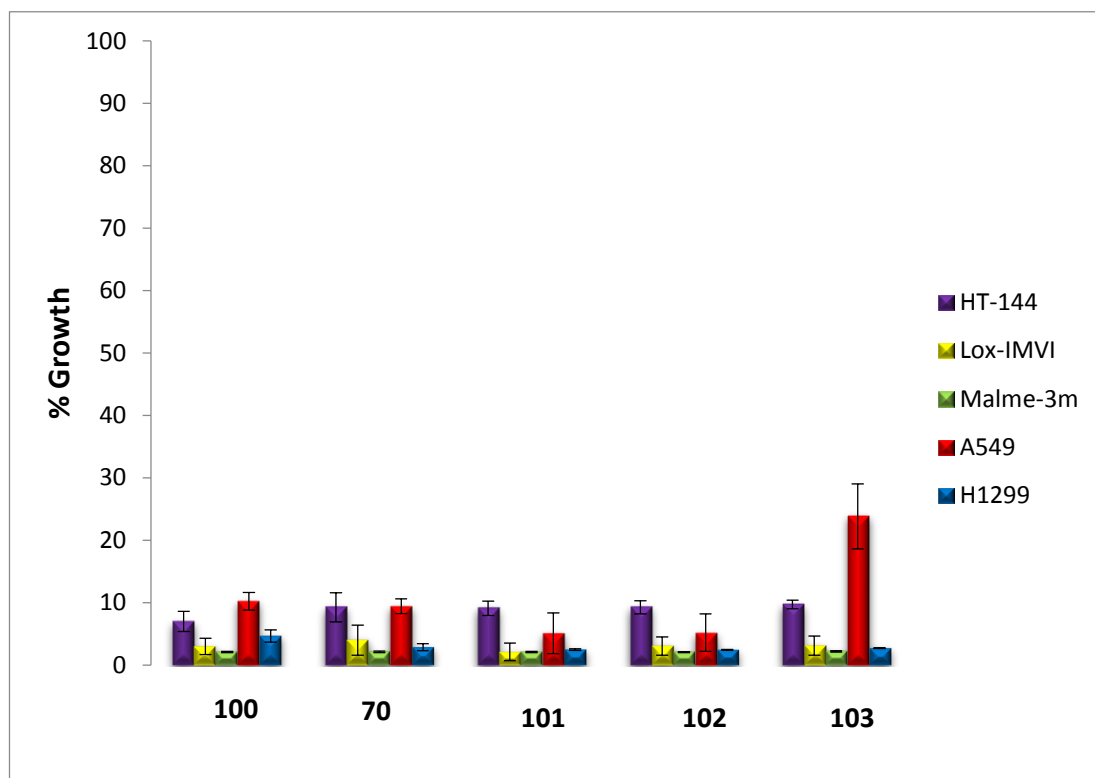


**Figure 3.1:** Evaluation of compounds **70**, **100-103** at 10  $\mu\text{M}$ . Growth is expressed relative to compounds treated with an equivalent volume of DMSO. Error bars represent the standard deviation of triplicate assays.

As can be seen in figure 3.1, all compound show excellent growth inhibition at 10  $\mu\text{M}$ , with growth inhibition above 70 % in all cell lines and for all compounds. Thus a further screen at 1  $\mu\text{M}$  was performed for all compounds tested (figure 3.2). At 1  $\mu\text{M}$  growth inhibition can be seen to be above 60 % for only the *N*-(6-ferrocenyl-2-naphthoyl)-glycine-glycine methyl ester **100** and the *N*-(6-ferrocenyl-2-naphthoyl)-glycine-glycine ethyl ester **70**, with compounds **101**, **102** and **103** all having less than 10 % growth inhibition at this concentration. Therefore both the methyl and ethyl esters were selected for further biological evaluation.

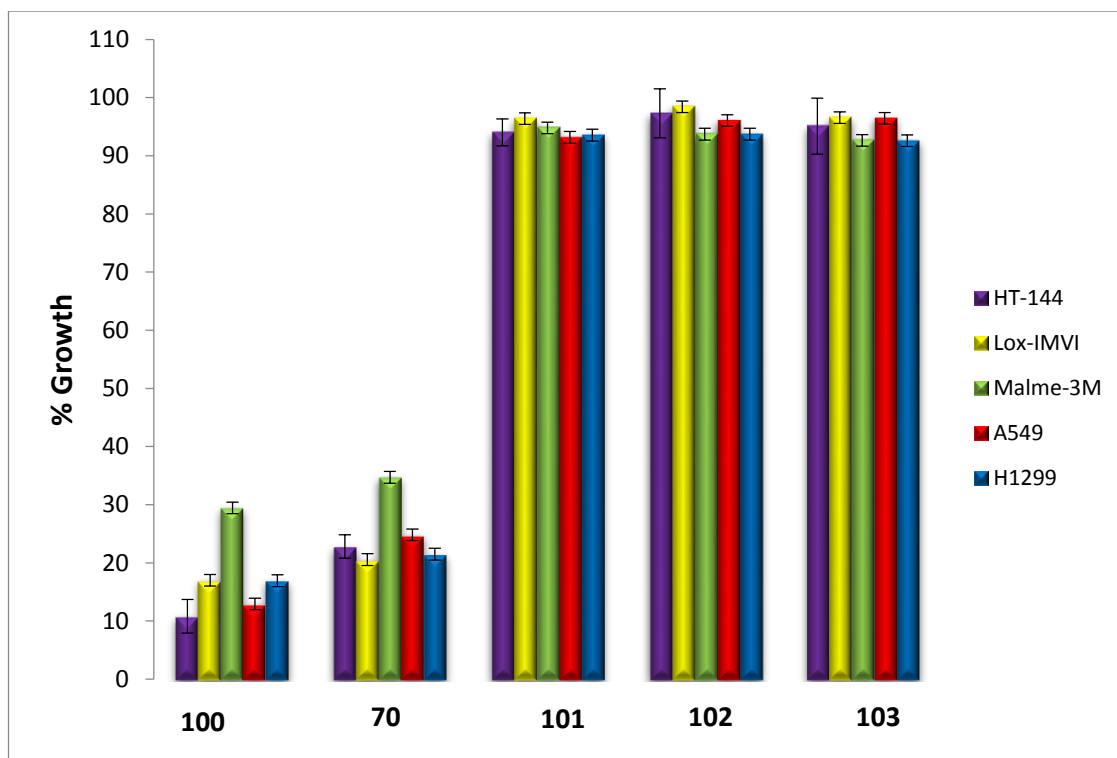


**Figure 3.2:** Evaluation of compounds **70**, **100-103** at 1  $\mu\text{M}$ . Growth is expressed relative to compounds treated with an equivalent volume of DMSO. Error bars represent the standard deviation of triplicate assays.

### 3.2.1 *In vitro* evaluation in A549 and H1299 lung cancer cell lines.

$\text{IC}_{50}$  values were then determined for compounds **100** and **70** along with cisplatin **22**. An excellent value of  $0.7 \pm 0.07 \mu\text{M}$  was obtained for **70** in the A549 cell line. The most active compound however was **100**, with a value of  $0.2 \pm 0.03 \mu\text{M}$ . A value of  $0.3 \pm 0.04$  was obtained for **100** in the H1299 cell line. This is higher than the literature value obtained for **70** at  $0.13 \pm 0.02$ , however both values were significantly lower than those obtained for cisplatin **22** at  $2.6 \pm 0.10$  and  $2.1 \pm 0.20 \mu\text{M}$ .



**Table 3.1:** Percentage growth of A549 cells in the presence of compounds **100-103** and IC<sub>50</sub> values.

A549	Compound	% growth at 10 $\mu\text{M}$	% growth at 1 $\mu\text{M}$	IC <sub>50</sub> ( $\mu\text{M}$ )
	<b>100</b>	10.0 $\pm$ 1.4	12.9 $\pm$ 0.4	0.2 $\pm$ 0.03
	<b>70</b>	9.4 $\pm$ 1.2	24.8 $\pm$ 1.9	0.7 $\pm$ 0.07
	<b>101</b>	5.1 $\pm$ 3.3	93.2 $\pm$ 1.8	
	<b>102</b>	5.2 $\pm$ 3.0	96.1 $\pm$ 3.4	
	<b>103</b>	23.8 $\pm$ 5.2	96.4 $\pm$ 7.9	
	<b>22</b>			2.6 $\pm$ 0.10

**Table 3.2:** Percentage growth of H1299 cells in the presence of compounds **100-103** and IC<sub>50</sub> values. \*Literature value for **70**<sup>8</sup>.

H1299	Compound	% growth at 10 $\mu\text{M}$	% growth at 1 $\mu\text{M}$	IC <sub>50</sub> ( $\mu\text{M}$ )
	<b>100</b>	4.7 $\pm$ 1.0	16.9 $\pm$ 2.0	0.3 $\pm$ 0.04
	<b>70</b>	2.9 $\pm$ 0.6	21.5 $\pm$ 3.3	0.13 $\pm$ 0.02*
	<b>101</b>	2.5 $\pm$ 0.1	93.6 $\pm$ 4.0	
	<b>102</b>	2.5 $\pm$ 0.1	93.7 $\pm$ 5.2	
	<b>103</b>	2.7 $\pm$ 0.0	92.6 $\pm$ 6.6	
	<b>22</b>			2.1 $\pm$ 0.20

### 3.2.2 *In vitro* evaluation in Lox-IMVI, Malme-3M and HT144 metastatic melanoma cell lines.

In the Lox-IMVI cell line IC<sub>50</sub> values of 0.2  $\pm$  0.06  $\mu\text{M}$  and 0.5  $\pm$  0.04  $\mu\text{M}$  were determined for **100** and **70** respectively (table 3.3). In the Malme-3M cell line values of 0.3  $\pm$  0.05  $\mu\text{M}$  and 0.5  $\pm$  0.02  $\mu\text{M}$  were determined for **100** and **70** (table 3.4), while in the HT144 cell line values of 0.2  $\pm$  0.02  $\mu\text{M}$  and 0.5  $\pm$  0.06  $\mu\text{M}$  were determined for **100** and **70** and (table 3.5). Values of approximately 2.9  $\pm$  0.90  $\mu\text{M}$ , 2.7  $\pm$  0.50  $\mu\text{M}$  and 3.0  $\pm$  0.40  $\mu\text{M}$  were obtained for cisplatin in each cell line. As can be seen **100** and **70** were considerably more active than cisplatin **22** across all cell lines.

**Table 3.3:** Percentage growth of Lox-IMVI cells in the presence of compounds **70**, **100-103** and IC<sub>50</sub> values.

Lox-IMVI	Compound	% growth at 10 $\mu\text{M}$	% growth at 1 $\mu\text{M}$	IC <sub>50</sub> ( $\mu\text{M}$ )
	<b>100</b>	3.0 $\pm$ 1.3	17.0 $\pm$ 2.6	0.2 $\pm$ 0.06
	<b>70</b>	4.0 $\pm$ 2.4	20.6 $\pm$ 4.7	0.5 $\pm$ 0.04
	<b>101</b>	2.1 $\pm$ 1.4	96.4 $\pm$ 3.4	
	<b>102</b>	3.0 $\pm$ 1.5	98.4 $\pm$ 3.6	
	<b>103</b>	3.1 $\pm$ 1.5	96.5 $\pm$ 2.3	
	<b>22</b>			2.9 $\pm$ 0.90

**Table 3.4:** Percentage Growth of Malme-3M cells in the presence of compounds **70**, **100-103** and IC<sub>50</sub> values.

Malme-3M	Compound	% growth at 10 $\mu\text{M}$	% growth at 1 $\mu\text{M}$	IC <sub>50</sub> ( $\mu\text{M}$ )
	<b>100</b>	2.1 $\pm$ 0.1	29.5 $\pm$ 3.2	0.3 $\pm$ 0.05
	<b>70</b>	2.1 $\pm$ 0.1	34.7 $\pm$ 3.5	0.5 $\pm$ 0.02
	<b>101</b>	2.1 $\pm$ 1.4	94.8 $\pm$ 6.3	
	<b>102</b>	2.1 $\pm$ 0.1	93.7 $\pm$ 6.5	
	<b>103</b>	2.2 $\pm$ 0.1	92.6 $\pm$ 6.6	
	<b>22</b>			2.7 $\pm$ 0.50

**Table 3.5:** Percentage Growth of HT-144 cells in the presence of compounds **70**, **100-103** and IC<sub>50</sub> values.

HT144	Compound	% growth at 10 $\mu\text{M}$	% growth at 1 $\mu\text{M}$	IC <sub>50</sub> ( $\mu\text{M}$ )
	<b>100</b>	7.0 $\pm$ 1.6	10.8 $\pm$ 2.9	0.2 $\pm$ 0.02
	<b>70</b>	9.2 $\pm$ 2.3	22.8 $\pm$ 2.0	0.5 $\pm$ 0.06
	<b>101</b>	9.1 $\pm$ 1.2	94.0 $\pm$ 2.3	
	<b>102</b>	9.2 $\pm$ 1.1	97.3 $\pm$ 4.2	
	<b>103</b>	9.7 $\pm$ 0.7	95.1 $\pm$ 4.8	
	<b>22</b>			3.0 $\pm$ 0.40

### 3.2.3 *In vitro* evaluation in normal human dermal fibroblast (NHDF) cells.

Toxicity is a common side effect of chemotherapeutic agents. Platinum compounds in particular are known for their harsh side effects<sup>9,10</sup>. IC<sub>50</sub> values were determined for **100** and **70** as well as cisplatin **22** in normal human dermal fibroblast cells (NHDF) (table 3.6) to determine their toxicity to normal cells. Normal human dermal fibroblast are non cancerous cells which are isolated from the dermis of the juvenile foreskin or adult skin on the face, breasts, abdomen and thighs. They are often used in wound healing studies and dermatological research as well as in cancer and tissue engineering.

Standard deviations are calculated based on triplicate assays. As standard deviations overlap the student's t test was performed to determine significant difference between results. The student's t test is used to determine significant difference between two sets of data. A value of  $p < 0.05$  indicates a strong probability against the two sets of data having no significant difference. For **70**  $p < 0.05$  indicating that there is significant difference, however for **100** it cannot be shown that there is significant difference in the toxicity from cisplatin **22**.

However we can see from the results that **100** and **70** are much more active in cancer cells than on NDHF cells. While **100** and **70** both have IC<sub>50</sub>'s of less than 1  $\mu\text{M}$  across all cell lines, the activity decreases to above 10  $\mu\text{M}$  in the NHDF cells. This indicates that they have some selectivity for cancer cells.

**Table 3.6:** IC<sub>50</sub> values of compounds **100** and **70** in normal human dermal fibroblast cells.

Cell Line	Compound	IC <sub>50</sub> ( $\mu\text{M}$ )	$\pm$
NDHF	Cisplatin	10.0	1.8
	<b>70</b>	14.2	2.4
	<b>100</b>	12.0	3.8

### 3.2.4 *In vitro* evaluation in resistant cell lines.

Along with toxicity, resistance is among the problems associated with commonly used chemotherapeutic drugs<sup>11, 12</sup>. Resistance may be intrinsic or acquired. The development of resistance to one chemotherapeutic agent may contribute to the development of resistance to another due to similarities in the mode of action. With our target compounds we wish to retain or improve the cytotoxic activity of these drugs while reducing the side effects such as

resistance. As resistance is common, evaluation in resistant cell lines could identify niches where these compounds may be of use. Thus we have examined the effect of compounds **100** and **70** in resistant cell lines. For lung cancer the A549 cell line resistant to cisplatin **22** (A549/Cpt) was studied and for melanoma the Malme-3M cell line resistant to temozolomide **132** (Malme-3M/TMZ) was used (table 3.7).

**Table 3.7:** IC<sub>50</sub> values of compounds **100** and **70** in resistant cell lines.

Cell Line	<b>100</b> (μM)	<b>70</b> (μM)	<b>22</b> (μM)
<b>A549</b>	0.2 ± 0.04	0.7 ± 0.04	3.6 ± 0.70
<b>A549/Cpt</b>	0.4 ± 0.10	2.4 ± 0.60	6.2 ± 0.90

Cell Line	<b>100</b> (μM)	<b>70</b> (μM)	<b>132</b> (μM)
<b>Malme-3M</b>	0.3 ± 0.05	0.5 ± 0.10	209.0 ± 27.00
<b>Malme-3M/TMZ</b>	0.3 ± 0.10	2.8 ± 0.50	483.0 ± 32.00

For the resistant A549 lung cancer cell line IC<sub>50</sub> values of 0.4 ± 0.10 μM and 2.4 ± 0.60 μM were obtained for **100** and **70**, while the resistant Malme-3M cell line gave IC<sub>50</sub> values of 0.3 ± 0.05 μM and 2.8 ± 0.50 μM respectively. When compared with the A549 cells the A549/Cpt cells showed 1.72 fold resistance to cisplatin **22** with an IC<sub>50</sub> of 3.6 ± 0.70 μM in A549 and 6.2 ± 0.90 μM in A549/Cpt cells. The Malme-3M/TMZ showed 2.3 fold resistance to temozolomide **132** with an IC<sub>50</sub> of 209 ± 27.00 μM in Malme-3M cells compared with Malme-3M/TMZ cells. Cross resistance can be seen for **70** in each cell line. In the lung cancer cell line the IC<sub>50</sub> value increases 3.4 times from 0.7 ± 0.04 μM to 2.4 ± 0.60 μM while in the melanoma cell line it increases 5.6 times from 0.5 ± 0.10 μM to 2.8 ± 0.50 μM. For compound **100** a twofold increase is seen in the lung cancer cell line with an increase from 0.2 ± 0.04 μM to 0.4 ± 0.10 μM. However in the melanoma cell line the IC<sub>50</sub> values remained constant for both resistant and normal cell lines at 0.3 ± 0.05 μM, suggesting that this compound is not susceptible to the same mechanism of acquired temozolomide **132** resistance in the Malme-3M cell line.

### 3.2.6 Apoptosis Assays

Apoptosis is programmed cell death. It is the cells main method of selective cell removal. It controls cell numbers and removes infected, stressed or damaged cells. During apoptosis

stress induced damage does not kill cells directly but rather triggers an apoptotic signalling pathway that leads to controlled cell death. Necrosis is an unregulated form of traumatic cell death caused by cellular injury<sup>13</sup>. The majority of human cancers are characterised by an inability to undergo apoptosis. Therefore we would like to selectively trigger apoptosis over necrosis<sup>14</sup>.

There are several known methods for determining apoptosis, among them are electron microscopy, the TUNEL assay and cell cycle analysis. Also used are microfluidic devices, single molecule spectroscopy and electrochemical devices. These techniques have been reviewed<sup>15</sup>. Here we have used both flow cytometry and the TUNEL assay to determine if cell death is apoptotic.

### **3.2.6.1 Cell cycle analysis**

The cell cycle consists of 4 stages, synthesis (S), mitosis (M), and two gap phases (G1) and (G2). Cells while non-dividing remain in (G0). The boundary between G1 and S phases is the main check point for cells. It is at this point that the cell must decide to divide or die. It is possible to determine the stages of the cell cycle due to changes in the concentration of DNA in the nucleus. The Guava cell cycle assay uses the fluorescent nuclear DNA stain propidium iodide (PI) to measure the quantity of DNA in each stage of the cell cycle. Resting cells in the G0/G1 phase contain two copies of each chromosome. As the cell progresses towards mitosis they begin to synthesis DNA (S phase) until the DNA content has doubled (G2/M phase). These cells will then fluoresce with twice the intensity. Cells in which the DNA has fragmented or degraded, such as apoptotic cells, appear as sub G0.

Cell cycle analysis was performed for one cell line of each the lung cancer and melanoma cells lines, A549 for the lung cancer cell line and HT144 for the melanoma cell line, as well as on control samples. The cells were treated with **100** at concentrations of 2, 1, 0.5, 0.25, 0.125 and 0.06125  $\mu\text{M}$ .

In the A549 cell line (figure 3.3) a significant increase in the sub G0 cells can be seen at as low as 0.125  $\mu\text{M}$ , with a corresponding decrease in the G1/G0 phase. This can be seen most markedly at the 2  $\mu\text{M}$  concentration where we can see an approximately 15 fold increase in the Sub G0 phase, with a decrease in the G1/G0 of nearly one third when compared with the control.

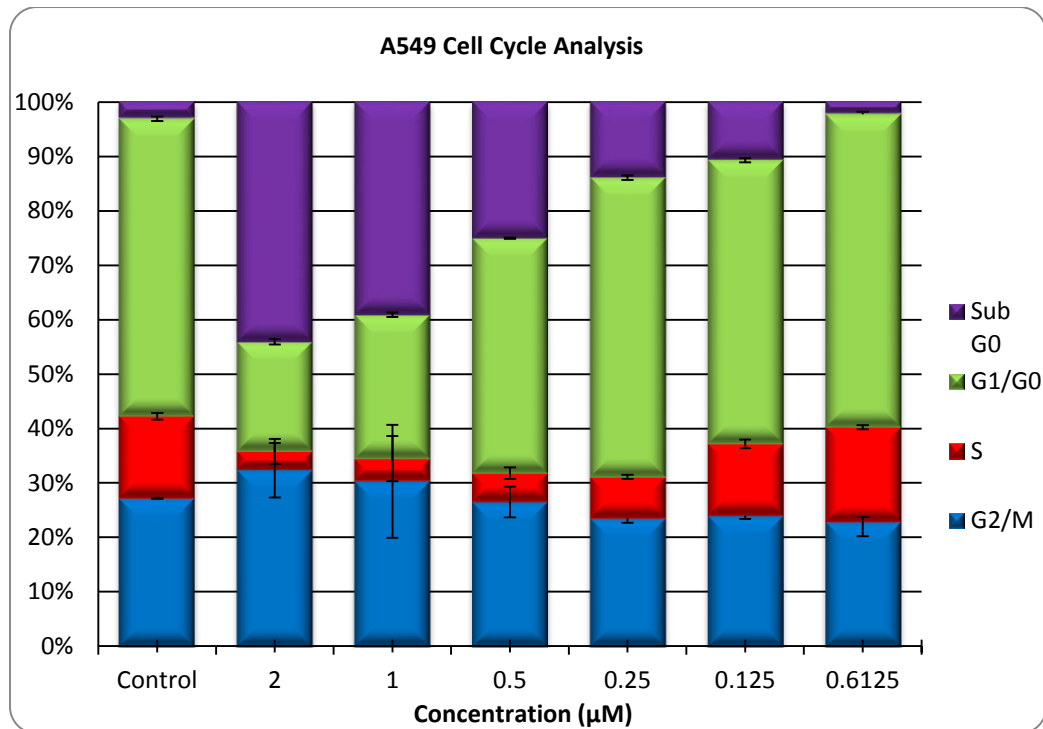


**Figure 3.3:** Graph of cell cycle distribution for A549 after incubation with **100**.

Similar results can be seen for the HT144 cells (figure 3.4). Again we can see a large increase in the Sub G0 population with a corresponding decrease in the G1/G0 population. These results are suggestive of apoptosis in the A549 and HT144 cell lines since apoptosis is characterised by DNA fragmentation and consequently a decrease in nuclear DNA content. However further studies of early and late apoptotic cells are required to confirm that cell death is occurring by apoptotic cell death.

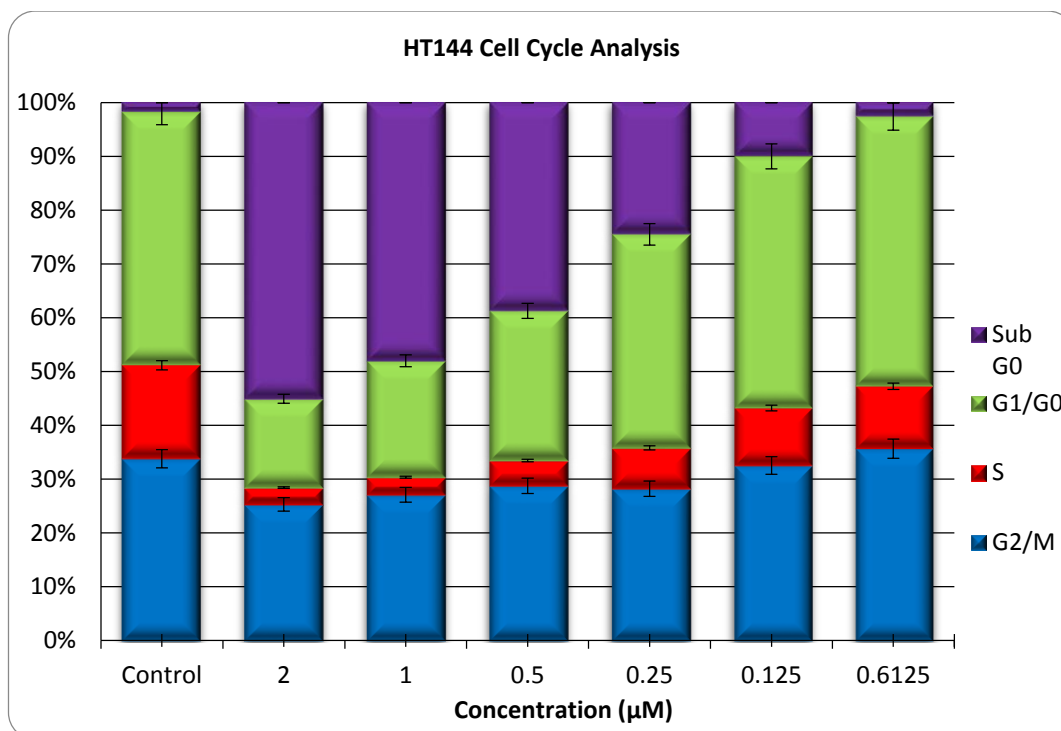


**Figure 3.4:** Graph of cell cycle distribution for HT-144 cells after incubation with 100.

### 3.2.6.2 TUNEL Assay

In order to further confirm the death of cells by apoptosis TUNEL assays were performed in addition to cell cycle analysis. This assay measures late stage apoptosis. It detects DNA fragmentation which results from apoptotic signalling cascades through a quantitative fluorescence assay. Nicks in DNA are labelled with bromo-deoxyuridine (BrdU) by terminal deoxynucleotidyl transferase (TdT) at the 3'-hydroxyl ends. This allows the cells undergoing apoptosis to be differentiated from cells undergoing necrosis. This test when performed correctly should label only cells in the last stage of apoptosis<sup>16,17</sup>.

The assays were again performed for A549 and HT144 cell lines. They were carried out at 2, 1, 0.5, 0.25 μM of *N*-(6-ferrocenyl-2-naphthoyl)-glycine-glycine methyl ester. These were accompanied with a 1 μM carboplatin control, a DMSO control and untreated cells. In the A549 cell line (figure 3.5), at concentrations ranging from 0.5 to 2 μM, cell death can be mainly attributed to apoptosis, with it making up approximately 80% of all cell death at the 2 μM concentration.

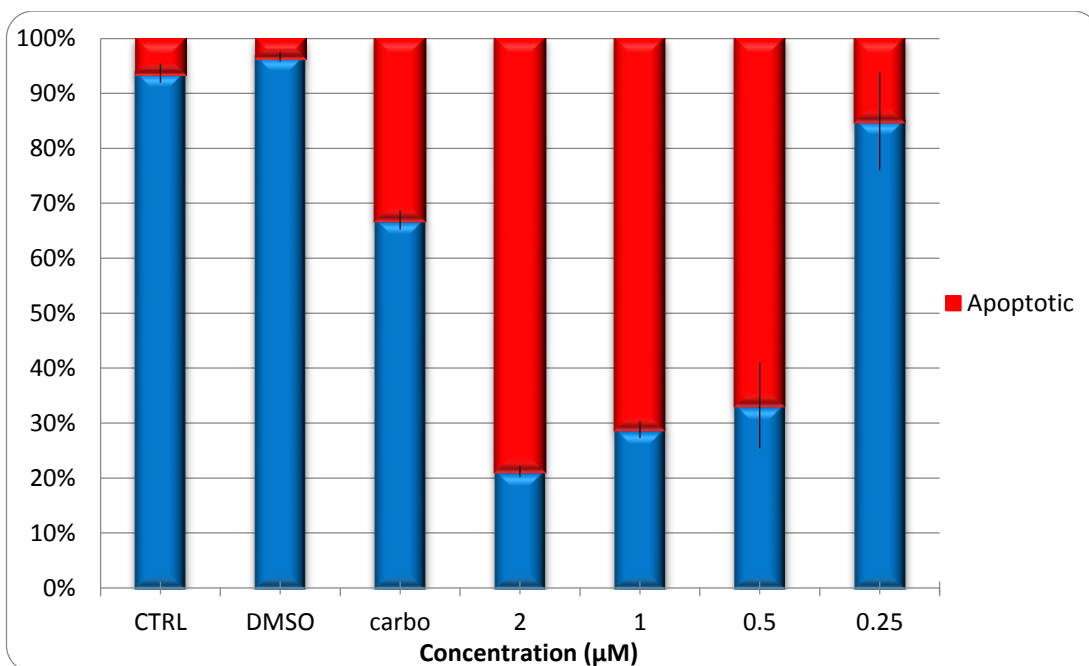


**Figure 3.5:** Graph showing apoptotic versus non apoptotic cell death in A549 cells after incubation with **100**.

In the HT144 cell line we can see similar results to the A549 cell line (figure 3.6). At concentrations from 0.5 to 2 μM cell death is occurring mainly through apoptosis with 80 % of cell death occurring due to apoptosis in the 1 and 2 μM ranges. These results further confirm the results of the cell cycle analysis and it can be seen that the *N*-(6-ferrocenyl-2-naphthoyl)-glycine-glycine esters induce cell death through apoptosis.

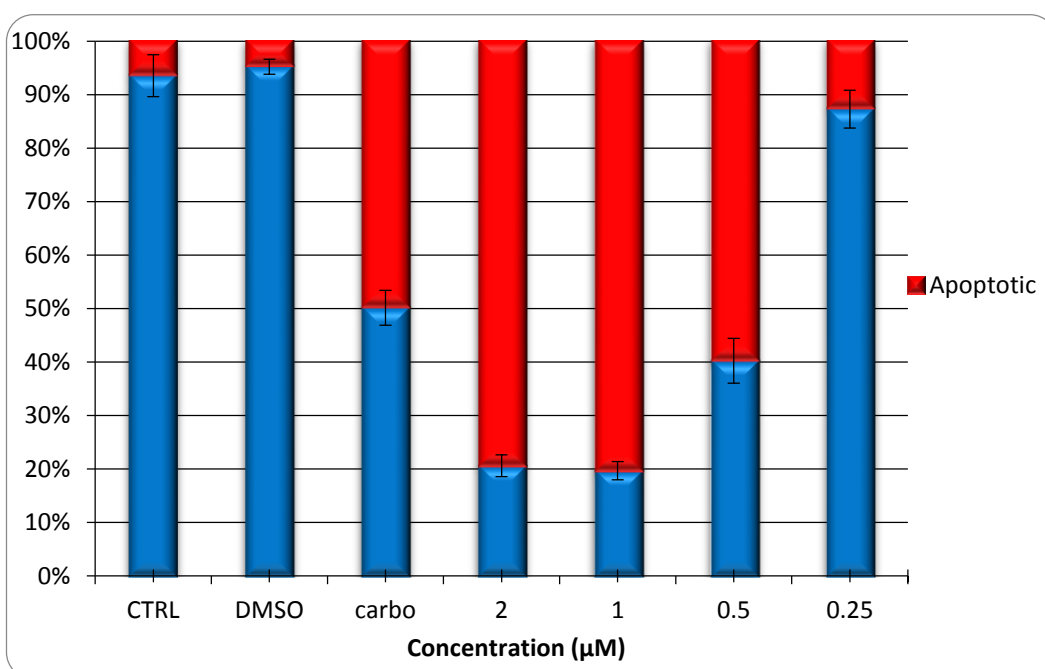


**Figure 3.6:** Graph showing apoptotic versus non apoptotic cell death in HT-144 cells after incubation with **100**.



### 3.3 Biological evaluation *N*-{*para*-(ferrocenyl)cinnamoyl} and *N*-{*para*-(ferrocenyl)benzoyl} amino acid and dipeptide derivatives.

A preliminary screen was performed for *N*-{*para*-(ferrocenyl)-benzoyl}-glycine-glycine esters and *N*-{*para*-(ferrocenyl)cinnamoyl} dipeptide ethyl esters at 10 and 1  $\mu$ M in the HT144 melanoma cell line (table 3.8). While these compounds showed some growth inhibition at 10  $\mu$ M with compounds **113**, **115**, **116**, **120** and **121** having greater than 50 % growth inhibition, none of the compounds tested showed significant growth inhibition at 1  $\mu$ M. Therefore no IC<sub>50</sub> values were determined for the *N*-{*para*-(ferrocenyl)-benzoyl}-glycine-glycine esters and *N*-{*para*-(ferrocenyl)cinnamoyl} dipeptide ethyl esters.

**Table 3.8:** % growth inhibition of compounds **109-113** and **115-117** at 10 and 1  $\mu$ M in the HT144 cell line.

HT144	Compound	% Growth 10 $\mu$ M	% Growth 1 $\mu$ M
	<b>113</b>	16.84	90.91
	<b>114</b>	74.42	86.06
	<b>115</b>	7.98	76.82
	<b>116</b>	11.40	92.9
	<b>117</b>	75.32	87.98
	<b>120</b>	14.82	66.44
	<b>121</b>	16.50	76.52
	<b>122</b>	53.53	86.96

### 3.4 Solubility studies

The aromatic portion of the ferrocenyl peptide bioconjugates make the molecule quite lipophilic. Whilst this may be useful for crossing biological membranes, it presents some problems with water solubility. For *in vitro* studies the compounds were administered dissolved in DMSO. In order to progress the biological evaluation of the ferrocenyl peptide conjugates to *in vivo* studies it was necessary to reduce the quantity of DMSO used for administration. Solubility studies were carried out for compound 100 with a selection of biological media in a ratio of 25 % DMSO to 75 % of the biological medium.

**Table 3.9:** % growth in A549 cells at 1  $\mu\text{M}$  of *N*-(6-ferrocenyl-2-naphthoyl)-glycine-glycine ethyl ester **70** using a variety of vehicles for delivery. The control group tested an equivalent amount of each vehicle without **70**.

Vehicles (25 % DMSO)	% growth	
	control	<b>70 (1 <math>\mu\text{M}</math>)</b>
80 mM Citrate Buffer	98.8 %	83.8 %
5% carboxymethyl cellulose	98.9 %	86.0 %
1 % carboxymethyl cellulose	96.8 %	60.2 %
50 % propylene glycol solution	103.1 %	96.1 %
Kolliphor EL	4.2 %	15.0 %

Compound **70** is known to have a growth inhibition of  $75.2 \pm 1.9$  % in A549 cells at 1  $\mu\text{M}$ . Kolliphor EL shows the greatest growth inhibition of the compounds tested with only 15 % growth, however the control group shows a growth inhibition of 95.8 % suggesting that the medium itself has an antiproliferative effect. Of the remaining vehicles tested 1 % carboxymethyl cellulose shows the greatest growth inhibition of 39.8 %. This is almost a 2 fold decrease in activity compared with administration in DMSO alone. This decrease in antiproliferative activity when diluted in a medium is not acceptable for the continuation of biological studies and a suitable alternative method of delivery is required.

PEGylation involves the covalent attachment of poly ethylene glycol (PEG) to another molecule. PEGylation offers improved water solubility and stability as well as reduced clearance by the kidneys leading to longer circulation time<sup>18</sup>. It has allowed the therapeutic application of molecules with limited water solubility, toxicity or a poor pharmacokinetic profile<sup>19</sup>. A PEGylated derivative of *N*-(6-ferrocenyl-2-naphthoyl)-glycine-glycine ethyl ester was prepared by Dr. Andy Harry<sup>1</sup>. It was found to be water soluble to 10 mM, however an  $\text{IC}_{50}$  value could not be obtained up to a concentration of 20  $\mu\text{M}$  in A549 cells.

### 3.5 Conclusions

The aims of this research were to extend the SAR study of the ferrocenyl peptide conjugates, to investigate the mode of action and to begin *in vivo* studies. In order to advance the project it was necessary to carry out preliminary evaluation of the new compounds synthesised.

The *N*-(6-ferrocenyl-2-naphthoyl)-glycine-glycine esters all showed excellent activity at 10  $\mu\text{M}$ . The *N*-(6-ferrocenyl-2-naphthoyl)-glycine-glycine ethyl ester **70** and the *N*-(6-ferrocenyl-2-naphthoyl)-glycine-glycine methyl ester **100** showed the greatest growth inhibition at 1  $\mu\text{M}$  and  $\text{IC}_{50}$ 's were obtained.  $\text{IC}_{50}$  values were in the range 0.2 - 0.3  $\mu\text{M}$  in all the cell lines for **100** whilst the  $\text{IC}_{50}$  values for **70** ranged from 0.5 - 0.7  $\mu\text{M}$ . **100** proved to be more active than

**70** in all the cell lines tested apart from H1299, for which the literature value is given. When tested at 1  $\mu\text{M}$ , none of the *N*-{*para*-(ferrocenyl)cinnamoyl} and *N*-{*para*-(ferrocenyl)benzoyl} amino acid and dipeptide derivatives showed significant growth inhibition and thus  $\text{IC}_{50}$ 's were not obtained.

From this it can be concluded that the naphthoyl linker is required for activity. It is likely that the extra conjugation of the system makes it a better linker than either the benzyl or the cinnamoyl linker. The loss of the bottom section of the second naphthalene ring may have introduced more flexibility into the molecule which may also have resulted in the loss of activity. Of the SAR study of the ester portion of the molecule it is apparent that an increase in ester chain length decreases the activity of the molecule. As the methyl ester is more active than the ethyl ester in 4 of the 5 cell lines with the propyl failing to significantly inhibit growth at 1  $\mu\text{M}$ , it is likely that the ester is cleaved in the cell and that the active form of the compound is actually the free acid.

Compounds were less active on normal human dermal fibroblast cells and showed a toxicity similar to cisplatin. When tested in resistant cell lines **70** showed cross resistance in both camptothecin resistant A459 cells and temozolomide resistant Malme-3M cell but **100** showed no cross resistance in the temozolomide resistant cell line suggesting it may overcome the mechanism of resistance to temozolomide in this cell line. Cell cycle analysis and TUNEL assays show that compounds induce cell death via apoptosis in both lung cancer and melanoma cell lines.

Solubility studies show that the compounds are very hydrophobic and require a high concentration of an organic solvent such as DMSO for administration. This presented considerable difficulties when preparing compounds for *in vivo* evaluation. A PEGylated derivative was prepared which increased activity, however it failed to achieve an  $\text{IC}_{50}$  value up to 20  $\mu\text{M}$ . In order to progress the biological evaluation to *in vivo* studies further modification of the compounds or optimisation of a drug delivery method or targeting system is required.

## Experimental procedures

### Cells and reagents

Growth Media and Foetal Calf Serum (FCS) were obtained from Sigma-Aldrich. Cell lines were maintained at 37 °C with 5 % CO<sub>2</sub>.

Cell Name	Source	Cell Type	Media + Additives
<b>HT144</b>	ATCC	Melanoma	RPMI + 10 % FCS
<b>Lox-IMVI</b>	NCI	Melanoma	RPMI + 10 % FCS
<b>Malme-3M</b>	NCI	Melanoma	RPMI + 10 % FCS
<b>Malme-3M-TMZ</b>	NICB Cell Bank	Temozolomide Resistant Melanoma	RPMI + 10 % FCS
<b>Sk-Mel-28</b>	NCI	Melanoma	RPMI + 10 % FCS
<b>A549</b>	ATCC	Adenocarcinoma	DMEM/Ham's F12 + 10 % FCS
<b>A549-Cpt</b>	NICB Cell Bank	Carboplatin resistant Adenocarcinoma	DMEM/Ham's F12 + 10 % FCS
<b>H1299</b>	ATCC	Non-small Cell Lung Carcinoma	RPMI + 10 % FCS + 10 mM L-Glutamine
<b>SKBR3</b>	ATCC	Breast Cancer	RPMI + 10 % FCS
<b>MDA-MB-361</b>	ATCC	Breast Cancer	RPMI + 10 % FCS
<b>NHDF</b>	Clonetics	Normal human dermal fibroblast	DMEM + 10 % FCS

### Proliferation assays

Proliferation was measured using an acid phosphatase assay.  $1 \times 10^3$  cells/well were seeded in 96-well plates, except for HT144 and Malme-3M which were seeded at  $2 \times 10^3$  cells/well. Plates were incubated overnight at 37 °C followed by addition of drug at the appropriate concentrations and incubated for a further 5 days until wells were 80 % to 90 % confluent. All media was removed and the wells were washed once with PBS (Sigma). 10 mM paranitrophenol phosphate substrate (Sigma-Aldrich) in 0.1 M sodium acetate buffer (Sigma) with 0.1 % Triton X (Sigma) pH 5.5 was added to each well and incubated at 37 °C for 2 hours. 50  $\mu$ L of 1 M NaOH (Sigma) was added and the absorbance was read at 405 nM (reference – 620 nM).

### **Cell cycle analysis**

2.5 x 10<sup>4</sup> cells were seeded per well in 24-well plates and incubated overnight at 37 °C. After 24 hours appropriate concentrations of test compound were added to the wells. Plates were then incubated at 37 °C for a further 72 hours. Media was collected and the wells washed once with PBS (Sigma). Cells were trypsinised and added to the media collected for each sample. Cells were centrifuged at 300 x g for 5 minutes and the media was aspirated. The cell pellet was re-suspended in 150 µL PBS and transferred to a round bottomed 96 well plate. The plate was centrifuged at 300 x g for 5 minutes and the supernatant aspirated leaving approximately 15 µL in each well. The remaining volume was used to resuspend the cells and 200 µL of ice cold 70 % ethanol (Fluka) was added. The plates were then stored at -20 °C for 2 hours. After fixing, the cells were centrifuged at 450 x g for 5 minutes, the supernatant removed, washed with 200 µL of PBS and centrifuged again at 450 x g. The PBS was then removed and 200 µL of Guava Cell Cycle reagent (Millipore) was added to each well. The cells were mixed by pipetting and stored at room temperature shielded from light for 30 minutes. Cells were analysed on the Guava EasyCyte (Guava Technologies).

### **TUNEL assay**

2.0 x 10<sup>4</sup> cells were seeded per well in 24-well plates and incubated overnight at 37 °C, followed by addition of test compound at the appropriate 51 concentrations. After 72 hours, media was removed and the wells washed once with PBS (Sigma). Cells were trypsinised and resuspended in 1 mL of media before being transferred to an eppendorf. Cells were centrifuged at 300 x g for 5 minutes and the medium was aspirated. The pellet was re-suspended in 150 µL of PBS and transferred to a round bottomed 96 well plate. 50 µL of 4 % para-formaldehyde (Sigma) prepared in PBS was added to the wells and mixed. Cells were incubated at 4 °C for 60 minutes. The plate was centrifuged at 300 x g for 5 minutes and the supernatant aspirated leaving approximately 15 µL in each well. The remaining volume was used to resuspend the cells and 200 µL of ice cold 70 % ethanol (Fluka) was added to the cells. The plates were then stored at -20 °C for at least 2 hours (maximum 2 weeks). After fixation, the cells including positive and negative controls (Millipore) were centrifuged at 300 x g for 5 minutes. The supernatant was aspirated, and the cells washed with 200 µL of wash buffer (Millipore) and then centrifuged again at 300 x g for 5 minutes. The wash buffer was aspirated and 25 µL of DNA labelling mix (Millipore) was added to each well and the cells mixed. The plates were covered with parafilm and incubated for 60 minutes at 37 °C. 200 µL

of rinsing buffer (Millipore) was then added to each well and the plates centrifuged at 300 x g for 5 minutes. The supernatant was aspirated and 50  $\mu$ L of anti-BrdU staining mix (Millipore) added to each well, with the plate stored in the dark at room temperature for 30 minutes. At the end of the incubation 150  $\mu$ L of rinsing buffer was added to each well. Cells were analysed on the Guava EasyCyte (Guava Technologies). Positive and negative controls were performed with each assay.

### **Statistical analysis**

IC<sub>50</sub> values were calculated using CalcuSyn Software (BioSoft). Student t-test (two tailed with unequal variance) was used to compare the activity of test compounds to their corresponding control group.

## References

- 
- <sup>1</sup> J. Murphy, Masters Thesis, DCU, **2014**.
  - <sup>2</sup> M. Butler, *Animal Cell Technology*, first edition, Open University press, **1987**.
  - <sup>3</sup> I. R. Freshney, *Culture of animal cells*, sixth edition, Wiley-Blackwell, **2011**.
  - <sup>4</sup> M. Clynes, *Animal Cell Culture Technique*, first edition, Springer, **1998**.
  - <sup>5</sup> A. Martin, Ph.D Thesis, DCU, **1992**.
  - <sup>6</sup> R. H. Shoemaker, *Nature Cancer Reviews*, **2006**, 6, 813-823.
  - <sup>7</sup> A. Martin, M. Clynes, *In Vitro Cellular and Developmental Biology*, **1991**, 27A (3), 183-184.
  - <sup>8</sup> A. Mooney, R. Tiedt, T. Maghoub, N. O'Donovan, J. Crown, B. White, P. T. M. Kenny, *Journal of Medicinal Chemistry*, **2012**, 55 (11), 5455-5466.
  - <sup>9</sup> J. T. Hartmann, H. P. Lipp, *Expert Opinions in Pharmacotherapy*, **2003**, 4(6), 889-901.
  - <sup>10</sup> E. Cvitkovic, *Cancer Treatment Reviews*, **1998**, 24, 265-281.
  - <sup>11</sup> D. J. Stewart, *Critical Reviews in Oncology/Haematology*, **2007**, 63, 12-31.
  - <sup>12</sup> B. Koberle, M. T. Tomicic, S. Usanova, B. Kaina, *Biochimica et Biophysica Acta*, **2010**, 1806, 172-182.
  - <sup>13</sup> P. Saikumar, Z. Dong, V. Mikhailov, M. Denton, J. M. Weinberg, M. A. Venkatachalam, *American Journal of Medicine*, **1999**, 107, 489-506.
  - <sup>14</sup> J. M. Matés, J. A. Segura, F. J. Alonso, J. Márquez, *Archives of Toxicology*, **2012**, 86(11), 1649-1665.
  - <sup>15</sup> M. M. Martinez, D. R. Reif, D. Pappas, *Analytical Methods*, **2010**, 2, 996-1004.
  - <sup>16</sup> A. Negoescu, P. Lorimier, F. Labat-Moleur, C. Drouet, C. Robert, C. Guillermet, C. Brambilla, E. Brambilla, *Journal of Histochemistry and Cytochemistry*, **1996**, 44(9), 959-968.
  - <sup>17</sup> A. Negoescu, C. Guillermet, P. Lorimier, E. Brambilla, F. Labat-Moleur, *Biomedical Pharmacotherapy*, **1998**, 52(6), 252-258.
  - <sup>18</sup> I. W. Hamley, *Biomacromolecules*, **2014**, 15, 1543- 1549.
  - <sup>19</sup> G. Pasut, F. M. Veronese, *Journal of Controlled Release*, **2012**, 161 (2), 461 – 472.

## Chapter 4

### Mode of action studies and drug targeting

#### 4.1 Introduction

The structure activity relationship of the ferrocenyl bioconjugates has been extensively studied. Corry *et al.* investigated the effect of the substitution pattern on the benzene ring and of modifying the peptide chain<sup>1, 2</sup>, while Mooney *et al.* investigated the effect of replacement of the benzoyl ring with a naphthoyl linker<sup>3, 4, 5</sup>. Harry *et al.* investigated the introduction of an ethynyl spacer and substitution of the cyclopentadienyl ring<sup>6, 7</sup>. Recent work has extended the SAR study to include modification of the ester portion of the molecule. A structure has been obtained which shows a high toxicity *in vitro*. The *N*-(6-ferrocenyl-2-naphthoyl)-glycine-glycine methyl ester has been found to have an excellent activity with IC<sub>50</sub> values of 0.2 ± 0.03 µM in A459 and 0.3 ± 0.04 µM in H1299 lung cancer cells, 0.2 ± 0.06 µM in LOX-IMVI, 0.3 ± 0.05 µM in Mal-Me and 0.2 ± 0.02 µM in HT144 melanoma cells.

Further work on the ferrocenyl bioconjugates will require the transition of biological testing from *in vitro* to *in vivo* models. The *in vitro* biological evaluation carried out on the *N*-(6-ferrocenyl-2-naphthoyl)-glycine-glycine esters has highlighted two key areas for the development of this class of compounds.

Firstly, further investigation of the mode of action of these compounds is required. The biological evaluation discussed in chapter 3 has shown that the *N*-(6-ferrocenyl-2-naphthoyl)-glycine-glycine esters generate DNA damage causing cell death and confirmed that this cell death is apoptotic. However to date it has not been confirmed how this DNA damage is generated. One potential mode of action for these compounds is DNA intercalation. Ethidium bromide displacement assays were carried out to determine if this was a possible mechanism for the generation of DNA damage. It has been proposed that the compounds may cause DNA damage by the generation of reactive oxygen species. To further elucidate the mode of action of these compounds a high performance liquid chromatographic (HPLC) study of guanine oxidation has been undertaken to investigate the generation of ROS.



Secondly, biological evaluation has highlighted that the compounds limited water solubility presents a barrier to the further study of this class of compounds by *in vivo* studies. As a considerable amount of structure optimisation has been undertaken, a method of increasing the compounds water solubility without dramatically altering the structure of the compounds is highly desirable. A system whereby the limited water solubility is overcome by attaching the compound to a targeting molecule is proposed. This may also increase the specificity of the drug while allowing greater accumulation in cancer tissues.

#### **4.1.1 Cancer Cells**

Cancer cells are formed when normal cells lose the regulatory mechanisms which control their growth and multiplication. Several genetic faults can lead to cancer such as the activation of oncogenes and the suppression of antioncogenes Proto-oncogenes code for proteins which are involved in cell division and differentiation. When these become mutated and the cell becomes cancerous they are referred to as oncogenes. When DNA becomes damaged certain proteins detect the damage and block DNA replication until the damage is repaired. If it cannot be repaired the cell undergoes apoptosis. Tumour suppressor genes or antioncogenes code for these proteins. If a gene becomes damaged and the defects are replicated, the chances of a cell becoming cancerous are increased. Hanahan and Weinberg<sup>8,9</sup> identify 6 biological capabilities acquired by tumour cells as the hallmarks of cancer; self sufficiency in growth signals, insensitivity to growth inhibitory signals, evasion of apoptosis, the development of cell immortality, sustained angiogenesis and the ability to metastasise.

#### **4.1.2. The cell cycle**

The cell cycle consists of four phases; G<sub>1</sub>, S, G<sub>2</sub> and M phase (figure 4.1)<sup>10</sup>. During G<sub>1</sub> (gap 1) the cell is growing in size and preparing to replicate its DNA. During S phase, synthesis occurs and DNA is replicated. After this the cell enters the second gap phase, G<sub>2</sub>. Here it prepares itself for division. Copied DNA is checked and any damaged copies are repaired. During M phase mitosis occurs and the cell divides to produce two daughter cells each with a full set of chromosomes. From here the cells either enter G<sub>1</sub> again or go to G<sub>0</sub>, a dormant phase.

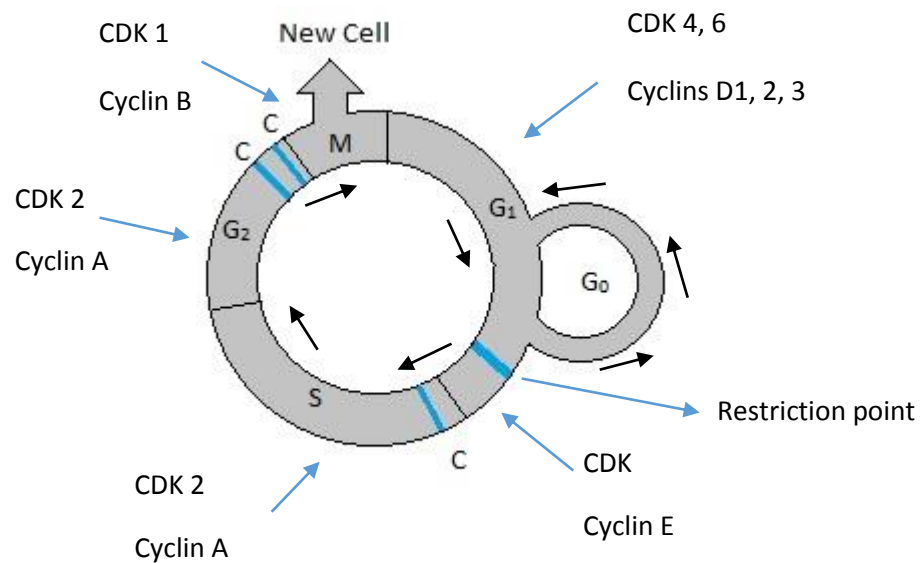


**Figure 4.1:** The cell cycle.

There are various points during the cell cycle at which a decision is made whether to advance to the next phase. The restriction point frequently becomes abnormal in tumour cells. There are also several checkpoints at the start of S phase and the end of G<sub>2</sub> where DNA is checked and either repaired or the cell undergoes apoptosis. These can also be defective in tumour cells.

Cell cycle control is regulated by proteins called cyclins and enzymes called cyclin dependant kinases (CDKs). Binding of a cyclin with its CDK advances the cell from one stage to the next. Cell cycle progression is controlled by sequential activation of cyclins and CDKs and is inhibited by CDK inhibitors. Restraining proteins are present which can modify the effect of cyclins including p15 and p16. These block the activity of cyclin D-CDK complex. P21 which is controlled by p53 monitors the health of the cell and DNA integrity.

#### 4.1.3. Abnormal signalling pathways

The decision for a cell to grow and divide depends on signals it receives from surrounding cells, the most important of which come from hormones called growth factors. Most cancers suffer from a defect in the signalling pathway which instructs for the transcription

of the proteins and enzymes required for growth and division. Many cancers are capable of producing their own growth factors whilst other cancers can produce abnormal receptors which are always switched on without the need for growth factors. Receptors may also be overexpressed making the cell sensitive to low levels of growth factors. External hormones counter the effects of growth factors and signal the inhibition of cell growth and division. An insensitivity to these can also increase the risk of a cell becoming cancerous.

#### **4.1.4. Apoptosis**

There are both intrinsic and extrinsic pathways for apoptosis. The intrinsic pathway can be triggered by DNA damage from exposure to chemicals, drugs or oxidative stress. When the cell detects increased levels of damage it increases the production of tumour suppressor protein p53. At sufficient levels it will trigger apoptosis<sup>11</sup>.

Extrinsic factors such as a lack of growth factors or hormones may cause apoptosis. Death activator proteins may also bind to cell membrane proteins called tumour necrosis factor receptors (TNF-R) which triggers apoptosis. It may also be triggered by T-lymphocytes. When they detect damaged cells they inject the cell with an enzyme called granzyme which initiates apoptosis. Metastatic cancer cells have undergone genetic changes which allow them to avoid this process.

#### **4.1.5. Cell immortality**

The lifetime of normal cells is determined by the number of times their DNA can divide; usually 50-60 divisions. Cancer cells may become 'immortal' with no limit to the number of times they can divide. This is due to the structure of chromatin. The telomere is a polynucleotide region at the 3' end of a chromosome. It contains several thousand repeats of a short 6 base sequence. About 50 to 100 bases are lost from the telomere during each replication because DNA polymerase is unable to completely replicate the ends. Eventually the telomere becomes too short to function and the DNA becomes unstable triggering apoptosis. Cancer cells produce an enzyme called telomerase which allows them to break free of this restriction and become immortal. Telomerase has the ability to add hexagonal nucleotide repeats on to the end of DNA and thus maintain its length. It is expressed in over 90 % of human cancers<sup>12</sup>.

#### **4.1.6. Angiogenesis**

As cancer cells grow they need a supply of nutrients, hormones and growth factors from the blood to continue to grow and divide. Almost all cells are located within 100  $\mu\text{m}$  of a capillary blood vessel. As a cancer grows its cells become further and further from the blood supply resulting in a lack of resources and a lack of oxygen, particularly in tumours. Hypoxia occurs when there is not enough oxygen to supply the tissue. Hypoxia-inducible factors (HIF) are produced and upregulate the release of vascular endothelial growth factor (VEGF) and fibroblast growth factor (FGF-2). These stimulate nearby blood vessels to divide leading to the branching of capillaries known as angiogenesis. The chance of metastasis is increased because the newly developing endothelial cells may release proteins such as interleukin-6 which stimulate metastasis. Blood vessels which result from angiogenesis are abnormal, dilated, leaky, disorganised in structure with excessive branching and erratic blood flow<sup>13</sup>.

#### **4.1.7. Metastasis**

Malignant cancers are dangerous because they have developed the ability to break away from the tumour and enter the circulation allowing them to develop anywhere in the body. Normal cells have cell adhesion molecules on their surface which ensure that they adhere to similar cells and the extracellular matrix. Molecules called integrins are involved in the anchoring process. When a cell becomes detached apoptosis is triggered. Metastasised cancer cells are missing cell adhesion molecules, they do not undergo apoptosis on detachment and have the ability to attach to the extracellular matrix in other parts of the body.

### **4.2. DNA binding assays**

#### **4.2.1. Targeting DNA**

Many important drugs target nucleic acids, especially in the fields of anticancer and antibacterial therapy. DNA is known to be the cellular target for many cytotoxic anticancer agents and understanding how drugs interact with DNA is currently an active research area. Targeting DNA affects protein interaction with DNA and can cause inhibition of transcription and replication and DNA repair processes. Many of the anticancer chemotherapeutic drugs that are used today are DNA damaging agents. Targeting of DNA

has been shown to cause relatively potent and selective destruction of tumour cells. The clinical potential of DNA damaging agents is limited by their adverse side effects while their genotoxicity increases the tendency for the formation of secondary cancers.

DNA present in the body takes the form of a double helix. Each strand is composed of the four nucleosides adenine (A), thymine (T), guanine (G) and cytosine (C) attached to a deoxyribose sugar and a phosphate backbone. Within each strand nucleotides are joined by phosphodiester linkages and the strands are held together by hydrogen bonds. Adenine forms 2 hydrogen bonds with thymine, while cytosine forms 3 hydrogen bonds with guanine (figure 4.2). The region where the two strands are close to each other is called the minor groove and is deep and narrow, while the region where the strands are far apart is called the major groove and is shallow and wide.

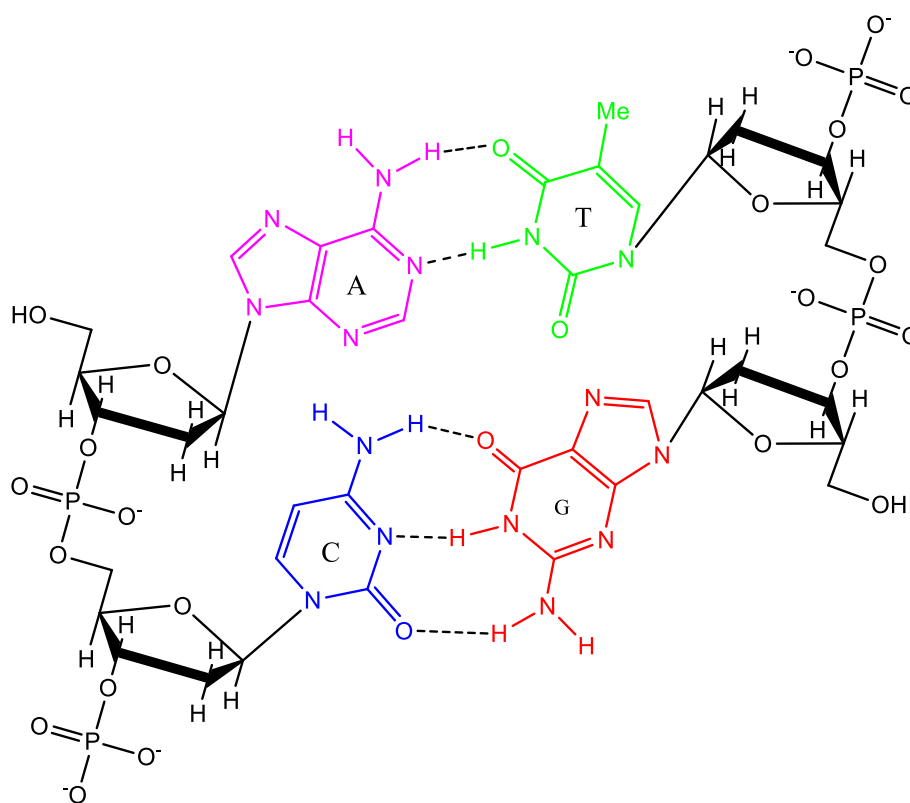


**Figure 4.2:** Structure of DNA illustrating bonding within the molecule.

#### 4.2.2 DNA binding.

Most anticancer drugs currently used exert their antitumour effect through either covalent or non-covalent binding with DNA. DNA binding agents can be classified by the type of

interactions they have with DNA. This includes covalent binding and non-covalent binding. Alkylating agents such as cisplatin **22** bind covalently with DNA. Non covalent bonding results in a reversible interaction with nucleic acids. Non covalent interactions interrupt replication and transcription and lead to cell death. There are six potential modes for non-covalent interaction with the DNA strand<sup>14</sup>. These are 1; intercalation with DNA bases in the major groove, 2; intercalation with DNA bases in the minor groove, 3; threading intercalation interactions, 4; interactions with the DNA major groove, 5; interactions with the DNA minor groove and 6; electrostatic interactions with the anionic sugar phosphate backbone of DNA. These can be broadly classed as either intercalators, groove binders and more recently backbone binders. Strong interactions fall into two categories; intercalation and hydrogen bonding interactions in the DNA grooves. While most compounds display specificity for either groove binding or intercalation some compounds can exhibit both modes.

#### 4.2.2.1 Classical DNA intercalators

Classical intercalators contain planar aromatic or heteroaromatic features which insert between neighbouring base pairs of the DNA double helix and bind through  $\pi$  stacking<sup>15</sup>. DNA base pairs form the top and bottom intercalation sites. This type of intercalator includes ethidium bromide **133**, proflavine **134** and benzopyrene **135** (figure 4.3). This mode of DNA binding was first proposed by Lerman in 1961<sup>16</sup> to explain the strong interaction with DNA of aromatic dyes such as acridine.

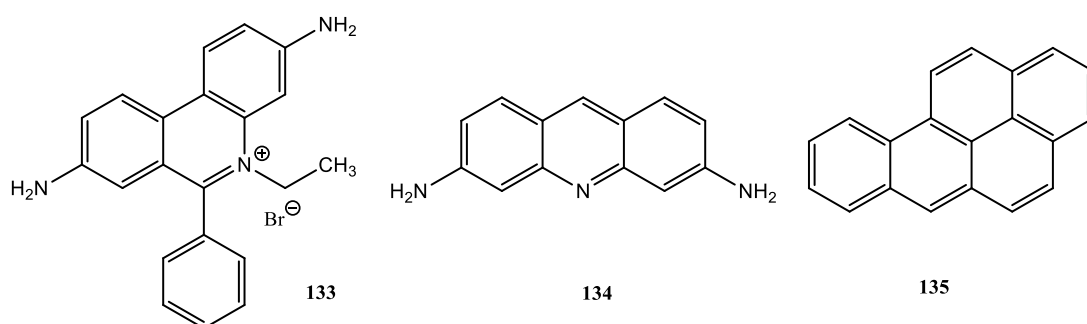


**Figure 4.3:** Classical intercalators; ethidium bromide **133**, proflavine **134**, benzopyrene **135**.

Ethidium bromide **133** is an intercalator which also functions as a fluorescent tag. On binding to DNA it fluoresces orange intensely under UV light. When unbound its fluorescence is quenched by molecules of water which are removed upon binding with the

hydrophobic DNA. Proflavine **134** is an antibacterial compound of the class of aminoacridines. It was used in WWI and WWII to treat deep surface wounds. Proflavine is completely ionised at pH7 and interacts with bacterial DNA. It interacts with base pairs through van der Waals interactions and aminium cations form ionic bonds with the negatively charged phosphate groups on the backbone<sup>10</sup>. Benzopyrene **135** is a component of burnt foods and cigarette smoke.

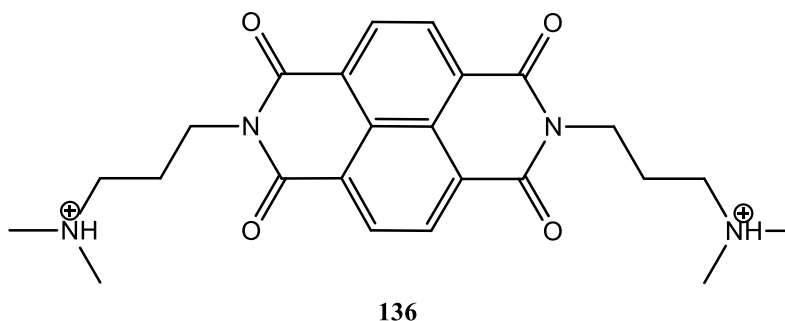
Intercalation is known to occur without breaking hydrogen bonds between base pairs and obeys the nearest neighbour exclusion principle; when DNA is saturated with intercalators, every second potential intercalation site on the DNA helix remains vacant. In order for intercalation to occur the DNA base pairs separate 3.4 Å to form a cavity for the incoming planar ligand. Localised left handed unwinding of the DNA sequence occurs. The ethidium cation unwinds DNA by about 26° while the proflavine cation unwinds it by 17°<sup>14</sup>. Intercalation lengthens, widens, stiffens and unwinds the DNA. This results in unwinding of the DNA and distortion of the conformation of the DNA backbone. It therefore interrupts the DNA protein interaction and results in frameshift mutations.

Intercalation is considered to be the result of hydrophobic interaction. The hydrophobic aromatic molecule is drawn to the hydrophobic environment of the base pairs away from the hydrophilic aqueous environment. Intercalation complexes are stabilised by frontier orbital interactions between the lowest unoccupied molecular orbital (LUMO) of the intercalator and the highest occupied molecular orbital (HOMO) of the adjacent purine bases<sup>17</sup>. An increase in complex stability is seen when the aromatic intercalator is a cation. Computational studies on proflavine indicate that the positive charge causes a lowering in the energy of the LUMO energy of the ligand, favouring the interaction with the HOMO of the DNA bases<sup>18</sup>. Classical intercalators may also contain ionised groups which interact with the phosphate backbone.

The extended planar aromatic system is usually required for a potential drug to act as a successful intercalator. With less extended systems intercalation can be prevented through the clashing of the ancillary ligands with the phosphodiester backbone. This may result in only partial intercalation.

#### 4.2.2.2 Threading intercalators

Threading intercalators usually have two side chains on opposite sides of a planar aromatic system. The aromatic system is inserted between the base pairs while one cationic substituent binds with the major groove and one with the minor. A threading intercalator occupies and interacts strongly with both the major and minor grooves of DNA simultaneously. Interactions of the side chains with the major and minor grooves add to the stability of the complex. An example of this is naphthalene diimide **136**<sup>14</sup>.



#### 4.2.2.3 Groove binders

While intercalators insert between DNA bases, groove binding agents bind to either the major or minor grooves of DNA. Groove binders must have flexible structures and the distortion caused is smaller than that caused by classical intercalators (figure 4.4).



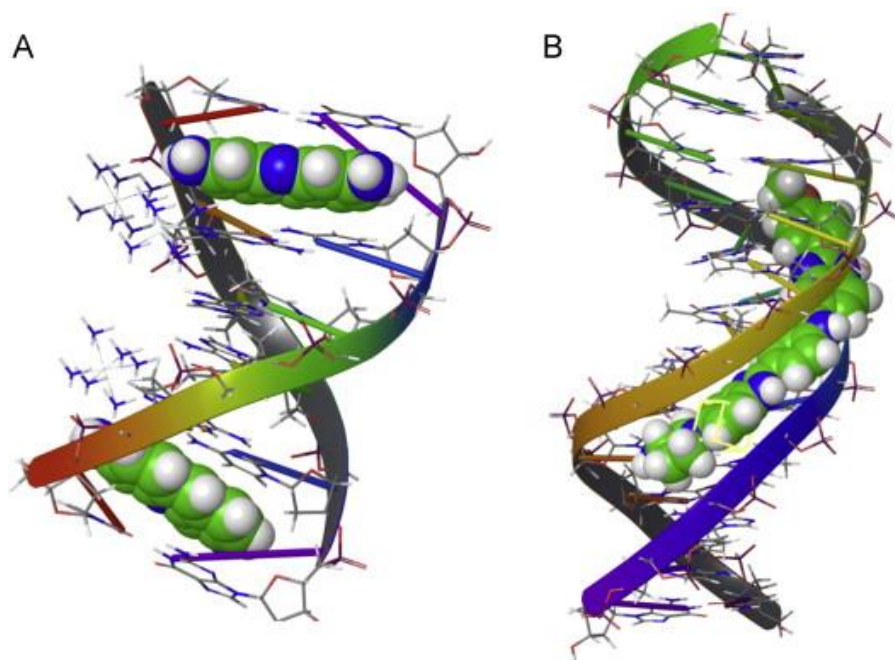


**Figure 4.4:** Classical intercalation of proflavine between base pairs of DNA (A) and groove binding of the minor groove of DNA by a tris-benzimidazole drug (B)<sup>19</sup>.

The environment of each of the grooves differ. The major grooves have multiple interaction sites and a stronger binding ability for guest molecules. It is 11.6 Å wide and 8.5 Å deep and offers easy access to bulky molecules. The minor grooves are smaller in size with a depth of 8.2 Å and have less binding sites. As most drug molecules are small molecules this is the main binding site.

Some compounds bind to the minor groove by van der Waals interactions and hydrogen bonding interactions. Minor groove binding drugs typically have several aromatic rings such as pyrrole, furan or benzene connected by bonds possessing torsional freedom. They are usually narrow curved shaped (figure 4.5).

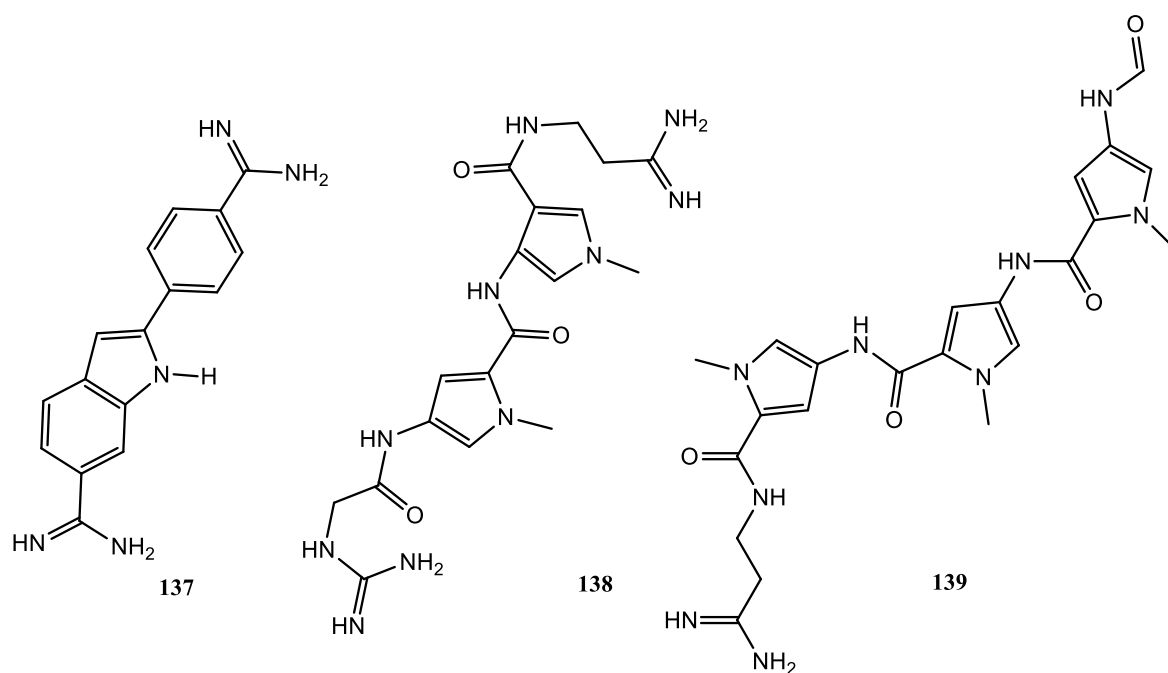
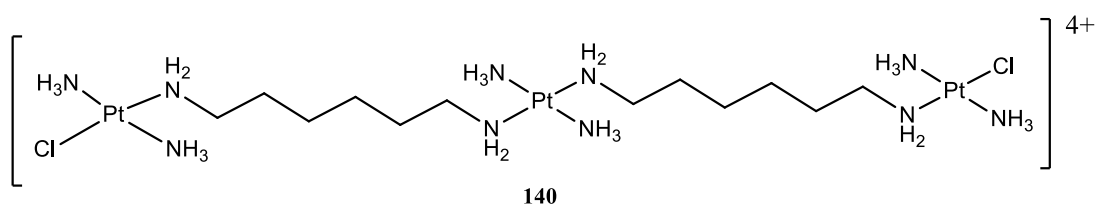


**Figure 4.5:** Groove binders; dapi **137**, netropsin **138** and dystamycin **139**.

#### 4.2.2.4 Electrostatic backbone binders

The stability of folded DNA requires interaction with metal cations such as  $Mg^{2+}$  or  $Na^+$  from solution. Interaction of organic cationic molecules with DNA neutralises the phosphate charges. These charge interactions depend on the salt concentration of the solution. At physiological pH they are weak for molecules without intercalating or groove bonding modes. It does have an impact on the binding energy of highly charged molecules such as proteins.



Drugs operating via this type of interaction are among the most recently discovered<sup>20</sup>. Triplatin NC **140** has three cationic platinum (II) centres and hydrogen bonding functionalities linked by flexible hydrophobic segments. It does not intercalate nor bind either groove. It binds to the phosphate oxygen atoms and associates with the backbone. It forms a bidentate NH-O-NH complex known as a 'phosphate clamp' with DNA through

hydrogen bonding. It displays both ‘backbone tracking’ and ‘groove spanning’ forms of binding (figure 4.6). It has been shown to have micromolar *in vitro* activity in human ovarian cancer cells<sup>21</sup> and *in vivo* activity against ovarian carcinoma xenografts.

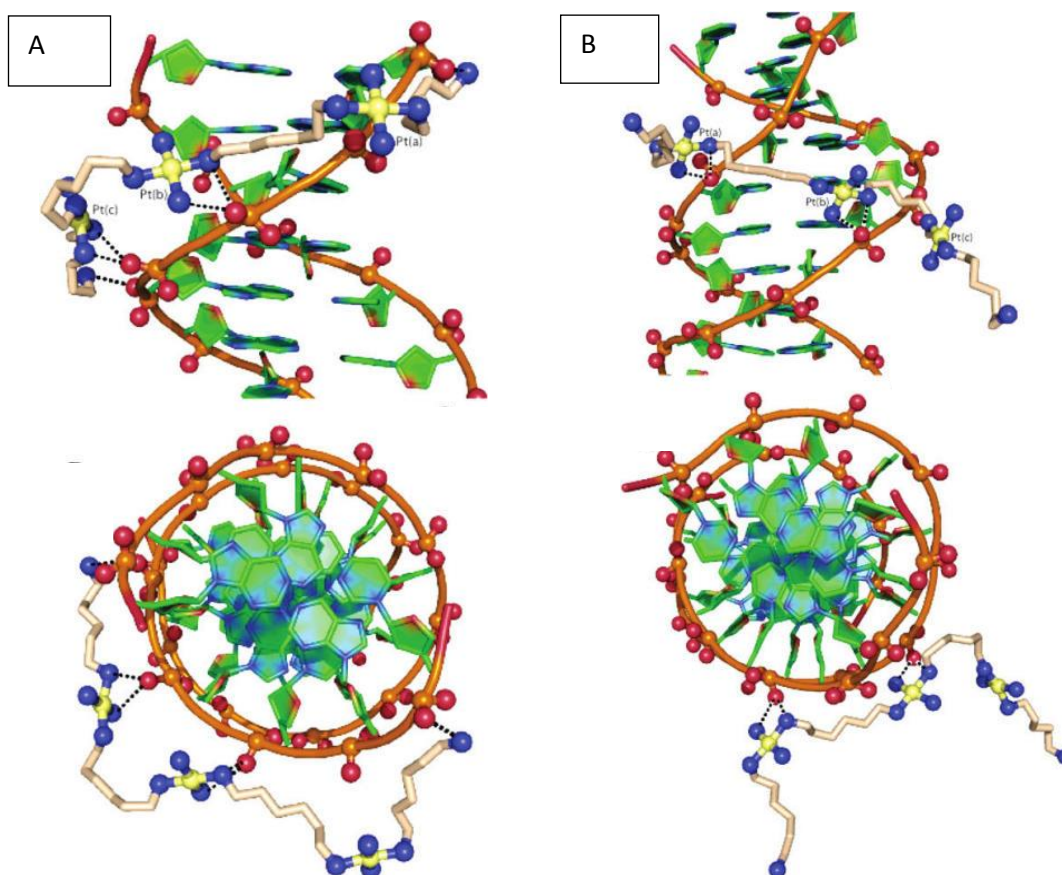


**Figure 4.6:** Interaction of Triplatin NC **140** with the phosphate backbone of DNA. A; ‘backbone tracking’ and B; ‘groove spanning’ modes. Views perpendicular to the helix and along the helix are shown.

#### 4.2.2.5 Metallointercalators

The covalent attachment of organic intercalators to transition metal complexes produces metallointercalators which may interact with DNA in a novel way that could affect biological activity<sup>22</sup>. Metal complexes with  $\delta$  bonded ligands with aromatic side arms as intercalators or organometallic complexes with  $\pi$  bonded arenes as intercalators can have dual functions. Where the aromatic side arms or arene ligands can intercalate between DNA bases while the metal coordinates directly to a DNA base. Metal complexes with sigma

bonded side arms can act by both binding to DNA via metal coordination and through intercalation of the attached ligand. Metallointercalators have been shown to act by intercalation or insertion. While metallointercalators unwind the DNA and insert their planar ligands between the DNA bases, metalloinserters eject the DNA bases of a single base pair and their planar ligand acts as a  $\pi$  stacking replacement for the base pair.

#### 4.2.3 *N*-(6-ferrocenyl-2-naphthoyl) amino acid and dipeptide esters as potential intercalating agents.

Sartorius and Schneider investigated the intercalation potential of 38 small molecule ligands based on benzene, naphthalene and quinolone with double stranded calf thymus DNA<sup>23</sup>. Naphthalene shaped ligands showed similar affinities regardless of the presence of nitrogen atoms or charges within the aromatic system. It was shown that quinolinium and naphthalene derivatives only intercalate if they bear a positively charged side chain and had similar binding constants. Amide functions were insufficient to enable naphthalene intercalation. They found no evidence for non-classical intercalation by partial insertion and no intercalation of phenyl units occurs unless forced to by other binding units.

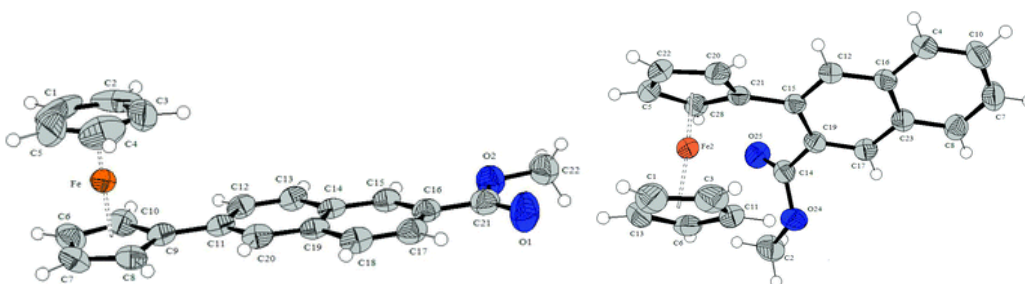


**Figure 4.7:** The *N*-(6-ferrocenyl-2-naphthoyl) derivatives adopt a planar conformation<sup>4</sup>, while the *N*-(3-ferrocenyl-2-naphthoyl) derivatives are forced to adopt a strained conformation due to steric hinderance.

The methyl-6-ferrocenylnaphthalene-2-carboxylate **82** (figure 4.7) was shown to have a planar conformation with similar results observed for the *N*-{*para*-(ferrocenyl) benzoyl} derivatives<sup>24</sup>. The methyl-3-ferrocenylnaphthalene-2-carboxylate however, is forced out of the plane with ferrocene and is accompanied by a corresponding decrease in activity. While the planar conformation of these drugs is desirable for intercalation, it is possible that they may not undergo classical or threading intercalation. Despite this, the affinity of

naphthalene for DNA is quite possible through groove binding interactions or other interactions with DNA.

A potential method for investigating the DNA binding capacity of ferrocenyl bioconjugates is the ethidium bromide fluorescing quenching assay. Fluorescence enhancement or quenching can be observed upon interaction of ethidium bromide with nucleic acids. A simple method for an ethidium bromide fluorescence quenching assay has been reported in the literature<sup>25</sup>. Calf thymus DNA (ctDNA) is treated with ethidium bromide which fluoresces on binding to DNA. Upon displacement of ethidium bromide by the reagent under investigation a decrease in fluorescence is observed corresponding to the amount of bound intercalator. An Ethidium bromide/Hoecht 33258 competitive binding assay can be used to determine the preference for intercalation versus groove binding.

### **4.3. Redox modulation in cancer therapy.**

#### **4.3.1 Reactive oxygen species (ROS).**

Reactive oxygen species (ROS) are constantly generated in living organisms; as by-products of respiration in the mitochondria, through redox cycling involving Fenton reactions by heavy metals, exposure to chemotherapeutic agents, transition metals and chemical oxidants. They are also produced by macrophages and neutrophils at the sites of infection and inflammation. In normal cells they are required for cell signalling before elimination. ROS include the superoxide anion ( $O_2^-$ ), hydrogen peroxide ( $H_2O_2$ ), the hydroxyl radical ( $OH^\bullet$ ) and ozone ( $O_3$ ). Accumulation of ROS within the cell can lead to oxidative stress.

The first factors in the defence against ROS are antioxidants. Natural antioxidants are the cells defence mechanism to scavenge radical species. Endogenous antioxidants include glutathione (GSH), enzymatic superoxide dismutase (SOD), catalase (CAT), glutathione peroxidases (GPXs), thioredoxins (TRX) and peroxiredoxins (PRXs). Other antioxidants such as ascorbic acid (vitamin C), tocopherol (vitamin E),  $\beta$ -carotene (vitamin A) and polyphenol metabolites may be obtained from the diet.

The damaging effects of these ROS on the cell depends on both their intracellular concentration and the levels of endogenous antioxidant species within the cell. Oxidative stress is implicated in a number of human diseases such as neurodegenerative diseases,

inflammatory diseases, cardiovascular disease, allergies, immune system dysfunction, diabetes, aging and cancer.

#### **4.3.2 Oxidative stress and cancer**

Cancer cells have an accelerated metabolism and thus require higher ROS concentrations to function. Cancer cells exhibit increased intrinsic ROS stress due to oncogenic stimulation, increased metabolic activity, and mitochondrial malfunction. When the balance between the oxidant and antioxidant species is lost, accumulation of ROS occurs and the cell is subjected to oxidative stress. This may lead to the damage of intracellular species including DNA, RNA and proteins.

This balance may be manipulated in cancer therapy. Targeting the redox chemistry of the cell has been suggested as potentially an effective strategy<sup>26</sup>. In order to exploit the higher level of oxidative stress in cancer cells both antioxidant and prooxidant therapy have been employed<sup>27</sup>.

A large number of metal anticancer agents have a potential redox arm to their mechanism of action. Combination therapy in conjunction with redox modulators could increase anti-cancer activity and potentially lower the dosage of metal complexes required.

#### **4.3.3. Antioxidant therapy**

Antioxidants are the cellular mechanism of defence against oxidative stress and ROS. They modulate redox homeostasis within the cell. Dietary antioxidants have been shown to have a protective effect against cancer development. Treatment with antioxidants has been shown to be effective in combating tumour cells *in vitro* however they have had little clinical success as a standalone therapy<sup>28</sup>. Antioxidants have however been used in combination with chemotherapy to reduce harmful side effects of chemotherapeutic agents. It was believed that antioxidant treatment would negatively impact treatment with chemotherapy and radiotherapy however they have been shown in some cases to have a synergistic effect<sup>29</sup>.

#### **4.3.4 Prooxidant therapy**

Although oxidative stress leads to tumour formation, it can also increase the sensitivity to treatment. Cancer cells may adapt to the higher concentration of ROS by upregulating

detoxification enzymes. Therefore in order to be effective a cancer treatment must increase the ROS concentration past a threshold that is incompatible with cell viability.

A crucial problem to be solved for the treatment of cancer with ROS is how to target ROS production selectively in cancer tissues. The mitochondrial respiratory chain is a major source of ROS generation in cells and mitochondrial DNA is particularly vulnerable to ROS mediated damage. During oxidative phosphorylation electrons are passed through the mitochondrial complexes and a proton gradient is established across the inner mitochondrial membrane as an energy source for respiration. When electrons escape from the electron transport chain they can react with oxygen to form superoxide. In this manner superoxide is continuously generated and can react to form  $H_2O_2$  and other ROS. Mitochondria are therefore considered the major source of cellular ROS. Under normal conditions these are regulated by a system of antioxidants.

Overproduction of cellular ROS or a reduction in the ability of the cell to eliminate them can result in oxidative stress. This can cause significant cellular damage such as lipid peroxidation, oxidative DNA modifications, protein oxidation and enzyme inactivation. Accumulation of ROS in cancer cells may exhaust the capacity of antioxidant defences. Because normal cells have lower levels of ROS stress they have a greater capacity to cope with increased levels of oxidative stress than cancer cells. It is therefore possible to use agents which generate ROS and cause ROS accumulation to preferentially kill cancer cells. Strategies to kill cancer cell through ROS induction can include either direct exposure to ROS generating agents, inhibition of antioxidant enzymes or a combination of both.

#### **4.3.4.1. Agents that generate ROS.**

Many currently used, well established, anticancer agents have been shown to cause increased cellular ROS generation in addition to their primary mechanism of action, including arsenic trioxide  $As_2O_3$  (ATO) , cisplatin, oxaliplatin, 5-fluorouracil and paclitaxel.

Arsenic trioxide is currently used in the treatment of acute promyelocytic leukaemia and has been shown to generate ROS through hindering mitochondrial electron transport and increasing superoxide radical generation in human leukaemia cells<sup>30</sup>.

While cisplatin activity has been attributed to its ability to alkylate DNA it has also been shown to cause increased intracellular ROS<sup>31</sup>. Only 1 % of intravenously administered cisplatin has been shown to reach the nucleus<sup>32</sup>. Up to 60 % is thought to react with GSH. Both GSH and cisplatin-GSH adducts may inhibit selenoenzyme thioredoxin reductase (TrxR), which has NADPH binding sites. Cisplatin also alters mitochondrial function, depleting NADPH which may increase OH• and O<sub>2</sub><sup>-</sup>. Depleted levels of GSH have also been shown to increase cisplatin induced apoptosis<sup>33</sup>.

5-fluorouracil and oxaliplatin have been linked to ROS production. In a study of patients with colorectal cancer, patients were treated with 5-fluorouracil and oxaliplatin in combination therapy. Generation of oxidative stress was measured by urinary excretion of 8-oxo-7,8-dihydro-2-deoxyguanosine (8-oxodG) and 8 oxoguanine. It was found that treatment elevated levels by around 15 %<sup>34</sup>.

Similarly paclitaxel has been shown to have some ROS mediated activity. It was found that ROS generated by paclitaxel accumulate outside of the cell while intracellular levels remain unchanged. This causes a cytotoxic bystander effect whereby surrounding cells which have not been exposed to paclitaxel itself are damaged. This has also been shown to occur for other microtubule agents such as vincristine and taxotere<sup>35</sup>.

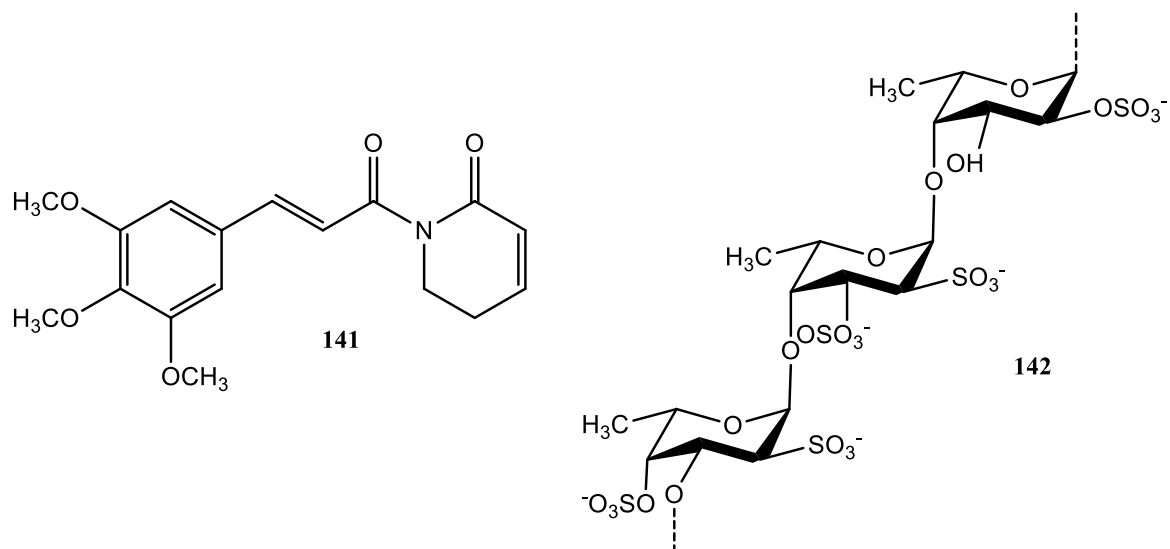
Similarly ROS have been shown to play a role in mediating apoptosis many other chemotherapeutic agents including anthracyclins such as daunorubicin<sup>36</sup> and doxorubicin<sup>37</sup>, bleomycin<sup>38</sup>, synthetic retinoids<sup>39</sup>, bortezomib<sup>40</sup>, dithiophene<sup>41</sup> and irradiation<sup>42</sup>.

Among compounds still in development piperlongumine **141**, a recently patented small molecule which has been shown to selectively kill cancer cells through the generation of oxidative stress, production of ROS and generation of apoptosis has been extensively studied in preclinical studies<sup>43</sup>. It is believed to generate ROS selectively in cancer cells over normal cells by acting on oxidative stress response enzymes which are unregulated in cancer cells.

Fucoidan **142** is a molecule extracted mainly from brown seaweed. It is a polysaccharide with L-fucose and sulphate ester groups and a number of variant structures have been identified including that extracted from *F. vesiculosus*<sup>44</sup>. It has recently been shown to have



some ROS activity<sup>45</sup>. Fucoidan was shown to increase ROS production in a MCF-7 cells and induce apoptosis by an ROS dependant mechanism.

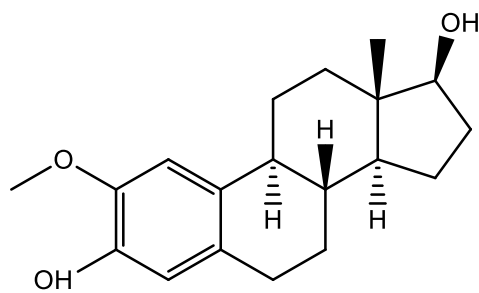


#### 4.3.4.2 Agents that inhibit antioxidants.

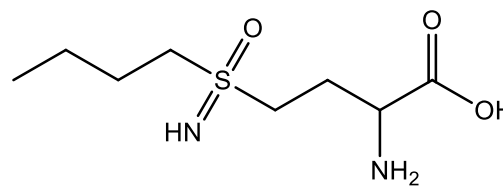
Antioxidant inhibitors were proposed in 1998 by Kong and Lillehei<sup>46</sup>. Treatment with antioxidant inhibitors can increase in the potency of a drug when co administered and thus reduce the dosage required. This reduction of the dose required may be beneficial in that it also results in a reduction of the associated side effects. Administration of an antioxidant inhibitor may also help to overcome drug resistance by resensitising resistant cells.

Arsenic trioxide, as well as generating ROS can inhibit glutathione peroxidase resulting in increased  $H_2O_2$ . In a study on human prostate cancer cells in combination with IR it has been shown to generate an increased level of ROS compared to either treatment alone<sup>47</sup>.

2-Methoxy estradiol (2-ME) **143** causes accumulation of ROS by inhibition of super oxide dismutase SOD. It is a natural metabolite of estradiol and has undergone several phase two clinical trials. It has been tested in hormone resistant prostate cancer<sup>48, 49</sup> has been tested alone and in combination with sunitinib against renal cell carcinoma<sup>50</sup> and been used in combination with bevacizumab against metastatic carcinoid tumours<sup>51</sup>. It has however had mixed results, with some studies showing low response rate and some toxicity. Further analogues are still undergoing development.



143



144

Buthionine sulfoximine (BSO) **144** inhibits the synthesis of  $\gamma$ -glutamylcystine, a precursor of BSO, which decreases the level of glutathione (GSH) produced. It has been shown to reduce intracellular GSH levels *in vitro* and *in vivo* and has been shown to increase the sensitivity of cancer cells to chemotherapeutic agents which rely on GSH detoxification.

Recently it has been demonstrated to increase the potency of organometallic ruthenium, iridium and osmium complexes in A2780 human ovarian cancer cells when co-incubated by up to 16 fold. Dependence on concentration was shown to be nonlinear with concentrations above an optimum dose showing no further improvement<sup>26</sup>. When used alone in high concentrations it has been shown to increase ROS to the point of inducing apoptosis<sup>52</sup> however at high concentrations it can deactivate certain anticancer drugs such as paclitaxel<sup>53</sup>.

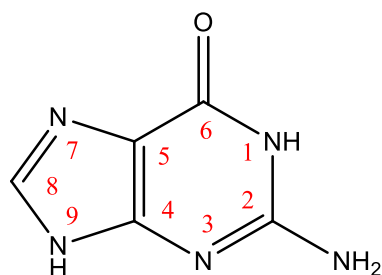
It has been shown to sensitize HL-60 and NB4 cells to ATO and it has been used in phase I clinical trials in combination with melphalan<sup>54</sup>.

#### 4.3.5 Oxidative DNA damage.

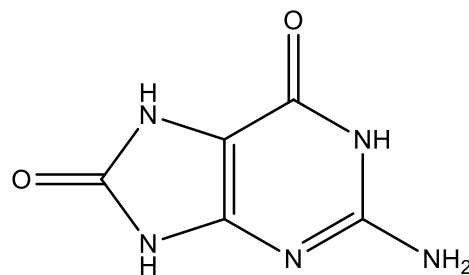
DNA may be damaged by spontaneous reactions such as hydrolysis, by products of metabolism such as reactive oxygen and nitrogen species or by exogenous chemical and physical agents. Types of DNA damage produced include double and single strand breaks, mismatches, inter or intrastrand crosslinks as well as chemical modifications to the bases or sugar moieties. The cellular response to oxidative DNA damage may include DNA repair, cell cycle arrest and apoptosis.

Guanine **145** has the lowest oxidation potential of the four bases and is thus the most easily damaged. When the cell is exposed to oxidative stress DNA damage is often

generated in the form of 7, 8-dihydro-8-oxo-guanine (8-oxoguanine) **146**. It is considered to be the clinical biomarker for oxidative stress<sup>55</sup>. Guanine may be oxidised at the C4, C5 or C8 position. At the C4 or C5 position, a radical 4 or 5 hydroxyguanine species is formed which readily reforms guanine. The C8 position, however, gives G-8OH which can undergo further oxidation to 8-oxoguanine. 8-Oxoguanine has a carbonyl group on the C8 carbon and a hydrogen atom on the N7 position. 8-oxoguanine has a lower oxidation potential and can be further oxidised.



**145**



**146**

When present during DNA replication 8-oxoguanine on the replicating strand results in frequent incorporation of adenine in the opposite strand (figure 4.8). This results in C:G to A:T transversion mutations which are one of the most common mutation in lung, breast, ovarian , gastric, and colorectal cancers. In one small cell lung cancer cell line C:G to A:T transversion mutations were identified as 34 % of all somatic mutations present<sup>56</sup>. It was also identified as the second most prevalent mutation in melanoma cells<sup>57</sup>.

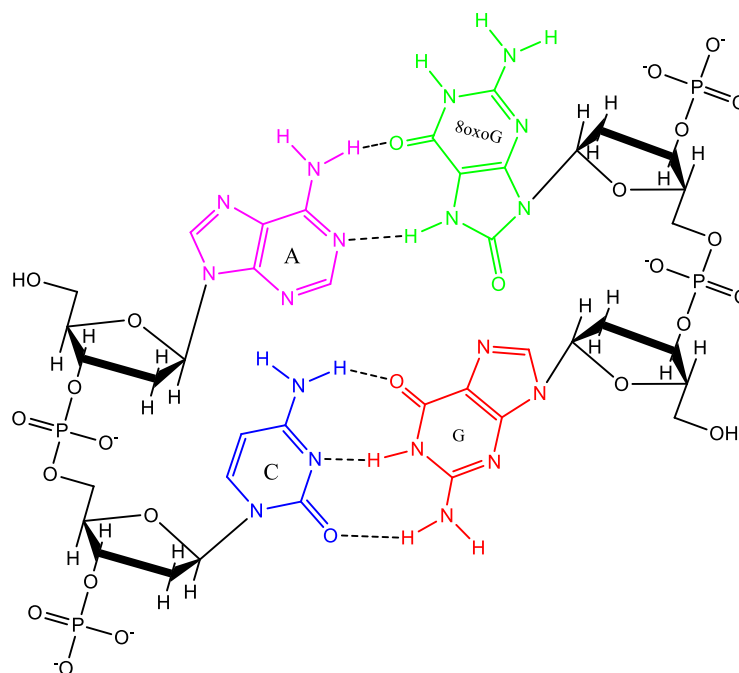


**Figure 4.8:** Structure of 8-oxoguanine incorporated opposite adenine in DNA strand<sup>58</sup>.

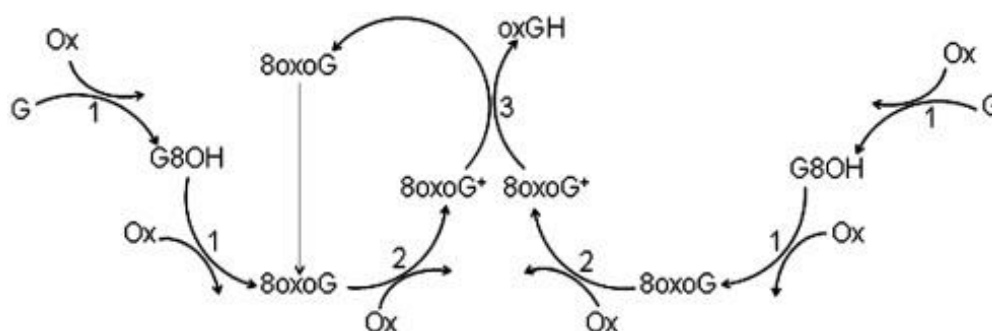
Guanine may be oxidised to 8-oxoguanine *in vivo* by hydroxyl radicals generated through Fenton chemistry within the cell. The majority of iron in the body is bound in either haemoglobin or myoglobin where the metal is responsible for the binding and release of oxygen. Its most important property is the ability to redox cycle under physiological conditions. However, as it may also generate free hydroxyl radicals, it must always be tightly bound in a non-redox form by proteins such as ferritin or transferrin when being stored or transported<sup>59</sup>. Neither  $O_2^-$  nor  $H_2O_2$  are strongly oxidising agents and they can react with few cellular components, however, when they come into contact with labile iron a Fenton type reaction may occur generating hydroxyl radicals (equation 4.1).  $H_2O_2$  is generated from  $O_2^-$  by SOD. A hydroxyl radical is formed when iron reacts with  $H_2O_2$ . It is a very strong oxidising agent and reacts rapidly near the site of formation.  $H_2O_2$  can diffuse through biological membranes in the cell and easily reach nuclear DNA.



The rate of formation of 8-oxoguanine from free guanine **125** and DNA using Fenton chemistry was previously studied<sup>60</sup>. It was shown that 8-oxoguanine **126** was produced from Fenton reagent in oscillating concentrations. As it was not formed in a linear fashion

increasing over time, it is likely that many reactions may be occurring simultaneously and that 8-oxoguanine is consumed and regenerated. This was attributed to a complex mechanism involving further oxidation. As 8-oxoguanine has a lower oxidation potential than guanine it is highly susceptible to further oxidation. Since the 8-oxoguanine is eventually consumed it was proposed that it is only an intermediate in the oxidation of guanine.

In a similar study nickel (II) catalysed oxidative damage to guanine and DNA was measured by HPLC-UV-EC<sup>61</sup> giving a similar oxidation profile. A simplified mechanism (Scheme 4.1) was proposed based on the mass spectrometric analysis of further known oxidation products of guanine, however the exact pathway has not been fully elucidated yet and the products generated may be pH dependant. Oxidation of guanine to 8-oxoguanine occurs through a two step oxidation. Further oxidation gives a highly reactive 8oxoG<sup>+</sup> moiety, two molecules of which react to give oxidised guandinohydantoin (oxGH) and regenerate 8-oxoguanine (scheme 4.1).



**Scheme 4.1:** Proposed mechanism for the generation of an 8-oxoguanine from guanine<sup>61</sup>.

Iron mediated further oxidation of DNA bases and nucleosides has previously been studied. Oxidised guandinohydantoin (Gh<sup>ox</sup>) and spiroiminodihydantoin (Sp) were found to be the major products of iron mediated 8-oxoguanine and 8-oxo-7,8-dihydro-2-deoxyguanosine (8oxodG) oxidation respectively with oxaluric acid being a minor product<sup>62</sup>. It was proposed that the ROS generated by the iron reactions are not responsible for the initiation of 8-oxoguanine oxidation, rather metal complexation to 8-oxoguanine occurs generating the reactive intermediate 8oxoGua<sup>++</sup>. Followed by the addition of H<sub>2</sub>O<sub>2</sub> this gives Gh<sup>ox</sup> or Sp in the case of 8oxodG. It was found that levels of these more stable oxidation products

remained almost constant over a 96 hour period with only minor further oxidation products detected.

Among the best currently available methods for the determination of oxidative DNA damage is high performance liquid chromatography with electrochemical detection (HPLC-EC). It generates very low levels of artifactual oxidation and is qualitative and sensitive<sup>63</sup>. The electrochemical method of detection is carried out with a flow through an EC cell –the eluent and sample flow through a small area close to auxiliary and working electrodes (figure 4.9). Analysis is carried out at a constant potential with the current measured as a function of time. Guanine and 8-oxoguanine can both theoretically be detected by UV detection however UV cannot detect levels of 8-oxoguanine at the concentrations found in biological samples. 8-Oxoguanine can therefore be selectively detected by electrochemical detection using a voltage at which only 8-oxoguanine is oxidised at the electrode. This is easily achieved due to 8-oxoguanine having a lower oxidation potential than guanine.

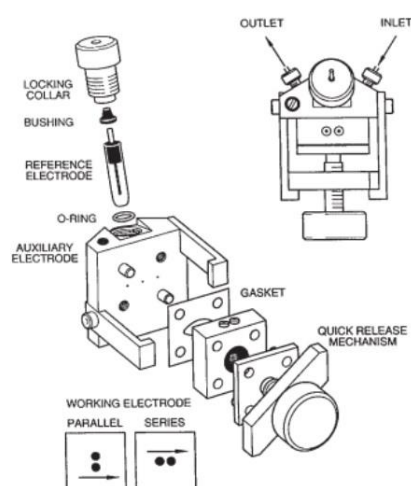


**Figure 4.9:** ECD schematic reproduced from the handbook of electrochemistry<sup>64</sup>.

#### 4.3.6 Guanine oxidation studies

Redox modulation by has been proposed as a potentially effective method in the treatment of cancer offering multiple targets and selectivity over normal cells. Significant research has been carried out on the redox chemistry of metal anticancer complexes in the treatment of cancer<sup>26</sup>. The generation of ROS by many commonly used chemotherapy agents can be

seen to generate DNA damage and induce apoptosis, which likely contributes to their cytotoxic effect in addition to their established mode of action.

A potential mechanism by which ferrocenyl peptide conjugates may exert their cytotoxicity is through oxidative DNA damage by the generation of Fenton reaction induced ROS. Ferricenium salts have been shown to produce hydroxyl radicals and cause oxidative DNA damage<sup>65</sup>. Given that ferrocene has the ability to undergo a one electron oxidation at biological potentials to the ferricenium ion and that ferricenium salts have been shown to exhibit anti tumour activity, it seems a logical strategy to investigate the ability of ferrocenyl peptide conjugates to generate oxidative DNA damage.

#### **4.3.6.1 *N*-(ferrocenylmethylamino acid) fluorinated benzene carboxamide derivatives.**

As part of the extended SAR study of ferrocenyl bioconjugates a series of *N*-(ferrocenylmethylamino acid) fluorinated benzene carboxamide derivatives were synthesised by Butler *et al.* concurrently with the *N*-(6-ferrocenyl-2-naphthoyl) dipeptide esters<sup>66</sup>. This was a continuation of research carried out by Kelly *et al.* who prepared a series of *N*-(ferrocenylmethyl)-fluorinated benzene carboxamide derivatives. Fluorinated benzene carboxamides were prepared by condensation of ferrocenyl methylamine with the corresponding fluorinated benzene carboxmides. The substitution pattern of fluorine was varied using 2-fluoro, 3-fluoro, 4-fluoro, 2- and 6-fluoro and 2-, 3-, 4-, 5- and 6-fluorobenzoic acids. The compounds were tested against MDA-MB-435-SF estrogen receptor positive breast cancer cells<sup>67</sup>. IC<sub>50</sub> values were obtained for selected compounds. The most active compound was *N*-(ferrocenylmethyl)-4-fluorobenzene carboxamide with an IC<sub>50</sub> value in the range of 11-14 μM.

Similarly to the *N*-(6-ferrocenyl-2-naphthoyl) amino acid and dipeptide esters the *N*-(ferrocenylmethylamino acid) fluorinated benzene carboxamide derivatives consist of 1; a redox active ferrocene core and 2; an amino acid linker component to interact with biological systems within the cell via hydrogen bonding. They also contain 3; a fluorinated aromatic component (figure 4.10). The incorporation of C-F bonds is a recognised strategy often employed in the development of pharmaceuticals<sup>68</sup>. The success of fluorine

substitution is evident from the large number of fluorinated drugs approved by the FDA and currently being used as anticancer, antidepressant, antiviral and anesthetic agents. There are generally two consequences of introducing fluorine into a potential drug molecule. Firstly there are the physicochemical properties. Fluorine has the ability to modulate electronic, lipophilic and steric parameters that can critically influence the pharmacological properties of a potential drug molecule. The introduction of a fluorine atom will generally increase lipophilicity, decrease basicity and alter the hydrogen bonding interactions of a molecule. Secondly, there is the influence of fluorine substitution on the biological stability through altering the metabolism of the drug molecule. In this study the position and also the number of fluorine atoms on the aromatic ring were investigated and several analogues were shown to have an anti-proliferative effect.

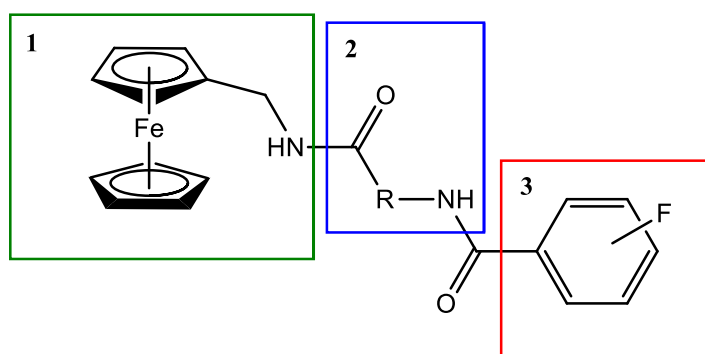
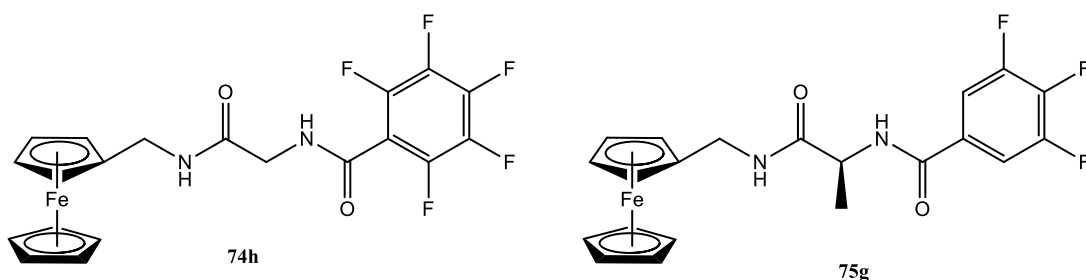


**Figure 4.10:** Structure of the *N*-(ferrocenylmethylamino acid) fluorinated benzene carboxamides.

The SAR study was extended by the introduction of amino acids and altering the number and substitution pattern of fluorine atoms on the benzene ring. Glycine, L-alanine and  $\beta$ -alanine were used as the amino acid linker and a fluorinated benzene ring with varying substitution patterns of 2-fluoro, 3-fluoro, 4-fluoro, 2- and 4-fluoro, 2- and 6-fluoro, 3- and 5-fluoro, 3,4,5-fluoro and 2,3,4,5-fluorobenzene carboxamide were used as the aromatic. All compounds were tested at 10  $\mu$ M in MCF-7 cells.  $IC_{50}$  values were obtained for selected compounds. The  $\beta$ -alanine compounds showed no activity at 10  $\mu$ M. The best activities were obtained for glycine and L-alanine derivatives which had more than one fluorine substituent on the benzene ring. The *N*-(ferrocenylmethylalanine)-3,4,5-trifluorobenzene carboxamide **75g** and *N*-(ferrocenylmethylglycine)-pentafluorobenzene carboxamide **74h**

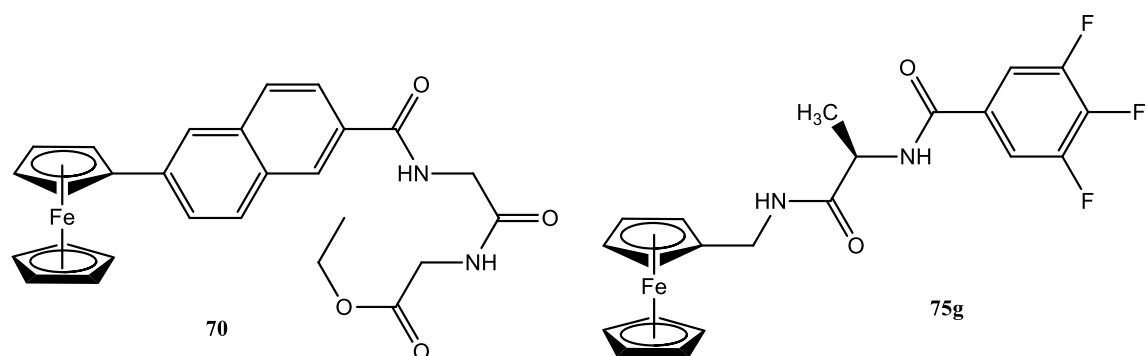


derivatives were found to be the most active with  $IC_{50}$ 's of 2.84  $\mu$ M and 10.3  $\mu$ M respectively.



#### 4.3.7 *N*-(6-ferrocenyl-2-naphthoyl)-glycine-glycine ethyl ester (**70**) and *N*-(ferrocenylmethyl-L-alanine)-3,4,5-trifluorobenzene carboxamide (**75g**) mediated DNA damage.

*N*-(6-ferrocenyl-2-naphthoyl)-glycine-glycine ethyl ester **70** and *N*-(ferrocenylmethyl-L-alanine)-3,4,5-trifluorobenzene carboxamide **75g** were selected as the most active compounds in the *N*-(ferrocenylnaphthoyl) dipeptide ester and *N*-(ferrocenylmethyl amino acid) fluorinated benzene-carboxamide series respectively. *N*-(6-ferrocenyl-2-naphthoyl)-glycine-glycine ethyl ester had an  $IC_{50}$  of 0.13  $\mu$ M in H1299 lung cancer cells and an  $IC_{50}$  of 1.10  $\mu$ M in Sk-Mel-28 melanoma cells<sup>5</sup>, while *N*-(ferrocenylmethyl-L-alanine)-3,4,5-trifluorobenzene carboxamide had an  $IC_{50}$  of 2.84  $\mu$ M in an MCF-7 breast cancer cell line<sup>66</sup>. Guanine oxidation studies were undertaken on both compounds to investigate if they could operate through this mode of action and if both series exhibited the same mode of action.



To investigate if the compounds generated Fenton reaction mediated ROS, the rate of 8-oxoguanine formation from guanine was monitored. Guanine was oxidised using either *N*-(6-ferrocenyl-2-naphthoyl)-glycine-glycine ethyl ester **70** or *N*-(ferrocenylmethyl-L-alanine)-3,4,5-trifluorobenzene carboxamide **75g** and H<sub>2</sub>O<sub>2</sub> and incubated at 37°C. Samples were taken in duplicate every 30 seconds after addition over a period of 15 minutes. Each sample was injected in triplicate and analysed by HPLC-EC using an electrochemical detector at +550mV versus Ag/AgCl. The separations were performed using the protocols previously established for the separation of DNA bases<sup>69</sup>.

The iron mediated Fenton oxidation of guanine and the kinetic profile of 8-oxoguanine formed as a result has previously been investigated, utilising FeSO<sub>4</sub> as the model iron complex<sup>62</sup>. To examine if the *N*-(6-ferrocenyl-2-naphthoyl)-glycine-glycine ethyl ester and *N*-(ferrocenylmethyl-L-alanine)-3,4,5-trifluorobenzene carboxamide induced guanine oxidation via a similar mechanism, kinetic 8-oxoguanine formation profiles were compared using both ferrocenyl conjugates and FeSO<sub>4</sub> complexes.

Control experiments were carried out utilising each of the iron complexes in the absence of peroxide, and peroxide in the absence of iron, to verify that any oxidation was Fenton mediated. Additionally, they ensured that no artifactual oxidation was occurring from the sample preparation or analysis methodology. For these experiments, deionised water was used to sequentially replace each of the reagents used. The highest background reading for these controls is plotted as the base line in figures 4.11, 4.12 and 4.13. Error bars show the standard deviation of duplicate samples injected in triplicate.

Incubation of free guanine with FeSO<sub>4</sub> and peroxide lead to oscillating concentrations of 8-oxoguanine over the incubation as previously reported. The formation is significantly higher than the control baselines, confirming the oxidation is Fenton mediated. The 8-oxoguanine concentration maxima were 1.39 μM at 6 minutes and 2.29 μM at 8.5 minutes (figure 4.11). This trend is analogous to that reported previously. These maxima occur with a different oscillation frequency, which can be attributed to differences in solution pH (previously these maxima were reported at 4 and 15 minutes respectively).

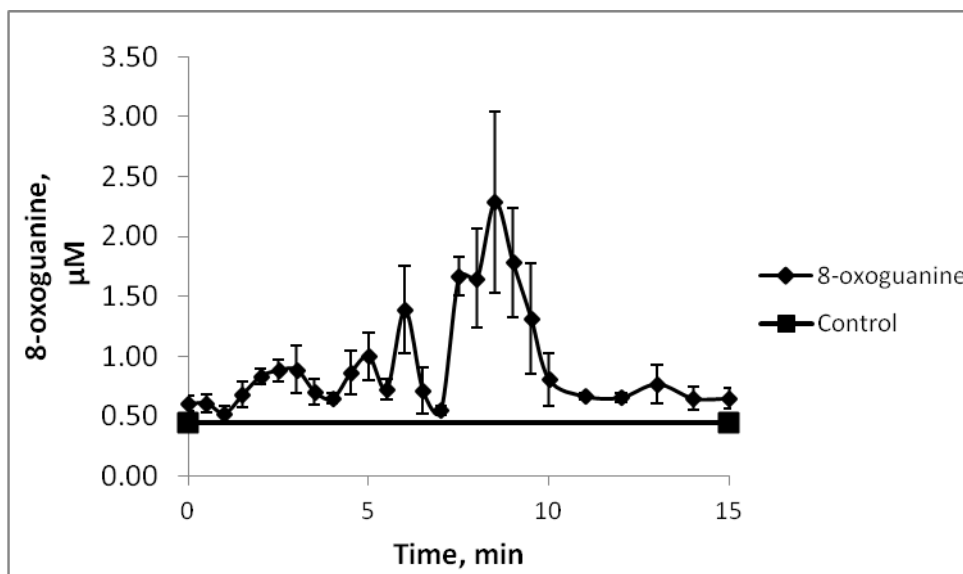


**Figure 4.11:** 8-oxoguanine concentration as a function of time after incubation of free guanine with reagents Fe(II) and H<sub>2</sub>O<sub>2</sub> at 37 °C. The mean of each of the duplicate samples injected in triplicate is taken.

Incubation of free guanine with **70** or **75g** and peroxide, which were suspected to result in Fenton mediated oxidation, also resulted in the formation of oscillating concentrations of 8-oxoguanine over the incubation period, as found with FeSO<sub>4</sub>. In both cases, the formation is significantly higher than the control baselines, clearly illustrating that both the iron complex and peroxide are required to form this concentration of 8-oxoguanine, confirming that the oxidation of guanine was Fenton mediated.

The maximum concentration of 8-oxoguanine formed using **70** was 0.62 µM and was reached after 30 seconds with a concentration of 0.56 µM at 2 minutes (figure 4.12). Following initial maxima the concentration of 8-oxoguanine decreased but continued to oscillate with concentrations increasing again towards 15 minutes.

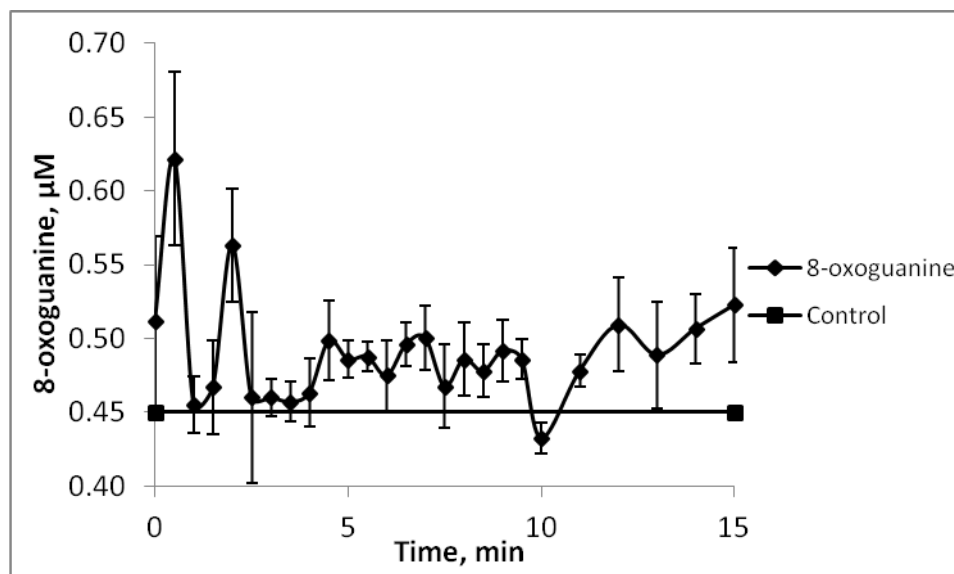


**Figure 4.12:** 8-Oxoguanine concentration as a function of time after incubation of free guanine with *N*-(6-ferrocenyl-2-naphthoyl)-glycine-glycine ethyl ester **70** and H<sub>2</sub>O<sub>2</sub> at 37 °C.

The maximum concentration of 8-oxoguanine formed using **75g** was 0.72 µM on addition of the peroxide (Figure 4.13). The oxidation profile is similar to **70**, in respect to maxima being generated almost immediately on addition of peroxide, however in the case of **75g**, after 2 minutes the concentration of 8-oxoguanine decreases but continues to oscillate for the rest of the incubation period while remaining low.

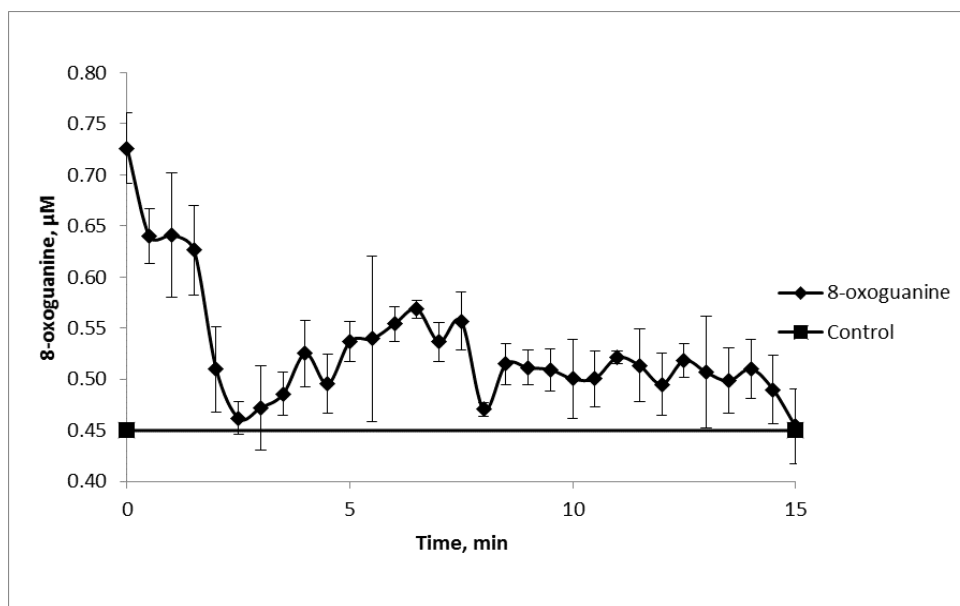


**Figure 4.13:** 8-Oxoguanine concentration as a function of time after incubation of free guanine with *N*-(ferrocenylmethyl-L-alanine)-3,4,5-trifluorobenzene carboxamide) **75g** and H<sub>2</sub>O<sub>2</sub> at 37 °C.

The concentrations of 8-oxoguanine generated by **70** and **75g** are both significantly lower than that of the FeSO<sub>4</sub>. Ferrocene may produce a weaker response than the FeSO<sub>4</sub> due to the presence of the cyclopentadienyl ligands and the size of the molecule. However the generation of 8-oxoguanine by both compounds illustrates that the oxidation is occurring by Fenton chemistry and that they are capable of generating DNA damage via a ROS mediated mechanism.

The oscillation period for 8-oxoguanine mediated by **70** and **75g** differs from that of FeSO<sub>4</sub>, however after the initial maxima, the 8-oxoguanine concentration continues to oscillate for the rest of the incubation period, with concentrations consistently higher than control levels, further confirming that oxidation is Fenton mediated.

## 4.4 Drug targeting

### 4.4.1 Introduction.

Among the problems encountered in the development of useful chemotherapeutics is a lack of specificity. Many commonly used chemotherapeutics are non-selective for cancer cells and thus a higher dose must be administered. This results in unwanted side effects and toxicity. Drug targeting gives increased specificity of delivery and therefore an

increased dose of the cytotoxic compound to the tumour relative to the rest of the body. Recently focus has switched to use of targeting molecules which are essential to the growth of the tumour. Vitamin B<sub>12</sub>, folic acid, biotin and riboflavin are essential for the division of all cells but more particularly for the growth of tumours.

Vitamin B<sub>12</sub> (cobalamin) is a complex molecule consisting of a nucleotide moiety and a planar corrin ring which contains a central cobalt (III) atom. It is an essential nutrient cofactor required for DNA synthesis. Active forms of cobalamin include methylcobalamin and adenosylcobalamin. The more stable cyanocobalamin is used in vitamin supplements and hydroxocobalamin is the most common form taken in in the diet. Both of these can be converted to the active forms *in vivo*. The use of dietary uptake pathway of B<sub>12</sub> to deliver pharmaceuticals has received attention since the 1970's with much work undertaken by Russell *et al.* in the 1990's.

Upon ingestion vitamin B<sub>12</sub> is bound by transcobalamin I which is released by salivary glands and gastric mucosa and transported to the duodenum. Pancreatic enzymes digest the transcobalamin I receptor and it is bound to intrinsic factor which facilitates transport across the intestine. It is then transported by transcobalamin II in the blood plasma and internalised by the cell by endocytosis at the transcobalamin II receptor<sup>70</sup>.

Conjugation of molecules to B<sub>12</sub> has been successful at 3 major sites: peripheral propionamide sites on the corrin ring (although the highlighted site is the only one which will not interfere with transport and binding), through the 5'-hydroxy group of the ribose unit and through the phosphate unit (figure 4.14).

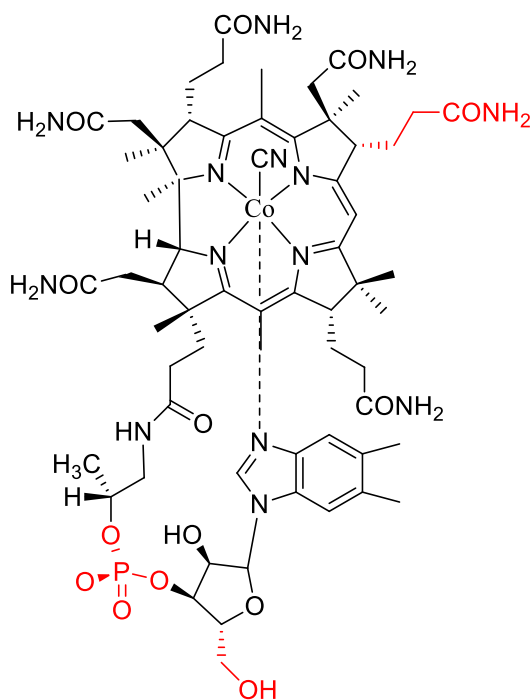


**Figure 4.14:** Location of successful conjugation sites on vitamin B<sub>12</sub> highlighted in red.

The transcobalamin receptor II has been reported to be over expressed in leukemic cells, lymphoma cells, breast, lung, bone, thyroid, colon, prostate and brain cells. The receptor is undetectable on non-dividing cells but highly expressed when cells are stimulated to divide. The degree of over expression has been shown to correlate with the stage of tumour growth with the highest found on stage IV tumours. The uptake of vitamin B<sub>12</sub> into tumours has been monitored using fluorescent labels. Most tumours have been shown to over express, however some do not. The binding of fluorinated polymers leads to rapid internalisation and accumulation to levels ranging from 2 to 30 times higher than the non-conjugated polymers.

There are two limitations of using B<sub>12</sub> as a targeting agent. Firstly the dose which can be delivered is quite small. Only one molecule of the active drug may be delivered with each molecule of vitamin B<sub>12</sub> and only a limited amount of B<sub>12</sub> can be transported into the cell before all the cellular receptors have been used up. Secondly the small size of the B<sub>12</sub>-drug complex means that it will be excreted by the kidneys. This causes the drug to be reabsorbed by the proximal tubules and accumulate in the kidney.

These limitations can be overcome by using polymer bound drug complexes which would both increase the dose of the target drug per molecule of vitamin B<sub>12</sub> and increase the size of the complex allowing exploitation of the enhanced permeability and retention (EPR) effect. The EPR effect allows spontaneous accumulation of the cytotoxic or passive targeting. In tumours the endothelial wall lining the blood vessels becomes more permeable and lymphatic drainage is poor. Large molecules loaded with a pharmaceutical agent can transport the active agent into the area with increased permeability where the active drug can be released from the carrier. The EPR effect is typically seen for large molecules of over 40 kDa in molecular weight. Small molecules are not retained and return to circulation by diffusion.

The vitamin B<sub>12</sub> delivery pathway has been extensively researched in the delivery of protein and peptide drugs as it avoids the problems of degradation in the stomach and inadequate absorption<sup>71</sup>.

The effect of targeting on the delivery of cytotoxins was investigated *in vitro* and *in vivo* using methotrexate<sup>72</sup>. The drug was linked to hydroxypropylmethacrylic acid (HPMA) and the polymer drug conjugate was modified with B<sub>12</sub>. In the case of methotrexate, it was found that the methotrexate polymer conjugate was more effective than either methotrexate alone or a direct B<sub>12</sub> conjugate of the drug. The B<sub>12</sub> drug polymer conjugate was slightly less active.

Howard *et al.* prepared a chlorambucil cobalamin derivative in 1997 to investigate the release of cobalamin conjugates by solvolysis<sup>73</sup>. This group has also worked on doxorubicin conjugates.

A cobalamin-colchicine conjugate was linked by a hydrazone linker by Bagnato *et al.* Upon uptake by the cell the linker was hydrolysed in the lysosome<sup>74</sup>. The active drug causes cell death by microtubule stabilisation. The conjugate showed preferential uptake by cancer cells and exhibited a nanomolar LC<sub>50</sub> against breast, brain and melanoma cells *in vitro*. The conjugate was found to be highly water soluble.

#### **4.4.2 Drug targeting for the *N*-(6-ferrocenyl-2-naphthoyl) dipeptide derivatives.**

Although the generation of ROS has been shown to have some specificity for cancer tissues due to elevated levels of oxidative stress, additional tumour targeting could increase



specificity of the ferrocenyl peptide conjugates. The incorporation of a molecule of vitamin B<sub>12</sub> was proposed as a potential strategy to both enhance the specificity and increase the water solubility and bioavailability of the ferrocenyl peptide conjugates. The *N*-(6-ferrocenyl-2naphthoyl) dipeptide esters have shown excellent activity *in vitro*, however their low water solubility has prevented advancement to *in vivo* studies. As rapidly dividing cells require high levels of B<sub>12</sub> for thymidine synthesis for DNA replication before cell division, cobalamin can be covalently modified to allow the attachment of various drugs without affecting the corrin ring pharmacophore which is recognised by the B<sub>12</sub> transport proteins, thus increasing uptake by the cells.

Although the incorporation of the drug candidate into a large biological molecule may reduce the quantity of active drug delivered, the quantity of active drug delivered to the target site could potentially be increased thus reducing the quantity necessary for activity. In this case a direct B<sub>12</sub>-drug conjugate was prepared in conjunction with Dr. Fabio Zobi of the University of Switzerland.

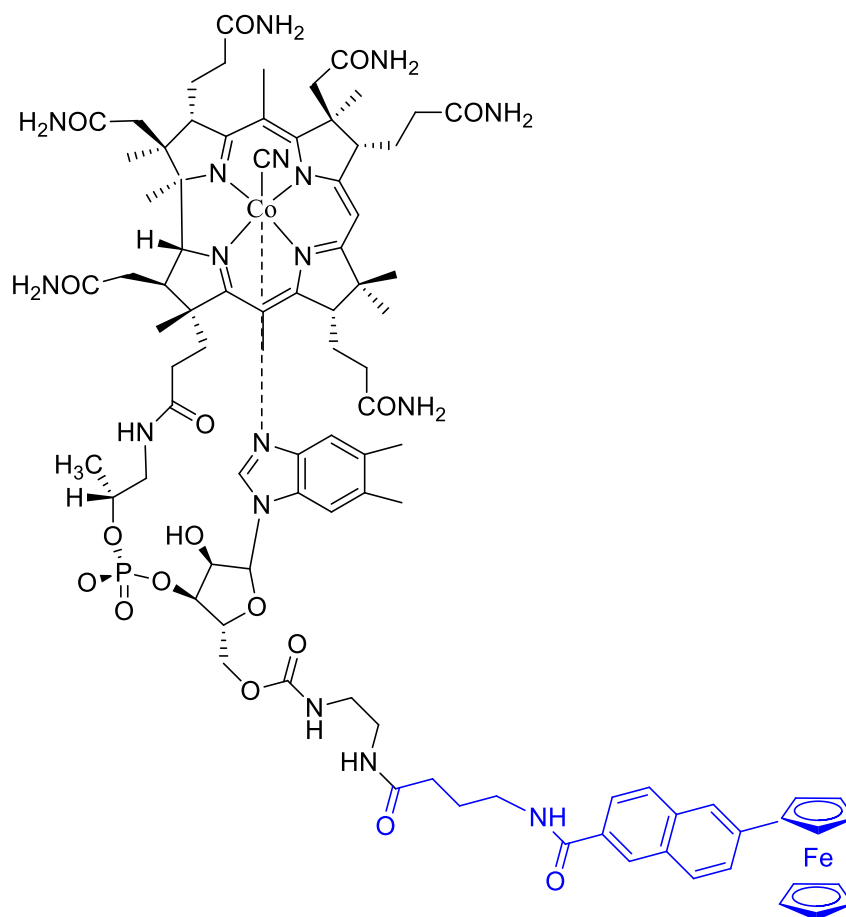


**Figure 4.15:** Structure of B<sub>12</sub>-N-(6-ferrocenyl-2-naphthoyl)- $\gamma$ -aminobutyric acid conjugate.

To date the *N*-(6-ferrocenyl-2-naphthoyl)- $\gamma$ -aminobutyric acid has been conjugated to Vitamin B<sub>12</sub> (figure 4.15). The compound was prepared in approximately 15-20 % yield via HPLC. The coupling was carried out via activation of the *N*-(6-ferrocenyl-2-naphthoyl)- $\gamma$ -aminobutyric acid with carbonyldiimidazole (CDI) and attachment to the Vitamin B<sub>12</sub> complex. The compound was identified by mass spectrometry (figure 4.16).

Further work will include coupling of other compounds including *N*-(6-ferrocenyl-2-naphthoyl)-glycine-glycine, followed by *in vitro* testing in both melanoma and lung cancer cell lines. This strategy presents a promising method for the solubilisation and targeting of this class of compounds for future potential *in vivo* studies.

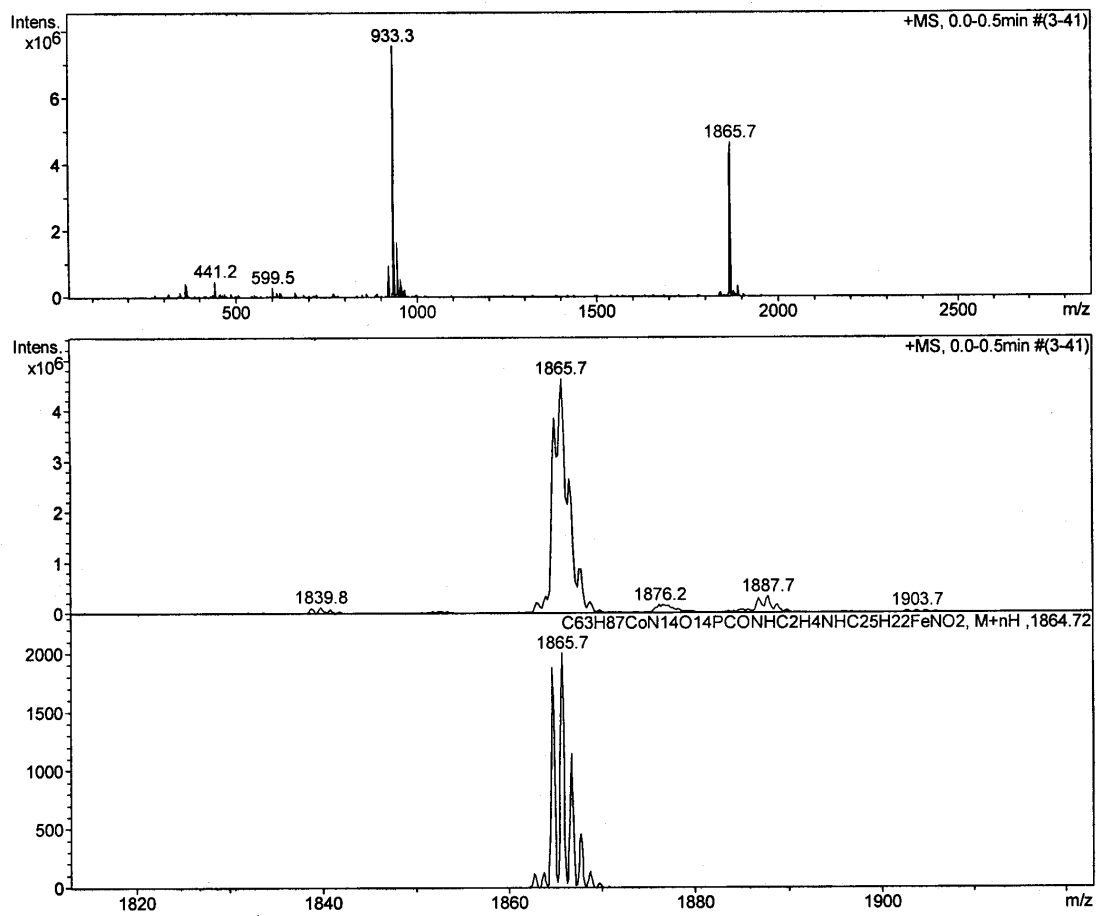


**Figure 4.16:** Mass spectrum of the B<sub>12</sub>-N-(6-ferrocenyl-2-naphthoyl)- $\gamma$ -aminobutyric acid conjugate.

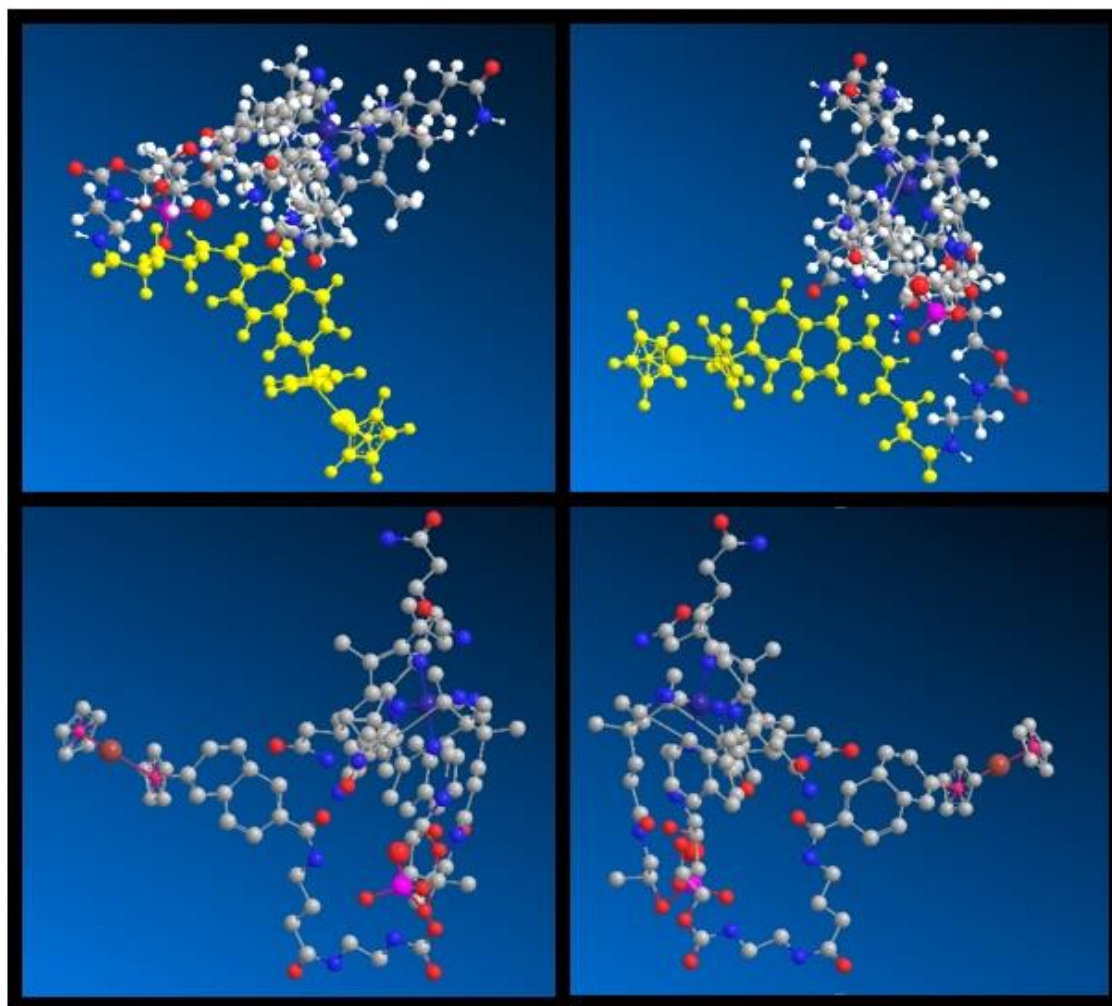


**Figure 4.17:** Chem draw 3D model of the  $B_{12}$ -*N*-(6-ferrocenyl-2-naphthoyl)- $\gamma$ -aminobutyric acid conjugate.

A chemdraw 3D model (figure 4.17) shows the  $B_{12}$ -*N*-(6-ferrocenyl-2-naphthoyl)- $\gamma$ -aminobutyric acid conjugate. The ferrocenyl moiety is exposed and should easily be able to undergo oxidation. The amino acid side chain also appears to protrude significantly from the main body of the  $B_{12}$  complex. This should allow for cleavage of the active drug by esterases or amidases in the cell.

## 4.5 Conclusions

Future work for the development of the *N*-(6-ferrocenyl-2-naphthoyl) amino acid and dipeptide esters will necessarily require the transition of biological testing from *in vitro* to *in vivo* models. This transition will require firstly an in depth understanding of how these compounds elicit their cytotoxic activity and secondly a reliable method for their delivery and uptake in cancer tissue.

We have established in chapter 3 that our compounds are capable of generating apoptosis by cell cycle analysis and TUNEL assays. One of the proposed mechanisms of action for these compounds is the generation of reactive oxygen species. In chapter 4 we have looked at the ability of these compounds to cause oxidative DNA damage via the generation of ROS as well as their potential as intercalating agents.

It is clear that the *N*-(6-ferrocenyl-2-naphthoyl) amino acid and dipeptides act through more than one mode of action. It has been proposed that the increase in conjugation when the benzoyl linker was replaced with the naphthoyl linker, lowered the oxidation potential of the ferrocene moiety, thus increasing the cytotoxicity of the molecule. However a decrease in the measured oxidation potential of these complexes is not always accompanied by an increase in cytotoxicity. It has been seen that *N*-(3-ferrocenyl-2-naphthoyl) dipeptide esters possess lower redox potentials than *N*-(6-ferrocenyl-2-naphthoyl) dipeptide esters while displaying less cytotoxicity<sup>75</sup>. Still, the oxidation potentials of both are significantly lower than those of the ferrocenyl dipeptide derivatives lacking a conjugated linker<sup>76</sup>.

It is likely that other features of these derivatives contribute to the cytotoxic activity. Classical intercalators typically possess an extended planar system and studies with naphthalene type ligands have shown that they are often poor intercalators. However, intercalation of the compounds is possible. Hydrogen bond donors and acceptors in the peptide chain could then interact with DNA bases in the centre of the helix. The bulky ferrocene core (10.5 Å) will not fit into the major groove of DNA (8.5 Å), however it is possible that the planar rings and side chain may play a part in its binding through hydrogen bonding or other non-covalent bonding with DNA. Given the low oxidation potential of these derivatives it is also possible that the ferrocene moiety in its oxidised Fe<sup>3+</sup> state could interact with the phosphate backbone. The *N*-(6-ferrocenyl-2-naphthoyl)

derivatives have been found to be planar which is desirable for DNA intercalation, whereas the *N*-(3-ferrocenyl-2-naphthoyl) derivatives which are less active are bent out of the plane with ferrocene due to the steric hindrance between the ferrocene moiety and the dipeptide chain. This loss of activity accompanied by the loss of planarity supports the currently suggested mode of action.

Thus there are at least two potential modes of action both of which could interfere with replication. These may act alone or in synergy to elicit the cytotoxic response from cancer cells. It is plausible that both intercalation and the generation of reactive oxygen species by the bound drug may occur simultaneously. Ethidium bromide displacement assays may offer a valuable insight into this potential mode of action and how the ferrocenyl bioconjugates elicit their cytotoxic activity.

A method for delivery and targeting of the *N*-(6-ferrocenyl-2-naphthoyl) amino acid and dipeptide esters has been proposed which should require minimal changes to the structure of these compounds. The incorporation of a B<sub>12</sub> conjugate represents a promising strategy to overcome the compounds water solubility issues while also offering a potential method for both targeting and increasing uptake in cancer tissues. The B<sub>12</sub> conjugate will be tested in both lung cancer and melanoma cell lines.

## Experimental Procedures

### Guanine oxidation

10 mM guanine prepared in 84 % 50 mM ammonium acetate, 85 mM acetic acid buffer and 16 % 1 M NaOH was incubated with 1 mM Iron (II) sulphate ( $\text{FeSO}_4 \cdot 6\text{H}_2\text{O}$ ) or 1 mM *N*-(6-ferrocenyl-2-naphthoyl)-glycine-glycine ethyl ester and 0.5 M hydrogen peroxide ( $\text{H}_2\text{O}_2$ ) at 37 °C with constant stirring. Aliquots of 100  $\mu\text{l}$  were taken in duplicate at various incubation times. The reaction was quenched with 1 mL cold ethanol. The solution was dried immediately under a stream of nitrogen gas. Samples were stored at -20 °C until further use. Prior to analysis they were redissolved in 1 mL 84 % 50 mM ammonium acetate, 85 mM acetic acid buffer and 16 % 1 M NaOH. Samples were injected in triplicate.

### HPLC-EC analysis of 8-oxoguanine formation

For 8-oxoguanine analysis, the HPLC System consisted of a Varian ProStar 230 solvent delivery module and a Varian ProStar 310 UV-VIS detector. A Phenomenex Onyx Monolithic C18 reversed phase column (100 x 4.6 mm) with 1 cm guard column was used. The eluent comprised 1.2 % acetonitrile (ACN), 50 mM ammonium acetate and was adjusted to pH 4.6 with glacial acetic acid. It was run at a flow rate of 4 mL  $\text{min}^{-1}$  with an injection volume of 20  $\mu\text{l}$ . The column temperature was ambient and 8-oxoguanine formation was monitored using an electrochemical detector at a detection potential of +550 mV versus an Ag/AgCl reference electrode.

### Controlled experiments

Control incubations were performed with guanine to ensure that no artificial oxidation was caused by the reaction conditions. Each of the reagents was replaced with deionised water to insure that none of them could generate oxidative damage individually.

## References

- 
- <sup>1</sup>A. J. Corry, N. O'Donovan, A. Mooney, D. O'Sullivan, D. K. Rai, P. T. M. Kenny, *Journal of Organometallic Chemistry*, **2009**, 694, 880-885.
- <sup>2</sup>A. J. Corry, A. Mooney, D. O'Sullivan, P. T. M. Kenny, *Inorganica Chimica Acta*, **2009**, 362, 2957-2961.
- <sup>3</sup>A. Mooney, A. J. Corry, D. O'Sullivan, D. K. Rai, P. T. M. Kenny, *Journal of Organometallic Chemistry*, **2009**, 694, 886-894.
- <sup>4</sup>A. Mooney, A. J. Corry, C. N. Ruairc, T. Mahgoub, D. O'Sullivan, N. O'Donovan, J. Crown, S. Varughese, S. M. Draper, D. K. Rai, P. T. M. Kenny, *Dalton Transactions*, **2010**, 39, 8228-8239.
- <sup>5</sup>A. Mooney, R. Tiedt, T. Mahgoub, N. O'Donovan, J. Crown, B. White, P. T. M. Kenny, *Journal of Medicinal Chemistry*, **2012**, 55 (11), 5455-5466.
- <sup>6</sup>A. G. Harry, J. Murphy, W. E. Butler, R. Tiedt, A. Mooney, J. C. Manton, M. T. Pryce, N. O'Donovan, N. Walsh, J. Crown, D. K. Rai, P. T. M. Kenny, *Journal of Organometallic Chemistry*, **2013**, 734, 86-92.
- <sup>7</sup>A. G. Harry, W. E. Butler, J. C. Manton, M. T. Pryce, N. O'Donovan, J. Crown, D. K. Rai, P. T. M. Kenny, *Journal of Organometallic Chemistry*, **2014**, DOI: 10.1016/j.jorganchem.2014.04.027.
- <sup>8</sup>D. Hanahan and R. A. Weinberg, *Cell*, **2000**, 100, 57-70.
- <sup>9</sup>D. Hanahan and R. A. Weinberg, *Cell*, **2011**, 144, 646-674.
- <sup>10</sup>G. L. Patrick, *An Introduction to Medicinal Chemistry*, fifth edition, Oxford university press, **2013**.
- <sup>11</sup>G. Evans and T. Littlewood, *Science*, **1998**, 281, 1317-1322.
- <sup>12</sup>M. A. Blasco, *Nature Reviews Genetics*, **2005**, 6 (8), 611-622.
- <sup>13</sup>P. Baluk, H. Hashizume and D. M. McDonald, *Current Opinion in Genetics & Development*, **2005**, 15 (1), 102-111.
- <sup>14</sup>L. Strekowski, B. Wilson, *Mutation Research*, **2007**, 623, 3-13.
- <sup>15</sup>H. K. Liu, P. J. Sadler, *Accounts of Chemical Research*, **2011**, 44 (5), 349-359.
- <sup>16</sup>L. S. Lerman, *Journal of Molecular Biology*, **1961**, 3 (1), 18-30.
- <sup>17</sup>S. E. Patterson, J. M. Coxon, L. Strekowski, *Bioorganic and Medicinal Chemistry*, **1997**, 5 (2), 277-281.



- 
- <sup>18</sup>R. Ruiz, B. Garcia, G. Ruisi, A. Silvestri, G. Barone, *Journal of Molecular Structure: THEOCHEM*, **2009**, 915 (1-3), 86-92.
- <sup>19</sup>G. Barone, A. Terenzi, A. Lauria, A. M. Almerico, J. M. Leal, N. Busto, B. García, *Coordination Chemistry Reviews*, **2013**, 257 (19-20), 2848-2862.
- <sup>20</sup>S. Komeda, T. Moulaei, K. K. Woods, M. Chikuma, N. P. Farrell, L. D. Williams, *Journal of the American Chemical Society*, **2006**, 128 (50), 16092-16103.
- <sup>21</sup>A. L. Harris, J. J. Ryan and N. Farrell, *Molecular Pharmacology*, **2006**, 69 (2), 666-672.
- <sup>22</sup>M. Sirajuddin, S. Ali, A. Badshah, *Journal of Photochemistry and Photobiology B: Biology*, **2013**, 124, 1-19.
- <sup>23</sup>J. Sartorius, H. J. Schneider, *Perkin Transactions 2*, **1997**, 11, 2319-2327.
- <sup>24</sup>D. Savage, J. F. Gallagher, Y. Ida, P. T. M. Kenny, *Inorganic Chemistry Communications*, **2002**, 5 (12), 1034-1040.
- <sup>25</sup>H. K. Liu, P. J. Sadler, *Accounts of Chemical Research*, **2011**, 44 (5), 349-359.
- <sup>26</sup>I. Romero-Canelón, P. J. Sadler, *Inorganic Chemistry*, **2013**, 52, 12276-12291.
- <sup>27</sup>V. Sosa, T. Moliné, R. Somoza, R. Paciucci, H. Kondoh, M. E. Lleonart, *Ageing Research Reviews*, **2013**, 12, 376-390.
- <sup>28</sup>M. Goodman, R. M. Bostick, O. Kucuk, D. P. Jones, *Free Radical Biology and Medicine*, **2011**, 51 (5), 1068-1084.
- <sup>29</sup>R. W. Moss, *Integrative Cancer Therapies*, **2006**, 5 (1), 63-82.
- <sup>30</sup>H. Pelicano, L. Feng, Y. Zhou, J. S. Carew, E. O. Hileman, W. Plunkett, M. J. Keating, P. Huang, *The Journal of Biological Chemistry*, **2003**, 278 (39), 37832-37839.
- <sup>31</sup>A. Miyajima, J. Nakashima, K. Yoshioka, M. Tachibana, H. Tazaki, M. Muri, *British Journal of Cancer*, **1997**, 76 (2), 206-210.
- <sup>32</sup>A. Eastman, *Biochemistry*, **1986**, 25, 3912-3915.
- <sup>33</sup>M. E. Rodriguez-Garcia, A. G. Quiroga, J. Castro, A. Ortiz, P. Aller, F. Mata, *Toxicological Sciences*, **2009**, 111 (2), 413-423.
- <sup>34</sup>S. Afazal, S. A. Jensen, J. B. Sørensen, T. Henriksen, A. Weimann, H. E. Poulsen, *Cancer Chemotherapy Pharmacology*, **2012**, 69, 301-307.
- <sup>35</sup>J. Alexandre, Y. Hu, W. Lu, *Cancer Research*, **2007**, 67, 3512-3517.
- <sup>36</sup>J. Serrano, C. M. Palmeira, D. W. Kuehl, K. B. Wallace, *Biochimica et Biophysica acta-bioenergetics*, **1999**, 1411 (1), 201-205.

- 
- <sup>37</sup>W. P. Tsang, S. P. Y. Chau, S. K. Kong, K. P. Fung, T. T. Kwok, *Life Sciences*, **2003**, 73 (16), 2047-2058.
- <sup>38</sup>H. Hug, S. Strand, A. Grambihler, G. Galle, V. Hack, W. Stremmel, P. H. Krammer, P. R. Galle, *Journal of Biological Chemistry*, **1997**, 272 (45), 28191-28193.
- <sup>39</sup>J. M. Wu, A. M. DiPietrantonio, T. C Hsieh, *Apoptosis*, **2001**, 6 (5), 377-388.
- <sup>40</sup>Y. H. Ling, L. Liebes, Y. Y. Zou, R. Perez-Soler, *Journal of Biological Chemistry*, **2003**, 278 (36), 33714-33713.
- <sup>41</sup>I. B. Levadeba, Z. Z. Su, D. Sarkar, R. V. Gopalkirishnan, S. Waxman, A. Yacoub, P. Dent, P. B. Fischer, *Oncogene*, **2005**, 24 (4), 585-596.
- <sup>42</sup>W. H. Chan, J. S. Yu, *Journal of Cellular Biochemistry*, **2000**, 78, 73-84.
- <sup>43</sup>D. P. Bezerra, C. Pessoa, M. O. DeMoraes, N. Saker-Nato, E. R. Silveira, L. V. Costa-Lotufo, *European Journal of Pharmaceutical Sciences*, **2013**, 48, 453-463.
- <sup>44</sup>A. M. Banafa, S. Roshan, Y. Liu, H. Chen, M. Chen, G. Yang, G. He, *Journal of Huazhong University of Science and Technology: Medical Sciences*, **2013**, 33 (5), 717-724.
- <sup>45</sup>Z. Zhang, K. Teryua, H. Eto, S. Shirahata, *PLoS ONE*, **2011**, 6 (11), e27441.
- <sup>46</sup>Q. Kong, K. O. Lillehei, *Medical Hypotheses*, **1998**, 51, 405-409.
- <sup>47</sup>H. W. Chiu, Y. A. Chen, S. Y. Ho, Y. J. Wang, *PLoS ONE*, **2012**, 7 (2), e31579.
- <sup>48</sup>C. Sweeney, G. Liu, C. Yiannoutsos, J. Kolesar, D. Horvath, M. J. Stabb, K. Fife, V. Armstrong, A. Treston, C. Sidor, G. Wilding, *Clinical Cancer Research*, **2005**, 11, 6625-6633.
- <sup>49</sup>M. R. Harrison, N. M. Hahn, R. Pili, W. K. Oh, H. Hammers, C. Sweeney, K. M. Kim, S. Perlman, J. Arnott, C. Sider, G. Wilding, G. Liu, *Investigational New Drugs*, **2011**, 29 (6), 1464-1475.
- <sup>50</sup>J. Y. Bruce, J. Eickhoff, R. Pili, T. Logan, M. Carducci, J. Arnott, A. Treston, G. Wilding, G. Liu, *Investigational New Drugs*, **2012**, 30 (2), 794-802.
- <sup>51</sup>M. K. Kulke, J. A. Chan, J. A. Meyerhardt, A. X. Zhu, T. A. Abrams, L. S. Blazzkowsky, E. Regan, C. Sidor, C. S. Fuchs, *Cancer Chemotherapy and Pharmacology*, **2011**, 68 (2), 293-300.
- <sup>52</sup>C. P. Anderson, C. P. Reynolds, *Bone Marrow Transplantation*, **2002**, 30 (3), 135-140.
- <sup>53</sup>J. E. Liebmann, S. M Hahn, J. A. Cook, C. Lipschultz, J. B. Mitchell, D. C. Kaufmann, *Cancer Research*, **1993**, 53 (9), 2066-2070.

- 
- <sup>54</sup>P. J. O'Dwyer, T. C. Hamilton, F. P. LaCreta, J. M. Gallo, D. Kilpatrick, T. Halbherr, J. Brennan, M. A. Bookman, J. Hoffman, R. C. Young, R. L. Comis, R. F. Ozols, *Journal of Clinical Oncology*, **1996**, 14 (1), 249-256.
- <sup>55</sup>B. Van Loon, E. Markkanen, U. Hubscher, *DNA Repair*, **2010**, 9, 604-616.
- <sup>56</sup>E. D. Pleasance, P. J. Stephens, S. O'Meara, D. J. McBride, A. Meynert, D. Jones, M. L. Lin, D. Beare, K. W. Lau, C. Greenman, I. Varela, S. Nik-Zainal, H. R. Davies, G. R. Ordenez, L. J. Mudie, C. Latimer, S. Edkins, L. Stebbings, L. Chen, M. Jia, C. Leroy, J. Marshall, A. Menzies, A. Butler, J. W. Teague, J. Mangion, Y. A. Sun, S. F. McLaughlin, H. E. Peckham, E. F. Tsung, G. L. Costa, C. C. Lee, J. D. Minna, A. Gazdar, E. Birney, M. D. Rhodes, K. J. McKernan, M. R. Stratton, P. A. Futreal, P. J. Campbell, *Nature*, **2010**, 463, 184-190.
- <sup>57</sup>E. D. Pleasance, R. K. Cheetham, P. J. Stephens, D. J. McBride, S. J. Humphray, C. D. Greenman, I. Varela, M. L. Lin, G. R. Ordenez, G. R. Bignell, K. Ye, J. Ali-paz, M. J. Bauer, D. Beare, A. Butler, R. J. Carter, L. Chen, A. J. Cox, S. Edkins, P. I. Kokko-Gonzales, N. A. Gormley, R. J. Grocock, C. D. Haudenschild, M. M. Hims, T. James, M. Jia, Z. Kingsbury, C. Leroy, J. Marshall, A. Menzies, L. J. Mudie, Z. Ning, T. Royce, O. B. Shulz-Trieglaff, A. Spiridou, L. A. Stebbings, L. Szajkowski, J. Teague, D. Williamson, L. Chin, M. T. Ross, P. J. Campbell, D. R. Bentley, P. A. Futreal, M. R. Stratton, *Nature*, **2010**, 463, 191-196.
- <sup>58</sup>L. A. Lipscomb, M. E. Peek, M. L. Morningstar, S. M. Verghis, E. M. Miller, A. Rich, J. M. Essigmann, L. D. Williams, *Proceedings of the Natural Academy of Sciences*, **1995**, 92, 719.
- <sup>59</sup>T. S. Koskenkorva-Frank, G. Weiss, W. H. Koppenol, S. Burckhardt, *Free Radical Biology and Medicine*, **2013**, 65, 1175-1194.
- <sup>60</sup>B. White, M. R. Smyth, J. D. Stewart, J. F. Rusling, *Journal of the American Chemical Society*, **2003**, 125, 6604-6605.
- <sup>61</sup>M. C. Kelly, G. Whitaker, B. White, M. R. Smyth, *Free Radical Biology and Medicine*, **2007**, 42, 1680-1689.
- <sup>62</sup>B. White, M. C. Tarun, N. Gathergood, J. F. Rusling, M. R. Smyth, *Molecular Biosystems*, **2005**, 1, 373-381.
- <sup>63</sup>C. M. Gedik, S. P. Boyle, S. G. Wood, N. J. Vaughan, A. R. Collins, *Carcinogenesis*, **2002**, 23, 2129-2133.
- <sup>64</sup>C. Zoski, *Handbook of Electrochemistry*, first edition, Elsevier, Oxford, UK, **2006**.
- <sup>65</sup>G. Tabbì, C. Cassino, G. Cavigiolio, D. Colangelo, A. Ghiglia, I. Viano, D. Osella, *Journal of Medicinal Chemistry*, **2002**, 45, 5786-5796.

- 
- <sup>66</sup>W. E. Butler, P. N. Kelly, A. G. Harry, R. Tiedt, B. White, R. Devery, P. T. M. Kenny, *Applied Organometallic Chemistry*, **2013**, 27, 361-365.
- <sup>67</sup>P. N. Kelly, A. Prêtre, S. Devoy, I. O'Reilly, R. Devery, A. Goel, J. Gallagher, A. J. Lough, P. T. M. Kenny, *Journal Of Organometallic Chemistry*, **2007**, 692, 1327-1331.
- <sup>68</sup>A. G. Myers, L. McKinstry, J. K. Barbay, J. L. Gleason, *Tetrahedron Letters*, **1998**, 39, 133.
- <sup>69</sup>M. C. Kelly, B. White, M. R. Smyth, *Journal of Chromatography B-Analytical Technologies in the Biomedical and Life Sciences*, **2008**, 863 (1), 181-186.
- <sup>70</sup>L. Randaccio, S. Geremia, N. Demitri, J. Wuerges, *Molecules*, **2010**, 15, 3228-3259.
- <sup>71</sup>A. K. Petrus, T. J. Fairchild, R. P. Doyle, *Angewente Chemie International Edition*, **2009**, 48, 1022-1028.
- <sup>72</sup>G. Russell-Jones, K. McTavish, J. McEwan, J. Rice, D. Nowotnik, *Journal of Inorganic Biochemistry*, **2004**, 98, 1625-1633.
- <sup>73</sup>W. A. Howard, A. Bayomi, E. Natarajan, M. A. Aziza, O. ElAhmady, C. B. Grissom, F. G. West, *Bioconjugate Chemistry*, **1997**, 8 (4), 498-502.
- <sup>74</sup>J. D. Baganto, A. L. Eilers, R. A. Hortton, C. B. Grissom, *Journal of Organic Chemistry*, **2004**, 69 (26), 8987-8996.
- <sup>75</sup>A. Mooney, A. J. Corry, D. O'Sullivan, D. K. Rai, P. T. M. Kenny, *Journal of Organometallic Chemistry*, **2009**, 694, 886-894.
- <sup>76</sup>M. J. Sheehy, J. F. Gallagher, M. Yamashita, Y. Ida, J. White-Colangelo, J. Johnson. R. Orlando, P. T. M. Kenny, *Inorganic Chemistry Communications*, **2002**, 5 (12), 1034 – 1040.

## **Appendix A– Abbreviations and units**

**A**

A	absorbance; adenine
ACE	angiotensin converting enzyme
ACN	acetonitrile
Ag/AgCl	silver/silver chloride (reference electrode)
AMP	antimicrobial peptide
Anal.	Analysis
ATO	arsenic trioxide

**B**

BMS	Bristol Myers Squibb
Boc	<i>tert</i> -butoxycarbonyl
Br.	broad (spectral)
BSO	buthionine sulfoximinme

**C**

C	cytosine
Calc.	calculated
CAT	catalase
CDCl <sub>3</sub>	deuterated chloroform
CDK	cyclin dependant kinase
Cl	chlorine
Co	cobalt
Cp	cyclopentadienyl
C <sub>q</sub>	quaternary carbon
Cu	copper
C=O	carbonyl

**D**

d	doublet (spectral)
D-Ala	D-alanine

DCM	dichloromethane
DCU	Dublin City University
dd	double doublets (spectral)
decomp.	decomposition
DEPT	distortionless enhancement by polarisation transfer
DHFR	dihydrofolate reductase
DMSO- <i>d</i> <sub>6</sub>	deuterated dimethylsulfoxide
DNA	deoxyribonucleic acid

## E

e-	electron
EAT	Ehrlich ascites tumour
ECD	electrochemical detector
<i>E. coli</i>	<i>Escherichia coli</i>
EDC	<i>N</i> -(3-dimethylaminopropyl)- <i>N</i> '-ethylcarbodiimide hydrochloride
EMEM	Eagle's minimum essential medium
EPR	enhanced permeability and retention
ER	estrogen receptor
ER (+)	estrogen receptor positive cells
ER (-)	estrogen receptor negative cells
ESI	electrospray ionisation
Et <sub>3</sub> N	triethylamine
EtOH	ethanol

## F

FACS	fluorescence activated cell sorting
FCS	foetal calf serum
FDA	food and drug administration
Fe	iron
Fe (II)	ferrous ion
Fe (III)	ferric ion

FeSO <sub>4</sub>	Iron sulphate
FGF	fibroblast growth factor
<b>G</b>	
G	guanine
G <sub>0</sub> /G <sub>1</sub> /G <sub>2</sub>	gap phase
GABA	γ-aminobutyric acid
Gly	glycine
GPX	glutathione peroxidase
GSH	glutathione
<b>H</b>	
H	hydrogen
H <sub>2</sub> O	water
H <sub>2</sub> O <sub>2</sub>	hydrogen peroxide
HCl	hydrochloric acid
HDACi	histone deacetylase inhibitor
HIF	hypoxia inducible factor
HO•	hydroxyl radical
HOMO	highest occupied molecular orbital
HPMA	hydropropylmethacrylic acid
HPLC	high performance liquid chromatography
HRB	Health Research Board
HSQC	heteronuclear single quantum coherence
<b>I</b>	
IC <sub>50</sub>	half maximal inhibitory concentration
IR	infra red
<b>J</b>	
<i>J</i>	coupling constant (spectral)



## K

## L

L	path length (in cm)
L-Ala	L-alanine
LBD	ligand binding domain
LNC	lipid nanocapsules
LUMO	lowest unoccupied molecular orbital

## M

<i>m</i>	<i>meta</i>
m	multiplet (spectral)
M	mitosis phase
MDR	multiple drug resistance
MeOH	methanol
MgSO <sub>4</sub>	magnesium sulphate
MIC	minimum inhibitory concentration
MLCT	metal-ligand charge transfer
Mp	melting point
MS	mass spectrometry
MTT	3-(4,5-dimethylthiazol-2-yl)-2, 5-dipheyltetrazolium bromide
<i>m/z</i>	mass to charge ratio

## N

N	nitrogen
NaNO <sub>2</sub>	sodium nitrite
NaOH	sodium hydroxide
NADP	nicotinamide adenine dinucleotide phosphate
NCI	National Cancer Institute

NHDF	normal human dermal fibroblast
NHS	<i>N</i> -hydroxysuccinimide
NICB	National Institute for Cellular Biotechnology
NMR	nuclear magnetic resonance
No.	number
NSCLC	non small cell lung cancer

## O

O	oxygen
OD	optical density
OEt	ethoxy
OH	hydroxyl
OMe	methoxy
OPOA	8-oxo-8-(phenylamino)octanoic acid

## P

<i>P</i>	<i>para</i>
<i>P. aeruginosa</i>	<i>Pseudomonas aeruginosa</i>
PEG	poly ethyleneglycol
Pgp	P-glycoprotein
PRX	peroxiredoxin
PSA	N <sup>1</sup> -phenylsuberamide

## Q

q	quartet (spectral)
qt	quintet (spectral)

## R

RBA	relative binding affinity
RNA	ribonucleic acid
ROS	reactive oxygen species

Ru	ruthenium
<b>S</b>	
s	singlet (spectral)
S	synthesis phase
SAHA	suberoylanilide hydroxamic acid
SAR	structure activity relationship
Sar	sarcosine
<i>S. aureus</i>	<i>Staphylococcus aureus</i>
SCLC	small cell lung cancer
SERM	selective estrogen receptor modulator
Sn	tin
SOCl <sub>2</sub>	thionyl chloride
SOD	superoxide dismutase
SPPS	solid phase peptide synthesis
<b>T</b>	
t	triplet (spectral); thymine
$T_c$	Coalescence temperature
TFA	trifluoroacetic acid
Ti	titanium
TMS	tetramethylsilane
TNF-R	tumour necrosis factor receptor
TRX	thioredoxin
TUNEL	terminal deoxynucleotidyl transferase dUTP nick end labeling
<b>U</b>	
UV	ultraviolet
<b>V</b>	
VEGF	vascular endothelial growth factor

Vis            visible

## Z

z            charge

### Miscellaneous

(E)           Entegen (opposite)

(Z)           Zusammen (together)

$\alpha$ H           alpha hydrogen

$\epsilon$             extinction coefficient

$\lambda_{\max}$         maximum absorbance

$\eta^5\text{-C}_5\text{H}_4$         mono substituted cyclopentadienyl ring

$\eta^5\text{-C}_5\text{H}_5$         unsubstituted cyclopentadienyl ring

$\pm$             plus/minus

$\sim$             approximately

<            less than

>            greater than

## Units

Å	Angstrom
cm	centimetre
cm <sup>-1</sup>	wavenumber(s)/per centimetre
g	gram
h	hour
Hz	hertz
l	litre
M	molar
MHz	megahertz
mg	milligrams
ml	millilitre
mm	millimeters
Nm	nanometers
mM	millimolar
mmol	millimole
mol	mole
µg	microgram
µg mL <sup>-1</sup>	microgram per millilitre
µl	microliter
µm	micrometer
µM	micromolar
nm	nanometer
nM	nanomolar
°	degrees
°C	degrees Celcius
Ppm	parts per million
s	second
δ	chemical shift (ppm)
%	percentage

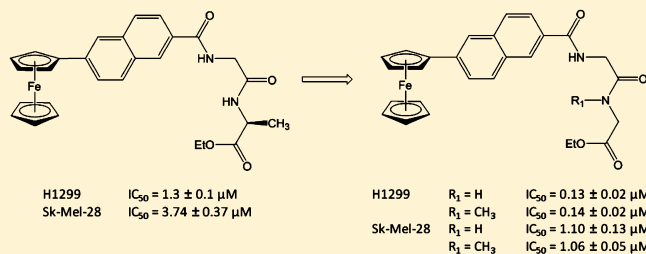


## Appendix B - Publications

Structure–Activity Relationship and Mode of Action of *N*-(6-Ferrocenyl-2-naphthoyl) Dipeptide Ethyl Esters: Novel Organometallic Anticancer CompoundsÁine Mooney,<sup>†,‡</sup> Rachel Tiedt,<sup>†,‡</sup> Thamir Maghoub,<sup>‡</sup> Norma O'Donovan,<sup>‡</sup> John Crown,<sup>‡,§</sup> Blánaid White,<sup>†</sup> and Peter T. M. Kenny<sup>\*,†,‡</sup><sup>†</sup>School of Chemical Sciences, Dublin City University, Dublin 9, Ireland<sup>‡</sup>National Institute for Cellular Biotechnology, Dublin City University, Dublin 9, Ireland<sup>§</sup>Department of Medical Oncology, St. Vincent's University Hospital, Dublin 4, Ireland

## Supporting Information

**ABSTRACT:** In this article, we report the findings of a comprehensive structure–activity relationship study of *N*-(6-ferrocenyl-2-naphthoyl) dipeptide ethyl esters, in which novel analogues were designed, synthesized, and evaluated *in vitro* for antiproliferative effect. Two new compounds, **2** and **16**, showed potent nanomolar activity in the H1299 NSCLC cell line, with exceptional IC<sub>50</sub> values of 0.13 and 0.14 μM, respectively. These compounds were also found to have significant activity in the Sk-Mel-28 malignant melanoma cell line (IC<sub>50</sub> values of 1.10 and 1.06 μM, respectively). Studies were also conducted to elucidate the mode of action of these novel organometallic anticancer compounds. Cell cycle analysis in the H1299 cell line suggests these compounds induce apoptosis, while guanine oxidation studies confirm that **2** is capable of generating oxidative damage via a ROS-mediated mechanism.



## INTRODUCTION

The medicinal application of ferrocene derivatives is currently a thriving area of research,<sup>1</sup> with applications in the area of cancer research being the most popular and well-researched.<sup>2</sup> To date, the most promising ferrocene-based drug candidates have been reported by Jaouen and co-workers;<sup>3</sup> these anticancer compounds contain a [3]-ferrocenophane motif and have a potent *in vitro* antiproliferative effect in breast and prostate cancer cell lines.

Our work is focused on developing a series of novel ferrocenyl-peptide bioconjugates that were found to exert a strong antiproliferative effect on the H1299 nonsmall cell lung cancer (NSCLC) cell line during preliminary *in vitro* studies.<sup>4</sup> These ferrocenyl-peptide bioconjugates are composed of three key moieties, namely, (i) an electroactive core, (ii) a conjugated aromatic linker, (iii) an amino acid or peptide derivative that can interact with other molecules via hydrogen bonds. One key feature of ferrocene is the ease by which it undergoes oxidation to form the ferricenium cation (Fc → Fc<sup>+</sup>). This occurs in a reversible manner and is accommodated readily by the loss/gain of an electron from a nonbonding high energy molecular orbital. The redox properties of ferrocene have often been implicated in its cytotoxicity.<sup>5</sup> Indeed, ferricenium salts that are known to inhibit tumor growth have been shown to produce hydroxyl (HO•) radicals under physiological conditions, leading to oxidatively damaged DNA.<sup>6</sup> In the case of our ferrocenyl-peptide bioconjugates, the presence of the conjugat-

ing aromatic linker between the ferrocene and peptide units lowers the redox potential to within the range of biologically accessible potentials, allowing for the interconversion between the ferrocene and ferricenium species. The catalytic generation of intracellular reactive oxygen species (ROS) such as the HO• radical offers an attractive and alternative method to target and kill cancer cells.<sup>7</sup>

In a previous study, we identified *N*-(6-ferrocenyl-2-naphthoyl)-glycine-L-alanine ethyl ester **1**, as a potential drug candidate since it has an *in vitro* antiproliferative effect that is comparable with cisplatin in the H1299 NSCLC cell line (IC<sub>50</sub> value = 1.3 ± 0.1 μM).<sup>8</sup> We have since conducted further studies in order to seek molecules that may have an even higher efficacy than **1**. Recently, we reported a study of *N*-(ferrocenyl)naphthoyl amino acid esters which found that *N*-(6-ferrocenyl-2-naphthoyl)-γ-aminobutyric acid ethyl ester was two times more potent than **1** in the H1299 NSCLC cell line (IC<sub>50</sub> value = 0.62 ± 0.07 μM).<sup>9</sup> This compound was also tested for *in vitro* antiproliferative activity in the Sk-Mel-28 malignant melanoma cell line and was found to have an encouraging IC<sub>50</sub> value of 1.41 ± 0.04 μM. We herein report the results of a comprehensive structure–activity relationship (SAR) study of *N*-(6-ferrocenyl-2-naphthoyl) dipeptide ethyl esters that was conducted concomitantly. In addition, we report the results of

Received: March 22, 2012

Published: May 1, 2012

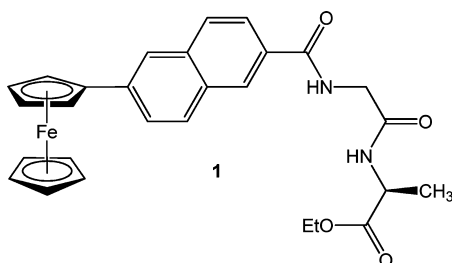


cell cycle analysis and guanine oxidation studies that were conducted to elucidate the mode of action of these novel organometallic anticancer compounds.

## RESULTS AND DISCUSSION

**Structure–Activity Relationship of 1.** For our initial SAR study, we focused our attention on preparing a set of peptide chain analogues of **1** (Chart 1) to probe the steric and

**Chart 1.** *N*-(6-Ferrocenyl-2-naphthoyl)-glycine-*L*-alanine Ethyl Ester **1**



stereochemical requirements for potent antiproliferative activity. Previous studies of *N*-(ferrocenyl)benzoyl dipeptide derivatives had indicated that the *in vitro* antiproliferative effect is best when the small, neutral  $\alpha$ -amino acids glycine and *L*-alanine are present in the peptide chain.<sup>4c</sup> However, the effect of the incorporation of  $\alpha$ -amino acids with either branched alkyl or aromatic side chains into the dipeptide chain has yet to be investigated. A set of peptide chain analogues **2–8** containing either glycine or *L*-alanine as the first amino acid (aa) residue, and either glycine, *L*-alanine, *L*-leucine or *L*-phenylalanine as the second aa residue, were prepared by solution-phase peptide coupling of 6-ferrocenyl-naphthalene-2-carboxylic acid to the appropriate free *N*-terminal dipeptide ethyl ester, using EDC/HOBt as the coupling reagent (Scheme 1). Inversion of the stereocenter of **1** was also investigated by preparing the inverse peptide chain analogue **9**. This was easily achieved by incorporating *D*-alanine as the second aa residue in the dipeptide chain **9a**, prior to solution-phase peptide coupling to 6-ferrocenyl-naphthalene-2-carboxylic acid using EDC/HOBt (Scheme 2).

**In Vitro Evaluation in the H1299 NSCLC Cell Line.** The *in vitro* antiproliferative effect of the peptide chain analogues **2–9** was evaluated by performing a comprehensive screen at a single dose (10  $\mu$ M) in the H1299 NSCLC cell line (Table 1).

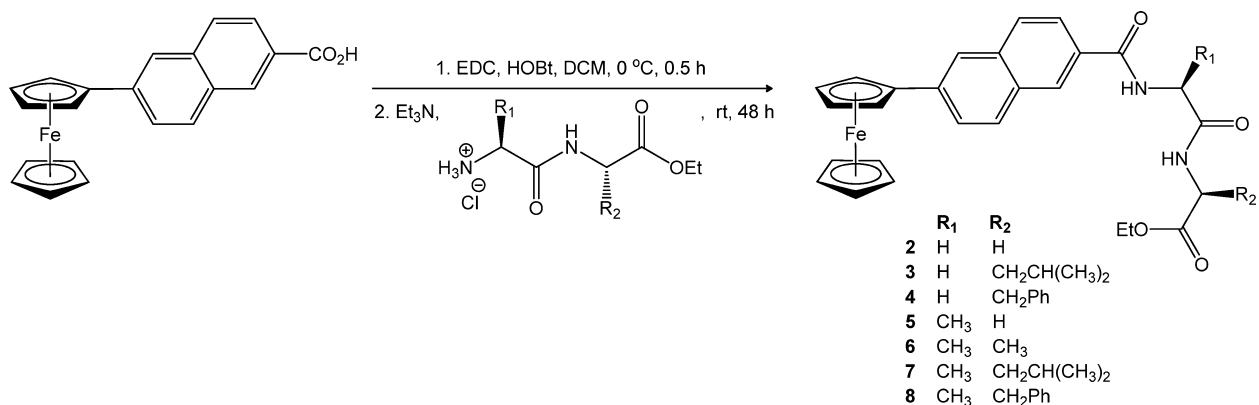
Compound **1** was also included in the screening to allow for the direct comparison of antiproliferative effect. At 10  $\mu$ M, compounds **1–9** were all found to strongly inhibit cell proliferation in the H1299 cell line. The weakest antiproliferative effect was observed for **8**; however, this compound still achieved an appreciable level of cell growth inhibition (>50%). Four compounds in particular were shown to inhibit cell growth by almost 99%. Interestingly, none of these compounds contained either *L*-leucine or *L*-phenylalanine in the dipeptide chain. This indicates that although incorporation of bulkier amino acids is not completely detrimental to the antiproliferative effect, the presence of small, neutral aa residues glycine and *L*-alanine within the dipeptide chain is more favorable for biological activity.

Since compounds **1–9** were all found to inhibit cell growth by at least 50%, it was necessary to repeat the screening at the lower dose of 1  $\mu$ M in order to identify the most potent derivatives. This second round of screening identified three compounds that inhibited cell growth by more than 50%: compounds **1** (~70% growth inhibition), **2** (~95% growth inhibition), and **9** (~55% growth inhibition). IC<sub>50</sub> values were determined for analogues **2** and **9** in the H1299 cell line. The inverse peptide chain analogue **9** was found to be four times more potent than **1**, with an IC<sub>50</sub> value of  $0.33 \pm 0.02 \mu$ M. Thus, the *in vitro* antiproliferative activity of **1** was optimized by inverting the stereochemistry of the C-terminal  $\alpha$ -carbon atom. This increase in antiproliferative effect may be a consequence of the increased resistance of **9** to degradation by proteases.<sup>10</sup>

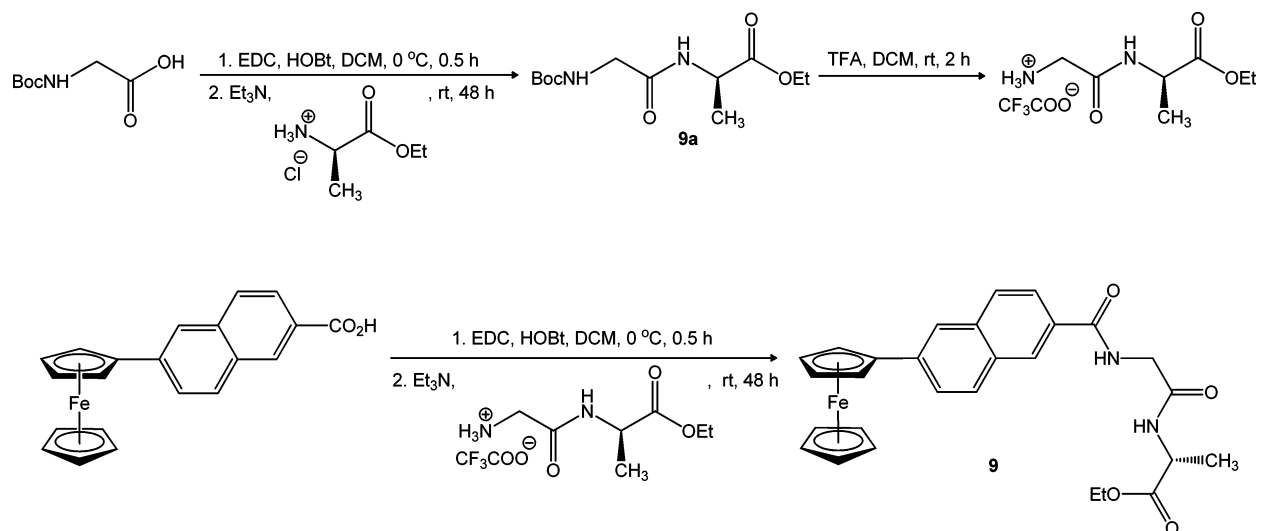
An exceptional IC<sub>50</sub> value of  $0.13 \pm 0.02 \mu$ M was calculated for **2**; the antiproliferative effect of this analogue is an order of magnitude greater than that of both cisplatin (IC<sub>50</sub> value of  $1.5 \pm 0.1 \mu$ M) and **1** in the H1299 cell line. Previous studies determined an IC<sub>50</sub> value of 20  $\mu$ M for *N*-{ortho-(ferrocenyl)-benzoyl}-glycine-glycine ethyl ester in the same cell line.<sup>4d</sup> Thus, in this instance, over a 150-fold improvement in biological activity has been achieved by replacing the benzoyl linker with the naphthoyl linker. This is an extremely encouraging finding; there are only a number of other ferrocenyl compounds that have been reported recently in the literature to have comparable IC<sub>50</sub> values, and these derivatives have been tested in breast and prostate cancer cell lines.<sup>3</sup>

**In Vitro Evaluation in Sk-Mel-28 Malignant Melanoma Cell Line.** The *in vitro* antiproliferative effect of compounds **1–9** was also evaluated in the Sk-Mel-28 malignant melanoma

**Scheme 1.** Synthesis of Peptide Chain Analogues **2–8**



Scheme 2. Synthesis of Inverse Peptide Chain Analogue 9

Table 1. Percentage Cell Growth of H1299 Cells in Presence of Compounds 1–9 and IC<sub>50</sub> Values<sup>a</sup>

compd	R <sub>1</sub>	1st aa	2nd aa	% cell growth at 10 μM	% cell growth at 1 μM	IC <sub>50</sub> <sup>b</sup> (μM)
1	Fc <sup>c</sup>	Gly	L-Ala	0.4 ± 0.7	31.3 ± 12.1	1.3 ± 0.1 <sup>d</sup>
2	Fc	Gly	Gly	0.5 ± 0.8	4.4 ± 0.9	0.13 ± 0.02
3	Fc	Gly	L-Leu	4.9 ± 0.9	103.2 ± 11.0	
4	Fc	Gly	L-Phe	16.2 ± 5.3	102.9 ± 22.2	
5	Fc	L-Ala	Gly	0.4 ± 0.7	118.0 ± 9.1	7.8 ± 0.2 <sup>d</sup>
6	Fc	L-Ala	L-Ala	0.1 ± 0.6	85.8 ± 5.7	3.7 ± 0.6 <sup>d</sup>
7	Fc	L-Ala	L-Leu	13.0 ± 3.5	107.4 ± 16.1	
8	Fc	L-Ala	L-Phe	40.7 ± 8.0	98.8 ± 10.9	
9	Fc	Gly	D-Ala	1.9 ± 0.7	44.8 ± 3.0	0.33 ± 0.02
cisplatin						1.5 ± 0.1

<sup>a</sup>Mean of at least three independent experiments ± standard deviation. <sup>b</sup>IC<sub>50</sub> values were only determined for compounds having an antiproliferative effect, on H1299 at 1 μM, greater than 50%. <sup>c</sup>Fc = ferrocenyl ( $\eta^5$ -C<sub>5</sub>H<sub>4</sub>-Fe-C<sub>5</sub>H<sub>5</sub>). <sup>d</sup>Values are from ref 8.

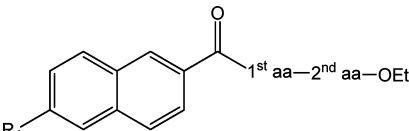
cell line at a single dose of 10 μM (Table 2). The Sk-Mel-28 cell line was found to be more resistant to treatment with 1–9 than the H1299 cell line. Only three compounds were found to inhibit cell growth by more than 50%: compounds 1 (~99% growth inhibition), 2 (~80% growth inhibition), and 9 (~85% growth inhibition). IC<sub>50</sub> values of 3.74 ± 0.37 μM, 1.10 ± 0.13 μM, and 1.83 ± 0.04 μM were calculated for compounds 1, 2, and 9, respectively. Although the antiproliferative effect of these compounds is not as strong in the Sk-Mel-28 cell line as in the H1299 cell line, these results are promising nonetheless since metastatic melanoma is notoriously resistant to chemotherapeutic drugs.<sup>11</sup>

**Structure–Activity Relationship of 2.** Considering the remarkable antiproliferative effect of 2, we decided to continue our SAR study by focusing on optimizing the biological activity of this compound. To determine if the unique chemistry of the redox active ferrocene unit was critical to the antiproliferative effect of 2, a nonorganometallic analogue 10 was prepared by solution-phase peptide coupling of 2-naphthoic acid to glycine–glycine ethyl ester hydrochloride, using EDC/HOBT (Scheme 3).

Previous studies of the *N*-(ferrocenyl)benzoyl peptide derivatives indicated that β-alanine and γ-aminobutyric acid could be of use as a potential isosteric replacement for glycine in the peptide chain.<sup>12</sup> For this reason, these two nonessential aa residues were incorporated into the dipeptide chain to yield a set of peptide chain analogues 11–14 (Chart 2).

Our final strategy was to prepare *N*-methylated derivatives of 2. This was achieved by incorporating the unusual aa sarcosine (*N*-methyl-glycine) into the dipeptide chain to yield the peptide chain analogues 15–17 (Chart 2). *N*-Methylation is a strategy widely used by scientists to alter pharmacological properties of peptides, such as metabolic stability, selectivity, potency, and bioavailability.<sup>13</sup> The inclusion of *N*-methyl amino acids within the dipeptide chain may also yield information concerning the importance of hydrogen bond formation for biological activity since the presence of an *N*-methyl group blocks the ability of the nitrogen atom to act as a hydrogen bond donor (HBD).

These unusual and nonessential aa residues were incorporated into compounds 11–17 by first of all preparing the Boc-protected dipeptide ethyl esters 11a–17a. This was achieved by

**Table 2. Percentage Cell Growth of Sk-Mel-28 Cells in the Presence of Compounds 1–9 and IC<sub>50</sub> Values<sup>a</sup>**


compd	R <sub>1</sub>	1st aa	2nd aa	% cell growth at 10 μM	IC <sub>50</sub> <sup>b</sup> (μM)
1	Fc <sup>c</sup>	Gly	L-Ala	0.7 ± 0.8	3.74 ± 0.37
2	Fc	Gly	Gly	19.0 ± 5.6	1.10 ± 0.13
3	Fc	Gly	L-Leu	79.0 ± 18.2	
4	Fc	Gly	L-Phe	95.4 ± 10.7	
5	Fc	L-Ala	Gly	74.7 ± 23.8	
6	Fc	L-Ala	L-Ala	55.9 ± 34	
7	Fc	L-Ala	L-Leu	86.3 ± 15.8	
8	Fc	L-Ala	L-Phe	102.6 ± 3.9	
9	Fc	Gly	D-Ala	15.6 ± 4.0	1.83 ± 0.04

<sup>a</sup>Mean of at least three independent experiments ± standard deviation.

<sup>b</sup>IC<sub>50</sub> values were only determined for compounds having an antiproliferative effect, on Sk-Mel-28 at 10 μM, greater than 50%.

<sup>c</sup>Fc = ferrocenyl (η<sup>5</sup>-C<sub>5</sub>H<sub>4</sub>-Fe-C<sub>5</sub>H<sub>5</sub>).

solution-phase peptide coupling of the appropriate Boc-protected aa to the corresponding aa ethyl ester hydrochloride using EDC/HOBt (Scheme 4). Removal of the Boc-protecting groups from **11a–17a** was achieved using an excess of trifluoroacetic acid in dichloromethane. The Boc-deprotected dipeptides were then coupled to 6-ferrocenylnaphthalene-2-carboxylic acid in the usual manner.

#### In Vitro Evaluation in H1299 and Sk-Mel-28 Cell Lines.

The in vitro antiproliferative effect of compounds **10–17** was evaluated at a single dose of 1 μM in the H1299 cell line and 10 μM in the Sk-Mel-28 cell line (Table 3). Nonorganometallic analogue **10** did not exhibit an inhibitory effect on cell growth in either cell line. This dramatic loss of antiproliferative effect upon removal of the ferrocene unit from **2** demonstrates conclusively that this organometallic unit is essential for in vitro biological activity.

For the peptide chain analogues **11–14**, compound **11** was the only derivative to exert an antiproliferative effect in the Sk-Mel-28 cell line (~85% growth inhibition); however, this compound did not have any inhibitory effect on cell growth in the H1299 cell line. Compounds **12–14** failed to inhibit cell growth in either cell line. Thus, the isosteric replacement of the glycine residues in **2** with either β-alanine or γ-aminobutyric acid does not improve the in vitro biological activity.

In the case of the *N*-methylated analogues **15–17**, compound **15** exhibited a strong antiproliferative effect in the Sk-Mel-28 cell line (~97% growth inhibition) but did not have any effect on cell growth in the H1299 cell line. Compound **16**, however, was shown to be a potent inhibitor of cell growth in both the H1299 (~95% growth inhibition) and Sk-Mel-28

(~85% growth inhibition) cell lines. Compound **17** failed to inhibit cell growth in either cell line. Thus, compound **16** was the only derivative for which IC<sub>50</sub> values were calculated: 0.14 ± 0.02 μM in the H1299 cell line and 1.06 ± 0.05 μM in the Sk-Mel-28 cell line. These IC<sub>50</sub> values are comparable with those determined for compound **2**. Therefore, *N*-methylation of the first glycine residue does not alter the observed in vitro antiproliferative effect. This could prove to be a valuable modification for future studies since *N*-methyl derivatives are more resistant to degradation by proteases in vivo.<sup>13</sup> However, *N*-methylation of the second glycine residue results in a loss of potency in the H1299 cell line, while *N*-methylation of both residues produces a fall in antiproliferative effect in both cell lines. Thus, the ability of the nitrogen atom in the second glycine residue to act as a HBD is clearly important for biological activity.

**Cell Cycle Analysis.** Cell cycle analysis was performed on control samples and H1299 cells treated with the two most active compounds, **2** and **16**, at concentrations of 0.5 μM and 1.0 μM (Figure 1). Table 4 summarizes the percentage of H1299 cells in each stage of the cell cycle following incubation with **2** for a period of 48 and 72 h. After 48 h, H1299 cells treated with 0.5 μM of **2** showed a significant increase in the sub-G0/G1 population (*p* = 0.006). There was also a significant decrease in the number of cells in the S phase of the cell cycle (*p* = 0.017). The sub-G0/G1 population was found to increase by approximately 2-fold when the concentration of **2** was increased to 1.0 μM. At this higher concentration, the increase in the sub-G0/G1 peak was accompanied by a concomitant decrease in the G0/G1 (*p* = 0.001) and S phase (*p* = 0.005) cell populations. Similar observations were made following incubation with **2** for 72 h; there was a significant increase in the sub-G0/G1 population of H1299 cells treated with 0.5 μM (*p* = 0.032) and 1.0 μM (*p* = 0.006) of **2**.

The cell cycle distribution of H1299 cells incubated with **16** for a period of 48 and 72 h follows a similar pattern (Figure 2 and Table 5). After 48 h, there was a significant increase in the sub-G0/G1 population (*p* = 0.040) accompanied by a decrease in the number of cells in the S (*p* = 0.009) phase of the cell cycle, following treatment with the lower concentration (0.5 μM) of **16**. Doubling the concentration of **16** to 1.0 μM also doubled the sub-G0/G1 population. At this higher concentration, there was also a significant decrease in the number of cells in the G0/G1 (*p* = 0.0004) and S (*p* = 0.002) phases of the cell cycle. After 72 h of incubation, there was a significant increase in the sub-G0/G1 population of H1299 cells treated with 0.5 μM (*p* = 0.012) and 1.0 μM (*p* = 0.015) of **16**.

Thus, the exposure of H1299 cells to compounds **2** and **16** leads in both cases to an accumulation of hypodiploid cells (cells with a lower nuclear DNA content compared to that of normal diploid cells). These findings suggest that both compounds most likely induce apoptosis in H1299 cells since apoptotic cells are characterized by DNA fragmentation and

#### Scheme 3. Synthesis of Nonorganometallic Analogue **10**

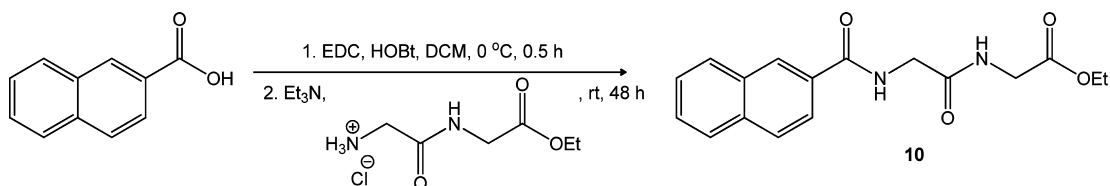
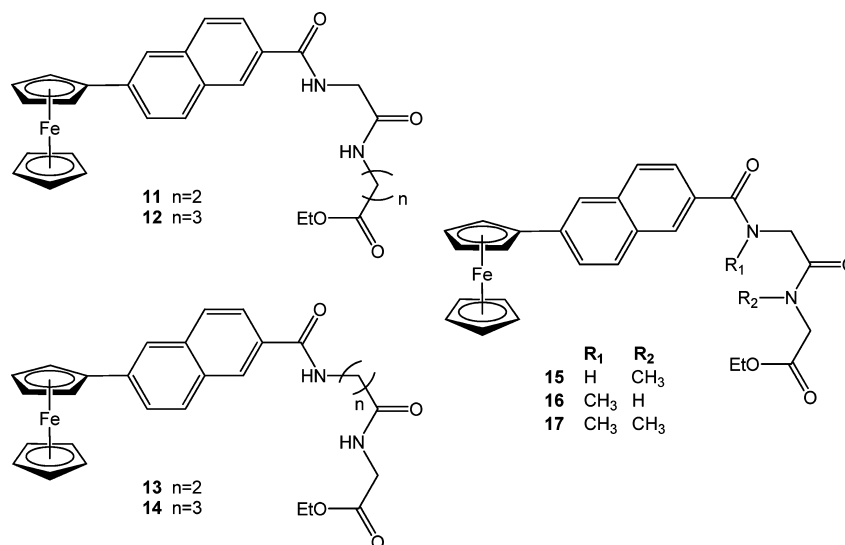
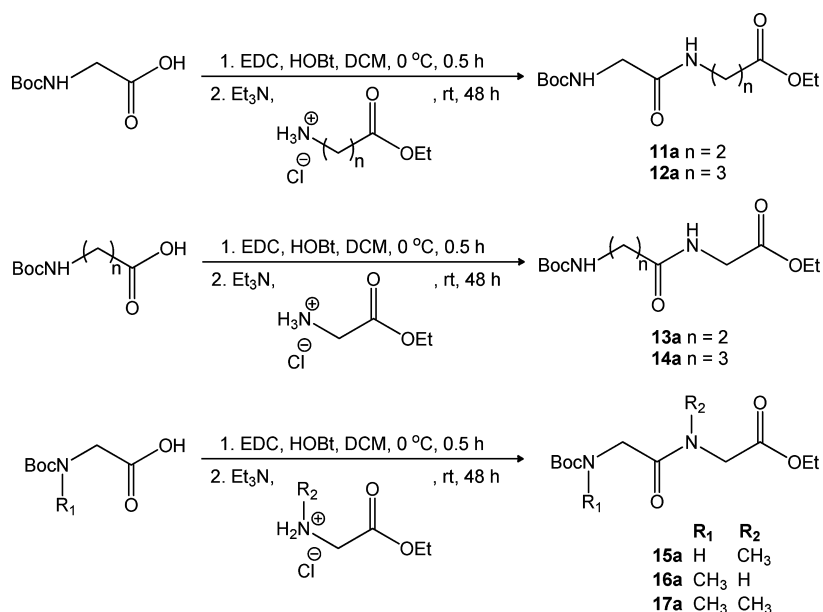


Chart 2. Peptide Chain Analogues 11–17



Scheme 4. Synthesis of Boc-Protected Dipeptide Ethyl Esters 11a–17a



consequently a decrease in nuclear DNA content. Similar observations have been made for the ferrocenyl derivative, ferrociphenol in the MCF-7 breast cancer cell line.<sup>14</sup> However, further flow cytometry studies that specifically measure the levels of early and late apoptotic cells would be required to confirm the induction of apoptosis by these novel compounds, as the presence of hypodiploid cells is not conclusive proof of apoptotic death.<sup>15</sup>

**Guanine Oxidation Studies.** A potential mechanism by which these novel organometallic anticancer compounds may induce DNA damage is by the catalytic generation of ROS. This is possible via a Fenton-type reaction, in which HO<sup>•</sup> radicals are generated from the superoxide dismutation product, hydrogen peroxide (H<sub>2</sub>O<sub>2</sub>). To investigate this, the rate of Fenton reaction mediated 8-oxo-7,8-dihydroguanine (8-oxoGua)<sup>16</sup> formation from guanine was monitored. Guanine was chosen as it has the lowest oxidation potential of all the DNA bases and

is considered the clinical biomarker for oxidatively damaged DNA.<sup>17</sup>

The Fenton-mediated oxidation of guanine and the kinetic profile of 8-oxoGua formed as a result have previously been investigated using iron(II) sulfate (FeSO<sub>4</sub>) and H<sub>2</sub>O<sub>2</sub> to generate HO<sup>•</sup> radicals.<sup>18</sup> To examine if compound **2** induces guanine oxidation via a similar mechanism, kinetic 8-oxoGua formation profiles were obtained by incubating free guanine with (i) FeSO<sub>4</sub> and H<sub>2</sub>O<sub>2</sub> at 37 °C (Figure 3), and (ii) **2** and H<sub>2</sub>O<sub>2</sub> at 37 °C (Figure 4). Samples were taken in duplicate over 15 min. Each sample was injected in triplicate and analyzed by HPLC-UV-EC using an electrochemical detector to detect 8-oxoGua at +550 mV versus Ag/AgCl. Control experiments were also carried out using either FeSO<sub>4</sub> or **2** in the absence of H<sub>2</sub>O<sub>2</sub> and H<sub>2</sub>O<sub>2</sub> in the absence of both iron compounds, to verify that any oxidation was Fenton-mediated. Additionally, they ensured that no artifactual oxidation was occurring from the sample preparation or analysis methodology.

Table 3. Percentage Cell Growth of H1299 and Sk-Mel-28 Cells in the Presence of Compounds 10–17 and IC<sub>50</sub> Values<sup>a</sup>

compd	R <sub>1</sub>	1st aa	2nd aa	% cell growth at 1 μM in H1299	IC <sub>50</sub> (μM) in H1299	% cell growth at 10 μM in Sk-Mel-28	IC <sub>50</sub> <sup>b</sup> (μM) in Sk-Mel-28
10	H	Gly	Gly	87.6 ± 18.4		95.6 ± 10.9	
11	Fc <sup>c</sup>	Gly	β-Ala	72.9 ± 5.2		14.8 ± 3.5	
13	Fc	Gly	GABA	97.5 ± 14.3		62.5 ± 30.7	
12	Fc	β-Ala	Gly	87.7 ± 8.1		98.4 ± 7.6	
14	Fc	GABA	Gly	102.8 ± 4.6		89.1 ± 17.8	
15	Fc	Gly	Sar	98.1 ± 4.4		3.2 ± 3.4	
16	Fc	Sar	Gly	4.8 ± 1.4	0.14 ± 0.02	15.7 ± 9.86	1.06 ± 0.05
17	Fc	Sar	Sar	102.2 ± 16.4	1.5 ± 0.1	65.0 ± 29.8	

<sup>a</sup>Mean of at least three independent experiments ± standard deviation. <sup>b</sup>IC<sub>50</sub> values were only determined for compounds having an antiproliferative effect, on H1299 at 1 μM, greater than 50%. <sup>c</sup>Fc = ferrocenyl ( $\eta^5$ -C<sub>5</sub>H<sub>4</sub>-Fe-C<sub>5</sub>H<sub>5</sub>).

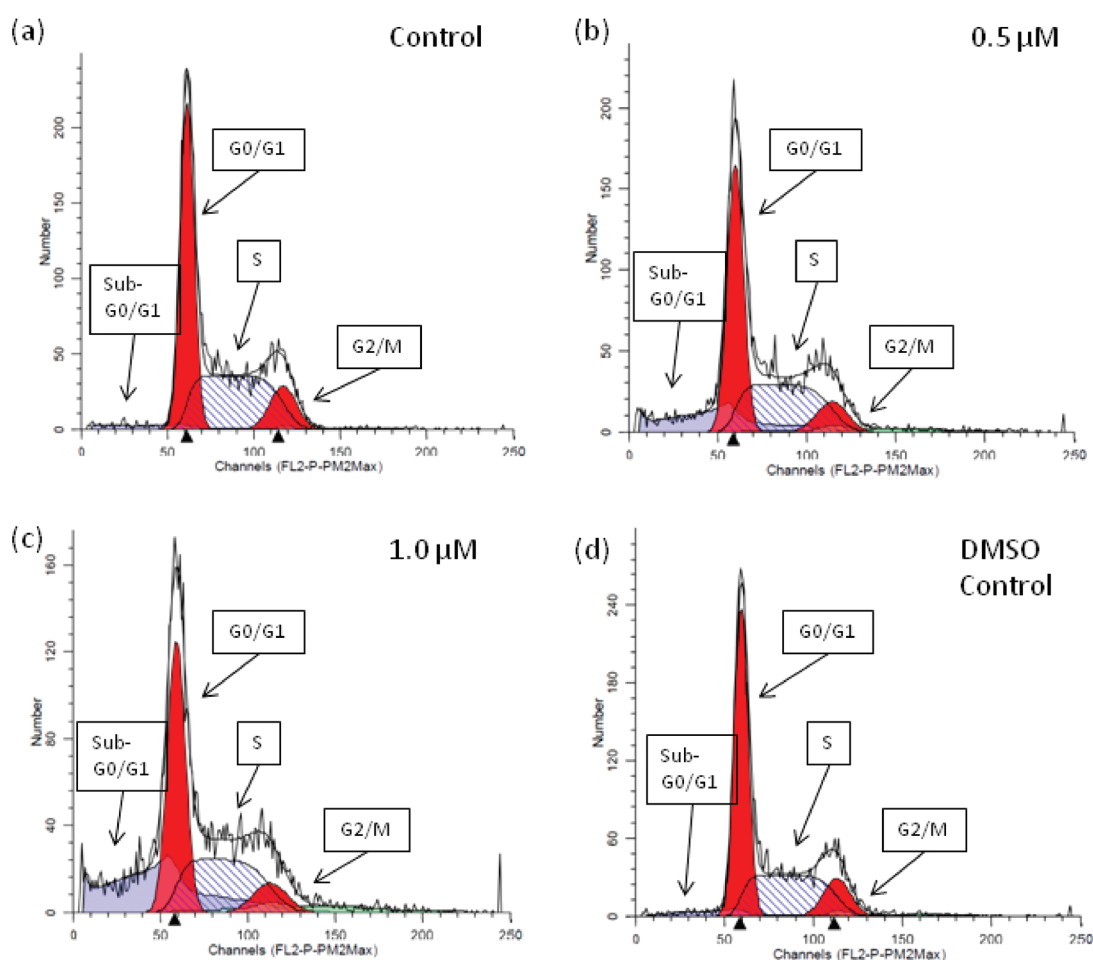


**Figure 1.** Sample graphs of H1299 cell cycle distribution after 72 h: (a) control, (b) 0.5 μM solution of **2**, (c) 1.0 μM solution of **2**, and (d) DMSO control. The data obtained from the flow cytometry was analyzed using ModFit software. This software calculates the number of diploid cells in G0/G1, S, and G2/M phases of the cell cycle, as well as cell debris and cell aggregates. Hypodiploid cells appear as a sub-G0/G1 peak.

Incubation of free guanine with (i) FeSO<sub>4</sub> and H<sub>2</sub>O<sub>2</sub> led to oscillating concentrations of 8-oxoGua over the incubation period as previously reported.<sup>18</sup> The formation is significantly higher than the control baselines, confirming the oxidation is Fenton-mediated. The 8-oxoGua concentration maxima were

1.39 μM at 6 min and 2.29 μM at 8.5 min. This trend is analogous to that reported previously. These maxima occur with a different oscillation frequency, which can be attributed to differences in solution pH (previously, these maxima were reported at 4 and 15 min, respectively).

**Table 4. Cell Cycle Distribution of H1299 Cells Incubated with 2 for 48 or 72 h, Then Analyzed by Flow Cytometry<sup>a</sup>**

	sub G0/G1	G0/G1	S	G2/M
48 h				
control	4.6 ± 1.1	40.9 ± 0.7	44.9 ± 1.8	9.6 ± 1.9
0.5 μM	11.9 ± 0.3**	39.6 ± 2.0	39.2 ± 0.8*	9.4 ± 1.4
1.0 μM	21.8 ± 1.6**	34.5 ± 0.8**	37.1 ± 1.2**	6.7 ± 1.4
DMSO control	5.3 ± 0.9	40.8 ± 0.9	44.4 ± 2.9	9.6 ± 1.3
72 h				
control	2.4 ± 0.3	46.6 ± 0.4	41.3 ± 0.8	9.7 ± 1.2
0.5 μM	7.5 ± 1.7*	44.5 ± 2.0	39.2 ± 1.8	8.9 ± 2.0
1.0 μM	12.2 ± 1.5**	41.5 ± 3.1	37.9 ± 1.6*	8.4 ± 2.3
DMSO control	2.2 ± 0.4	47.9 ± 3.1	40.2 ± 3.6	9.7 ± 0.9

<sup>a</sup>Standard deviations have been calculated using data obtained from three independent experiments. Student's *t*-test was performed to determine significance: \* denotes  $p < 0.05$ ; \*\* denotes  $p < 0.01$ , when comparing treatment with the control or DMSO control.

Incubation of free guanine with (ii) 2 and H<sub>2</sub>O<sub>2</sub>, which was suspected to result in Fenton-mediated oxidation, also resulted in the formation of oscillating concentrations of 8-oxoGua over the incubation period. Again, the formation is significantly

higher than the control baselines, clearly illustrating that both 2 and H<sub>2</sub>O<sub>2</sub> are required to form this concentration of 8-oxoGua and confirming that the oxidation of guanine was Fenton-mediated. The maximum concentrations of 8-oxoGua formed with 2 were 0.62 μM after 30 s and 0.56 μM at 2 min. The concentration of 8-oxoGua generated by 2 is significantly lower than that generated by FeSO<sub>4</sub>. Ferrocene may produce a weaker response than the FeSO<sub>4</sub> due to the presence of the cyclopentadienyl ligands and the size of the molecule. However, the generation of 8-oxoGua by 2 illustrates that the oxidation is occurring by Fenton chemistry and that 2 is generating oxidative damage via a ROS-mediated mechanism.

The oscillation period for 8-oxoGua formation mediated by 2 differs from that of FeSO<sub>4</sub>. After the initial maxima at 0.5 and 2 min, the 8-oxoGua concentration continues to oscillate for the rest of the incubation period, with concentrations consistently higher than control levels, further confirming that oxidation is Fenton-mediated.

## CONCLUSIONS

Our comprehensive structure–activity relationship study has shown that *N*-(6-ferrocenyl-2-naphthoyl) dipeptide ethyl esters are promising novel organometallic anticancer compounds. We have established the structural modifications that have a

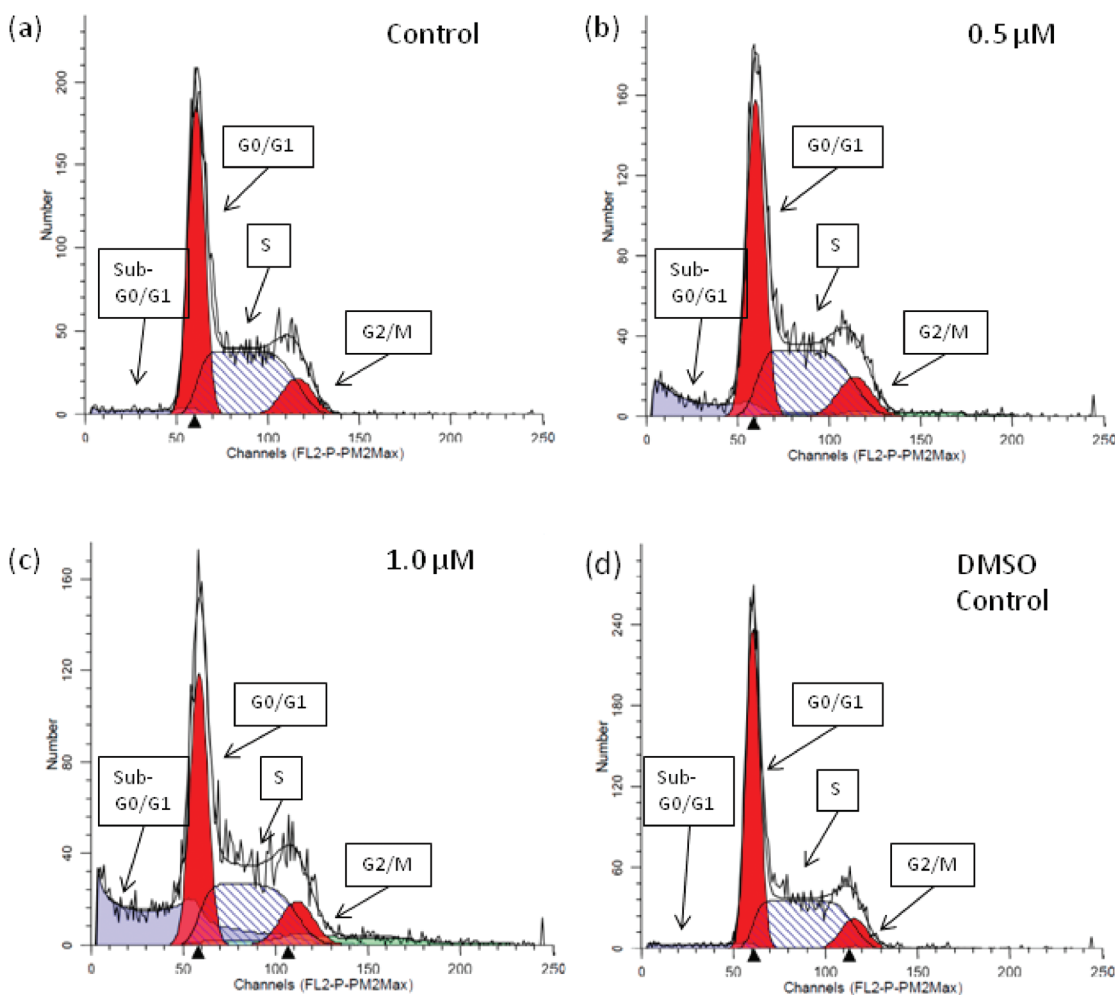


**Figure 2.** Sample graphs of H1299 cell cycle distribution after 72 h: (a) control, (b) 0.5 μM solution of 16, (c) 1.0 μM solution of 16, and (d) DMSO control. The data obtained from flow cytometry was analyzed using ModFit software. This software calculates the number of diploid cells in G0/G1, S, and G2/M phases of the cell cycle, as well as cell debris and cell aggregates. Hypodiploid cells appear as a sub-G0/G1 peak.

Table 5. Cell Cycle Distribution of H1299 Cells Incubated with 16 for 48 or 72 h, Then Analyzed by Flow Cytometry<sup>a</sup>

	sub G0/G1	G0/G1	S	G2/M
		48 h		
control	3.6 ± 0.4	40.5 ± 0.6	46.4 ± 1.3	9.6 ± 1.0
0.5 μM	11.3 ± 2.8*	37.2 ± 2.0	41.3 ± 1.3**	10.2 ± 2.5
1.0 μM	19.5 ± 3.0**	34.0 ± 0.7**	38.9 ± 1.4**	7.6 ± 1.3
DMSO control	4.7 ± 1.0	39.8 ± 1.6	45.7 ± 2.9	9.8 ± 2.9
		72 h		
control	2.9 ± 0.2	42.4 ± 1.1	43.9 ± 0.1	10.8 ± 1.0
0.5 μM	6.0 ± 0.7*	41.1 ± 1.0	42.0 ± 1.0	10.8 ± 0.6
1.0 μM	11.3 ± 1.9*	38.4 ± 0.4*	40.3 ± 0.5**	10.1 ± 1.1
DMSO control	2.0 ± 0.4	44.0 ± 1.8	43.0 ± 0.7	11.0 ± 0.7

<sup>a</sup>Standard deviations have been calculated using data obtained from three independent experiments. Student's *t*-test was performed to determine significance: \* denotes  $p < 0.05$ ; \*\* denotes  $p < 0.01$ , when comparing treatment with the control.

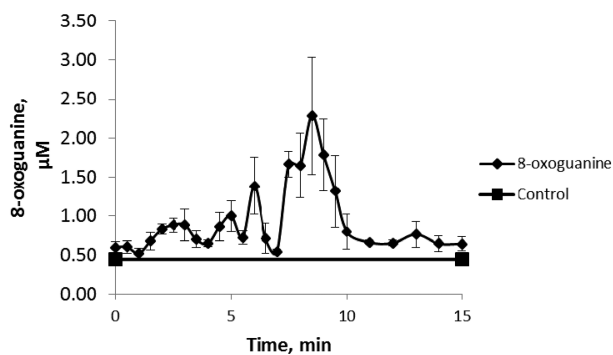


Figure 3. Concentration of 8-oxoGua formed as a function of time after the incubation of guanine with  $\text{FeSO}_4$  and  $\text{H}_2\text{O}_2$  at 37 °C. Error bars show the standard deviation of duplicate samples injected in triplicate.

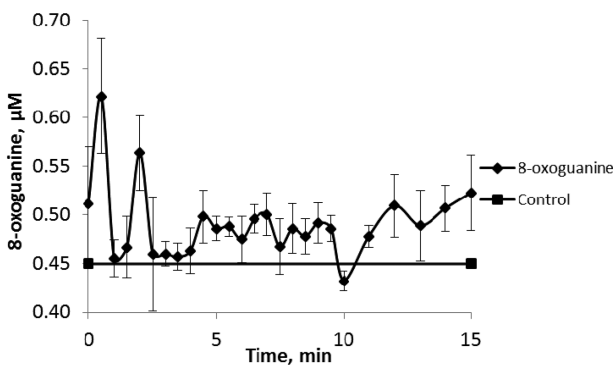


Figure 4. Concentration of 8-oxoGua formed as a function of time after the incubation of guanine with 2 and  $\text{H}_2\text{O}_2$  at 37 °C. Error bars show the standard deviation of duplicate samples injected in triplicate.

positive impact and those that have a negative impact on the biological activity of these novel compounds. We have also clearly demonstrated that the organometallic ferrocene unit is essential for in vitro biological activity. Our study has identified two new compounds (2 and 16) that have a potent nanomolar activity in H1299 NSCLC cell line, with  $\text{IC}_{50}$  values of 0.13 and 0.14 μM, respectively. These compounds also have significant activity in the Sk-Mel-28 malignant melanoma cell line ( $\text{IC}_{50}$  values of 1.10 and 1.06 μM, respectively).

With regard to the proposed mode of action of these novel compounds, cell cycle analysis in the H1299 cell line has shown 2 and 16 to cause a significant increase in the sub-G0/G1 peak, which is suggestive of apoptosis. This observation is

encouraging since the production of intracellular ROS has been shown to lead to cancer cell apoptosis.<sup>19</sup>

Guanine oxidation studies confirm that 2 is capable of causing oxidative damage to guanine, and it does so by the generation of  $\text{HO}^\bullet$  radicals from  $\text{H}_2\text{O}_2$ . This finding is also consistent with the proposed mode of action. Further studies with ds-DNA are now required to demonstrate that 2 is capable of generating oxidatively damaged DNA. In addition, studies to detect the generation of intracellular ROS by these novel compounds are currently in progress.

## EXPERIMENTAL SECTION

**Chemistry.** All chemicals were purchased from Sigma-Aldrich, Lennox Chemicals, Fluorochem Limited, or Tokyo Chemical Industry UK Limited, and used as received. Commercial grade reagents were used without further purification. When necessary, all solvents were purified and dried prior to use. Riedel-Haën silica gel was used for thin layer and column chromatography. Melting points were determined using a Stuart melting point (SMP3) apparatus and are uncorrected. Optical rotation measurements were made on a Perkin-Elmer 343 Polarimeter and are quoted in units of  $10^{-1} \text{ deg cm}^2 \text{ g}^{-1}$ . Infrared spectra were recorded on a Perkin-Elmer Spectrum 100 FT-IR with ATR. UV-vis spectra were recorded on a Hewlett-Packard 8452 A diode array UV-vis spectrophotometer.  $^1\text{H}$  and  $^{13}\text{C}$  NMR spectra were recorded in deuterated solvents on either a Bruker Avance 400 NMR or a Bruker Avance Ultrashield 600 NMR. The  $^1\text{H}$  and  $^{13}\text{C}$  NMR chemical shifts are reported in ppm (parts per million). Tetramethylsilane (TMS) or the residual solvent peaks have been used as an internal reference. All coupling constants (*J*) are in Hertz. The abbreviations for the peak multiplicities are as follows: s (singlet), d (doublet), dd (doublet of doublets), t (triplet), q (quartet), qt (quintet), m (multiplet), and br (broad). Electrospray ionization mass spectra were performed on a Micromass LCT mass spectrometer or a Brüker Daltonics Esquire-LC ion trap mass spectrometer. Tandem mass spectra were obtained on a Micromass Quattro micro LC-MS/MS triple quadrupole mass spectrometer. Elemental analyses (C, H, N) of the target compounds, which were performed at the Microanalysis Laboratory at University College Dublin, are within 0.4% of the calculated values, confirming  $\geq 95\%$  purity. As reported previously for related compounds,<sup>20</sup> fractional moles of ethyl acetate and/or water could not be prevented despite 24–72 h of drying in vacuum.

Cyclic voltammograms were recorded in anhydrous acetonitrile (Sigma-Aldrich), with 0.1 M tetrabutylammonium perchlorate (TBAP) as a supporting electrolyte, using a CH Instruments 600a electrochemical analyzer (Pico-Amp Booster and Faraday Cage). The experiments were carried out at room temperature. A three-electrode cell consisting of a glassy carbon working electrode, a platinum wire counter electrode, and an Ag/AgCl reference electrode was used. The glassy carbon electrode was polished with 0.3 μm alumina followed by 0.05 μm alumina between each experiment to remove any surface

contaminants. The scan rate was 0.1 V s<sup>-1</sup>. The concentration range of the ferrocene compounds was 1.0 mM in acetonitrile. The E<sup>0</sup> values obtained for the test samples were referenced relative to the ferrocene/ferrocenium redox couple.

**General Procedure for the Synthesis of *N*-(Ferrocenyl)-naphthoyl Dipeptide Ethyl Esters.** 6-Ferrocenyl-naphthalene-2-carboxylic acid was treated in DCM at 0 °C with 1.3 equiv of *N*-(3-dimethylaminopropyl)-*N'*-ethylcarbodiimide hydrochloride and 1.3 equiv of 1-hydroxybenzotriazole. After 30 min, an excess of triethylamine (5 mL) and 1 equiv of the corresponding dipeptide ethyl ester salt were added to the solution; the resulting mixture was raised to room temperature, and the reaction was allowed to proceed for 48 h. The reaction mixture was washed with water, and the DCM layer was then dried over MgSO<sub>4</sub>. The solvent was removed in vacuo to give a residue that was then purified by silica gel column flash chromatography, eluting with a 1:1 mixture of hexane/ethyl acetate.

***N*-(6-Ferrocenyl-2-naphthoyl)-glycine-glycine Ethyl Ester 2.** Orange solid (0.33 g, 83%); mp 179–180 °C; E<sup>0</sup> 47 mV vs Fc/Fc<sup>+</sup>. IR ν<sub>max</sub> (KBr): 3407, 3340, 1732, 1654, 1650, 1558, 1494, 1213 cm<sup>-1</sup>. UV-vis λ<sub>max</sub> CH<sub>3</sub>CN: 375 (ε 3485), 450 (ε 1497) nm. <sup>1</sup>H NMR (400 MHz, DMSO-*d*<sub>6</sub>): 8.94 (1H, t, *J* = 5.6 Hz, -CONH-), 8.46 (1H, s, ArH), 8.38 (1H, t, *J* = 5.6 Hz, -CONH-), 8.06 (1H, s, ArH), 7.92–7.97 (3H, m, ArH), 7.82 (1H, dd, *J* = 1.6 and 8.4 Hz, ArH), 4.96 {2H, t, *J* = 1.6 Hz, *ortho* on (η<sup>5</sup>-C<sub>5</sub>H<sub>4</sub>)}, 4.45 {2H, t, *J* = 1.6 Hz, *meta* on (η<sup>5</sup>-C<sub>5</sub>H<sub>4</sub>)}, 4.10 (2H, q, *J* = 7.2 Hz, -OCH<sub>2</sub>CH<sub>3</sub>), 4.05 (5H, s, η<sup>5</sup>-C<sub>5</sub>H<sub>5</sub>), 3.98 (2H, d, *J* = 5.6 Hz, -NHCH<sub>2</sub>-), 3.87 (2H, d, *J* = 5.6 Hz, -NHCH<sub>2</sub>-), 1.20 (3H, t, *J* = 7.2 Hz, -OCH<sub>2</sub>CH<sub>3</sub>); <sup>13</sup>C NMR (100 MHz, DMSO-*d*<sub>6</sub>): 169.8 (C=O), 169.6 (C=O), 166.5 (C=O), 138.8, 134.5, 130.6, 130.4, 128.7, 127.6, 127.3, 125.9, 124.6, 122.7, 84.0, 69.5, 69.4, 66.6, 60.4 (-ve DEPT), 42.5 (-ve DEPT), 40.7 (-ve DEPT), 14.0; HRMS (ESI<sup>+</sup>) *m/z* 499.1320 calcd. [M + H]<sup>+</sup>; found, 499.1296. Anal. (C<sub>27</sub>H<sub>26</sub>N<sub>2</sub>O<sub>4</sub>Fe) C, H, N.

***N*-(6-Ferrocenyl-2-naphthoyl)-glycine-L-leucine Ethyl Ester 3.** Orange solid (0.32 g, 58%); mp 160–161 °C; E<sup>0</sup> 60 mV vs Fc/Fc<sup>+</sup>; [α]<sub>D</sub><sup>20</sup> -12 (c 0.06 in CH<sub>3</sub>CN); IR ν<sub>max</sub> (neat) 3298, 2955, 1744, 1682, 1644, 1624, 1512, 1184 cm<sup>-1</sup>. UV-vis λ<sub>max</sub> (CH<sub>3</sub>CN): 370 (ε 3336), 445 (ε 1422) nm. <sup>1</sup>H NMR (400 MHz, DMSO-*d*<sub>6</sub>): 8.82 (1H, t, *J* = 5.6 Hz, -CONH-), 8.44 (1H, s, ArH), 8.34 (1H, d, *J* = 8.4 Hz, -CONH-), 8.06 (1H, s, ArH), 7.93–7.97 (3H, m, ArH), 7.82 (1H, dd, *J* = 1.2 and 8.4 Hz, ArH), 4.96 {2H, t, *J* = 2.0 Hz, *ortho* on (η<sup>5</sup>-C<sub>5</sub>H<sub>4</sub>)}, 4.45 {2H, t, *J* = 2.0 Hz, *meta* on (η<sup>5</sup>-C<sub>5</sub>H<sub>4</sub>)}, 4.30–4.35 (1H, m, -NHCH-), 4.07–4.13 (7H, m, -OCH<sub>2</sub>CH<sub>3</sub>, η<sup>5</sup>-C<sub>5</sub>H<sub>5</sub>), 3.93–3.99 (2H, m, -NHCH<sub>2</sub>-), 1.48–1.72 (3H, m, -CH<sub>2</sub>CH-), 1.19 (3H, t, *J* = 7.2 Hz, -OCH<sub>2</sub>CH<sub>3</sub>), 0.86–0.92 {6H, m, -CH(CH<sub>3</sub>)<sub>2</sub>}. <sup>13</sup>C NMR (100 MHz, DMSO-*d*<sub>6</sub>): 172.5 (C=O), 169.1 (C=O), 166.5 (C=O), 138.8, 134.5, 130.7, 130.5, 128.7, 127.5, 127.3, 125.9, 124.5, 122.7, 84.1, 69.4, 66.6, 60.4 (-ve DEPT), 50.3, 42.2 (-ve DEPT), 40.1 (-ve DEPT), 24.2, 22.7, 21.4, 14.0; HRMS (ESI<sup>+</sup>) *m/z* 555.1946 calcd. [M + H]<sup>+</sup>; found, 555.1931. Anal. (C<sub>31</sub>H<sub>34</sub>N<sub>2</sub>O<sub>4</sub>Fe) C, H, N.

***N*-(6-Ferrocenyl-2-naphthoyl)-glycine-L-phenylalanine Ethyl Ester 4.** Orange solid (0.15 g, 56%); mp 53–54 °C; E<sup>0</sup> 59 mV vs Fc/Fc<sup>+</sup>; [α]<sub>D</sub><sup>20</sup> +18 (c 0.06 in CH<sub>3</sub>CN); IR ν<sub>max</sub> (neat) 3290, 3062, 1735, 1640, 1521, 1298, 1209 cm<sup>-1</sup>. UV-vis λ<sub>max</sub> (CH<sub>3</sub>CN): 370 (ε 2894), 445 (ε 1242) nm. <sup>1</sup>H NMR (400 MHz, DMSO-*d*<sub>6</sub>): 8.86 (1H, t, *J* = 5.6 Hz, -CONH-), 8.43–8.47 (2H, m, -CONH-, ArH), 8.10 (1H, s, ArH), 7.97–8.00 (3H, m, ArH), 7.86 (1H, dd, *J* = 1.2 and 8.4 Hz, ArH), 7.23–7.33 (5H, m, -CH<sub>2</sub>Ph), 5.00 {2H, t, *J* = 1.6 Hz, *ortho* on (η<sup>5</sup>-C<sub>5</sub>H<sub>4</sub>)}, 4.49–4.56 {3H, m, -NHCH-, *meta* on (η<sup>5</sup>-C<sub>5</sub>H<sub>4</sub>)}, 3.93–4.10 (9H, m, -OCH<sub>2</sub>CH<sub>3</sub>, η<sup>5</sup>-C<sub>5</sub>H<sub>5</sub>, -NHCH<sub>2</sub>-), 2.98–3.13 (2H, m, -CH<sub>2</sub>Ph), 1.15 (3H, t, *J* = 7.2 Hz, -OCH<sub>2</sub>CH<sub>3</sub>). <sup>13</sup>C NMR (100 MHz, DMSO-*d*<sub>6</sub>): 171.4 (C=O), 169.1 (C=O), 166.4 (C=O), 138.8, 136.9, 134.5, 130.7, 130.4, 129.1, 128.7, 128.2, 127.5, 127.3, 126.6, 125.9, 124.5, 122.7, 84.1, 69.4, 66.6, 60.5 (-ve DEPT), 53.7, 42.3 (-ve DEPT), 36.9 (-ve DEPT), 14.1; HRMS (ESI<sup>+</sup>) *m/z* 588.1711 calcd. [M]<sup>+</sup>; found, 588.1693. Anal. (C<sub>34</sub>H<sub>32</sub>N<sub>2</sub>O<sub>4</sub>Fe·0.6C<sub>4</sub>H<sub>8</sub>O<sub>2</sub>·0.15H<sub>2</sub>O) C, H, N.

***N*-(6-Ferrocenyl-2-naphthoyl)-L-alanine-glycine Ethyl Ester 5.** See ref 8.

***N*-(6-Ferrocenyl-2-naphthoyl)-L-alanine-L-alanine Ethyl Ester 6.** See ref 8.

***N*-(6-Ferrocenyl-2-naphthoyl)-L-alanine-L-leucine Ethyl Ester 7.** Orange solid (0.10 g, 23%); mp 73–74 °C; E<sup>0</sup> 60 mV vs Fc/Fc<sup>+</sup>; [α]<sub>D</sub><sup>20</sup> +29 (c 0.06 in CH<sub>3</sub>CN); IR ν<sub>max</sub> (neat) 3282, 3089, 1734, 1633, 1530, 1187 cm<sup>-1</sup>. UV-vis λ<sub>max</sub> (CH<sub>3</sub>CN): 370 (ε 3064), 445 (ε 1298) nm. <sup>1</sup>H NMR (400 MHz, DMSO-*d*<sub>6</sub>): 8.58 (1H, d, *J* = 7.2 Hz, -CONH-), 8.46 (1H, s, ArH), 8.29 (1H, d, *J* = 7.2 Hz, -CONH-), 8.05 (1H, s, ArH), 7.90–7.97 (3H, m, ArH), 7.79–7.86 (1H, m, ArH), 4.95 {2H, t, *J* = 1.6 Hz, *ortho* on (η<sup>5</sup>-C<sub>5</sub>H<sub>4</sub>)}, 4.60 (1H, qt, *J* = 7.2 Hz, -NHCH-), 4.44 {2H, t, *J* = 1.6 Hz, *meta* on (η<sup>5</sup>-C<sub>5</sub>H<sub>4</sub>)}, 4.26–4.32 (1H, m, -NHCH-), 4.00–4.14 (7H, m, -OCH<sub>2</sub>CH<sub>3</sub>, η<sup>5</sup>-C<sub>5</sub>H<sub>5</sub>), 1.48–1.73 (3H, m, -CH<sub>2</sub>CH-), 1.39 (3H, d, *J* = 7.2 Hz, -CH<sub>3</sub>), 1.17 (3H, t, *J* = 7.2 Hz, -OCH<sub>2</sub>CH<sub>3</sub>), 0.86–0.93 {6H, m, -CH(CH<sub>3</sub>)<sub>2</sub>}. <sup>13</sup>C NMR (100 MHz, DMSO-*d*<sub>6</sub>): 172.7 (C=O), 172.4 (C=O), 166.0 (C=O), 138.7, 134.5, 130.6, 130.5, 128.7, 127.6, 127.2, 125.9, 124.7, 122.7, 84.1, 69.4, 66.6, 60.4 (-ve DEPT), 50.4, 48.6, 39.7 (-ve DEPT), 24.2, 22.7, 21.4, 17.9, 14.0; HRMS (ESI<sup>+</sup>) *m/z* 569.2103 calcd. [M + H]<sup>+</sup>; found, 569.2095. Anal. (C<sub>32</sub>H<sub>36</sub>N<sub>2</sub>O<sub>4</sub>Fe) C, H, N.

***N*-(6-Ferrocenyl-2-naphthoyl)-L-alanine-L-phenylalanine Ethyl Ester 8.** Orange solid (0.12 g, 23%); mp 75 °C; E<sup>0</sup> 59 mV vs Fc/Fc<sup>+</sup>; [α]<sub>D</sub><sup>20</sup> +36 (c 0.06 in CH<sub>3</sub>CN); IR ν<sub>max</sub> (neat) 3282, 2963, 1736, 1634, 1526, 1260, 1187 cm<sup>-1</sup>. UV-vis λ<sub>max</sub> (CH<sub>3</sub>CN): 370 (ε 2774), 445 (ε 1188) nm. <sup>1</sup>H NMR (400 MHz, DMSO-*d*<sub>6</sub>): 8.58 (1H, d, *J* = 7.2 Hz, -CONH-), 8.45 (1H, s, ArH), 8.36 (1H, d, *J* = 7.2 Hz, -CONH-), 8.06 (1H, s, ArH), 7.93–7.97 (3H, m, ArH), 7.82 (1H, dd, *J* = 1.6 and 8.4 Hz, ArH), 7.17–7.25 (5H, m, -CH<sub>2</sub>Ph), 4.96 {2H, t, *J* = 2.0 Hz, *ortho* on (η<sup>5</sup>-C<sub>5</sub>H<sub>4</sub>)}, 4.60 (1H, qt, *J* = 7.2 Hz, -NHCH-), 4.43–4.50 {3H, m, -NHCH-, *meta* on (η<sup>5</sup>-C<sub>5</sub>H<sub>4</sub>)}, 4.00–4.08 (7H, m, -OCH<sub>2</sub>CH<sub>3</sub>, η<sup>5</sup>-C<sub>5</sub>H<sub>5</sub>), 2.96–3.07 (2H, m, -CH<sub>2</sub>Ph), 1.36 (3H, d, *J* = 7.2 Hz, -CH<sub>3</sub>), 1.10 (3H, t, *J* = 7.2 Hz, -OCH<sub>2</sub>CH<sub>3</sub>). <sup>13</sup>C NMR (100 MHz, DMSO-*d*<sub>6</sub>): 172.6 (C=O), 171.3 (C=O), 166.0 (C=O), 138.8, 137.0, 134.5, 130.6, 130.4, 129.1, 128.7, 128.2, 127.6, 127.2, 126.5, 125.9, 124.7, 122.7, 84.1, 69.4, 66.6, 60.4 (-ve DEPT), 53.7, 48.6, 36.6 (-ve DEPT), 17.8, 14.1; HRMS (ESI<sup>+</sup>) *m/z* 602.1868 calcd. [M]<sup>+</sup>; found, 602.1841. Anal. (C<sub>35</sub>H<sub>34</sub>N<sub>2</sub>O<sub>4</sub>Fe·0.45C<sub>4</sub>H<sub>8</sub>O<sub>2</sub>) C, H, N.

***N*-(6-Ferrocenyl-2-naphthoyl)-glycine-D-alanine Ethyl Ester 9.** Orange solid (0.19 g, 41%); mp 73–74 °C; E<sup>0</sup> 63 mV vs Fc/Fc<sup>+</sup>; [α]<sub>D</sub><sup>20</sup> +5 (c 0.05 in CH<sub>3</sub>CN); IR ν<sub>max</sub> (neat): 3290, 3084, 1733, 1640, 1529, 1450, 1206 cm<sup>-1</sup>. UV-vis λ<sub>max</sub> CH<sub>3</sub>CN: 370 (ε 3048), 445 (ε 1288) nm. <sup>1</sup>H NMR (400 MHz, DMSO-*d*<sub>6</sub>): 8.83 (1H, t, *J* = 5.6 Hz, -CONH-), 8.44 (1H, s, ArH), 8.39 (1H, d, *J* = 7.2 Hz, -CONH-), 8.06 (1H, s, ArH), 7.94–7.97 (3H, m, ArH), 7.83 (1H, dd, *J* = 1.6 and 8.4 Hz, ArH), 4.97 {2H, t, *J* = 2.0 Hz, *ortho* on (η<sup>5</sup>-C<sub>5</sub>H<sub>4</sub>)}, 4.46 {2H, t, *J* = 2.0 Hz, *meta* on (η<sup>5</sup>-C<sub>5</sub>H<sub>4</sub>)}, 4.31 (1H, qt, *J* = 7.2 Hz, -NHCH-), 3.91–4.14 (9H, m, -OCH<sub>2</sub>CH<sub>3</sub>, η<sup>5</sup>-C<sub>5</sub>H<sub>5</sub>, -NHCH<sub>2</sub>-), 1.31 (3H, d, *J* = 7.2 Hz, -CH<sub>3</sub>), 1.20 (3H, t, *J* = 7.2 Hz, -OCH<sub>2</sub>CH<sub>3</sub>). <sup>13</sup>C NMR (100 MHz, DMSO-*d*<sub>6</sub>): 172.5 (C=O), 168.9 (C=O), 166.4 (C=O), 138.8, 134.5, 130.7, 130.5, 128.9, 127.5, 127.3, 125.9, 124.5, 122.7, 84.1, 69.4, 66.6, 60.4 (-ve DEPT), 47.7, 42.2 (-ve DEPT), 17.1, 14.0; HRMS (ESI<sup>+</sup>) *m/z* 512.1398 calcd. [M]<sup>+</sup>; found, 512.1397. Anal. (C<sub>28</sub>H<sub>28</sub>N<sub>2</sub>O<sub>4</sub>Fe·0.45C<sub>4</sub>H<sub>8</sub>O<sub>2</sub>) C, H, N.

***N*-(2-Naphthoyl)-glycine-glycine Ethyl Ester 10.** 2-Naphthoic acid (0.18 g, 1.0 mmol) was treated in DCM at 0 °C with *N*-(3-dimethylaminopropyl)-*N'*-ethylcarbodiimide hydrochloride (0.25 g, 1.3 mmol) and 1-hydroxybenzotriazole (0.18 g, 1.3 mmol). After 30 min, an excess of triethylamine (5 mL) and glycine-glycine ethyl ester hydrochloride (0.20 g, 1.0 mmol) was added to the solution; the resulting mixture was raised to room temperature, and the reaction was allowed to proceed for 48 h. The reaction mixture was washed with water, and the DCM layer was then dried over MgSO<sub>4</sub>. The solvent was removed in vacuo to give a residue that was then purified by silica gel flash chromatography, eluting with a 1:1 mixture of hexane/ethyl acetate. The title compound was obtained as a white solid (0.28 g, 89%); mp 128–129 °C; IR ν<sub>max</sub> (neat) 3264, 3056, 1738, 1646, 1633, 1619, 1546, 1203 cm<sup>-1</sup>. <sup>1</sup>H NMR (400 MHz, DMSO-*d*<sub>6</sub>): 9.05 (1H, t, *J* = 5.6 Hz, -CONH-), 8.58 (1H, s, -ArH), 8.46 (1H, t, *J* = 5.6 Hz, -CONH-), 8.10–8.02 (4H, m, -ArH), 7.71–7.64 (2H, m, -ArH), 4.15 (2H, q, *J* = 7.2 Hz, -OCH<sub>2</sub>CH<sub>3</sub>), 4.04 (2H, d, *J* = 5.6 Hz, -NHCH<sub>2</sub>-), 3.92 (2H, d, *J* = 5.6 Hz, -NHCH<sub>2</sub>-), 1.25 (3H, t, *J* = 7.2 Hz, -OCH<sub>2</sub>CH<sub>3</sub>). <sup>13</sup>C NMR (100 MHz, DMSO-*d*<sub>6</sub>): 169.8 (C=O), 169.6



(C=O), 166.5 (C=O), 134.2, 132.1, 131.3, 128.8, 127.8, 127.7, 127.62, 127.59, 126.7, 124.2, 60.4 (-ve DEPT), 42.5 (-ve DEPT), 40.7 (-ve DEPT), 14.0; HRMS (ESI<sup>+</sup>) *m/z* 315.1345 calcd. [M + H]<sup>+</sup>; found, 315.1360. Anal. (C<sub>17</sub>H<sub>18</sub>N<sub>2</sub>O<sub>4</sub>) C, H, N.

**N-(6-Ferrocenyl-2-naphthoyl)-glycine-β-alanine Ethyl Ester 11.** Orange solid (0.20 g, 43%); mp 148–149 °C; E<sup>0</sup> 61 mV vs. Fc/Fc<sup>+</sup>. IR ν<sub>max</sub> (neat): 3312, 3084, 1728, 1677, 1639, 1625, 1538, 1185 cm<sup>-1</sup>. UV-vis λ<sub>max</sub> CH<sub>3</sub>CN: 370 (ε 3006), 450 (ε 1288) nm. <sup>1</sup>H NMR (400 MHz, acetone-*d*<sub>6</sub>): 8.32 (1H, s, ArH), 8.01 (1H, t, J = 5.6 Hz, -CONH-), 7.93 (1H, s, ArH), 7.78–7.86 (3H, m, ArH), 7.71 (1H, dd, J = 1.6 and 8.4 Hz, ArH), 7.34 (1H, br. s, -CONH-), 4.79 {2H, t, J = 2.0 Hz, *ortho* on (η<sup>5</sup>-C<sub>5</sub>H<sub>4</sub>)}, 4.30 {2H, t, J = 2.0 Hz, *meta* on (η<sup>5</sup>-C<sub>5</sub>H<sub>4</sub>)}, 3.91–3.97 (9H, m, -OCH<sub>2</sub>CH<sub>3</sub>, η<sup>5</sup>-C<sub>5</sub>H<sub>5</sub>, -NHCH<sub>2</sub>-), 3.35 (2H, q, J = 6.8 Hz, -CH<sub>2</sub>CH<sub>2</sub>-), 2.40 (2H, t, J = 6.8 Hz, -CH<sub>2</sub>CH<sub>2</sub>-), 1.06 (3H, t, J = 7.2 Hz, -OCH<sub>2</sub>CH<sub>3</sub>). <sup>13</sup>C NMR (100 MHz, acetone-*d*<sub>6</sub>): 172.2 (C=O), 169.9 (C=O), 167.7 (C=O), 140.3, 136.1, 132.2, 131.7, 129.7, 128.5, 128.4, 126.9, 125.3, 123.9, 85.4, 70.4, 70.3, 67.6, 60.8 (-ve DEPT), 44.1 (-ve DEPT), 35.9 (-ve DEPT), 34.9 (-ve DEPT), 14.5; HRMS (ESI<sup>+</sup>) *m/z* 512.1398 calcd. [M]<sup>++</sup>; found, 512.1410. Anal. (C<sub>28</sub>H<sub>28</sub>N<sub>2</sub>O<sub>4</sub>Fe·0.2C<sub>4</sub>H<sub>8</sub>O<sub>2</sub>·0.1H<sub>2</sub>O) C, H, N.

**N-(6-Ferrocenyl-2-naphthoyl)-glycine-γ-aminobutyric Acid Ethyl Ester 12.** Orange solid (0.18 g, 38%); mp 140–142 °C; E<sup>0</sup> 65 mV vs. Fc/Fc<sup>+</sup>. IR ν<sub>max</sub> (neat): 3374, 3246, 3082, 1704, 1672, 1638, 1566, 1538 cm<sup>-1</sup>. UV-vis λ<sub>max</sub> CH<sub>3</sub>CN: 375 (ε 3070), 450 (ε 1312) nm. <sup>1</sup>H NMR (400 MHz, acetone-*d*<sub>6</sub>): 8.32 (1H, s, ArH), 8.01 (1H, t, J = 5.6 Hz, -CONH-), 7.94 (1H, s, ArH), 7.78–7.86 (3H, m, ArH), 7.71 (1H, dd, J = 1.6 and 8.4 Hz, ArH), 7.33 (1H, br. s, -CONH-), 4.78 {2H, t, J = 2.0 Hz, *ortho* on (η<sup>5</sup>-C<sub>5</sub>H<sub>4</sub>)}, 4.30 {2H, t, J = 2.0 Hz, *meta* on (η<sup>5</sup>-C<sub>5</sub>H<sub>4</sub>)}, 3.90–3.96 (9H, m, -OCH<sub>2</sub>CH<sub>3</sub>, η<sup>5</sup>-C<sub>5</sub>H<sub>5</sub>, -NHCH<sub>2</sub>-), 3.15 (2H, q, J = 6.8 Hz, -CH<sub>2</sub>CH<sub>2</sub>-), 2.22 (2H, t, J = 7.2 Hz, -CH<sub>2</sub>CH<sub>2</sub>CH<sub>2</sub>-), 1.66 (2H, qt, J = 7.2 Hz, -CH<sub>2</sub>CH<sub>2</sub>CH<sub>2</sub>-), 1.06 (3H, t, J = 7.2 Hz, -OCH<sub>2</sub>CH<sub>3</sub>). <sup>13</sup>C NMR (100 MHz, acetone-*d*<sub>6</sub>): 173.5 (C=O), 169.8 (C=O), 167.7 (C=O), 140.3, 136.1, 132.2, 131.8, 129.7, 128.5, 128.4, 126.9, 125.4, 123.9, 85.4, 70.4, 70.3, 67.6, 60.6 (-ve DEPT), 44.1 (-ve DEPT), 39.1 (-ve DEPT), 32.0 (-ve DEPT), 25.8 (-ve DEPT), 14.5; HRMS (ESI<sup>+</sup>) *m/z* 527.1633 calcd. [M + H]<sup>+</sup>; found, 527.1622. Anal. (C<sub>29</sub>H<sub>30</sub>N<sub>2</sub>O<sub>4</sub>Fe) C, H, N.

**N-(6-Ferrocenyl-2-naphthoyl)-β-alanine-glycine Ethyl Ester 13.** Orange solid (0.16 g, 34%); mp 171–172 °C; E<sup>0</sup> 60 mV vs. Fc/Fc<sup>+</sup>; IR ν<sub>max</sub> (neat) 3357, 3282, 3073, 1735, 1678, 1633, 1600, 1540, 1214 cm<sup>-1</sup>. UV-vis λ<sub>max</sub> CH<sub>3</sub>CN: 370 (ε 2758), 450 (ε 1154) nm. <sup>1</sup>H NMR (400 MHz, acetone-*d*<sub>6</sub>): 8.28 (1H, s, ArH), 7.92 (1H, s, ArH), 7.76–7.84 (4H, m, -CONH-, ArH), 7.69 (1H, dd, J = 1.6 and 8.8 Hz, ArH), 7.51 (1H, br. s, -CONH-), 4.78 {2H, t, J = 1.6 Hz, *ortho* on (η<sup>5</sup>-C<sub>5</sub>H<sub>4</sub>)}, 4.29 {2H, t, J = 1.6 Hz, *meta* on (η<sup>5</sup>-C<sub>5</sub>H<sub>4</sub>)}, 4.02 (2H, q, J = 7.2 Hz, -OCH<sub>2</sub>CH<sub>3</sub>), 3.92 (5H, s, η<sup>5</sup>-C<sub>5</sub>H<sub>5</sub>), 3.84 (2H, d, J = 5.6 Hz, -NHCH<sub>2</sub>-), 3.59 (2H, q, J = 6.4 Hz, -CH<sub>2</sub>CH<sub>2</sub>-), 2.47 (2H, t, J = 6.4 Hz, -CH<sub>2</sub>CH<sub>2</sub>-), 1.09 (3H, t, J = 7.2 Hz, -OCH<sub>2</sub>CH<sub>3</sub>). <sup>13</sup>C NMR (100 MHz, acetone-*d*<sub>6</sub>): 172.4 (C=O), 170.8 (C=O), 167.3 (C=O), 140.0, 135.9, 132.4, 132.2, 129.6, 128.4, 128.1, 126.9, 125.4, 123.9, 85.5, 70.4, 70.3, 67.6, 61.4 (-ve DEPT), 41.7 (-ve DEPT), 37.2 (-ve DEPT), 36.3 (-ve DEPT), 14.5; HRMS (ESI<sup>+</sup>) *m/z* 512.1398 calcd. [M]<sup>++</sup>; found, 512.1384. Anal. (C<sub>28</sub>H<sub>28</sub>N<sub>2</sub>O<sub>4</sub>Fe·0.25C<sub>4</sub>H<sub>8</sub>O<sub>2</sub>·0.1H<sub>2</sub>O) C, H, N.

**N-(6-Ferrocenyl-2-naphthoyl)-γ-aminobutyric Acid-Glycine Ethyl Ester 14.** Orange solid (0.14 g, 27%); mp 150–151 °C; E<sup>0</sup> 60 mV vs. Fc/Fc<sup>+</sup>. IR ν<sub>max</sub> (neat): 3256, 3081, 1750, 1656, 1634, 1622, 1575, 1551, 1201 cm<sup>-1</sup>. UV-vis λ<sub>max</sub> CH<sub>3</sub>CN: 370 (ε 2700), 450 (ε 1112) nm. <sup>1</sup>H NMR (400 MHz, DMSO-*d*<sub>6</sub>): 8.67 (1H, t, J = 5.6 Hz, -CONH-), 8.45 (1H, s, ArH), 8.38 (1H, t, J = 6.0 Hz, -CONH-), 8.11 (1H, s, ArH), 7.94–8.01 (3H, m, ArH), 7.87 (1H, dd, J = 1.6 and 8.4 Hz, ArH), 5.02 {2H, t, J = 2.0 Hz, *ortho* on (η<sup>5</sup>-C<sub>5</sub>H<sub>4</sub>)}, 4.50 {2H, t, J = 2.0 Hz, *meta* on (η<sup>5</sup>-C<sub>5</sub>H<sub>4</sub>)}, 4.08–4.17 (7H, m, -OCH<sub>2</sub>CH<sub>3</sub>, η<sup>5</sup>-C<sub>5</sub>H<sub>5</sub>), 3.88 (2H, d, J = 5.6 Hz, -NHCH<sub>2</sub>-), 3.37–3.42 (2H, m, -CH<sub>2</sub>CH<sub>2</sub>CH<sub>2</sub>-), 2.30 (2H, t, J = 7.2 Hz, -CH<sub>2</sub>CH<sub>2</sub>CH<sub>2</sub>-), 1.87 (2H, qt, J = 7.2 Hz, -CH<sub>2</sub>CH<sub>2</sub>CH<sub>2</sub>-), 1.25 (3H, t, J = 7.2 Hz, -OCH<sub>2</sub>CH<sub>3</sub>). <sup>13</sup>C NMR (100 MHz, DMSO-*d*<sub>6</sub>): 172.5 (C=O), 170.0 (C=O), 166.2 (C=O), 138.6, 134.4, 131.1, 130.7, 128.7, 127.3,

127.2, 125.9, 124.5, 122.7, 84.1, 69.4, 66.6, 60.3 (-ve DEPT), 40.6 (-ve DEPT), 39.0 (-ve DEPT), 32.7 (-ve DEPT), 25.3 (-ve DEPT), 14.0; HRMS (ESI<sup>+</sup>) *m/z* 527.1633 calcd. [M + H]<sup>+</sup>; found, 527.1611. Anal. (C<sub>29</sub>H<sub>30</sub>N<sub>2</sub>O<sub>4</sub>Fe) C, H, N.

**N-(6-Ferrocenyl-2-naphthoyl)-glycine-sarcosine Ethyl Ester 15.** Orange solid (0.20 g, 43%); mp 64–65 °C; E<sup>0</sup> 63 mV vs. Fc/Fc<sup>+</sup>. IR ν<sub>max</sub> (neat): 3300, 2928, 1739, 1626, 1507, 1480, 1200 cm<sup>-1</sup>. UV-vis λ<sub>max</sub> CH<sub>3</sub>CN: 370 (ε 2670), 450 (ε 1098) nm. <sup>1</sup>H NMR (400 MHz, DMSO-*d*<sub>6</sub>): 8.72, 7.45–7.51 (1H, t, J = 5.6 Hz, m, -CONH-, rotamers), 8.44–8.48 (1H, m, ArH), 8.05–8.07 (1H, m, ArH), 7.81–7.98 (4H, m, ArH), 4.95–4.97 {2H, m, *ortho* on (η<sup>5</sup>-C<sub>5</sub>H<sub>4</sub>)}, 4.44–4.46 {2H, m, *meta* on (η<sup>5</sup>-C<sub>5</sub>H<sub>4</sub>)}, 3.96–4.36 (11H, m, -OCH<sub>2</sub>CH<sub>3</sub>, η<sup>5</sup>-C<sub>5</sub>H<sub>5</sub>, Gly CH<sub>2</sub>, Sar CH<sub>2</sub>, rotamers), 3.12, 3.01, 2.88 (3H, s, br. s, Sar CH<sub>3</sub>, rotamers), 1.18–1.26 (3H, m, -OCH<sub>2</sub>CH<sub>3</sub>, rotamers). <sup>13</sup>C NMR (100 MHz, DMSO-*d*<sub>6</sub>): 171.2 (C=O), 169.2 (C=O), 166.4 (C=O), 138.8, 134.5, 133.4, 130.7, 128.7, 128.2, 127.4, 125.9, 124.4, 122.7, 84.1, 69.4, 66.6, 60.9 (-ve DEPT), 60.5 (-ve DEPT), 49.3 (-ve DEPT), 40.8 (-ve DEPT), 35.2, 34.5, 30.7, 14.0; HRMS (ESI<sup>+</sup>) *m/z* 512.1398 calcd. [M]<sup>++</sup>; found, 512.1398. Anal. (C<sub>28</sub>H<sub>28</sub>N<sub>2</sub>O<sub>4</sub>Fe) C, H, N.

**N-(6-Ferrocenyl-2-naphthoyl)-sarcosine-glycine Ethyl Ester 16.** Red solid (0.18 g, 35%); mp 66–67 °C; E<sup>0</sup> 55 mV vs. Fc/Fc<sup>+</sup>. IR ν<sub>max</sub> (neat): 3291, 2930, 1745, 1677, 1623, 1507, 1396, 1196 cm<sup>-1</sup>. UV-vis λ<sub>max</sub> CH<sub>3</sub>CN: 370 (ε 2492), 450 (ε 988) nm. <sup>1</sup>H NMR (600 MHz, DMSO-*d*<sub>6</sub>): 8.61, 8.53 (1H, 2xbr. s, -CONH-, rotamers), 8.11 (1H, s, ArH), 7.95–8.03 (3H, m, ArH), 7.87 (1H, d, J = 8.4 Hz, ArH), 7.54–7.58 (1H, m, ArH), 5.01 {2H, t, J = 1.8 Hz, *ortho* on (η<sup>5</sup>-C<sub>5</sub>H<sub>4</sub>)}, 4.49–4.52 {2H, m, *meta* on (η<sup>5</sup>-C<sub>5</sub>H<sub>4</sub>)}, 3.96–4.26 (11H, m, -OCH<sub>2</sub>CH<sub>3</sub>, η<sup>5</sup>-C<sub>5</sub>H<sub>5</sub>, Gly CH<sub>2</sub>, Sar CH<sub>2</sub>, rotamers), 3.08 (3H, s, Sar CH<sub>3</sub>), 1.27 (3H, t, J = 7.2 Hz, -OCH<sub>2</sub>CH<sub>3</sub>). <sup>13</sup>C NMR (150 MHz, DMSO-*d*<sub>6</sub>): 171.1 (C=O), 169.7 (C=O), 168.6 (C=O), 138.2, 133.4, 132.4, 130.7, 128.3, 126.5, 125.9, 125.0, 124.8, 122.8, 84.1, 69.41, 69.38, 66.6, 60.5 (-ve DEPT), 59.7 (-ve DEPT), 53.9 (-ve DEPT), 49.7 (-ve DEPT), 40.7 (-ve DEPT), 39.3, 34.1, 14.1; HRMS (ESI<sup>+</sup>) *m/z* 512.1398 calcd. [M]<sup>++</sup>; found, 512.1399. Anal. (C<sub>28</sub>H<sub>28</sub>N<sub>2</sub>O<sub>4</sub>Fe·0.2C<sub>4</sub>H<sub>8</sub>O<sub>2</sub>·0.25H<sub>2</sub>O) C, H, N.

**N-(6-Ferrocenyl-2-naphthoyl)-sarcosine-sarcosine Ethyl Ester 17.** Orange solid (0.05 g, 12%); mp 68–69 °C; E<sup>0</sup> 58 mV vs. Fc/Fc<sup>+</sup>. IR ν<sub>max</sub> (neat): 2926, 1739, 1663, 1626, 1479, 1394, 1198 cm<sup>-1</sup>. UV-vis λ<sub>max</sub> CH<sub>3</sub>CN: 370 (ε 2106), 450 (ε 836) nm. <sup>1</sup>H NMR (600 MHz, DMSO-*d*<sub>6</sub>): 8.08–8.11 (1H, m, ArH), 7.86–8.02 (4H, m, ArH), 7.54, 7.42–7.46 (1H, d, J = 8.4 Hz, m, ArH, rotamers), 5.01 {2H, s, *ortho* on (η<sup>5</sup>-C<sub>5</sub>H<sub>4</sub>)}, 3.87–4.51 {13H, *meta* on (η<sup>5</sup>-C<sub>5</sub>H<sub>4</sub>), -OCH<sub>2</sub>CH<sub>3</sub>, η<sup>5</sup>-C<sub>5</sub>H<sub>5</sub>, Sar CH<sub>2</sub>, Sar CH<sub>2</sub>, rotamers}, 3.03–3.16 (3H, m, Sar CH<sub>3</sub>, rotamers), 2.88–3.01 (3H, m, Sar CH<sub>3</sub>, rotamers), 1.24–1.32, 1.00 (3H, m, s, J = 7.2 Hz, -OCH<sub>2</sub>CH<sub>3</sub>, rotamers). <sup>13</sup>C NMR (150 MHz, DMSO-*d*<sub>6</sub>): 171.0 (C=O), 169.1 (C=O), 168.1 (C=O), 138.1, 133.4, 132.5, 130.3, 128.2, 127.5, 126.3, 125.9, 124.7, 122.8, 84.2, 69.40, 69.38, 66.6, 60.58 (-ve DEPT), 60.54 (-ve DEPT), 52.48 (-ve DEPT), 49.60 (-ve DEPT), 49.23 (-ve DEPT), 48.36 (-ve DEPT), 38.34, 35.19, 34.47, 34.35, 14.1; HRMS (ESI<sup>+</sup>) *m/z* 526.1555 calcd. [M]<sup>++</sup>; found, 526.1536. Anal. (C<sub>29</sub>H<sub>30</sub>N<sub>2</sub>O<sub>4</sub>Fe·0.5C<sub>4</sub>H<sub>8</sub>O<sub>2</sub>) C, H, N.

**Biological Assays: Cell Lines.** Sk-Mel-28 was obtained from the Department of Developmental Therapeutics, National Cancer Institute (NCI) and H1299 from the American Tissue Culture Centre (ATCC). Cell lines were grown in RPMI-1640 supplemented with 10% fetal calf serum (FCS) at 37 °C in a 5% CO<sub>2</sub> humidified chamber.

**In Vitro Proliferation Assays.** Cells in the exponential phase of growth were harvested by trypsinization, and a cell suspension of 1 × 10<sup>4</sup> cells/mL was prepared in fresh culture medium. The cell suspension (100 μL) was added to a flat bottom 96-well plate (Costar, 3599), plates were agitated gently in order to ensure even dispersion of cells over the surface of the wells, and then cells were incubated for an initial 24 h in a 37 °C, 5% CO<sub>2</sub> incubator to allow cell attachment to the wells. A 10 mM stock solution of a test sample was prepared in dimethyl sulfoxide; dilute solutions of the test sample were prepared at 2X final concentration by spiking the cell culture medium with a calculated amount of the stock solution. Then, 100 μL aliquot of each dilute solution was added to each well of the plate, the plate

was gently agitated, and then incubated at 37 °C, 5% CO<sub>2</sub> for 5–6 days, until cell confluency reached 80–90%. Assessment of cell survival in the presence of the compounds 1–17 was determined by the acid phosphatase assay.<sup>21</sup> The acid phosphatase assay is highly sensitive and is easier to perform than the neutral red assay as it involves fewer steps and fewer reagents. It is also more convenient than the MTT assay because of the inherent problem of removal of the medium from the insoluble crystals. The reproducibility between replicate wells is excellent in the acid phosphatase assay, and in many cases, it has been shown to be better than the neutral red assay and the MTT assay. The percentage cell growth in the presence of each compound was determined relative to the control cells. The concentration of compounds causing 50% growth inhibition (IC<sub>50</sub> of the compound) was determined using CalcuSyn (Biosoft, UK).

**Cell Cycle Assays.** H1299 cells were plated at a density of 2.5 × 10<sup>4</sup> cells/well in 24-well plates, in RPMI-1640 media containing 10% FCS. After 24 h, the cells were treated with the test compound. Dimethyl sulfoxide (DMSO) control wells were included in each assay. After 48 and 72 h, the media was collected into microcentrifuge tubes, and the wells were washed with PBS, which was also collected. Cells were trypsinized and added to the media collected for each sample. The tubes were centrifuged at 300g for 5 min, and the media were aspirated. The cell pellets were resuspended in PBS, and each cell suspension was transferred to a well of a round bottomed 96 well plate. The plate was centrifuged at 450g for 5 min and the supernatant aspirated leaving approximately 20 μL in each well. The remaining volume was used to resuspend the cells, and 200 μL of ice cold 70% ethanol was added gradually to each well. The plates were then stored at 4 °C overnight. After fixing, the cells were stained according to the protocol for the Guava Cell Cycle assay. Cells were analyzed on Guava EasyCyte (Guava Technologies), and the data was analyzed using Modfit LT software (Verity).

**Statistical Analysis.** Analysis of the response to treatment was performed using Student's *t*-test (two-tailed with unequal variance), and *p*-value <0.05 was considered statistically significant.

**Guanine Oxidation Studies: Chemicals.** Guanine was purchased from Sigma-Aldrich. 8-Oxo-7,8-dihydroguanine was purchased from Cayman Chemicals. Deionized water was purified using an ELGA purelab ultrasystem to a specific resistance of greater than 18.2 MΩ cm. All other chemicals were of analytical grade and used without further purification. All buffers and HPLC mobile phases were filtered through a 47 mm, 0.45 μm polyvinylidene fluoride (PVDF) micropore filter (Sartorius Stedim Biotech) before use.

**Oxidation of Guanine.** Ten millimolar guanine prepared in 84% 50 mM ammonium acetate, 85 mM acetic acid buffer, and 16% 1 M NaOH were incubated with 1 mM iron(II) sulfate (FeSO<sub>4</sub>·6H<sub>2</sub>O) or 1 mM *N*-(6-ferrocenyl-2-naphthoyl)-glycine-glycine ethyl ester 2 and 0.5 M hydrogen peroxide (H<sub>2</sub>O<sub>2</sub>) at 37 °C with constant stirring. Aliquots of 100 μL were taken in duplicate at various incubation times. The reaction was quenched with 1 mL of cold ethanol. The solution was dried immediately under a stream of nitrogen gas. Samples were stored at –20 °C until further use. Prior to analysis they were redissolved in 1 mL of 84% 50 mM ammonium acetate, 85 mM acetic acid buffer, and 16% 1 M NaOH. Samples were injected in triplicate.

**HPLC-UV-EC Analysis of 8-oxoGua Formation.** For 8-oxoGua analysis, the HPLC System consisted of a Varian ProStar 230 solvent delivery module and a Varian ProStar 310 UV–vis detector. A Phenomenex Onyx Monolithic C18 reversed phase column (100 × 4.6 mm) with 1 cm guard column was used. The eluent comprised 1.2% acetonitrile (ACN) and 50 mM ammonium acetate and was adjusted to pH 4.6 with glacial acetic acid. It was run at a flow rate of 4 mL min<sup>–1</sup> with an injection volume of 20 μL. The column temperature was ambient, and 8-oxoGua formation was monitored using an electrochemical detector at a detection potential of +550 mV versus an Ag/AgCl reference electrode.

**Controlled Experiments.** Control incubations were performed with guanine to ensure that no artificial oxidation was caused by the reaction conditions. Each of the reagents was sequentially replaced with deionized water to ensure that none of them could generate

oxidative damage individually. The highest background reading for these controls is plotted as the baseline in Figures 3 and 4.

## ■ ASSOCIATED CONTENT

### 📄 Supporting Information

Preparation details and spectroscopic data of Boc-protected dipeptide ethyl esters 9a and 11a–17a; a table containing the elemental analysis data of the novel compounds 2–4 and 7-17. This material is available free of charge via the Internet at <http://pubs.acs.org>.

## ■ AUTHOR INFORMATION

### Corresponding Author

\*School of Chemical Sciences, Dublin City University, Glasnevin, Dublin 9, Ireland. Phone: + 353 1 700 5689. Fax: + 353 1 700 5503. E-mail: peter.kenny@dcu.ie.

### Notes

The authors declare no competing financial interest.

## ■ ACKNOWLEDGMENTS

Á.M. would like to thank the Embark Initiative and IRCSET for all their support. This research was partly supported by the Health Research Board, Grant Reference Number HRA/09/86. We thank Dr. M. Pryce for the provision of access to the potentiostat and E. Harvey for technical assistance.

## ■ ABBREVIATIONS USED

8-oxoGua, 8-oxo-7,8-dihydroguanine; β-Ala, β-alanine; D-Ala, D-alanine; ds-DNA, double stranded DNA; EDC, N-(3-dimethylaminopropyl)-N'-ethylcarbodiimide hydrochloride; Et<sub>3</sub>N, triethylamine; Fc, ferrocene; Fc<sup>+</sup>, ferricenium ion; FeSO<sub>4</sub>, iron(II) sulfate; H<sub>2</sub>O<sub>2</sub>, hydrogen peroxide; HO•, hydroxyl radical; HOBt, 1-hydroxybenzotriazole; MgSO<sub>4</sub>, magnesium sulfate; NSCLC, nonsmall cell lung cancer; Sar, sarcosine

## ■ REFERENCES

- (1) Fouda, M. F. R.; Abd-Elzاهر, M. M.; Abdelsamaia, R. A.; Labib, A. A. On the Medicinal Chemistry of Ferrocene. *Appl. Organomet. Chem.* **2007**, *21*, 613–625.
- (2) (a) Gasser, G.; Ott, I.; Metzler-Nolte, N. Organometallic Anticancer Compounds. *J. Med. Chem.* **2011**, *54*, 3–25. (b) Ornelas, C. Application of Ferrocene and its Derivatives in Cancer Research. *New J. Chem.* **2011**, *35*, 1973–1985.
- (3) (a) Plazuk, D.; Vessieres, A.; Hillard, E. A.; Buriez, O.; Labbe, E.; Pigeon, P.; Plamont, M. A.; Amatore, C.; Zakrzewski, J.; Jaouen, G. A [3]-Ferrocenophane Polyphenol Showing a Remarkable Antiproliferative Activity on Breast and Prostate Cancer Cell Lines. *J. Med. Chem.* **2009**, *52*, 4964–4967. (b) Gormen, M.; Plazuk, D.; Pigeon, P.; Hillard, E. A.; Plamont, M.-A.; Top, S.; Vessières, A.; Jaouen, G. Comparative Toxicity of [3]-Ferrocenophane and Ferrocene Moieties on Breast Cancer Cells. *Tetrahedron Lett.* **2010**, *51*, 118–120. (c) Gormen, M.; Pigeon, P.; Top, S.; Vessieres, A.; Plamont, M.-A.; Hillard, E. A.; Jaouen, G. Facile Synthesis and Strong Antiproliferative Activity of Disubstituted Diphenylmethylidene-[3]-Ferrocenophanes on Breast and Prostate Cancer Cell Lines. *MedChemComm* **2010**, *1*, 149–151.
- (4) (a) Goel, A.; Savage, D.; Alley, S. R.; Kelly, P. N.; O'Sullivan, D.; Mueller-Bunz, H.; Kenny, P. T. M. The Synthesis and Structural Characterization of Novel *N*-Meta-Ferrocenyl Benzoyl Dipeptide Esters: The X-ray Crystal Structure and *in vitro* Anticancer Activity of *N*-[Meta-Ferrocenyl]benzoyl-L-Alanine-Glycine Ethyl Ester. *J. Organomet. Chem.* **2007**, *692*, 1292–1299. (b) Corry, A. J.; Goel, A.; Alley, S. R.; Kelly, P. N.; O'Sullivan, D.; Savage, D.; Kenny, P. T. M. *N*-ortho-Ferrocenyl Benzoyl Dipeptide Esters: Synthesis, Structural

Characterization and *in vitro* Anticancer Activity of *N*-{Ortho-(Ferrocenyl)benzoyl}-Glycine-L-Alanine Ethyl Ester and *N*-{Ortho-(Ferrocenyl)benzoyl}-L-Alanine-Glycine Ethyl Ester. *J. Organomet. Chem.* **2007**, *692*, 1405–1410. (c) Corry, A. J.; O'Donovan, N.; Mooney, Á.; O'Sullivan, D.; Rai, D. K.; Kenny, P. T. M. Synthesis, Structural Characterization, *in vitro* Anti-Proliferative Effect and Cell Cycle Analysis of *N*-(Ferrocenyl)benzoyl Dipeptide Esters. *J. Organomet. Chem.* **2009**, *694*, 880–885. (d) Corry, A. J.; Mooney, Á.; O'Sullivan, D.; Kenny, P. T. M. Synthesis, Characterization and *in vitro* Anticancer Activity of *N*-(Ferrocenyl)benzoyl Tri- and Tetrapeptide Esters. *Inorg. Chim. Acta* **2009**, *362*, 2957–2961.

(5) Neuse, E. W. Macromolecular Ferrocene Compounds as Cancer Drug Models. *J. Inorg. Organomet. Polym. Mater.* **2005**, *15*, 3–32.

(6) Tabbi, G.; Cassino, C.; Cavigiolo, G.; Colangelo, D.; Ghiglia, A.; Viano, I.; Osella, D. Water Stability and Cytotoxic Activity Relationship of a Series of Ferricenium Derivatives. ESR Insights on the Radical Production During the Degradation Process. *J. Med. Chem.* **2002**, *45*, 5786–5796.

(7) Trachootham, D.; Alexandre, J.; Huang, P. Targeting Cancer Cells by ROS-Mediated Mechanisms: a Radical Therapeutic Approach? *Nat. Rev. Drug Discovery* **2009**, *8*, 579–591.

(8) Mooney, Á.; Corry, A. J.; O'Sullivan, D.; Rai, D. K.; Kenny, P. T. M. The Synthesis, Structural Characterization and *in vitro* Anticancer Activity of Novel *N*-(3-Ferrocenyl-2-Naphthoyl) Dipeptide Ethyl Esters and Novel *N*-(6-Ferrocenyl-2-Naphthoyl) Dipeptide Ethyl Esters. *J. Organomet. Chem.* **2009**, *694*, 886–894.

(9) Mooney, Á.; Corry, A. J.; Ni Ruairc, C.; Mahgoub, T.; O'Sullivan, D.; O'Donovan, N.; Crown, J.; Varughese, S.; Draper, S. M.; Rai, D. K.; Kenny, P. T. M. Synthesis, Characterisation and Biological Evaluation of *N*-(Ferrocenyl)naphthoyl Amino Acid Esters as Anticancer Agents. *Dalton Trans.* **2010**, *39*, 8228–8239.

(10) Adessi, C.; Soto, C. Converting a Peptide into a Drug: Strategies to Improve Stability and Bioavailability. *Curr. Med. Chem.* **2002**, *9*, 963–978.

(11) Eustace, A. J.; Crown, J.; Clynes, M.; O'Donovan, N. Preclinical Evaluation of Dasatinib, a Potent Src Kinase Inhibitor, in Melanoma Cell Lines. *J. Transl. Med.* **2008**, *6*, 53–64.

(12) Corry, A. J. Novel Ferrocenyl Benzoyl Peptide Esters as Anticancer Agents and Ferrocenoyl Self-Assembled Monolayers as Anion Sensors. Ph.D. Thesis, Dublin City University, 2009.

(13) Grauer, A.; Konig, B. Peptidomimetics: A Versatile Route to Biologically Active Compounds. *Eur. J. Org. Chem.* **2009**, 5099–5111.

(14) Nguyen, A.; Marsaud, V.; Bouclier, C.; Top, S.; Vessieres, A.; Pigeon, P.; Gref, R.; Legrand, P.; Jaouen, G.; Renoir, J. M. Nanoparticles Loaded with Ferrocenyl Tamoxifen Derivatives for Breast Cancer Treatment. *Int. J. Pharm.* **2008**, *347*, 128–135.

(15) Riccardi, C.; Nicoletti, I. Analysis of Apoptosis by Propidium Iodide Staining and Flow Cytometry. *Nat. Protoc.* **2006**, *1*, 1458–1461.

(16) Cooke, M. S.; Loft, S.; Olinski, R.; Evans, M. D.; Bialkowski, K.; Wagner, J. R.; Dedon, P. C.; Moller, P.; Greenberg, M. M.; Cadet, J. Recommendations for Standardized Description of and Nomenclature Concerning Oxidatively Damaged Nucleobases in DNA. *Chem. Res. Toxicol.* **2010**, *23*, 705–707.

(17) (a) van Loon, B.; Markkanen, E.; Hubscher, U. Oxygen as a Friend and Enemy: How to Combat the Mutational Potential of 8-oxo-Guanine. *DNA Repair* **2010**, *9*, 604–616. (b) Peoples, M. C.; Karnes, H. T. Recent Developments in Analytical Methodology for 8-Hydroxy-2'-Deoxyguanosine and Related Compounds. *J. Chromatogr. B* **2005**, *827*, 5–15.

(18) White, B.; Smyth, M. R.; Stuart, J. D.; Rusling, J. F. Oscillating Formation of 8-oxoGuanine During DNA Oxidation. *J. Am. Chem. Soc.* **2003**, *125*, 6604–6605.

(19) Kirshner, J. R.; He, S. Q.; Balasubramanyam, V.; Kepros, J.; Yang, C. Y.; Zhang, M.; Du, Z. J.; Barsoum, J.; Bertin, J. Elesclomol Induces Cancer Cell Apoptosis Through Oxidative Stress. *Mol. Cancer Ther.* **2008**, *7*, 2319–2327.

(20) Goel, A.; Savage, D.; Alley, S. R.; Hogan, T.; Kelly, P. N.; Draper, S. M.; Fitchett, C. M.; Kenny, P. T. M. The Synthesis and Structural Characterization of *N*-Para-Ferrocenyl Benzoyl Dipeptide

Esters: The X-ray Crystal Structure of *N*-{Para-(Ferrocenyl)benzoyl}-L-Alanine-Glycine Ethyl Ester. *J. Organomet. Chem.* **2006**, *691*, 4686–4693.

(21) Martin, A.; Clynes, M. Acid Phosphatase: Endpoint for *in vitro* Toxicity Tests. *In Vitro Cell. Dev. Biol.* **1991**, *27A*, 183–184.

# The synthesis, structural characterization and biological evaluation of *N*-(ferrocenylmethyl amino acid) fluorinated benzene-carboxamide derivatives as potential anticancer agents

William E. Butler<sup>a,b</sup>, Paula N. Kelly<sup>a,b</sup>, Andy G. Harry<sup>b</sup>, Rachel Tiedt<sup>a,b</sup>, Blanaid White<sup>b</sup>, Rosaleen Devery<sup>c</sup> and Peter T. M. Kenny<sup>a,b,\*</sup>

A series of *N*-(ferrocenylmethyl amino acid) fluorinated benzene-carboxamide derivatives 4b–i and 5b–i have been synthesized by coupling ferrocenylmethyl amine 3 with various substituted *N*-(fluorobenzoyl) amino acid derivatives using the standard *N*-(3-dimethylaminopropyl)-*N'*-ethylcarbodiimide hydrochloride, 1-hydroxybenzotriazole protocol. The amino acids employed in this study were glycine and L-alanine. All of the compounds were fully characterized using a combination of <sup>1</sup>H NMR, <sup>13</sup>C NMR, <sup>19</sup>F NMR, distortionless enhancement by polarization transfer (DEPT)-135, <sup>1</sup>H–<sup>1</sup>H correlation spectroscopy (COSY) and <sup>1</sup>H–<sup>13</sup>C COSY (heteronuclear multiple-quantum correlation) spectroscopy. The compounds were biologically evaluated on the oestrogen-positive MCF-7 breast cancer cell line. Compounds 4g, 4i, 5h and 5i exhibited cytotoxic effects on the MCF-7 breast cancer cell line. *N*-(Ferrocenylmethyl-L-alanine)-3,4,5-trifluorobenzene-carboxamide (5h) was the most active compound, with an IC<sub>50</sub> value of 2.84 μM. Compounds 4i, 5h and 5i had lower IC<sub>50</sub> values than that found for the clinically employed anticancer drug cisplatin (IC<sub>50</sub> = 16.3 μM against MCF-7). Guanine oxidation studies confirmed that 5h was capable of generating oxidative damage via a reactive oxygen species-mediated mechanism. Copyright © 2013 John Wiley & Sons, Ltd.

Supporting information may be found in the online version of this article.

**Keywords:** ferrocene; bioorganometallic chemistry; breast cancer; MCF-7

## Introduction

Interest in metal complexes with biological applications has grown at a phenomenal rate since the serendipitous discovery of the inhibition of cell division by Pt complexes in 1965, and the subsequent identification of *cis*-dichlorodiamineplatinum(II) or cisplatin as an effective anticancer drug.<sup>[1]</sup> A recent review article has categorized the diverse range of metal anticancer compounds according to their mode of action.<sup>[2]</sup> Some of the most promising novel non-platinum metal anticancer agents are emerging from the field of bioorganometallic chemistry.<sup>[3]</sup> A perspective article on organometallic anticancer compounds has been published recently.<sup>[4]</sup> Ferrocene is perhaps the quintessential organometallic molecule and indeed was the first example of the well-known 'metallocene' compounds to be discovered.<sup>[5]</sup> Ferrocene is also a particularly attractive candidate for incorporation into biomolecules and biologically active compounds because of its aromatic character, redox properties and low toxicity. The redox properties of ferrocene have often been implicated in its cytotoxicity.<sup>[6]</sup> Indeed, ferricenium salts that are known to inhibit tumour growth have been shown to produce hydroxyl (HO·) radicals under physiological conditions, leading to oxidatively damaged DNA.<sup>[7]</sup> The catalytic generation of intracellular reactive oxygen species (ROS) such as the HO· radical offers an attractive and alternative method to target and kill cancer cells.<sup>[8]</sup>

The medicinal application of ferrocene derivatives is currently a thriving area of research, with countless reports showing their activity *in vitro* and *in vivo* against several diseases, including fungal and bacterial infections, human immunodeficiency virus (HIV), malaria and cancer.<sup>[9]</sup> Perhaps the most popular and well-researched application of ferrocene and its derivatives is in the area of cancer research.<sup>[10]</sup> Over the past decade Jaouen and co-workers have comprehensively investigated the *in vitro* anticancer activity of ferrocifen, a ferrocenyl analogue of tamoxifen, and various related derivatives.<sup>[11]</sup> Their most promising drug candidates contain a [13]-ferrocenophane motif and have a potent *in vitro* antiproliferative effect in breast and prostate cancer cell lines.<sup>[12–14]</sup> This research group has reported the antiproliferative effects of ferrocenyl benzoyl and ferrocenyl naphthoyl bioconjugates in the H1299 lung cancer cell line.<sup>[15–21]</sup> Also in a previous study we reported the biological activity of novel *N*-(ferrocenylmethyl) benzene-carboxamide derivatives.<sup>[22]</sup> We now report the results

\* Correspondence to: P. T. M. Kenny, School of Chemical Sciences, Dublin City University, Dublin 9, Ireland. Email: peter.kenny@dcu.ie

a National Institute for Cellular Biotechnology, DCU, Dublin 9, Ireland

b School of Chemical Sciences, DCU, Dublin 9, Ireland

c School of Biotechnology, DCU, Dublin 9, Ireland

of a structure–activity relationship (SAR) study of a series of *N*-(ferrocenylmethyl amino acid) fluorinated benzene-carboxamide derivatives. The incorporation of C-F bonds is a recognized strategy often employed in the development of pharmaceuticals.<sup>[23]</sup> The success of fluorine substitution is evident from the large number of fluorinated drugs approved by the US Food and Drug Administration and currently being used as anticancer, antidepressant, antiviral and anaesthetic agents. There are generally two consequences of introducing fluorine into a potential drug molecule. Firstly, there are the physicochemical properties. Fluorine has the ability to modulate electronic, lipophilic and steric parameters that can critically influence the pharmacological properties of a potential drug molecule. The introduction of a fluorine atom will generally increase lipophilicity, decrease basicity and alter the hydrogen bonding interactions of a molecule. Secondly, there is the influence of fluorine substitution on the biological stability through altering the metabolism of the drug molecule. In this study the position and also the number of fluorine atoms on the aromatic ring were investigated and several analogues were shown to have an antiproliferative effect. In addition, we report guanine oxidation studies that were conducted to elucidate the mode of action of the *N*-(ferrocenylmethyl amino acid) fluorinated benzene-carboxamide derivatives.

## Results and Discussion

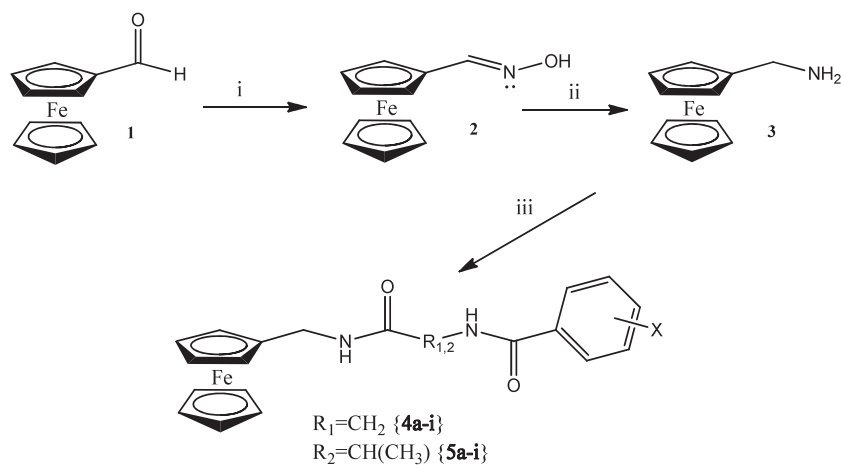
The parent compound ferrocenylmethylamine **3** was synthesized from ferrocenecarboxaldehyde **1** via the ferrocene oxime **2** intermediate (Scheme 1). The condensation of ferrocenylmethyl amine with *N*-(fluorobenzoyl) amino acids in the presence of *N*-(3-dimethylaminopropyl)-*N'*-ethylcarbodiimide hydrochloride (EDC) and 1-hydroxybenzotriazole (HOBT) yielded the corresponding *N*-(ferrocenylmethyl amino acid) fluorobenzene-carboxamides **4b–i** and **5b–i** as orange/yellow compounds. All of the compounds gave analytical and spectroscopic data in accordance with the proposed structures Fig 1. All of the proton and carbon chemical shifts for compounds **4a–i** and **5a–i** were unambiguously assigned by a combination of distortionless enhancement by polarization transfer (DEPT)-135 and <sup>1</sup>H–<sup>13</sup>C correlation spectroscopy (COSY) (heteronuclear multiple-quantum

correlation). The <sup>1</sup>H NMR and <sup>13</sup>C NMR spectra for the compounds showed peaks in the ferrocene region characteristic of a mono-substituted ferrocene moiety.<sup>[24]</sup>

The aromatic signals in the <sup>1</sup>H NMR spectra of the *N*-(ferrocenylmethyl amino acid)-fluorinated benzene-carboxamide derivatives varied, depending on the position and number of fluorine atoms on the benzoyl moiety. The aromatic protons of the benzene ring appear in the range  $\delta$  7.75–7.50 for **4a** and  $\delta$  7.90–7.45 for the **5a** derivative. For the mono-, di- and trifluorobenzoyl derivatives, the protons of the fluorobenzoyl rings exhibit <sup>1</sup>H–<sup>19</sup>F coupling interactions and appear as complex multiplets in the range  $\delta$  7.99–7.14 for derivatives **4b–h**, while for derivatives **5b–h** these signals appear as complex multiplets in the range of  $\delta$  8.02–7.13. The <sup>13</sup>C NMR spectra of the *N*-(ferrocenylmethyl amino acid) fluorinated benzene-carboxamide derivatives **4a–i** and **5a–i** show signals typical of a monosubstituted ferrocene moiety. The <sup>13</sup>C–<sup>19</sup>F coupling can be seen in the <sup>13</sup>C NMR and DEPT-135 spectra of the fluorinated compounds. Complete spectroscopic data for the compounds are presented as supporting information. As the compounds were not amenable to electron ionization measurements, electrospray ionization mass spectrometry (ESI-MS) was employed in the analysis. In the ESI mass spectra both radical cations, [M]<sup>+</sup> as well as [M + H]<sup>+</sup> species were observed. An intense fragment ion was also present at *m/z* 199 and is due to the [FcCH<sub>2</sub>]<sup>+</sup> cation.

The *in vitro* activity of the compounds **4a–i** and **5a–i** against the oestrogen receptor-positive breast cancer cell line MCF-7 was evaluated using the acid phosphatase assay as previously described.<sup>[25]</sup> The acid phosphatase assay is highly sensitive and is easier to perform than the neutral red assay as it involves fewer steps and fewer reagents. It is also more convenient than the MTT assay because of the inherent problem of removal of the medium from the insoluble crystals. Reproducibility between replicate wells is also excellent in the acid phosphatase assay.

The percentage cell growth in the presence of each compound was determined relative to the control cells. The concentration of compounds causing a 50% growth inhibition (IC<sub>50</sub> of the compound) was determined using Calcsyn (Biosoft, UK). In a previous study a series of *N*-(ferrocenylmethyl) fluorobenzene-carboxamide derivatives were synthesized and biologically evaluated on the human breast cancer cell line MDA-MB-435-S-F.



**Scheme 1.** Synthesis of *N*-(ferrocenylmethyl amino acid) fluorinated benzene-carboxamide derivatives: (i) NH<sub>2</sub>OH, HCl, EtOH; (ii) LiAlH<sub>4</sub>, THF; (iii) EDC, HOBT, *N*-(fluorobenzoyl) amino acid derivative, CH<sub>2</sub>Cl<sub>2</sub>, 48 h. **4** and **5a** X = H, **b** X = 2F, **c** X = 3F, **d** X = 4F, **e** X = 2F and 6F, **f** X = 2F and 4F, **g** X = 3F and 5F, **h** X = 3F, 4F and 5F, **i** X = 2F, 3F, 4F, 5F and 6F.

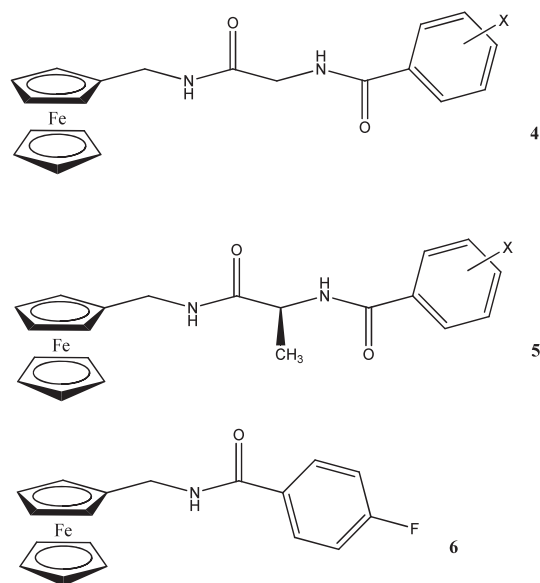


**Figure 1.** *N*-(Ferrocenylmethylglycine)-fluorinated benzene-carboxamide derivatives **4b–i** and *N*-(ferrocenylmethyl-L-alanine)-fluorinated benzene carboxamide derivatives **5b–i**, **b** X = 2F, **c** X = 3F, **d** X = 4F, **e** X = 2F and 6F, **f** X = 2F and 4F, **g** X = 3F and 5F, **h** X = 3F, 4F and 5F, **i** X = 2F, 3F, 4F, 5F and 6F and *N*-(ferrocenylmethyl)-4-fluorobenzene-carboxamide (**6**).

The most active compound was *N*-(ferrocenylmethyl)-4-fluorobenzene-carboxamide (**6**), which had an  $IC_{50}$  value in the range of 11–14  $\mu\text{M}$ .<sup>[23]</sup> Therefore this compound was used as a comparative standard for the current biological evaluation in conjunction with the positive control drug cisplatin. In a preliminary screen on the MCF-7 human breast cancer cell line the following compounds were tested at 10  $\mu\text{M}$  concentration: **4a**, **4d**, **4g**, **4h**, **4i**, **5a**, **5d**, **5g**, **5h** and **5i**. Of the 10 compounds screened, the four most active compounds were selected for further evaluation namely: **4g** (57% inhibition), **4i** (69% inhibition), **5h** (63% inhibition) and **5i** (42% inhibition). The percent inhibition of the other compounds was deemed to be too low and was not evaluated further, e.g. **4h** (11% inhibition) and **5d** (17% inhibition).

The compounds **4g**, **4i**, **5h** and **5i** were then selected for  $IC_{50}$  studies. The four *N*-(ferrocenylmethyl amino acid) fluorinated benzene-carboxamides were shown to exert an antiproliferative effect on the MCF-7 cell line, as three of the derivatives are considerably more active than compound **6** (Table 1). Compounds **4i**, **5h** and **5i** also had lower  $IC_{50}$  values than that found for the clinically employed anticancer drug cisplatin (Table 1).<sup>[26]</sup> A potential mechanism by which *N*-(ferrocenylmethyl-L-alanine)-3,4,5-trifluorobenzene-carboxamide may induce DNA damage is by the generation of a reactive oxygenated species via the Fenton reaction. To investigate this, the rate of Fenton reaction-mediated 8-oxoguanine formation from the DNA nucleotide base guanine was monitored. Guanine was chosen as it has the lowest oxidation potential of all the DNA bases and is considered the clinical biomarker for oxidative DNA damage.<sup>[26,27]</sup> Guanine was oxidized using *N*-(ferrocenylmethyl-L-alanine)-3,4,5-trifluorobenzene-carboxamide (**5h**) and  $\text{H}_2\text{O}_2$  at 37°C. Samples were taken in duplicate over 15 min. Each sample was injected in triplicate and analysed by high-performance liquid chromatography–electrochemical detection using an electrochemical detector at +550 mV versus Ag/AgCl. The iron-mediated Fenton oxidation of guanine and the kinetic profile of

**Table 1.**  $IC_{50}$  data of *N*-(ferrocenylmethylamino acid)-fluorinated benzene-carboxamide derivatives, **4g**, **4i**, **5h**, **5i**, *N*-(ferrocenylmethyl)-4-fluorobenzene-carboxamide **6** and cisplatin

Compound name	$IC_{50}$ value ( $\mu\text{M}$ ) (RSD %)
Cisplatin	16.3 $\pm$ 17%
<i>N</i> -(Ferrocenylmethyl)-4-fluorobenzene-carboxamide ( <b>6</b> )	24.8 $\pm$ 12%
<i>N</i> -(Ferrocenylmethylglycine)-3,5-difluorobenzene-carboxamide ( <b>4g</b> )	46.5 $\pm$ 11%
<i>N</i> -(Ferrocenylmethylglycine)-2,3,4,5,6-pentafluorobenzene-carboxamide ( <b>4i</b> )	11.1 $\pm$ 12%
<i>N</i> -(Ferrocenylmethyl-L-alanine)-3,4,5-trifluorobenzene-carboxamide ( <b>5h</b> )	2.84 $\pm$ 10%
<i>N</i> -(Ferrocenylmethyl-L-alanine)-2,3,4,5,6-pentafluorobenzene-carboxamide ( <b>5i</b> )	10.3 $\pm$ 12%

8-oxoguanine formed as a result have previously been investigated, utilizing  $\text{FeSO}_4$  as the model iron complex.<sup>[27]</sup> To examine whether the *N*-(ferrocenylmethyl-L-alanine)-3,4,5-trifluorobenzene-carboxamide (**5h**) induced guanine oxidation via a similar mechanism, kinetic 8-oxoguanine formation profiles were compared using both iron complexes. Control experiments were carried out utilizing both the iron complexes in the absence of peroxide, and peroxide in the absence of iron, to verify that any oxidation was Fenton mediated. Additionally, they ensured that no artifactual oxidation was occurring from the sample preparation or analysis methodology. For these experiments, deionized water was used to sequentially replace each of the reagents used. The highest background reading for these controls is plotted as the base line (Figs 2 and 3) Error bars show the standard deviation of duplicate samples injected in triplicate. Incubation of free guanine with  $\text{FeSO}_4$  and peroxide lead to oscillating concentrations of 8-oxoguanine over the incubation, as previously reported.<sup>[27]</sup> The formation is significantly higher than the control baselines, confirming that the oxidation is Fenton mediated. The 8-oxoguanine concentration maxima were 1.39  $\mu\text{M}$  at 6 min and 2.29  $\mu\text{M}$  at 8.5 min. This trend is analogous to that reported previously.<sup>[28]</sup> These maxima occur with a different oscillation frequency, which can be attributed to differences in solution pH (previously these maxima were reported at 4 and 15 min respectively). Incubation of free guanine with *N*-(ferrocenylmethyl-L-alanine)-3,4,5-trifluorobenzene-carboxamide and peroxide, which was suspected to result in Fenton-mediated oxidation, also resulted in the formation of oscillating concentrations of 8-oxoguanine over the incubation period, as found with  $\text{FeSO}_4$ . Again, the formation is significantly higher than the control base lines, clearly illustrating that both the iron complex and peroxide are required to form this concentration of 8-oxoguanine, confirming that the oxidation of guanine was Fenton mediated.

The maximum concentration of 8-oxoguanine achieved was 0.72  $\mu\text{M}$ . The concentration of 8-oxoguanine generated by *N*-(ferrocenylmethyl-L-alanine)-3,4,5-trifluorobenzene-carboxamide (**5h**) is significantly lower than that of the  $\text{FeSO}_4$ . Ferrocene may produce a weaker response than the  $\text{FeSO}_4$  due to the presence of the cyclopentadienyl ligands and the size of the molecule. However, the generation of 8-oxoguanine by *N*-(ferrocenylmethyl-L-alanine)-3,4,5-trifluorobenzene-carboxamide (**5h**) illustrates that the oxidation is occurring by Fenton chemistry and generating DNA damage via a reactive oxygenated species (ROS)-mediated mechanism. The oscillation period for 8-oxoguanine mediated by the

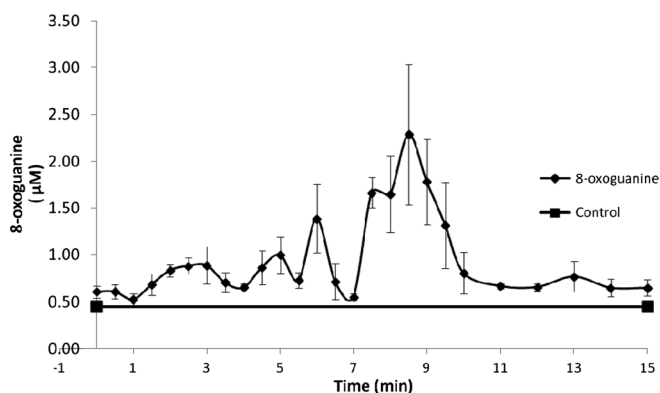


**Figure 2.** 8-Oxoguanine concentration as a function of time after incubation of free guanine with reagents Fe(II) and H<sub>2</sub>O<sub>2</sub> at 37°C.

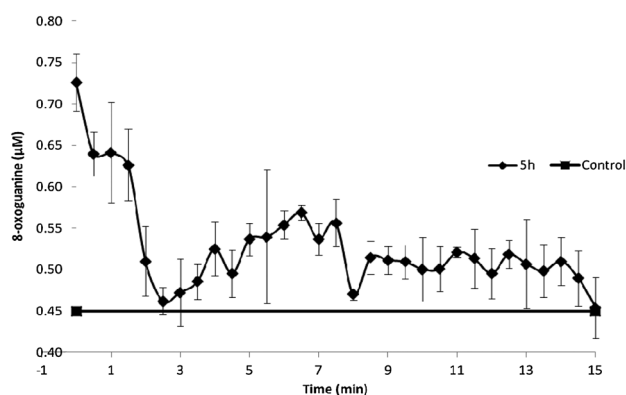


**Figure 3.** 8-Oxoguanine concentration as a function of time after incubation of free guanine with *N*-(ferrocenylmethyl-L-alanine)-3,4,5-trifluorobenzene-carboxamide (**5h**) and H<sub>2</sub>O<sub>2</sub> at 37°C.

*N*-(ferrocenylmethyl-L-alanine)-3,4,5-trifluorobenzene-carboxamide (**5h**) differs from that of FeSO<sub>4</sub>. After the initial maxima at 0.0 and up to 2 min, the 8-oxoguanine concentration continues to oscillate for the rest of the incubation period, with concentrations consistently higher than control levels, further confirming that oxidation is Fenton mediated.

## Conclusion

The *N*-(ferrocenylmethyl amino acid) fluorinated benzene-carboxamide derivatives which have shown anti-proliferative activity have more than one fluorine atom on the aromatic ring. *N*-(Ferrocenylmethyl-L-alanine)-3,4,5-trifluorobenzene-carboxamide (**5h**) was the most active compound and had an IC<sub>50</sub> value of 2.84 µM. *N*-(Ferrocenylmethylglycine)-2,3,4,5,6-pentafluorobenzene-carboxamide (**4i**) and *N*-(ferrocenylmethyl-L-alanine)-2,3,4,5,6-pentafluorobenzene-carboxamide (**5i**) had IC<sub>50</sub> values of 11.1 µM and 10.3 µM respectively. The three derivatives are considerably more active than *N*-(ferrocenylmethyl)-4-fluorobenzene-carboxamide **6** and also had lower IC<sub>50</sub> values than that found for the clinically employed anticancer drug cisplatin. These results show that the inclusion of the amino acids, glycine and L-alanine, in combination with the position and

number of fluorine atoms, plays a vital role in increasing the biological activity and anticancer effect of these compounds. Guanine oxidation studies confirmed that *N*-(ferrocenylmethyl-L-alanine)-3,4,5-trifluorobenzene-carboxamide (**5h**) is capable of generating oxidative damage via a ROS-mediated mechanism. The ease of preparation and stability of these compounds together with the encouraging cytotoxicity against the oestrogen receptor-positive breast cancer cell line MCF-7 clearly promote further research in this area. We are currently in the process of synthesizing other derivatives with the aim of improving cytotoxicity and identifying derivatives with lower IC<sub>50</sub> values.

## Experimental

### Materials and Methods

All chemicals were purchased from Sigma-Aldrich, Lennox Chemicals, Fluorochem Ltd or Tokyo Chemical Industry UK Ltd and used as received. Commercial-grade reagents were used without further purification. When necessary, all solvents were purified and dried prior to use. Riedal-Haën silica gel was used for thin-layer chromatography and column chromatography. Melting points were determined using a Griffin melting point apparatus and are uncorrected. Optical rotation measurements were made on a PerkinElmer 343 polarimeter and are quoted in units of 10<sup>-1</sup> deg cm<sup>2</sup> g<sup>-1</sup>. Infrared spectra were recorded on either a Nicolet 405 FT-IR spectrometer or a PerkinElmer 100 FT-IR spectrometer with ATR. UV-visible spectra were recorded on a Hewlett-Packard 8452A diode array UV-visible spectrophotometer. NMR spectra were obtained on a Bruker AC 400 NMR spectrometer operating at 400 MHz for <sup>1</sup>H NMR, 376 MHz for <sup>19</sup>F NMR and 100 MHz for <sup>13</sup>C NMR. The <sup>1</sup>H and <sup>13</sup>C NMR chemical shifts (δ) are relative to tetramethylsilane and the <sup>19</sup>F NMR chemical shifts (δ) are relative to trifluoroacetic acid. All coupling constants (*J*) are in hertz (Hz). The abbreviations for the peak multiplicities are as follows: s (singlet), d (doublet), t (triplet), q (quartet), qt (quintet), st (sextet) and m (multiplet). ESI mass spectra were performed on either a Micromass LCT mass spectrometer or a Brüker Daltonics Esquire-LC ion trap mass spectrometer. Elemental analysis was carried out by the microanalytical laboratory at University College Dublin.

### General Procedure for the Synthesis of Compounds 4a-i and 5a-i

#### Synthesis of *N*-(ferrocenylmethyl-L-alanine)-3,4,5-trifluorobenzene-carboxamide (**5h**)

1-Hydroxybenzotriazole (0.55 g, 4.07 mmol) was added to a solution of ferrocenylmethyl amine (1.15 g, 5.34 mmol), *N*-(3-dimethylaminopropyl)-*N'*-ethylcarbodiimide hydrochloride (0.61 g, 3.18 mmol) and triethylamine (2 ml) in dichloromethane (40 ml) at 0°C. After 30 min, *N*-(3,4,5-trifluorobenzoyl)-L-alanine (1.27 g, 5.14 mmol) was added and the reaction was stirred at room temperature for 72 h. Diethyl ether (100 ml) was then added. The organic layer was then washed with water, dried over MgSO<sub>4</sub> and the solvent was removed *in vacuo*. The compound was purified by column chromatography (eluant 2:1 hexane-ethyl acetate) and isolated as red crystals (1.10 g, 46.6%); m.p. 134–136°C. [α]<sub>D</sub><sup>20</sup> = +32° (c 0.005, ACN); UV-visible λ<sub>max</sub> ACN: (320, 432) IR: *u*<sub>max</sub> (KBr): 3279, 3075, 1641, 1621, 1559, 1455, 1232, 1043, 1001, 889 cm<sup>-1</sup>; <sup>1</sup>H NMR (400 MHz) δ (DMSO-d<sub>6</sub>): 8.78 (1H, d, *J* = 7.2 Hz, Ar-CO-NH), 8.25 (1H, t, *J* = 6 Hz, FcCH<sub>2</sub>NH), 7.93–7.85 (2H, m, Ar-H), 4.53–4.46 {1H, m, NH-CH(CH<sub>3</sub>)}, 4.19–4.17 {7H, m, (η<sup>5</sup>-C<sub>5</sub>H<sub>5</sub>)

and *ortho* on ( $\eta^5$ -C<sub>5</sub>H<sub>4</sub>), 4.10 {2H, t, *J* = 2 Hz, *meta* on ( $\eta^5$ -C<sub>5</sub>H<sub>4</sub>), 4.05–3.95 (2H, m, FcCH<sub>2</sub>), 1.41 {3H, d, *J* = 7.2 Hz, NH-CH(CH<sub>3</sub>)}; <sup>13</sup>C NMR (100 MHz)  $\delta$  (DMSO-d<sub>6</sub>): 170.3 (CO), 167.7 (CO), 155.9–155.7 (C3,C5), 147.5–147.4 (C4), 130.2–130.0 (C1), 112.7–112.5 (C2,C6), 86.2 (Fc), 68.3 (Fc), 67.4 (Fc), 67.1 (Fc), 49.7 (CH), 37.5 (CH<sub>2</sub>, –ve DEPT), 17.9 (CH<sub>3</sub>); <sup>19</sup>F (376 MHz, DMSO):  $\delta$  –134.6 (2F, m), –157.1 (1F, m). Anal. Calcd for C<sub>21</sub>H<sub>19</sub>F<sub>3</sub>FeN<sub>2</sub>O<sub>2</sub>: C, 56.78; H, 4.31; N, 6.31. Found: C, 56.62; H, 4.28; N, 5.98. *m/z* (ESI) 444.07 [M]<sup>+</sup>. C<sub>21</sub>H<sub>19</sub>F<sub>3</sub>FeN<sub>2</sub>O<sub>2</sub> requires 444.075.

### General Procedure for *In Vitro* Cytotoxicity Assays

Confluent cells in the exponential growth phase were harvested by trypsination and a cell suspension of  $5 \times 10^4$  cells ml<sup>-1</sup> was prepared in fresh culture medium. The cell suspension (40  $\mu$ l) was added to a flat-bottom 96-well plate (Costar 3599), followed by culture medium (60  $\mu$ l). The plate was slightly agitated in order to ensure complete dispersion of the cells. The cells were then incubated for an initial 24 h in a 37°C, 5% CO<sub>2</sub> incubator to allow the adhesion of cells to flat-bottom wells. The compounds for testing were prepared in 1 mM stock solutions. The different concentrations used in the preliminary scans and for the further IC<sub>50</sub> data studies were made up accordingly by adding the desired amount of compound stock solution to fresh culture media. Once the compounds and media were added to the 96-well flat-bottom plates, the plate was gently agitated and then incubated at 37°C, 5% CO<sub>2</sub>, for 4–5 days until cell confluency reached over 85%. Assessment of cell survival in the presence of test sample was determined by the acid phosphatase assay. For the full comprehensive screen, cell growth percentage in the presence of each sample was calculated relative to the DMSO control cells. For the preliminary studies and IC<sub>50</sub> data studies, the concentration of drug that causes 50% growth inhibition was determined by plotting the percentage survival of cells (relative to control cells) against the concentration of the test sample. In relation to IC<sub>50</sub> data studies, IC<sub>50</sub> values were calculated using Calcsyn software (Biosoft, UK).

### Supporting information

Supporting information may be found in the online version of this article.

### Acknowledgements

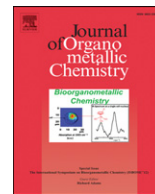
W. E. Butler would like to thank the National Institute of Cellular Biotechnology and the School of Chemical Sciences at Dublin City University, Glasnevin, Dublin 9, for their facilities and cooperation

in conducting this research. This research was partly supported by the Health Research Board, Grant Reference Number HRA/09/86.

### References

- [1] B. Rosenberg, L. Vancamp, T. Krigas, *Nature* **1965**, *205*, 698.
- [2] T. Gianferrara, I. Bratsos, E. Alessio, *Dalton Trans.* **2009**, *37*, 7588.
- [3] C. G. Hartinger, P. J. Dyson, *Chem. Soc. Rev.* **2009**, *38*, 391.
- [4] G. Gasser, I. Ott, N. Metzler-Nolte, *J. Med. Chem.* **2011**, *54*, 3.
- [5] T. J. Kealy, P. L. Pauson, *Nature* **1951**, *168*, 1039.
- [6] E. W. Neuse, *J. Inorg. Organomet. Poly. Mat.* **2005**, *15*, 3.
- [7] G. Tabbi, C. Cassino, G. Cavigliolo, D. Colangelo, A. Ghiglia, I. Viano, D. Osella, *J. Med. Chem.* **2002**, *45*, 5786.
- [8] D. Trachootham, J. Alexandre, P. Huang, *Nat. Rev. Drug Dis.* **2009**, *8*, 579.
- [9] M. F. R. Fouda, M. M. Abd-Elzaher, R. A. Abdelsamaia, A. A. Labib, *Appl. Organomet. Chem.* **2007**, *21*, 613.
- [10] C. Ornelas, *New J. Chem.* **2011**, *35*, 1973.
- [11] A. Nguyen, A. Vessieres, E. A. Hillard, S. Top, P. Pigeon, G. Jaouen, *Chimia* **2007**, *61*, 716.
- [12] D. Plazuk, A. Vessieres, E. A. Hillard, O. Buriez, E. Labbe, P. Pigeon, M.-A. Plamont, C. Amatore, J. Zakrzewski, G. Jaouen, *J. Med. Chem.* **2009**, *52*, 4964.
- [13] M. Gormen, D. Plazuk, P. Pigeon, E. A. Hillard, M.-A. Plamont, S. Top, A. Vessieres, G. Jaouen, *Tetrahedron Lett.* **2010**, *51*, 118.
- [14] M. Gormen, P. Pigeon, S. Top, A. Vessieres, M.-A. Plamont, E. A. Hillard, G. Jaouen, *MedChemComm.* **2010**, *1*, 149.
- [15] A. Goel, D. Savage, S. R. Alley, P. N. Kelly, D. O'Sullivan, H. Mueller-Bunz, P. T. M. Kenny, *J. Organomet. Chem.* **2007**, *692*, 1292.
- [16] A. J. Corry, A. Goel, S. R. Alley, P. N. Kelly, D. O'Sullivan, D. Savage, P. T. M. Kenny, *J. Organomet. Chem.* **2007**, *692*, 1405.
- [17] A. J. Corry, N. O'Donovan, Á. Mooney, D. O'Sullivan, D. K. Rai, P. T. M. Kenny, *J. Organomet. Chem.* **2009**, *694*, 880.
- [18] A. J. Corry, A. Mooney, D. O'Sullivan, P. T. M. Kenny, *Inorg. Chim. Acta* **2009**, *362*, 2957.
- [19] Á. Mooney, A. J. Corry, D. O'Sullivan, D. K. Rai, P. T. M. Kenny, *J. Organomet. Chem.* **2009**, *694*, 886.
- [20] Á. Mooney, A. J. Corry, C. Ní Ruairc, T. Maghoub, D. O'Sullivan, N. O'Donovan, J. Crown, S. Varughese, S. M. Draper, D. K. Rai, P. T. M. Kenny, *Dalton Trans.* **2010**, *39*, 8228.
- [21] Á. Mooney, R. Tiedt, T. Maghoub, N. O'Donovan, J. Crown, B. White, P. T. M. Kenny, *J. Med. Chem.* **2012**, *55*, 5455.
- [22] P. N. Kelly, A. Prêtre, S. Devoy, I. O'Reilly, R. Devery, A. Goel, J. F. Gallagher, A. J. Lough, P. T. M. Kenny, *J. Organomet. Chem.* **2007**, *692*, 1327.
- [23] A. G. Myers, L. McKinstry, J. K. Barbay, J. L. Gleason, *Tetrahedron Lett.* **1998**, *39*, 133.
- [24] D. Savage, S. R. Alley, A. Goel, T. Hogan, Y. Ida, P. N. Kelly, L. Lehmann, P. T. M. Kenny, *Inorg. Chem. Commun.* **2006**, *9*, 1267.
- [25] A. Martin, M. Clynes, *In Vitro Cell. Dev. Biol. Anim.* **1991**, *27*, 183.
- [26] Z. Dvorak, P. Starha, Z. Sindelar, Z. Travniczek, *Toxicol. In Vitro* **2012**, *26*, 480.
- [27] B. Van Loom, E. Markkanen, U. Hubscher, *DNA Repair* **2010**, *9*, 604.
- [28] M. C. Peoples, H. T. Karnes, *J. Chromatogr. B* **2005**, *827*, 5.





## The synthesis, structural characterization and *in vitro* anti-cancer activity of novel *N*-{6-(ferrocenyl) ethynyl-2-naphthoyl} amino acid and dipeptide ethyl esters

Andy G. Harry<sup>a</sup>, James Murphy<sup>b</sup>, William E. Butler<sup>a,b</sup>, Rachel Tiedt<sup>b</sup>, Áine Mooney<sup>a,b</sup>, Jennifer C. Manton<sup>a</sup>, Mary T. Pryce<sup>a</sup>, Norma O'Donovan<sup>b</sup>, Naomi Walsh<sup>b</sup>, John Crown<sup>c</sup>, Dilip K. Rai<sup>d</sup>, Peter T.M. Kenny<sup>a,b,\*</sup>

<sup>a</sup>School of Chemical Sciences, Dublin City University, Dublin 9, Ireland

<sup>b</sup>National Institute for Cellular Biotechnology, Dublin City University, Dublin 9, Ireland

<sup>c</sup>Dept. of Medical Oncology, St. Vincent's University Hospital, Dublin 4, Ireland

<sup>d</sup>Dept. of Food Biosciences, Teagasc Food Research Centre, Ashtown, Dublin 15, Ireland

### ARTICLE INFO

#### Article history:

Received 25 October 2012

Received in revised form

29 November 2012

Accepted 30 November 2012

#### Keywords:

Ferrocene

Bioorganometallic chemistry

Dipeptides

Cytotoxicity

Lung cancer

### ABSTRACT

*N*-{6-(Ferrocenyl) ethynyl-2-naphthoyl} amino acid and dipeptide ethyl esters **2–8** were prepared by coupling 6-(ferrocenyl) ethynyl-2-naphthoic acid **1** to the amino acid ethyl ester GABA(OEt) and the dipeptide ethyl esters GlyGly(OEt), GlyAla(OEt), SarGly(OEt), SarAla(OEt), ProGly(OEt) and ProAla(OEt) using the standard *N*-(3-dimethylaminopropyl)-*N'*-ethylcarbodiimide hydrochloride (EDC), 1-hydroxybenzotriazole (HOBt) protocol. All the compounds were fully characterized using a combination of <sup>1</sup>H NMR, <sup>13</sup>C NMR, DEPT-135 and <sup>1</sup>H–<sup>13</sup>C COSY (HMQC) spectroscopy, electrospray ionization mass spectrometry (ESI-MS) and cyclic voltammetry (CV). Compounds, **2–8** showed micromolar activity in the H1299 NSCLC cell line, with IC<sub>50</sub> values in the range of 3.2–7.2 μM.

© 2012 Elsevier B.V. All rights reserved.

### 1. Introduction

Ferrocene is a particularly attractive candidate for incorporation into biomolecules and biologically active compounds due to its aromatic character, redox properties and low toxicity [1–3]. The redox properties of ferrocene have often been implicated in its cytotoxicity [4]. Ferricenium salts that are known to inhibit tumour growth have been shown to produce hydroxyl (HO•) radicals under physiological conditions, leading to oxidatively damaged DNA [5]. The catalytic generation of intracellular reactive oxygen species (ROS) such as the HO• radical offers an attractive and alternative method to target and kill cancer cells [6].

The medicinal application of ferrocene derivatives is currently an active area of research, with countless reports showing their activity *in vitro* and *in vivo* against several diseases including fungal and bacterial infections, human immunodeficiency virus (HIV),

malaria and cancer [7]. Perhaps the most popular and well-researched application of ferrocene and its derivatives is in the area of cancer research [8]. Over the past decade Jaouen and co-workers have comprehensively investigated the *in vitro* anti-cancer activity of ferrocifen, a ferrocenyl analogue of tamoxifen, and various related derivatives [9]. Their most promising drug candidates contain a [3]-ferrocenophane motif and have a potent *in vitro* anti-proliferative effect in breast and prostate cancer cell lines [10–12]. This research group has reported the anti-proliferative effects of ferrocenyl benzoyl and ferrocenyl naphthoyl bioconjugates in the H1299 lung cancer cell line [13–19]. These *N*-(ferrocenyl)benzoyl and naphthoyl dipeptide esters consist of three components, namely: (i) an electroactive core, (ii) a conjugated linker that lowers the oxidation potential of the ferrocene moiety and (iii) an amino acid or peptide derivative that can interact with other biomolecules *via* secondary interactions such as hydrogen bonding. In an effort to improve the cytotoxicity of these derivatives, we are currently modifying the conjugated linker moiety and conducting variations of the peptide chain. The compounds prepared in this study have an ethynyl group linked to the ferrocene and the naphthoyl spacer group.

\* Corresponding author. School of Chemical Sciences, Dublin City University, Dublin 9, Ireland. Tel.: +353 1 7005689; fax: +353 1 7005503.

E-mail address: [peter.kenny@dcu.ie](mailto:peter.kenny@dcu.ie) (P.T.M. Kenny).

Herein, we report the synthesis and structural characterization of novel *N*-{6-(ferrocenyl) ethynyl-2-naphthoyl} amino acid and dipeptide ethyl esters. The dipeptide ethyl esters GlyGly(OEt), SarGly(OEt) and GlyAla(OEt) were employed in this investigation as they were shown to have IC<sub>50</sub> values of 0.13, 0.14 and 1.3 μM respectively, in the H1299 lung cancer cell line. The dipeptide ethyl esters SarAla(OEt), ProGly(OEt) and ProAla(OEt) were selected as they are closely related analogues of the most active compounds.

The synthesis of the new ferrocenyl bioconjugates involved Sonogashira coupling of ethynyl ferrocene to generate 6-(ferrocenyl) ethynyl-2-naphthoic acid [20]. A series of dipeptide esters were coupled to the 6-(ferrocenyl) ethynyl-2-naphthoic acid to generate the new class of compounds which were characterized by a combination of <sup>1</sup>H NMR, <sup>13</sup>C NMR, DEPT-135, <sup>1</sup>H–<sup>13</sup>C COSY spectroscopy, cyclic voltammetry and mass spectrometry. In addition, we present the *in vitro* anti-cancer activity of compounds 2–8 against the human lung carcinoma cell line H1299.

## 2. Results and discussion

### 2.1. Synthesis

#### 2.1.1. Synthesis of *N*-{6-(ferrocenyl) ethynyl-2-naphthoyl} amino acid and dipeptide ethyl esters 2–8

6-(Ferrocenyl) ethynyl-2-naphthoic acid **1** was prepared by coupling ethynyl ferrocene to 6-bromo-2-naphthoic acid via the Sonogashira reaction [20]. The <sup>1</sup>H NMR spectrum showed signals for the aromatic ring protons at δ 8.13 (1H, s) and between δ 7.95–7.48 (5H, m) for the 2,6-disubstituted naphthalene ring system. The carboxylic acid proton was present at δ 12.87. The ferrocenyl *ortho* and *meta* protons on the (η<sup>5</sup>-C<sub>5</sub>H<sub>4</sub>) ring were observed at δ 4.27 and δ 4.19, respectively, and an intense signal was present at δ 4.19 for the (η<sup>5</sup>-C<sub>5</sub>H<sub>5</sub>) ring. The free *N*-terminal amino acid GABA(OEt) and the free *N*-terminal dipeptide ethyl esters GlyGly(OEt), GlyAla(OEt), SarGly(OEt), SarAla(OEt), ProGly(OEt) and ProAla(OEt) were coupled to 6-(ferrocenyl) ethynyl-2-naphthoic acid **1** using EDC and HOBT in the presence of excess triethylamine in dichloromethane (Scheme 1). EDC was used in preference to the less expensive coupling reagent *N,N'*-dicyclohexylcarbodiimide (DCC) as its reaction by-products are easier to remove compared to those of DCC, namely dicyclohexylurea (DCU). Purification by column chromatography furnished the pure products in yields of 11–32% and all compounds gave spectroscopic data in accordance with the proposed structures. The relatively low yields of products obtained are partly due to the

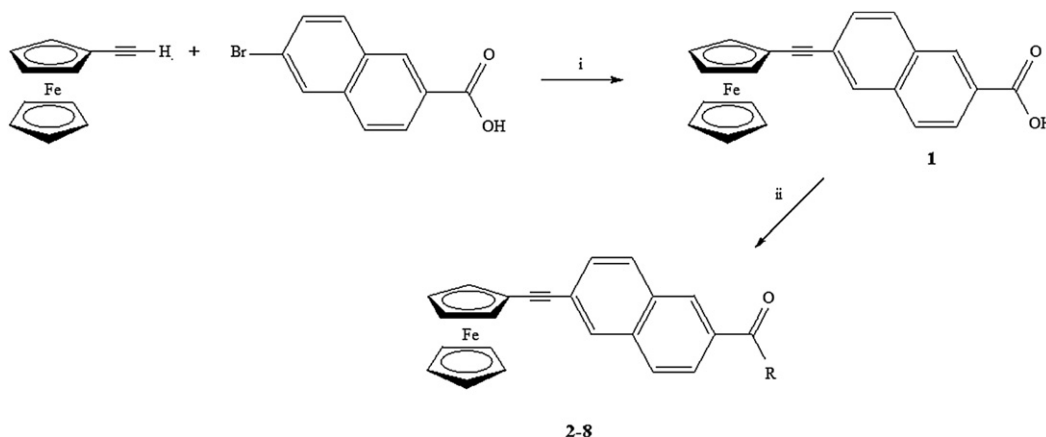
coupling procedure. The first step in amide bond formation in the coupling protocol is formation of the *O*-acylisourea ester intermediate. This intermediate is highly reactive and thus, side-reactions can pose a serious problem and can result in extensive racemisation resulting in low yields. The addition of HOBT stabilizes the *O*-acylisourea ester intermediate thus suppressing side reactions, however the addition does not result in 100% suppression. As the reaction proceeds upon addition of the amino acid and dipeptide ethyl esters the HOBT is displaced resulting in the formation of compounds 2–8. As a result of the complexity of the reaction which is associated with the competing reactions, low yields for compounds 2–8 were obtained. Also in the EDC/HOBT coupling reaction when primary amine amino acid and dipeptide ethyl esters, namely, GABA(OEt), GlyGly(OEt) and GlyAla(OEt) are used, the yields are generally higher than that of the secondary amine dipeptide ethyl esters SarGly(OEt), SarAla(OEt), ProGly(OEt) and ProAla(OEt). For example the percentage yield of *N*-{6-(ferrocenyl) ethynyl-2-naphthoyl}-glycine-glycine ethyl ester **3** obtained was 28% whereas the percentage yield of *N*-{6-(ferrocenyl) ethynyl-2-naphthoyl}-sarcosine-glycine ethyl ester **5** was only 13%.

The *N*-{6-(ferrocenyl) ethynyl-2-naphthoyl} amino acid and dipeptide ethyl esters 2–8 were characterized by a combination of IR, UV–Vis, <sup>1</sup>H NMR, <sup>13</sup>C NMR, DEPT-135 and <sup>1</sup>H–<sup>13</sup>C COSY (HMQC) spectroscopy and cyclic voltammetry (CV). Electrospray ionization (ESI) mass spectrometry in conjunction with tandem mass spectrometry (MS/MS) was also employed in the analysis.

### 2.2. <sup>1</sup>H and <sup>13</sup>C spectroscopic analysis

All the proton and carbon chemical shifts for compounds 2–8 were unambiguously assigned by a combination of DEPT-135 and <sup>1</sup>H–<sup>13</sup>C COSY (HMQC). The <sup>1</sup>H and <sup>13</sup>C NMR spectra for compounds 2–8 showed peaks in the ferrocene region characteristic of a monosubstituted ferrocene moiety [21–25]. The *ortho* protons on the cyclopentadiene ring attached to the (–C≡C–) spacer moiety appear in the region δ 4.4 to δ 4.72, the *meta* protons occur in the range δ 4.33 to δ 3.9 and usually overlap with the unsubstituted (η<sup>5</sup>-C<sub>5</sub>H<sub>5</sub>) ring which also appears between δ 4.33 and δ 3.90.

The <sup>13</sup>C NMR spectra of compounds 2–8 show signals in the region δ 63.6 to δ 74.2 indicative of a monosubstituted ferrocene unit. The *ipso* carbon of the (η<sup>5</sup>-C<sub>5</sub>H<sub>4</sub>) ring appears in the range of δ 63.6 to δ 67.8. This signal is absent in the DEPT-135 spectra. The carbon atoms of the ethynyl group appear in the range of δ 85.0 to δ 91.4 and are also



**Scheme 1.** Synthesis of *N*-{6-(ferrocenyl) ethynyl-2-naphthoyl} amino acid and dipeptide ethyl esters 2–8, (i) TEA, PPh<sub>3</sub>, Bis(triphenylphosphine)palladium(II) dichloride, THF, Cu(I) (ii) EDC, HOBT, triethylamine, amino acid and dipeptide ethyl esters, R = GABA(OEt) **2**, GlyGly(OEt) **3**, GlyAla(OEt) **4**, SarGly(OEt) **5**, SarAla(OEt) **6**, ProGly(OEt) **7** and ProAla(OEt) **8**.

absent in the DEPT-135 spectra. The carbon atoms of the aromatic naphthalene ring are non-equivalent and therefore ten signals are visible in the region of  $\delta$  120.8 to  $\delta$  135.8 for compounds **2–8**. The quaternary carbon atoms of the aromatic ring and the methylene carbon atoms of derivatives **2–8** were identified by DEPT-135. Complete spectroscopic data for all the compounds is presented in the experimental section.

### 2.3. Mass spectrometry

Soft ionization techniques such as electrospray ionization (ESI) mass spectrometry permit the analysis of thermolabile and non-volatile analytes [26]. Electrospray ionization (ESI) mass spectrometry was employed in the analysis of compounds **2–8** and confirmed the correct relative molecular mass for all the compounds.

Tandem mass spectrometry was used to determine the fragmentation pattern of *N*-{6-(ferrocenyl) ethynyl-2-naphthoyl}-glycine-glycine ethyl ester **3**. In the MS/MS spectrum of *N*-{6-(ferrocenyl) ethynyl-2-naphthoyl}-glycine-glycine ethyl ester **3** the sequence specific fragment ions are present at  $m/z$  335,  $m/z$  363,  $m/z$  391 and  $m/z$  419 (Fig. 1). The product ions at  $m/z$  335 and  $m/z$  363 correspond to the *N*-{6-(ferrocenyl) ethynyl-2-naphthyl} and *N*-{6-(ferrocenyl) ethynyl-2-naphthoyl} subunits respectively figure. However, the expected  $a_1$  and  $b_1$  product ions at  $m/z$  392 and  $m/z$  420 were not observed, instead  $a_1 - 1$  and  $b_1 - 1$  product ions were observed at  $m/z$  391 and  $m/z$  419 respectively. Obviously a hydrogen atom has also been lost during the fragmentation process. This is unusual as these  $a_1$  and  $b_1$  fragment ions are usually produced without loss of a hydrogen atom [27]. The formation of  $a_1 - 1$  and  $b_1 - 1$  ions in the mass spectra of *N*-{*para*-(ferrocenyl)benzoyl}-glycine-*L*-alanine ethyl ester was investigated by tandem mass spectrometry and deuterium labelling studies. The results showed that  $b_1 - 1$  product ions arise from the loss of a hydrogen atom attached to the nitrogen and not to the  $\alpha$ -carbon of the glycine residue [28].

### 2.4. Electrochemistry

The CV curves for compounds **2–8** exhibit quasi-reversible behaviour similar to the Fc/Fc<sup>+</sup> redox couple. The  $E^{\circ'}$  (oxidation potential) values for the *N*-{6-(ferrocenyl) ethynyl-2-naphthoyl} amino acid and dipeptide ethyl esters **2–8** showed values in the 119–162 mV range (versus Fc/Fc<sup>+</sup>). The values for compounds **2–8** are higher than those reported for the *N*-{6-(ferrocenyl-2-naphthoyl} derivatives (42–56 mV versus Fc/Fc<sup>+</sup>), but are lower than ferrocenyl

dipeptide ester derivatives [17,19]. For example, Fc-Ala-Ala-OMe, was reported as  $E^{\circ'} = 230$  mV (vs Fc/Fc<sup>+</sup>) [29].

### 2.5. In vitro anti-cancer activity of **2–8**

The *N*-{6-(ferrocenyl) ethynyl-2-naphthoyl} amino acid and dipeptide ethyl esters **2–8** have been prepared as part of an ongoing SAR study. The *in vitro* anti-proliferative effect of compounds **2–8** was studied in the H1299 non-small cell lung cancer (NSCLC) cell line. Proliferation was measured using the acid phosphatase assay. Thus  $1 \times 10^3$  cells per well were seeded in 96 well plates. The plates were incubated overnight at 37 °C followed by addition of the compound at a concentration of 10  $\mu$ M and incubated for a further 5 days. The results of this biological study are reported in Table 1 and are expressed as % cell growth inhibition relative to the untreated controls. The % cell growth inhibition was lowest for compound **2** at 68% and highest for compounds **6** and **8** at 94% cell growth inhibition. The IC<sub>50</sub> values for derivatives **2–8** were then determined by the acid phosphatase assay as previously described [30]. This colorimetric end-point assay is an indirect measure of cytotoxicity which evaluates the enzyme activity of cells after a given treatment period. Acid phosphatase is an enzyme which dephosphorylates *p*-nitrophenyl phosphate substrate converting it to *p*-nitrophenol which in the presence of strong alkali can be quantified colorimetrically. The cells were treated with the *N*-{6-(ferrocenyl) ethynyl-2-naphthoyl} amino acid and dipeptide ethyl esters **2–8** at a range of concentrations (from 1  $\mu$ M to 100  $\mu$ M) and were incubated for 5 days until cell confluency reached 80–90%. Cell survival was established through determination of the acid phosphatase activity of surviving cells and growth inhibition calculated relative to controls (untreated cells). The results for compounds **2–8** are depicted in Fig. 2 and Table 2 displays the IC<sub>50</sub> values for derivatives **2–8** and the control drug cisplatin.

It can be seen from Fig. 2 that the *N*-{6-(ferrocenyl) ethynyl-2-naphthoyl} amino acid and dipeptide ethyl esters **2–8** all exert a cytotoxic effect on the human lung carcinoma cell line H1299. All seven derivatives have an IC<sub>50</sub> value that is lower than 7.2  $\mu$ M. The most active compound was *N*-{6-(ferrocenyl) ethynyl-2-naphthoyl}-sarcosine-*L*-alanine ethyl ester which had an IC<sub>50</sub> value of 3.2  $\mu$ M. It is interesting to note that this compound has the lowest  $E^{\circ'}$  value of 119 mV. However for compounds **2–5** the presence of the ethynyl moiety had a negative effect of anti-proliferative effect compared to analogous compounds prepared previously lacking the ethynyl group [17–19]. For

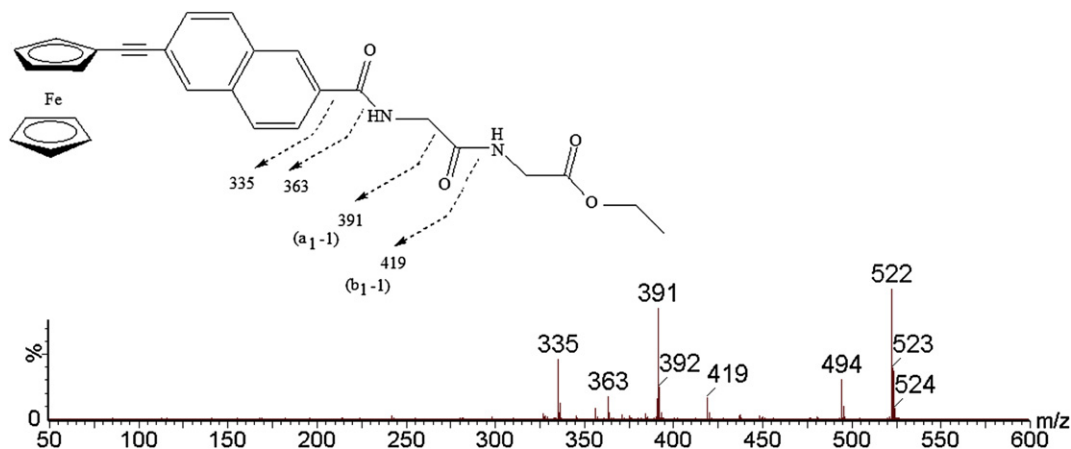


Fig. 1. MS/MS spectrum of *N*-{6-(ferrocenyl) ethynyl-2-naphthoyl}-glycine-glycine ethyl ester **3**.

**Table 1**

% Growth inhibition values for compounds **2–8** against human lung carcinoma cell line H1299.

Compound name	% Growth inhibition
<i>N</i> -{6-(Ferrocenyl) ethynyl-2-naphthoyl}- $\gamma$ -aminobutyric acid ethyl ester <b>2</b>	68
<i>N</i> -{6-(Ferrocenyl) ethynyl-2-naphthoyl}-glycine-glycine ethyl ester <b>3</b>	89
<i>N</i> -{6-(Ferrocenyl) ethynyl-2-naphthoyl}-glycine-L-alanine ethyl ester <b>4</b>	84
<i>N</i> -{6-(Ferrocenyl) ethynyl-2-naphthoyl}-sarcosine-glycine ethyl ester <b>5</b>	90
<i>N</i> -{6-(Ferrocenyl) ethynyl-2-naphthoyl}-sarcosine-L-alanine ethyl ester <b>6</b>	94
<i>N</i> -{6-(Ferrocenyl) ethynyl-2-naphthoyl}-L-proline-glycine ethyl ester <b>7</b>	82
<i>N</i> -{6-(Ferrocenyl) ethynyl-2-naphthoyl}-L-proline-L-alanine ethyl ester <b>8</b>	94

example for *N*-{6-(ferrocenyl) ethynyl-2-naphthoyl}- $\gamma$ -aminobutyric acid ethyl ester the  $IC_{50}$  value is 7.2  $\mu$ M whereas for *N*-{6-ferrocenyl-2-naphthoyl}- $\gamma$ -aminobutyric acid ethyl ester the  $IC_{50}$  value was 0.62  $\mu$ M. The *in vitro* cytotoxicity of the platinum(II)-based anti-cancer drug cisplatin was also evaluated against the H1299 cell line, and was found to have an  $IC_{50}$  value of  $1.5 \pm 0.1 \mu$ M (Table 2). Thus, compounds **2–8** are less cytotoxic *in vitro* than the clinically employed anti-cancer drug cisplatin.

### 3. Conclusions

In conclusion, the novel *N*-{6-(ferrocenyl) ethynyl-2-naphthoyl} amino acid and dipeptide ethyl esters **2–8** were synthesized and fully characterized by a range of NMR spectroscopic techniques, mass spectrometry and cyclic voltammetry. Compounds **2–8** were tested *in vitro* against the human lung carcinoma cell line H1299. Compounds **2–8** showed micromolar activity in the H1299 NSCLC cell line, with  $IC_{50}$  values in the range of 3.2–7.2  $\mu$ M. However insertion of the ethynyl group had a negative effect on the anti-proliferative effect compared to analogous compounds prepared previously lacking the ethynyl group.

### 4. Experimental

#### 4.1. General procedures

All chemicals were purchased from Sigma–Aldrich, Lennox Chemicals, Fluorochem Limited or Tokyo Chemical Industry UK

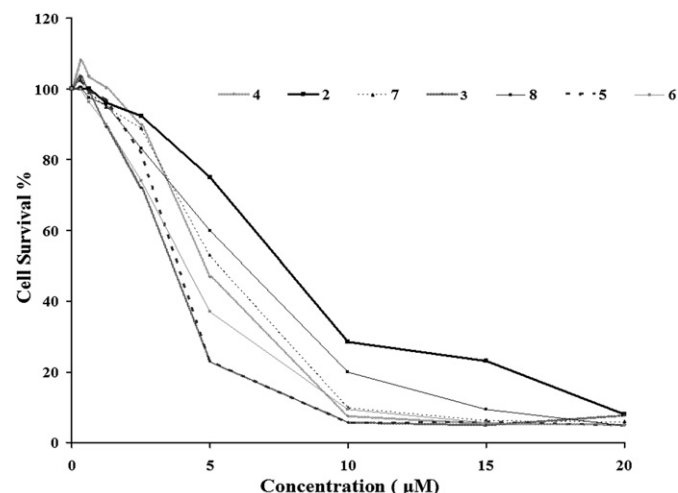


Fig. 2. Cytotoxicity of derivatives **2–8**.

**Table 2**

$IC_{50}$  values for compounds **2–8** and cisplatin against human lung carcinoma cell line H1299.

Compound	$IC_{50}$ value ( $\mu$ M)
Cisplatin	$1.5 \pm 0.1$
<i>N</i> -{6-(Ferrocenyl) ethynyl-2-naphthoyl}- $\gamma$ -aminobutyric acid ethyl ester <b>2</b>	$7.2 \pm 1.5$
<i>N</i> -{6-(Ferrocenyl) ethynyl-2-naphthoyl}-glycine-glycine ethyl ester <b>3</b>	$5.0 \pm 4.1$
<i>N</i> -{6-(Ferrocenyl) ethynyl-2-naphthoyl}-glycine-L-alanine ethyl ester <b>4</b>	$5.0 \pm 3.6$
<i>N</i> -{6-(Ferrocenyl) ethynyl-2-naphthoyl}-sarcosine-glycine ethyl ester <b>5</b>	$4.7 \pm 3.7$
<i>N</i> -{6-(Ferrocenyl) ethynyl-2-naphthoyl}-L-proline-glycine ethyl ester <b>6</b>	$3.2 \pm 6.6$
<i>N</i> -{6-(Ferrocenyl) ethynyl-2-naphthoyl}-L-proline-L-alanine ethyl ester <b>7</b>	$5.1 \pm 1.3$
<i>N</i> -{6-(Ferrocenyl) ethynyl-2-naphthoyl}-L-proline-L-alanine ethyl ester <b>8</b>	$3.8 \pm 2.0$

Limited; and used as received. Commercial grade reagents were used without further purification. When necessary, all solvents were purified and dried prior to use. Riedel-Haën silica gel was used for thin layer and column chromatography. Melting points were determined using a Stuart melting point (SMP3) apparatus and are uncorrected. Optical rotation measurements were made on a Perkin–Elmer 343 Polarimeter and are quoted in units of  $10^{-1} \text{ deg cm}^2 \text{ g}^{-1}$ . Infrared spectra were recorded on a Perkin–Elmer Spectrum 100 FT-IR with ATR. UV–Vis spectra were recorded on a Hewlett Packard 8452 A diode array UV–Vis spectrophotometer.  $^1\text{H}$  and  $^{13}\text{C}$  NMR spectra were recorded in deuterated solvents on a Bruker Avance 400 NMR. The  $^1\text{H}$  and  $^{13}\text{C}$  NMR chemical shifts are reported in ppm (parts per million). Tetramethylsilane (TMS) or the residual solvent peaks were used as an internal reference. All coupling constants ( $J$ ) are in Hertz. Electrospray ionisation mass spectra were performed on a Micromass LCT mass spectrometer. Tandem mass spectra were obtained on a Micromass Quattro micro™ LC–MS/MS triple quadrupole mass spectrometer.

Cyclic voltammograms were recorded in anhydrous acetonitrile (Sigma–Aldrich), with 0.1 M tetrabutylammonium hexafluorophosphate (TBAPF<sub>6</sub>) as a supporting electrolyte, using a CH Instruments 600a electrochemical analyzer (Pico-Amp Booster and Faraday Cage). The experiments were carried out at room temperature. A three-electrode cell consisting of a glassy carbon working-electrode, a platinum wire counter-electrode and an Ag/AgCl reference electrode was used. The glassy carbon electrode was polished with 0.3  $\mu$ m alumina followed by 0.05  $\mu$ m alumina, between each experiment to remove any surface contaminants. The scan rate was  $0.1 \text{ V s}^{-1}$ . The concentration range of the ferrocene compounds was 1.0 mM in acetonitrile. The  $E^{\circ}$  values obtained for the test samples were referenced relative to the ferrocene/ferricenium redox couple.

#### 4.2. General procedure for the synthesis of the starting materials

##### 4.2.1. 6-Ferrocenyl ethynyl-2-naphthoic acid **1**

Ethynyl ferrocene (2.00 g, 9.52 mmol) and 6-bromo-2-naphthoic acid (2.39 g, 9.52 mmol) were mixed together and dissolved in 50 ml of a 1:1 mixture of dry triethylamine and tetrahydrofuran under nitrogen for 10 min. Triphenylphosphine (0.20 g, 0.76 mmol), bis(triphenylphosphine)palladium(II) dichloride (0.28 g, 0.38 mmol) and copper(I) iodide (0.07 g, 0.38 mmol) were mixed together and added to the reaction mixture. The reaction mixture was stirred for 10 min and refluxed at 80  $^{\circ}\text{C}$  for 12 h. The reaction mixture was vacuum

filtered. The solvent was removed *in vacuo* to yield the crude product. The crude product was purified by column chromatography (eluant 1:1 hexane:ethyl acetate) to yield the desired product as a red solid (2.34 g, 64%), mp 167–169 °C.

$^1\text{H NMR}$  (400 MHz)  $\delta$  (DMSO- $d_6$ ): 12.87 (1H, s,  $-\text{COOH}$ ), 8.13 (1H, s, ArH), 7.95–7.48 (5H, m, (ArH)), 4.60 (2H, t,  $J = 2.0$  Hz, *ortho* on  $\eta^5\text{-C}_5\text{H}_4\text{-C}\equiv\text{C}-$ ), 4.27 (2H, t,  $J = 2.0$  Hz *meta* on  $\eta^5\text{-C}_5\text{H}_4\text{-C}\equiv\text{C}-$ ), 4.19 (5H, s,  $\eta^5\text{-C}_5\text{H}_5$ ).

$^{13}\text{C NMR}$  (100 MHz)  $\delta$  (DMSO- $d_6$ ): 172.7 (C=O), 134.9 (C<sub>q</sub>), 134.6 (C<sub>q</sub>), 134.0 (C<sub>q</sub>), 132.2 (C<sub>q</sub>), 131.6, 130.3, 128.1, 128.0, 127.8, 120.8, 90.3 ( $\eta^5\text{-C}_5\text{H}_4\text{-C}\equiv\text{C}-$ ), 85.7 ( $\eta^5\text{-C}_5\text{H}_4\text{-C}\equiv\text{C}-$ ), 71.4 (C<sub>ortho</sub>  $\eta^5\text{-C}_5\text{H}_4\text{-C}\equiv\text{C}-$ ), 69.9 ( $\eta^5\text{-C}_5\text{H}_5$ ), 68.7 (C<sub>meta</sub>  $\eta^5\text{-C}_5\text{H}_4\text{-C}\equiv\text{C}-$ ), 65.8 (C<sub>ipso</sub>  $\eta^5\text{-C}_5\text{H}_4\text{-C}\equiv\text{C}-$ ).

#### 4.3. General procedure for the synthesis of *N*-{6-(ferrocenyl) ethynyl-2-naphthoyl} amino acid and dipeptide ethyl esters

##### 4.3.1. *N*-{6-(Ferrocenyl) ethynyl-2-naphthoyl}- $\gamma$ -aminobutyric acid ethyl ester **2**

6-(Ferrocenyl) ethynyl-2-naphthoic acid (1.00 g, 2.63 mmol) was dissolved in dichloromethane (100 ml) at 0 °C. *N*-(3-dimethylaminopropyl)-*N'*-ethylcarbodiimide hydrochloride (0.50 g, 2.63 mmol), 1-hydroxybenzotriazole (0.36 g, 2.63 mmol) and triethylamine (6 ml) were added and the reaction mixture was allowed to stir at 0 °C for 45 min. The reaction mixture was then allowed to stir at room temperature for 48 h. The reaction mixture was washed with water and brine. The organic layer was dried over MgSO<sub>4</sub>. The solvent was removed *in vacuo* to yield the crude product. The crude product was purified by column chromatography (eluant 1:1 hexane:ethyl acetate) and recrystallisation from hexane:ethyl acetate yielded the desired product as a red solid (0.42 g, 32%), m.p. 71–73 °C;  $E^\circ = 131$  mV (vs Fc/Fc<sup>+</sup>).

Mass spectrum: found: [M + Na]<sup>+</sup> 516.1255.

C<sub>29</sub>H<sub>27</sub>NO<sub>3</sub>FeNa requires: 516.1340.

I.R.  $\nu_{\text{max}}$  (KBr): 3283 (NH), 2205 (C≡C), 1726 (C=O<sub>ester</sub>), 1605 (C=O<sub>amide</sub>) cm<sup>-1</sup>.

UV–Vis  $\lambda_{\text{max}}$  EtOH: 268 ( $\epsilon$  308) nm.

$^1\text{H NMR}$  (400 MHz)  $\delta$  (CDCl<sub>3</sub>): 8.18 (1H, s, ArH), 7.81 (1H, s, ArH), 7.75–7.49 (5H, m, (CONH), (ArH)), 4.47 (2H, t,  $J = 1.6$  Hz, *ortho* on  $\eta^5\text{-C}_5\text{H}_4\text{-C}\equiv\text{C}-$ ), 4.19–4.18 (7H, m, (*meta* on  $\eta^5\text{-C}_5\text{H}_4\text{-C}\equiv\text{C}-$ ), ( $\eta^5\text{-C}_5\text{H}_5$ )), 4.04 (2H, q,  $J = 7.2$  Hz,  $-\text{OCH}_2\text{CH}_3$ ), 3.46 (2H, q,  $J = 5.6$  Hz,  $-\text{NHCH}_2\text{CH}_2\text{CH}_2-$ ), 2.37 (2H, t,  $J = 6.8$  Hz,  $-\text{NHCH}_2\text{CH}_2\text{CH}_2-$ ), 1.87 (2H, quin,  $J = 6.4$  Hz,  $-\text{NHCH}_2\text{CH}_2\text{CH}_2-$ ), 1.15 (3H, t,  $J = 7.2$  Hz,  $-\text{OCH}_2\text{CH}_3$ ).

$^{13}\text{C NMR}$  (100 MHz)  $\delta$  (CDCl<sub>3</sub>): 171.5 (C=O), 167.4 (C=O), 131.5 (C<sub>q</sub>), 130.1 (C<sub>q</sub>), 129.1 (C<sub>q</sub>), 128.9 (C<sub>q</sub>), 128.2, 127.6, 127.7, 126.0, 125.1, 123.0, 89.2 ( $\eta^5\text{-C}_5\text{H}_4\text{-C}\equiv\text{C}-$ ), 85.0 ( $\eta^5\text{-C}_5\text{H}_4\text{-C}\equiv\text{C}-$ ), 71.9 (C<sub>ortho</sub>  $\eta^5\text{-C}_5\text{H}_4\text{-C}\equiv\text{C}-$ ), 69.2 ( $\eta^5\text{-C}_5\text{H}_5$ ), 68.4 (C<sub>meta</sub>  $\eta^5\text{-C}_5\text{H}_4\text{-C}\equiv\text{C}-$ ), 63.8 (C<sub>ipso</sub>  $\eta^5\text{-C}_5\text{H}_4\text{-C}\equiv\text{C}-$ ), 60.0 ( $-\text{OCH}_2\text{CH}_3$ , -ve DEPT), 39.0 ( $-\text{NHCH}_2\text{CH}_2\text{CH}_2-$ , -ve DEPT), 31.2 ( $-\text{NHCH}_2\text{CH}_2\text{CH}_2-$ , -ve DEPT), 23.3 ( $-\text{NHCH}_2\text{CH}_2\text{CH}_2-$ , -ve DEPT), 13.1 ( $-\text{OCH}_2\text{CH}_3$ ).

##### 4.3.2. *N*-{6-(Ferrocenyl) ethynyl-2-naphthoyl}-glycine-glycine ethyl ester **3**

Glycine-glycine ethyl ester hydrochloride (0.42 g, 2.63 mmol) was used as a starting material. The crude product was purified by column chromatography (eluant 1:1 hexane:ethyl acetate) and recrystallisation from hexane:ethyl acetate yielded the desired product as a red solid (0.38 g, 28%), m.p. 128–130 °C;  $E^\circ = 141$  mV (vs Fc/Fc<sup>+</sup>).

Mass spectrum: [M + Na]<sup>+</sup> found: 545.1130.

C<sub>29</sub>H<sub>26</sub>N<sub>2</sub>O<sub>4</sub>FeNa requires: 545.1140.

I.R.  $\nu_{\text{max}}$  (KBr): 3261 (NH), 2204 (C≡C), 1736 (C=O<sub>ester</sub>), 1658 (C=O<sub>amide</sub>), 1603 (C=O<sub>amide</sub>) cm<sup>-1</sup>.

UV–Vis  $\lambda_{\text{max}}$  EtOH: 278 ( $\epsilon$  310) nm.

$^1\text{H NMR}$  (400 MHz)  $\delta$  (CDCl<sub>3</sub>): 8.13 (1H, s, ArH), 7.95–7.48 (7H, m, (ArH), ( $-\text{CONH}-$ ), ( $-\text{CONH}-$ )), 4.61 (2H, t,  $J = 2.0$  Hz, *ortho* on  $\eta^5\text{-C}_5\text{H}_4\text{-C}\equiv\text{C}-$ ), 4.30 (2H, t,  $J = 2.0$  Hz, *meta* on  $\eta^5\text{-C}_5\text{H}_4\text{-C}\equiv\text{C}-$ ), 4.19–4.15 (11H, m, ( $\eta^5\text{-C}_5\text{H}_5$ ), ( $-\text{NHCH}_2\text{CO}-$ ), ( $-\text{NHCH}_2\text{CO}-$ ), ( $-\text{OCH}_2\text{CH}_3$ )), 1.23 (3H, t,  $J = 7.2$  Hz,  $-\text{OCH}_2\text{CH}_3$ ).

$^{13}\text{C NMR}$  (100 MHz)  $\delta$  (CDCl<sub>3</sub>): 172.7 (C=O), 170.9 (C=O), 169.6 (C=O), 133.9 (C<sub>q</sub>), 132.6 (C<sub>q</sub>), 131.0 (C<sub>q</sub>), 130.2 (C<sub>q</sub>), 129.6, 129.3, 128.9, 128.1, 127.8, 125.8, 90.3 ( $\eta^5\text{-C}_5\text{H}_4\text{-C}\equiv\text{C}-$ ), 84.7 ( $\eta^5\text{-C}_5\text{H}_4\text{-C}\equiv\text{C}-$ ), 72.1 (C<sub>ortho</sub>  $\eta^5\text{-C}_5\text{H}_4\text{-C}\equiv\text{C}-$ ), 70.0 ( $\eta^5\text{-C}_5\text{H}_5$ ), 69.7 (C<sub>meta</sub>  $\eta^5\text{-C}_5\text{H}_4\text{-C}\equiv\text{C}-$ ), 67.8 (C<sub>ipso</sub>  $\eta^5\text{-C}_5\text{H}_4\text{-C}\equiv\text{C}-$ ), 61.6 ( $-\text{OCH}_2\text{CH}_3$ , -ve DEPT), 42.3 ( $-\text{NHCH}_2\text{CO}-$ , -ve DEPT), 40.1 ( $-\text{NHCH}_2\text{CO}-$ , -ve DEPT), 14.8 ( $-\text{OCH}_2\text{CH}_3$ ).

##### 4.3.3. *N*-{6-(Ferrocenyl) ethynyl-2-naphthoyl}-glycine-L-alanine ethyl ester **4**

Glycine-L-alanine ethyl ester hydrochloride (0.46 g, 2.63 mmol) was used as a starting material. The crude product was purified by column chromatography (eluant 1:1 hexane:ethyl acetate) and recrystallisation from hexane:ethyl acetate yielded the desired product as a red solid (0.23 g, 16%), m.p. 58–60 °C;  $E^\circ = 139$  mV (vs Fc/Fc<sup>+</sup>); [ $\alpha$ ]<sub>D</sub><sup>20</sup> =  $-14^\circ$  ( $c$  0.1, EtOH).

Mass spectrum: [M + Na]<sup>+</sup> found: 559.1305.

C<sub>30</sub>H<sub>28</sub>N<sub>2</sub>O<sub>4</sub>FeNa requires: 559.1398.

I.R.  $\nu_{\text{max}}$  (KBr): 3287 (NH), 2204 (C≡C), 1734 (C=O<sub>ester</sub>), 1658 (C=O<sub>amide</sub>), 1625 (C=O<sub>amide</sub>) cm<sup>-1</sup>.

UV–Vis  $\lambda_{\text{max}}$  EtOH: 242 ( $\epsilon$  316) nm.

$^1\text{H NMR}$  (400 MHz)  $\delta$  (CDCl<sub>3</sub>): 8.21 (1H, s, ArH), 7.87–7.51 (7H, m, (ArH), ( $-\text{CONH}-$ ), ( $-\text{CONH}-$ )), 4.48–4.47 (3H, m, ( $-\text{CHCH}_3$ ), (*ortho* on  $\eta^5\text{-C}_5\text{H}_4\text{-C}\equiv\text{C}-$ )), 4.19–4.07 (11H, m, (*meta* on  $\eta^5\text{-C}_5\text{H}_4\text{-C}\equiv\text{C}-$ ), ( $\eta^5\text{-C}_5\text{H}_5$ ), ( $-\text{OCH}_2\text{CH}_3$ ), ( $-\text{NHCH}_2\text{CO}-$ )), 1.36 (3H, d,  $J = 7.2$  Hz,  $-\text{CHCH}_3$ ), 1.28 (3H, t,  $J = 6.8$  Hz,  $-\text{OCH}_2\text{CH}_3$ ).

$^{13}\text{C NMR}$  (100 MHz)  $\delta$  (CDCl<sub>3</sub>): 171.8 (C=O), 169.1 (C=O), 167.9 (C=O), 134.5 (C<sub>q</sub>), 131.5 (C<sub>q</sub>), 130.8 (C<sub>q</sub>), 130.4 (C<sub>q</sub>), 129.3, 128.9, 128.0, 127.7, 124.3, 123.4, 90.4 ( $\eta^5\text{-C}_5\text{H}_4\text{-C}\equiv\text{C}-$ ), 84.9 ( $\eta^5\text{-C}_5\text{H}_4\text{-C}\equiv\text{C}-$ ), 71.3 (C<sub>ortho</sub>  $\eta^5\text{-C}_5\text{H}_4\text{-C}\equiv\text{C}-$ ), 70.1 ( $\eta^5\text{-C}_5\text{H}_5$ ), 69.5 (C<sub>meta</sub>  $\eta^5\text{-C}_5\text{H}_4\text{-C}\equiv\text{C}-$ ), 65.9 (C<sub>ipso</sub>  $\eta^5\text{-C}_5\text{H}_4\text{-C}\equiv\text{C}-$ ), 60.3 ( $-\text{OCH}_2\text{CH}_3$ , -ve DEPT), 48.9 ( $-\text{CHCH}_3$ ), 43.1 ( $-\text{NHCH}_2\text{CO}-$ , -ve DEPT), 17.2 ( $-\text{CHCH}_3$ ), 13.7 ( $-\text{OCH}_2\text{CH}_3$ ).

##### 4.3.4. *N*-{6-(Ferrocenyl) ethynyl-2-naphthoyl}-sarcosine-glycine ethyl ester **5**

Sarcosine-glycine ethyl ester hydrochloride (0.46 g, 2.63 mmol) was used as a starting material. The crude product was purified by column chromatography (eluant 1:1 hexane:ethyl acetate) and recrystallisation from hexane:ethyl acetate yielded the desired product as a red solid (0.19 g, 13%), m.p. 32–34 °C;  $E^\circ = 162$  mV (vs Fc/Fc<sup>+</sup>).

Mass spectrum: found: [M + Na]<sup>+</sup> 559.1307.

C<sub>30</sub>H<sub>28</sub>N<sub>2</sub>O<sub>4</sub>FeNa requires: 559.1398.

I.R.  $\nu_{\text{max}}$  (KBr): 3284 (NH), 2205 (C≡C), 1744 (C=O<sub>ester</sub>), 1676 (C=O<sub>amide</sub>), 1605 (C=O<sub>amide</sub>) cm<sup>-1</sup>.

UV–Vis  $\lambda_{\text{max}}$  EtOH: 252 ( $\epsilon$  313) nm.

$^1\text{H NMR}$  (400 MHz)  $\delta$  (CDCl<sub>3</sub>): 7.92–7.49 (7H, m, ( $-\text{CONH}-$ ), (ArH)), 4.48 (2H, s, *ortho* on  $\eta^5\text{-C}_5\text{H}_4\text{-C}\equiv\text{C}-$ ), 4.30–3.90 (13H, m, (*meta* on  $\eta^5\text{-C}_5\text{H}_4\text{-C}\equiv\text{C}-$ ), ( $\eta^5\text{-C}_5\text{H}_5$ ), ( $-\text{N}(\text{CH}_3)\text{CH}_2\text{CO}-$ ), ( $-\text{NHCH}_2\text{CO}-$ ) ( $-\text{OCH}_2\text{CH}_3$ )), 3.10 (3H, s,  $-\text{N}(\text{CH}_3)\text{CH}_2\text{CO}-$ ), 1.19 (3H, t,  $J = 7.2$  Hz,  $-\text{OCH}_2\text{CH}_3$ ).

$^{13}\text{C NMR}$  (100 MHz)  $\delta$  (CDCl<sub>3</sub>): 172.7 (C=O), 170.4 (C=O), 167.2 (C=O), 133.6 (C<sub>q</sub>), 132.7 (C<sub>q</sub>), 131.9 (C<sub>q</sub>), 130.8 (C<sub>q</sub>), 129.5, 128.5, 128.1, 127.3, 125.0, 122.9, 90.1 ( $\eta^5\text{-C}_5\text{H}_4\text{-C}\equiv\text{C}-$ ), 85.9 ( $\eta^5\text{-C}_5\text{H}_4\text{-C}\equiv\text{C}-$ ), 71.8 (C<sub>ortho</sub>  $\eta^5\text{-C}_5\text{H}_4\text{-C}\equiv\text{C}-$ ), 70.5 ( $\eta^5\text{-C}_5\text{H}_5$ ), 69.5 (C<sub>meta</sub>  $\eta^5\text{-C}_5\text{H}_4\text{-C}\equiv\text{C}-$ ), 65.4 (C<sub>ipso</sub>  $\eta^5\text{-C}_5\text{H}_4\text{-C}\equiv\text{C}-$ ), 61.7 ( $-\text{OCH}_2\text{CH}_3$ , -ve DEPT), 48.2 ( $-\text{N}(\text{CH}_3)\text{CH}_2\text{CO}-$ , -ve DEPT), 41.2 ( $-\text{NHCH}_2\text{CO}-$ , -ve DEPT), 38.4 ( $-\text{N}(\text{CH}_3)\text{CH}_2\text{CO}-$ ), 14.2 ( $-\text{OCH}_2\text{CH}_3$ ).

#### 4.3.5. *N*-[6-(Ferrocenyl) ethynyl-2-naphthoyl]-sarcosine-*L*-alanine ethyl ester **6**

Sarcosine-*L*-alanine ethyl ester hydrochloride (0.50 g, 2.63 mmol) was used as a starting material. The crude product was purified by column chromatography (eluant 1:1 hexane:ethyl acetate) and recrystallisation from hexane:ethyl acetate yielded the desired product as a red solid (0.19 g, 13%), m.p. 59–61 °C;  $E^{\nu}$  = 119 mV (vs Fc/Fc<sup>+</sup>);  $[\alpha]_D^{20}$  = -23° (c 0.1, EtOH).

Mass spectrum:  $[M + Na]^+$  found: 573.1879.

C<sub>31</sub>H<sub>30</sub>N<sub>2</sub>O<sub>4</sub>FeNa requires: 573.1555.

I.R.  $\nu_{\max}$  (KBr): 3308 (NH), 2206 (C≡C-), 1732 (C=O<sub>ester</sub>), 1625 (C=O<sub>amide</sub>), 1538 (C=O<sub>amide</sub>) cm<sup>-1</sup>.

UV-Vis  $\lambda_{\max}$  EtOH: 261 ( $\epsilon$  304) nm.

<sup>1</sup>H NMR (400 MHz)  $\delta$  (CDCl<sub>3</sub>): 7.93–7.50 {7H, m, (-CONH-), (ArH)}, 4.53–4.40 {3H, m, (ortho on  $\eta^5$ -C<sub>5</sub>H<sub>4</sub>-C≡C-), (-CHCH<sub>3</sub>)}, 4.20–4.10 {11H, m, (meta on  $\eta^5$ -C<sub>5</sub>H<sub>4</sub>-C≡C-), ( $\eta^5$ -C<sub>5</sub>H<sub>5</sub>)}, (-N(CH<sub>3</sub>)CH<sub>2</sub>CO-), (-OCH<sub>2</sub>CH<sub>3</sub>)}, 3.07 {3H, s, -N(CH<sub>3</sub>)CH<sub>2</sub>CO-}, 1.38 (2H, d,  $J$  = 7.2 Hz, -CHCH<sub>3</sub>), 1.21 (3H, t,  $J$  = 7.2 Hz, -OCH<sub>2</sub>CH<sub>3</sub>).

<sup>13</sup>C NMR (100 MHz)  $\delta$  (CDCl<sub>3</sub>): 172.0 (C=O), 170.2 (C=O), 169.1 (C=O), 134.4 (C<sub>q</sub>), 132.7 (C<sub>q</sub>), 131.6 (C<sub>q</sub>), 130.6 (C<sub>q</sub>), 129.4, 128.5, 128.0, 127.3, 125.0, 123.9, 91.3 ( $\eta^5$ -C<sub>5</sub>H<sub>4</sub>-C≡C-), 84.7 ( $\eta^5$ -C<sub>5</sub>H<sub>4</sub>-C≡C-), 71.1 (C<sub>ortho</sub>  $\eta^5$ -C<sub>5</sub>H<sub>4</sub>-C≡C-), 69.7 ( $\eta^5$ -C<sub>5</sub>H<sub>5</sub>), 68.2 (C<sub>meta</sub>  $\eta^5$ -C<sub>5</sub>H<sub>4</sub>-C≡C-), 66.2 (C<sub>ipso</sub>  $\eta^5$ -C<sub>5</sub>H<sub>4</sub>-C≡C-), 61.9 (-OCH<sub>2</sub>CH<sub>3</sub>, -ve DEPT), 49.7 (-CHCH<sub>3</sub>), 45.1 (-N(CH<sub>3</sub>)CH<sub>2</sub>CO-, -ve DEPT), 38.2 (-N(CH<sub>3</sub>)CH<sub>2</sub>CO-, -ve DEPT), 19.0 (-CHCH<sub>3</sub>), 13.8 (-OCH<sub>2</sub>CH<sub>3</sub>).

#### 4.3.6. *N*-[6-(Ferrocenyl) ethynyl-2-naphthoyl]-*L*-proline-glycine ethyl ester **7**

*L*-Proline-glycine ethyl ester hydrochloride (0.53 g, 2.63 mmol) was used as a starting material. The crude product was purified by column chromatography (eluant 1:1 hexane:ethyl acetate) and recrystallisation from hexane:ethyl acetate yielded the desired product as a red solid (0.22 g, 15%), m.p. 53–55 °C;  $E^{\nu}$  = 153 mV (vs Fc/Fc<sup>+</sup>);  $[\alpha]_D^{20}$  = +27° (c 0.1, EtOH).

Mass spectrum:  $[M + Na]^+$  found: 585.1467.

C<sub>32</sub>H<sub>30</sub>N<sub>2</sub>O<sub>4</sub>FeNa requires: 585.1555.

I.R.  $\nu_{\max}$  (KBr): 3313 (NH), 2205 (C≡C-), 1735 (C=O<sub>ester</sub>), 1652 (C=O<sub>amide</sub>), 1604 (C=O<sub>amide</sub>) cm<sup>-1</sup>.

UV-Vis  $\lambda_{\max}$  EtOH: 254 ( $\epsilon$  317) nm.

<sup>1</sup>H NMR (400 MHz)  $\delta$  (CDCl<sub>3</sub>): 7.96–7.38 {7H, m, (ArH), (-CONH-)}, 4.82 (1H, t,  $J$  = 5.2 Hz, -N(CH<sub>2</sub>CH<sub>2</sub>CH<sub>2</sub>)CHCO-), 4.47 (2H, s, ortho on  $\eta^5$ -C<sub>5</sub>H<sub>4</sub>-C≡C-), 4.21–4.18 {7H, m, (meta on  $\eta^5$ -C<sub>5</sub>H<sub>4</sub>-C≡C-), ( $\eta^5$ -C<sub>5</sub>H<sub>5</sub>)}, 4.16 (2H, q,  $J$  = 7.2 Hz, -OCH<sub>2</sub>CH<sub>3</sub>), 4.00 (2H, d,  $J$  = 5.6 Hz, -NHCH<sub>2</sub>CO-), 3.61–3.50 (2H, m, -N(CH<sub>2</sub>CH<sub>2</sub>CH<sub>2</sub>)CHCO-, 2.40–1.70 (4H, m, -N(CH<sub>2</sub>CH<sub>2</sub>CH<sub>2</sub>)CHCO-), 1.21 (3H, t,  $J$  = 7.2 Hz, -OCH<sub>2</sub>CH<sub>3</sub>).

<sup>13</sup>C NMR (100 MHz)  $\delta$  (CDCl<sub>3</sub>): 171.7 (C=O), 171.0 (C=O), 169.2 (C=O), 133.7 (C<sub>q</sub>), 131.5 (C<sub>q</sub>), 130.6 (C<sub>q</sub>), 129.4 (C<sub>q</sub>), 128.1, 127.9, 127.0, 127.2, 124.9, 123.0, 90.1 ( $\eta^5$ -C<sub>5</sub>H<sub>4</sub>-C≡C-), 84.8 ( $\eta^5$ -C<sub>5</sub>H<sub>4</sub>-C≡C-), 71.0 (C<sub>ortho</sub>  $\eta^5$ -C<sub>5</sub>H<sub>4</sub>-C≡C-), 70.1 ( $\eta^5$ -C<sub>5</sub>H<sub>5</sub>), 69.1 (C<sub>meta</sub>  $\eta^5$ -C<sub>5</sub>H<sub>4</sub>-C≡C-), 64.9 (C<sub>ipso</sub>  $\eta^5$ -C<sub>5</sub>H<sub>4</sub>-C≡C-), 61.4 (-OCH<sub>2</sub>CH<sub>3</sub>, -ve DEPT), 50.8 (-N(CH<sub>2</sub>CH<sub>2</sub>CH<sub>2</sub>)CHCO-, -ve DEPT), 47.6 (-N(CH<sub>2</sub>CH<sub>2</sub>CH<sub>2</sub>)CHCO-, -ve DEPT), 42.5 (-NHCH<sub>2</sub>CO-, -ve DEPT), 27.4 (-N(CH<sub>2</sub>CH<sub>2</sub>CH<sub>2</sub>)CHCO-, -ve DEPT), 25.0 (-N(CH<sub>2</sub>CH<sub>2</sub>CH<sub>2</sub>)CHCO-, -ve DEPT), 13.2 (-OCH<sub>2</sub>CH<sub>3</sub>).

#### 4.3.7. *N*-[6-(Ferrocenyl) ethynyl-2-naphthoyl]-*L*-proline-*L*-alanine ethyl ester **8**

*L*-Proline-*L*-alanine ethyl ester hydrochloride (0.56 g, 2.63 mmol) was used as a starting material. The crude product was purified by column chromatography (eluant 1:1 hexane:ethyl acetate) and recrystallisation from hexane:ethyl acetate yielded the desired product as a red solid (0.17 g, 11%), m.p. 56–58 °C;  $E^{\nu}$  = 133 mV (vs Fc/Fc<sup>+</sup>);  $[\alpha]_D^{20}$  = -67° (c 0.1, EtOH).

Mass spectrum: found:  $[M + Na]^+$  599.1639.

C<sub>33</sub>H<sub>32</sub>N<sub>2</sub>O<sub>4</sub>FeNa requires: 599.1711.

I.R.  $\nu_{\max}$  (KBr): 3285 (NH), 2202 (C≡C-), 1736 (C=O<sub>ester</sub>), 1672 (C=O<sub>amide</sub>), 1608 (C=O<sub>amide</sub>) cm<sup>-1</sup>.

UV-Vis  $\lambda_{\max}$  EtOH: 270 ( $\epsilon$  311) nm.

<sup>1</sup>H NMR (400 MHz)  $\delta$  (CDCl<sub>3</sub>): 8.12 (1H, s, ArH), 7.96–7.54 {6H, m, (ArH), (-CONH-)}, 4.72–4.65 {3H, m, (-N(CH<sub>2</sub>CH<sub>2</sub>CH<sub>2</sub>)CHCO-), (ortho on  $\eta^5$ -C<sub>5</sub>H<sub>4</sub>-C≡C-)}, 4.55–4.45 (1H, m, -CHCH<sub>3</sub>), 4.33 (2H, s, meta on  $\eta^5$ -C<sub>5</sub>H<sub>4</sub>-C≡C-), 4.33–4.12 {7H, m, ( $\eta^5$ -C<sub>5</sub>H<sub>5</sub>)}, (-OCH<sub>2</sub>CH<sub>3</sub>), 3.61–3.49 (2H, m, -N(CH<sub>2</sub>CH<sub>2</sub>CH<sub>2</sub>)CHCO-), 2.40–1.70 (4H, m, -N(CH<sub>2</sub>CH<sub>2</sub>CH<sub>2</sub>)CHCO-), 1.38 (3H, d,  $J$  = 4.4 Hz, -CHCH<sub>3</sub>), 1.17 (3H, t,  $J$  = 7.2 Hz, -OCH<sub>2</sub>CH<sub>3</sub>).

<sup>13</sup>C NMR (100 MHz)  $\delta$  (CDCl<sub>3</sub>): 172.1 (C=O), 169.7 (C=O), 168.2 (C=O), 134.5 (C<sub>q</sub>), 133.5 (C<sub>q</sub>), 132.8 (C<sub>q</sub>), 131.6 (C<sub>q</sub>), 130.1, 128.4, 128.0, 127.1, 124.7, 121.0, 90.1 ( $\eta^5$ -C<sub>5</sub>H<sub>4</sub>-C≡C-), 85.8 ( $\eta^5$ -C<sub>5</sub>H<sub>4</sub>-C≡C-), 71.9 (C<sub>ortho</sub>  $\eta^5$ -C<sub>5</sub>H<sub>4</sub>-C≡C-), 70.2 ( $\eta^5$ -C<sub>5</sub>H<sub>5</sub>), 69.4 (C<sub>meta</sub>  $\eta^5$ -C<sub>5</sub>H<sub>4</sub>-C≡C-), 67.6 (C<sub>ipso</sub>  $\eta^5$ -C<sub>5</sub>H<sub>4</sub>-C≡C-), 61.9 (-OCH<sub>2</sub>CH<sub>3</sub>, -ve DEPT), 60.1 (-N(CH<sub>2</sub>CH<sub>2</sub>CH<sub>2</sub>)CHCO-, -ve DEPT), 50.7 (-N(CH<sub>2</sub>CH<sub>2</sub>CH<sub>2</sub>)CHCO-, -ve DEPT), 48.5 (-CHCH<sub>3</sub>), 27.2 (-N(CH<sub>2</sub>CH<sub>2</sub>CH<sub>2</sub>)CHCO-, -ve DEPT), 25.0 (-N(CH<sub>2</sub>CH<sub>2</sub>CH<sub>2</sub>)CHCO-, -ve DEPT), 19.2 (-CHCH<sub>3</sub>), 14.0 (-OCH<sub>2</sub>CH<sub>3</sub>).

### 4.4. General procedure for in vitro cytotoxicity assays

#### 4.4.1. Biological assays. Cell line

H1299 was obtained from the American Tissue Culture Centre (ATCC). The cell line was grown in RPMI-1640 supplemented with 10% foetal calf serum (FCS) and 1% Sodium Pyruvate at 37 °C in a 5% CO<sub>2</sub> humidified chamber.

#### 4.4.2. In vitro proliferation assays

Cells in the exponential phase of growth were harvested by trypsinisation and a cell suspension of 1 × 10<sup>3</sup> cells per ml was prepared in fresh culture medium. The cell suspension (100  $\mu$ L) was added to a flat bottom 96-well plate (Costar, 3599), the plates were agitated gently in order to ensure even dispersion of cells over the surface of the wells, and then the cells were incubated for an initial 24 h in a 37 °C, 5% CO<sub>2</sub> incubator, to allow cell attachment to the wells. A 10 mM stock solution of a test sample was prepared in dimethyl sulfoxide; dilute solutions of the test sample were prepared at 2 $\times$  final concentration by spiking the cell culture medium with a calculated amount of the stock solution.

100  $\mu$ L aliquots of each dilute solution was added to each well of the plate, the plate was gently agitated, and then incubated at 37 °C, 5% CO<sub>2</sub> for 5 days, until cell confluency reached 80–90%. Assessment of cell survival in the presence of the compounds **2–8** was determined by the acid phosphatase assay [30]. The acid phosphatase assay is highly sensitive and is easier to perform than the neutral red assay as it involves fewer steps and fewer reagents. It is also more convenient than the MTT assay because of the inherent problem of removal of the medium from the insoluble crystals. The reproducibility between replicate wells is excellent in the acid phosphatase assay and in many cases it has been shown to be better than the neutral red assay and the MTT assay.

The percentage cell growth in the presence of each compound was determined relative to the control cells. The concentration of compounds causing a 50% growth inhibition (IC<sub>50</sub> of the compound) was determined using CalcuSyn (Biosoft, UK).

### Acknowledgements

This research was partly supported by the Health Research Board, Grant Reference Number HRA/09/86.

### References

- [1] T. Gianferrara, I. Bratsos, E. Alessio, Dalton Trans. 37 (2009) 7588.

- [2] C.G. Hartinger, P.J. Dyson, *Chem. Soc. Rev.* 38 (2009) 391.
- [3] G. Gasser, I. Ott, N. Metzler-Nolte, *J. Med. Chem.* 54 (2011) 3.
- [4] E.W. Neuse, *J. Inorg. Organomet. Poly. Mater.* 15 (2005) 3.
- [5] G. Tabbi, C. Cassino, G. Cavigliolo, D. Colangelo, A. Ghiglia, I. Viano, D. Osella, *J. Med. Chem.* 45 (2002) 5786.
- [6] D. Trachootham, J. Alexandre, P. Huang, *Nat. Rev. Drug Dis.* 8 (2009) 579.
- [7] M.F.R. Fouda, M.M. Abd-Elzaher, R.A. Abdelsamaia, A.A. Labib, *Appl. Organomet. Chem.* 21 (2007) 613.
- [8] C. Ornelas, *New J. Chem.* 35 (2011) 1973.
- [9] A. Nguyen, A. Vessieres, E.A. Hillard, S. Top, P. Pigeon, G. Jaouen, *Chimia* 61 (2007) 716.
- [10] D. Plazuk, A. Vessieres, E.A. Hillard, O. Buriez, E. Labbe, P. Pigeon, M.-A. Plamont, C. Amatore, J. Zakrzewski, G. Jaouen, *J. Med. Chem.* 52 (2009) 4964.
- [11] M. Gormen, D. Plazuk, P. Pigeon, E.A. Hillard, M.-A. Plamont, S. Top, A. Vessières, G. Jaouen, *Tetrahedron Lett.* 51 (2010) 118.
- [12] M. Gormen, P. Pigeon, S. Top, A. Vessieres, M.-A. Plamont, E.A. Hillard, G. Jaouen, *MedChemComm* 1 (2010) 149.
- [13] A. Goel, D. Savage, S.R. Alley, P.N. Kelly, D. O'Sullivan, H. Mueller-Bunz, P.T.M. Kenny, *J. Organomet. Chem.* 692 (2007) 1292.
- [14] A.J. Corry, A. Goel, S.R. Alley, P.N. Kelly, D. O'Sullivan, D. Savage, P.T.M. Kenny, *J. Organomet. Chem.* 692 (2007) 1405.
- [15] A.J. Corry, N. O'Donovan, Á. Mooney, D. O'Sullivan, D.K. Rai, P.T.M. Kenny, *J. Organomet. Chem.* 694 (2009) 880.
- [16] A.J. Corry, A. Mooney, D. O'Sullivan, P.T.M. Kenny, *Inorg. Chim. Acta* 362 (2009) 2957.
- [17] Á. Mooney, A.J. Corry, D. O'Sullivan, D.K. Rai, P.T.M. Kenny, *J. Organomet. Chem.* 694 (2009) 886.
- [18] Á. Mooney, A.J. Corry, C. Ní Ruairc, T. Maghoub, D. O'Sullivan, N. O'Donovan, J. Crown, S. Varughese, S.M. Draper, D.K. Rai, P.T.M. Kenny, *Dalton Trans.* 39 (2010) 8228.
- [19] Á. Mooney, R. Tiedt, T. Maghoub, N. O'Donovan, J. Crown, B. White, P.T.M. Kenny, *J. Med. Chem.* 55 (2012) 5455.
- [20] K. Sonogashira, *J. Organomet. Chem.* 653 (2002) 46–49.
- [21] M.J. Sheehy, J.F. Gallagher, M. Yamashita, Y. Ida, J. White-Colangelo, J. Johnson, R. Orlando, P.T.M. Kenny, *J. Organomet. Chem.* 689 (2004) 1511.
- [22] D. Savage, G. Malone, J.F. Gallagher, Y. Ida, P.T.M. Kenny, *J. Organomet. Chem.* 690 (2005) 383.
- [23] D. Savage, N. Neary, G. Malone, S.R. Alley, J.F. Gallagher, P.T.M. Kenny, *Inorg. Chem. Commun.* 8 (2005) 429.
- [24] D. Savage, G. Malone, S.R. Alley, J.F. Gallagher, A. Goel, P.N. Kelly, H. Mueller-Bunz, P.T.M. Kenny, *J. Organomet. Chem.* 691 (2006) 463.
- [25] D. Savage, S.R. Alley, A. Goel, T. Hogan, Y. Ida, P.N. Kelly, L. Lehmann, P.T.M. Kenny, *Inorg. Chem. Commun.* 9 (2006) 1267.
- [26] J.B. Fenn, *J. Am. Soc. Mass. Spectrom.* 4 (1993) 524.
- [27] K. Biemann, *Biomed. Environ. Mass. Spectrom.* 16 (1988) 99.
- [28] A. Goel, P.T.M. Kenny, *Rapid Commun. Mass. Spectrom.* 22 (2008) 2398.
- [29] W. Bauer, K. Polborn, W. Beck, *J. Organomet. Chem.* 579 (1999) 269.
- [30] A. Martin, M. Clynes, *In Vitro Cell. Dev. Biol.* 27A (1991) 183.